



HAL
open science

Synthesis, structural investigations and evaluation of pyrazine sensitizers for lanthanides emitting in near-infrared and novel phosphine derivatives

Monika Bouet

► **To cite this version:**

Monika Bouet. Synthesis, structural investigations and evaluation of pyrazine sensitizers for lanthanides emitting in near-infrared and novel phosphine derivatives. Organic chemistry. Université d'Orléans; Jagiellonian University, 2012. English. NNT: . tel-01786831

HAL Id: tel-01786831

<https://theses.hal.science/tel-01786831>

Submitted on 6 May 2018

HAL is a multi-disciplinary open access archive for the deposit and dissemination of scientific research documents, whether they are published or not. The documents may come from teaching and research institutions in France or abroad, or from public or private research centers.

L'archive ouverte pluridisciplinaire **HAL**, est destinée au dépôt et à la diffusion de documents scientifiques de niveau recherche, publiés ou non, émanant des établissements d'enseignement et de recherche français ou étrangers, des laboratoires publics ou privés.

**ÉCOLE DOCTORALE 549, SANTÉ, SCIENCES BIOLOGIQUES ET
CHIMIE DU VIVANT**

Institut de Chimie Organique et Analytique (UMR 7311)

THÈSE présentée par :
Monika Cieřlikiewicz-Bouet

Soutenue le : **18 Octobre 2012**

pour obtenir le grade de : **Docteur de l'Université d'Orléans**

Discipline : Chimie Organique

**Synthesis, structural investigations
and evaluation of pyrazine sensitizers for
lanthanides emitting in near-infrared
and novel phosphine derivatives**

THÈSE dirigée par :

Ms Isabelle GILLAIZEAU
Mr Krzysztof LEWIŃSKI

Professeur, Université d'Orléans
Professeur, Université Jagellonne de Cracovie

RAPPORTEURS :

Mr Sylvain JUGE
Ms Anna TRZECIAK

Professeur, Université de Bourgogne
Professeur, Université de Wrocław

JURY (*y reporter tous les membres de jury présents à la soutenance*):

Ms Isabelle GILLAIZEAU
Mr Sylvain JUGE
Mr Krzysztof LEWIŃSKI
Mr Olivier MARTIN
Mr Stéphane PETOUD
Ms Grażyna STOCHEL
Ms Anna TRZECIAK

Professeur, Université d'Orléans
Professeur, Université de Bourgogne
Professeur, Université Jagellonne de Cracovie
Professeur, Université d'Orléans
Directeur de Recherche INSERM, CBM
Professeur, Université Jagellonne de Cracovie
Professeur, Université de Wrocław

Acknowledgments

At the very beginning I would like to acknowledge the Supervisors of my thesis: Prof. Isabelle Gillaizeau and Prof. Krzysztof Lewiński for their accordance to realize the work in the laboratory, under their assistance and help. Without their kind supervision and the application in the International Programme–Double Master this work would not be possible. The great words of thanks to the Directors of both research centers, where I performed thesis: Prof. Grażyna Stochel, the Dean of the Faculty of Chemistry and Prof. Olivier Martin, the Director of the Institute of Organic and Analytical Chemistry.

I am very grateful to Prof. Anna Trzeciak from the University of Wrocław and Prof. Jacek Młynarski from the Jagiellonian University as well as Prof. Sylvain Jugé - University of Bourgogne for the interest they have contributed to this work by agreeing to review the thesis.

I would like to acknowledge the French Embassy in Warsaw for the financial support for the thesis co-tutelle and the French Organization “Association pour la Recherche sur le Cancer (ARC)” for financing the last year of this thesis.

The kind words of thanks should be directed to Dr. Stéphane Petoud and Dr. Sandrine Villette for their help and assistance in spectroscopic investigations realized in the Center of Molecular Biophysics, Dr. Vincent Aucagne and Dr. Agnès Delmas for the possibility to work with cyclopeptides.

I would like to acknowledge also Prof. Gérard Coudert and Dr. Pascal Bouyssou for their kindness, help in solving difficult NMR problems and other, not only chemical, dilemmas. I am grateful to the SFC team: Dr. Caroline West and Dr. Eric Lesellier for chiral analysis. The great words of thanks for all personnel of the laboratory 5 in ICOA, who I met and with whom I spent a lot of very fruitful time, to Nicolas Gigant, Elise Cleaveau, Jérôme Blu, Ela Niemiec, Kasia Kucwaj, Bartek Szmyd, Edyta Korbut and others Master students. My kind words are directed to my colleagues: Christelle Pillard, Myriam Lefoix, Nathalie Percina, Sandrine Grosse, Mathieu Perrier, Jérôme Coste, other PhD students, with whom I was sharing time: Matthieu, Sandrine, Fabien, Thibault, Emmanuel and also personnel for IUT Chimie, Mme Coudrat et Mme Iziz for good and fruitful time spent on the teaching. My kind words of thanks are addressed to all people that I met and shared a time in the corridors of ICOA: Marie-Madelaine Le Floch, Yann Vital, Jean-Marie Robert, Stéphane Retif, Laoge Thao, Allain-Michel Croze.

Finally, the kind words of thanks to my beloved husband Alexis and my family for their support and compassion, comprehension and kindness.

Abbreviations

¹³ C NMR	carbon-13 nuclear magnetic resonance
¹ H NMR	proton-1 nuclear magnetic resonance
³¹ P NMR	phosphorus-31 nuclear magnetic resonance
ATP	adenosine triphosphorane
BINAP	2,2'-bis(diphenylphosphin)-1,1'- bisnaphthyl
Boc group	<i>tert</i> -butoxycarbonyl group
Boc ₂ O	di- <i>tert</i> - butyldicarbonate
CCD	charge coupled device – analogue shift register
Celite [®]	the perlite product for filtration
Cs ₂ CO ₃	cesium carbonate
CuAAC	Copper(I)-catalyzed Azide-Alkyne Cycloaddition
DEAD	diethylacetylene dicarboxylate
DIOP	2,3-O-isopropylidene-2,3-dihydroxyl-4-bis(diphenylophosphino)butane
DIPAMP	1,2'-bis[(methoxyphenyl)(phenylophosphino)]ethane
DMAD	dimethylacetylene dicarboxylate
DMAP	dimethylaminopyridine
DMF	dimethylformamide
DMF	<i>N,N</i> -dimethylformamide
DMSO	dimethylsulfoxide
DNA	deoxyribonucleic acid
DO3A	1,4,7,10-tetraazacyclododecan-1,4,7-triacetic acid
dppfPdCl ₂	1,1'-bis(diphenylophosphino)ferrocene dichloropalladium
EtOAc	ethyl acetate
F(hkl)	structure factor
GooF	goodness of fit parameter
HEPES buffer	4-(2-hydroxyethyl)-1-piperazineethanesulfonic acid buffer
HMPA	hexamethylphosphoramide
HPLC	high pressure liquid chromatography
HRMS	high resolution mass spectrometry
iPr ₂ NEt	diisopropylethylamine
K ₂ CO ₃	potassium carbonate
LDA	lithium diisopropylamide
L-DOPA	(<i>S</i>)-2-amino-3-(3,4-dihydroxyphenyl)propanoic acid
LiHMDS	lithium hexamethyldisilylamide
MoK α	molybdenum radiation
MS	mass spectrometry
Ms	mesyl
MW	molecular weight
MWv	microwave conditions of reaction
<i>n</i> – BuLi	<i>n</i> - butyl lithium
NIR	Near Infrared
ORTEP	program for a plotting a single molecule (Oak Ridge Thermal Ellipsoid Plot)
PAMP	methylphenyl- <i>o</i> -anisylphosphine
PBS buffer	phosphate buffered saline
PE	petroleum ether
QUINAP	1-(2-Diphenylphosphino-1-naphthyl)isoquinoline
R value	residual factor and also reliability factor
R ₁	residual normal factor
RNA	ribonucleic acid
SFC	Supercritical Fluid Chromatography
<i>t</i> – BuOK	potassium <i>tert</i> -butoxide
TBAF	Tetra- <i>n</i> -butylammonium fluoride
TEA	triethylamine
TFA	Trifluoroacetic acid
THF	tetrahydrofuran
THPTA	tris(hydroxypropyl)triazolylmethyl-amine
TIS	triisopropyl silane
TLC	thin layer chromatography
TMS	tetramethylsilan
Ts	tosyl
wR ₂	residual weight factor

Table of content

Acknowledgments.....	3
Abbreviations	5
Table of content	7
General introduction.....	11
Chapter 1.....	19
I. Bibliographic introduction.....	21
I.1. Applications of organophosphorus compounds	22
I.1.1. Organophosphorus compounds as nucleophilic and Brønsted acid organocatalysts	22
I.1.2. Chiral ligands for reactions catalyzed by transition metals	24
I.1.3. Biological importance of organophosphorus compounds.....	26
I.1.3.a. Peptidomimetics.....	26
I.1.3.b. Phosphorus compounds as bioactive agents	28
I.1.3.c. Phosphine containing amino acids	29
I.2. Formation of organophosphorus compounds	31
I.2.1. General introduction	31
I.2.2. Phospha-Michael reaction	32
I.2.3. Hydrophosphonylation/hydrophosphorylation.....	34
I.2.4. Carbon-phosphorus transition metal-catalyzed cross-coupling	36
I.2.4.a. Historical introduction.....	36
I.2.4.b. Phosphine oxides and phosphines as coupling agents.....	37
I.2.4.c. Phosphine boranes as coupling agents.....	38
I.2.4.d. Triphenylphosphine as coupling agents	40
I.2.4.e. Phosphine chlorides as coupling agents	41
I.2.4.f. Alkyl sp derivatives as coupling partners	42
I.2.4.g. Alkyl sp ³ derivatives as coupling partners	42
I.2.4.h. Asymmetric examples	43
I.3. Summary	44
II. Results and discussion.....	45
II.1. C-P cross-coupling reaction	45
II.1.1. Introduction.....	45
II.1.2. Objectives of the project	46
II.1.3. The interest of enol phosphates in Pd-catalyzed couplings	46
II.2. Results of C-P coupling reaction	48
II.2.1. Protection step	48

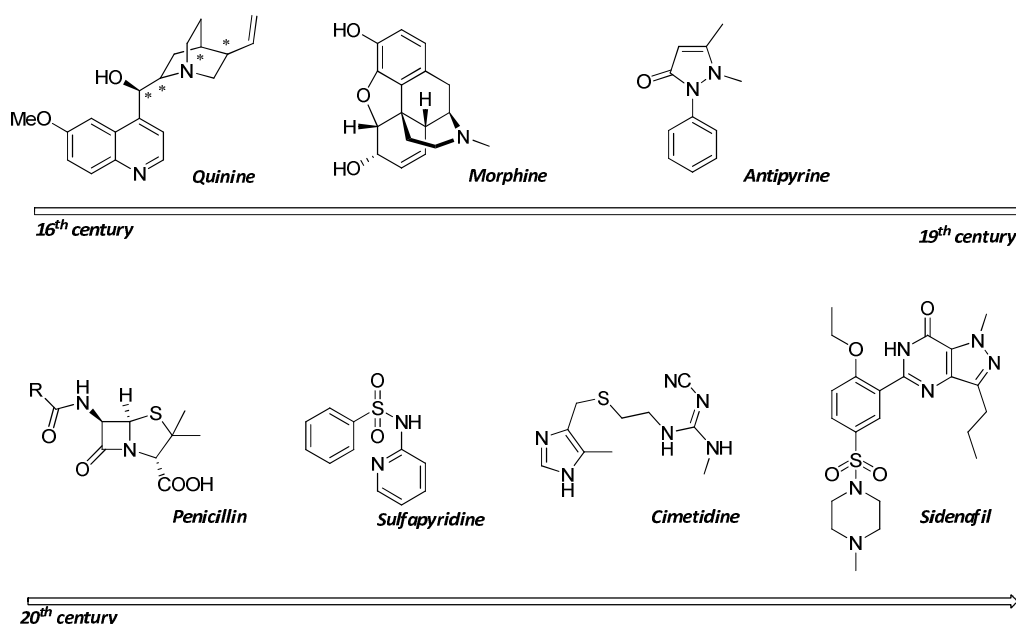
II.2.2. Preparation of enol phosphates	49
II.2.3. C-P cross-coupling reaction	50
II.2.3.a. The first approach and optimization of conditions	50
II.2.3.b. C-P cross-coupling reaction on the chiral phosphine boranes	52
II.2.3.c. Reaction with the (<i>S</i>)-(ortho-anisyl)phenylphosphine borane 13a	52
II.2.3.d. Reaction with the (2 <i>S</i> ,5 <i>S</i>)-2,5-diphenylphospholane borane complex 13b	54
II.2.3.e. Reaction with the (2 <i>S</i> ,5 <i>S</i>)-2,5-diphenylphospholane oxide 13c	54
II.2.4. Conclusion and perspectives of C-P coupling reaction	56
II.3. Nucleophilic addition onto acyclic enecarbamates - an access to P-containing non-natural amino acids	58
II.3.1. Bibliographic background	58
II.3.2. Objectives	60
II.3.3. Results of the nucleophilic addition	60
II.3.3.a. Synthesis details	60
II.3.3.b. Preparation of acyclic enecarbamates	61
II.3.3.c. Literature examples of nucleophilic addition onto double bond	63
II.3.3.d. Nucleophilic addition reaction	64
II.3.3.e. Oxidation of phosphine-based derivatives	66
II.3.3.f. Attempts with chiral phosphines	67
II.3.4. Conclusion and perspectives of C-P coupling reaction	69
III. Crystal structure determination	70
III.1. Introduction	70
III.1.1. Crystallization and quality of crystals	70
III.1.2. Data collection and data reduction	71
III.1.3. Structure determination	73
III.1.4. Structure refinement and analysis	74
III.2. Crystal structure of products after direct C-P coupling	75
III.3. Crystal structure of compounds from the family of P-containing non-natural amino acids	80
Chapter 2	85
I. Bibliography	87
I.1. Lanthanides - introduction	87
I.2. Lanthanide complexes	89
I.3. Jablonski Diagram and antenna effect	90
I.4. Antennae for lanthanide sensitization	94
I.5. Advantage of lanthanide markers for biological applications	95
I.6. Lanthanide sensitizers based on cyclen derivatives	96
I.7. Examples of lanthanides application in NIR probing	100
II. Result and discussion: chromophores based on pyrazinic core	105

II.1. Background	105
II.2. Previous work	107
II.3. Spectroscopic properties	109
II.4. Reactivity of 2,5-dibenzo[<i>b</i>]thiophenyl-pyrazine and construction of sensitizers for lanthanides with pyrazinic core	109
II.4.1. Objectives of project	109
II.4.2. DO3A derivative as a convenient chelator for lanthanides	110
II.5. First approach - Construction of sensitizers <i>via</i> cycloaddition reaction	111
II.5.1. Bibliographic background: Diels-Alder reaction	111
II.5.2. Objectives	113
II.5.3. Results and discussion of Diels-Alder reaction	113
II.5.4. Cleavage of <i>tert</i> -butoxycarbonyl groups	116
II.5.5. Aromatization of the polycyclic system	117
II.5.6. Attempts to attach the DO3A moiety	118
II.5.7. Summary	119
II.6. Second approach	120
II.6.1. Construction of spacing arm <i>via</i> cross-coupling reaction	120
II.6.1.a. Bibliographic background: Sonogashira cross-coupling	121
II.6.1.b. Application of Sonogashira coupling on the compounds 65 and 66	123
II.6.1.c. Background of copper-catalyzed cycloaddition - application "click reaction"	123
II.6.1.d. Attempts of alkyne deprotection and click reaction	125
II.6.1.e. Tests of copper-catalyzed cycloaddition	127
II.6.1.f. Attempts of deprotection	128
II.6.2. Summary	129
II.7. Construction of the spacing arm starting from a key aldehyde function	129
II.7.1. Wittig-Horner-Emmons olefination reaction	129
II.7.1.a. Formation of pyrazinic core	132
II.7.1.b. Reduction of ester and formation of compatible function to attach the DO3A	134
II.7.1.c. Reduction of nitrile, formation of amide and S _N on cyclen derivative	137
II.7.1.d. Deprotection and complexation step	138
II.7.2. Reduction of aldehyde and reactivity of obtained alcohol	139
II.7.3. Reductive amination	142
II.7.3.a. Short introduction	142
II.7.3.b. Examples of reductive amination onto the aldehyde 76	142
II.8. Spectroscopic properties of compounds 91 and 92	145
II.8.1. Absorption and emission spectra	145
II.8.2. Emission spectra and determination of energy levels	146
II.8.3. Quantum yields and luminescence lifetimes	148

II.8.4. Conclusion	149
III. Results and discussion: Sensitizers based on azo compounds	150
III.1. Bibliography.....	150
III.2. The synthesis of azo compounds.....	152
III.2.1. Formation of diazonium salt and azo coupling	152
III.2.2. The Mills reaction.....	154
III.2.3. The Wallach reaction	156
III.2.4. Other reaction providing the azo compounds	157
III.3. Objectives	160
III.4. Formation of azo compounds.....	161
III.5. Reductive amination with pyrazinic aldehyde.....	164
III.6. Creation of the spacing arm	165
III.7. Nucleophilic substitution with DO3A	166
III.8. Deprotection of acetic acid groups in DO3A	167
III.9. Formation of lanthanide complexes.....	168
III.10. Vectorization of lanthanide complex by the mean of cyclopeptide RGD.....	171
III.10.1. Cyclopeptide RGD and its role in cancer cell vectorization	171
III.10.2. Cycloaddition reaction with peptide RGD	172
III.11. Spectroscopic properties of azo compounds	174
III.11.1. Absorption spectra	174
III.11.2. Emission spectra in the NIR region – luminescence of lanthanide	178
III.11.3. Emission spectra in UV-Vis – fluorescence of chromophore	181
III.11.4. Lifetime measurements	182
III.11.5. Summary	183
IV. Conclusion and perspectives	184
Experimental part	193
I. General methods.....	195
II. General procedures.....	197
Annexes.....	269
I. Determination of the enantiomeric excess of chiral compounds	271
I.1. Analysis of organophosphorus chiral compounds by SFC.....	271
I.2. SFC separation of racemic mixtures of phosphine-containing non-natural amino acids.....	274
Streszczenie.....	275
Résumé.....	285
Bibliography	295

General introduction

quinine analogues. Morphine was isolated by the pharmacist Friedrich Wilhelm Sertürner (1783-1841) in 1806. The first synthetic heterocyclic medicament seemed to be antipyrine (called also phenazon) discovered in 1887 by Ludwig Knorr (1859-1921). This compound was used as analgesic and antipyretic drug for fever treatment, until the apparition of non-steroidal anti-inflammatory compounds. The discovery of penicillin in 1928 by Alexander Fleming has revolutionized the medicinal chemistry by entering on the market antibiotics which can deal with a large spectrum of bacterial diseases (such as syphilis). This drug was largely produced and used during the II World War against bacterial infections of wounds, saving estimated 12% - 15% of lives. As a continuation in this research, sulfapyridine – the first synthetic antibiotic has been obtained in 1938.³ Otherwise, at the end of 1970's the first medicament synthesized on the large scale the hundreds of tones was cimetidine (Tagamet[®]) – the antagonist of H₂ receptor, largely used for heartburns and peptic ulcers. It was the first “blockbuster of the history” - the medicament which gained pharmaceutical companies more than billions of dollars. Finally, the sildenafil citrate (Viagra[®]) launched in 1998 as a drug for erectile dysfunction and pulmonary arterial hypertension belongs to the most common recent medicaments.



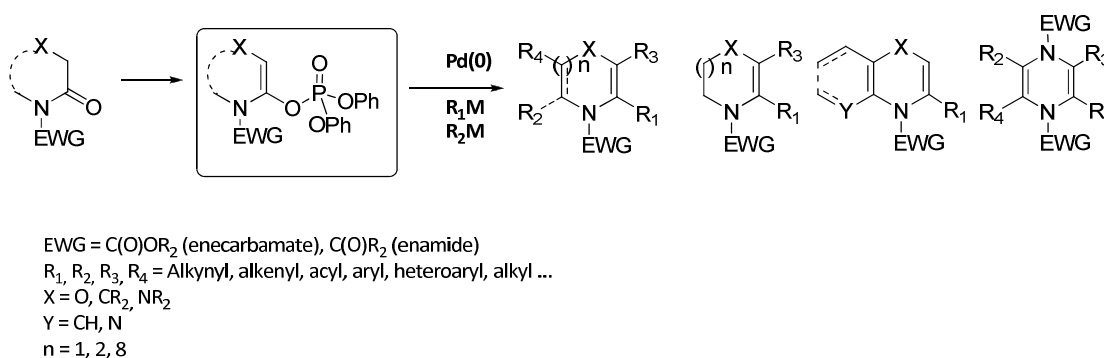
Scheme 2 Examples of heterocyclic N-containing drugs

Due to the rich chemistry of nitrogen containing compounds and their evident biological interest, synthesizing N-heterocycles has been a central and important theme within organic chemistry. Encarbamates or enamides, a class of deactivated enamines, are versatile intermediates for the synthesis of alkaloids and nitrogen-containing heterocycles.

Among the available methodologies for the preparation of enamides or encarbamates, the palladium catalyzed cross-coupling reaction of the corresponding enol ether appears a very fruitful

³ A. Burger, *Medicinal Chemistry*, Wiley-Interscience, 1970.

approach. Several research groups (e.g. Nicolaou,⁴ Skrydstrup,⁵Fuwa⁶) have indeed demonstrated that lactam- and imide-derived vinyl phosphates represent versatile intermediates for the construction of various enamides. The ability to easily convert enol phosphates into a myriad of functional motifs of synthetic relevance is well-known. The capacity of these synthetic intermediates to undergo cross-coupling reactions in the presence of various heteroatoms makes them attractive functional groups for the construction of diverse substituted heterocyclic systems. This methodology has been elaborated since several years in our team to prepare a number of original privileged heterocyclic structures (e.g. 1,4-dihydropyridines, 1,4-oxazines, 1,4-dihydropyrazines) bearing an enecarbamate moiety (Scheme 3).



Scheme 3

Considering the great expertise and investigations undertaken in the field of synthesis and reactivity of enecarbamates in our laboratory, we will focus on the extension of this methodology onto the original heterocycles with diverse applications. The first part of this dissertation will be devoted to the reactivity of enecarbamates and enamides in the reaction of direct C-P cross-coupling and nucleophilic addition of phosphide anions in order to create novel building blocks containing phosphorus atom. The second part of this work will concern the synthesis and characterization of original chromophores based on the pyrazinic core derived from the dihydropyrazine moiety. These chromophores are envisaged to be efficient sensitizers of lanthanide cations and, therefore, may be applied as organic antennae for molecular imaging in near infrared.

Chapter 1 Organophosphorus heterocyclic compounds: carbon - phosphorus bond formation

The synthesis of new P-containing compounds is an ever-growing subject in recent organic chemistry. In the first chapter, we will describe the possible methods of introduction the P-atom to the

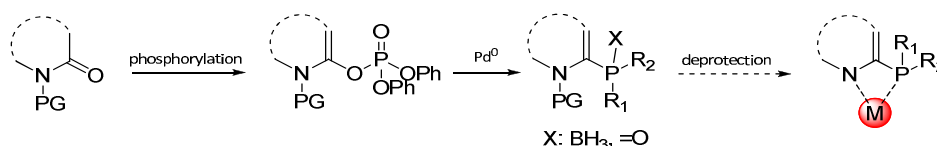
⁴ K. C. Nicolaou, K. Namoto, *Chem. Commun.*, **1998**, 1757.

⁵ (a) A. L. Hansen, J.-P. Ebran, T. Gøgsig, T. Skrydstrup, *Chem. Commun.*, **2006**, 4137; (b) A. L. Hansen, J.-P. Ebran, T. M. Gøgsig, T. Skrydstrup, *J. Org. Chem.*, **2007**, 72, 6464.

⁶ H. Fuwa, M. Sasaki, *J. Org. Chem.*, **2009**, 74, 212.

heterocyclic scaffold and we will focus on the importance of P-containing products in the asymmetric catalysis and the domain of bioactive compounds.

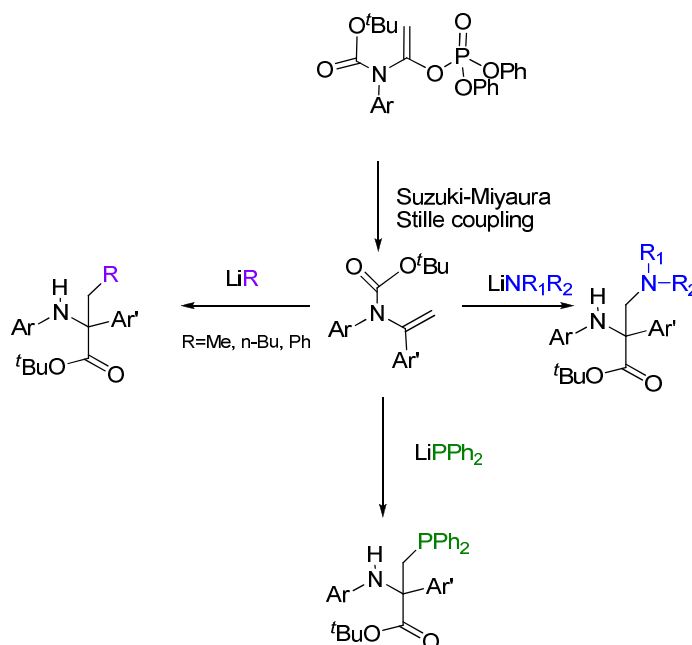
Our scope is to introduce the phosphorus atom to the enecarbamate and enamide moiety in an efficient and stereospecific way by the means of two particular reactions: the C-P cross-coupling reaction catalyzed by palladium complexes and the nucleophilic addition of lithiated phosphines onto the double bond of acyclic enecarbamates. In the first approach, starting from commercial available lactames, we have envisaged the three-step synthesis of α -enamido phosphane derivatives (Scheme 4).



Scheme 4

This methodology is based on the reactivity of enol phosphates, derived from protected lactames and already studied in our laboratory.⁷ The proposed strategy may thus provide an access to phosphinoheterocyclic compounds based on privileged structures with potential biological interest.

The second part of this chapter will discuss about the phospholithiation reaction onto the acyclic enecarbamates, derived from enol phosphates of various amides. Inspired by the anterior work previously described in the laboratory,⁸ we have envisaged the addition of nucleophilic phosphorus agent onto the enecarbamate moiety providing a spontaneous migration of the alkyloxycarbonyl group to lead to derivatives of non-natural amino acids. Thus, we would like to confirm the strategy and enlarge the scope for the non-natural β -phospho α -amino acids (Scheme 5).



Scheme 5 Strategy to synthesize analogues of non-natural amino acids

⁷ F. Lepifre, S. Clavier, P. Bouyssou, G. Coudert, *Tetrahedron*, **2001**, *57*, 6969.

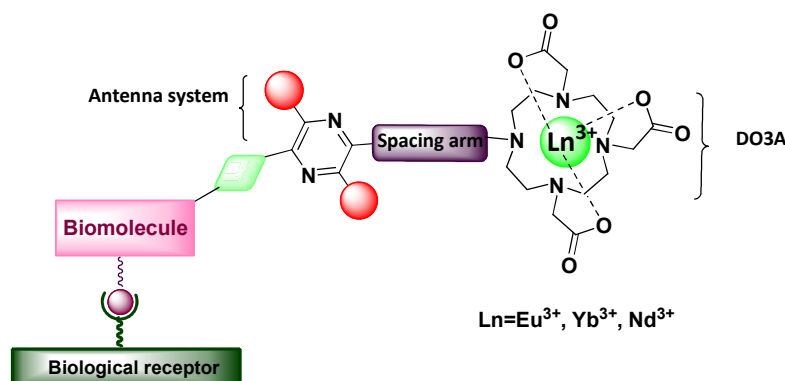
⁸ B. Cottineau, I. Gillaizeau, J. Farard, M.-L. Auclair, G. Coudert, *Synlett*, **2007**, *12*, 1925.

This synthesis is also based on the reactivity of enol phosphates, derived from the *N*-Boc protected amide. The involved strategy gives an easy access to precursors of non-natural amino acids and offers the potential advantage by directly introducing further diversity onto the molecules as a result of the original choice of starting primary amine, the partner for the cross-coupling and the phospholithium reagent.

Chapter 2 Sensitizers for lanthanide complexes: an original access to novel pyrazine chromophores

The lanthanide complexes begin to mark a territory in the domain of molecular imaging, especially nowadays with the great development of techniques and devices compatible with the near infrared domain. The emission of lanthanide complexes in the near infrared fits the spectral region called biological window for tissues, and it is undisturbed by the emission of biological fluids, tissues and hemoglobin. Moreover, the use of NIR photons allow the discrimination from autofluorescence in biological tissue as these do not have native NIR emission, give good signal to noise ratio and can pass through the tissue until few centimeters without damages to the biological systems. An important limitation to take advantage of the luminescence of lanthanide complexes is that their direct excitation is inefficient and they require a sensitizer molecule attached to them to provoke the energy transfer in the system.

In the second chapter of this dissertation, we will focus on the original way of synthesis of pyrazinic chromophores as sensitizers for lanthanide complexes. Taking advantage from the proven high reactivity of the 1,4-dihydropyrazine moiety,⁹ derived from 2,5-piperazinedione, we intend to functionalize this scaffold in a versatile way and introduce numerous functional groups in order to construct the sensitizing system. As a chelating ligand for lanthanides we have chosen macrocyclic compound DO3A (1,4,7,10-tetraazacyclododecan-1,4,7-triacetic acid) because of its great affinity for lanthanide cations and hence the possibility of formation of thermodynamically and kinetically stable complexes.



Scheme 6 Sensitizers based on pyrazinic core

⁹ M. Chaignaud, I. Gillaizeau, N. Ouhamou, G. Coudert, *Tetrahedron*, **2008**, *64*, 8059.

We envisage the formation of sensitizers in two distinct ways:

- ✓ by the functionalization of the dihydropyrazine moiety under anionic conditions by using standard transformations, deprotection and aromatization providing the pyrazinic core
- ✓ *via* cycloaddition Diels-Alder reaction with different dienophiles leading to more complex conjugated heterocyclic systems.

The formation of specific linker called "spacing arm" between the chromophore center and the chelate will be widely studied (Scheme 6). The spectroscopic properties of new complexes, such as absorption, emission in near-infrared and quantum yields will be studied in the Center of Molecular Biophysics in collaboration with S. Petoud.¹⁰

The last part will be devoted to the synthesis and characterization of azo-dyes derivatives as potential sensitizers for lanthanides (Fig.1). This conjugated system may be applied as chromophore alone or in conjunction with the pyrazinic core.

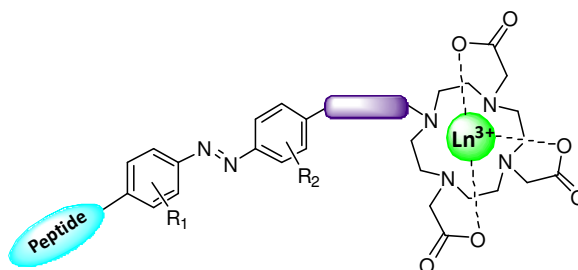


Fig. 1 Sensitizer based on azo derivatives

In order to denote the biological application, we will attach our sensitizers to the biomolecule to test the activity of vector molecule in the biological system. The cyclopeptide RGD is a model compound showing the high affinity to cancer cells and therefore it became a valuable target for our investigations.

¹⁰ H. Uh, S. Petoud, *CR Chimie*, **2010**, *13*, 668.

Chapter 1

I. Bibliographic introduction

Over 240 years have passed since the discovery of elemental phosphorus. For centuries before the modern chemistry was defined, alchemists were searching the prescription for the philosophers' stones – substances that will allow turn every inexpensive metal into gold. With this aim, in 1669 German alchemist Henning Brand and his co-workers were undertaking the long and arduous process of isolation of some matter from urine sample and accidentally they discovered a new element. After its particular property – glowing at dark and burning brilliantly – it was called “phosphorus” which in Greek means “light-bearing” or “light bearer”. Starting from this discovery, the elemental phosphorus and its inorganic and organic compounds have found an important role in the chemistry. The great structural and electronic diversity of organophosphorus compounds and their specific chemical behavior make them particular reagents in modern synthetic organic chemistry.¹¹ Moreover, optically active organophosphorus products are also building blocks for the synthesis of natural products¹² and play an important role as ligands or catalyst in different enantioselective transformations.¹³ From the biological point of view, compounds containing phosphorus play a crucial role for process of energy transmission in living organism under the form of adenosine triphosphate (ATP) as well as phospholipids which create the cell membrane and are responsible for signal transduction. They are a part of living organisms' genetic instructions as a phosphate in the nucleic acids DNA and RNA. Taking into account their particular properties in the field of signal transduction and organism growth, they found an application as fertilizers for plants and also as pesticides irreversibly inactivating an enzyme acetylcholinesterase, which is essential to nerve function of insects, humans and other animals. Likewise, organophosphorus is present in phosphoproteins and peptidomimetics. Considering the interesting chemical behavior and versatile biological features of organophosphorus compounds, a great need exists to develop new methods for preparation of this class of products.

A limited number of reactions for organophosphorus compound synthesis are reported in the modern chemistry. Apart from well-known Michaelis-Arbuzov and Michaelis-Becker reaction, the phospho-Michael addition is probably one of the most important tools for C-P bond formation. Also, transition metal catalyzed cross-coupling reactions are worth mentioning.

The importance of these compounds can be regarded in their great utility in organic synthesis,¹⁴ nucleophilic¹⁵ and Brønsted acidic¹⁶ organocatalysts, chiral ligands for transition metals¹⁷ and peptidomimetics.¹⁸

¹¹ P. Savignac, B. Iorga, *Modern Phosphonate Chemistry*, CRC, New York, **2003**.

¹² M. Mikołajczyk, P. Bałczewski, *Top. Curr. Chem.*, **2003**, 223, 161.

¹³ A. Börner, *Phosphorus Ligands in Asymmetric Catalysis: Synthesis and Applications*, Wiley-VCH, Weinheim, **2008**.

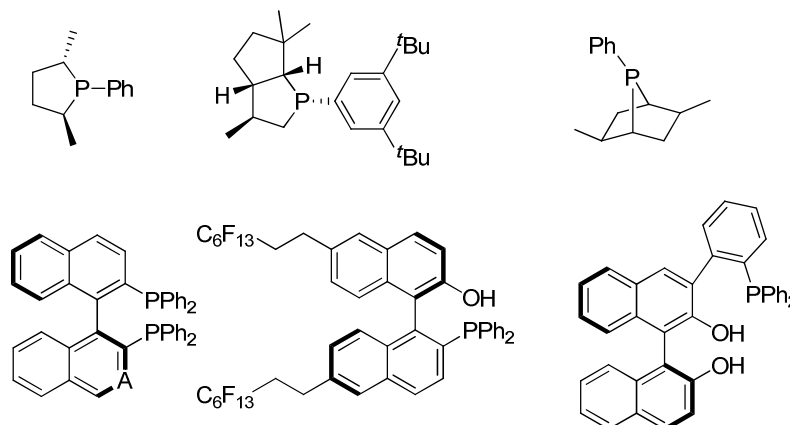
¹⁴ (a) W.S. Wadsworth Jr., W.D. Emmons, *J. Am. Chem. Soc.* **1961**, 83, 1733; (b) B.H. Lipshutz, D.W. Chung, B. Rich, R. Corral, *Org. Lett.*, **2006**, 8, 5069; (c) M. Shi, Y.-H. Liu, *Org. Biomol. Chem.*, **2006**, 4, 1468.

¹⁵ (a) N.T. McDougal, S.E. Schauls, *J. Am. Chem. Soc.*, **2003**, 125, 12094; (b) Y.K. Chung, G.C. Fu, *Angew. Chem. Int. Ed.*, **2009**, 48, 2225.

I.1. Applications of organophosphorus compounds

I.1.1. Organophosphorus compounds as nucleophilic and Brønsted acid organocatalysts

The term organocatalyst refers to low-weight organic molecules composed of carbon, hydrogen, oxygen, nitrogen, sulphur or phosphorus, which are able to accelerate chemical reactions. Among these organocatalysts, phosphines found their important role due to the great tunability from the electronic and steric point of view and owing to chirality that can be induced on the phosphorus atom.¹³ Acyclic phosphines retain chirality on the P-atom at room temperature, contrary to amines. Among the most widely used phosphine organocatalyst are both cyclic and acyclic ones, particularly compounds presented on the Scheme 7.



Scheme 7 Phosphine organocatalysts

The range of stereoselective syntheses catalyzed by trivalent phosphorus compounds covers the acylation, desymmetrization reaction and asymmetric transformations starting from prochiral substrates. Examples of typical C-C bond formation reactions catalyzed by phosphine organocatalyst are: Michael-type addition called Morita-Baylis-Hillman reaction¹⁹ and its aza-equivalent,²⁰ alkyne to 1,3-diene isomerisation,²¹ Umpolung γ -addition, [3+2] cycloaddition²² and [4+2] annulation.²³ In addition, phosphoramidites have proven to be efficient organocatalyst for the Michael reaction.²⁴

In 2004, the research groups of Akiyama²⁵ and Terada²⁶ independently reported the first application of a new class of chiral phosphoric Brønsted acids as catalyst in Mannich reaction (Fig. 2).

¹⁶ (a) T. Akiyama, J. Itoh, K. Yokota, K. Fuchibe, *Angew. Chem. Int. Ed.*, **2004**, *43*, 1566; (b) M. Rueping, A. P. Antonchick, T. Theissmann, *Angew. Chem. Int. Ed.*, **2006**, *45*, 3683; (c) S. Hoffmann, A. M. Seayad, B. List, *Angew. Chem. Int. Ed.*, **2005**, *44*, 7424; (d) S. Hoffmann, S. Nicoletti, B. List, *J. Am. Chem. Soc.*, **2006**, *128*, 13074; (e) S. J. Connon, *Angew. Chem. Int. Ed.*, **2006**, *45*, 3909.

¹⁷ W. Tang, X. Zhang, *Chem. Rev.*, **2003**, *103*, 3029.

¹⁸ (a) F. Palacios, C. Alonso, J. M. Santos, *Chem. Rev.*, **2005**, *105*, 899; (b) J. G. Allen, F. R. Atherton, M. J. Hall, C. H. Hassall, S. W. Holmes, L. W. Lambert, L. J. Nisbet, P. S. Ringrose, *Nature*, **1978**, *272*, 56; (c) S. Fushimi, K. Furihata, H. Seto, *J. Antibiot (Tokyo)*, **1989**, *42*, 1019.

¹⁹ (a) K. Morita, Z. Suzuki, H. Hirose, *Bull. Chem. Soc. Jpn*, **1968**, *41*, 2815; (b) T. Hayase, T. Shibata, K. Soai, Y. Wakatsuki, *Chem. Commun.*, **1998**, 1271.

²⁰ M. Shi, L.-H. Chen, C.-Q. Li, *J. Am. Chem. Soc.*, **2005**, *127*, 3790.

²¹ (a) B. M. Trost, U. Kazmaier, *J. Am. Chem. Soc.*, **1992**, *114*, 7933; (b) C. Guo, X. Lu, *J. Chem. Soc., Perkin Trans. 1*, **1993**, 1921.

²² (a) C. Zhang, X. Lu, *J. Org. Chem.*, **1995**, *60*, 2906; (b) J. E. Wilson, G. C. Fu, *Angew. Chem. Int. Ed.*, **2006**, *45*, 1426.

²³ (a) X.-F. Zhu, J. Lan, O. Kron, *J. Am. Chem. Soc.*, **2003**, *125*, 4716; (b) R. P. Wurz, G. C. Fu, *J. Am. Chem. Soc.*, **2005**, *127*, 12234.

²⁴ R. B. Grossman, S. Comesse, R. M. Rasne, K. Hattori, M. N. DeLong, *J. Org. Chem.*, **2002**, *68*, 871.

²⁵ T. Akiyama, J. Itoh, K. Yokota, K. Fuchibe, *Angew. Chem. Int. Ed.*, **2004**, *43*, 1566.

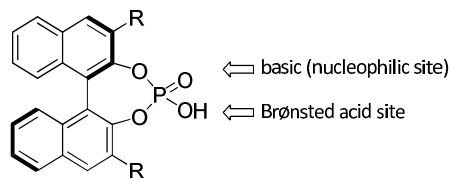
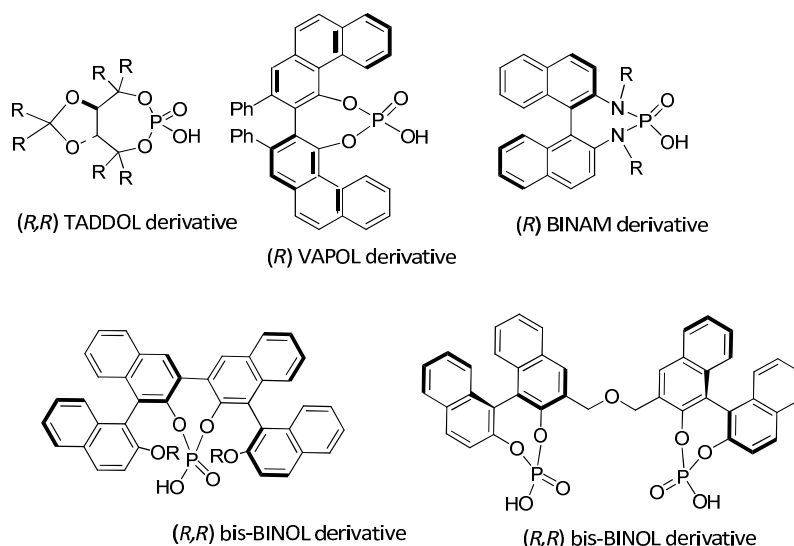


Fig. 2 Chiral phosphoric acid

This axially chiral phosphoric acid has a particular characteristic; the phosphorus atom is built into seven-membered ring, which prevents free rotation around the P-O bond and fixes conformation of Brønsted acid. The phosphate derivative with appropriate acidity can activate potential substrates *via* protonation and increases their electrophilicity. Subsequent attack of a nucleophile can result in the formation of enantioenriched products *via* stereochemical communication between the cationic protonated substrate and the chiral phosphate anion. Moreover, the phosphoryl oxygen atom has basic properties and thus chiral BINOL phosphate can act as bifunctional catalyst.

The development of new asymmetric transformations requires new chiral catalysts with different electronic and steric properties. Therefore, the number of phosphoric acids derived from TADDOL, VAPOL, BINAM and bis-BINOL has been prepared (Scheme 8).



Scheme 8 Examples of phosphoric acid catalysts

The first asymmetric organocatalytic reductive amination using phosphoric acid derivatives was described by MacMillan *et al.*²⁷ Simultaneously, these organocatalysts were applied in many other transformations, such as cascade transfer hydrogenation of quinolinones,²⁸ asymmetric hydrophosphonylation,²⁹ cycloaddition reaction, for example aza-Diels–Alder reaction for preparation nitrogen containing heterocycles,³⁰ dihydropyridine synthesis³¹ and much more, which will not be depicted in this thesis.

²⁶ D. Uraguchi, M. Terada, *J. Am. Chem. Soc.*, **2004**, *126*, 5356.

²⁷ R. I. Storer, D. E. Carrera, Y. Ni, D. W. C. MacMillan, *J. Am. Chem. Soc.*, **2006**, *128*, 84.

²⁸ M. Rueping, A. P. Antonchick, T. Tiessmann, *Angew. Chem. Int. Ed.*, **2006**, *45*, 3683.

²⁹ T. Akiyama, H. Morita, J. Itoh, K. Fushibe, *Org. Lett.*, **2005**, *7*, 2583.

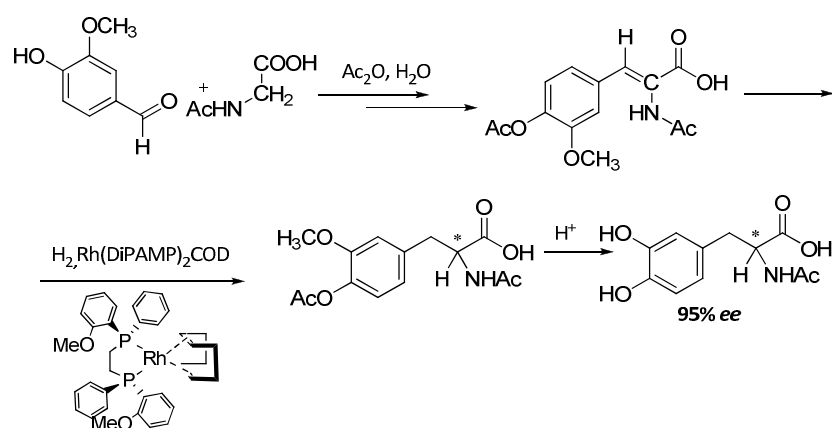
³⁰ T. Akiyama, Y. Tamura, J. Itoh, H. Morita, K. Fuchibe, *Synlett.*, **2006**, 141.

All presented examples of application of BINOL phosphoric acid shows its potential to activate various imine compounds, however with less reactive substrates like carbonyl compounds its acidity is insufficient. Guided by this idea, the group of Yamamoto has introduced a strong electron acceptor, such as *N*-triflate in the place of hydroxyl group and has created a new stronger Brønsted acid – a chiral *N*-triflyl phosphoramidate.³² This organocatalyst was first tested with success in the asymmetric Diels-Alder reaction of α,β -unsaturated ketones with silyloxydienes,²⁸ asymmetric Nazarov cyclization.³³

I.1.2. Chiral ligands for reactions catalyzed by transition metals

The increasing demand to produce enantiomerically pure pharmaceuticals, agrochemicals and other fine chemicals has inspired the field of asymmetric catalysis. The domain of asymmetric synthesis can be divided into chiral organocatalysis, enzymatic asymmetric synthesis and transition metal-catalyzed synthesis, which plays a major role nowadays. Phosphorus-containing compounds are one of the most common group among ligands for transition metals, due to their great variability, the possibility to bear chirogenic center on the *P* or *C*-atom and their ability to make complexes with many different metals, such as Pd, Rh, Ru, Ir, Pt, Ti, Zr and Au.

Since the first application of phosphine heterogenous ligand for asymmetric hydrogenation by Knowles^{34a} and Horner^{34b}, the great progress in this domain has been made. Although the first results showed poor enantioselectivity, the next investigations were encouraging and led to the application of C_2 -symmetric chelating bisphosphine ligands DIPAMP in Rh-catalyzed asymmetric hydrogenation of dehydroamino acids and in the industrial production of drug for the Parkinson's disease – L-DOPA (3,4-dihydroxy (*S*)-phenylalanine) (Scheme 9).³⁵



Scheme 9 The first chiral synthesis of (L)-DOPA

³¹ J. Jiang, J. Yu, X.-X. Sun, Q.-Q. Rao, L.-Z. Gong, *Angew. Chem. Int. Ed.*, **2008**, *47*, 2458.

³² D. Nakashima, H. Yamamoto, *J. Am. Chem. Soc.*, **2006**, *128*, 9626.

³³ M. Rueping, W. Leawsuwan, A. P. Antonchick, B. J. Nachtsheim, *Angew. Chem. Int. Ed.*, **2007**, *46*, 2097.

³⁴ (a) S. W. Knowles, M. J. Sabacky, *Chem. Commun.*, **1968**, 1445; (b) L. Horner, H. Siegel, H. Büthe, *Angew. Chem. Int. Ed. Engl.*, **1968**, *7*, 941.

³⁵ (a) W. S. Knowles, *Acc. Chem. Res.*, **1983**, *16*, 106; (b) W. S. Knowles, *Angew. Chem. Int. Ed.*, **2002**, *41*, 1999.

Kagan *et al.*³⁶ first introduced the concept of C_2 -symmetry in ligands with the development of the phosphine ligand DIOP for Rh-catalyzed asymmetric hydrogenation of enamides to give rise to the corresponding amino acids. A significant advance in the field of asymmetric catalysis was also achieved with the preparation of 1,2-bis(phospholano)ethane BPE and 1,2-bis(phospholano)benzene DuPHOS by the group of Burk.³⁷

In 1980, the group of Noyori and Takaya presented a synthesis of atropisomeric C_2 -symmetric bisphosphine ligand BINAP and its use in the Rh-catalyzed asymmetric hydrogenation of α -(acylamino)acrylic acids.³⁸ Their discovery did not gain much attention until BINAP was applied as the Ru-complex in the asymmetric hydrogenation of functionalized olefins and ketones. It appeared that this catalytic system is able to reduce ketones in the presence of carbon-carbon double bond with high selectivity,³⁹ which was a great challenge until these days.

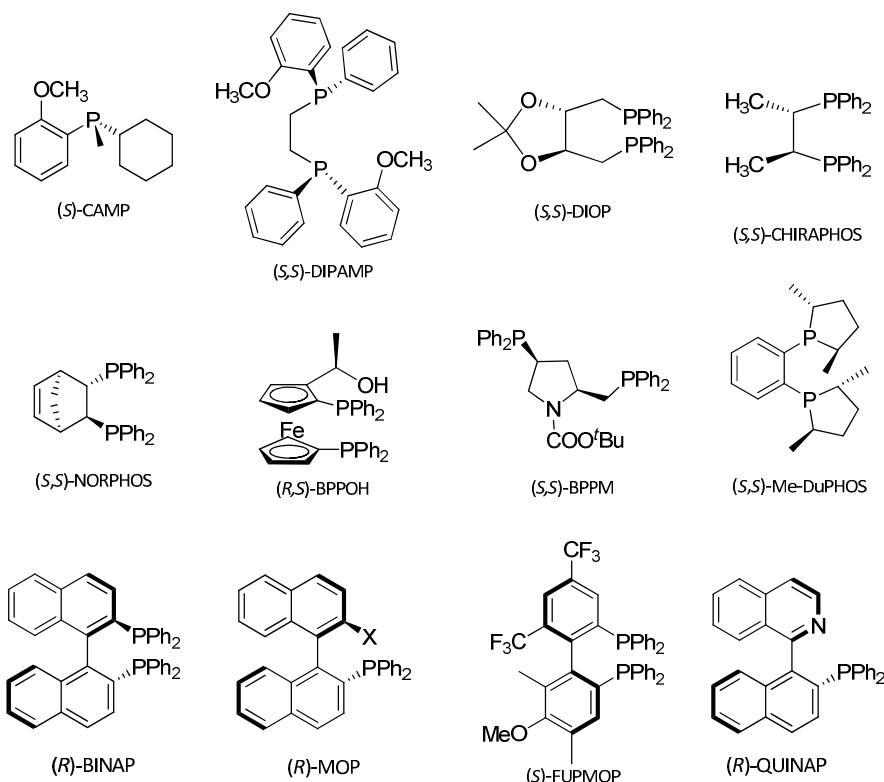


Fig. 3 Examples of chiral ligands

Chiral ligands containing phosphorus atom might be classified into three main categories depending on the position of chiral centre:

- ✓ Ligands with axial chirality, such as BINAP or MOP
- ✓ Ligands presenting a chiral carbon-backbone, i.e. DIOP or DuPHOS
- ✓ Ligands with *P*-chirogenic centre like DIPAMP or CAMP.

³⁶ (a) T. P. Dang, H. B. Kagan, *J. Chem. Soc. Chem. Commun.*, **1971**, 481; (b) T. Satyanarayana, S. Abraham, H. B. Kagan, *Angew. Chem. Int. Ed.*, **2009**, *48*, 456.

³⁷ M. J. Burk, J. E. Feaster, W. A. Nugent, R. L. Harlow, *J. Am. Chem. Soc.*, **1993**, *115*, 10125.

³⁸ A. Miyashita, A. Yasuda, H. Takaya, K. Toriumi, T. Ito, T. Souchi, R. Noyori, *J. Am. Chem. Soc.*, **1980**, *102*, 7932.

³⁹ T. Ohkuma, H. Ooka, T. Ikariya, R. Noyori, *J. Am. Chem. Soc.*, **1995**, *117*, 10417.

Each of these categories has their own particularities, which makes it specific for the chosen asymmetric reaction. Ligands bearing chirality on the *P*-atom ensure the direct contact between the asymmetric center and the transition metal (i.e. the reaction site), achieving high enantioselectivity with great affinity to the hydrogen for electron-rich catalyst such as trialkylated *P*-chirogenic ones. They enable also elevated turnover numbers, which reduce the usage of catalyst to few molar percents. In the ligands with the chirality on the carbon atom the phenomenon of the *pseudo*-chirality on the phosphorus atom is present. Thanks to that, these ligands show high activity to the corresponding metal complex and independent enantioselection for the conformation properties of the chelate cycle. Exceeding high enantioselectivities were achieved in the hydrogenation of a variety of unsaturated systems with these ligands. Modifications of electronic/steric properties of ligands presenting axial chirality are more difficult to manage due to the cumbersome procedures for structural modification of the ligand scaffold, however, once the proper structure is acquired, they are excellent catalyst for the asymmetric hydrogenation of C=C, C=O and N-C bond, and also for asymmetric C-C bond formation. Moreover, ever-growing interest in this domain increases the family of axial ligands with new heterocyclic representatives such as QUINAP (Fig. 3).

Thousands of new catalytic complexes has been synthesized and tested for asymmetric hydrogenation,⁴⁰ but also for palladium catalyzed allylic alkylation,⁴¹ asymmetric oxygenation, as well as nucleophilic additions of organometallic reagents to aldehydes,⁴² ketones and imines, conjugate addition, aldol reaction, Diels-Alder reactions, 1,3-dipolar additions, enyne cyclization and olefin metathesis.⁴³

I.1.3. Biological importance of organophosphorus compounds

I.1.3.a. Peptidomimetics

A molecule bearing identifiable similarity to a peptide, preferably with a low molecular weight, which can act as a ligand or a biological receptor to imitate or inhibit the effect of a natural peptide, is called peptidomimetic. Among many chemical transformations of amino acids to obtain modified ones for construction of peptidomimetics, an introduction of phosphorus atom plays an important role. For a long time "phosphorus analogues" of the amino acids, in which carboxylic group was replaced by phosphonic, phosphinic or phosphonate group, have attached special interest in the preparation of isosteric or bioisosteric analogues of number of natural products. Particularly, β -aminophosphonic⁴⁴

⁴⁰ S. Prevost, S. Gauthier, M. C. C. de Andrade, C. Mordant, A. R. Touati, P. Lesot, P. Savignac, T. Ayard, P. Phansavath, V. Ratovelomana-Vidal, J.-P. Genêt, *Tet.:Asym.*, **2010**, *21*, 1436.

⁴¹ I. G. Rios, A. Rosas-Hernandez, E. Martin, *Molecules*, **2011**, *16*, 970.

⁴² Y. Wei, M. Shi, *Acc.Chem. Res.*, **2010**, *43*, 1005.

⁴³ C. Lexter, D. Burtscher, B. Perner, E. Tzur, N. G. Lemcoff, C. Slugov, *J. Org. Chem.* **2011**, *696*, 2466.

⁴⁴ (a) F. Orsini, G. Sello, M. Sisti, *Curr Med Chem*, **2010**, *17*, 264; (b) E. D. Naydenova, P. T. Todorov, K. D. Troev, *Amino Acids.*, **2010**, *38*, 23.

acids as isosteres of β -amino acids (Fig.4) became valuable and interesting products with biological and biochemical properties: as enzymes' inhibitors,⁴⁵ antibacterial agents⁴⁶ and anti HIV agents.⁴⁷

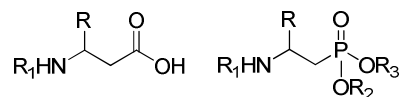


Fig. 4 Isosteric analogues of amino acids

Aminophosphonic acids can be obtained on the way of carbon-phosphorus bond formation such as reactions between aminoalkyl halides and phosphinites⁴⁸ (the Arbuzov reaction), the nucleophilic addition of phosphorus derivatives to small heterocycles,⁴⁹ the hydrophosphinylation to α -amino aldehydes⁵⁰ and the addition of phosphorus derivatives to unsaturated C-C and C-N bond.⁵¹ A great deal of different transformations to obtain aminophosphonates exists also, but this topic will not be discussed here.

Below, few examples of organophosphorus compounds playing role of peptidomimetics will be presented. First of them is HIV-1 protease inhibitor (Fig. 5a) designed and synthesized by the group of Janda,⁵² showing a great antagonist potential ($K_i = 8.2$ nM *in vitro* against protease). Second peptidomimetic (Fig. 5b) belongs also to the class of HIV protease inhibitors.^{51b}

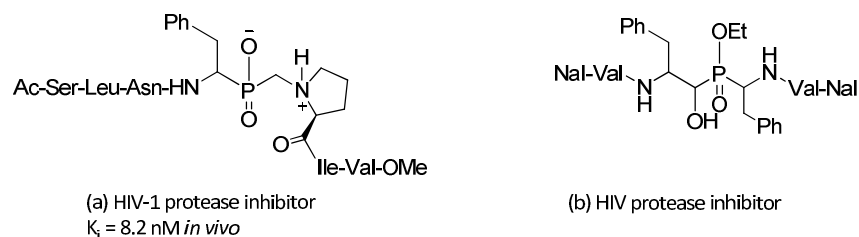


Fig. 5 Examples of HIV proteases inhibitors

Another citation of active peptidomimetics is human renin inhibitor and norstatine renin inhibitor (Fig. 6).

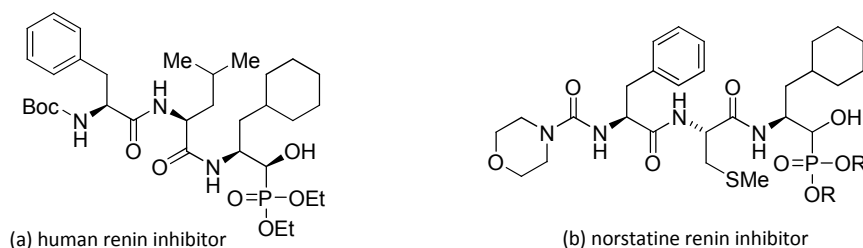


Fig. 6 Examples of active peptidomimetics

⁴⁵ W. W. Smith, P. A. Bartlett, *J. Am. Chem. Soc.*, **1998**, *120*, 4622.

⁴⁶ J. G. Allen, F. R. Artherton, M. J. Hall, C. H. Hassall, S. W. Holmes, R. W. Lambert, L. J. Nisbet, P. S. Ringrose, *Nature*, **1978**, *272*, 56.

⁴⁷ E. Alonso, E. Alonso, A. Solis, C. del Pozo, *Synlett*, **2000**, 698.

⁴⁸ H. Gali, K. R. Prabhu, S. R. Karra, K. V. Katti, *J. Org. Chem.*, **2000**, *65*, 676.

⁴⁹ F. Palacios, A. M. Ocha de Retana, E. Martinez de Marigorta, J. M. de los Santo, *Org. Prep. Proc. Int.*, **2002**, *34*, 219.

⁵⁰ (a) D. V. Patel, K. Reilly-Gauvin, D. E. Ryono, C. A. Free, W. L. Rogers, S. A. Smith, J. M. DeForrest, R. S. Oehl, E. W. Pertillo Jr., *J. Med. Chem.*, **1995**, *38*, 4557; (b) B. Stowasser, K.-H. Budt, L. Jian-Qi, A. Peyman, D. Ruppert, *Tetrahedron Lett.*, **1992**, *33*, 6625.

⁵¹ C. de Risi, D. Perrone, A. Dondoni, G. P. Pollini, V. Vertolasi, *Eur. J. Org. Chem.*, **2003**, 1904.

⁵² S. Ikeda, J. A. Ashley, P. Wirsching, K. D. Janda, *J. Am. Chem. Soc.*, **1992**, *114*, 7604.

Recently, antiviral agent HPMPC - 9-[(2S)-3-hydroxy-2-phosphonomethoxypropyl] adenine has been introduced to the short chain peptide to create peptidomimetic playing role of the prodrug⁵³ for treatment for human cytomegalovirus (HCMV) (Fig.7).

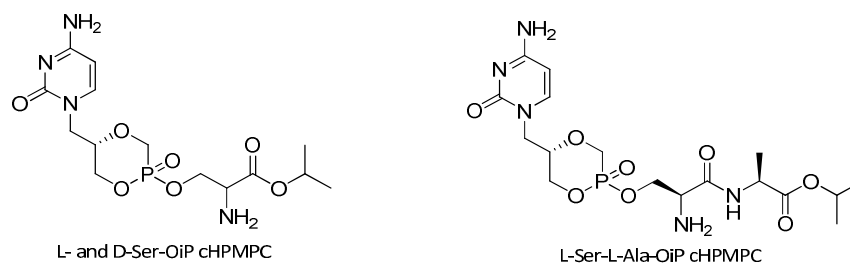


Fig. 7 Examples of peptidomimetic playing role of prodrugs

I.1.3.b. Phosphorus compounds as bioactive agents

Other classes of compounds containing phosphorus are organophosphates or in other words organic esters of phosphoric acid. Many of the most important biomolecules are organophosphates, including DNA, RNA and cofactors essential for proper functioning of organisms (i.e. thiamine diphosphate - vitamin B₁). Organophosphates are also the basis of insecticides, herbicides and nerve gases, because they act as inhibitors of acetylcholinesterase AChE, an enzyme degrading the neurotransmitter - acetylcholine. They poison an enzyme by phosphorylation reaction. The effector organ becomes overstimulated by the excess of acetylcholine, what provokes the perturbation in the nervous system. Some examples of organophosphates are Sarin (propan-2-yl methylphosphonofluoridate) - the paralyzing gas used as a chemical weapon during II World War, the insecticide Malathion, the herbicide Glyphosate or Glufosinate (Fig.8).

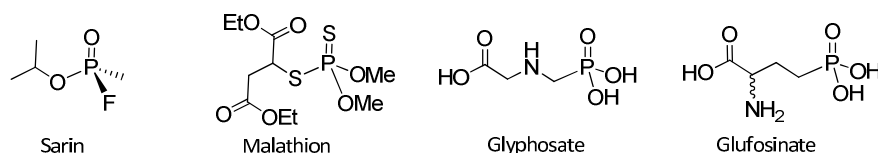


Fig. 8 Organophosphates as inhibitors of acetylcholinesterase

Notwithstanding, organophosphates have got also significant role in the pharmaceutical field: Fosinopril (Fig. 9a) shows a valuable hypertensive activity, naphthylmethylphosphonate (Fig.9b) is an inhibitor of insulin receptor tyrosine kinase, the phosphinopeptide analogue of the glutathionylspermidine GSP (Fig. 9c) reveals potent tripanocidal activity through inhibition of GSP synthetase and fosfomicin - the broad spectrum antibiotic produced by certain *Streptomyces* species (Fig.9d).

⁵³ L. W. Peterson, M. Sala-Rabanal, I. S. Krylov, M. Serpi, B. A. Kashemirov, C. E. McKenna, *Molecular Pharmaceutics*, **2010**, *7*, 2349.

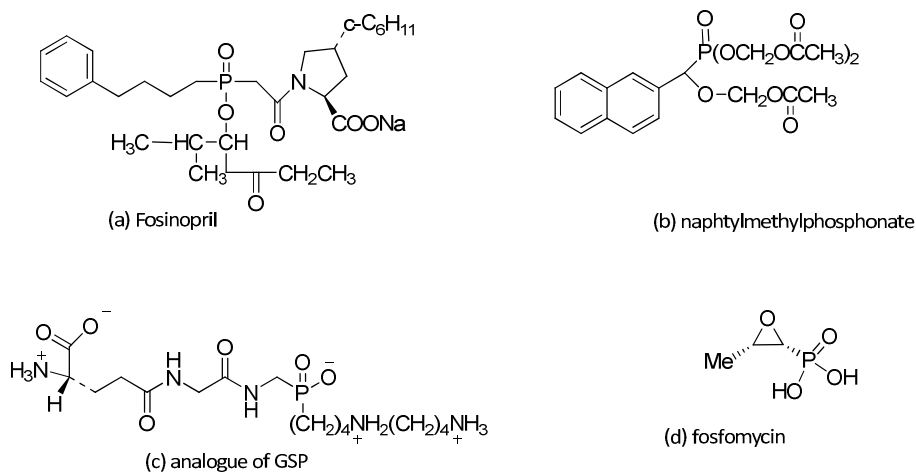
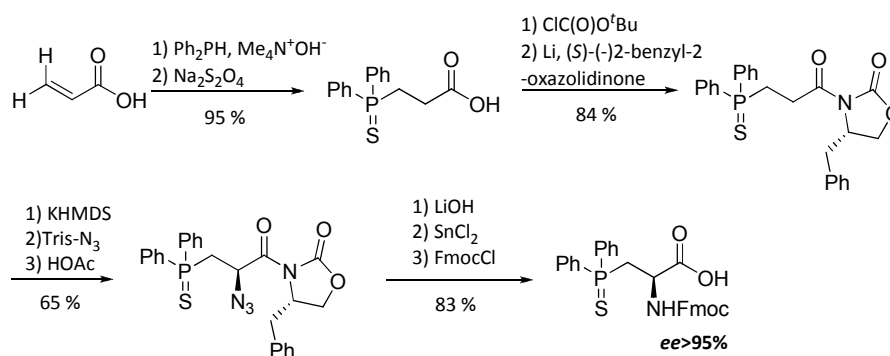


Fig. 9 Pharmaceuticals organophosphates

I.1.3.c. Phosphine containing amino acids

In 1994, the group of Gilbertson pioneered the chemistry of phosphine-containing peptides and their application in asymmetric catalysis.⁵⁴ The original approach to phosphine-containing serine derivatives was developed based on Evan's chiral oxazolidinone chemistry (Scheme 10).



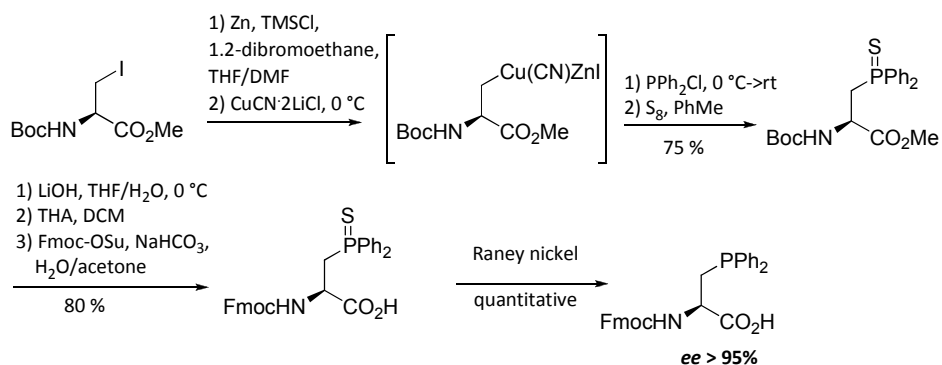
Scheme 10 Synthesis of phosphine sulfide containing serine based on Evans' oxazolidinone methodology

Several phosphines was prepared according to this methodology, however several steps required chromatography purification were limiting agents for wide applicability of this method. A more direct pathway was developed to transform (S)-serine into a highly functionalized Knochel cuprate,⁵⁵ which easily reacts with chlorophosphine derivatives (Scheme 11). A number of compounds bearing different phosphines (i. e. aromatic or alkyl groups) were prepared.⁵⁶ To avoid oxidation of the phosphine, the protection of P-atom must be undertaken. Methods of reduction of phosphine oxide or deprotection of borane group proved to be inefficient, notwithstanding it was found that phosphine sulfides are excellent protectors and they can be cleaved at the final step with Raney nickel or by sulfur methylation by HMPT.

⁵⁴ R. S. Gilbertson, G. Chen, M. MacLoughlin, *J. Am. Chem. Soc.*, **1994**, *116*, 4481.

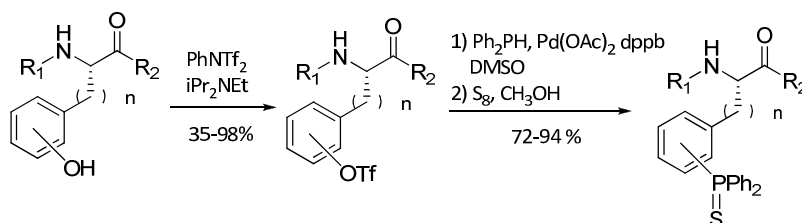
⁵⁵ P. Knochel, M. Ch. P. Yeh, S. C. Berk, J. Talbert, *J. Org. Chem.*, **1988**, *53*, 2390.

⁵⁶ (a) S. J. Greenfield, S. R. Gilbertson, *Synthesis*, **2001**, *15*, 2337; (b) A. Agarkov, S. J. Greenfield, D. Xie, R. Pawlick, G. Starkley, S. R. Gilbertson, *Peptide Science*, **2006**, *84*, 48.



Scheme 11 Synthesis of diphenylphosphinoserine

Gilbertson's group has described also synthesis of phosphine analogues of proline, tyrosine and phenylglycine. For the aromatic amino acids, the methodology with cross-coupling of corresponding triflates has been applied. This approach enables to achieve desired phosphine derivatives after two steps with excellent yields (Scheme 12).⁵⁷



Scheme 12 Synthesis of aromatic acids containing diphenylphosphino sulfide

While the reaction is very efficient for single amino acid it also presents the possibility for the conversion of tyrosine to its phosphine derivative in already constructed larger peptides.^{57a} Presented methodology have been applied to the synthesis of libraries of building blocks for construction of peptides, especially β -turn ones to control the selectivity of palladium-catalyzed allylation.⁵⁸ Peptides possessing both helical and β -turn secondary structure (Fig. 10) were examined in rhodium-catalyzed asymmetric hydrogenation, however selectivities obtained with these systems were low and varied widely depending on the solvent used as well as the mobility of the catalyst.^{56b}

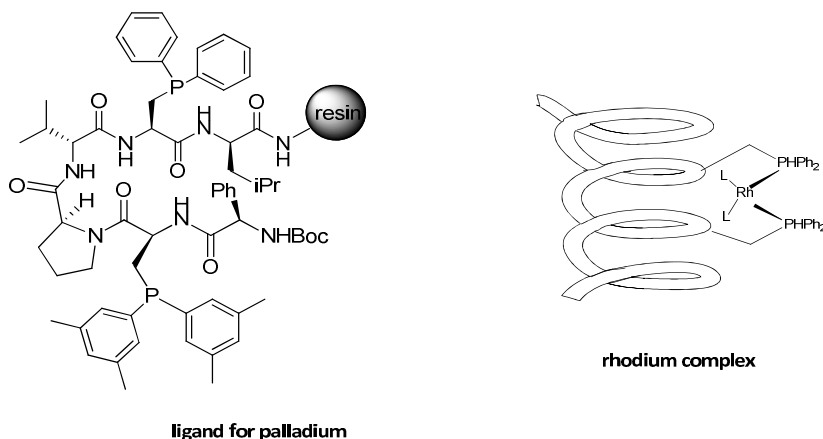


Fig. 10 Phosphine-containing peptides as catalysts

⁵⁷ S. R. Gilbertson, G. W. Starkey, *J. Org. Chem.*, **1996**, *61*, 2922.

⁵⁸ A. Agarkov, S. J. Greenfield, T. Ohishi, S. E. Collibee, S. R. Gilbertson, *J. Org. Chem.*, **2004**, *69*, 8077.

Also, the team of Jugé described the application of oxazolines, derived from L-serine, for the hemisynthesis of the racemic β -phosphorus amino acids (Fig. 11).⁵⁹

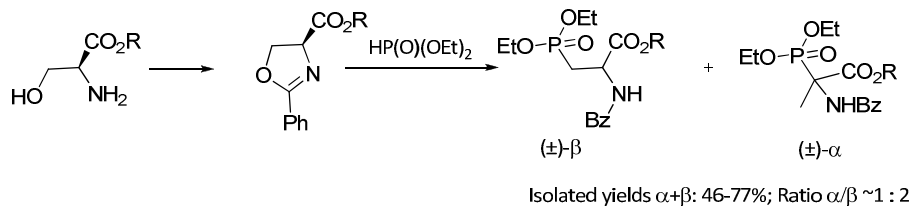


Fig. 11 Strategy for hemisynthesis of β -phosphorus amino acids

They elaborated the methodology to introduce the ferrocenylphosphide borane to the L-aspartic acid, which is used as an electrochemical probe to detect autoantibodies in multiple sclerosis.⁶⁰

I.2. Formation of organophosphorus compounds

I.2.1. General introduction

The great interest of developing novel organophosphorus compounds exists since the first synthesis of phosphonates from alkyl halides and phosphinite by German chemist August Michaelis in 1898 (Fig.12).

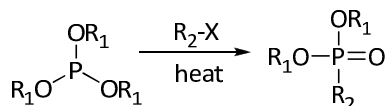
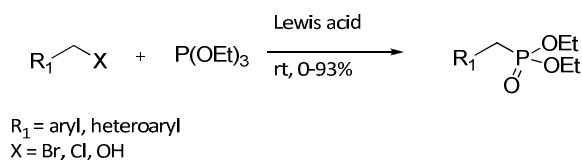


Fig. 12 Scheme of Arbuzov reaction

Aleksandr Arbuzov extended this reaction on the whole group of various phosphinates and phosphine oxides. The first step involves nucleophilic attack by the phosphorus on the alkyl halide, followed by the halide ion dealkylation of the resulting trialkoxyphosphonium salt. However, this reaction is useful from the synthetic point of view, it requires very drastic reaction conditions, like heating in the reflux of alkyl halides; therefore many of variation exists nowadays. One of them is the Lewis acid-mediated Michaelis-Arbuzov reaction at room temperature,⁶¹ which leads to arylmethyl and heteroarylmethyl phosphonates with excellent yields (Scheme 13).



Scheme 13 Michaelis-Arbuzov reaction assisted by Lewis acid

⁵⁹ (a) F. Meyer, A. Laaziri, A. M. Papini, J. Uziel, S. Jugé, *Tetrahedron: Asymm.*, **2003**, *14*, 2229; (b) F. Meyer, A. Laaziri, A. M. Papini, J. Uziel, S. Jugé, *Tetrahedron*, **2004**, *60*, 3593.

⁶⁰ F. Real-Fernandez, A. Colson, J. Bayardon, F. Nuti, E. Peroni, R. Meunier-Prest, F. Lolli, M. Chello, C. Daracel, S. Jugé, A. M. Papini, *Peptide Science*, **2008**, *90*, 488.

⁶¹ G.G. Rajeshwaran, M. Nandakumar, R. Sureshbabu, A. K. Mohanakrishnan, *Org. Lett.*, **2011**, *13*, 1270.

During the years prior to 1980 only few important methods for the C-P bond formation appeared. Starting with pioneering work of Hirao⁶² on palladium(0) catalyzed coupling of aryl and vinyl bromides with dialkyl phosphinites, many of new improved methods arose. Among them, the phospho-Michael reaction, the hydrophosphination reaction and the cross-coupling with the variety of nucleophilic phosphorus containing agents are considerable.

I.2.2. Phospha-Michael reaction

Similar to the Michaelis-Arbuzov and the Michaelis-Becker reaction (reaction of trialkyl phosphites with alkyl halides and of alkali salts of dialkyl phosphonates with alkyl halides, respectively), the phospho-Michael addition certainly represents versatile method for formation of P-C bonds. The phospho-Michael reaction is an addition of a phosphorus nucleophile to an olefinic acceptor. This reaction offers the possibility to access a number of diversely functionalized products, since many different electrophiles and P nucleophiles can be combined.

Acceptors for phospho-Michael addition may be classified into five groups, depending on to the character of olefin, it may be: an acceptor bearing carbonyl or carboxyl group, an acceptor with a nitro group, with a sulfoxide or sulfone, with a phosphonate or phosphane oxide or alkynic acceptor. From the other hand, nucleophiles engaged in the reaction might be triaryl- or trialkylphosphines, phosphinites, phosphine boranes, etc...⁶³

The Michael addition of a trivalent phosphorus nucleophile to an acrylic acid leads to the phosphobetain (Fig.13), which could be isolated and its structure could be confirmed by X-ray analysis.⁶⁴ The same results were obtained with cinammic acid and its derivatives, however with butyl methacrylate only anionic polymerization was observed, which means that the initially formed adduct is highly reactive and the polymerization step is faster than the addition itself.

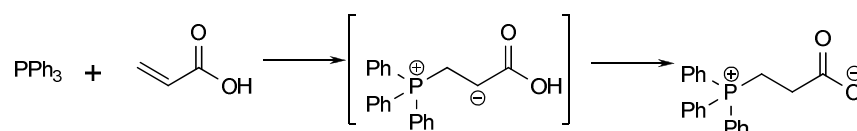


Fig. 13 Phospha-Michael addition between triphenylphosphine and acrylic acid

In order to avoid the polymerization or degradation of obtained betain, the proton source is applied to trap this agent as a phosphonium salt. Cristau *et al.*⁶⁵ reported a phospho-Michael addition of triphenylphosphine to the α,β -unsaturated ketones in the presence of hydrobromide (Fig. 14).

⁶² (a) T. Hirao, T. Masunaga, Y. Ohshiro, T. Agawa, *Tetrahedron Lett.*, **1980**, 21, 3595; (b) T. Hirao, T. Masunaga, N. Yamada, Y. Ohshiro, T. Agawa, *Bull. Chem. Soc. Jpn.*, **1982**, 55, 909.

⁶³ D. Enders, A. Saint-Dizier, M.-I. Lannou, A. Lenzen, *Eur. J. Org. Chem.*, **2006**, 29.

⁶⁴ C. Larpent, H. Patin, *Tetrahedron*, **1988**, 44, 6107.

⁶⁵ H.-J. Cristau, J.-P. Vors, H. Christol, *Tetrahedron Lett.*, **1961**, 20, 2377.

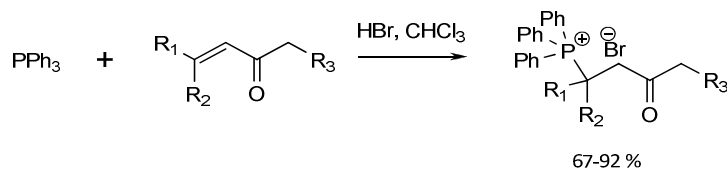


Fig. 14 Phospha-Michael reaction

Nucleophiles with P-H have also been used in the phospha-Michael addition. Among them the phenylphosphines Ph_2PH and PhPH_2 are most often cited - either in form of their lithium salts or in the presence of KO^tBu as a catalyst. Helmchen *et al.*⁶⁶ reported an addition of Ph_2PLi to (-)-(1*R*)-*tert*-butyl myrtenate in a diastereoselective manner, providing chiral phosphine ligand in four steps with good yield (Fig. 15).

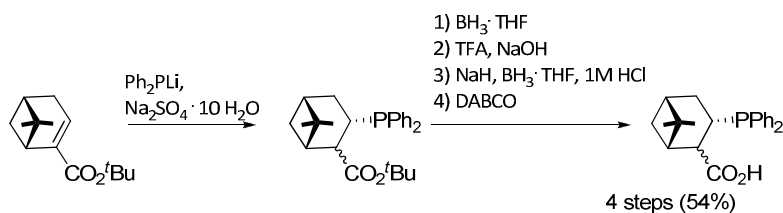


Fig. 15 Phospha-Michael addition on (-)-(1*R*)-*tert*-butyl myrtenate

The phospha-Michael addition of Ph_2PLi to *tert*-butyl crotonate followed by cleavage of the ester gave the racemic mixture of acid, which can be separated by recrystallization with chiral salt (Fig. 16).⁶⁷

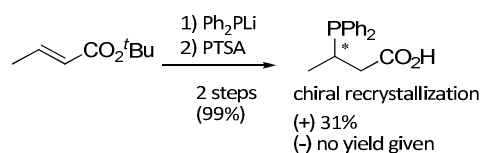


Fig. 16 Phospha-Michael addition with Ph_2PLi

Also, the phosphine-borane can act as nucleophile in phospha-Michael addition. The borane moiety is regarded as a protecting group, because it prevents oxidation of the phosphorus atom and can be cleaved in the presence of an excess of a highly nucleophilic amine (Et_2NH , morpholine, DABCO). The 1,4-addition to unsaturated amides using $\text{Ph}_2\text{P}(\text{BH}_3)\text{Li}$ was studied by Quirion *et al.*⁶⁸ The nucleophilic attack of lithiated diphenylphosphine-borane to the double bond occurs to give tertiary phosphine-boranes in good yields and with high diastereoisomeric excesses (Fig. 17).

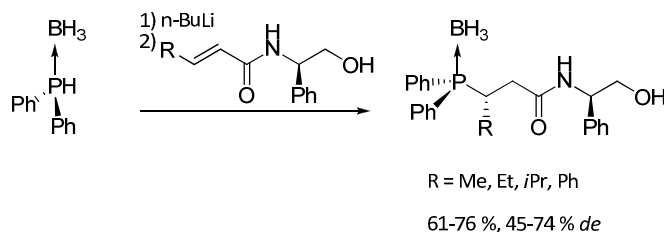


Fig. 17 Phospha-Michael addition with $\text{Ph}_2\text{P}(\text{BH}_3)\text{Li}$

⁶⁶ G. Knühl, P. Sennhenn, G. Helmchen, *J. Chem. Soc., Chem. Commun.*, **1995**, 1845.

⁶⁷ T. Minami, Y. Okada, T. Otaguro, S. Tawaraya, T. Furuichi, T. Okauchi, *Tetrahedron: Asymmetry*, **1995**, *6*, 2469.

⁶⁸ M. Léautey, G. Castelot-Deliencourt, P. Jubault, X. Pannecoucke, J.-C. Quirion, *Tetrahedron Lett.*, **2002**, *43*, 9237.

The asymmetric C-P bond formation was achieved under heterogenous conditions *via* a iron(III) oxide - mediated phospho-Michael conjugate addition of chiral phosphinite to alkylidene malonates⁶⁹ (Fig.18).

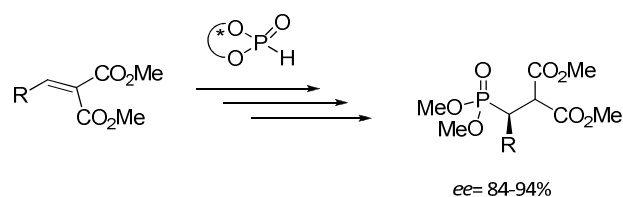
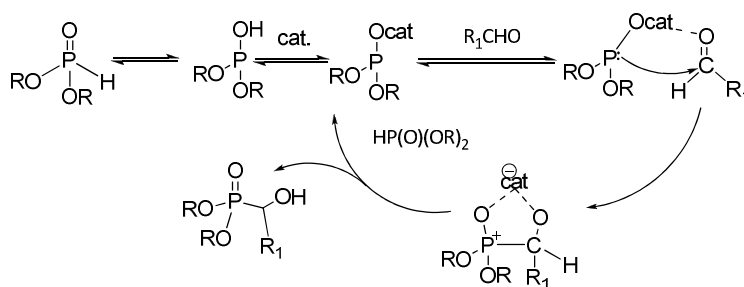


Fig. 18 Chiral phospho-Michael addition

The use of a Brønsted base bicyclic guanidine catalyst was also reported for this reaction between aromatic phosphine oxides and nitrostyrene⁷⁰ with very remarkable enantioselectivity. The same author studies the catalytic mechanism and origins of enantioselectivity of this kind of catalyst in phospho-Michael reaction.⁷¹ Examples of intermolecular phospho-Michael reaction of cyclic and acyclic alkenyl sulfoximines⁷² and α,β -unsaturated aldehydes⁷³ exist in the recent literature.

I.2.3. Hydrophosphonylation/hydrophosphorylation

The addition reaction of H-phosphonates to activated double bond by electron withdrawing group is called hydrophosphonylation. This reaction is often promoted by transition metal catalysts, radical initiators, strong bases or Lewis acid-microwave initiation.⁷⁴ In this group of transformations, we can distinguish Pudovik reaction,⁷⁵ the conversion of dialkyl phosphites to α -hydroxy phosphonates in the presence of carbonyl compounds. The mechanism of this reaction involves the deprotonation of phosphorus agent forming a dialkyl phosphate anion, which reacts as a nucleophile toward electrophilic carbonyl carbon (Scheme 14).



Scheme 14 Mechanism of Pudovik reaction

⁶⁹ L. Tedeschi, D. Enders, *Org. Lett.*, **2001**, 22, 3515.

⁷⁰ X. Fu, Z. Jiang, C.-H. Tan, *Chem. Commun.*, **2007**, 5058.

⁷¹ B. Cho, C.-H. Tan, M. W. Wong, *Org. Biomol. Chem.*, **2011**, 9, 4550.

⁷² F. Lemasson, H.-J. Gais, J. Runsink, G. Raabe, *Eur. J. Org. Chem.*, **2010**, 2157.

⁷³ X. Luo, Z. Zhou, X. Li, X. Liang, J. Ye, *RCS Adv.*, **2011**, 1, 698.

⁷⁴ (a) C. Baillie, J. Xiao, *J. Curr. Org. Chem.*, **2003**, 7, 477; (b) M. Tanaka, *Top. Curr. Chem.*, **2004**, 232, 25; (c) J.-L. Montchamp, *J. Organomet. Chem.* **2005**, 690, 2388; (d) D. Enders, A. Saint-Dizier, Lannou, M.-I.; Lenzen, A. *Eur. J. Org. Chem.*, **2006**, 29; (e) F. Alonso, I. P. Beletskaya, M. Yus, *Chem. Rev.* **2004**, 104, 3079; (f) I. P. Beletskaya, M. A. Kazankova, *Russ. J. Org. Chem.* **2002**, 38, 1391; (g) L. Coudray, J.-L. Montchamp, *Eur. J. Org. Chem.* **2008**, 3601.

⁷⁵ N. Pudovik, A. Arbuzov, *Dokl. Akad. Nauk. SSSR*, **1950**, 73, 327.

Diverse metal complexes have been used as effective catalyst for this transformation, such as lanthanides or titanium.⁷⁶ Recently, MoO₂Cl₂ has been reported as a novel catalyst for C-P bond formation during hydrophosphonylation of different aromatic and aliphatic aldehydes⁷⁷ in solvent-free conditions with good to high yields.

Furthermore, Balaraman *et al.* presented the protocol for regio-/stereo-selective hydro-/hydrothiophosphonylation in ionic liquid medium.⁷⁸ Several examples of Baylis-Hillman adducts in the presence of TBAF in [BMIM]⁺[PF₆]⁻ were depicted in this work, leading to γ -hydroxyphosphonates with good yield (Fig.19).

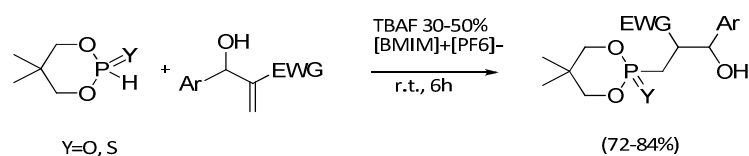


Fig. 19 Example of hydrophosphonylation

The group of Knochel⁷⁹ elaborated an application of *t*-BuOK - catalyzed addition of phosphines to functionalized alkenes, which allows an access to polyfunctional phosphine derivatives. Moreover, their methodology has been expanded to the preparation of novel chiral N,P-ligands, which were applied to enantioselective Ir-catalyzed hydrogenation.⁸⁰

The regio- and stereoselective hydrophosphination reaction of alkynes with phosphine boranes was presented by A.-C. Gaumont.⁸¹ This methodology gives an access to vinylphosphines - a ligand building blocks for homogenous catalysis.

The first asymmetric organocatalytic electrophilic phosphination has been reported by Nielsen *et al.*⁸² as a reaction of α -substituted cyanoacetates with diarylphosphine chlorides with catalytic amounts of cinchona alkaloids (DHQD)₂PYR as organocatalysts. Furthermore, obtained optically active α -phosphinated cyanoacetates were transformed into protected chiral α -phosphino β -amino acids by using one-pot procedure (Fig.20). These products could be also regarded as precursors for new N,P-ligands.

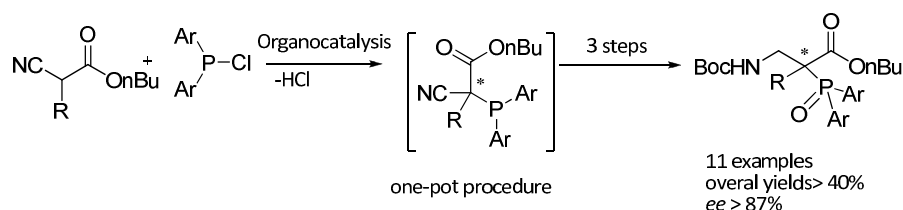


Fig. 20 Asymmetric catalytic phosphination

⁷⁶ F. Yang, D. Zhao, J. Lan, P. Xi, L. Yang, S. Xiang, J. You, *Angew. Chem. Int. Ed.*, **2008**, *47*, 5646.

⁷⁷ R. G. de Noronha, P. J. Costa, C. C. Romão, M. J. Calhorda, A. C. Fernandes, *Organometallics*, **2009**, *28*, 6206.

⁷⁸ E. Balaraman, V. Srinivas, K. C. Swamy, *Tetrahedron*, **2009**, *65*, 7603.

⁷⁹ T. Bunlaksananusorn, P. Knochel, *Tetrahedron Lett.*, **2002**, *43*, 5817.

⁸⁰ T. Bunlaksananusorn, K. Polbron, P. Knochel, *Angew. Chem. Int. Ed.*, **2003**, *42*, 3941.

⁸¹ D. Mimeau, A.-C. Gaumont, *J. Org. Chem.*, **2003**, *68*, 7016.

⁸² M. Nielsen, C. B. Jacobsen, K. A. Jørgensen, *Angew. Chem. Int. Ed.*, **2011**, *50*, 3211.

I.2.4. Carbon-phosphorus transition metal-catalyzed cross-coupling

I.2.4.a. Historical introduction

The group of cross-coupling reactions catalyzed by metal complexes is well-known in organic synthesis since the Cadiot-Chodkiewicz reaction between a terminal alkyne and halogen derivative in 1957.⁸³ Thereafter, plenty of new methods have been described, with different coupling partners and operating conditions. However, the issue of coupling between heteroatoms has been raised quite recently. Pioneering work in this field has been performed by the Hirao group⁶³ and stated the palladium catalyzed couplings between aryl or vinyl halides and dialkyl phosphinites, affording dialkyl arylphosphonates and dialkyl vinylphosphonates (Fig. 21). The reaction conditions for these early experiments were: Pd(PPh₃)₄ in catalytic amount of 5 mol % and triethylamine as a base. Reactions were carried out neat or in toluene; the geometry of the double bond was maintained in the case of vinyl compound.

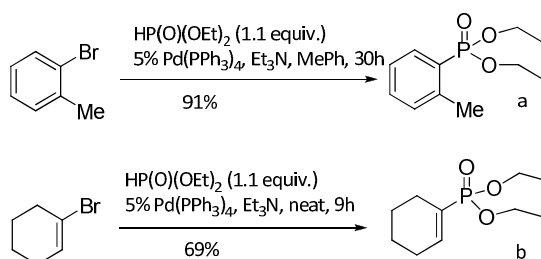
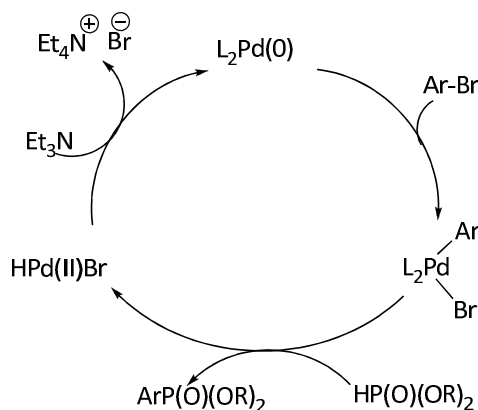


Fig. 21 First examples of C-P coupling reaction

The mechanism of this reaction proposed by the Hirao group states an oxidative addition of the Pd(0) complex to the aryl bromide bond (Scheme 15). Attack of the phosphinite forms expected product, while triethylamine liberates the Pd(0) from the complex HPd(II)Br. The significant amounts of salt (EtO)₂PO⁻ Et₃NH⁺ are present in the reaction mixture; which lowers the yield.



Scheme 15 Mechanism presented by Hirao

Tunney and Stille⁸⁴ were the first to describe direct phosphine synthesis using palladium catalyzed carbon-phosphorus bond formation. Diphenyl(trimethylsilyl)phosphine and

⁸³ (a) W. Chodkiewicz, *Ann. Chim. Paris*, **1957**, 2, 819; (b) P. Cadiot, W. Chodkiewicz, *Chemistry of Acetylenes*; H. G. Viehe Ed., Marcel Dekker: New York, **1969**, 597.

⁸⁴ S. E. Tunney, K. J. Stille, *J. Org. Chem.*, **1987**, 52, 748.

diphenyl(trimethylstannyl)phosphine were brought into reaction with aryl halides in the presence of $\text{PdCl}_2(\text{PPh}_3)_2$ or $\text{PdCl}_2(\text{MeCN})_2$ as catalyst in benzene (Fig.22).

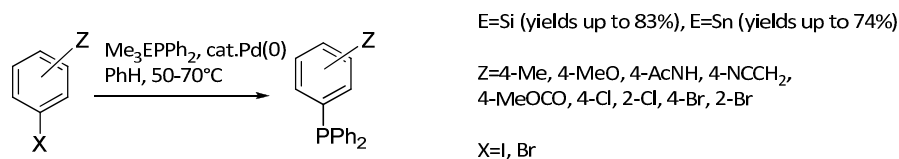
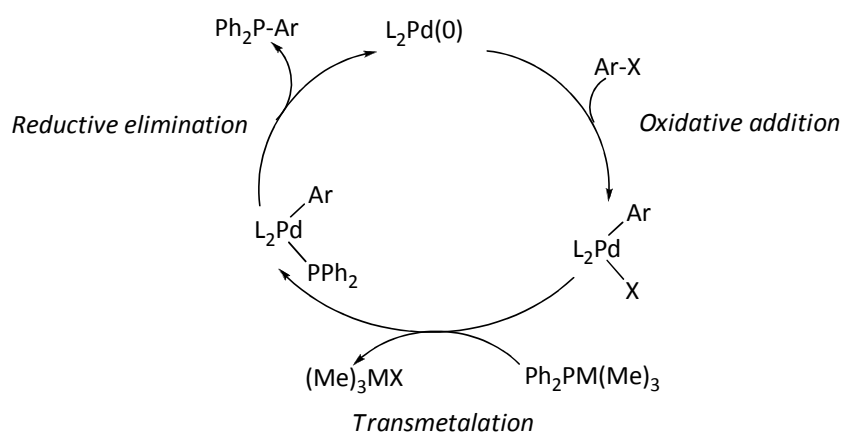


Fig. 22 Phosphine synthesis presented by Tunney and Stille

The mechanism presented by Stille is comparable to the Hirao catalytic cycle; it is more advanced due to recognition of probable intermediates in palladium chemistry and their role in steps of oxidative addition, transmetalation and reductive elimination (Scheme 16).



Scheme 16 Mechanism presented by Tunney and Stille

Modern methods of organic synthesis might consider these two protocols somewhat outdated with quite toxic solvents and harsh thermal conditions, however a contribution of these strategies in a C-P bond formation is significant and enable a great progress in this area.

Below, most significant examples of C-P metal catalyzed cross-coupling will be presented with the division of phosphorus-containing agents on the phosphines and phosphine oxides, phosphine boranes, triphenylphosphine, phosphine chlorides, and also to form the $\text{C}(\text{sp})\text{-P}$ bond, $\text{C}(\text{sp}^3)\text{-P}$ bond and some asymmetric examples.

I.2.4.b. Phosphine oxides and phosphines as coupling agents

Herein, some examples of phosphine synthesis from phosphine oxides and lower phosphines will be presented. The ability to convert phenol into phosphorus species by the aryl triflates intermediates was first presented by Morgans in 1990⁸⁵ and has been widely exploited by numbers of researcher for the preparation of chiral phosphines. Morgans and co-workers showed that 3-4 equiv. of a phosphoarylating agent such as diphenylphosphine oxide and 6 equiv. of diisopropylethylamine combined with the catalytic system of $\text{Pd}(\text{OAc})_2/\text{dppp}/\text{HCOONa}$ carries out the stereospecific

⁸⁵ L. Kurz, G. Lee, D. Morgans Jr., M. J. Waldyke, T. Ward, *Tetrahedron Lett.*, **1990**, 31, 6321.

conversion of (-)-BINOL ditriflate to its monophosphorylated derivative in good yield. After hydrolysis of second triflate and phosphorus deoxygenation step, this methodology gives an access stereospecifically to triarylphosphines.

A synthesis of one of the most efficient phosphorus-containing chiral ligand BINAP (2,2'-bis(diphenylphosphino)-1,1'-binaphthyl) is a good example of direct arylation of secondary and primary amines. BINAP was synthesized for the first time by Noyori in early 1980s.⁸⁶ Since this time many attempts have been undertaken, one of them is catalytic pathway proposed by Merck,⁸⁷ starting from BINOL ditriflate with diphenylphosphine and NiCl₂/dppe in DMF in the presence of DABCO as a base (Fig.23).

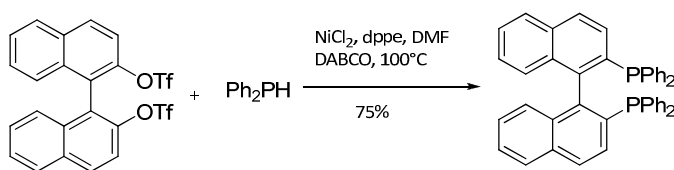


Fig. 23 BINAP synthesis presented by Noyori

Another interesting example of direct phosphination is synthesis of phosphine-containing amino acids⁵⁷ described already in the paragraph I.1.3c. The catalytic transformation of tyrosine and hydroxyphenylglycine derivatives, and also thyrosine-containing peptides was effected by cross-coupling of the corresponding trifluoromethylsulfonates with diphenyl phosphine in DMSO.

I.2.4.c. Phosphine boranes as coupling agents

Some phosphines oxidize easily in the presence of O₂ from the air and they are difficult to handle. In order to circumvent this objection, the protection of phosphorus atom with borane group was undertaken. The phosphine-borane adducts are solid substances stable in air, where phosphorus atom is protected from oxidation. However, various transformations, like arylation or vinylation, on the P-center or in the α- or β-position of one of the phosphorus substituents, are possible. The approach was introduced by Imamoto and Oshiki in 1992⁸⁸ who showed that (S)_P - and (R)_P - menthylphosphine-boranes can undergo palladium catalyzed C-P bond formation with *o*-iodoanisole. The reaction conditions provoke either retention or inversion of phosphorus configuration. Fig.24 presents experimental prove, that in the case of acetonitrile solution, the chiral center remains intact, but using ethereal solvents (i.e. THF) or toluene, the inversion of configuration occurs.

⁸⁶ A. Miyashita, A. Yasuda, H. Takaya, K. Toriumi, T. Ito, T. Souchi, R. Noyori, *J. Am. Chem. Soc.*, **1980**, *102*, 7932.

⁸⁷ D. Cai, J. F. Payack, D. R. Bender, D. L. Hughes, T. R. Verhoeven, P. J. Reider, *J. Org. Chem.*, **1994**, *59*, 7180.

⁸⁸ T. Imamoto, T. Oshiki, T. Onozawa, M. Matsuo, T. Hikosaka, M. Yanagawa, *Heteroat. Chem.*, **1992**, *3*, 563.

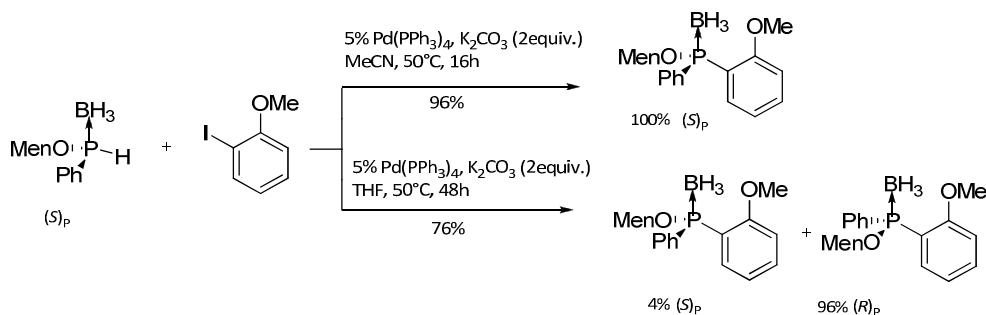


Fig. 24 Stereoselectivity depending on the solvent in the reaction with phosphine-boranes

Aryl triflates and nonaflates are reactive with secondary phosphine-boranes (Fig.25).⁸⁹ However, the authors describe that this procedure cannot be applied to compounds containing heterocyclic nitrogen because the presence of N-atom decomplexes the phosphine of its borane.

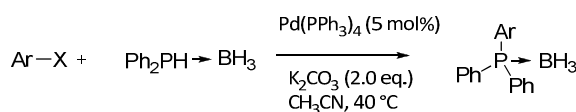


Fig. 25 Cross-coupling with aryl triflates and nonaflates with phosphine-boranes

Apart from palladium catalyst, mild arylation of phosphine-boranes is favored by addition of a catalytic amount of copper(I) iodide.⁹⁰ Yields of this reaction are high, even at room temperature, which is explained by the formation of stable intermediate - copper phosphide. Moreover, mild conditions ensure arylation of a chiral phosphine-borane with a high enantioselectivity (*ee* 94.5-99%).⁹¹

Other example of secondary phosphine functionalisation includes the conversion of vinyl triflates to vinylphosphines, which can be transformed to the more stable borane complex (Fig.26).⁹²

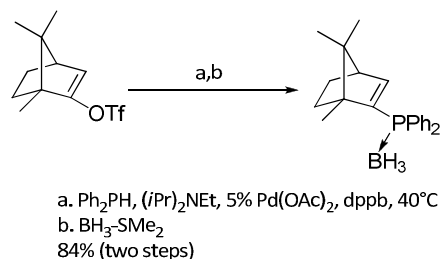


Fig. 26 Synthesis of vinylphosphine-boranes by Starkley

Lately, the group of Gaumont showed that vinylphosphine-borane complexes are accessible directly by the cross-coupling with secondary phosphine-boranes.⁹³ Series of experiments with different bases (K_2CO_3 , K_3PO_4) and different heating conditions have been undertaken to choose the best ones (Fig. 27). Also, some examples showing enantioselectivity of this reaction was presented.⁹⁴

⁸⁹ B. H. Lipshutz, D. J. Buzard, C. S. Yun, *Tetrahedron Lett.*, **1999**, 40, 201.

⁹⁰ M. Al-Masum, T. Livinghouse, *Tetrahedron Lett.*, **1999**, 40, 7731.

⁹¹ M. Al-Masum, G. Kumaraswamy, T. Livinghouse, *J. Org. Chem.*, **2000**, 65, 4776.

⁹² S. R. Gilbertson, Z. Fu, G. W. Starkley, *Tetrahedron Lett.*, **1999**, 40, 8509.

⁹³ D. Julienne, J.-F. Lohier, O. Delacroix, A.-C. Gaumont, *J. Org. Chem.*, **2007**, 72, 2247.

⁹⁴ D. Julienne, O. Delacroix, A.-C. Gaumont, *C. R. Chimie*, **2010**, 13, 1099.

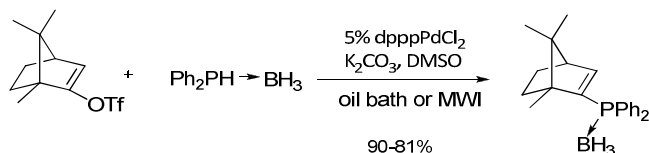


Fig. 27 Synthesis of vinylphosphine-boranes by Gaumont

The borane protecting group is very convenient for phosphorus compounds, because its deprotection can be easily achieved to give quantitatively P(III) compound with complete retention of configuration on the phosphorus center.⁹⁵

I.2.4.d. Triphenylphosphine as coupling agents

Chan⁹⁶ has proved that triphenylphosphine might play a role in the direct formation of tertiary phosphorus ligands as the diarylphosphinating agent (Fig. 28).

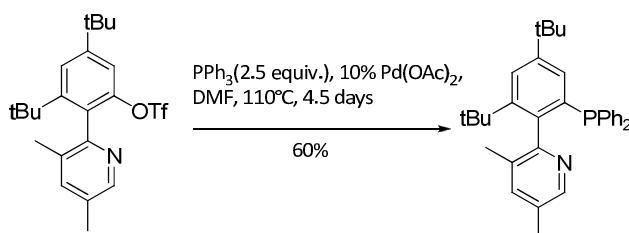
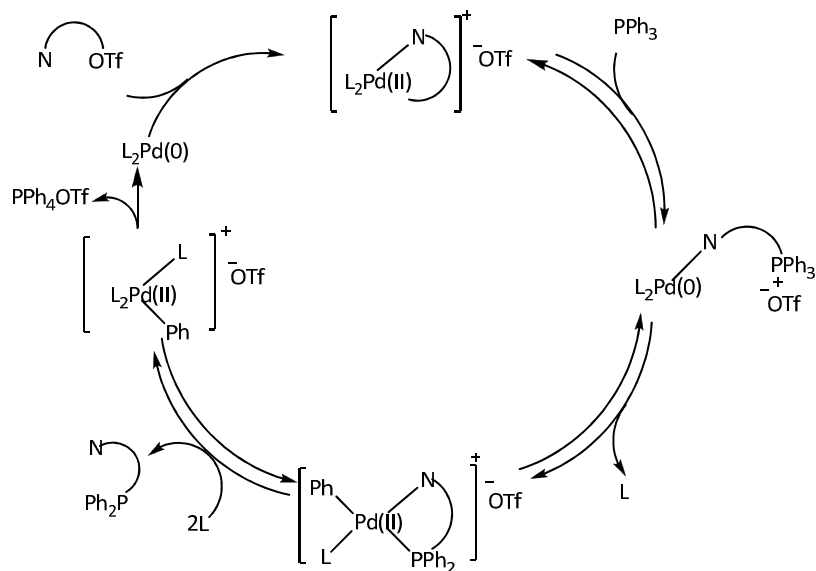


Fig. 28 Cross-coupling with triphenylphosphine

In fact, palladium catalyzes in this reaction an aryl exchange on the phosphorus atom, attaching a functionalized aryl part to the expense of a phenyl group. The conversion of aryl bromides or triflates to phosphines offers products in the 25-50% yield, however application of this methodology to the synthesis of atropisomeric biaryl N,P-ligands increases the recovery of product to 50-68%, presumably due to implication and coordinative interaction of the pyridyl nitrogen in the catalytic mechanism (Scheme 17).

⁹⁵ (a) J. Uziel, C. Darcel, D. Moulin, C. Bauduin, S. Jugé, *Tetrahedron: Asymmetry*, **2001**, 12, 1441 ; (b) S. Jugé, M. Stephan, J. A. Laffitte, J. P. Genêt, *Tetrahedron Let.*, **1990**, 31, 6357.

⁹⁶ F. Y. Kwong, K. S. Chan, *Organometallics*, **2001**, 20, 2570.



Scheme 17 Mechanism proposed by Chan

According to Chan, the proximal nitrogen participates in complexation of palladium(II) and also provokes the oxidative addition of the palladium into existing P-C bond. It was shown that more than two equivalents of triarylphosphine are required for a complete transformation. The liberation of P,N-ligand causes a formation of Pd phenyl complex, the last one undergoes reductive elimination and releases tetraphenylphosphonium triflate (which could be isolated from the reactional mixture) and regenerates the palladium(0) complex.

I.2.4.e. Phosphine chlorides as coupling agents

Other alternative partners for C-P cross-coupling are phosphine chlorides. First attempts of an application of diphenylphosphine chloride in the nickel-catalyzed cross-coupling are reported by Cristau.⁹⁷ An improvement to his methodology has been brought by Laneman by the addition of stoichiometric amounts of zinc.⁹⁸ Aryl and vinyl halides as well as sulfonates and benzylic halides can react with diphenylphosphine chloride to yield the corresponding tertiary phosphines in good yields (Fig. 29). The role of zinc is, from one hand, to reduce Ni(II) to Ni(0) but also, to form the intermediate Ph_2PZnCl prior to the transmetalation step.

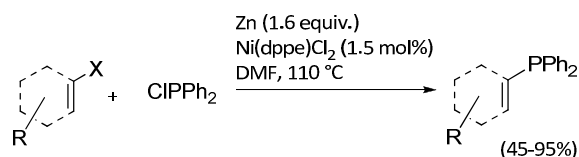


Fig. 29 Cross-coupling reaction with phosphine chloride

The methodology presented by Laneman provides the opportunity to the preparation of wide range of phosphines starting from sterically hindered aryl halides or sulfonates. Better yields are obtained with aryl triflates than with aryl halides.

⁹⁷ H.-J. Cristau, A. Chêne, H. Christol, *J. Organomet. Chem.*, **1980**, *185*, 283.

⁹⁸ D. J. Ager, B. E. East, A. Eisenstadt, S. A. Laneman, *Chem. Comm.*, **1997**, 23590.

I.2.4.f. Alkyl sp derivatives as coupling partners

Cross-coupling reaction catalyzed by transition metals providing to $C(sp^2)$ -P bond formation is by far the most widespread, however some examples of coupling between $C(sp)$ -P appeared in recent years. Beletskaya presented nickel-, palladium- and copper-catalyzed couplings of terminal alkynes with chlorophosphines.⁹⁹ The mechanism of this transformation is similar to the Sonogashira cross-coupling; here the initial step is the oxidative addition of the chlorophosphine to the metal complex, forming phosphido complex. After the exchange on the aforementioned complex, the phosphinioalkyne is liberated. The copper-catalyzed reaction can be applied to alkynes with heteroaryl substituents.^{100b} This reaction works also with weaker electrophiles such as $(RO)_2P$ or $(R_2N)_nPCl_{3-n}$. The second example of this type of coupling is work of Yamaguchi¹⁰⁰ on reactions with terminal alkynes and diphosphines under rhodium catalysis in the presence of nitrobenzenes (Fig.30). The role of nitrobenzene is here to activate P-P bond for the transition metal catalysis.

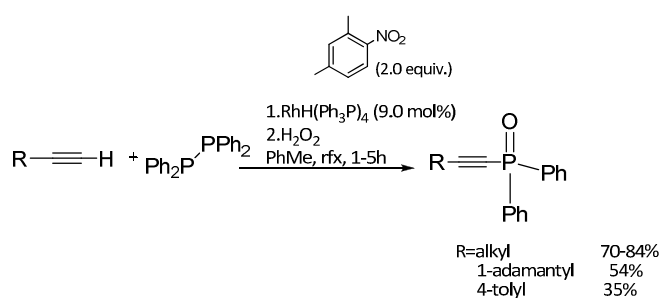


Fig. 30 Cross-coupling reaction $C(sp)$ -P

I.2.4.g. Alkyl sp^3 derivatives as coupling partners

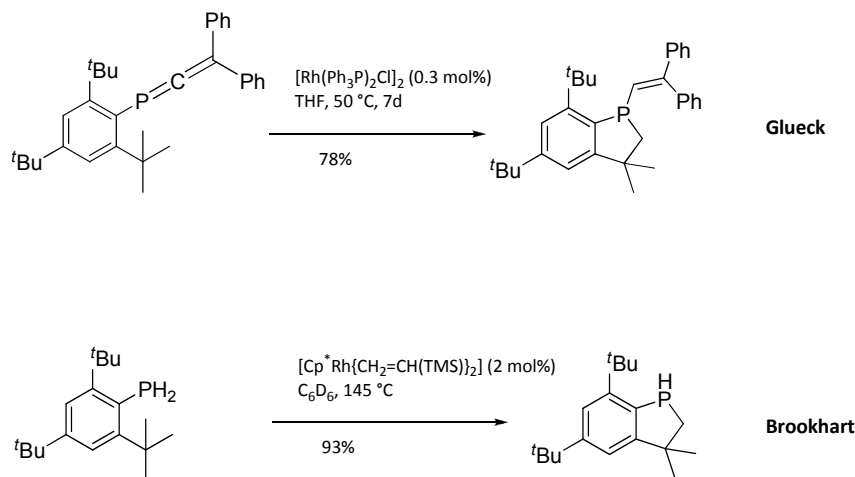
In order to perform $C(sp^3)$ -P couplings, benzylic halides can be applied. Laneman *et al.*⁷⁹ presented the coupling reaction with benzylic bromide and diphenylphosphine chloride under nickel catalysis in the presence of zinc dust. Montchamp *et al.*¹⁰¹ utilized benzylic and heterobenzylic chlorides in the Pd-catalyzed coupling with the anilinium salt of hypophosphorus acid to give substituted phosphinates with good to moderate (in case of heterobenzylic substrates) yields. Also phosphination of allylic alcohols and allylic chlorides with hypophosphorus acid was reported by the same group. C-H bond activation and subsequent $C(sp^3)$ -P coupling under rhodium catalyst¹⁰² was observed by Glueck using 2,4,6-tri(*tert*-butyl)phenyl phosphacumulenes and by Brookhart using phosphines (Scheme 18).

⁹⁹ (a) I. P. Beletskaya, M. A. Kazankova, I. V. Efimova, *Org. Lett.*, **2003**, 5, 4309; (b) V. V. Afanasiev, I. P. Beletskaya, M. A. Kazankova, I. V. Efimova, M. U. Antipin, *Synthesis*, **2003**, 2835.

¹⁰⁰ M. Arisawa, M. Onoda, C. Hori, M. Yamaguchi, *Tetrahedron Lett.*, **2006**, 47, 5211.

¹⁰¹ K. Bravo-Altamirano, Z. Huang, J.-L. Montchamp, *Tetrahedron*, **2006**, 61, 6315.

¹⁰² (a) M.-A. David, S. N. Paisner, D. S. Glueck, *Organometallics*, **1995**, 14, 17; (b) V. P. W. Böhm, M. Brookhart, *Angew. Chem. Int. Ed.*, **2001**, 40, 4694.



Scheme 18 Cross-coupling reaction C(sp³)-P

I.2.4.h. Asymmetric examples

The last part discussed here will concern asymmetric cross-coupling reactions with racemic phosphines and phosphorus-containing compounds. The first example of C-P coupling between secondary phosphine and phenyl iodide was reported by Glueck,¹⁰³ catalyzed by the Pd-complex of (*R,R*)-MeDuPHOS (Fig. 31). The chiral product was obtained with 78% of enantiomeric excess; detailed studies of the reaction kinetics suggest that enantiodetermining step occurs after Pd-P bond formation.

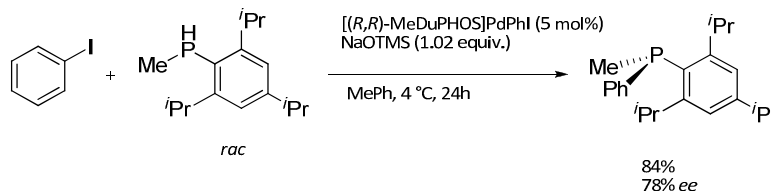
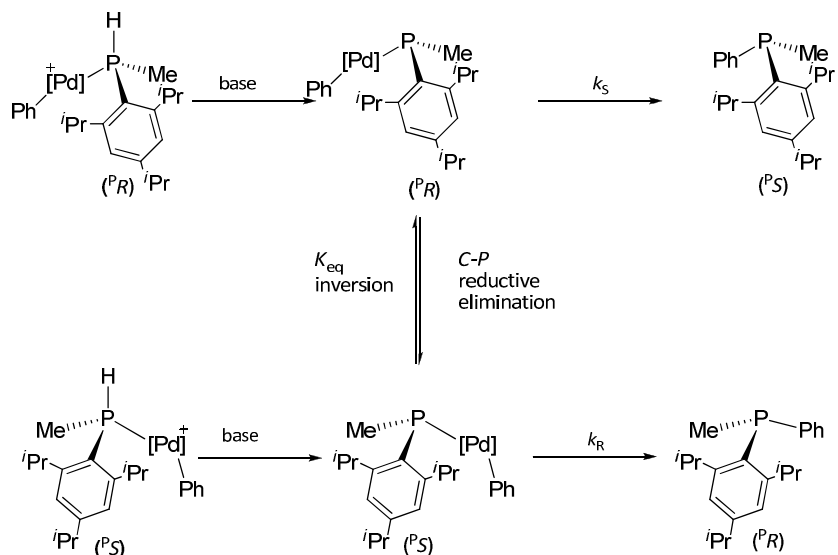


Fig. 31 Asymmetric C-P coupling

The interconversion of diastereoisomers through inversion at the phosphorus atom was proven to be much more fast than C-P bond formation by reductive elimination ($K_{eq} \gg k_R$ and k_S). The reaction depends on both the equilibrium ratio and the relative rates of the reductive elimination. It was shown that the major enantiomer (^{*P*}*S*) is formed from the major diastereoisomer (^{*P*}*R*), but also it was found that minor enantiomer suffers reductive elimination three times faster, though this slightly diminishes enantioselectivities (Scheme 19).

¹⁰³ J. R. Moncarz, N. F. Laritcheva, D. S. Glueck, *J. Am. Chem. Soc.*, **2002**, *124*, 13356.



Scheme 19 Stereoselectivity of C-P coupling

Also phosphine boranes were tested in asymmetric cross-couplings starting from racemic product. Intensive mechanistic studies were performed by Glueck¹⁰⁴, however in this case enantiomeric excess was lower. An intramolecular variant of asymmetric C-P bond formation was presented by the same authors,¹⁰⁵ giving an access to benzophospholanes with moderate level of enantioselectivity. Also racemic silylphosphines¹⁰⁶ served as substrate for this type of reaction, giving products with high *ee*. Other transition metals than Pd such as Pt or Ru were also tested for asymmetric couplings of C(sp³)-hybridized coupling partners. Glueck¹⁰⁷ showed that platinum(II) Me-DuPHOS reacts similar to palladium complex; from the other hand, Bergman and Toste¹⁰⁸ have introduced ruthenium catalyst to the enantioselective preparation of *P*-stereogenic phosphines from *para*- and *ortho*-substituted benzylic chlorides, heteroaryls and non-benzylic electrophiles.

I.3. Summary

In this bibliographic part, we have presented the importance of phosphorus-containing compounds in the field of organic synthesis (as organocatalyst and ligands for transition-metal asymmetric reactions) and in the domain of biologically active products. We have depicted possible strategies of synthesis of mentioned products, putting emphasis particularly on the cross-coupling reaction and the versatility of possible coupling partners.

On the next pages of this dissertation, we will describe the preparation of original compounds containing phosphorus atom, applying two methodologies depicted previously: the C-P coupling of asymmetric phosphorus-containing compounds on N-heterocycles and the nucleophilic addition of the lithium phosphide on the acyclic enecarbamates.

¹⁰⁴ J. R. Moncarz, T. J. Brunker, D. S. Glueck, R. D. Sommer, A. L. Rheingold, *J. Am. Chem. Soc.*, **2003**, *125*, 1180.

¹⁰⁵ T. J. Brukner, B. J. Anderson, N. F. Blank, D. S. Glueck, A. L. Rheingold, *Org. Lett.*, **2007**, *9*, 1109.

¹⁰⁶ V. S. Chan, R. G. Bergman, F. D. Toste, *J. Am. Chem. Soc.*, **2007**, *129*, 15122.

¹⁰⁷ C. Scriban, D. S. Glueck, *J. Am. Chem. Soc.*, **2006**, *128*, 2788; C. Scriban, D. S. Glueck, J. A. Golen, A. L. Rheingold, *Organometallics*, **2007**, *26*, 1788.

¹⁰⁸ V. S. Chan, I. C. Steward, R. G. Bergman, F. D. Toste, *J. Am. Chem. Soc.*, **2006**, *128*, 2786.

II. Results and discussion

II.1. C-P cross-coupling reaction

II.1.1. Introduction

As it was described before in the bibliographic part, the transition metal cross-coupling reaction plays a major role for construction of C-P bond. It exist vast number of literature examples of different electrophiles as partners for coupling reaction, such as halogenated derivatives and triflates, or even tosylates. The group of Gaumont⁹⁴ has reported the palladium-catalyzed C-P coupling between vinyl triflates and phosphine-boranes providing vinylphosphine-boranes in efficient way (Fig. 32).

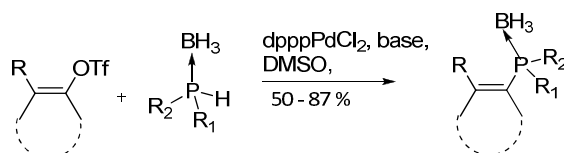


Fig. 32

They expand their methodology to the vinyl tosylates (Fig. 33) as a less expensive and more stable counterparts.¹⁰⁹ The presented systematical work on activated and unactivated vinyl tosylates showed the usefulness of their approach.

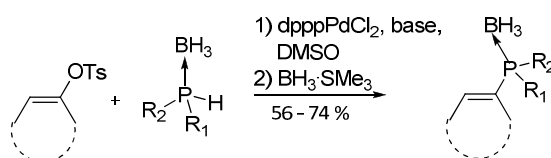


Fig. 33

Considering the nucleophilic partners for C-P coupling, the oxidized species are also available. Equally, the cyclic phospholane moiety elaborated and largely studied by the group of Toffano in the cross-coupling between the diphenylphospholane oxides and boranes and aryl triflates (Fig. 34).¹¹⁰

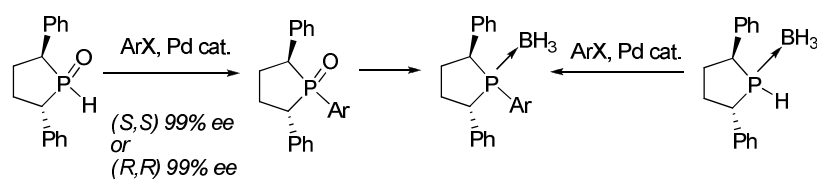


Fig. 34

For the best of our knowledge, any citation of phosphates as substrates for C-P cross-coupling reaction was given. That was the reason to test the vinyl phosphate – derivatives into the reaction of direct C-P coupling.

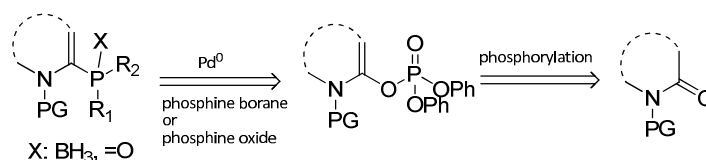
¹⁰⁹ D. Julienne, O. Delacroix, A.-C. Gaumont, *Phosphorus, Sulfur and Silicon*, **2009**, *184*, 846.

¹¹⁰ (a) C. Dobrota, A. Durand, M. Toffano, *Eur. J. Org. Chem.*, **2008**, *14*, 2439; (b) J.-C. Fiaud, M. Toffano, C. Dobrota, J.-C. Fiaud, *Eur. J. Org. Chem.*, **2006**, 650; (c) F. Guillen, M. Rivard, M. Toffano, J.-Y. Legros, J.-C. Daran, J.-C. Fiaud, *Tetrahedron*, **2002**, *58*, 5895.

Only few examples of C-P coupling with electrophiles containing N-atom incorporated into heterocycles is reported. Notably, this arises from the reactivity of these substrates in cross-coupling reaction. With our investigation, we wanted to fill this gap and show the potential of N-containing vinyl phosphates as a substrate in palladium catalyzed cross-coupling reaction.

II.1.2. Objectives of the project

In the aim of the construction of novel alkenyl α -amidophosphines *via* a direct C-P cross-coupling reaction, we envisage a three-step methodology. First, the starting lactam would be protected permitting the possibility to form the enol ether which would be trapped by chlorophosphate to furnish the corresponding enol phosphate. Finally, the palladium catalyzed reaction of C-P cross-coupling could occur to get the desired phosphine borane or phosphine oxides (Scheme 20).



Scheme 20

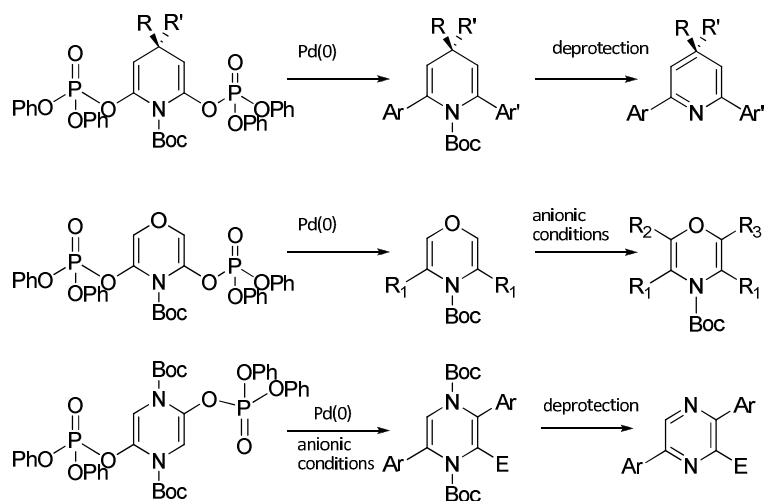
We envisage introducing phosphines with chiral phosphorus and then, conducting the structural investigations determining the stereospecificity of reactions. Therefore, final part of this project will be devoted to the X-ray diffraction studies of obtained products.

II.1.3. The interest of enol phosphates in Pd-catalyzed couplings

For several years, in order to develop synthetic routes to original nitrogen-containing derivatives, the laboratory of Pr. I. Gillaizeau has undertaken a research program directed toward expanding the range of lactam- and imide-derived vinyl phosphates available to the organist chemist. The ability to easily convert alkenyl phosphates into a myriad of functional motifs of synthetic relevance is well-known. In particular, this moiety has proved to be a robust and versatile partner for a range of cross-coupling reactions mediated by Pd(0) and Ni(0) (Heck, Hiyama, Negishi, Sonogashira, Stille and Suzuki-Miyaura reactions). Enol phosphates have in fact, in a few cases, proved to work better in such reactions than their triflate counterparts owing to higher stability, higher reaction yield, and easier work up. Even if the oxidative addition step to the catalyst is less favorable with this reagent, use of electron rich tertiary phosphines can provide yields comparable to those obtained with the traditional electrophiles. The ability of these synthetic intermediates to undergo cross-coupling reactions in the presence of various heteroatoms makes them indeed attractive functional groups for the construction of various substituted heterocyclic systems.^{7,8,111} Enol phosphate has thus become a

¹¹¹ (a) C. Buon, P. Bouyssou, G. Coudert, *Tetrahedron Lett.*, **1999**, *40*, 701; (b) F. Lepifre, C. Buon, R. Rabot, P. Bouyssou, G. Coudert, *Tetrahedron Lett.*, **1999**, *40*, 6373.

powerful tool and has engendered a number of versatile methods for the total synthesis of natural products and other biologically active targets. This methodology allowed to prepare a range of original privileged heterocyclic structures with high diversity (e.g. 1,4-dihydropyridines, 1,4-oxazines, 1,4-dihydropyrazines) and which are advanced synthetic intermediate for the synthesis of biologically active derivatives (Scheme 21).¹¹²



Scheme 21

The first application of enol phosphates was reported by Nicolaou *et al.*¹¹³ in 1997 for the synthesis of cyclic ethers by the mean of palladium-catalyzed cross couplings of lactones *via* their enol derivatives (Fig. 35).

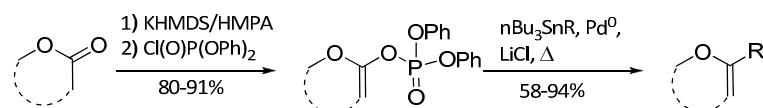


Fig. 35

Another example is the coupling of enol phosphates synthesized from 4-piperidinone with arylboronic acids in the Suzuki-Miyaura coupling to give an access to 4-substituted tetrahydropyridines (Fig. 36).¹¹⁴

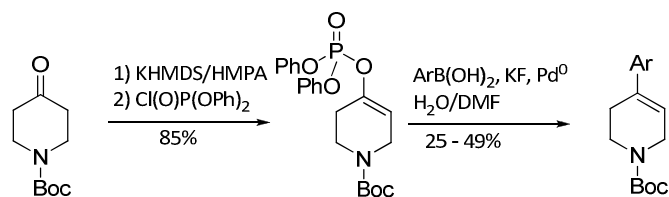


Fig. 36

¹¹² (a) D. Mousset, I. Gillaizeau, A. Sabatié, P. Bouyssou, G. Coudert, *J. Org. Chem.*, **2006**, *71*, 5993; (b) E. Cleaveau, I. Gillaizeau, J. Blu, A. Bruel, G. Coudert, *J. Org. Chem.*, **2007**, *72*, 4832; (c) M. Chaignaud, I. Gillaizeau, N. Ouhamou, G. Coudert, *Tetrahedron*, **2008**, *64*, 8059.

¹¹³ K. C. Nicolaou, G.-Q. Shi, J. L. Gunzner, P. Gärtner, Z. Yang, *J. Am. Chem. Soc.*, **1997**, *119*, 5467.

¹¹⁴ U. S. Larsen, L. Martiny, M. Begtrup, *Tetrahedron Lett.*, **2005**, *46*, 4261.

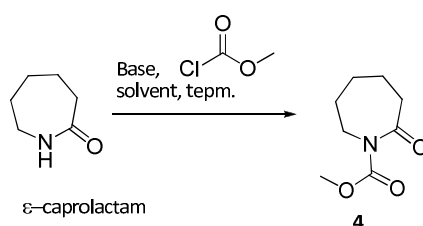
II.2. Results of C-P coupling reaction

II.2.1. Protection step

In order to apply lactams to the preparation of enol phosphates, it is necessary to protect the NH function. We predicted to block this group with a carbamate, an electron withdrawing group activating the α -proton near to a carbonyl function.

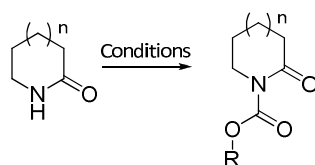
Starting materials for the construction of new P-containing compounds were commercially available 6- and 7-membered ring lactams, respectively δ -valerolactam and ϵ -caprolactam. The standard method with di-*tert*-butyl dicarbonate in the presence of catalyst DMAP gave satisfactory results, however to enlarge the scope, the corresponding methyl carbamates were also synthesized. In order to optimize reaction conditions with methyl chloroformate as electrophile, several different bases and solvents were tested (Table 1) with ϵ -caprolactam.

Table 1 Protection of ϵ -caprolactam



Entry	Base (Equiv.)	Solvent	Temp.	Time	Yield [%]
1	NaH (2.2)	DMF	RT	20 h	0%
2	TEA (2.0)	THF	RT	20 h	0 %
3	<i>t</i> BuOK (1.6)	Et ₂ O	0 °C	16 h	32%
4	<i>n</i> -BuLi (1.1)	THF	-78 °C	2 h	66%

The best result of protection for 7-membered lactam was *n*-BuLi as a base at -78 °C yielding expected carbamate **4** with 66% yield. The same conditions were also applied to the 6-membered counterpart, yielding the methyl 2-oxopiperidine-1-carboxylate **3** (68%). *Tert*-butyl carbamates of 6- and 7-membered ring lactams were obtained with good yields (70% and 65%, respectively) after purification by column chromatography (Table 2).

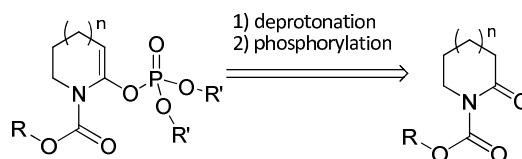
Table 2 Protection of lactames

Cond.:(a) Boc_2O (1.10 equiv.), DMAP (0.05 equiv.), MeCN, rt, 24h;
 (b) MeOCOCl (1.10 equiv.), $n\text{-BuLi}$ (1.10 equiv.), THF, -78°C , 2h

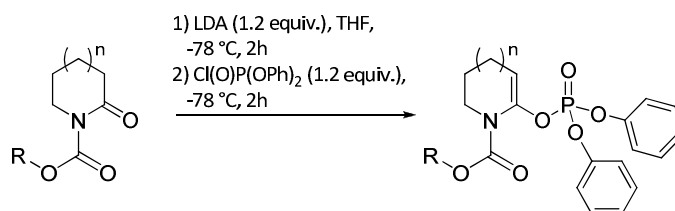
Entry	Conditions	R, n	Product.	Yield [%]
1	(a)	R= <i>t</i> Bu, n=1	1	70%
2		R= <i>t</i> Bu, n=2	2	65 %
3	(b)	R=Me, n=1	3	68%
4		R=Me, n=2	4	66%

II.2.2. Preparation of enol phosphates

The formation of enol phosphates from starting carbamates was conducted in reaction conditions described in the literature.¹¹²⁻¹¹³



The reaction of deprotonation of protected lactames **1-4** was carried out under anionic condition in anhydrous tetrahydrofuran at -78°C , in the presence of 1.2 equiv. of LDA. 1.2 equiv. of electrophile were then introduced to trap the created lithiated anion. Diphenylchlorophosphate was chosen as an electrophile for this reaction due to the high stability of enol phosphates of our products during purification by column chromatography and the storage. These conditions already tested for *Boc*-protected derivatives gave very good results with methyl carbamates (Table 3).

Table 3 Formation of enol phosphates

Entry	Substrate	R, n	Product	Yield [%]
1	1	R=tBu, n=1	5	90*
2	2	R=tBu, n=2	6	58
3	3	R=Me, n=1	7	83
4	4	R=Me, n=2	8	89

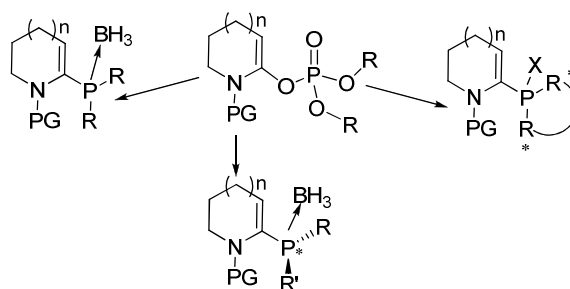
* Product decomposes immediately after reaction so the yield is calculated from the conversion of starting material

Results depicted in the Table 3 show that vinyl phosphates with methyl carbamate protecting group give better yields (83% and 89% yields) and they are more stable during the purification (the product **5** - vinyl phosphate of 6-membered lactam was degrading during the chromatography on neutralized silica gel).

II.2.3. C-P cross-coupling reaction

II.2.3.a. The first approach and optimization of conditions

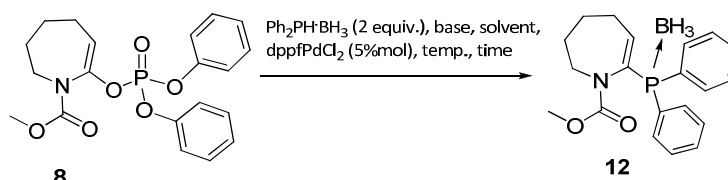
In order to obtain original alkenyl- α -amidophosphines, cross-coupling reaction was performed on the enol phosphate intermediates (**5-8**). We intended first to test the reaction with the achiral diphenylphosphine borane substrate and then move to the series with chiral phosphorus atom. The coupling with the cyclic phospholane oxide or boranes was also predicted (Scheme 22).

**Scheme 22**

Although some examples of coupling between vinyl triflates and phosphine boranes exist in the literature, to the best of our knowledge any of them was given for the vinyl phosphate. The major advantage of our strategy lies in the fact that direct precursors of the free phosphine function can be easily introduced in the α -position to the nitrogen-containing heterocycle.

Using conditions similar to those reported for triflate reagents⁹⁴ we conducted preliminary essays onto the 7-membered ring phosphate **8** and diphenylphosphine borane - commercial product. The first coupling was carried out in DMSO, in the presence of 2.0 equiv. of potassium carbonate and 5mol% of dppfPdCl₂ as a catalyst, at 60 °C for 3 hours yielding desired phosphine with 38% efficiency. This reaction was the starting point to improve the yield and shorten the time of reaction. All tested conditions were presented in the Table 4.

Table 4 Optimization of cross-coupling conditions



Entry	Base	Solvent	Temp. / time	Yield [%] ^a
1	K ₂ CO ₃	DMSO	60°C / 3h	38
2	K ₂ CO ₃	DMSO	60°C (MWI) / 15 min.	11
3	K ₂ CO ₃	DMSO	60°C (MWI) / 30 min.	0
4	K ₂ CO ₃	CH ₃ CN	60°C / 24h	51
5	Cs ₂ CO ₃	DMSO	60°C / 24h	60
6	Cs ₂ CO ₃	CH ₃ CN	60°C / 2h	95
7	Cs ₂ CO ₃	CH ₃ CN ^b	60°C / 1h	90

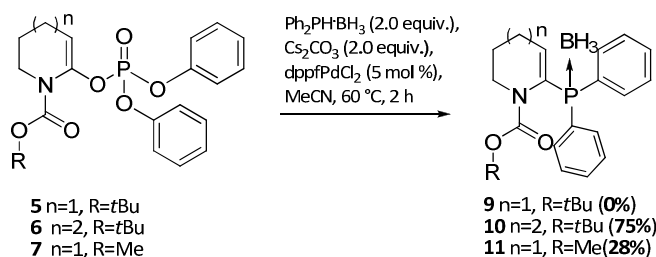
(a) Isolated yields after purification by column chromatography in air. MWI = microwave irradiation. (b) Reaction carried out with a catalyst (IMes)Pd(η 3-2-methylallyl)Cl¹¹⁵

As we can see in the Table 4, the change of weak inorganic base K₂CO₃ for a stronger one Cs₂CO₃ increases the yield of reaction almost twice (Entry 5). Comparing tested solvents, the best results were obtained in polar solvent with high dielectric constant, acetonitrile (Entry 6) instead of DMSO (Entry 5). We performed reactions with classical thermal heating and microwave irradiation activation (MWI), however in this case, contrary to what we could expect, the lower yield was observed (Entry 2 and 3); due to the significant decomposition of starting phosphate. Using another catalyst - (IMes)Pd(η 3-2-methylallyl)Cl developed by Nolan et al.,¹¹⁵ our result was the same as with dppfPdCl₂ (Entry 7). Therefore, the best operational conditions were: the reaction of 1.0 equiv. of enol phosphate with 2.0 equiv. of phosphine borane, then the addition of 2.0 equiv. of Cs₂CO₃, 5 mol% of dppfPdCl₂ and heating for 2 hours at 60 °C.

These optimized conditions were then applied to other vinyl phosphates **5-7** to afford products with moderate yields 75% and 28 % (Scheme 23). In the case of *tert*-butyl 6-(diphenoxyphosphoryloxy)-3,4-

¹¹⁵ O. Navarro, Y. Oonishi, R. A. Kelly, D. E. Stevens, O. Briel, S. P. Nolan, *J. Organomet. Chem.*, **2004**, 689, 3722.

dihydropyridine-1(2*H*)-carboxylate **5** desired product was not formed, probably because of the low stability of phosphate in reaction conditions.



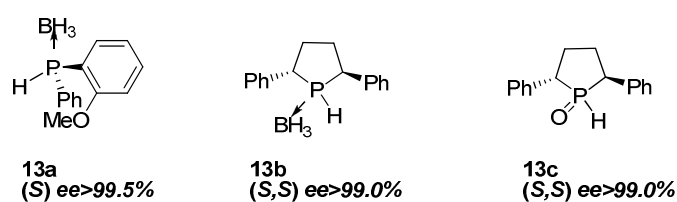
Scheme 23

The first attempt showed that enol phosphate derivatives might be a potential substrate in the C-P cross-coupling reaction with phosphine boranes. In the next part of this chapter we will describe the extension of our methodology for the chiral secondary phosphines.

We predicted also that decomplexation could occur during the coupling reaction, therefore the supplementary $\text{BH}_3\cdot\text{Me}_2\text{S}$ was also added in order to increase the amount of attempted phosphine borane **9-12**. Unfortunately, only unsubstituted enecarbamates resulting from the reduction of the enol phosphate moiety and degradation products were recovered.

II.2.3.b. C-P cross-coupling reaction on the chiral phosphine boranes

The next step of our investigation was an application of enol phosphates to the cross-coupling with asymmetric phosphine boranes and phosphine oxides. The partners for the coupling were enantiomerically pure (*S*)-(*ortho*-anisyl)phenylphosphine borane **13a** largely studied by the group of Jugé¹¹⁶ and phospholane borane **13b** and oxide **13c** elaborated by the group of Fiaud and Toffano.¹¹¹



Scheme 24

The product **13a** is an example of *P*-chirogenic compounds and **13b-13c** presents the asymmetry placed on carbon center which provoke the reorganization around the phosphorus atom (Scheme 24).

II.2.3.c. Reaction with the (*S*)-(*ortho*-anisyl)phenylphosphine borane **13a**

The first attempt was undertaken with phosphine borane **13a** and 7-membered ring enol phosphate **8** in the already elaborated conditions (Table 5); however the expected product was isolated with poor yield 18%. After increasing the time of reaction from 5h15 to 22h only

¹¹⁶ C. Bauduin, D. Moulin, El B. Kaloun, C. Darcel, S. Jugé, *J. Org. Chem.*, **2003**, *68*, 4293.

decomposition of starting phosphate occurred (Entry 2). Finally, decreasing the quantity of catalyst to 5 mol% we obtained better yield (Entry 3).

Table 5

Entry	Time	dppPdCl ₂ [mol%]	Yield
1	5h15	10 %	18 % (racemisation)
2	22h	5 %	0 % (decomposition)
3	2h	5 %	58 % (racemisation)

Unfortunately, the reaction in thermal condition provokes the racemisation of *P*-atom. It may be explained by an inversion, under basic conditions, of the phosphine borane anion before ligand exchange in the coordination sphere of the palladium.¹¹⁷ The enantiomeric excess was verified before and after reaction by SFC chromatography on a chiral column, and showed that obtained product is a racemic mixture of enantiomers.

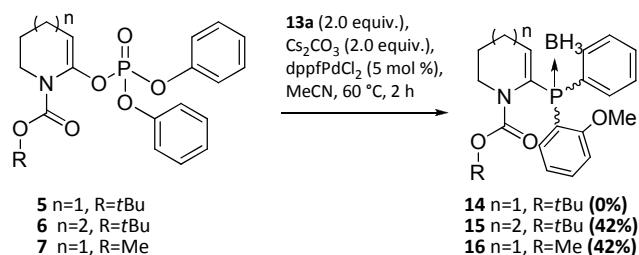


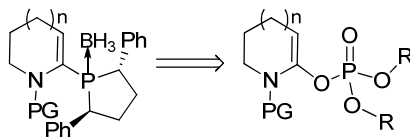
Fig. 37

The same situation was observed for the other phosphates **5-7** (Fig. 37). The racemic phosphine boranes **15** and **16** from enol phosphates with 6-membered ring *N*-COOMe and 7-membered ring *N*-Boc were acquired with 42% yields each. It was impossible to obtain *tert*-butyl 6-(diphenylphosphino)-3,4-dihydropyridine-1(2H)-carboxylate borane **14** in used conditions. Only the product of hydrolysis of phosphate was recovered. Considering the presented results of *C*-*P* coupling with chiral phosphine borane **13a**, the racemisation of products occurs in the case of coupling reaction in thermal conditions. In addition, obtained yields of isolated compounds are much lower, than in achiral series, probably due to the lesser reactivity of the phosphine **13a**, owing to the inductive donor effect of the methoxy group.

¹¹⁷ J. S. Harvey, V. Gouverneur, *Chem. Commun.*, **2010**, 46, 7477.

II.2.3.d. Reaction with the (2*S*,5*S*)-2,5-diphenylphospholane borane complex **13b**

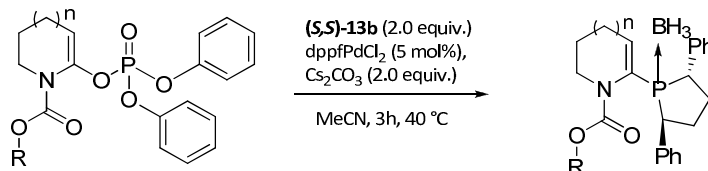
In this paragraph, we will consider the coupling reaction with phospholane bearing the chirality on two carbon center in α position to phosphorus atom. We anticipate, that this type of compound should not racemise under reaction conditions.



Scheme 25

With the coupling partner **13b**, the initial reaction condition has been taken from the previous work;¹¹¹ a reaction was carried out first with 7-membered ring enol phosphate **8** in acetonitrile at 40 °C, in the presence of K₂CO₃ as a base and dppfPdCl₂ as a catalyst, but only traces of good product were isolated. After changing the base for cesium carbonate and slightly increasing the time of reaction from 2 to 3 hours, desired products were obtained in moderate yields (Table 6).

Table 6 Cross-coupling reaction with **13b**



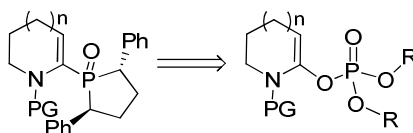
Entry	Substrate	R, n	Product	Yield [%]	ee [%]
1	5	R= <i>t</i> Bu, n=1	18	0	-
2	6	R= <i>t</i> Bu, n=2	19	35	99.5
3	7	R=Me, n=1	20	30	99.5
4	8	R=Me, n=2	21	46	99.5

As in previous case, the product **18** from 6-membered ring enol phosphate could not be obtained, even traces of expected product were not isolated, probably due to low stability of this phosphate in reaction conditions. Moreover, as reported by Toffano *et al.*,¹¹¹ the observed low yield could be explained by a lack of reactivity of the secondary phosphine **13b** and the possible decomplexation of the borane group. Other compounds **19-21** were afforded in moderate yields (30-46% yield) after purification by column chromatography on neutralized silica gel. Enantiomeric excess were established by chiral SFC analysis, they show that this time coupling reaction permitted to retain the chirality in the reaction.

II.2.3.e. Reaction with the (2*S*,5*S*)-2,5-diphenylphospholane oxide **13c**

Finally, (2*S*,5*S*)-2,5-diphenylphospholane oxide **13c** was applied to the cross-coupling with enol phosphates. This phosphine oxide is characterized by higher stability and reactivity than phosphine boranes due to its oxidation state and more acidic P-H hydrogen. The starting coupling conditions were

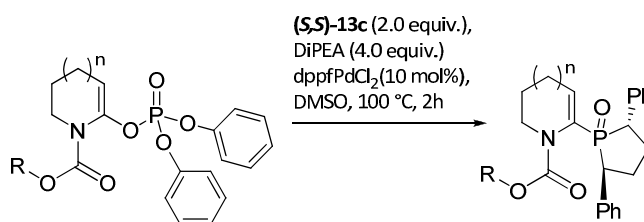
taken from the literature: diisopropylethylamine as a base, dppfPdCl₂ in distilled DMSO at 100 °C.¹¹¹



Scheme 26

It appeared that this procedure was appropriate for desired products, giving chiral phospholane oxide derivative with good yields (Table 7). The coupling reaction was performed on the enantiomer pairs (*S,S*) and (*R,R*) showing similar results in both cases.

Table 7 Cross-coupling reaction with **13c**



Entry	Substrate	R, n	Product	Yield [%]	ee [%]
1	5	R=tBu, n=1	22	28*	99.4
2	6	R=tBu, n=2	23	70	>99.5
3	7	R=Me, n=1	24	64	99.4
4	8	R=Me, n=2	25	70	99.7

* Yield was calculated for starting carbamate, because the enol phosphate after reaction was directly used for coupling.

All conducted reactions were clean and showed the whole transformation of starting enol phosphate within 2 hours. We were also pleased to observe that the higher reactivity of the phospholane oxide **13c** ensures the accomplishment of the C-P coupling with the hindered 6-membered ring phosphate **5**, although with a low yield (Entry 1). In the case of compound **24** X-ray diffraction analysis revealed that no epimerization at the benzylic carbon atom occurred.

In order to study the scope of this methodology and apply it to another *N*-containing heterocycles, we adopted the coupling reaction with (*S,S*)-2,5-diphenylphospholane oxide **13c** to bis-enol phosphates of dihydropyrazine. Based on the previously reported results of the functionalization of the dihydropyrazine ring and its possible aromatization into pyrazine,^{113c} we anticipated obtaining a diphosphine with a dihydropyrazine moiety as a bridge. To date, only a few papers have reported the synthesis of pyrazinyl phosphine derivative.¹¹⁸ To prove our concept we engaged bis-enol phosphate in

¹¹⁸ (a) F. Palacios, A. M. O. de Retana, J. I. Gil, R. L. de Munain, *Org. Lett.*, **2002**, *4*, 2405; (b) M. E. Fox, M. Jackson, I. C. Lennon, J. Klosin, K. A. Abboud, *J. Org. Chem.*, **2008**, *73*, 775; (c) E. L. Deal, C. Petit, J. L. Montchamp, *Org. Lett.*, **2011**, *13*, 3270.

optimized conditions to yield bis-phospholane oxide derivative with good yield (75%) in an enantiomerically pure form (Fig. 38).

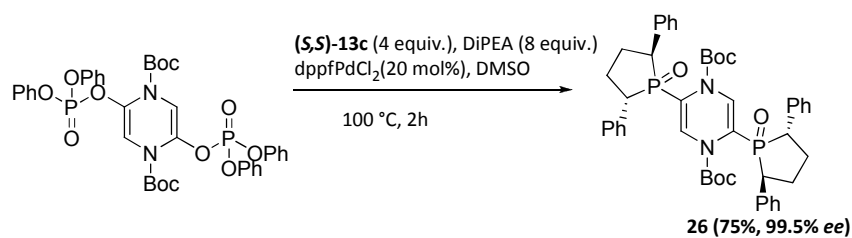
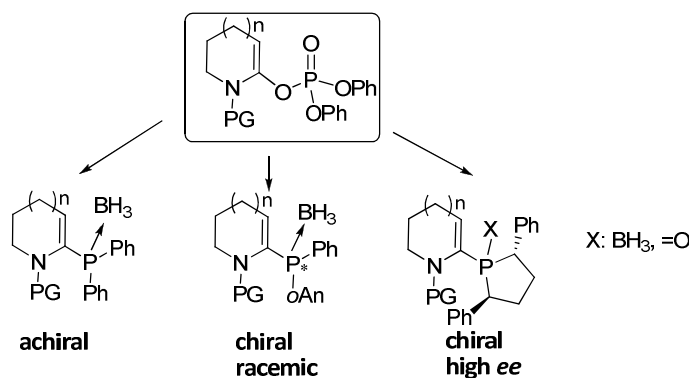


Fig. 38

This product was also sensitized with both enantiomers (*S,S*) and (*R,R*) giving similar results in both cases. The high enantiomeric excess was obtained in this reaction.

II.2.4. Conclusion and perspectives of C-P coupling reaction

This part of thesis dissertation presents a formation of novel products containing C-P bond in direct C-P cross-coupling reaction between vinylphosphates of corresponding 6- and 7-membered ring carbamates leading to original alkenyl- α -amidophosphines.¹¹⁹ This approach is showing the possibility of cross-coupling between secondary phosphine boranes or phospholane derivative and N-containing non-aromatic heterocycles in mild conditions with short reaction times. First attempts were conducted onto achiral phosphines in order to optimize the conditions and then, the methodology was spread onto the series of chiral phosphines, with chirogenic phosphorus and a chirality bearing on the C-atoms in α position to phosphorus.



During the optimization of reaction conditions we have met with some difficulties of racemisation of chiral phosphine borane **13a**. Nevertheless, in the series of asymmetric phospholane derivatives **13b** and **13c**, we managed to obtain the desired products with high enantiomeric excesses established by chiral SFC analysis (up to 99.7%) with fair to good yields. These products were used to optimized the condition of chiral separation in the Supercritical Fluid Chromatography.

¹¹⁹ M. Cieslikiewicz, A. Bouet, S. Jugé, M. Toffano, J. Bayardon, C. West, K. Lewinski, I. Gillaizeau, *Eur. J. Org. Chem.*, **2012**, 1101.

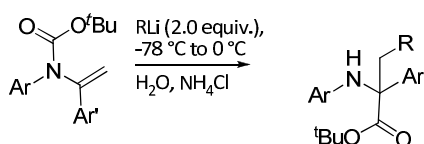
In a perspective to this project, the racemisation problem encountered in the case of carbon-phosphorus coupling could be elude by using the chiral catalyst for cross-coupling such as (*R*)-Tol-BINAP or (*S,S*)-Me-DuPHOS. The group of Gaumont *et al.*⁹⁴ presented recently the application of these catalytic systems to the enantioselective palladium C-P coupling between alkenyltriflate and secondary phosphine-borane complex.

II.3. Nucleophilic addition onto acyclic enecarbamates - an access to P-containing non-natural amino acids

II.3.1. Bibliographic background

Previous works in the laboratory were focused on the carbolithiation reaction onto acyclic enecarbamates derived from the vinylphosphates *via* a cross-coupling reaction.⁸ The key step in this methodology is the spontaneous internal migration of the alkyloxycarbonyl group from nitrogen atom to the quaternary carbon leading to aminoesters (Table 8). This approach gives an access to derivatives of amino acids with varied alkyl and N-containing substituents on β position.⁸

Table 8



Entry	Ar	Ar'	R	Yield [%]
1	Ph	Ph	Me	75
2	Ph	Ph	Ph	78
3	Ph	Ph	N(iPr) ₂	89
4	Ph	Ph	N(Me)(Bz)	51
5	<i>o</i> -MePh	Ph	Me	80
6	<i>o</i> -MePh	Ph	Ph	81
7	<i>m</i> -MeOPh	Ph	Me	68
8	<i>m</i> -MeOPh	Naph	Me	56
9	<i>o</i> -MePh	Ph	<i>n</i> -Bu	89
10	<i>o</i> -MePh	Ph	N(iPr) ₂	86

Theoretical investigations reported by Houk¹²⁰ and Bailey¹²¹ show that the initial step of intermolecular carbolithiation is an energetically favorable coordination of the lithium atom to π -system. This can be supported also by the concept of Complex-Induced Proximity Effect (CIPE), which elucidates the role of carbamate in the reaction mechanism.¹²² The lithiated intermediate provokes a spontaneous internal migration of *tert*-butyloxycarbonyl group *via* the formation of a strained aziridine cycle. As depicted in the Fig. 39, the equilibrium of the reaction is shifted into the direction of the aminoester creation when reaction is warmed up. After hydrolysis and work-up, desired products can be isolated.

¹²⁰ K. N. Houk, N. G. Rondan, P. V. R. Schleyer, E. Kaufman, T. J. Clark, *J. Am. Chem. Soc.*, **1985**, *107*, 2821.

¹²¹ W. F. Bailey, A. D. Khnaolkar, K. Gavaskar, T. V. Ovaska, K. Rossi, Y. Thiel, K. B. Wiberg, *J. Am. Chem. Soc.*, **1991**, *113*, 2925.

¹²² (a) D. R. Anderson, N. C. Faibish, P. Beak, *J. Am. Chem. Soc.*, **1999**, *121*, 7553; (b) K. M. Gross, P. Beak, *J. Am. Chem. Soc.*, **2001**, *123*, 315.

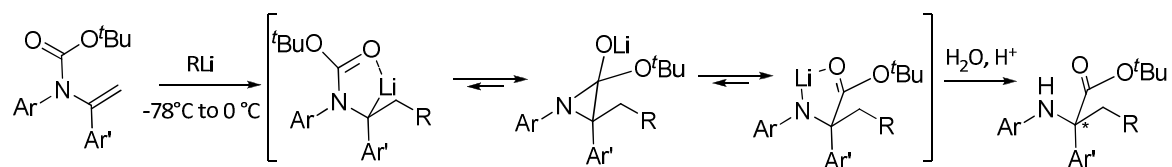
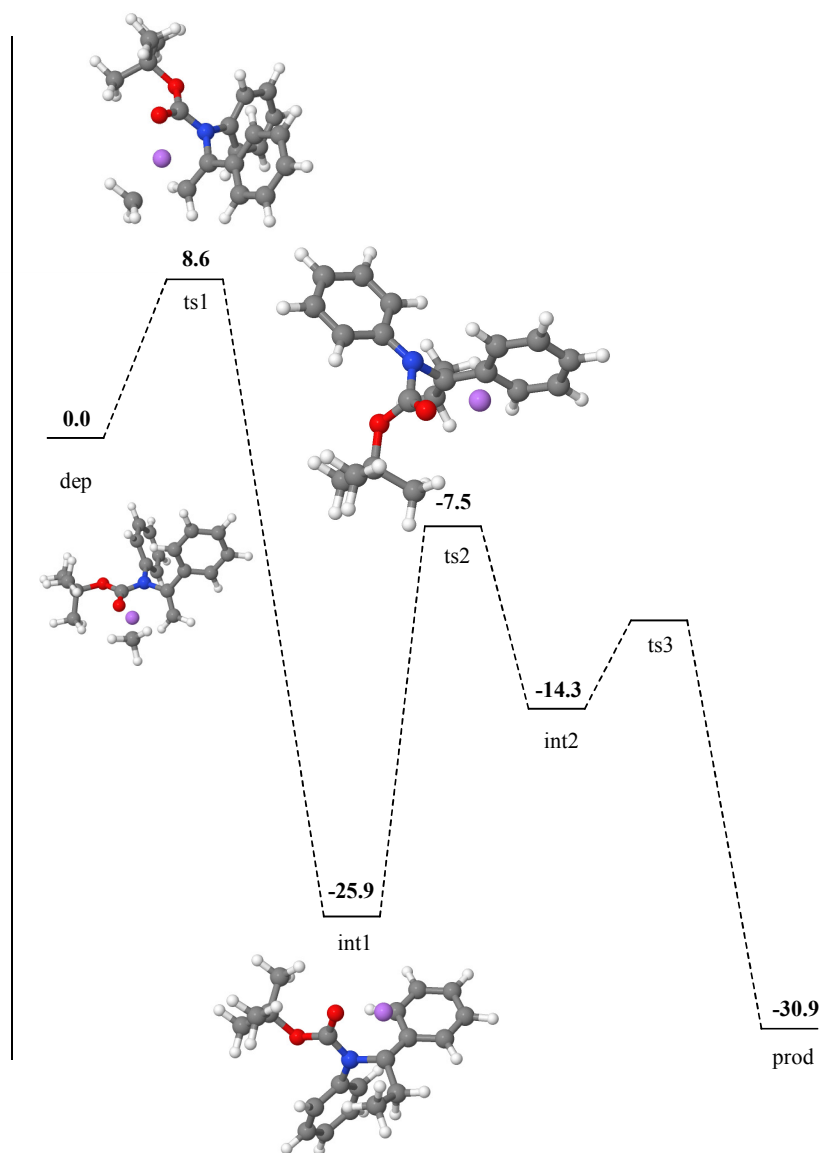


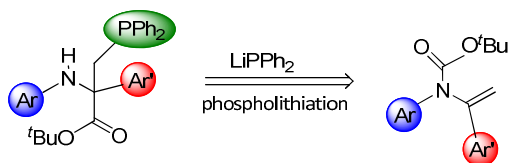
Fig. 39

According to theoretical calculations realized by Arnaud Martel from University of Le Mans, we have well distinguished three transition states during the reaction: (i) the lithium derivative addition, (ii) the formation of aziridine and (iii) opening of aziridine cycle and the same time, the intermolecular migration. As presented on the energetic schema below, the intermediate **int1** is energetically preferable than intermediate **int2**. The addition of lithiated agent is not a limiting step in this reaction. As well, the racemisation step is correlated with the aziridine cycle opening, which is not regioselective.



II.3.2. Objectives

Based on the above mentioned results, we envisage thus to introduce the phosphorus atom *via* phospholithiation reaction into the β position to quaternary carbon in order to enlarge the family of non-natural amino acids. This strategy is expected to offer the potential advantage of directly introducing further molecular diversity as a result of the original choice of the starting primary amine, the phosphorus reagent or the palladium coupling catalyst. The first part of this work will concern the preparation of acyclic enecarbamates from the corresponding vinylphosphates *via* a palladium cross-coupling reaction. The nucleophilic addition of lithiated phosphines onto the latter will be investigated in the second stage (Scheme 28).



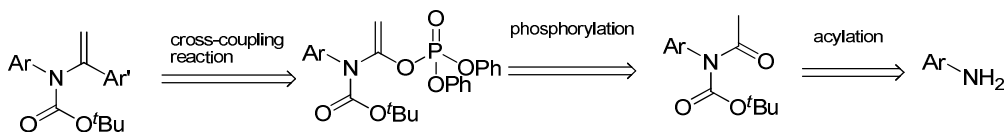
Scheme 28

This methodology will give an access to phosphine-containing amino acid, which can be valorized not only in the domain of biological compounds, but also as a useful building blocks for the synthesis of N,P-heterocycles and hybrid ligands.

II.3.3. Results of the nucleophilic addition

II.3.3.a. Synthesis details

Based on the results from anterior investigations on nucleophilic additions,⁸ we decided to synthesize a family of enecarbamates from commercially available anilines and benzylamines in three step transformation, going through vinylphosphates and palladium-catalyzed cross-coupling reaction.



Scheme 29

The series of enecarbamates with different aryl and heteroaryl substituents would be synthesized *via* this methodology. The vinylphosphates obtained from amides could be isolated with high yields. They are very convenient electrophilic partners for both Suzuki-Miyaura and Stille couplings. The last step - nucleophilic addition of lithiated phosphine would be carried out according to conditions established in our team (Scheme 29).

II.3.3.b. Preparation of acyclic enecarbamates

The first step consisted of the acylation of primary amine in acidic conditions in the presence of acetic anhydride, followed by the protection of the nitrogen atom with a *Boc* group in classical conditions (Fig. 40).

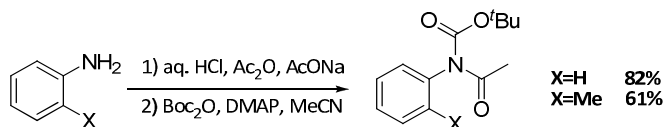


Fig. 40

Equally, the benzylamine was converted into the acetamide by refluxing in acetic anhydride, and after work-up, protected by *Boc* as previously described (Fig. 41).

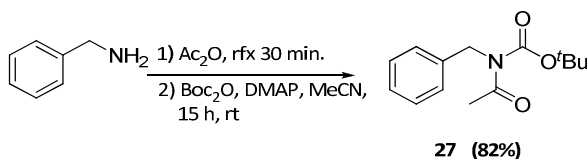


Fig. 41

Obtained acetylated carbamates were treated with LDA at -78 °C in anhydrous THF to give lithium enolates, which were quenched with diphenylchlorophosphate. This transformation gave an access to stable intermediates for numerous palladium-catalyzed cross-coupling reactions with excellent yields (Fig. 42).

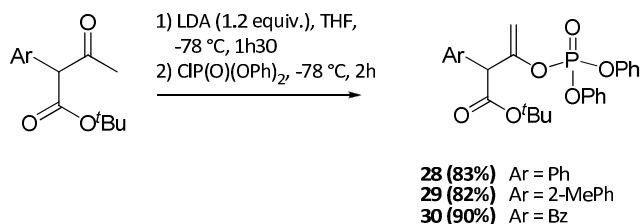
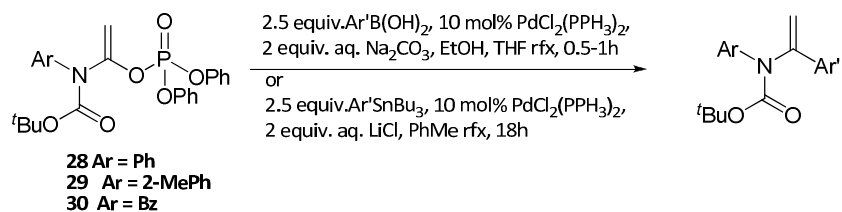


Fig. 42

Vinylphosphates **28-30** were subjected to the cross-coupling reaction as previously demonstrated⁸ to extend the scope of synthesized acyclic enecarbamates. Derivatives with various substituents on a position to the *N*-atom were synthesized, both heteroaryl such as benzothiophenyl, benzofuranyl or pyridinyl and aryl with *ortho*-fluoro group. Standard conditions for Suzuki-Miyaura and Stille cross-coupling reaction have been applied (Table 9).

Table 9 Cross-coupling reactions leading to acyclic enecarbamates



Entry	Substrate	Product	Product / Yield [%]
1			31 / 86
2			32 / 46
3			33 / 88
4			34 / 74
5			35 / 81
6			36 / 90
7			37 / 64
8			38 / 89
9			39 / 94
10			40 / 78
11			41 / 81

Applied reaction conditions were not optimized, however acyclic enecarbamates were obtained in fair to good yields. The best results were observed in the case of phenyl **36** and benzofuranyl moiety **38** (90 and 94% respectively), probably due to the palladium activation in the reactional system. The lowest yield was observed in the fluoro-substituted compounds **32** and **37** because of electron withdrawing character of substituent, as we suppose. Ten synthesized derivatives have been tested in the phospholithiation reaction presented above.

II.3.3.c. Literature examples of nucleophilic addition onto double bond

In the literature, only few examples of the nucleophilic addition of phosphines onto the unactivated double bond have been reported. One of them is the treatment of pyridines bearing unsaturation with diphenylphosphane (Ph_2PH) in the presence of a catalytic amount of potassium *tert*-butoxide in DMSO or *N*-methylpyrrolidinone (NMP). This strategy gave an access to the new family of N,P-ligands for asymmetric Ir-catalyzed reactions (Fig. 43).⁸¹

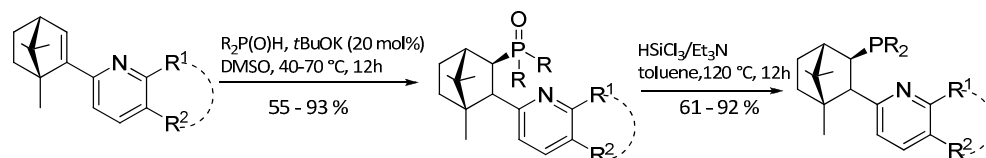


Fig. 43 P,N - ligands for asymmetric Ir-catalyzed reactions

Also, an organocatalytic asymmetric direct *ortho* phosphonylation of α,β -unsaturated aldehydes has been reported.¹²³ The catalytic reaction affords the phosphonates in good yields and high enantioselectivities for a broad range of enals, such as aliphatic, aromatic and heteroaromatic α,β -unsaturated aldehydes (Fig. 44).

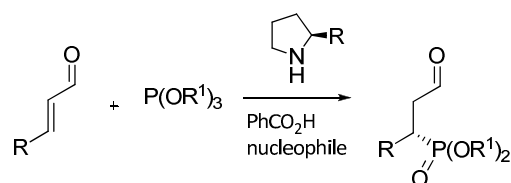


Fig. 44 Organocatalytic asymmetric phosphonylation of α,β -unsaturated aldehydes

Chiral β -phosphinocarboxylic acids can be obtained by addition of lithium diarylphosphides to α,β -unsaturated carboxylic esters.¹²⁴ Trofimov et al.¹²⁵ reported nucleophilic additions of phosphines and phosphine chalcogenides onto alkenes and alkynes in the superbasic system such as KOH/DMSO (Fig. 45).

¹²³ E. Maerten, S. Cabrera, A. Kjærsgaard, K. A. Jørgensen, *J. Org. Chem.*, **2007**, 72, 8893.

¹²⁴ G. Knühl, P. Sennhenn, G. J. Helmchen, *Chem. Comm.*, **1995**, 1845.

¹²⁵ S. N. Arbuzova, N. K. Gusarova, B. A. Trofimov, *Arkivoc*, **2006**, V, 12.

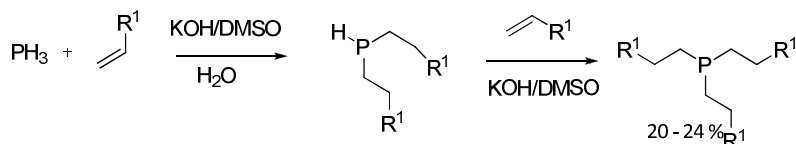


Fig. 45 Nucleophilic addition of phosphines to alkenes

II.3.3.d. Nucleophilic addition reaction

As previously reported, acyclic enecarbamates belong to the group of convenient electrophiles for nucleophilic addition.⁸ In our interest was to introduce the phosphorus atom in β -position to nitrogen and owing to the internal (N->C) alkyloxycarbonyl group migration, to synthesize the phosphine-containing non-natural α -amino acids.¹²⁶ This methodology permits to perform at the same time the addition of phosphine moiety and the reorganization in the starting molecule. Our approach is beneficial from the point of view of atom economy and allows the reduction of steps of reaction. As a model molecule, tert-butyl phenyl(1-phenylvinyl)carbamate **30** was chosen. In order to get nucleophilic phosphorus agent, diphenylphosphine was treated with lithium base such as *n*BuLi at -78°C . This diphenylphosphanide lithium was introduced by cannula to the degassed anhydrous solution of enecarbamate **31** at -78°C and left to react for 15 minutes during warming up to room temperature. The reaction was completed after this time, no starting material was observed in the reaction mixture and desired compound was isolated in 43% yield (Fig. 46). At the same time, some part of product with oxidized phosphine was recovered (confirmed by ^{31}P NMR).

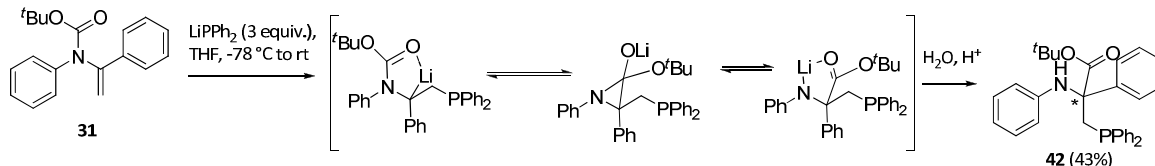


Fig. 46

Three equivalents of lithiated phosphine were used as an optimum to make a complete conversion of starting material in the shortest time.

As presented on the Fig. 46, during the spontaneous *Boc* transfer, the quaternary center is formed, notwithstanding the reaction is not enantioselective and we obtain the racemic mixture. In order to induce the stereoselectivity during the nucleophilic attack onto the double bond, the synthesized phosphinide anion was first complexed with (-)-sparteine. Nonetheless, also in these conditions, racemic mixture was obtained. These may testify that the carbanion formation is not regioselective and that the *Boc* is equally transferred on both sites on this anion.

¹²⁶ A. Bouet, M. Cieslikiewicz, K. Lewinski, G. Coudert, I. Gillaizeau, *Tetrahedron*, **2010**, *66*, 498.

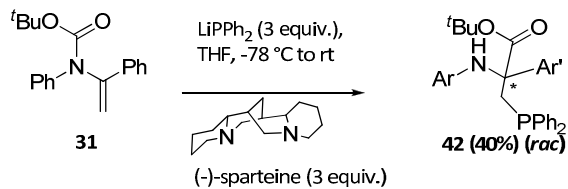
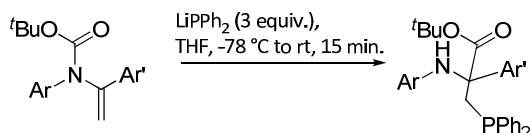


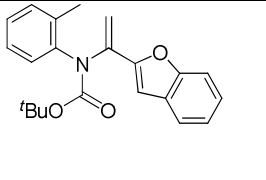
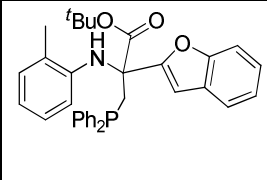
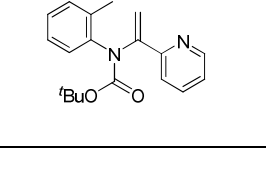
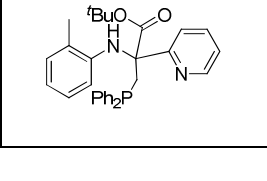
Fig. 47

Following the first results on the nucleophilic addition onto acyclic enecarbamate **30**, the same reaction conditions were applied for the rest of the products (Table 10). This gave a range of phosphine-containing aminoesters in fair to good yields.

Table 10 Phospholithiation reaction



Entry	Substrate	Product	Product/ Yield [%]
1			43 / 41
2			44 / 95
3			45 / 0
4			46 / 47
5			47 / 43
6			48 / 55
7			49 / 54

8			50 / 0
9			51 / 0

The best conversion was observed for the derivatives with benzo[*b*]thiophenyl group **44** (95%) and **49** (54%). However, yields of other transformation were quite moderate (41-55%). The phospholithiation reaction did not give expected product in the case of benzo[*b*]furan derivatives **45** and **50** and pyridinyl **51**, presumably due to the decomposition of starting enecarbamate in basic conditions.

In the case of *tert*-butyl benzyl(1-phenylvinyl)carbamate **40** only one product was observed - here the complete oxidation of phosphine occurred without the *Boc* migration (Fig. 48).

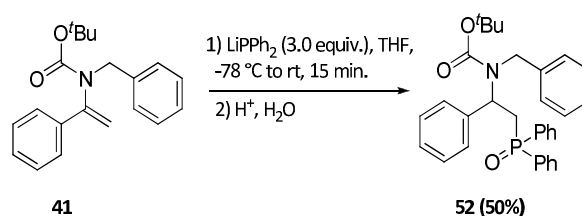


Fig. 48

Obtained results confirm the hypothesis of a possible nucleophilic addition of phosphide agents onto the double bond of enecarbamates and permit to enlarge the family of non-natural amino acids with the β -phosphino counterparts.

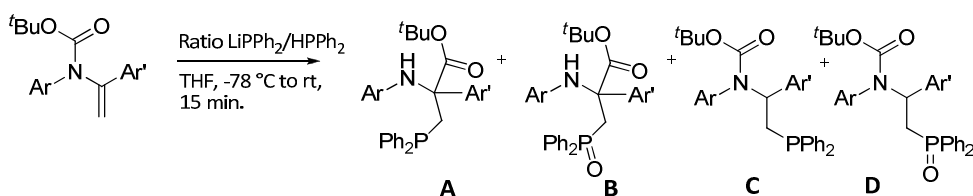
II.3.3.e. Oxidation of phosphine-based derivatives

A spontaneous oxidation of phosphine-based derivatives **43-51** was observed during the hydrolysis process, the purification step by column chromatography or simply while the contact with the air. It is well-known that stability for oxidation of mixed aryl-alkyl phosphines is lower than purely aryl one. However, the reduction of phosphine oxide may be performed in the presence of trichlorosilane/triethylamine in toluene.¹²⁷

This partial oxidation was responsible for lower yield of isolation of phosphine-derivatives. Notwithstanding, the benzyl enecarbamate **40** gave only the oxidized product without the *tBoc* group transfer. These results show that migration of alkyloxycarbonyl group and oxidation of phosphorus atom may be co-notated and may influence one to another. In the purpose of rationalizing these observations, we studied the ratio of free and lithiated phosphine and its effect on the conversion of starting enecarbamate (Table 11).

¹²⁷ Y. Uozumi, T. Hayashi, *J. Am. Chem. Soc.*, **1991**, *113*, 9887.

Table 11



Entry	Ratio $\text{LiPPh}_2/\text{HPPH}_2$	Starting enecarbamate	Ar	Ar'	Product ratio A/B/C/D [%]			
					A	B	C	D
1	3/0	30	Ph	Ph	100	0	0	0
2	1.5/1.5		Ph	Ph	39	0	35 (42a)	26 (42b)
3	1/2		Ph	Ph	30	0	62	8
4	3/0	34	Ph	Py	100	0	0	0
5	2/1		Ph	Py	0	0	0	100 (46a)
6	3/0	40	Bz	Ph	0	0	0	100

We started with *tert*-butyl phenyl(1-phenylvinyl)carbamate **30** limiting the quantity of the base and therefore introducing to the milieu the free phosphine, we observed the apparition of the non-transferred product **41a** almost in the same quantity of non-transferred oxidized one **41b**. By using more equivalents of free phosphine than lithiated phosphanide we increased the quantity of non-transferred product **41a** (Table 11, Entry 3). For pyridinyl derivative **34** the presence of only one equivalent of free phosphine was sufficient to provoke the formation of non-transferred oxidized product **45b**. Benzylic derivative **40** gives oxidized untransferred product even in the absence of free phosphine (Table 11, Entry 6). These results may be explained by the kinetic influence of *in situ* reprotonation which is significantly faster than the intermolecular migration of *Boc* group.

II.3.3.f. Attempts with chiral phosphines

At the end of our investigation, we wanted to introduce the chiral center to the system by the nucleophilic addition of chiral phosphine borane **13a** or phospholane oxide **13c**. The pyridinyl derivative **35**, chosen as a model, was treated with chiral phosphine borane in different conditions (*n*-BuLi, THF, -78°C or *t*BuOK, DMSO, 50°C as reported in the literature^{80,81}) but did not give any results. Only degradation of starting material was observed (Fig. 49).

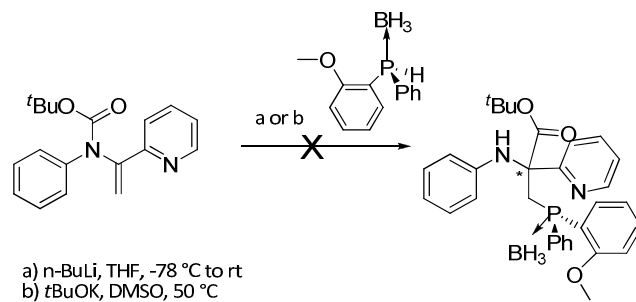


Fig. 49

At the same time, the phospholane oxide **13c** was tested in the nucleophilic addition reaction. However it was impossible to deprotonate this compound. Probably the acidity of hydrogen attached to phosphorus is not high enough to be deprotonated in applied reaction conditions (Fig. 50).

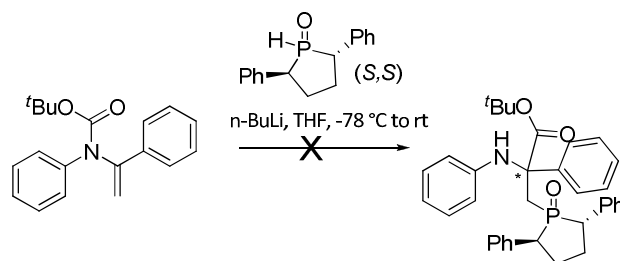
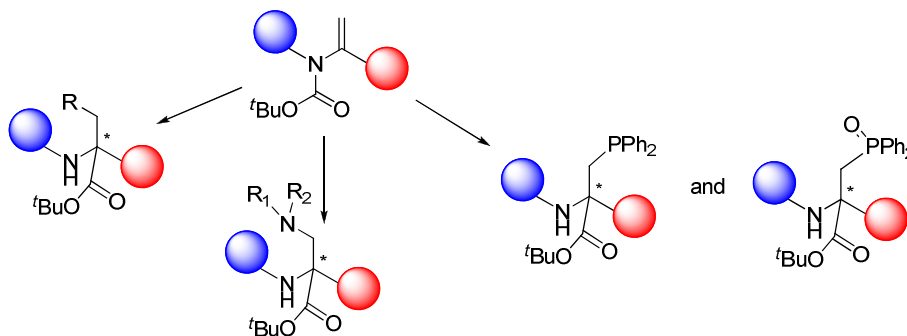


Fig. 50

Unfortunately, both envisaged reaction did not provide chiral phosphines and phospholane oxide. For the moment, the stereospecificity could not be introduced into the synthesized phosphine-derivatives.

II.3.4. Conclusion and perspectives of C-P coupling reaction

This part of thesis dissertation presents the formation of novel products containing C-P bond: β -phosphino α -amino acid derivatives on the way of nucleophilic addition onto the double bond of acyclic enecarbamates with concomitant spontaneous (C \rightarrow N) alkyloxy group migration.



Scheme 30

Phosphine-containing amino acid derivatives extended the family of non-natural amino acids already elaborated in our laboratory (Scheme 30). The reaction of phospholithiation permits to introduce the nucleophile phosphorus agent to the studied scaffold in good to excellent yields. In the course of these investigations, we have envisaged carrying out the phospholithiation in the enantioselective manner; however, the transition state postulated for the mechanism precludes the possibility of enantiocontrol. Moreover, the application of (-)-sparteine as a chiral ligand for lithium complex during the nucleophilic addition did not avoid the racemisation of products.

In perspectives to nucleophilic addition onto the double C=C bond of enecarbamates, we have anticipated to extend this reaction by using other nucleophilic heteroatom species such as silicon derivatives. The preliminary studies were encouraging (Fig.51).

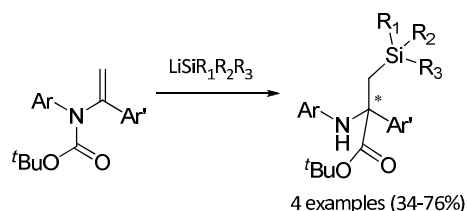


Fig. 51

Also, in order to deal with the enantioselectivity of internal migration during nucleophilic addition, the chirality could be introduced by protection of the amide within an asymmetric protecting group. Recently, the group of Clayden¹²⁸ showed that carbamate directed lithiation can be conducted in an enantioselective way.

¹²⁸ A. Page, J. Clayden, *Beilstein J. Org. Chem.*, **2011**, *7*, 1327.

III. Crystal structure determination

The determination of the structure by the X-ray diffraction comprises four steps:

- crystallization,
- collection and processing of diffraction data,
- solution of the phase problem,
- refinement and analysis of structure.

Each step will be briefly described here.

III.1. Introduction

III.1.1. Crystallization and quality of crystals

This is a crucial step for structure determination because without well diffracting crystals, X-ray diffraction methods cannot be applied. Several methods of crystallization exist, although in this work we will focus only on those that are most popular for small molecules, such as slow evaporation and the vapour diffusion.

The crystallization by slow solvent evaporation is a simple and efficient method for crystallization of small molecules. The crystal growth is controlled by choosing type of solvent, initial concentration, temperature of crystallization and rate of evaporation. If a crystallization solvent is too volatile, rapid evaporation leads to creation of many nuclei and crystals are too small or results in aggregation of the material. The evaporation can be slowed down by sealing the crystallization dish or lowering the temperature however, for some organic compounds this method still does not allow to obtain single crystals of sufficient size.

For molecules having mixed polar and non-polar character, the vapour diffusion method has been adapted. The compound has to be dissolved in the good solvent, placed in the open dish in the larger container next to reservoir containing other solvent poorly dissolving the compound. This container should be tightly closed in order to allow these two solvents to equilibrate. The non-solvent diffuses through vapour phase to the solvent and lowers solubility, which leads to crystallization of the compound.

The diffraction-quality crystal should be a single crystal without any occlusions or crystallization faults. In order to estimate quality of the crystal, we examine it under microscope using polarized light. If the ideal single crystal is not available, the fragment mechanically separated from larger sample might be used.

The size of crystal is also an important parameter, generally it should be large enough to give a high intensity of diffraction pattern, but not larger than the diameter of X-ray beam. It is important to correct the effect of absorption that increases with the size of the crystal. Absorption of X-rays, much like other forms of electromagnetic radiation, depends on the path length (crystal size) and the absorption coefficient. The absorption coefficient μ , depends both on the absorbing species present in

the crystal and the wavelength of X-rays used. The absorption of X-rays by matter in general decreases with decreasing wavelength, meaning that MoK_0 radiation will be less absorbed than CuK_α radiation and reflections intensity will be less affected by absorption. The effect of absorption is corrected either by analytical methods that require indexing the faces of the crystal or by comparing intensities from redundant measurements. Because of its simplicity, the second method is now method of choice for data collected on CCD detectors.

Other than absorption reason for using MoK_0 radiation is higher efficiency of data collection. Use of CuK_α radiation requires much larger angular θ range for collecting high-angle reflections necessary to determine the structure with atomic resolution and that makes data collection very time consuming. For all structures described here diffraction data were collected using MoK_0 radiation.

III.1.2. Data collection and data reduction

In order to get the best quality of diffraction data, during data collection crystal samples are cooled to temperature about 100 K (which equals -173°C) using a dry nitrogen stream. At low temperatures, crystals (especially those of macromolecules) are more stable, they do not lose solvent and are resistant to the effects of X-ray radiation. At the same time, the low temperature reduces dynamic disorder and atomic thermal vibrations, facilitating their subsequent location within the crystal structure.

During data collection the crystal is mounted on the goniometer head, which enables perfect positioning on the intersection of rotation axes and in the X-ray beam (Figure 52). The crystal is fixed to the tip of tiny glass needle with silicon grease or glue. In case of very little or very fragile crystals, they can be mounted on the nylon loop in a drop of mother liquor.

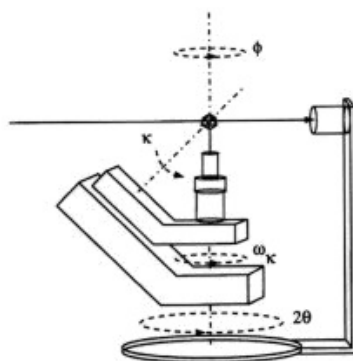
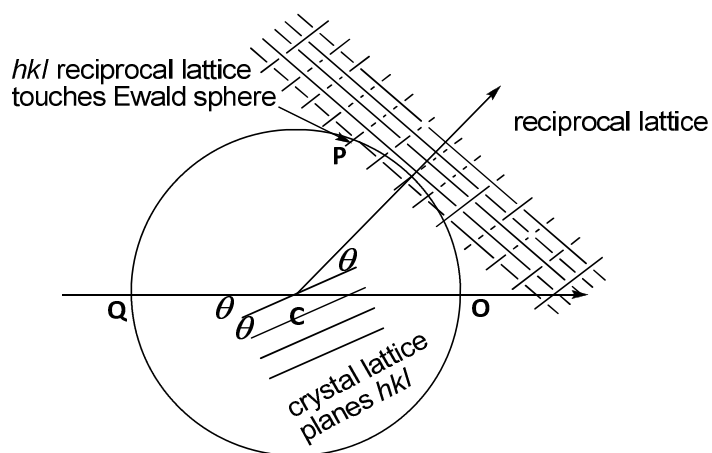


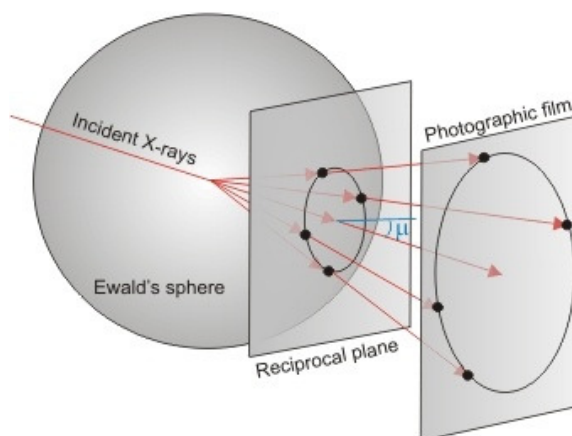
Fig. 52 Positioning of crystal in the X-ray beam

The diffraction pattern resulting from a scattering of X-rays on the crystal can be described in terms of geometrical distribution and intensity of diffraction spots. The description of diffraction conditions and interpretation of diffraction pattern geometry was proposed in 1913 by P. P. Ewald on the base of introduced by him reciprocal lattice and is known as a Ewald construction. Each reciprocal lattice point described by coordinates (h, k, l) corresponds to the set of lattice planes (hkl) . The Ewald sphere with a center **C** is a sphere of radius $1/\lambda$ passing through the origin **O** of the reciprocal lattice.

When the crystal is rotated, the crystal lattice as well as the reciprocal lattice rotates in the same way. The diffraction conditions for a plane (hkl) are satisfied when during the rotation a reciprocal lattice point (h, k, l) goes through the surface of Ewald sphere in point marked as **P** on the Figure 53a. This results in a Bragg reflection in the direction **CP**.



a



b

Fig. 53 Ewald sphere

As can be seen on Figure 53b, the diffraction pattern is a projection of reciprocal lattice points passing through the Ewald sphere when the crystal is rotated. Using reverse projection it is possible from positions of diffraction spots on detector to reproduce the position of reciprocal lattice points in 3-dimensional space and to determine lattice parameters and h, k, l indices corresponding to each diffraction spot.

The intensity $I(hkl)$ of reflection is proportional to the square of amplitude of the structure factor $F(hkl)$. The structure factor $F(hkl)$ can be described as a Fourier transform of electron density distribution $\rho(xyz)$ in the unit cell:

$$F(hkl) = V \iiint \rho(xyz) \exp\{2\pi i(hx + ky + lz)\} dx dy dz$$

Equation 1

In order to solve the crystal structure, the intensity of reflections must be determined with high accuracy. It is done by program that integrates intensity of signal for each pixel on CCD detector in the region where diffraction spot is expected and makes corrections for background level. For reflections that were recorded on several frames, average intensity is calculated. Corrections corresponding to absorption and measurement conditions are also introduced.

III.1.3. Structure determination

The electron density distribution can be calculated from the structure factors using reverse Fourier transform:

$$\rho(xyz) = \frac{1}{V} \sum_h \sum_k \sum_l F(hkl) \exp\{-2\pi i(hx + ky + lz)\}$$

Equation 2

Unfortunately, from diffraction data only amplitude $|F(hkl)|$ of the structure factor can be determined experimentally. The phase angle must be determined in indirect way using some other method. For small organic compounds the most popular and efficient is application of so called “direct methods”.

Direct methods are based on two assumptions:

- The electron-density function calculated from deduced phase angles should never be negative,
- The electron density map should have high values at/near the atomic position and have nearly zero value everywhere else.

First of all, normalized structure factors E need to be calculated from the observed magnitude $|F|$ of structure factors. Only reflections with high values of $|E|$ will be used to assign preliminary phases. The set of three reflections is selected for which indices satisfy the triplet relationship

$$\alpha(h) \approx \langle \alpha(h') + \alpha(h - h') \rangle_{h'}$$

Equation 3

From this relationship, given the two phases in the right-hand side, we can calculate an estimate of third phase. This method requires approximate values of phases for at least some reflections, so called starting set. Several strategies have been adopted for setting starting phases, including random choice. Probabilities for every triplet are calculated using the tangent formula and the most probably phases are used to calculate the E map that is the first approximation of the electron-density map (replacing $|F(hkl)|$ by $|E(hkl)|$). Distances between peaks are analysed for evidence of atomic connectivity and molecular fragments. The coordinates of these peaks represent the position of atoms and are used as an initial trial structure.

III.1.4. Structure refinement and analysis

Positions of atoms based on the Fourier maps are only approximate and therefore they need to be optimised by the refinement process. The method usually applied for structure of small organic compounds is the least squares method. The process is done by minimizing the sum of differences between structure factors calculated from the model and determined experimentally.

$$Q = \sum_{hkl} w(hkl) (|F_{obs}(hkl)| - k |F_{calc}(hkl)|)^2$$

Equation 4

The individual terms of the sum are usually weighted to take into account the precision of the observation. Each structure factor is a function of atomic coordinates and displacement parameters. The function Q has minimum when its derivative is equal zero. Because this function is non-linear, to find out best set of atomic parameters, the structure factors are expanded in a Taylor series, from which only linear terms are used.

$$|F_{calc}(hkl; u)| \approx |F_{calc}(hkl; u_0)| + \sum_i \varepsilon_i \left[\frac{\partial |F_{calc}(hkl; u)|}{\partial u_i} \right]_{u_0}$$

Equation 5

Each structure factor is approximated by equation that linearly depends on small differences ε between current value of parameter u_0 and its correct value u . Least squares method is applied to obtain the change ε of each parameter. As this value is only an approximation of real difference between current and correct value of the parameter, the procedure must be repeated iteratively until parameter changes are very small or zero. For successful refinement there should be at least 5 to 10 observations for each refined parameter. Progress of refinement and correctness of the model are reflected by decreasing differences between observed and calculated structure factors expressed by the R-factor:

$$R = \frac{\sum_{hkl} \left| |F_{obs}| - k |F_{calc}| \right|}{\sum_{hkl} |F_{obs}|}$$

For well determined and refined structure value of R should be close to 0.03 (3%). Higher values are also acceptable for structures containing disorder, partially occupied solvent and other irregularities. Low quality of crystal and errors during data collection also affect R-factor value.

For chiral molecules an important issue is determination of absolute structure. It is possible when the crystal contains atoms for which the anomalous dispersion effect is observed and Friedel's law is no longer satisfied. By comparing intensities of reflections with opposite hkl indices (Bijvoet pairs), it is possible to determine correct enantiomer. Another approach was introduced by H. D. Flack¹. Two structures corresponding to two enantiomers are refined simultaneously with weights x and $1-x$.

$$|I(hkl)| = (1-x)|F(hkl)|^2 + x|F(-h-k-l)|^2$$

Equation 7

The value of x called the Flack parameter indicates correctness of model. If the value is near 0 with a small standard uncertainty, the absolute structure given by the structure refinement is likely correct, and if the value is near 1, then the inverted structure is likely correct. If the value is near 0.5, the crystal may be racemic or twinned. This parameter, became one of a standard parameters confirming correctness of structures with non-centrosymmetric space group symmetry. Unfortunately, for MoK_α radiation the anomalous dispersion from light atoms is very weak and this method do not give reliable results.

III.2. Crystal structure of products after direct C-P coupling

Two products, **16** and **25**, were crystallized in order to determine their structure. First product, *tert*-butyl 7-((methoxyphenyl)(phenyl)phosphino)-2,3,4,5-tetrahydro-1*H*-azepine-1-carboxylate borane complex **16**, was dissolved in organic solvents having different polarities and crystallized by slow evaporation and phase diffusion. Crystallization conditions are presented in the Table 12.

Table 12

Entry	Solvents, temp.	Time of crystallization	Observations
1	DMSO:EtOAc (2:1), rt	two weeks	orange prismatic crystals
2	MeOH, 4 °C	one month	orange plate crystals
3	Acetone, 4 °C	one month	orange prisms, aggregated

The best crystals were obtained at room temperature from crystallization in DMSO and EtOAc in 2:1 ratio. Prismatic crystals were observed after two weeks, for X-ray experiment the crystal of size $0.20 \times 0.17 \times 0.05 \text{ mm}^3$ was selected (Fig. 54).

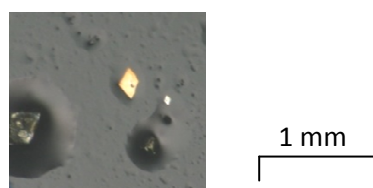


Fig. 54 The crystal form of product 16

The diffraction data for compound **16** were collected on Nonius KappaCCD diffractometer at 100 K using a graphite monochromatized MoK_α (45 kV, 20 mA) radiation, $\lambda = 0.7107 \text{ \AA}$. For cell

refinement and data reduction, the Denzo/Scalepack program package¹²⁹ was used. The multiscan absorption correction was applied to the data. The structure was solved by direct methods using SIR92¹³⁰ and refined by full-matrix least-squares on F^2 using the program SHELXL-97.¹³¹ Anisotropic displacement parameters were applied for non-hydrogen atoms. The hydrogen atoms were refined with isotropic displacement parameters set at 1.5 times that of bonded atoms for methyl or BH_3 groups and 1.2 times for ring atoms. Because high-angle reflections were on the level of noise, only reflections from Θ range up to 22.5° were used in the refinement. Hydrogen atoms bonded to the carbon skeleton were added on calculated positions, however H-atoms in the boron group were located on the electron density map and refined with restrained distances and angles. The crystal data and refinement parameters are presented in Table 14.

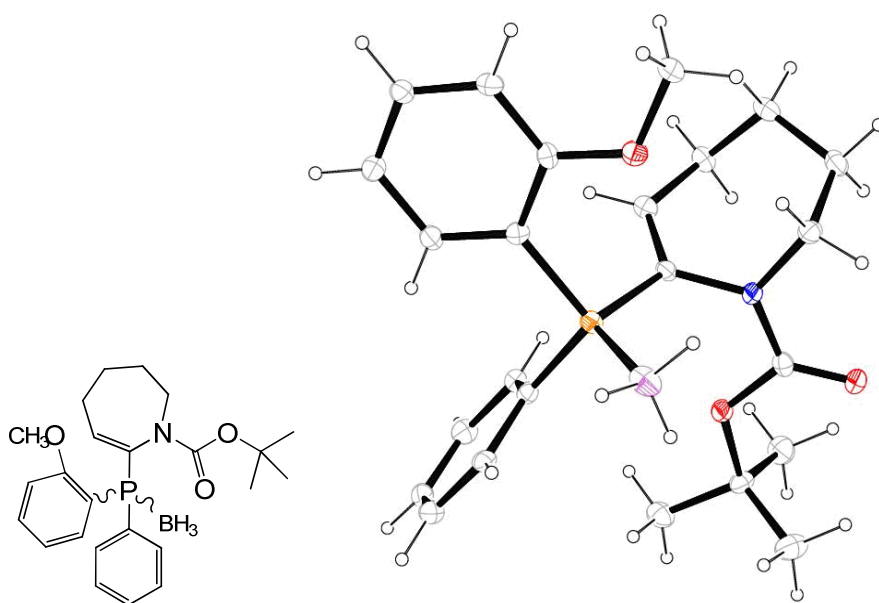


Fig. 55 Chemical structure and ORTEP presentation of compound **15** with displacement ellipsoids at 20% probability level

The crystal structure of desired product **16** and the arrangement of phenyl groups around P-atom is presented on Fig. 54. The presence of BH_3 group attached to the phosphorus atoms that has been confirmed by the structure, could not be determined reliably using spectroscopy. The crystals of compound **16** were centrosymmetric and contained racemic mixture of two enantiomers.

The product from the family of phospholane oxides – 7-((2*S*,5*S*)-1-oxo-2,5-diphenyl- λ_5 -phosphan-1-yl)-2,3,4,5-tetrahydro-azepine-1-carboxylic acid methyl ester **25** gave single crystal under crystallization conditions presented in the Table 13.

¹²⁹ (a) Z. Otwinowski, W. Minor, *Macromolecular Crystallography*, Part A; (b) C. W. Jr. Carter, R. M. Sweet, Eds.; Academic Press: New York, **1997**; *Methods in Enzymology*, Vol. 276, 307.

¹³⁰ A. Altomare, G. Cascarno, G. Giacovazzo, A. Guagliardi, M. C. Burla, G. Polidori, M. Camalli, *J. Appl. Cryst.*, **1994**, 27, 435.

¹³¹ G. M. Sheldrick, *Acta Crystallogr.*, **2008**, A64, 112.

Table 13

Entry	Solvents, temp.	Time of crystallization	Observations
1	DMSO:EtOAc (2:1), rt	one month	brown film
2	Chloroform, rt	one week	brown plates
3	Acetone, 4 °C	one month	brown needles
4	Toluene: acetone, 4 °C	one week	brown film and needles

The best single crystals of product **25**, light-brown plates, were obtained from saturated solution in chloroform at room temperature after 7 days of slow evaporation (Fig.56).



Fig. 56 The picture of crystal forms of product **24**, the single crystal chosen for experiment is marked with an arrow

A single crystal ($0.50 \times 0.30 \times 0.25 \text{ mm}^3$) was selected and attached to a tip of glass fiber with cyanopropene glue. The diffraction experiment was carried out at room temperature. The data were collected and processed as described above for compound **16**. The symmetry of space group $P2_12_12_1$ was determined on the base of systematic absences. The structure was solved by direct methods using SIR92.¹³⁰ The initial solution revealed positions of the P atom and the most of non-hydrogen atoms. The remaining atomic positions were determined from subsequent difference Fourier maps. and the refinement was performed as described above using reflections from the Θ range up to 27.5° . Details of crystal structure and refinement parameters are presented in Table 14.

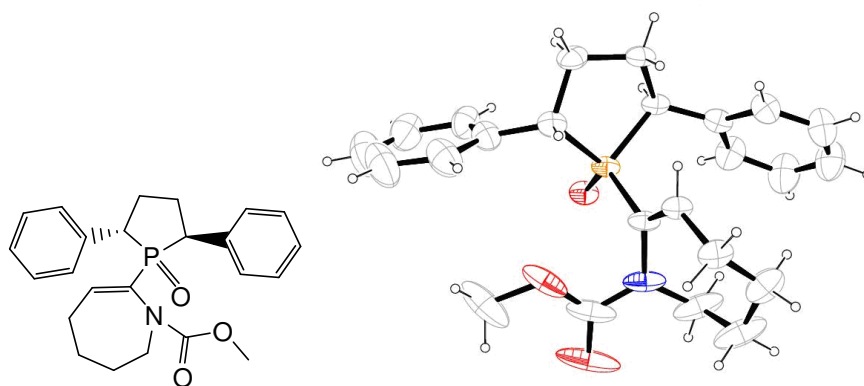


Fig. 57 The structure and an ORTEP presentation of compound **25** in RT with displacement ellipsoids at 20% probability level.

The crystal structure analysis gave an evidence for the absolute structure of product **25**. On the Fig. 57, carbon atoms attached to the phosphorus in the phospholane cycle are in the *S* configuration (as in starting phosphine **13c**), what means that during the applied cross-coupling reaction the stereoselectivity is retained. The value of Flack parameter equal 0.07 confirms that the absolute structure given by the structure refinement is likely correct.

Table 14 Crystallographical parameters

Product	16	25
Empirical formula	C ₂₄ H ₃₃ B N O ₃ P	C ₂₄ H ₂₈ N O ₃ P
Formula weight	425.29	409.44
Temperature	113(2) K	293(2) K
Wavelength	0.71070 Å	0.71070 Å
Crystal system	Monoclinic	Orthorhombic
Space group	P 2 ₁ /n	P2 ₁ 2 ₁ 2 ₁
Unit cell dimensions	a = 10.093(1) Å α = 90° b = 14.074(2) Å β = 92.048(9)° c = 16.437(3) Å γ = 90°	a = 9.501(5) Å α = 90° b = 12.105(5) Å β = 90° c = 19.615(5) Å γ = 90°
Volume	2333.4(6) Å ³	2256(2) Å ³
Z	4	4
Absorption coefficient	0.142 mm ⁻¹	0.145 mm ⁻¹
F(000)	912	872
Crystal size	0.20 x 0.17 x 0.05 mm ³	0.50 x 0.30 x 0.25 mm ³
Reflections collected	14659	19074
Independent reflections	2064 [R(int) = 0.0608]	5173 [R(int) = 0.0476]
Data / restraints / parameters	2064 / 6 / 273	3971 / 0 / 264
Goodness-of-fit on F ² (S)	1.144	1.027
Final R indices [I > 2σ(I)]	R1 = 0.0620, wR2 = 0.1252	R1 = 0.0437, wR2 = 0.1090
R indices (all data)	R1 = 0.0933, wR2 = 0.1447	R1 = 0.0668, wR2 = 0.1213
Flack parameter	-	0.07(13)

III.3. Crystal structure of compounds from the family of P-containing non-natural amino acids

The synthesized products, analogues of β -phosphino non-natural amino acids, were racemic mixtures and in this form they were crystallized. Compounds were dissolved in acetonitrile and crystallized by slow evaporation of solvent from saturated solutions at temperature 4 °C. The crystallization gave only aggregated crystals, from which parts of single crystals were mechanically separated and used for X-ray experiments. The diffraction data for **47** were collected on Nonius KappaCCD diffractometer using the same procedures as described above. For compound **52** data were collected on Oxford Diffraction SuperNova diffractometer using CuK α radiation ($\lambda = 1.5418 \text{ \AA}$) while for **46** the diffractometer was Oxford Diffraction Xcalibur with Mo X-ray source. The structures were solved by direct methods using *SIR-92* software and refined by full-matrix least squares on F^2 using the program *SHELXL-97*.

The first crystallized compound in the family of phosphine non-natural amino acids analogues was *tert*-butyl 3-(diphenylphosphino)-2-phenyl-2-(*o*-tolylamino)propanoate **47**. A single crystal selected for the diffraction experiment was colorless plate with dimensions 0.5x0.25x0.25 mm³. The systematic absences indicated symmetry of space group $P2_1/c$ which was confirmed by subsequent solution and refinement of the structure. The initial solution revealed positions of only P atoms and C atoms from the phenyl rings, the remaining atomic positions were determined from difference Fourier maps. The final refinement included anisotropic temperature factors of all non-hydrogen atoms. The H-atoms were refined using the riding model with isotropic displacement parameters set at 1.5 times that of a bonded atoms for methyl groups and 1.2 times for ring atoms. The crystal structure confirmed the presence of trivalent phosphorus atom and showed the arrangement of phenyl rings around the quaternary carbon. This structure was deposited in the Cambridge Crystallographic Data Center with the entry 748012.

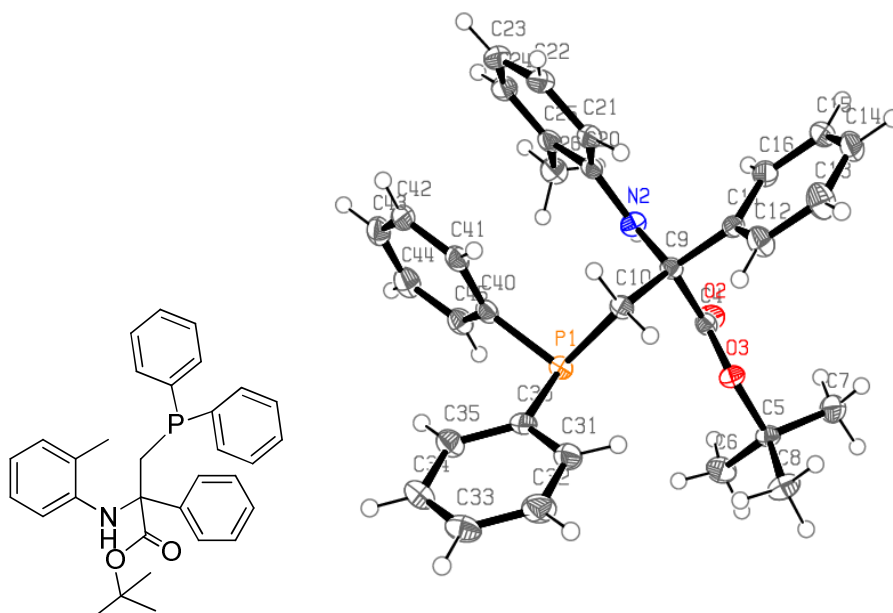


Fig. 58 The structure and ORTEP representation of compound 46 (ellipsoids drawn at 50% probability level)

The single crystals of product **52** were very thin needles, nevertheless it was possible to obtain diffraction pattern at 100 K using SuperNova diffractometer and CuK α radiation. The data collection and processing were performed in Oxford Diffraction headquarter with kind help of dr. Zoltan Gal from Oxford Diffraction Ltd, Yarnton, UK. This compound crystallizes in P2 $_1$ space group, and contains two molecules in the asymmetric part of the unit cell. Its crystal structure enables unambiguously to confirm the oxidation of phosphorus atom. This structure was deposited in the CCDC with the accession number 748216.

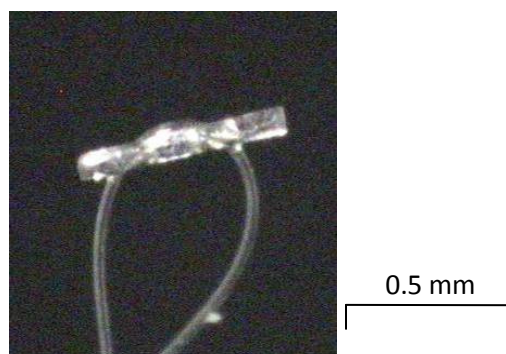


Fig. 59 Crystal of product 51 on the nylon loop

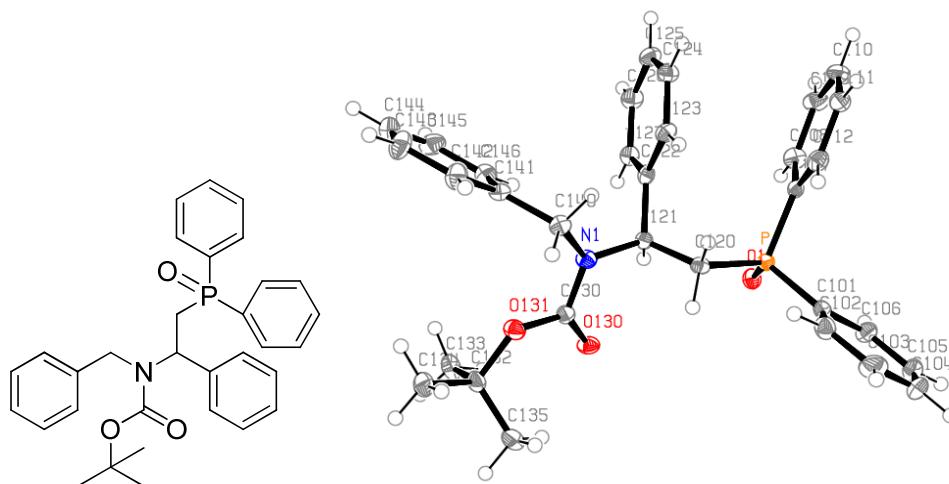


Fig. 60 The structure and ORTEP representation of compound 51 (ellipsoids drawn at 50 % probability level)

The last presented structure is a pyridine-derivative **46**. The piece of single crystal used for the diffraction experiment was obtained by slow diffusion between two solvents: acetonitrile and methanol at 4 °C. It was very small and of low quality (Fig. 61) but after the data collection at 100 K and data processing with omitting high-angle reflections, it was possible to solve the structure in monoclinic crystal system. The data collection and processing were performed in Oxford Diffraction headquarter with kind help of dr. Zoltan Gal from Oxford Diffraction Ltd, Yarnton, UK. After refinement process the reliable structure was obtained that has confirmed the chemical structure of expected product.

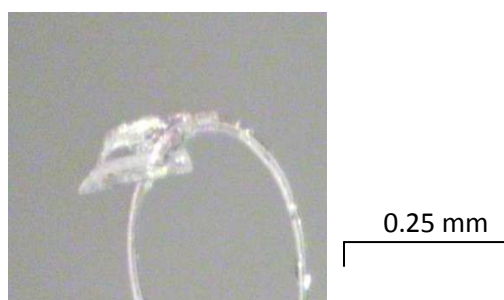


Fig. 61 Crystal of product 45 on the nylon loop

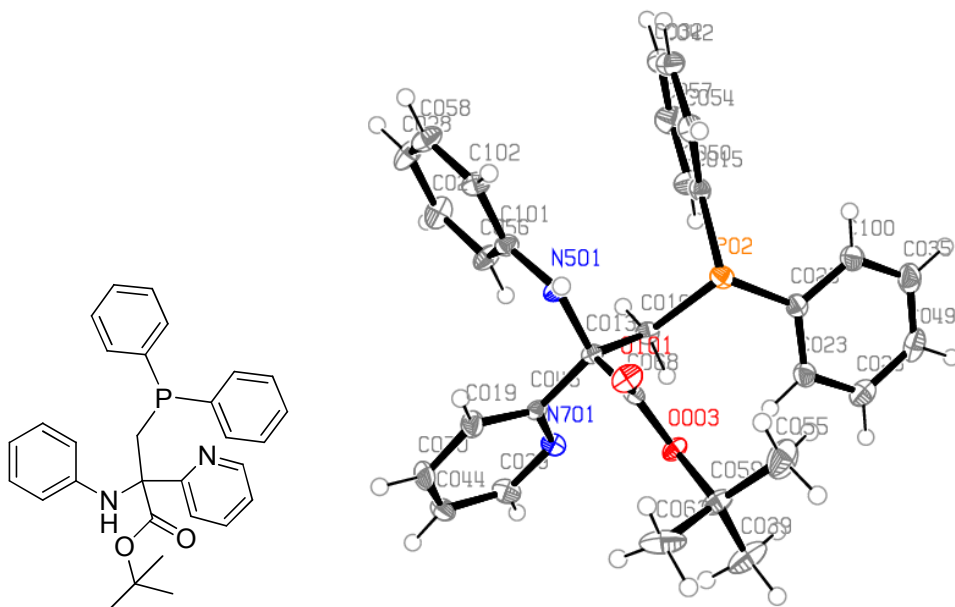


Fig. 62 The structure and ORTEP diagram of compound 45 (ellipsoids at 50 % probability level)

Table 15

Compound	47	52	46
Empirical formula	C ₃₂ H ₃₄ N O ₂ P	C ₃₂ H ₃₄ N O ₃ P	C ₃₀ H ₃₁ N ₂ O ₂ P
Formula weight	495.57	511.61	482.54
Temperature	100(2) K	100(2) K	100(2) K
Wavelength	0.7107 Å	1.5418 Å	0.7107 Å
Diffractometer	Nonius KappaCCD	Oxford Diffraction SuperNova	Oxford Diffraction Xcalibur
Crystal system	monoclinic	monoclinic	monoclinic
Space group	P 2 ₁ /c	P 2 ₁	P 2 ₁ /n
Unit cell dimensions	a = 19.798(2) Å b = 11.805(2) Å c = 11.620(4) Å α = 90° β = 94.025(10)° γ = 90°	a = 5.8788(5) Å b = 36.672(2) Å c = 12.357(8) Å α = 90° β = 90.42(1)° γ = 90°	a = 22.176(1) Å b = 11.575(4) Å c = 22.4137(1) Å α = 90° β = 115.608(6)° γ = 90°
Volume	2709.07(11) Å ³	2663.9(3) Å ³	5188.0(4) Å ³
Z	4	4	8
Density (calc.)	1.215 Mg/m ³	1.275 Mg/m ³	1.236 Mg/m ³
Absorption coefficient	0.130 mm ⁻¹	1.181 mm ⁻¹	0.135 mm ⁻¹
Crystal size	0.5 x 0.25 x 0.25 mm ³	0.47 x 0.23 x 0.04 mm ³	0.25 x 0.17 x 0.05 mm ³
Reflections collected / unique / obs [I > 2σ(I)]	11487 / 6191 / 4846	6743 / 5724 / 5518	16981 / 11106 / 5844
R [I > 2σ(I)]	R1 = 0.0404, wR2 = 0.1012	R1 = 0.0477, wR2 = 0.1310	R1 = 0.0415, wR2 = 0.0565
R (all data)	R1 = 0.0585, wR2 = 0.1179	R1 = 0.0492, wR2 = 0.1294	R1 = 0.0979, wR2 = 0.0632
Flack parameter		0.09(3)	
Goodness-of-fit on F ²	1.079	1.045	0.758
Largest diff. peak and hole	0.284 and -0.342 e. Å ⁻³	0.732 and -0.443 e. Å ⁻³	0.257 and -0.274 e. Å ⁻³

Chapter 2

I. Bibliography

I.1. Lanthanides - introduction

Lanthanides or lanthanoids (according to IUPAC nomenclature) are metallic elements of the *f* block of periodic table, comprising 15 species from lanthanum La (atomic number 57) through lutetium Lu (71). Etymology of their name comes from Greek and it means "lying hidden" (*lanthanein*), therefore their common name is "the rare-earth elements". In fact, the less abundant lanthanide - thulium occurs in the amount greater than arsenic or mercury and neodymium is more abundant than gold. However, the rarity of lanthanides is understood not in the term of scarcity, but with regard to difficulty in isolating certain elements in their pure form. The similarity of ionic radius between adjacent lanthanide metals makes it difficult to separate them from each other in naturally occurring ores or other mixtures.

The luminescent properties of several lanthanides have been investigated and put into practice in lighting and light conversion technologies such as lasers (Nd:YAG laser), cathode-ray and plasma displays or light-emitting diodes (cerium or europium doped LED). Recently, it appeared that particular luminescent properties of lanthanide ions could be exploited in applications ranging from biomedical to sensing areas and luminescence imaging. This opens a great possibility for the coordination chemistry of these ions.¹³² Stable trivalent lanthanide complexes are of considerable interest owing to their magnetic¹³³ and luminescent features.¹³⁴ Gd³⁺ complexes are paramagnetic at room temperature and they serve as contrast agents in magnetic resonance imaging (MRI). Also, a novel class of contrast based on the transfer of magnetization properties to the bulk water signal provides high sensitive Ln³⁺ based probes for MRI. This phenomenon called Chemical Exchange Saturation Transfer (CEST) permits to use the different contrast agents in the same MR-image to distinguish them by activation with characteristic irradiation frequency.¹³⁵

¹³² (a) S. V. Eliseeva, J.-C. G. Bünzli, *Chem. Soc. Rev.*, **2010**, 39, 189; (b) J.-C. G. Bünzli, S.V. Eliseeva, *J. Rare Earths*, **2010**, 28, 824; (c) J.-C. G Bünzli, *Chem. Rev.* **2010**, 110, 2729; (d) C. P. Montgomery, B. S. Murray, E. J. New, R. Pal, D. Parker, *Acc. Chem. Res.* **2009**, 42, 925; (e) K. Binnemans, *Chem. Rev.* **2009**, 109, 4283; (f) E. G. Moore, A. P. S. Samuel, K. N. Raymond, *Acc. Chem. Res.* **2009**, 42, 542; (g) C. M. G. Dos Santos, A.J. Harte, S.J. Quinn, T. Gunnlaugsson, *Coord. Chem. Rev.* **2008**, 252, 2512; (h) J.-C. G. Bünzli, C. Piguat, *Chem. Soc. Rev.*, **2005**, 34, 1048.

¹³³ (a) D. Parker, *Chem. Soc. Rev.*, **2004**, 33, 156; (b) D. Parker, R. S. Dickins, H. Puschmann, C. Crossland, J. A. K. Howard, *Chem. Res.*, **2002**, 102, 1977; (c) J.-C. G. Bünzli, *Acc. Chem. Res.*, **2006**, 39, 53.

¹³⁴ C. M. G. dos Santos, P. B. Fernandez, S. E. Plush, J. P. Leonard, T. Gunnlaugsson, *Chem. Commun.*, **2007**, 3389.

¹³⁵ S. Aime, S. G. Crich, E. Gianolio, G. B. Giovenzana, L. Tei, E. Terreno, *Coord. Chem. Rev.*, **2006**, 250, 1562.

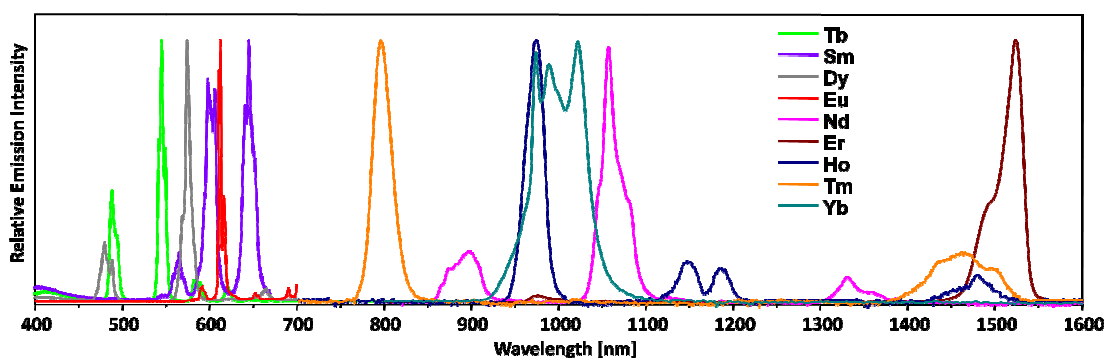


Fig. 63 Emission spectra of lanthanides complexed with tropolonate ligand¹³⁶

The luminescent properties of lanthanides give a range of applications from biomedical, through sensing area to optical imaging of cells and tissues *in vivo*. Remarkably, the most studied are complexes of europium and terbium exhibiting quite intense visible narrow emission bands (Fig. 63). Notwithstanding, the photophysical properties of near infrared (NIR) lanthanide emitters such as Sm³⁺, Dy³⁺, Pr³⁺, Ho³⁺, Yb³⁺, Nd³⁺ and Er³⁺ have become more and more investigated during the last ten years. Lanthanide cations emitting in near infrared are more efficient for the use in the human tissue than probes in visible range because they are much less absorbed in the tissue. The ratio signal to noise is much more important than for visible photons. Moreover, NIR photons diffract less than visible one in biological tissues¹³⁷ and they can pass through the tissue up to centimeters without harming it (less absorption and less diffusion). Similarly, NIR luminescence from ions such as Nd³⁺, Yb³⁺ or Er³⁺ provides a useful application as optical signal amplifier in telecommunication network.¹³⁸

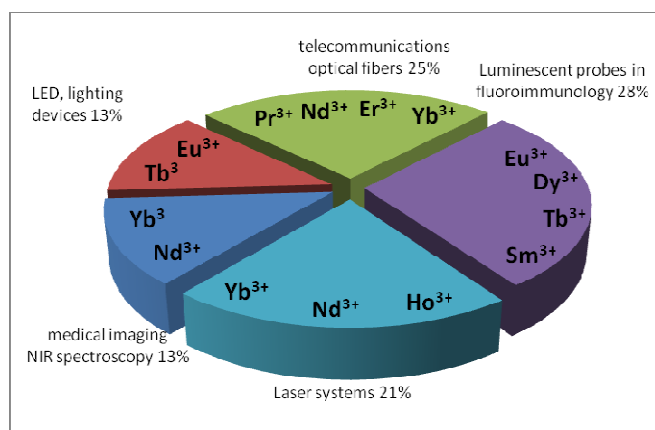


Fig. 64 Type of emission and related applications of lanthanides¹³⁹

¹³⁶ J. Zhang, P. D Badger, S. J. Geib, S. Petoud, *Angew. Chem. Int. Ed.*, **2005**, *44*, 2508.

¹³⁷ G. A. Wagnieres, W. M. Star, B. C. Wilson, *PhotochemPhotobiol.*, **1998**, *68*, 603.

¹³⁸ (a) Y. Oshishi, T. Kanamori, T. Kitagawa, S. Takashashi, E. Snitzer, G. H. Sigel, *Opt. Lett.*, **1991**, *16*, 1747; L. H. Slooff, A. Polman, M. P. O. Wolbers, F. van Veggel, D. N. Reinhoudt, J. W. Hofstraat, *J. Appl. Phys.*, **1998**, *83*, 497.

¹³⁹ L. Armelao, S. Quici, F. Barigelletti, G. Accorsi, G. Bottar, M. Cavazzini, E. Tondello, *Coord. Chem. Rev.*, **2010**, *254*, 487.

I.2. Lanthanide complexes

The coordination numbers of Ln^{3+} are in the range 3 - 12 depending on the steric requirement of the ligand and the size of the lanthanide cation, although the number 8 and 9 are the most frequent. Aqua ions of crystalline compounds are generally 9-coordinated with the tricapped trigonal prism as favored structure.

The choice of ligand for lanthanide complexation is very important. Aqueous solutions of non-complexed lanthanides are toxic for living organisms (because of accumulation in the lung tissue and bones)¹⁴⁰, therefore for the *in vivo* application, it is necessary to create complexes with high kinetic stability to avoid cation's liberation in aqueous media. The trivalent lanthanide ions are hard acceptors (according to the HSAB theory) and they form more stable complexes with *O*- and *N*-donor ligands. The most efficient coordination site for lanthanides needs to be formed by a number of donor atoms or groups arranged in a covalently organized structure. In relation to the dimensionality, they may be:

- ✓ monodimensional, like acyclic linear ligands (podands) or branched ones (polypodands),
- ✓ bidimensional macrocyclic ligands (coronands),
- ✓ tridimensional macrobicyclic and macropolycyclic ligands (cryptands).

A very important group of acyclic ligands is based on the polyaminopolycarboxylate system with four or more acetic groups covalently attached to a polyamino skeleton such as ethylenediaminetetraacetic acid EDTA or diethylenetriaminepentaacetic acid DTPA. This kind of lanthanide chelates found an application in Magnetic Resonance Imaging (MRI) commercialized as MagnevistTM or OmniscanTM (Fig. 64)¹⁴¹ and biological assays by means of Dissociation-Enhanced Lanthanide Fluorescence ImmunoAssay (DELFI A).¹⁴²

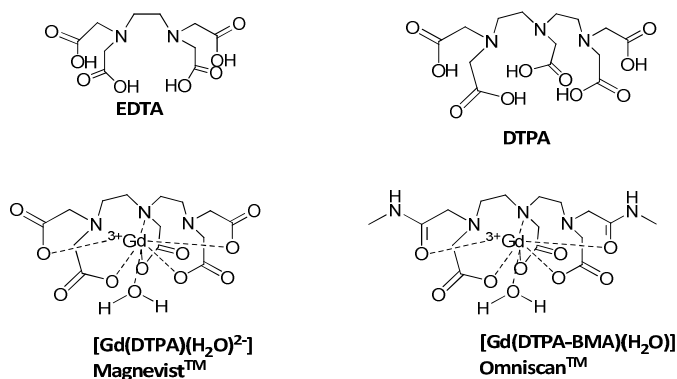


Fig. 65 Examples of Gd^{3+} chelates currently used as MRI agents

Cryptands are excellent candidates for the coordination of spherical lanthanide cations as long as they show complementarity of the dimension of the coordinating cavity with the size of metal cation (the "lock and key" criterion). Notwithstanding the control of the ligand topology based on this principle may fail in controlling the stability and selectivity of complexation with Ln^{3+} . Therefore,

¹⁴⁰ S. Hirano, K. T. Suzuki, *Environ. Health. Perspect.*, **1996**, *104*, 85.

¹⁴¹ K. W.-Y. Chan, W. T. Wong, *Coord. Chem. Rev.*, **2007**, *251*, 2428.

¹⁴² P.G. Sammes, G. Yahioglu, *Nat. Prod. Rep.*, **1996**, *13*, 1.

ligands showing intermediate character between highly organized "lock and key" based macropolycycles and the preorganized "induced fit" systems are very useful for lanthanide complexation. These ligands contain polyaza-macrocyclic core with pending anionic binding sites covalently linked to the secondary amine nitrogen atom of the ring. The stability of these complexes may be controlled by adjusting the ring size and the number and nature of binding arms to surround the lanthanide cation. Among all known lanthanide ligands, 1,4,7,10-tetraazacyclododecane-1,4,7,10-tetraacetic acid (DOTA) shows the highest stability constant ($\log K_{ML}$ in the range of 22-29). Four nitrogens of the cyclen ring bind cooperatively to the face of the square antiprism; they possess the same quadrangular conformation either in the free or complexed state.¹⁴³ Other aza-macrocycles such as 1,4,7-triazacyclononane or 1,4,8,11-tetraazacyclotetradecane (cyclam) having acetic pending groups are also applied in the lanthanide chelation, even if their thermodynamic and kinetic stability constants are lower than for cyclen (Fig. 66).

These complexes are used as contrast agents or luminescent labels for biological assays, depending on the lanthanide cation. Gadolinium DOTA complexes are efficient contrast agents for MRI.¹⁴⁴

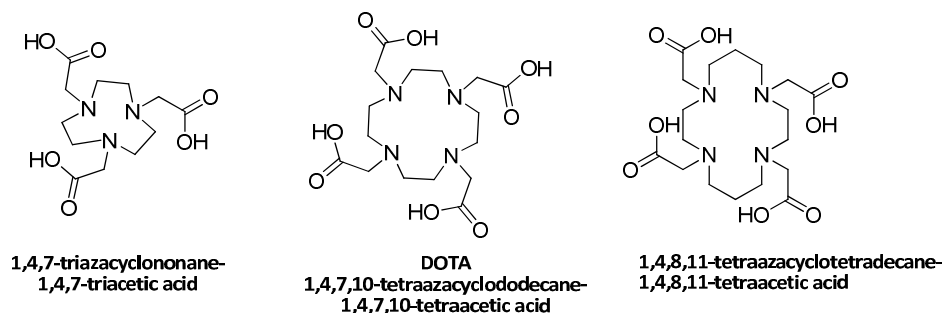


Fig. 66 Examples of polyaza-macrocyclic ligands

I.3. Jablonski Diagram and antenna effect

The luminescence activity of molecules can be described schematically by the energy diagram, presented for the first time at 1935 by Polish physicist Aleksander Jablonski, and after that called the Jablonski's diagram. This diagram illustrated the electronic states of the molecule and the transition between them (Scheme 31).

The absorption of energy by the chromophore system leads to the excitation on the higher vibrational level S_1 or S_2 . In a typical system, irradiation with a wide range of wavelengths (the UV or visible part) will generate an entire range of possible transitions and therefore, will populate the various vibrational energy levels of the excited state. The intensity of absorption represents the degree of probability of certain transitions and combined lines of these transitions construct the absorption spectrum of the molecule. Immediately after absorption of a photon, several processes can occur with different probabilities, but the most likely will be the relaxation to the lowest vibrational energy level of the first

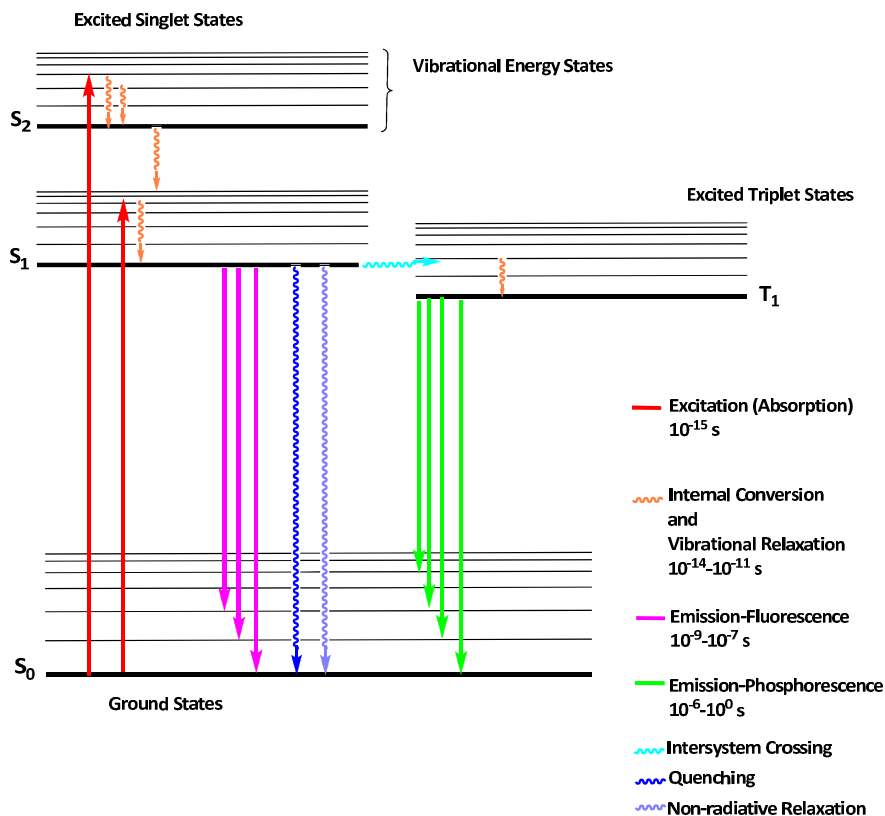
¹⁴³ S. Aime, A. S. Batsanov, M. Botta, J. A. K. Howard, D. Parker, K. Senanayake, G. Williams, *Inorg. Chem.*, **1994**, *33*, 4696.

¹⁴⁴ (a) D. Meyer, M. Sheaffer, B. Bonnemain, *Invest. Radiol.*, **1988**, *23*, S232; (b) K. Nwe, M. Bernardo, C. A. Regino, M. Williams, M. W. Brechbiel, *Bioorg. Med. Chem.*, **2010**, *18*, 5925.

excited state S_1 . This process is known as internal conversion or vibrational relaxation (loss of energy in the absence of light emission) and generally occurs in a picosecond's range or less. Due to fact that a significant number of vibration cycles may occur during the lifetime of excited state, all molecules virtually always undergo the complete vibrational relaxation during their excited states. An energy liberated over vibrational relaxation is converted into heat, which is absorbed by neighboring solvent molecules upon collisions with the excited state molecule.

The lifetime of excited electronic state S_1 is around a few nanoseconds. An excited molecule exists in the lowest excited singlet state S_1 for this time before finally it comes back to the ground state. If relaxation from this excited state is accompanied by emission of a photon, the process is formally known as fluorescence. The closely spaced vibrational energy levels of the ground state, when coupled with normal thermal motion, produce a wide range of photon energies during emission. As a result, fluorescence is normally observed as emission intensity over a band of wavelengths rather than a sharp line. Most fluorophores can repeat the excitation and emission cycle many hundreds to thousands of times before the highly reactive excited state molecule is photobleached, resulting in the destruction of fluorescence.

However, several other relaxation pathways that have varying degrees of probability compete with the fluorescence emission process. The excited state energy can be dissipated non-radiatively as heat, the excited fluorophore can collide with another molecule to transfer energy in a second type of non-radiative process, or a phenomenon known as intersystem crossing to the lowest excited triplet state can occur. The latter event is relatively rare, but ultimately results either in emission of a photon through phosphorescence or a transition back to the excited singlet ($T \rightarrow S_1$) state that yields delayed fluorescence. The phosphorescence and delayed fluorescence are phenomena much more slow than fluorescence; they may last even few seconds. The difference between them is the characteristic emission spectrum: for delayed fluorescence this spectrum is similar to the "normal" fluorescence one, while, because the triplet state has lower energy, the phosphorescence spectrum will be located at higher wavelengths.



Scheme 31 Jablonski Diagram

The luminescence of lanthanide complexes results from the oscillator strength of the $f-f$ transitions (forbidden by the Laporte's rule) and even if many lanthanide containing compounds display a reasonable quantum yield, the direct excitation of Ln^{3+} ions is almost impossible (the absorption coefficients for such trivalent cations is $\epsilon \approx 1\text{-}10 \text{ M}^{-1}\text{cm}^{-1}$). Therefore, the indirect excitation (called sensitization or antenna effect) needs to be adopted by the means of the chromophore (antenna). This proceeds in three steps:

- ✓ absorption of light by a chromophore and population of the lowest-lying singlet excited state (S),
- ✓ intersystem crossing (ISC) to the chromophore triplet level (T),
- ✓ energy transfer (ET) to the excited lanthanide state Ln^{3+*} which provokes its luminescence.

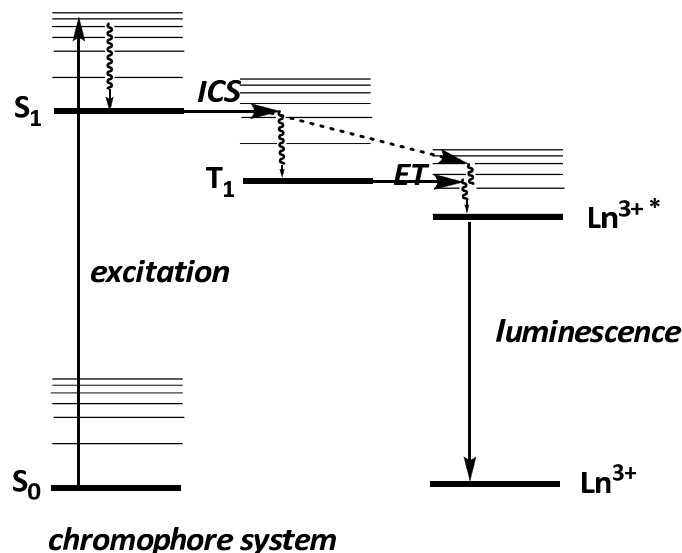


Fig. 67 The antenna effect for sensitization of the lanthanide luminescence

As presented on the schematic Jablonski Energy Diagram (Fig. 67), both the singlet and triplet states may transfer energy onto the metal ion, however, the singlet state S_1 is short lived and this process is therefore less efficient. The energy proximity between the chromophore triplet state and lanthanide excited state is taking into account. The overall efficiency of sensitized emission φ_{SE} is regulated by the intersystem crossing efficiency φ_{ISC} , the energy transfer efficiency φ_{ET} and the intrinsic metal center quantum yield of the lanthanide ion φ_{lum}^{MC} (Equation 8)

$$\varphi_{SE} = \varphi_{ISC} \varphi_{ET} \varphi_{lum}^{MC}$$

Equation 8

Besides, in aqueous solutions, in order to avoid non-radiative deactivation by quenching with O-H oscillators, the 8-9 coordination positions of Ln^{3+} should be shielded from solvent molecules. For this purpose, the comparison of luminescence results in water and deuterated water solutions need to be done to estimate the number of water molecules close to the lanthanide center. For example, for the $Nd(III)^{145}$ and $Yb(III)^{146}$ complexes following equations could be applied, where q is the number of coordinated water molecules and τ is the lifetime of complex:

$$q = A(\Delta k_{obs}) - C \text{ for } Nd^{3+}$$

Equation 9

$$q = A(\Delta k_{obs}) - B \text{ for } Yb^{3+}$$

Equation 10

$$\Delta k_{obs} = \frac{1}{\tau_{obs}}(H_2O) - \frac{1}{\tau_{obs}}(D_2O)$$

Equation 11

Where $A = 130 \text{ ns}$ for Nd^{3+} and $1 \mu\text{s}$ for Yb^{3+} , $B = 0.2 \mu\text{s}^{-1}$ and $C = 0.4$. Δk_{obs} is described in ns^{-1} for Nd^{3+} and in μs^{-1} for Yb^{3+} complex.

¹⁴⁵ (a) A. Beeby, B. P. Burton-Pye, S. Faulkner, G. R. Motson, J. Jeffery, J. A. McCleverty, M. D. Ward, *Dalton Trans.*, **2002**, 19, 1923; (b) Faulkner, A. Beeby, M. C. Carrie, A. Dadabhoy, A. M. Kenwright, P. G. Sammes, *Inorg. Chem. Commun.*, **2001**, 4, 187.

¹⁴⁶ A. Beeby, I. M. Clarkson, R. S. Dickins, S. Faulkner, D. Parker, L. Royle, A. S. de Sousa, J. A. G. Woods, *J. Chem. Soc., Perkin Trans.*, **1999**, 3, 493.

Therefore, in order to ensure efficient lanthanide sensitization the sensitizer-ligand must fulfill several requirements. From the one hand, thermodynamic, kinetic and structural features (complex stability, saturation of the coordination position of lanthanide) must be considered, but also the electronic properties of the sensitizer must be tuned with, to obtain effective energy transfer to the lanthanide metal center.

I.4. Antennae for lanthanide sensitization

The antenna for lanthanide sensitization might be an organic molecule or the system (the nanocrystal, the metal-organic framework or the dendrimer) collecting the energy and transferring it directly to the metal center, provoking the emission of lanthanide.¹⁴⁷ In this work, we will focus on the organic sensitizers.

In general, the organic antenna can be any aromatic or hetero-aromatic compound with highly π -conjugated system and superior absorption coefficient ϵ responsible for high light absorption. Also, it should be characterized by energy of triplet excited state that should be located at sufficient energy in respect to the lowest emitting level of the Ln^{3+} cation.¹⁴⁸ When the energy gap is smaller, the thermal deactivation occurs due to the back energy transfer towards the chromophore triplet level. The excitation wavelengths of chromophore should be above ~ 350 nm to facilitate the use of inexpensive excitation sources and avoid the harmful for biological tissues UV irradiation. Taking into account the position and nature of the chromophore, the energy transfer may occur either by Förster (FRET), Dexter and electron transfer mechanisms.¹⁴⁹ The difference between these types of energy transfer is the distance from donor to acceptor: in the Dexter and electron transfer mechanisms, the overlap of orbitals is needed, whereas in the Förster mechanism the transfer is through the space and it depends strongly on the spectral overlap of the emission of the donor and the absorption of the acceptor. An energy transfer by the Dexter and electron transfer mechanisms is efficient only at very small distances (< 10 Å), when the Förster energy transfer has been reported to occur over much longer distances.¹⁵⁰ In order to avoid the dissipation of energy in the system, the distance between the sensitizer and lanthanide cation should be short enough; the most efficient energy transfer can be obtained when the chromophore directly coordinates the metal centre. This goal can be achieved when antenna contains binding sites for the Ln^{3+} such as aza-aromatic compounds (bipyridine, phenantroline) or phenolate aromatics (2-hydroxyisophtalamide or 1-hydroxypyridin-2-one).¹⁵¹

¹⁴⁷ H. Uh, S. Petoud, *CR Chimie*, **2010**, *13*, 668.

¹⁴⁸ M. Latva, H. Takalo, V.-M. Mikkala, C. Matachescu, J. C. Rodriguez-Ubis, J. Kankare, *J. Lumin.*, **1997**, *75*, 149.

¹⁴⁹ (a) T. Förster, *Discuss. Faraday Soc.*, **1959**, *27*, 7; (b) D. L. Dexter, *J. Chem. Phys.*, **1953**, *21*, 836; (c) T. Lazarides, D. Sykes, S. Faulkner, A. Barbieri, M. D. Ward, *Chem. Eur. J.*, **2008**, *14*, 9389.

¹⁵⁰ W. de W. Horrocks, M.-J. Rhee, A. P. Snyder, D. R. Sudnick, *J. Am. Chem. Soc.*, **1980**, *102*, 3650.

¹⁵¹ (a) A. P. S. Samuel, E. G. Moore, M. Melchior, J. Xu, K. N. Raymond, *Inorg. Chem.*, **2008**, *47*, 7535; (b) E. G. Moore, J. Xu, C. J. Jocher, I. Castro-Rodriguez, K. N. Raymond, *Inorg. Chem.*, **2008**, *47*, 3105.

However, the too short distance between the triplet state of chromophore and the accepting level of the lanthanide cation may provoke the back energy transfer without efficient sensitization process.

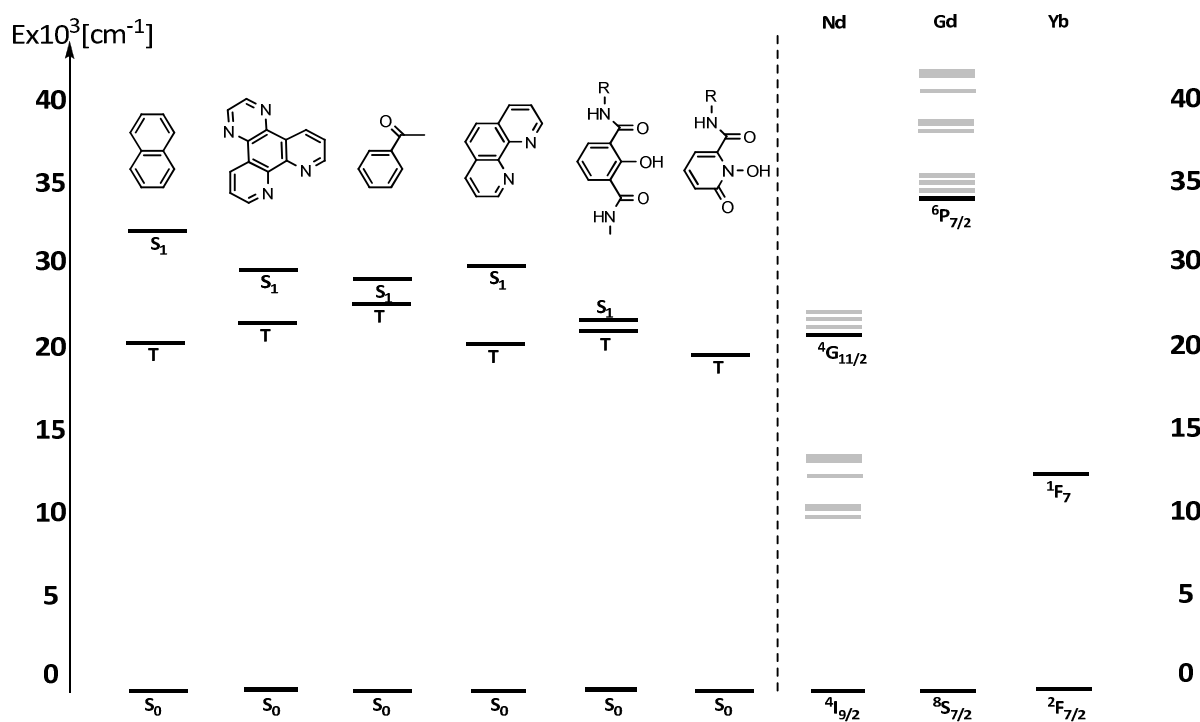


Fig. 68 The Dieke energy diagram of emissive levels of some lanthanide cations (Nd, Gd, Yb) and chromophores¹³⁹

Emissive levels of some chromophores were presented in comparison with the Dieke energy diagram of three of lanthanide cations particularly used in the medical imaging (Fig. 68). As presented on figure above, the lowest excited state of Gd^{3+} is about $32\ 000\text{cm}^{-1}$, which corresponds to energy in UV region. For gadolinium complexes containing chromophores with excitation band higher than 300 nm any transfer of energy cannot occur, for this reason the Gd^{3+} compounds are used to determine the triplet state of complex.

I.5. Advantage of lanthanide markers for biological applications

Fluorescence detection is among the most sensitive, versatile and least expensive techniques for biological applications. In the field of the fluorescence microscopy, there is a strong demand for luminescent imaging agents with advanced properties. Lanthanides are very promising for biological imaging for the following reasons:

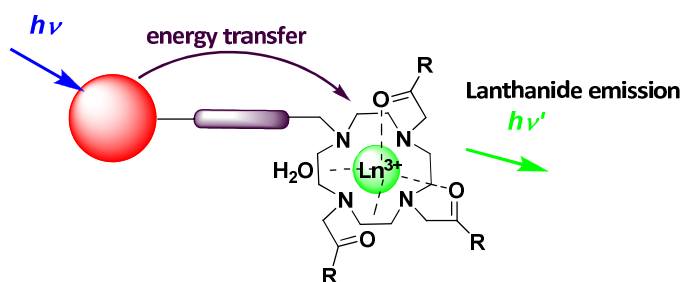
- Most described lanthanide complexes do not photobleach.¹³⁶ This prevents irreversible photoreactions when complex is irradiated.
- Lanthanide luminescence can be spectrally discriminated from other luminescent reporters (biological autofluorescence). They have a number of excited states allowing their emission to appear as sharp bands in the visible and near-infrared regions. This

advantage allows the individual detection of several lanthanide emitters during the same experiment (multiplex assay).

- Biological tissues do not have significant native NIR fluorescence, therefore the use of NIR eliminates background fluorescence, one of the most important issues for biological imaging. The use of NIR photons is also a good strategy to obtain higher resolution pictures than visible photons, as NIR light scatters less than visible light.

I.6. Lanthanide sensitizers based on cyclen derivatives

In the recent literature, a vast number of lanthanide sensitizers have been presented, however in this chapter we will focus on the lanthanide sensitizers bearing heterocycle framework and with cyclen chelating core, because of their applications in near-infrared optical imaging.¹⁵² As it was already stated, the DOTA complexes are kinetically and thermodynamically stable in aqueous conditions and furthermore, the substitution of one of the pending arm with organic aromatic molecule enables the formation of the sensitizer.



Scheme 32 The concept of lanthanide sensitizer based on DOTA complex

The first lanthanide sensitizers were absorbing in the UV region. The phenantroline¹⁵³ chromophore is an example of molecule that permits the efficient energy transfer to the lanthanide center and at the same time enters in the coordination sphere of the metal ion (Fig. 69). The limitation of this system was the excitation band at 280 nm, which exclude this compound from use for biological application.

¹⁵² (a) J.-C. G. Bünzli, *Chem. Rev.*, **2010**, *110*, 2729, (b) S. Faulkner, S. J. A. Pope, B. P. Burton-Pye, *Appl. Spectr. Reviews*, **2005**, *40*, 1.

¹⁵³ S. Quici, G. Marzanni, M. Cavazzini, P. L. Anelli, M. Botta, E. Gianolio, G. Accorsi, N. Armaroli, F. Barigelletti, *Inorg. Chem.*, **2002**, *41*, 2777.

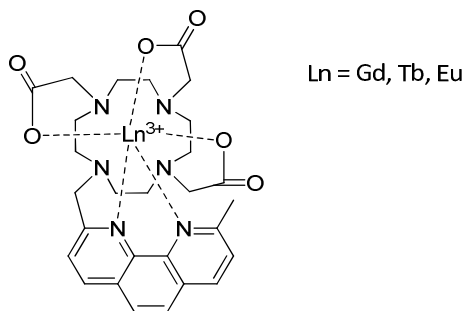


Fig. 69 The phenantroline sensitizer

Some inorganic transition-metal complexes have been used as sensitizers for lanthanide complexes. Beeby *et al.*¹⁵⁴ reported a porphyrin core with Pd(II) covalently bound to the chiral lanthanide complex, which effectively sensitizes the near-IR emission of Yb³⁺ and Nd³⁺ and has also a specific affinity to the nucleic acids. At the same time, the group of Klink¹⁵⁵ presented ferrocene and ruthenium tris(bipyridine) complexes as light-harvesting units for sensitization of lanthanide luminescence.

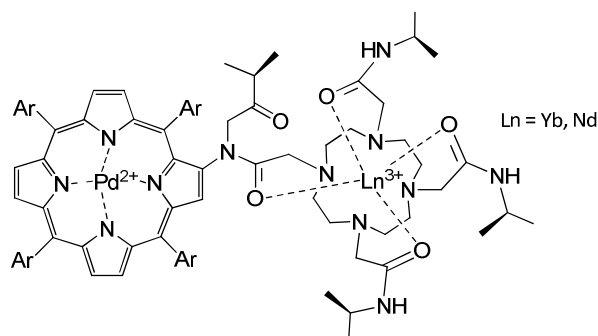


Fig. 70 The palladium porphyrin sensitizer for lanthanides

Investigations in the field of organic sensitizers with the absorption in the visible were pioneered by Li and Selvin¹⁵⁶ by the application of carbostyryl-124 chromophore (Fig. 71). This compound is attached to polyaminocarboxylate chelates for lanthanide cations such as DPTA, DOTA or TETA and shows a good efficiency of energy transfer to the metal center, both europium and terbium.

¹⁵⁴ A. Beeby, R. S. Dickins, S. FitzGerald, L. J. Govenlock, C. L. Maupin, D. Parker, J. P. Riehl, G. Siligardi, J. A. G. Williams, *Chem. Commun.*, **2000**, 1183.

¹⁵⁵ S. I. Klink, H. Keizer, F. C. J. M. van Veggel, *Angew. Chem. Int. Ed.*, **2000**, 39, 4319.

¹⁵⁶ M. Li, P. R. Selvin, *J. Am. Chem. Soc.*, **1995**, 117, 8132.

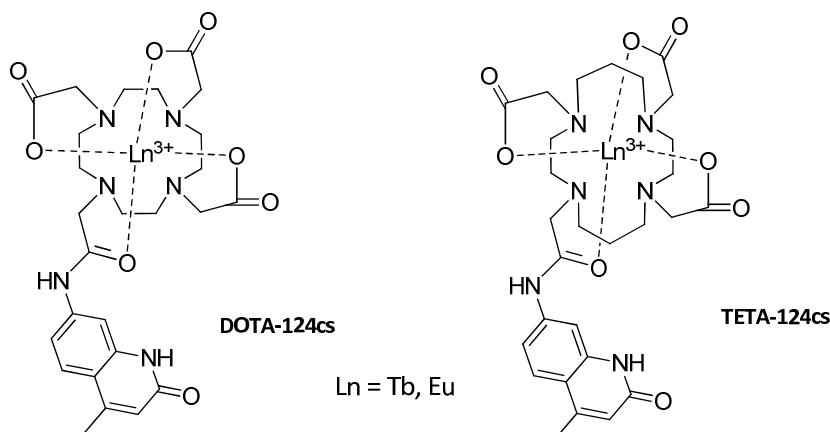


Fig. 71 The carbostyryl chromophores incorporated into DOTA complex

Another example is the complex of Eu^{3+} based on acridone derivatives (Fig. 72a) reported by Sammes *et al.*¹⁵⁷ This sensitizer shows high quantum yields after excitation with the visible light ($\lambda_{\text{exc}} = 380 \text{ nm}$). Faulkner¹⁵⁸ also presented efficient excitation of several lanthanides with the use of triazolophthalazine as an antenna (Fig. 72b). The observation of lanthanide emission has been made in visible (for Eu^{3+}) and near-infrared (Yb^{3+} , Nd^{3+} , Er^{3+}) part of spectrum.

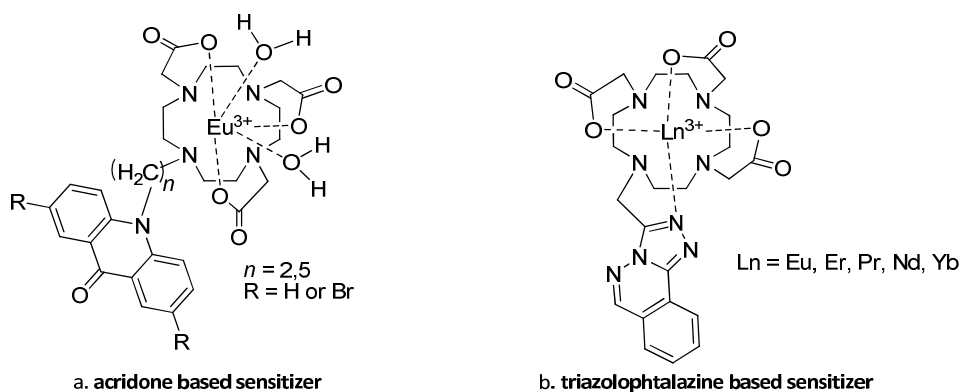


Fig. 72 Acridone and triazolophthalazine based sensitizers for lanthanides

The attachment of 8-hydroxyquinoline¹⁵⁹ and 8-benzyloxyquinoline¹⁶⁰ moiety to DOTA derivatives has been reported. The additional benzyloxy group displaces the water molecules from the lanthanide coordination sphere; however it does not improve the efficiency of sensitization.

¹⁵⁷ A. Dadabhoy, S. Faulkner, P. G. Sammes, *J. Chem. Soc., Perkin Trans. 2*, **2002**, 348.

¹⁵⁸ B. P. Burton-Pye, S. L. Heath, S. Faulkner, *Dalton Trans.*, **2005**, 146.

¹⁵⁹ F. Rizzo, A. Papagni, F. Meinardi, R. Tubino, M. Ottonelli, G. F. Musso, G. Dellapiane, *Synthetic Metals*, **2004**, *147*, 143.

¹⁶⁰ D. Maffeo, J. A. G. Williams, *Inorg. Chimica Acta*, **2003**, *355*, 127.

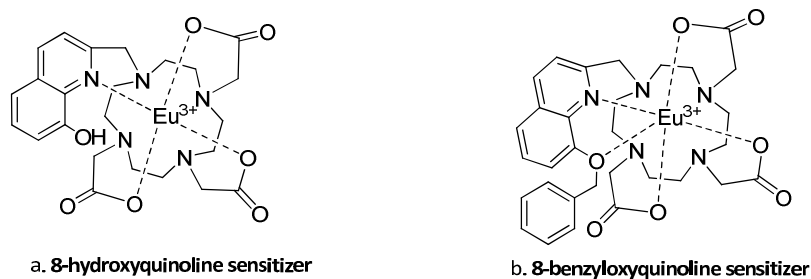


Fig. 73 8-hydroxyquinoline and 8-benzyloxyquinoline sensitizers for europium

Other organic chromophore - quinoxaline - proved to be a good sensitizer for lanthanide ion luminescence.¹⁶¹ In the case of this complex, the coordination of lanthanide cation is provided by carbonyl groups of amides replacing triacetic acids. Emission spectra of lanthanides after excitation at 320-390 nm were recorded. Also xanthone derivatives have been tested for the sensitization of terbium luminescence at 355 nm with cell permeable pyrazoyl-1-azaxanthone macrocyclic complexes.¹⁶²

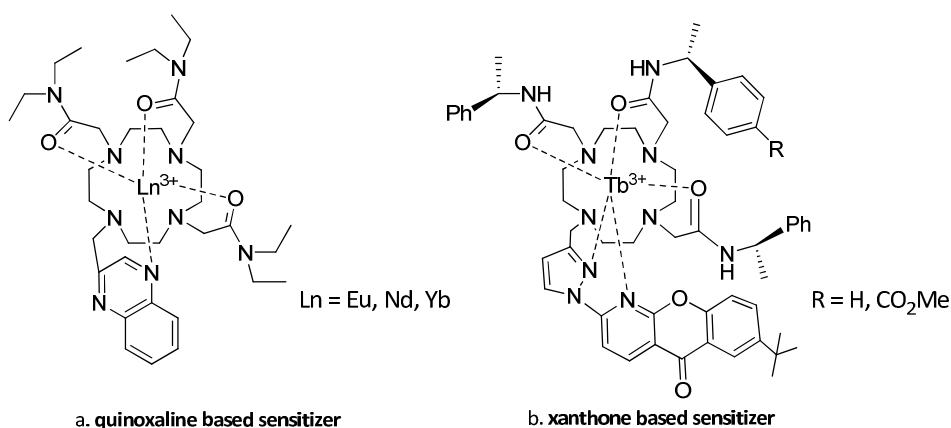


Fig. 74 Quinoxaline and xanthone-based sensitizer

The heterometallic lanthanide complex containing Yb³⁺ and Tb³⁺ cations has been reported by Faulkner *et al.*¹⁶³ This approach was achieved by sequential controlled deprotection (one DOTA unit was protected with *tert*-butyl esters and the second one - with ethyl esters) and complexation of orthogonally blocked ligand. The compound (Fig. 74) showed sensitized luminescence from both the Tb³⁺ and Yb³⁺ metal center in the visible and near-infrared, respectively.

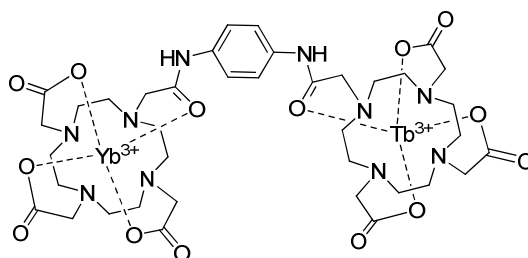


Fig. 75 Heterometallic lanthanide complex

¹⁶¹ M. Andrews, L. H. Laye, L. P. Harding, S. J. A. Pope, *Polyhedron*, **2008**, 27, 2365.

¹⁶² C. P. Montgomery, D. Parker, L. Lamarque, *Chem. Commun.*, **2007**, 3841.

¹⁶³ L.S. Natrajan, A.-J. L. Villaraza, A. M. Kenwright, S. Faulkner, *Chem. Commun.*, **2009**, 6020.

Alternatively, the building blocks containing various lanthanide cations may be connected by the simple organic reaction of diazotization and therefore enhance the wavelengths of excitation by increasing the conjugation of the system.¹⁶⁴ This methodology allows not only the preparation of heterometallic systems containing different lanthanides but also the simultaneous incorporation of a sensitizing chromophore (Fig. 76).

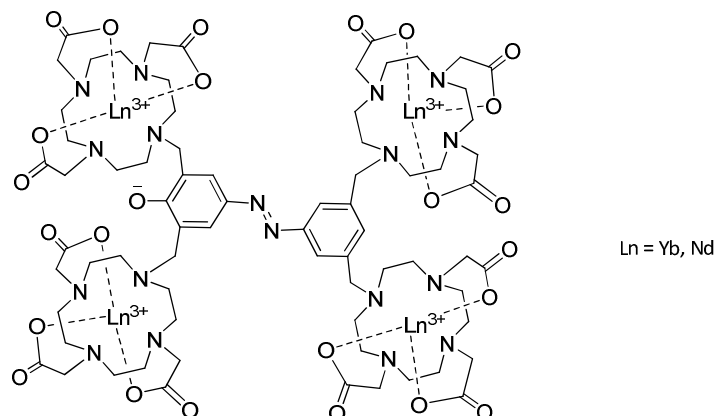


Fig. 76 Azo-dye derivatives of polymeric lanthanide complexes

Aita *et al.*¹⁶⁵ reported the NIR fluorescent ytterbium complex based on the pyridin-2-yl-diazenyl-5-amino-naphthalen-2-ol (PAN) (Fig. 77), which gives efficient lanthanide emission upon excitation at 530 nm. This complex is not fluorescent and has negligible fluorescence in the red to NIR region, which allows the complete energy transfer to the lanthanide chelate. In addition, this compound is stable in the large range of pH, therefore it reports high *in vivo* stability.

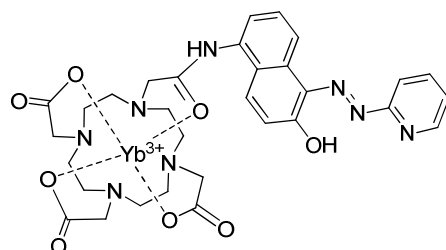


Fig. 77 Yb complex with pyridine-2-yl-diazenyl-5-amino-naphthalen-2-ol

Examples presented above did not cover whole literature in this domain; they are depicted here in order to illustrate the versatility of the approach and a vast possibility to extend this field.

I.7. Examples of lanthanides application in NIR probing

Some demonstrations of the application of NIR luminescent lanthanide complexes in bioanalytics and molecular imaging have appeared in recent years. This development is due to the

¹⁶⁴ M.P. Placidi, A-J.L. Villaraza, L.S. Natrajan, D. Sykes, A.M. Kenwright, S. Faulkner, *J. Am. Chem. Soc.* **2009**, *131*, 9916.

¹⁶⁵ K. Aita, T. Temma, Y. Kuge, K. Seki, H. Saji, *Luminescence*, **2010**, *25*, 19.

great progress in the domain of optoelectronics, with light sources and detectors suitable to work in the near-infrared region.

Lanthanide complexes can be pH, temperature or oxygen¹⁶⁶ sensitive and therefore may become useful sensors for cell imaging. A crown ether-modified Nd³⁺ cryptand¹⁶⁷ was proposed for barium ion detection. Unfortunately, this complex works as probe only in one organic solvent - acetonitrile and it requires UV excitations.

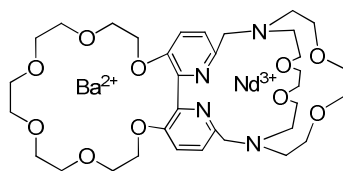
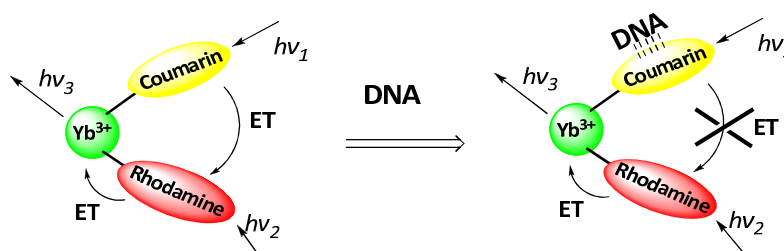


Fig. 78 Barium ion sensor based on lanthanide luminescence

The detection of nucleic acid strands by NIR luminescence is possible by the tuning of ytterbium emission in Pd-porphyrin-containing complexes (previously described in this document) or by the sensitivity of the intramolecular energy transfer in coumarin-rhodamine-modified Yb³⁺ complex.¹⁶⁸ The lanthanide is sensitized by rhodamine, which in turn is excited by energy transfer from a coumarin moiety. These three compounds operate on the principle of energy transfer cascade, spanning the UV-visible-near IR region of the spectrum, resulting in the large Stokes shifts. When double stranded DNA is interacting with coumarin, this system is disturbed and only NIR signal is observed.



Scheme 33 Principle of NIR-emitting DNA-probe

The europium(III) complex containing diaza-18-crown-6 ether and diaryl-alkyne-antenna-part reported by He *et al.*¹⁶⁹ works in the similar way as described earlier. This compound was demonstrated to be a specific fluorescence probe for the toxin isolated from the paralytic shellfish (saxitoxin). The binding of the toxin to the crown ether triggers a two-photon induced *f-f* emission of europium complex.

¹⁶⁶ D. Parker, P. K. Senanayake, J. A. G. Williams, *J. Chem. Soc., Perkin Trans. 2*, **1998**, 2129.

¹⁶⁷ J. B. Coldwell, C. E. Felton, L. P. Harding, R. Moon, J. A. Pope, C. Rice, *Chem. Commun.*, **2006**, 5048.

¹⁶⁸ A. Bodi, K. E. Borbas, J. I. Bruce, *Dalton Trans.*, **2007**, 4352.

¹⁶⁹ S. He, H. Li, Y.-W. Yip, C.-T. Yeung, Y. O. Fung, H.-K. Kong, H.-L. Yeung, G.-L. Law *et al.*, *Org. Lett.*, **2011**, *13*, 5036.

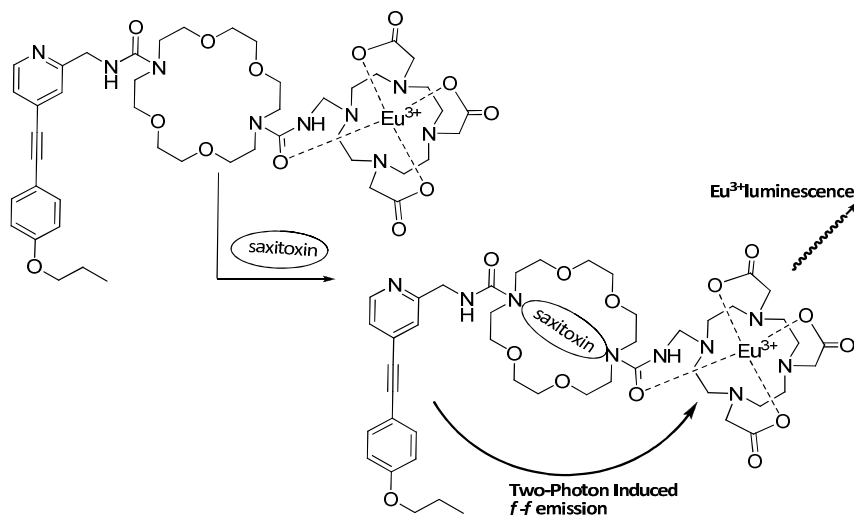


Fig. 79 Mechanism of saxitoxin detection

In addition, the lanthanide complexes have found applications in the domain of live cell imaging and *in vivo* detection. The particular Yb^{3+} complex with porphyrin chelate¹⁷⁰ has amphiphilic properties, which allow molecule to cross the membrane barrier and target the tumor cell by NIR luminescence. Furthermore, this molecule may act as dual-function probe, combining near-infrared luminescence for detecting and imaging with a singlet oxygen generation for photodynamic therapy on malignant cells.

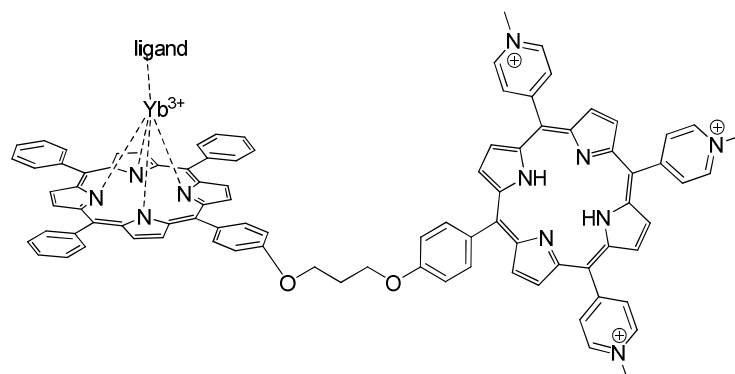


Fig. 80 Amphiphilic bisporphyrin Yb(III) complex

Another example of connection both bioanalysis and bioimaging applications with photodynamic therapy of cancer is photosensitizer with Yb^{3+} and Er^{3+} (Fig. 80).¹⁷¹ Upon irradiation at a specific wavelength, the sensitization of nanoparticles occurs and the singlet oxygen is produced at the same time, provoking the destruction of cancerous cells. This system has been tested on the breast cancer cells.

The lanthanide cations may be likewise complexed by dendrimers (repetitively branched molecules) type PAMAM (polyamidoamine). This kind of compounds allows the incorporation of many Ln^{3+} ions (7-8 cations with the coordination number equals 9) and naphthalimide molecules branched at the end of dendrimers to sensitize cations and therefore enhance the emission signal (Fig. 81).

¹⁷⁰ F.-L.Jiang, C.-T. Poon, W.-K. Wong, H.-K. Koon, N.-K. Mak, C. Y. Choi, D. W. J. Kwong, Y. Liu, *Chem. Bio. Chem.*, **2008**, 9, 1034.

¹⁷¹ P. Zhang, W. Steelant, M. Kumar, M. Scholfield, *J. Am. Chem. Soc.*, **2007**, 129, 4526.

Recently, luminescent dendrimer europium(III) complexes¹⁷² have been proved to accumulate preferentially within rat liver tumors. This imaging agent seems to be much more resistant for photobleaching than organic sensitizers.

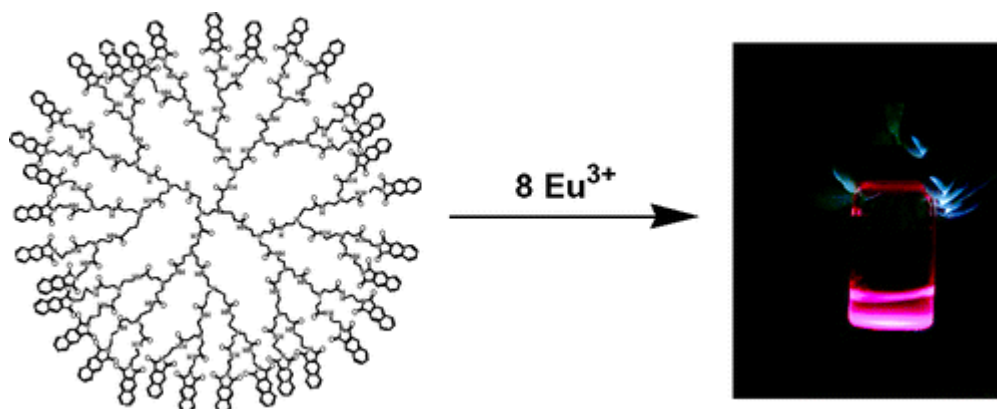
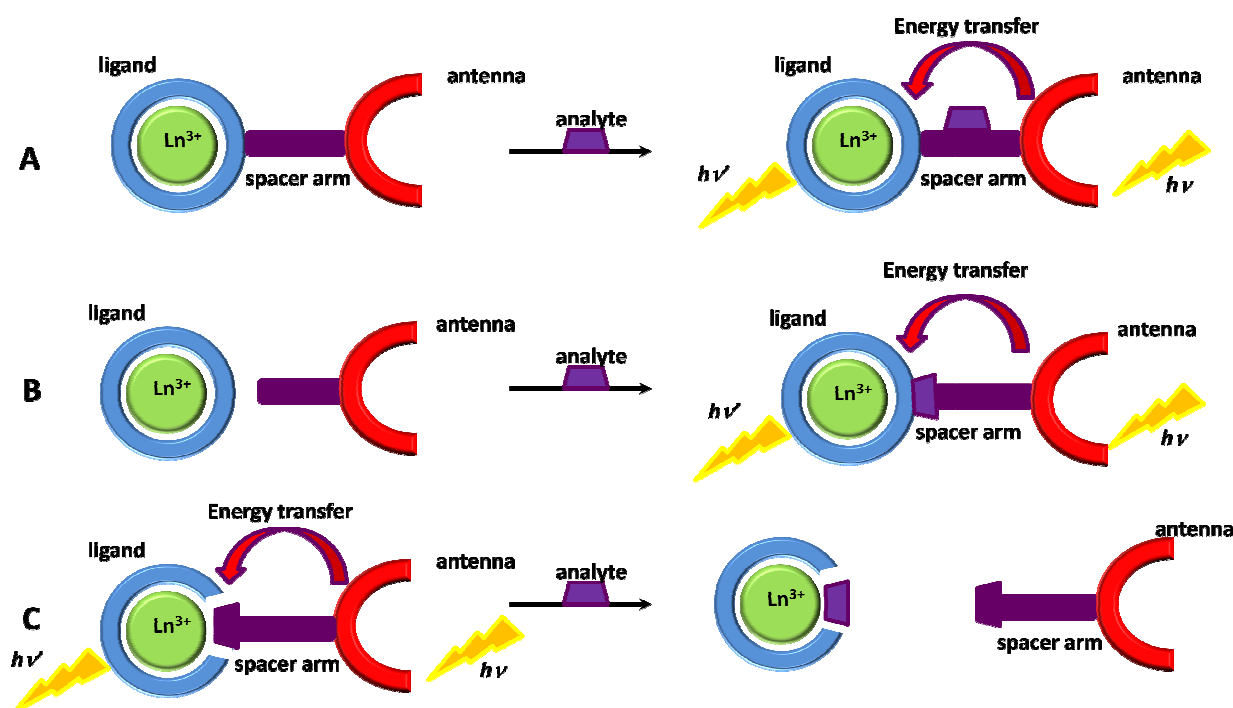


Fig. 81 PAMAM dendrimer

Lanthanide complexes have found commercial use as highly sensitive and selective probes in immunoassays and DNA assays such as DELFIA and FIAGEN probes. Complexes for time-resolved Förster resonance energy transfer (TR-FRET) and time-resolved fluorescence quenching assays (TR-FQA) are also commercially available. The new challenge is the construction of responsive lanthanide luminescent probes for cellular imaging.¹⁷³



Scheme 34 The possible ways of lanthanide luminescence modulation

Several possibilities exist for the modulation of the luminescence of lanthanide sensor by the distance separating the sensitizer from the chelating center (Scheme 34):

¹⁷² M. A. Alcala, C. M. Shade, H. Uh, S. Y. Kwan, M. Bishhof, Z. P. Thompson, K. A. Gogick, A. R. Meier, T. G. Strein, D. L. Bartlett, R. A. Modzelewski, Y. J. Lee, S. Petoud, C. K. Brown, *Biomaterials*, **2011**, 32, 9343.

¹⁷³ A. Thibon, V. C. Pierre, *Anal. Bioanal. Chem.*, **2009**, 394, 107.

- a. binding the analyte to the spacer arm brings lanthanide in close proximity to the Ln^{3+} and switches on the luminescence,
- b. the analyte provokes the conjugation of the antenna to the lanthanide complex and therefore enables the sensitization process,
- c. direct coordination of the analyte to the lanthanide removes a weakly coordinated antenna and turns off the lanthanide's luminescence.

An interesting example for lanthanide sensors for protease activity is antenna-chelator conjugate, which acts by emitting the strong luminescence signal once the protease cleaves the amide bond in the complex.¹⁷⁴ Also, the application of peptide bound DOTA[Tb^{3+}] complex for cyclin A probe was reported.¹⁷⁵ The concept of this sensor is based on the intermolecular lanthanide sensitization through the tryptophan residue placed in the surface of the peptide.

¹⁷⁴ S. Mizukami, K. Tonai, M. Kaneko, K. Kikuchi, *J. Am. Chem. Soc.*, **2008**, *130*, 14376.

¹⁷⁵ E. Pazos, D. Torrecilla, M. V. López, L. Castedo, J. L. Mascareñas, A. Vidal, M. E. Vásquez, *J. Am. Chem. Soc.*, **2008**, *130*, 9652.

II. Result and discussion: chromophores based on pyrazinic core

II.1. Background

The preparation and the valorization of new chromophores is a challenging task nowadays, taking into account the requirements that need to be fulfilled. The efficient sensitizer for lanthanide complexes needs to have well defined excitation and emission bands tailored for the lanthanide excitation. The synthesis pathway of this molecule should be simple and reproducible. Besides, it needs to be easily changeable giving access to different derivatives. From the photophysical point of view, it must be photostable to give a constant signal during the time of the experiments.

In the course of investigation on the synthesis of original *N*-containing heterocycles conducted in our laboratory, we were interested in the 1,4-dihydropyrazines motif. This moiety gives a direct access to a range of 2,5-disubstituted pyrazines after deprotection/aromatization step and *ipso facto* opens a great possibility to synthesize various pyrazinic chromophores with a broad variety of electronic structures.⁹

We can find some significant examples of the pyrazine ring system in biological organisms showing the luminescence properties. One of them is a coelenterazine isolated from marine organisms, including the sea pansy *Renilla*, the jellyfish *Aequorea* and the hydroid *Obelia*.¹⁷⁶ This pyrazinic framework is responsible for the chemiluminescence of these animals by reaction with oxygen and formation of coelenteramide anion in the excited state (Fig. 82).

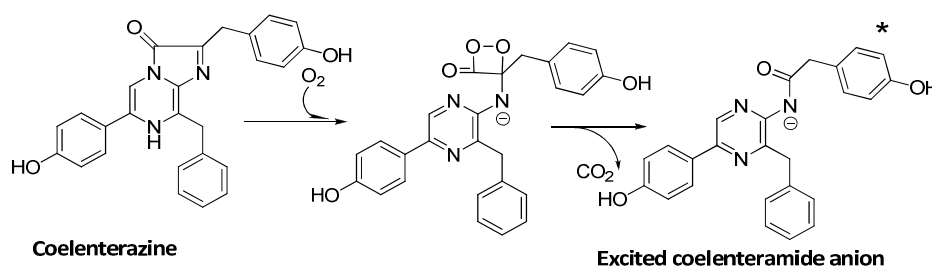


Fig. 82 The chemiluminescence of coelenterazine

The pyrazinic moiety has interesting photophysical properties, which have been proven useful in different fields of science. The photophysical features of pyrazine and its methylated derivatives at high pressure were examined first by Mitchell.¹⁷⁷ They showed that when the pressure increases, the intensity of $\pi \rightarrow \pi^*$ transition increases and at the same time, the fluorescence intensity increases. Also, the effect of substituents linked to the pyrazine in the position 2 and 5 were investigated¹⁷⁸ in series of polar and apolar solvents. One of tested molecules – dibenzofuran-2,2'-pyrazine in acetonitrile solution showed very high fluorescence quantum yields (more than 90 %) after excitation at 390 nm and with emission maximum above 410 nm (Fig. 83).

¹⁷⁶ (a) K. Hori, M. J. Cormier, *Proc. Natl. Acad. Sci. U.S.A.*, **1973**, *14*, 120; (b) O. Shimomura, F. H. Johnson, *Proc. Nat. Acad. Sci.*, **1975**, *72*, 1546; (c) C. M. Thomson, P. J. Herring, A. K. Campbell, *J. Biolumin. Chemilumin.*, **1997**, *8*, 87; (d) K. Jones, F. Hibbert, M. Keenan, *Trends Biotechnol.*, **1999**, *17*, 477; (e) J. W. Hastings, C. H. Johnson, *Methods Enzymol.*, **2000**, *305*, 75.

¹⁷⁷ D. J. Mitchell, G. B. Schuster, H. G. Drickamer, *J. Chem. Phys.*, **1979**, *70*, 2443.

¹⁷⁸ Z. Li, S. Wu, *J. Fluorescence*, **1997**, *7*, 237.

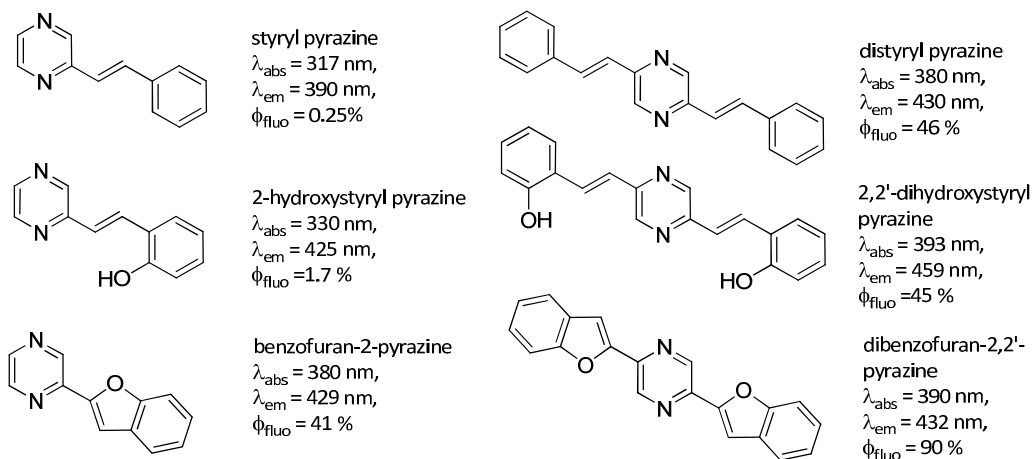


Fig. 83 Photophysical properties of pyrazine derivatives in acetonitrile solution¹⁷⁸

Moreover, the pyrazine may play a role as a ligand for transition metals such as ruthenium or rhodium (Fig. 84). One of the applications is construction of a light-absorber – electron-acceptor dyads with tridentate-bridge Ru-Rh complex of 2,3,5,6-tetrakis(2-pyridyl)pyrazine).¹⁷⁹ This system enables a construction of a wide assortment of supramolecular arrangements.

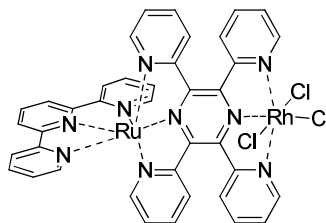


Fig. 84 Tridentate-bridged ruthenium-rhodium complex

The pyrazinic ring has been incorporated into the porphyrin system in order to create the light-harvesting assembly.¹⁸⁰ This structure is able to enhance the fluorescence of porphyrin about 77 times. The introduction of pyrazine moiety in the polymer structure such as polyfluorene has been reported lately¹⁸¹ as an efficient polymer light-emitting diode (PLED).

Recently, the pyrazine moiety has been applied as an original bis-pyridinylpyrazine chromophore for efficient sensitizing of Eu (III) and Sm (III) cations.¹⁸² This complex shows the red-shift of the maximum absorption wavelength compared to the usual terpyridine-based Ln(III) chelates. Moreover, a bioconjugation of non-symmetrical chelate provided a labelling marker for peptides (Fig. 85).

¹⁷⁹ J. D. Lee, L. M. Vrana, E. R. Bullock, K. J. Brewer, *Inorg. Chem.*, **1998**, 37, 3575.

¹⁸⁰ K. Sugou, K. Sasaki, K. Kitajima, T. Iwaki, Y. Kuroda, *J. Am. Chem. Soc.*, **2002**, 124, 1182.

¹⁸¹ W. Ming, L. Ying, X. ZhiYuan, W. LiXiang, *Science China, chemistry*, **2011**, 54, 656.

¹⁸² N. Maindron, S. Poupart, M. Hamon, J.-B. Langlois, N. Plé, L. Jean, A. Romieu, P.-Y. Renard, *Org. Biomol. Chem.*, **2011**, 9, 2357.

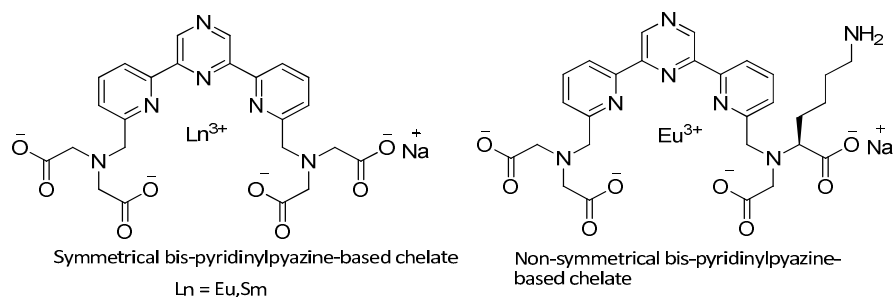


Fig. 85 Bis pyridinylpyrazine chromophores

Despite the relevant potential of pyrazine, its chemistry is under-developed in comparison with that of its isomers (i.e. dihydropyrazines) and pyridine. Given that non-flexible dimerization approach is the most often reported for the preparation of substituted 1,4-dihydropyrazines¹⁸³ and pyrazines, the development of new methods of their synthesis and their functionalization is still a great challenge.

II.2. Previous work

The antennae, that we propose to construct, are based on pyrazinic heterocyclic frameworks chosen as a luminescent moiety. This molecule is indeed hypothesized to emit a significant amount of photons in the red/ near-infrared region of electromagnetic spectrum. In previous investigation, realized in our laboratory,⁹ we have demonstrated that this diazinic skeleton could be functionalized in a controlled and selective way, which appears as a main advantage in term of flexibility. Taking advantage of our previous works, the original 1,4-dihydropyrazine bis-vinyl phosphate **A** was synthesized in good yields from piperazine-2,5-dione (Fig. 86). This vinyl phosphate **A** became a starting point for the numerous palladium catalyzed cross-coupling reactions in order to obtain "symmetrical" 2,5-disubstitued 1,4-dihydropyrazines. First, the reaction of Suzuki-Miyaura was tested with different boronic acids in the presence of 10 mol% of PdCl₂(PPh₃)₂, aqueous Na₂CO₃ (2M) and few drops of EtOH in the reflux of THF. Products with different heterocyclic substituents were obtained with good yields. Then, the Stille cross-coupling with tin reagents was performed, providing the 1,4-dihydropyrazines with heterocyclic and vinylic substituents.

¹⁸³ (a) X. Zhang, Z. Sui, *Tetrahedron*, **2006**, *47*, 5953; (b) D. Aparicio, O. A. Attanasi, P. Filippone, R. Ignacio, S. Lillini, F. Mantellini, F. Palacios, J. M. de los Santos, *J. Org. Chem.*, **2006**, *71*, 5897.

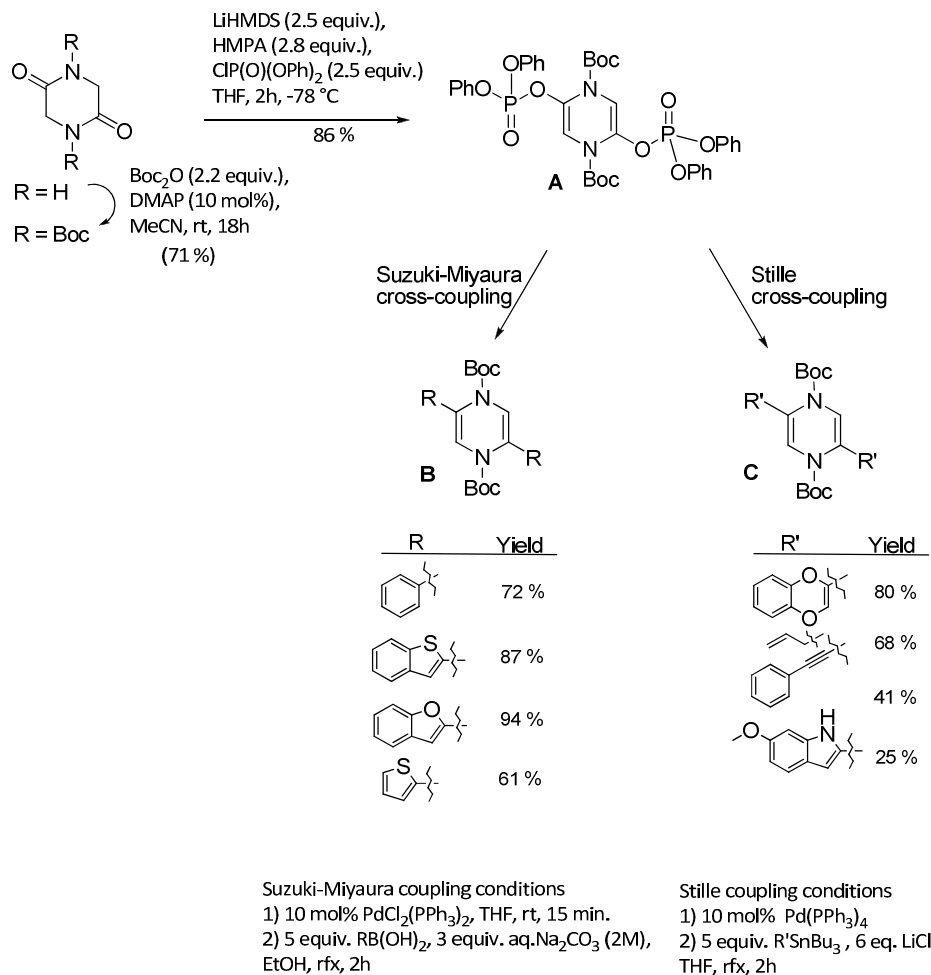


Fig. 86

The treatment of 2,5-disubstituted dihydropyrazines with anhydrous trifluoroacetic acid in dichloromethane for 2h afforded desired pyrazines with fair to good yields. The using TMSI instead of TFA improved the time of reaction providing the same conversion of starting dihydropyrazines (Fig. 87).

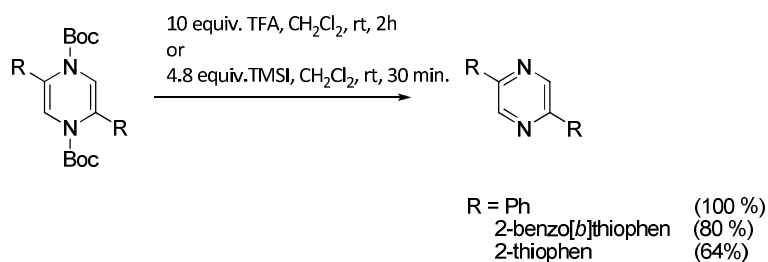


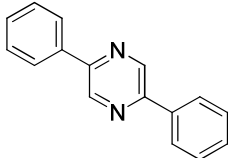
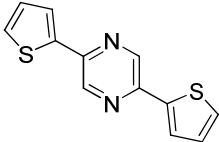
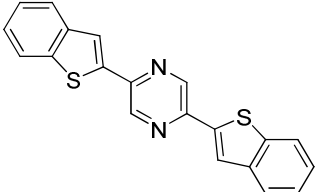
Fig. 87

The presented original strategy permits to synthesize 2,5-disubstituted pyrazines in three step synthesis starting from easily accessible products in a modifiable methodology.

II.3. Spectroscopic properties

The fluorescence properties of new synthesized pyrazines were tested and one of these compounds was selected for further investigation. These values may be compared to the derivative with benzofuranyl substituent presented before¹⁷⁸; where excitation on the maximum of the band at 390 nm leads to an emission band at 432 nm. A high quantum yield of fluorescence is observed ($\varphi_f = 90\%$) in acetonitrile solution.

Table 16 The comparison of photophysical properties of pyrazine derivatives⁹

Molecule			
	2,5-diphenylpyrazine	2,5-dithiophenylpyrazine	2,5-dibenzo[b]thiophenylpyrazine
λ_{abs} [nm]	326	367	390
λ_{em} [nm]	374	417	418 & 433
ϵ [$M^{-1}cm^{-1}$]	12000	94200	8300
φ_f [%] (CHCl ₃ solution)	5	15	40

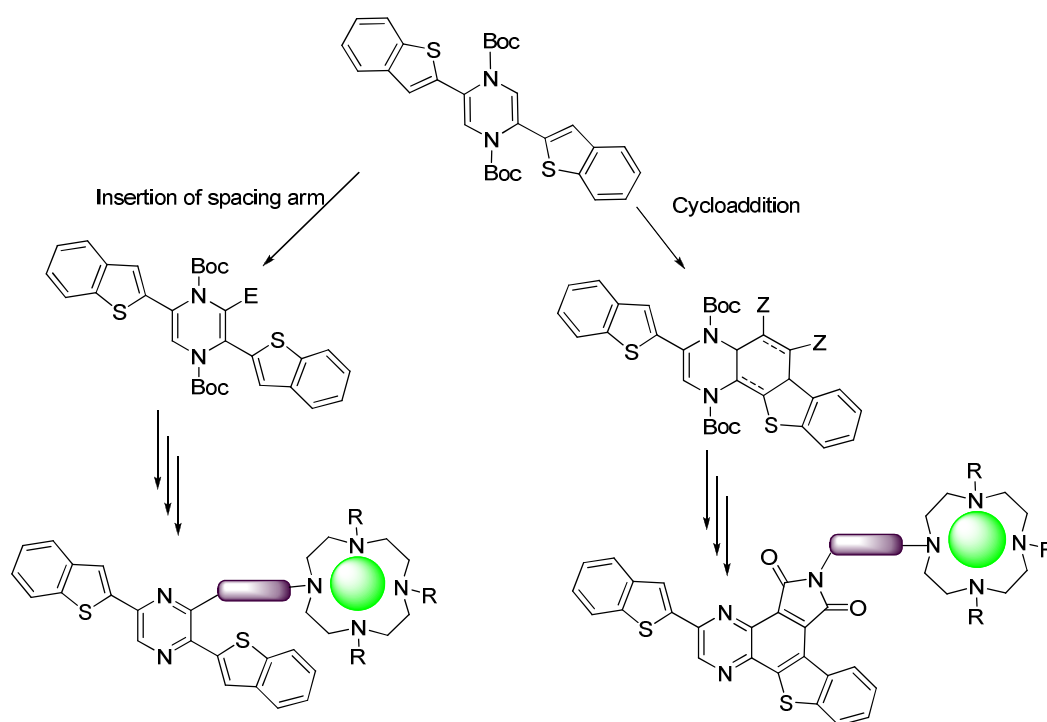
Results presented in Table 16 signify that among three synthesized pyrazine derivatives, the one bearing benzo[b]thiophenyl group possesses the best photophysical properties for the lanthanide sensitization, which means the lowest energy of excitation and emission with the highest quantum yield of fluorescence. This molecule became for us a starting point for the preparation of various dihydropyrazine systems.

II.4. Reactivity of 2,5-dibenzo[b]thiophenyl-pyrazine and construction of sensitizers for lanthanides with pyrazinic core

II.4.1. Objectives of project

Based on previous encouraging results and with the perspective of the valorization of pyrazine frameworks as a new NIR antenna, our objective was to introduce onto the dihydropyrazine moiety various relevant functional groups enabling to anchor *via* simple steps (e.g. click chemistry, nucleophilic substitution) the lanthanide chelator (DOTA). For our investigation, we have chosen the di-*tert*-butyl 2,5-di(benzo[b]thiophen-2-yl)pyrazine-1,4-dicarboxylate as the common moiety as it allows the preparation of various dihydropyrazinic systems (Scheme 35). In this aim, we have envisaged two possible routes for the preparation of the sensitizer: first *via* the Diels-Alder cycloaddition reaction using dihydropyrazine substituted with aryl group as a dienic partner and the

second one – *via* the functionalization of dihydropyrazine system under anionic conditions and by using standard transformations. A final step of deprotection/aromatization might be conducted to afford desired pyrazine moiety. As a system chelating lanthanides, we have chosen substituted cyclen derivative, taking into account the great stability of these complexes. With cyclen derivatives, the coordination cavity is achieved by the four nitrogen atoms of the ring and by four additional donor atoms located on each dangling arm. Moreover, this chelate is easily modulable, relatively stable on air and commercially available.



Scheme 35

II.4.2. DO3A derivative as a convenient chelator for lanthanides

1,4,7,10-tetraazacyclododecane-1,4,7,10-tetraacetic acid (also known as DOTA) is an organic compound derived from cyclen. This 12-membered tetraaza macrocycle is usually applied as a complexing agent, especially for lanthanide ions. The transition metal and lanthanide DOTA complexes have medical applications as contrast agents and cancer treatments.

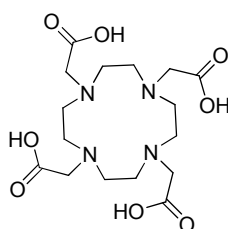


Fig. 88 DOTA

In our synthesis we used the three substituted cyclen moiety, in abbreviation DO3A, in order to have the possibility to attach our chromophore to the fourth *N*-atom. We have carried out the nucleophilic

substitution with 3.3 equiv. of *tert*-butyl bromoacetate, which was slowly added drop by drop to the mixture of cyclen with NaHCO₃. This method permitted us to substitute only three nitrogens and purify the product **53** as a free secondary amine after filtration and crystallization from toluene.¹⁸⁴

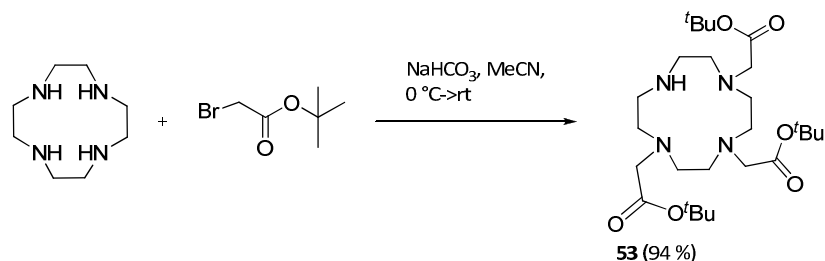
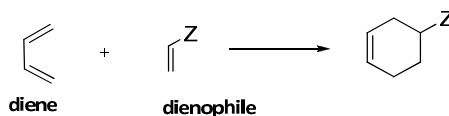


Fig. 89 The synthesis of DO3A

II.5. First approach - Construction of sensitizers *via* cycloaddition reaction

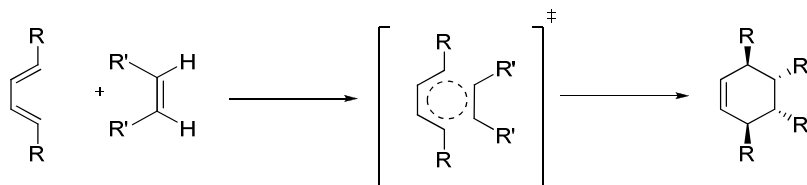
II.5.1. Bibliographic background: Diels-Alder reaction

Diels-Alder reaction is a [4+2] cycloaddition of a conjugated diene with a double or triple bond (the dienophile).¹⁸⁵ This electrocyclic reaction involves the 4 π -electrons of the diene and 2 π -electrons of the dienophile. The driving force of the reaction is the formation of new σ -bonds, which are energetically more stable than the π -bonds.



Scheme 36 Diels-Alder cycloaddition

With its broad scope and simplicity of operation, the Diels-Alder is the most powerful synthetic method for unsaturated six-membered rings. The Diels-Alder reaction occurs *via* single cyclic transition state with redistribution of bonding valence electrons. The cisoid conformation of the diene is a prerequisite for the cycloaddition step. Favored by a fixed cisoid geometry are those substrates where the diene is fitted into a ring (i.e. cyclopentadiene).



Scheme 37 Mechanism of Diels-Alder reaction

Overlap of the molecular orbitals (MOs) is required:

¹⁸⁴ S. Mizukami, K. Tono, M. Kaneko, K. Kikuchi, *J. Am. Chem. Soc.*, **2008**, *130*, 14376.

¹⁸⁵ O. Diels, K. Alder, *Justus Liebigs. Ann. Chem.*, **1928**, *460*, 98.

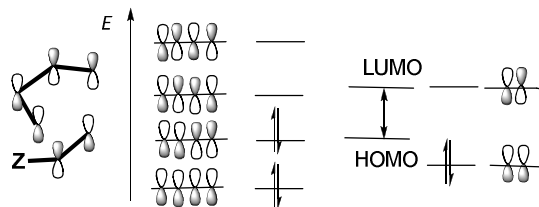


Fig. 90 Orbital explanation of Diels-Alder reaction

Overlap between the highest occupied MO of the diene (HOMO) and the lowest unoccupied MO of the dienophile (LUMO) is thermally allowed in the Diels-Alder reaction, provided the orbitals are of similar energy. The reaction is facilitated by electron-withdrawing groups on the dienophile, since this will lower the energy of the LUMO. Good dienophiles often bear one or two of the following substituents: CHO, COR, COOR, CN, C=C, Ph, or halogen. The diene component should be as electron-rich as possible.

There are "inverse demand" Diels Alder reactions that involve the overlap of the HOMO of the dienophile with the unoccupied MO of the diene. This alternative scenario for the reaction is favored by electron-donating groups on the dienophile and an electron-poor diene.

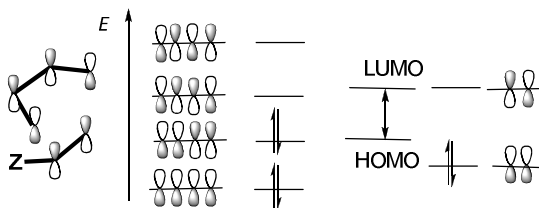
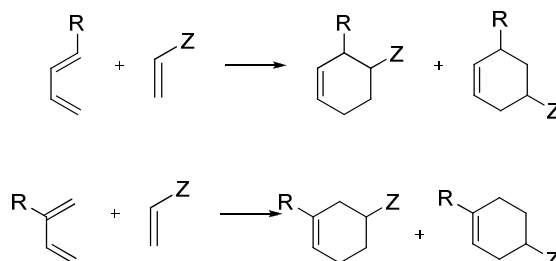


Fig. 91 Orbital explanation of "inverse demand" Diels-Alder reaction

From reaction of an unsymmetrically substituted diene and dienophile, different regioisomeric products can be formed. The so-called *ortho* and *para* isomers are formed preferentially. The observed regioselectivity can be explained by taking into account the frontier orbital coefficients of the reactants.¹⁸⁶



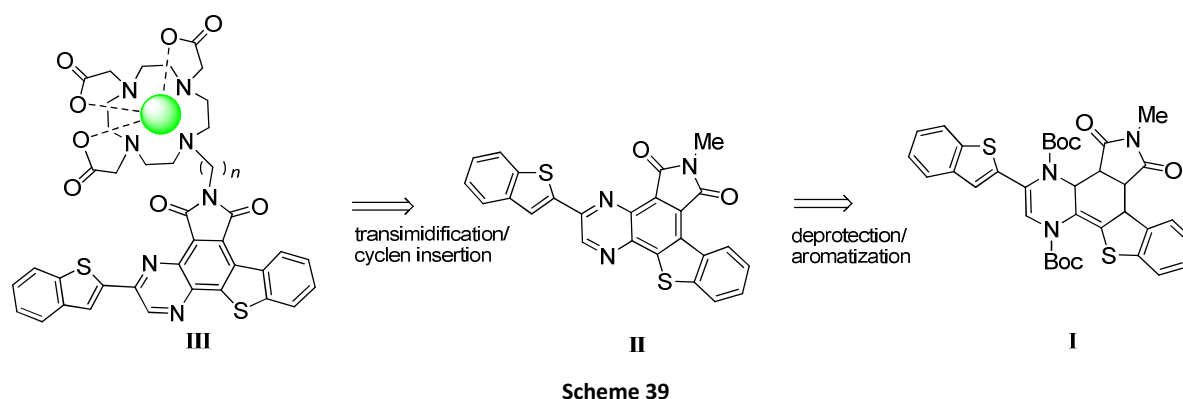
Scheme 38 Regioselectivity of Diels-Alder reaction

¹⁸⁶ I. Fleming, *Frontier Orbitals and Organic Chemical Reactions*, Wiley, London, 1976, p.110, 161.

II.5.2. Objectives

Based on the anterior work conducted in our team on the Diels-Alder cycloaddition of benzoxazines and benzodioxanes, which notably conducted to new heterocyclic compounds exhibited antitumor activity,¹⁸⁷ we have focused on the valorization of substituted dihydropyrazine derivative as a diene. The Diels-Alder cycloaddition followed by the complete aromatization of ring system will give an access to highly conjugated compound **II**. The deprotection and aromatization of cyclic scaffold provides to the pyrazino[*d*]naphto[1,2-*b*]thiophen system, which is highly conjugated therefore promising from the photophysical point of view. Indeed, the naphthalimide motif present in this structure has found an application as an antenna for dendrimers PAMAM.¹⁸⁸ Therefore, we decided to elaborate the sensitizer based on the cycloadduct attached to the cyclen chelate.

The spacer arm can be introduced to the system *via* trans-imidation step. Further modification of spacer and nucleophilic substitution with DO3A will afford the compound **III**, which after deprotection of *tert*-butyl esters may complex various lanthanide cations. The retrosynthetic pathway to obtain these molecules is presented on the Scheme 39.



II.5.3. Results and discussion of Diels-Alder reaction

Our starting molecule - dihydropyrazine substituted with benzo[*b*]thiophenyl groups shows a potential diene-character. A free rotation around the single bond is possible, however, the steric hindrance near the *tert*-butyl group favors the *trans* conformation (Fig. 91). We predicted that this dienic system may work well in thermal conditions.¹⁸⁹ We have started the screening process with 5 equiv. of *N*-methylmaleimide as a dienophile, heating the solution in toluene for several hours.

¹⁸⁷ (a) G. Coudert, F. Lepifre, D. H. Caignard, P. Renard, J. Hickman, A. Pierré, L. Kraus-Berthier, *FR 2002-12964 A* 18 oct. 2002 – WO 2003-FR3068 W 17 oct. 2003; (b) G. Coudert, N. Ayerbe, F. Lepifre, S. Routier, D. H. Caignard, P. Renard, J. Hickman, A. Pierré, S. Léonce, *FR 2002-12965 A* 18 oct. 2002 – WO 2003-FR3069 W 17 oct. 2003.

¹⁸⁸ M. A. Alcalá, S. Y. Kwan, C. M. Shade, M. Lang, H. Uh, M. Wang, S. G. Weber, D. L. Bartlett, S. Petoud, Y. J. Lee, *Nanomedicine*, **2011**, 7, 249.

¹⁸⁹ (a) A. Bourderioux, V. Bénétéau, J.-Y. Mérour, B. Baldeyrou, C. Ballot, A. Lansiaux, C. Bailly, R. Le Guével, C. Guillouzo, S. Routier, *Org. Biomol. Chem.*, **2008**, 6, 2108; (b) N. Ayerbe, S. Routier, I. Gillaizeau, S. Tardy, G. Coudert, *Lett. Org. Chem.*, **2010**, 7, 121.

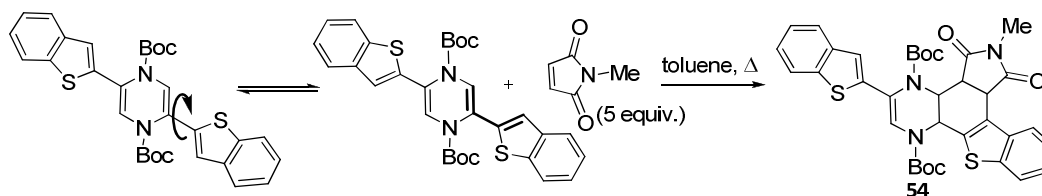
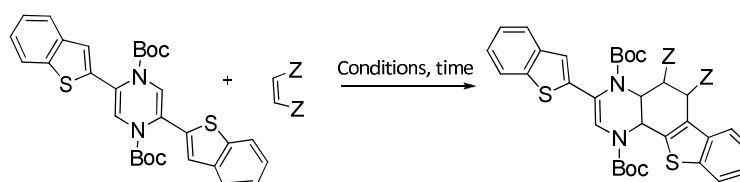


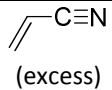
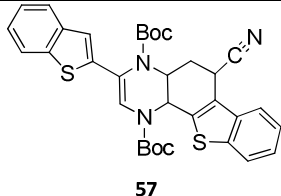
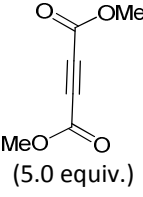
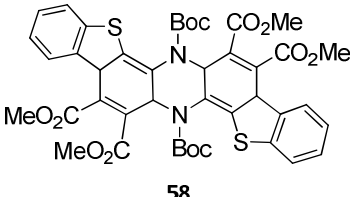
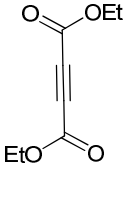
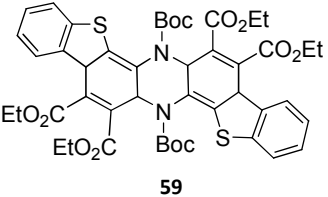
Fig. 92 Diels-Alder reaction with N-methylmaleimide

First, this reaction was tested under classical thermal conditions. The mixture was heated in toluene solution and with micro-wave activation in the sealed tube. Tested conditions of reaction were depicted in Table 17 (Entry 1-5). The structure of compound **54** was assigned as presented on Fig. 91, however, an isomer with aromatized benzo[*b*]thiophen is also possible. The two-dimensional NMR investigation (HSQC, HMBC) were performed, but results did not enable to clearly determine if this structure is correctly represented. Then, the methodology was extended for other dienophiles (maleimide, ethyl acrylate, acrylonitrile, dimethyl acetylenedicarboxylate (DMAD) and diethyl acetylenedicarboxylate (DEAD)).

Table 17 Diels-Alder reaction with dihydropyrazine as diene



Entry	Substrate	Conditions	Time	Product	Yield
1	 (5.0 equiv.)	Toluene, 140 °C	24 h	 54	58 %
2		Toluene, 110 °C	24 h		95 %
3		μ-waves, toluene, 160 °C, 140 W	45 min.		55 %
4		μ-waves, toluene, 160 °C, 140 W	1 h		41 %
5	 (5.0 equiv.)	Toluene, 110 °C	72 h	 55	62 %
6	 (excess)	110 °C, neat, sealed tube	48 h	 56	47 %

7	 (excess)	110 °C, neat, sealed tube	5 days	 57	19 %
8	 (5.0 equiv.)	Toluene, 150 °C	48 h	 58	37 %
9	 (5.0 equiv.)	Toluene, 150 °C,	5 days	 59	23 %

As we can notice, the optimal conditions were obtained with thermal heating at 110 °C for 24h (Table 17, Entry 2). In other applied conditions, remaining starting material was present in the reaction mixture and some part of degradation was observed. The microwave activation did not improve the yield of reaction; at the same time, the increase of the time of reaction (Table 17, Entry 4) decreased the yield of conversion, provoking the degradation of some starting material.

Interestingly, even using 5 equiv. of dienophile we did not observe the product of double cycloaddition (our starting material is a double dienic system). Probably, the energy delivered for this reaction is not sufficient or the double cycloadduct is too much constrained to be a stable molecule. Moreover, the steric hindrance play a role of constrain for the double cycloaddition.

Encouraged with the satisfactory results obtained with *N*-methylmaleimide, we have moved our investigation to other dienophiles. We have enlarged the scope of the Diels-Alder cycloaddition for dienophilic systems which permit the further modification of inserted groups in order to attach the chelate system for lanthanides. For this goal we have chosen maleimide, ethyl acrylate, acrylonitrile, and the activated dienophiles - dimethyl acetylenedicarboxylate (DMAD) and diethyl acetylenedicarboxylate (DEAD). We predicted to modify the ester and nitrile groups into the easily functionalizable alcohol or primary amine counterparts. The imide-moiety can be substituted by transimidation reaction leading to the product with longer terminal chain and a new functional group.

The results presented in Table 17 show that the most reactive dienophile in Diels-Alder reaction with our compound is *N*-methylmaleimide. Other products give much lower yields and the time of reaction was much longer. These may signify that starting dihydropyrazine derivative is not very active diene and it reacts well only with activated dienophile. In the case of non-substituted maleimide (Entry 5), the yield is much lower and the complete conversion of starting materials requires longer heating. Moreover, the resulted product is less stable due to free NH bond. Low yields of isolation of products

56 and **57** result from the lack of regioselectivity of reaction (Entry 6 and 7), these reactions gave the mixture of products of mono- and di-addition very difficult to separate by the column chromatography. Dimethyl and diethyl acetylenedicarboxylates showed only double cycloaddition with moderated yields, probably due to the steric hindrance.

Among all synthesized cycloadducts, the derivative with N-methylmaleimide has been involved in the further investigation, because of the great repeatability of the synthesis and the high yield of conversion. The compound **54** is stable in the air yellow solid, which allows easy storage and handling.

II.5.4. Cleavage of *tert*-butoxycarbonyl groups

The cleavage of *N*-Boc groups was carried out in acidic conditions in the presence of TFA at 0 °C in CH₂Cl₂. By using TMSI, a strong electrophile, instead of TFA, we managed to improve the yield of reaction. Both reactions gave the expected product **60** but the second method (using TMSI) was much more efficient (98 % in comparison with 32 % obtained after deprotection with TFA). During the deprotection, the aromatization step occurs with migration of the double bond. The structure of compound **60** was confirmed by the two-dimensional NMR experiments.

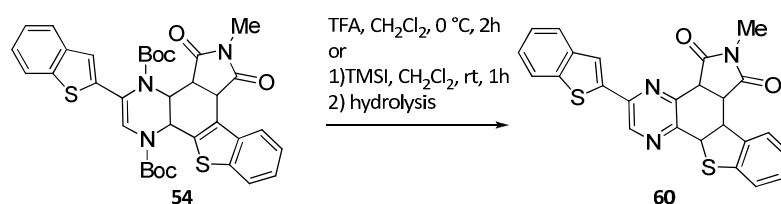
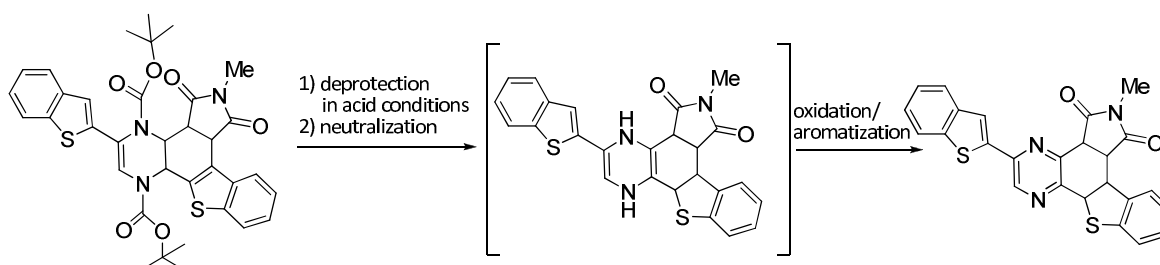


Fig. 93

The proposed mechanism is based on the stability of 1,4-dihydropyrazine moiety after elimination of *tert*-butyloxy carbamate group. This dihydropyrazine undergoes spontaneously the dehydrogenation/aromatization after aqueous work-up and provides the pyrazine scaffold directly.



Scheme 40

In order to validate the strategy for other cycloadducts, reaction of deprotection of the double adduct **58** has been carried out in the presence of TMSI in dichloromethane, and the elimination of *t*Boc group with complete aromatization of the 7-membered cyclic system occurred (Fig. 94).

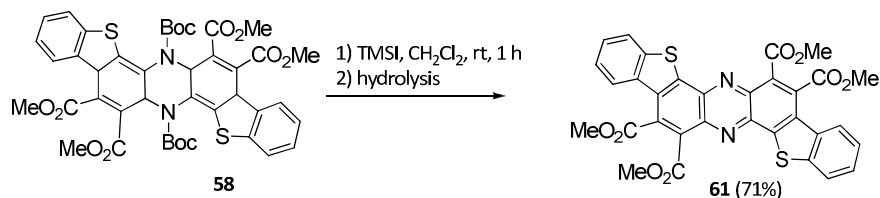


Fig. 94

II.5.5. Aromatization of the polycyclic system

In the aim to get the tetracyclic polyaromatic target compounds, a further aromatization step is needed. This transformation was carried out in the presence of 2 equiv. of DDQ (2,3-dichloro-5,6-dicyano-1,4-benzoquinone) as a mild oxidizing agent in toluene at 90 °C. However, as remaining starting material was present in the reaction mixture, additional of 2 equiv. of DDQ allowed the completion of reaction within 18 h to give after isolation and purification the desired product **62** on a quantitative way (Fig. 95).

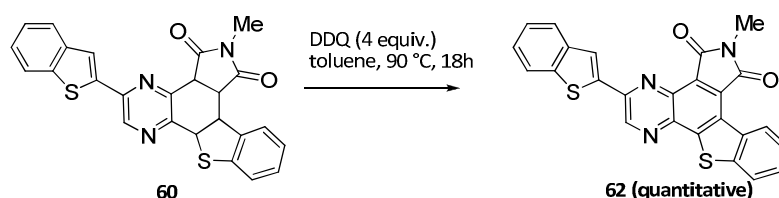


Fig. 95

In order to introduce the diversity on the maleimide nitrogen, we have envisaged to perform trans-imidation reaction in the presence of aminoalcohol or diamine derivative in order to introduce the aminopropyl or hydroxypropyl-group. According to the literature,¹⁸⁹ this reaction is possible for *N*-methyl imides constructed into the cyclic systems (Fig. 96).

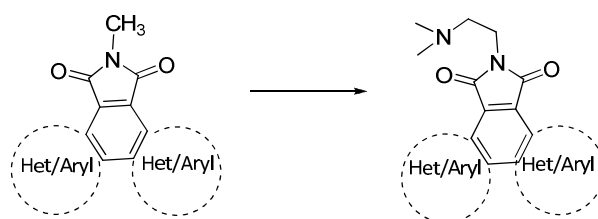


Fig. 96

In this aim, we have conducted the reaction of trans-imidation with *N*-methyl imide **62** in thermal conditions (110 °C) using 3-aminopropanol as solvent. The reaction took 3 hours and converted completely the starting material. The product isolated after precipitation and filtration appeared to be a double hydroxyamide formed by the double nucleophilic attack of the amine group on the open

diamide. By carrying out the reaction at 110 °C under classical heating in the presence of 3-aminopropanol used as solvent, after 3 hours we isolated the difunctionalized adduct in 86 % yield.

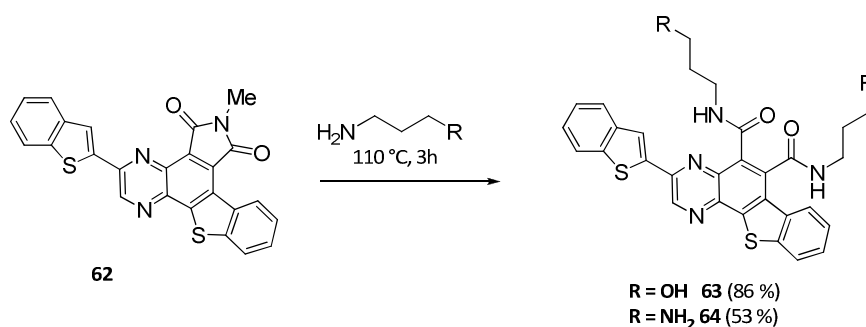


Fig. 97

By using 1,3-diaminopropane, similar results were obtained and the difunctionalized adduct was isolated with 53 % yield (Fig. 97).

In the aim to valorize these results, attempts were made to substitute both primary amine and hydroxyl-functions. We have predicted two possibilities: either the substitution of the hydroxyl groups by the halogen or the formation of esters from alcohols and amides from amino group with bromoacetic bromide. These envisaged products could be attached to the cyclen moiety by the nucleophilic substitution.

II.5.6. Attempts to attach the DO3A moiety

The first tested reaction was the Appel reaction¹⁹⁰ with carbon tetrabromide and triphenylphosphine in toluene at 60 °C. This reaction did not give expected product, only the degradation of starting alcohol. Also, the application of NBS (*N*-bromo succinimide) with PPh₃ in toluene was unsuccessful (Fig. 98).

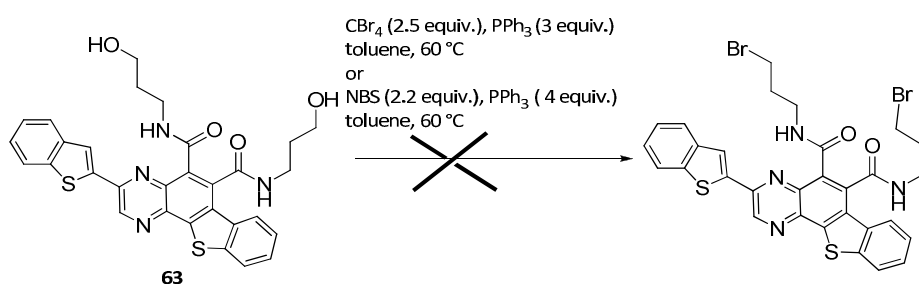


Fig. 98

From the other hand, we predicted the formation of the ester with bromoacetic bromide, this reaction should provide an ester with bromide terminal function. Tested condition (2.5 equiv. of bromoacetic bromide, 5 equiv. Et₃N, CH₂Cl₂ or THF as solvents at 50 to 80 °C) did not lead to the expected product; we observed the decomposition of starting alcohol **62**.

¹⁹⁰ R. Appel, *Angew.Chem. Int. Ed.*, **1975**, *14*, 801.

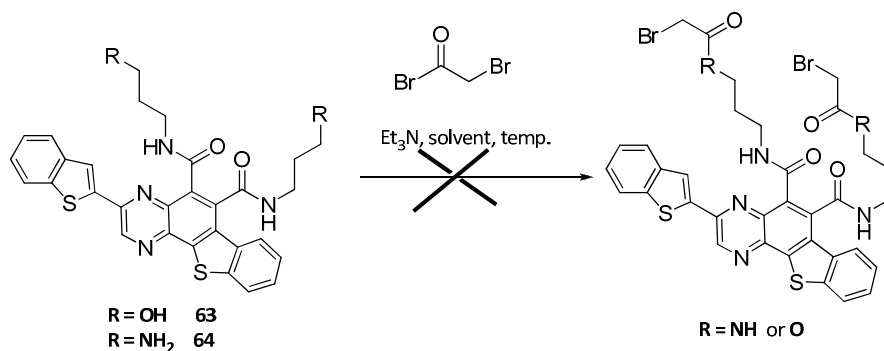


Fig. 99

The same situation was observed in the case of amino derivative **64**. The applied reaction conditions gave only decomposition of starting material (Fig. 99).

II.5.7. Summary

This part of dissertation was devoted to the construction of original antenna systems for lanthanide sensitization based on the condensed polycyclic systems. We were able to develop the synthesis of new polycyclic systems and valorize our starting dihydropyrazine as a valuable diene for the Diels-Alder reaction. Unfortunately, we did not manage to accomplish the goal due to the difficulties arising at the last step of undertaken strategy. We met the problem during the functionalization of hydroxy **63** and amino **64** derivatives to attach them to the DO3A moiety. However, we hope that this reaction may be substituted by other transformation making our polycyclic system valuable chromophore system.

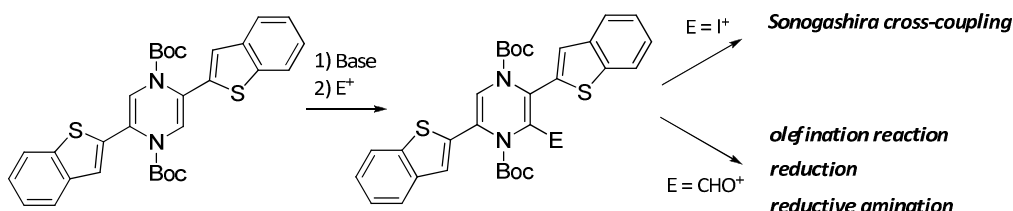
II.6. Second approach

In order to valorize the pyrazinic scaffold in the domain of chromophores for lanthanide sensitization, we wanted to introduce an "easy-to-modulate function", which would serve to construct the spacing arm between the light harvesting center and the chelator of lanthanide. Two different pathways were envisaged.

First, we could introduce a iodide atom, which could be advantageously used in the reaction of palladium-catalyzed cross-coupling (i.e. type Sonogashira). The Sonogashira cross-coupling could give an access to compounds with triple bond, which could be involved in a "click reaction".

Second, an aldehyde function could be submitted to further synthetic transformations (oxidation or reduction, olefination, reductive amination, etc.) and provides hydroxyl, amino, ester, nitrile groups for further modifications.

The both strategies were designed to provide a linkage between the chromophore center and a ligand for lanthanide cations.



Scheme 41 Possible functionalization of 1,4-dihydropyrazine

II.6.1. Construction of spacing arm *via* cross-coupling reaction

In order to construct the spacer by the cross-coupling reaction, the first step requires the introduction of a iodide atom onto the 1,4-dihydropyrazine derivative. The reaction of iodation was conducted under anionic conditions (-78 °C) in anhydrous THF in the presence of an excess of iodide (2.5 equiv.). This reaction provided uniquely to the mono-iodated product **65** in an efficient way (91 %). It is noteworthy that in the presence of HMPA used to stabilize formed anion, we obtained the 3,6-diiodo derivative (**66**) with an excellent yield (93 %).

The elaborated methodology enables to control the synthesis of dihydropyrazines substituted on three of four positions in the case of iodide derivatives. It is worth mentioning that the mixture of mono- and di-iodo-products is impossible to separate by the column chromatography.

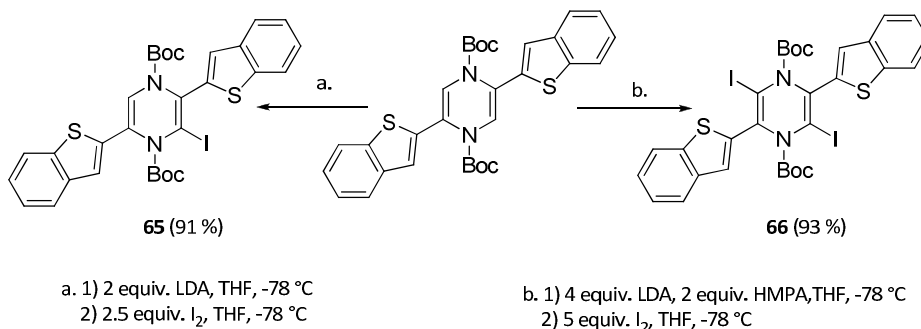
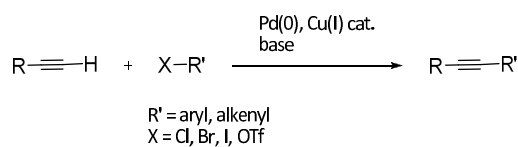


Fig. 100 Regioselective synthesis of mono- and diiodo- derivatives of 1,4-dihydropyrazine

These iodo-derivatives may be applied in the palladium-catalyzed cross-coupling reaction, i.e. Sonogashira type to introduce the triple bond useful from the point of view of cycloaddition reactions.

II.6.1.a. Bibliographic background: Sonogashira cross-coupling

This cross-coupling reaction between terminal alkyne and vinyl or aryl halides was first reported in 1975 by Japanese chemists Sonogashira and Hagihara.¹⁹¹

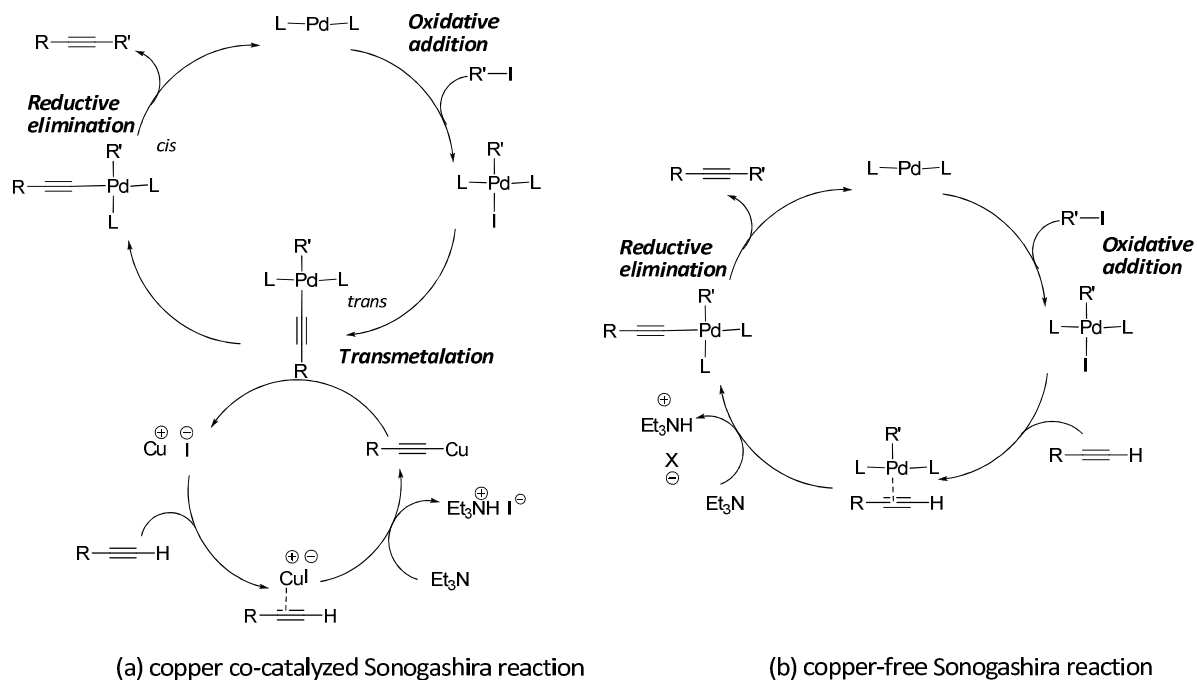


Scheme 42 Sonogashira coupling

The Sonogashira coupling requires Pd(0) complex as catalyst and Cu(I) as co-catalyst. The mechanism of this reaction is not fully understood but theoretical predication indicates an existence of two catalytic cycles (palladium cycle and copper-involved cycle).¹⁹²

¹⁹¹ K. Sonogashira, Y. Tohda, N. Hagihara, *Tetrahedron Lett.*, **1975**, 16, 4467.

¹⁹² R. Chinchilla, C. Nájera, *Chem. Rev.*, **2007**, 107, 874.



Scheme 43 Proposed mechanisms of Sonogashira reaction with copper co-catalyst (a) and without (b)

The main catalytic cycle starts with an oxidative addition to a pre-formed Pd(0) catalyst. Simultaneously, a copper acetylide is believed to be generated in a separate cycle through an activation of the alkyne by coordination of the copper catalyst to form a π -alkyne – Cu complex followed by deprotonation by a base (usually amine bases are applied for Sonogashira coupling). Generally the base is not sufficiently basic to deprotonate the alkyne on its own (pK_a of the base has to be greater than 25), thus a pre-coordination of the alkyne to the metal to form a π -alkyne – Cu complex is probably occurring prior to the formation of the copper acetylide. Formation of a π -alkyne complex facilitates deprotonation of the alkyne due to an increase of the acidity of the C-H bond. This copper acetylide is involved in the transmetalation step with Pd(II) complex. Organic ligands on the Pd center are in the *trans* orientation and they convert to the *cis* isomer. In the final step, the product is released in a reductive elimination, what regenerated Pd(0). The organocopper compound is formed after reaction with a base and continues to react with palladium complex to reconstitute copper halide. It exists also a "copper-free" variant of Sonogashira reaction, called the Heck-Cassar coupling.¹⁹³ In the mechanism of this transformation, the alkyne can be deprotonated by base, and the catalytic cycle can be proceeded as for copper version. However, this reaction depends strongly on the electronic properties of the employed alkyne and the choice of base.

The Sonogashira reaction is very useful transformation to construct the triple bond in complicated systems, enynes and enedynes, which serve as starting materials for cyclizations and synthesis of natural products.

¹⁹³ (a) H. A. Dieck, F. R. Heck, *J. Organomet. Chem.*, **1975**, 93, 259; (b) L. Cassar; *J. Organomet. Chem.*, **1975**, 93, 253.

II.6.1.b. Application of Sonogashira coupling on the compounds **65** and **66**

The Sonogashira coupling was carried out in standard conditions in the presence of trimethylsilylacetylene. The free terminal alkyne may be obtained after desilylation with TBAF.

We conducted our first attempt with $\text{PdCl}_2(\text{PPh}_3)_2$ (10 mol%) as catalyst and CuI (25 mol%) as co-catalyst in freshly distilled triethylamine as solvent with mono-iodide derivative **65**. The reaction mixture was heated at 50 °C and after 40 hours gave complete conversion of starting material. The acidic aqueous work-up and purification by column chromatography provided expected alkyne **67** in excellent yield 91 %.

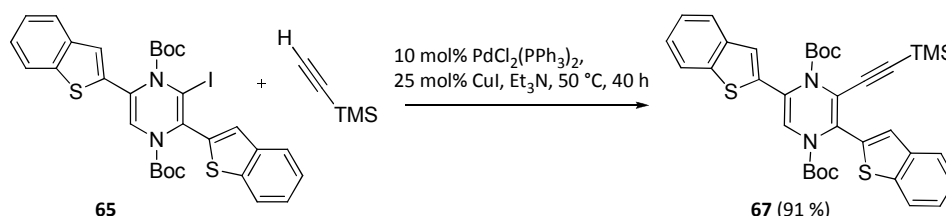


Fig. 101 Sonogashira coupling on the compound **66**

Starting from the diiodo derivative **66** and by doubling the quantity of reactants, we obtained the bis-trimethylsilylalkynyl derivative **68** with good yield (79 %). The reaction was completed after only 4h, the transformation appeared to be very clean and we did not observe any traces of mixed products.

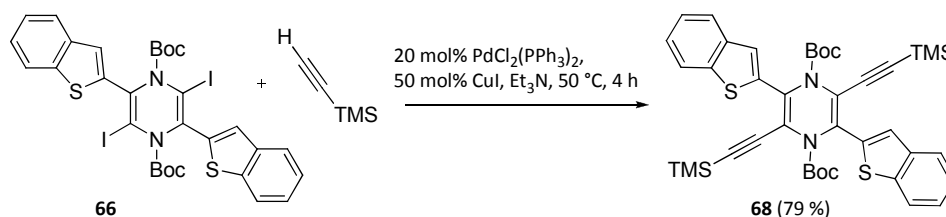


Fig. 102 Sonogashira coupling on the compound **67**

It should be noted that unsuccessful attempts were conducted in order to functionalize only one iodide atom by using 1 equiv. of alkyne derivative. However, in this case, only bis-coupled compound was isolated with unreacted starting material.

II.6.1.c. Background of copper-catalyzed cycloaddition - application "click reaction"

"Click Chemistry" is a term introduced by K. B. Sharpless in 2001 to describe reactions that are high yielding, wide in scope, create only by-products that can be removed without chromatography, are stereospecific, simple to perform, and can be conducted in easily removable or benign solvents. This concept was developed in parallel with the interest within the pharmaceutical, materials, and other industries in capabilities for generating large libraries of compounds for screening in discovery research.

Although meeting the requirements of a "click" reaction is a tall order, several processes have been ascribed to this category. Among them, we can mention nucleophilic ring opening reactions: epoxides, aziridines; non-aldol carbonyl chemistry: formation of ureas, oximes and hydrazones;

addition to carbon-carbon multiple bonds: especially oxidative addition and Michael additions of Nu-H substrates; and cycloaddition reactions: especially 1,3-dipolar cycloaddition. In this work, we will focus on the last transformation.

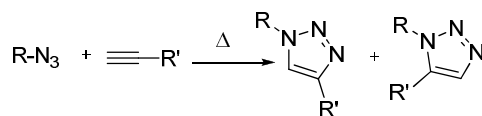


Fig. 103

The Huisgen 1,3-dipolar cycloaddition between azide and terminal alkyne often provides a mixture of two regioisomers of triazole (1,4 and 1,5 substituted) and it requires elevated temperatures. However, it is considered as an example of click chemistry just after one small modification: an application of metal catalysts. The copper(I)-catalyzed variant was first reported in 2002 in independent publications by Meldal¹⁹⁴ and Sharpless.¹⁹⁵ This reaction is better termed the Copper(I)-catalyzed Azide-Alkyne Cycloaddition (CuAAC). A copper-catalyzed variant can be conducted under aqueous conditions, even at room temperature.

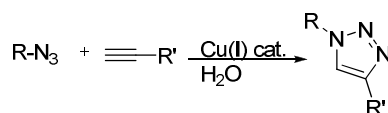


Fig. 104

The ruthenium-catalysed 1,3-dipolar azide-alkyne cycloaddition (RuAAC)¹⁹⁶ gives the 1,5-triazole. Unlike CuAAC in which only terminal alkynes reacted, in RuAAC both, terminal and internal alkynes can participate in the reaction. This suggests that ruthenium acetylides are not involved in the catalytic cycle.

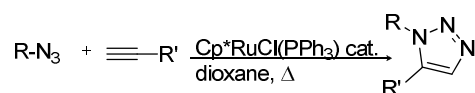


Fig. 105

Mechanism of CuAAC was first established by Sharpless *et al.*¹⁹⁷ based on the DFT calculations. The copper (I) species generated in situ forms a π complex with the triple bond of a terminal alkyne. In the presence of a base, the terminal hydrogen, being the most acidic is deprotonated first to give a Cu acetylide intermediate. The ligands employed are labile and are weakly coordinating. The azide displaces one ligand to generate a copper-azide-acetylide complex. At this point cyclization takes place. This is followed by protonation; the source of proton being the hydrogen which was pulled off from the terminal acetylene by the base. The product is formed by dissociation and the copper catalyst complex is regenerated for further reaction cycles.

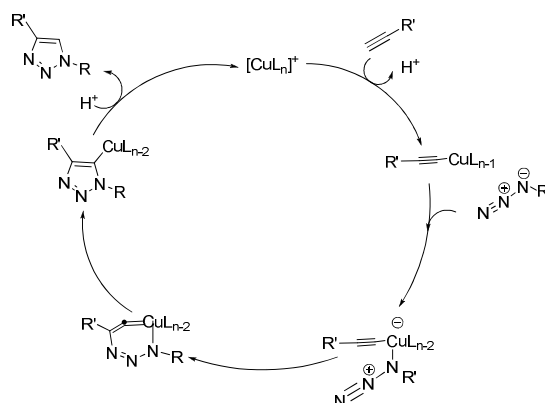
¹⁹⁴ C. W. Tornøe, C. Christensen, M. Meldal, *J. Org. Chem.*, **2002**, *67*, 3057.

¹⁹⁵ V. V. Rostovtsev, L. G. Green, V. V. Fokin, K. B. Sharpless, *Angew. Chem. Int. Ed.*, **2002**, *41*, 2596.

¹⁹⁶ B. C. Boren, S. Narayan, L. K. Rasmussen, L. Zhang, H. Zhao, Z. Lin, G. Jia and V. V. Fokin, *J. Am. Chem. Soc.*, **2008**, *130*, 8923.

¹⁹⁷ F. Himo, T. Lovell, R. Hilgraf, V. V. Rostovtsev, L. Noodleman, K. B. Sharpless, V. V. Fokin, *J. Am. Chem. Soc.*, **2005**, *127*, 210.

In the reaction without the catalyst, the alkyne remains a poor electrophile. Thus high energy barriers lead to slow reaction rates. The reaction is assisted by copper, which, when coordinated with the acetylide lowers the pKa of the alkyne C-H by up to 9.8 units. Under certain conditions, the reaction may be carried out even in the absence of a base.



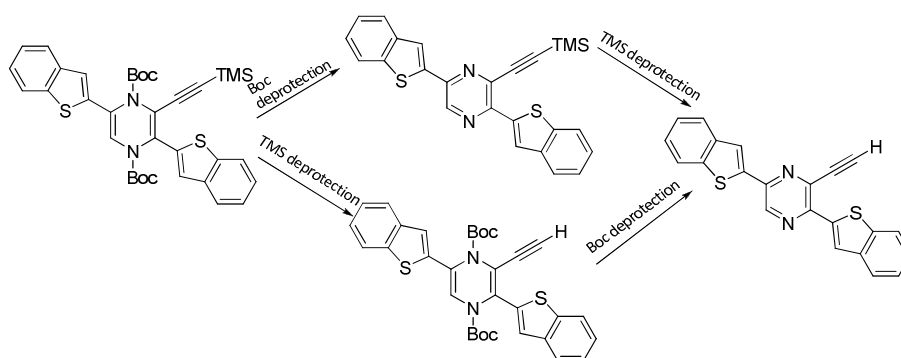
Scheme 44

The copper(I)-catalyzed cycloaddition is considered as bioorthogonal reaction due to the high specificity and the biocompatibility of reactants. It may be carried out in aqueous media; respective triazols may be obtained from biomolecules after simple modification. Neither azides nor alkynes react with other functional groups commonly present in biomolecules, there is no need for protecting groups.

In the course of our investigation, we envisaged the introduction of spacing arm by applying the “click reaction” with alkyne function already introduced onto the dihydropyrazine moiety, in order to insert different functional groups and then to attach the DO3A ligand.

II.6.1.d. Attempts of alkyne deprotection and click reaction

In the first attempt, we predicted the deprotection of the dihydropyrazine moiety, followed by the deprotection of TMS group, however this synthetic pathway could not be achieved. The complete degradation of starting product **67** was observed. We tested the deprotection of *tert*-butoxycarbonyl groups in acidic conditions in the presence of TFA (10 equiv.) in CH₂Cl₂ at room temperature and at 0 °C.



Scheme 45

Thus, we decided first to deprotect the TMS group and after the “click reaction”, and to remove the *t*Boc group to have an access to pyrazines. The trimethylsilyl group can be cleaved in the presence of tetrabutylammonium fluoride (TBAF) in mild conditions (0 °C to room temperature). We have tested this deprotection step on the compound **67** with 2.2 equiv. of TBAF, but even after long time of contact (3 days) we observe only partial conversion of starting material.

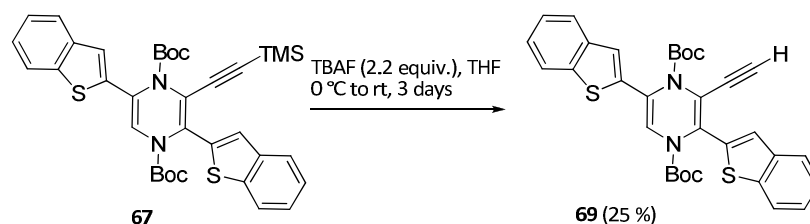
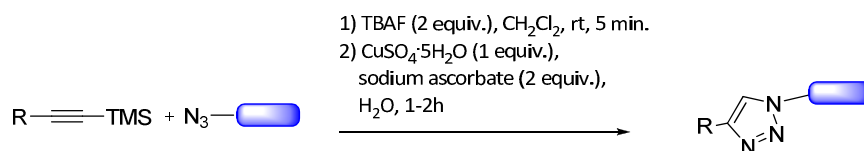


Fig. 106 Deprotection of compound 66

According to recent results described in the literature, we thought to perform a direct “click reaction” on the TMS-protected alkynes with the deprotection step *in situ*,¹⁹⁸ in order to optimize this step.



Scheme 46 Click reaction with TMS-protected alkyne

We decided to apply the same methodology to our compounds. We wanted to test the copper-catalyzed cycloaddition reaction on the easy to synthesized model compounds and at the same time, introduce the functional group at the end of chain. The azide from 2-(2-benzyloxy-ethoxy)-ethanol and 3-aminopropanol were formed in two-step synthesis. These compounds were predicted to introduce the hydroxy- and amino group to our dihydropyrazine derivatives.

We have started from 2-(2-benzyloxy-ethoxy)-ethanol, which was first treated with methanesulfonyl chloride in the presence of triethylamine to form mesylate, a good nucleofuge. This mesylate was used without any purification and submitted to nucleophilic substitution in the presence of sodium azide. This two-step synthesis gave a desired azide **70** in good yield (52 %).

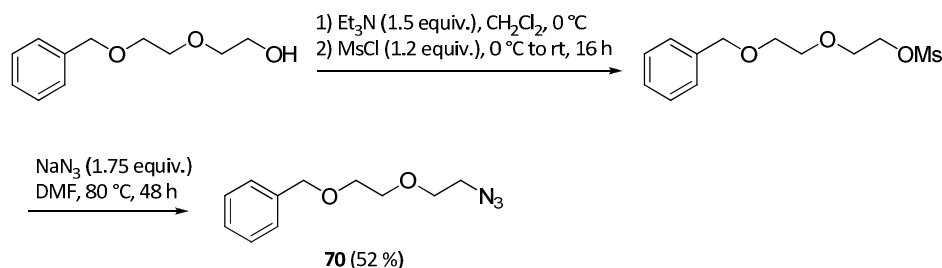


Fig. 107 Formation of [2-(2-azido-ethoxy)-ethoxymethyl]-benzene **70**

¹⁹⁸ C. Li, E. Henry, N. K. Mani, J. Tang, J.-C. Bronchon, E. Deprez, J. Xie, *Eur. J. Org. Chem.*, **2010**, 2395.

The same procedure was applied to 3-aminopropanol. In this case, we observed the formation of mesylate and of methylsulfonamide from the primary amino group **71**. This synthesis yielded only 20 % of good product.

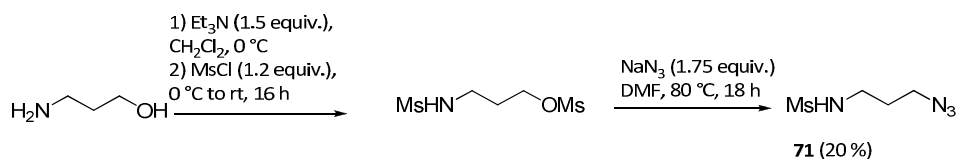


Fig. 108 Synthesis of *N*-(3-azidopropyl)methanesulfonamide **71**

These products are good partners of copper-catalyzed cycloaddition reaction, because they are water-soluble, potentially easy to deprotect giving access to free alcohol or amine possible to functionalize *via* DO3A substitution.

II.6.1.e. Tests of copper-catalyzed cycloaddition

The obtained products **67** and **68** were subsequently used in the “click reactions” with azides in the aim to create the linkage for the DO3A attachment. The copper-catalyzed cycloaddition was preferably chosen in view of its great bioavailability, the aqueous operational conditions and the possibility to introduce the diverse functional groups.

As it was previously presented, TMS-protected alkyne derivatives **67** and **68** were cleaved with difficulty. Notwithstanding we decided to use them directly in the click reaction, trying the *in situ* deprotection with an excess of TBAF (4 equiv. for one TMS group). Effectively, this procedure applied to the products **68** and **69** which provided respectively the cycloadducts **70** and **71** with mild yields (53 % and 45 %).

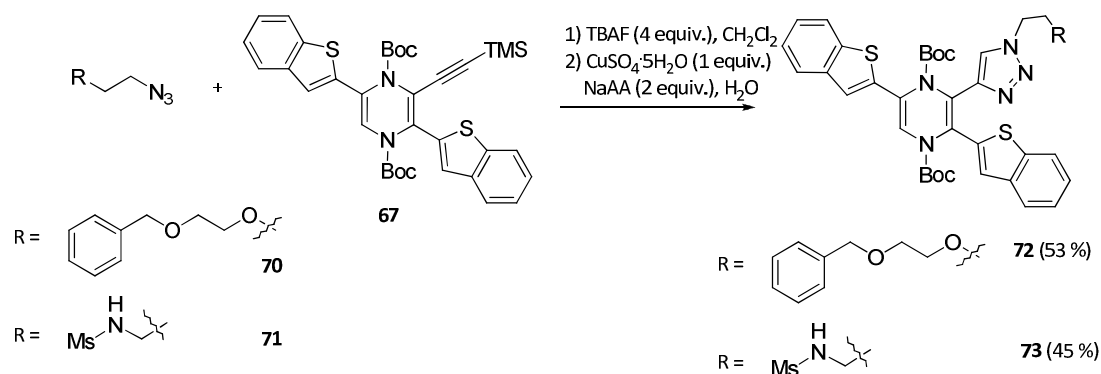


Fig. 109

The same strategy was applied to the double substituted alkyne **67** providing double cycloadducts **72** and **73** with lower yields (35 % and 30 % respectively). This was probably due to the steric hindrance around the pyrazinic core and the difficulty to form the catalytic copper-complex. From the other hand, we did not use any ligands for copper and that could also affect the results. These reactions should be optimized in order to improve the yield of the double cyclization.

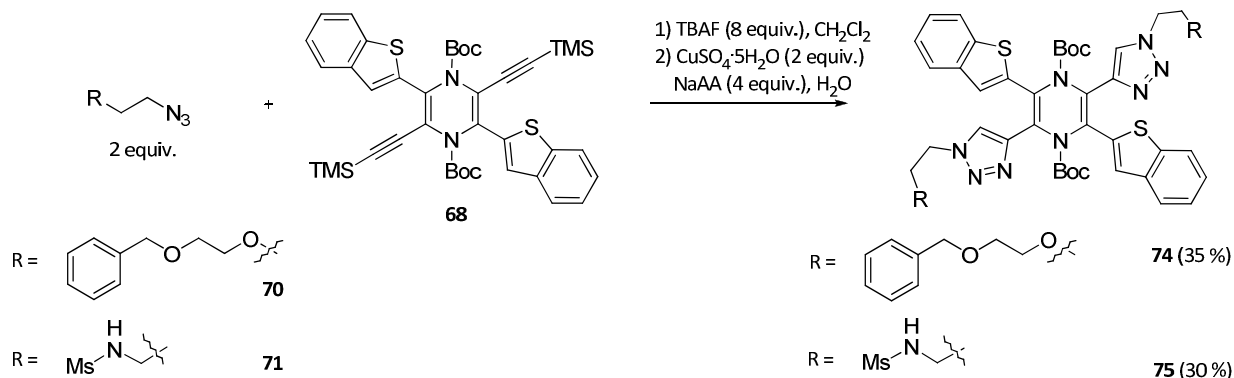


Fig. 110

II.6.1.f. Attempts of deprotection

The step leading to the antenna system is a deprotection of benzyl or mesyl group and *tert*-butyloxycarbamates. First, we tried to perform the deprotection step starting from compound **74** in the presence of 10 % Pd/C using an atmospheric pressure of H₂ at room and at elevated temperature. In each case, only starting materials were recovered; no trace of the expected product was observed.

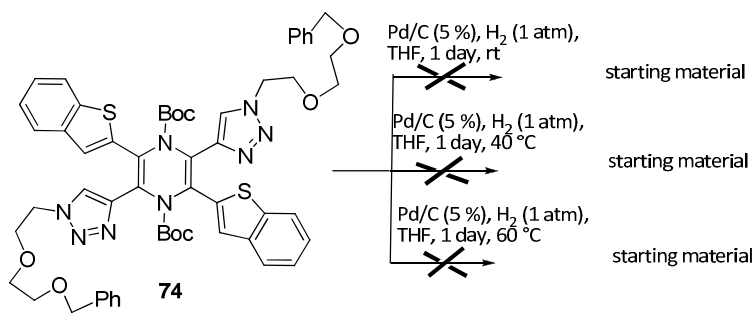


Fig. 111

At the same time, we were testing the deprotection reaction in acidic conditions, hoping that we would manage to unprotect two blocking functions in one step. The triisopropyl silane (TIS) was used as scavenger for free radicals. Unfortunately, this reaction also did not result in deprotection, even by using a large excess (10 and 45 equiv.) of trifluoroacetic acid at 0 °C or ambient temperature. The last attempt was to treat the cycloadduct **74** with the electrophile TMSI at 0 °C. This reaction provided complete decomposition of the starting product.

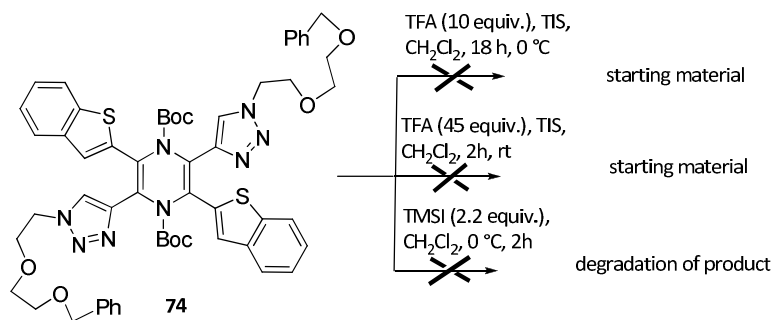


Fig. 112

These failed attempts did not allow achieving the construction of the spacing arm, to attach DO3A moiety. However, the application of other protecting functions may be considered. At the same time, we proved that the copper-catalyzed cycloaddition is possible for our model compounds. The proper protecting group should be applied.

II.6.2. Summary

In the above paragraph we were considering the usefulness of our dihydropyrazine system in the reaction of copper-catalyzed cycloaddition. Indeed, this molecule could be transformed after the iodation reaction into the alkyne - derivative and then directly used in the “click reaction” with diverse azides. However, we did not manage to unprotect our pyrazinic core. In the perspective of this part of project, we envisage to connect the derivatized cyclen molecule (**53**).

II.7. Construction of the spacing arm starting from a key aldehyde function

The formylation reaction permits the introduction of an aldehyde group onto the 1,4-dihydropyrazine system in the chosen position. This reaction was conducted under anionic conditions, treating the starting dihydropyrazine with 4.0 equiv. of LDA in the presence of 2.0 equiv. of HMPA. Introduction of DMF (5.0 equiv.) provided the aldehyde derivative **76** after a 5h reaction.

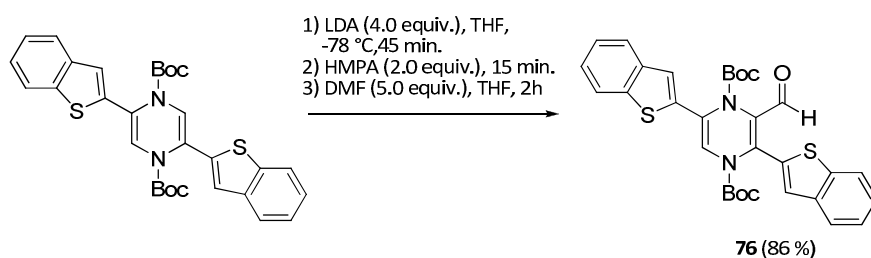
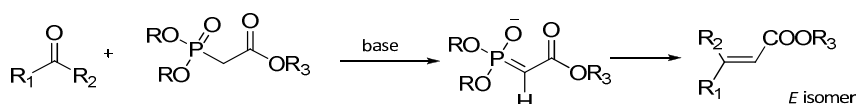


Fig. 113 Formylation reaction

We did not observe any product resulting of a double insertion of the aldehyde function, neither the deprotonation of thiophenic positions. The only by-product of this transformation was the carboxylic acid, which degraded directly after purification by flash chromatography. The aldehyde **74** was then subjected to Wittig-Horner-Emmons olefination reaction.

II.7.1. Wittig-Horner-Emmons olefination reaction

The Wittig - Horner reaction (called also Horner-Wadsworth-Emmons reaction) is the variant of the Wittig reaction for aldehydes or ketones with stabilized phosphorus ylides (phosphonate carbanions), which leads to olefins with excellent *E*-selectivity (Scheme 47).



Scheme 47

As first reported by Horner,¹⁹⁹ carbanionic phosphine oxide can be used; today carbanions from alkyl phosphonates are most often used. The latter are easily prepared by application of the Arbuzov reaction. The reactive carbanionic species are generated by treatment of the appropriate phosphonate with base (i.e. sodium hydride).

The reaction mechanism is similar to the mechanism of the Wittig reaction. The stereochemistry is set by a steric approach control, where the antiperiplanar approach of the carbanion to the carbon of the carbonyl group is favored when the smaller aldehydic hydrogen eclipses the bulky phosphoranyl moiety. This places the ester group syn to the aldehyde R group, but the incipient alkene assumes an *E*-orientation of these groups after rotation to form the oxaphosphetane.

The reaction of Wittig-Horner-Emmons is a very convenient transformation to get olefins with various terminal chains. Because of the reliability and wide applicability, the Wittig reaction and variations has become a standard tool for synthetic organic chemists. They are used as key steps in many organic syntheses of natural products,²⁰⁰ in the late stage of multi-step synthetic sequences.²⁰¹ A real advantage of this transformation is that both *Z* and *E* isomers of alkene are available by choosing the reaction conditions.

In the course of our work, diethylcyanomethyl phosphonate and triethyl phosphonoacetate has been chosen as active substrates for Horner-Wadsworth-Emmons (HWE) reaction because of their very active carbanions in α position to the phosphonate. As well, these substrates allow different modifications on the terminal functions leading to possible connection with the chelating system for lanthanides - DO3A.

First, the appropriate carbanion was formed in the presence of NaH, then the addition of aldehyde **76** provided after several hours desired products bearing a nitrile (**77**) and ester (**78**) group in a very efficient way (92 % and 80 %, respectively) (Fig. 114).

¹⁹⁹ L. Horner, H. Hoffmann, H. G. Wippel, G. Klahre, *Chem. Ber.*, **1959**, *92*, 2499.

²⁰⁰ K. C. Nicolau, M. W. Härter, J. L. Gunzner, A. Nadin, *Eu. J. Org. Chem.*, **1997**, *7*, 1283.

²⁰¹ G. Pattenden, A. Walter, S. J. Woodhead, *Natural Product Synthesis*, **2004**, *101*, 12024.

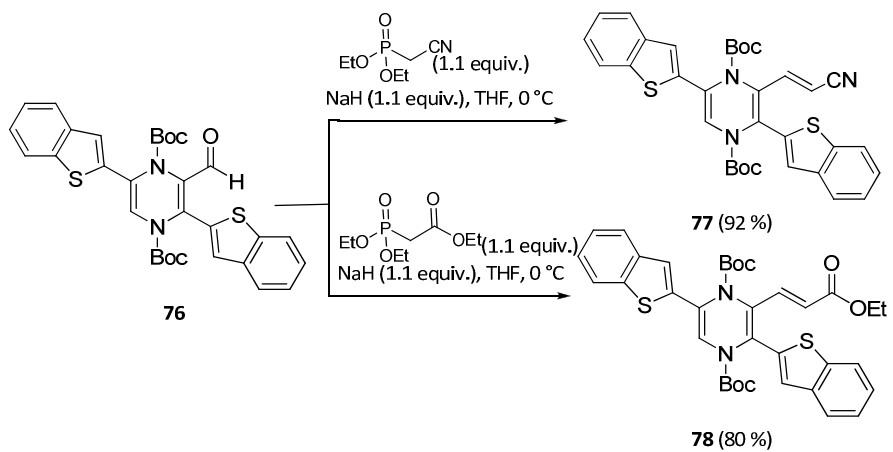


Fig. 114

The following step of spacing arm formation involves the deprotection of dihydropyrazine moiety leading to free pyrazine core.

II.7.1.a. Formation of pyrazinic core

The removal of *tert*-butylcarbamate function was undertaken in order to form aromatized pyrazinic core. Two possible protocols were tested: the treatment of TMSI (4.8 equiv.) at 0 °C and ambient temperature, and the deprotection in the presence of trifluoroacetic acid at 0 °C. The reaction in acidic conditions did not provide the good product in both cases, but the attack of strong electrophile TMSI led to the good unprotected pyrazine. The application of TMSI in anhydrous conditions on ester **78** gave the pyrazine **79** with reduced double bond in a 76 % yield.

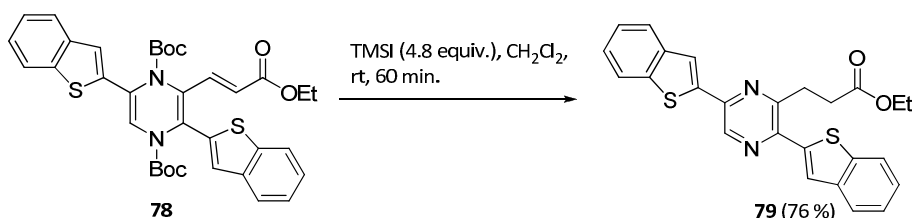


Fig. 115

However, in the case of nitrile derivative **77** we noticed a partial reduction of the double bond, depending on the quality of TMSI, the time of contact, and the temperature of reaction.

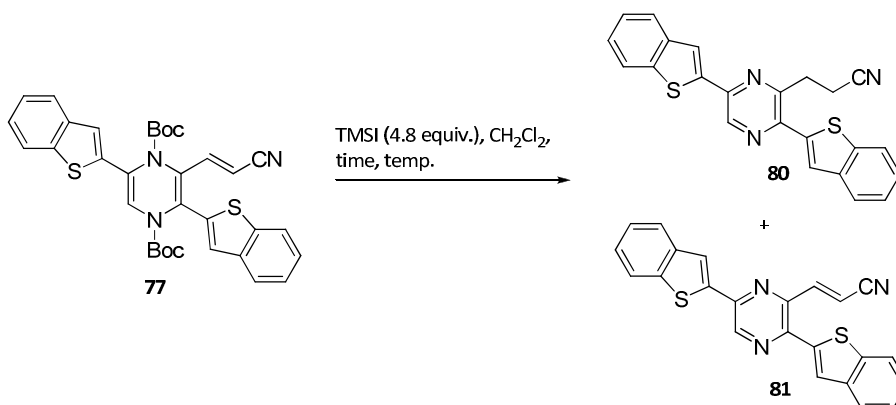


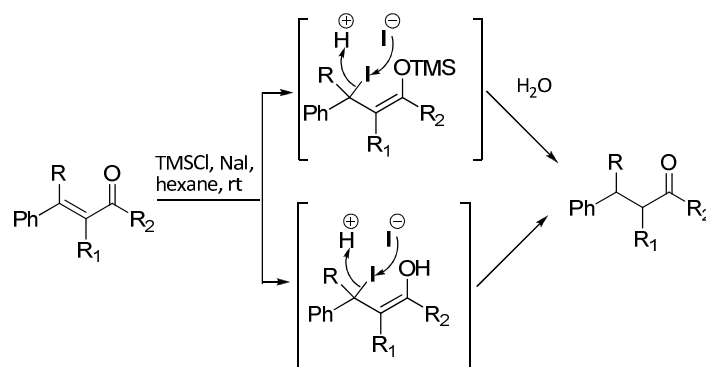
Table 18 Optimization of the deprotection reaction of nitrile

Entry	TMSI (equiv.)	Temp.	Time	Yield [%] (ratio 80:81)
1	4.8	rt	30 min.	72 (50:50)
2	4.8	rt	60 min.	76 (40:60)
3	6.0	0 °C	60 min.	61 (60:40)
4	6.0	0 °C	3 h	53 (100:0)
5	2.4	rt	60 min.	16 (50:50)

As it was presented in Table 18, the obtainment of reduced product varied largely in the applied conditions. Increasing the time of contact (Table 18, Entry 1 and 2), we observed the increase of quantity of unsaturated nitrile **81**. From the other hand, the increase of number of equivalents of TMSI provoked the reduction of double bond and provided the product **80** (Table 18, Entry 3 and 4). At the same time, the lower number of equivalents of TMSI gave equimolar mixture of products **80** and **81**.

The best results were obtained with freshly open bottle of TMSI, after stirring for 60 minutes at room temperature (Table 18, Entry 2).

Trying to understand the mechanism of deprotection and partial reduction of the double bond in the presence of TMSI, we found some examples in the literature, which describe similar phenomenon.²⁰² In the case of an α,β -unsaturated ester, the reaction is initiated by 1,4-addition of TMSI to produce a β -iodo enol silyl ether intermediate, whose allylic and benzylic iodo substituent will be extremely labile and attacked by an iodide anion existing in milieu, to generate the iodine molecule.



Scheme 48

Also we have described an experiment which proves that, by using the reactant TMSI, we can have a liberation of HI in these reaction conditions. To prove the presence of HI, we carried out an experiment with norbornen. We added the same number of equivalents of TMSI (4.8 equiv.), as in the typical deprotection reaction, to the solution of norbornen in CH_2Cl_2 and we observed the addition of HI onto the double bond. The same situation took place with freshly prepared TMSI from TMSCl and NaI in acetonitrile (Fig. 116).²⁰³

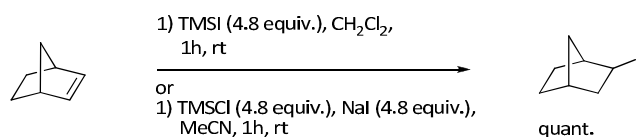


Fig. 116

Thus, the reaction of deprotection of ester **78** was carried out in the presence of norbornen. Taking into account that in the case of deprotection of this ester, the complete reduction of the double bond occurred, we wanted to trap the HI by addition of an equimolar amount of norbornen. However, the reaction of ester **78** with norbornen provided only the saturated pyrazinic ester **79** in 40 % yield and the iodo – bicycle[2.2.1]heptane. In the case of *in situ* produced TMSI from TMSCl and NaI, we obtained also the ester **79** in 51 % yield and a product of complete addition of HI to norbornen.

²⁰² (a) J. M. Robinson, G. T. Daniel, S. J. Hale, *J. Org. Chem.*, **1986**, *51*, 109; (b) T. Sakai, K. Miyata, M. Utaka, A. Takeda, *Bull. Chem. Soc. Jpn.*, **1987**, *60*, 1063.

²⁰³ S. Irifune, T. Kibayashi, Y. Ishii, M. Ogawa, *Synthesis*, **1988**, *5*, 366.

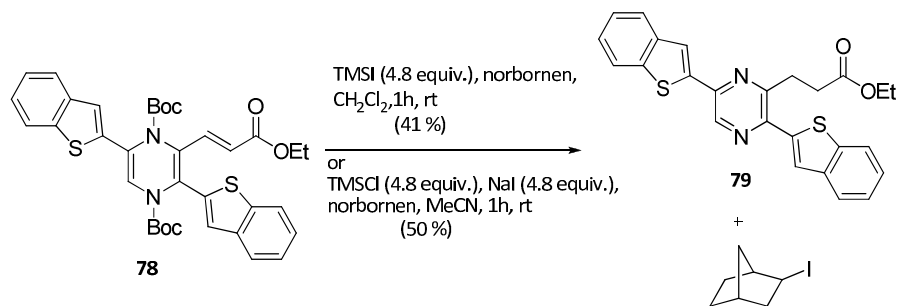
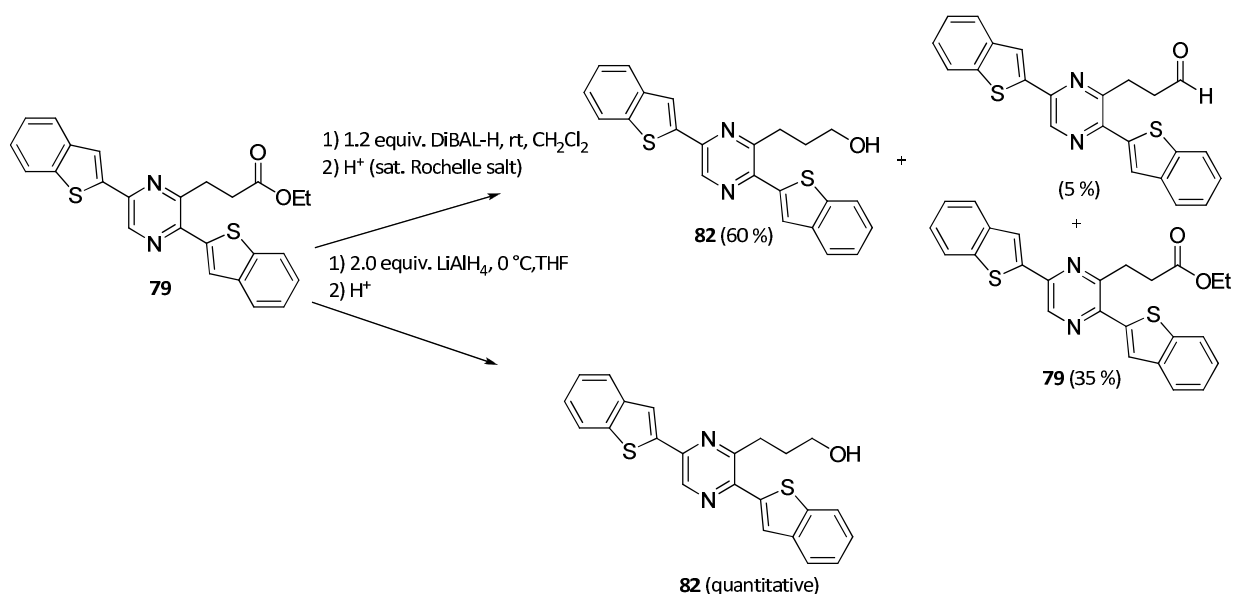


Fig. 117

These experiments proved that we have got a hydroiodide in the reaction, which is responsible for the reduction of the double bond. In the same time, we did not manage to avoid this reaction by addition of norbornene as a "sponge" for created HI.

II.7.1.b. Reduction of ester and formation of compatible function to attach the DO3A

The reduction of ester **79** was first conducted with DiBAL (1.2 equiv.) at 0 °C, but in these conditions, the starting material remained intact. After increasing the temperature to 20 °C, a mixture of aliphatic alcohol **82**, traces of aldehyde and an ester were obtained. The ratio of each compound was determined by ¹H NMR of the crude, but the isolation of an aldehyde derivative was not possible by column chromatography. Then, the complete reduction of α,β -unsaturated ester was conducted in anhydrous THF in the presence of LiAlH₄ (2.0 equiv.) at 0 °C to give quantitatively the alcohol **82**.



Scheme 49

For the next investigations, we focused on the alcohol **82**, which can be modified in the reaction of exchange of hydroxyl group to halogen (Br, I) or the esterification reaction with bromoacetic bromide. Our aim was to introduce a functional group compatible with the DO3A attachment.

The bromide derivative **83** was obtained using standard conditions (PPh₃, NBS, DMF, 30 min., 60 °C) or in the Appel conditions (PPh₃, CBr₄, DMF, 18h, rt) with respective yields (66 % and 80 %). The iodide **84** was isolated in 67 % yield by reacting the compound **82** in the presence of PPh₃, imidazole and I₂ in

toluene at 60 °C. As well, the treatment of alcohol **80** with bromoacetic bromide in the presence of Et₃N gave the bromo - ester **85** with correct efficiency (79 % yield).

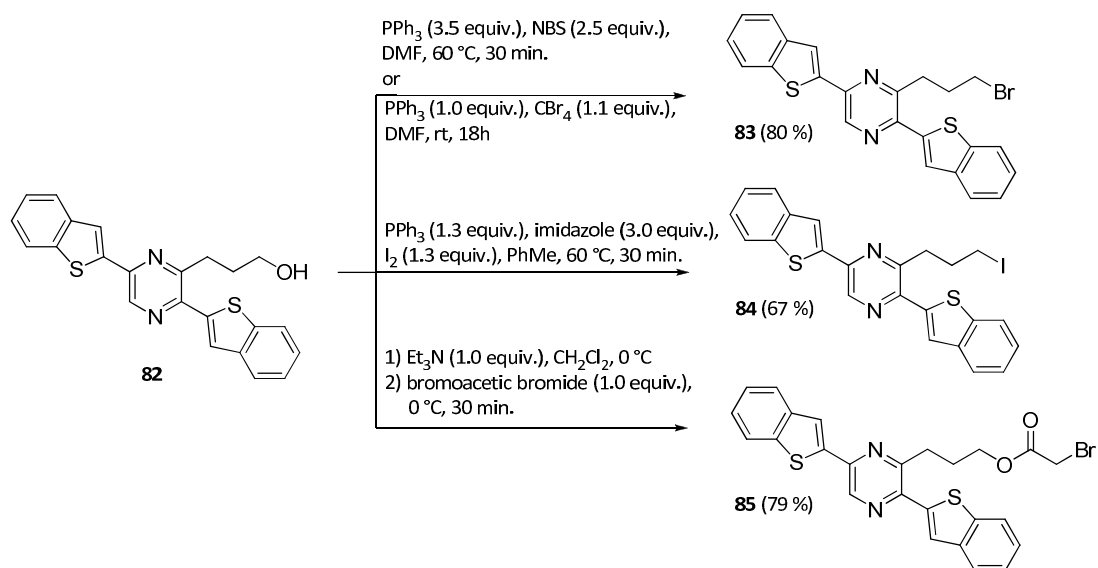


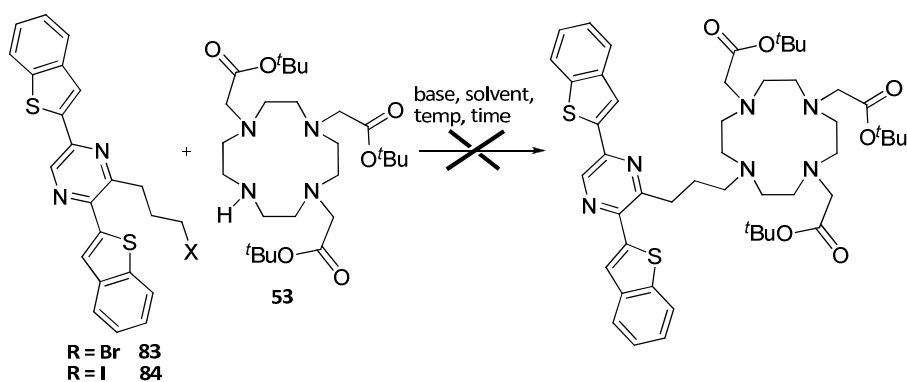
Fig. 118

Having in hand these newly synthesized electrophilic derivatives, they were submitted to nucleophilic substitution in the presence of cyclen DO3A derivative **53**. According to the literature conditions,¹⁵⁷ a first attempt was carried out in the presence of Et₃N (2.0 equiv.) in acetonitrile with bromide derivative **83**. A reaction was carried out for 60 h at 80 °C and with complete consumption of starting material **83**. However, after work-up and purification by column chromatography, only starting cyclen and the by-product were obtained. We supposed that bromide derivative **83** eliminates HBr in the long heating reaction and forms the (dibenzo[*b*]thiophen-2-yl)pyrazine bearing an allylic chain. We decided therefore to change the base for Na₂CO₃ and solvent for THF.²⁰⁴ However, in these conditions we observed also the formation of by-products instead of expected one. The same situation was observed with a stronger base K₂CO₃.²⁰⁵ That is why we abandoned the nucleophilic substitution with bromide derivative **83** and moved to the iodide **84**, supposed to show higher reactivity. First we attempted the substitution with triethylamine under reflux of acetonitrile, but without success. Next, we tested inorganic base K₂CO₃ and here, once again, we observed the elimination of halogen and we recovered intact DO3A product. These reactions failed because of the low nucleophilicity of the secondary amine - DO3A, and at the same time, the low stability of tested halogens' derivatives **83** and **84** in applied conditions.

²⁰⁴ M. Botta, S. Quici, G. Pozzi, G. Marzanni, R. Pagliarin, S. Barra, S. G. Crich, *Org. Biomol. Chem.*, **2004**, *2*, 570

²⁰⁵ N. Raghunani, G. P. Guntle, V. Gokhale, G. S. Nichol, E. A. Mash, B. Jagadish, *J. Med. Chem.*, **2010**, *18*, 6746

Table 19



Entry	X	Base	Solvent	Temp.	Time
1	Br	Et ₃ N	Acetonitrile	80 °C	60 h
2	Br	Na ₂ CO ₃	THF	66 °C	16 h
3	Br	K ₂ CO ₃	THF	66 °C	16 h
4	I	Et ₃ N	Acetonitrile	80 °C	60 h
5	I	K ₂ CO ₃	THF	66 °C	60 h

Finally, we decided to apply brominated ester **85**, a better source of electrophilic bromine, to carry out the nucleophilic substitution with the secondary amine. According to the literature,²⁰⁶ we dissolved the DO3A derivative in THF and suspended Na₂CO₃ to activate the secondary amine. Then, the solution of ester **85** was added and the mixture was heated for 20 h under reflux of THF. After this time, complete consumption of both starting materials was observed and desired DOTA derivative **86** was isolated in a good yield 73 %. This product was subjected to the deprotection of *tert*-butyl esters in order to liberate the acid functions, necessary for the metal complexation.

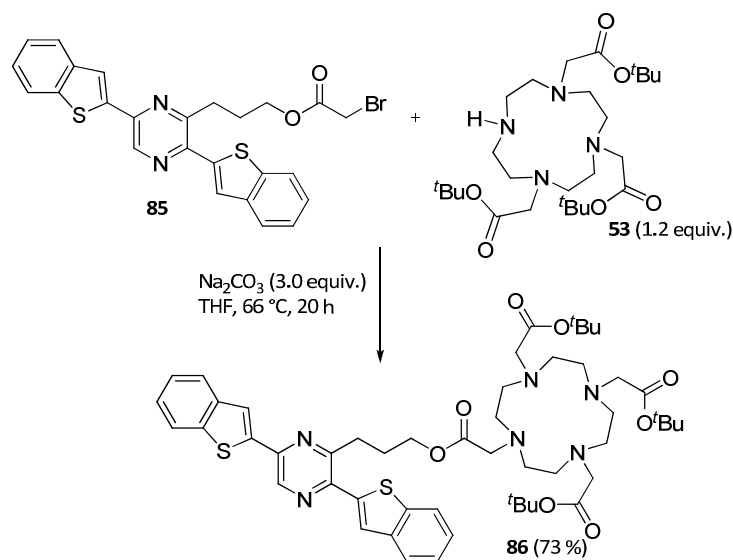


Fig. 119

²⁰⁶ C. Tu, E. A. Osborne, A. Y. Louie, *Tetrahedron*, **2009**, *65*, 1241.

II.7.1.c. Reduction of nitrile, formation of amide and S_N on cyclen derivative

At the same time, we have envisaged the connection of cyclen moiety *via* an amide bond. In this aim, we wanted to reduce the nitrile derivative **81** to obtain a primary amine. However, the reduction appeared to be more complicated than it was supposed. As it was explained in the paragraph II.7.1.a, after the deprotection of dihydropyrazine moiety with terminal nitrile group, the mixture of reduced and non-reduced product, impossible to separate by the column chromatography, was obtained. In the first approach, this mixture was directly applied to the reduction step in the presence of LiAlH₄ in THF at room temperature.

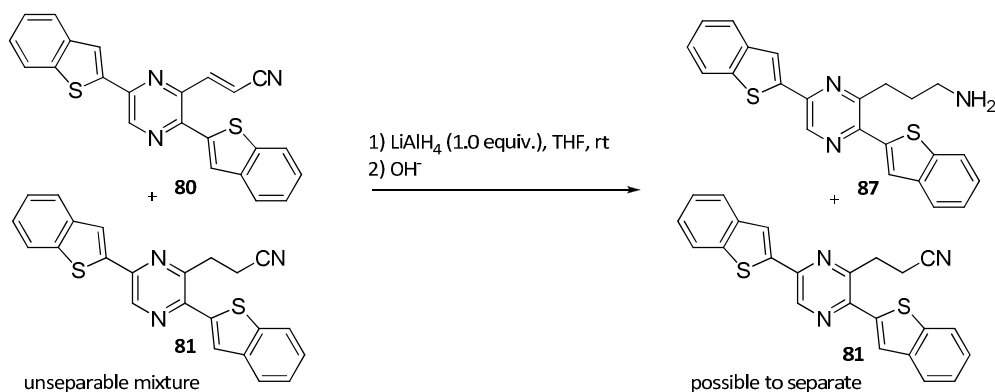
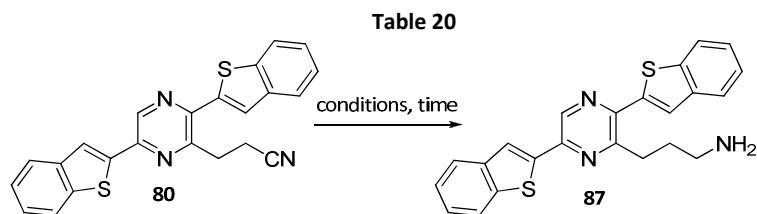


Fig. 120

We observed that some part of mixture (the unsaturated nitrile) undergoes the reduction, giving the amine **87**. Saturated nitrile **80** does not react in these conditions. However, during all the test of deprotection, we recovered much more of the saturated nitrile, than unsaturated one. Thus, we wanted to use this product in the reduction step, testing different conditions, presented in Table 20.



Entry	Conditions	Time	Results
1	1) LiAlH ₄ (2 equiv.), THF, t.a. 2) H ⁺ , H ₂ O	16h	No reaction
2	H ₂ , Pd/C, MeOH, rt	72h	Degradation
3	1) CoCl ₂ , MeOH, 0 °C 2) NaBH ₄ , 0 °C → rt 3) H ⁺ , H ₂ O	30 min. 1h	Degradation
4	NH ₂ NH ₂ ·H ₂ O, Ni Raney EtOH, 50 °C	18h	Degradation
5	H ₂ (80 psi), (CF ₃ CO) ₂ O, Ni Raney, THF, 30 °C	18h	Not isolable

The degradation of starting material was observed by using hydrogen under atmospheric pressure with Pd/C catalyst, using NaBH₄ with CoCl₂ and also in the presence of hydrazine with Ni Raney catalyst (Entry 2, 3 and 4). The reduction with Ni Raney in the presence of trifluoroacetic acid anhydride gave a non-isolable product.

The amine derivative **87**, obtained from the reduction of the mixture of nitrile derivatives (Fig. 120), was transformed into the amide **88** in a good yield (75 %) by reaction with bromoacetic bromide, according to conditions already described for ester derivative **85**. This amide was subjected to the nucleophilic substitution with DO3A, giving product **89** isolated in good yield (75 %) – Fig. 121.

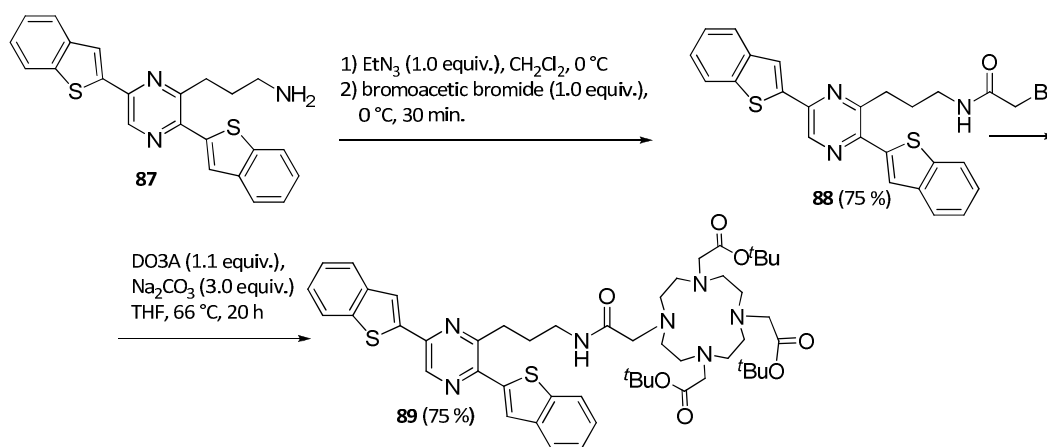


Fig. 121

II.7.1.d. Deprotection and complexation step

According to the literature,^{158,160} the cleavage of *tert*-butyl esters may be conducted in an excess of trifluoroacetic acid in dichloromethane at 0 °C. We applied these conditions to ester derivative **84**. After overnight stirring, we did not observe any conversion of starting materials. Therefore, we warmed the reaction to room temperature without any success. By increasing the temperature to reflux of CH₂Cl₂, the cleavage of pyrazinc ester was observed. The use of formic acid at room temperature afforded a complete decomposition of starting material.

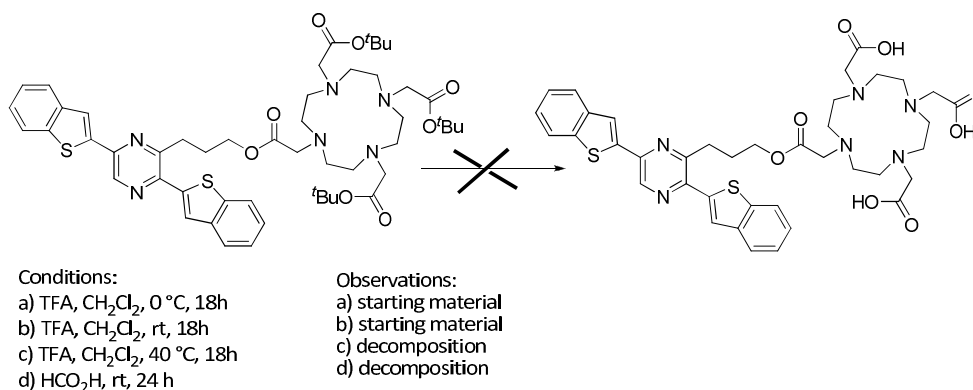


Fig. 122

These results indicate that the ester derivative **86** will be difficult to unprotect without the cleavage of molecule and a change of protecting group in cyclen derivative should be envisaged.

Subsequently, we moved forward to the amide product **89** regarding the higher stability of amide bond to the cleavage in acidic conditions. The product **89** was dissolved in a mixture TFA/CH₂Cl₂ (50/50 % vol) with 2%vol of triisopropylsilane as scavenger for formed carbocations. The reaction took 16 hours and gave expected triacetic acid **90** in an excellent yield (94 %).

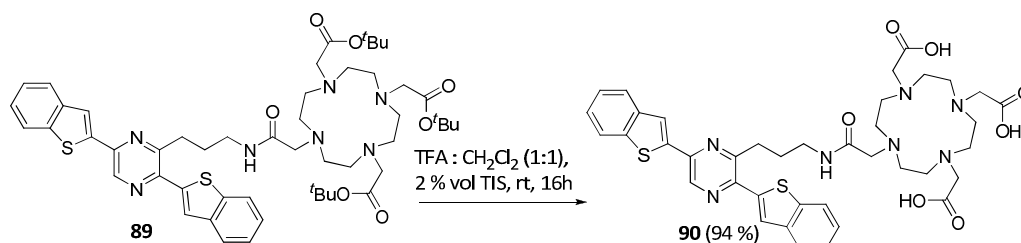


Fig. 123

This product was directly involved in the complexation reaction with triflate salts of neodymium, ytterbium and gadolinium in order to get lanthanide complexes. The complexation reaction was carried out in methanol, in equimolar amounts of chelate and lanthanide salt, by heating at 50 °C for 16 hours.

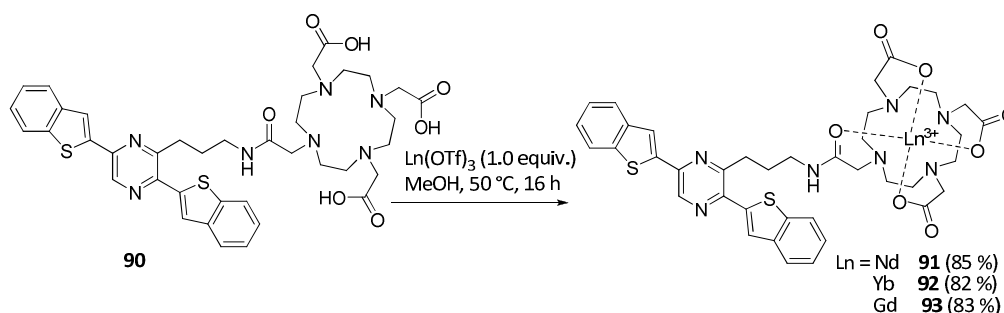
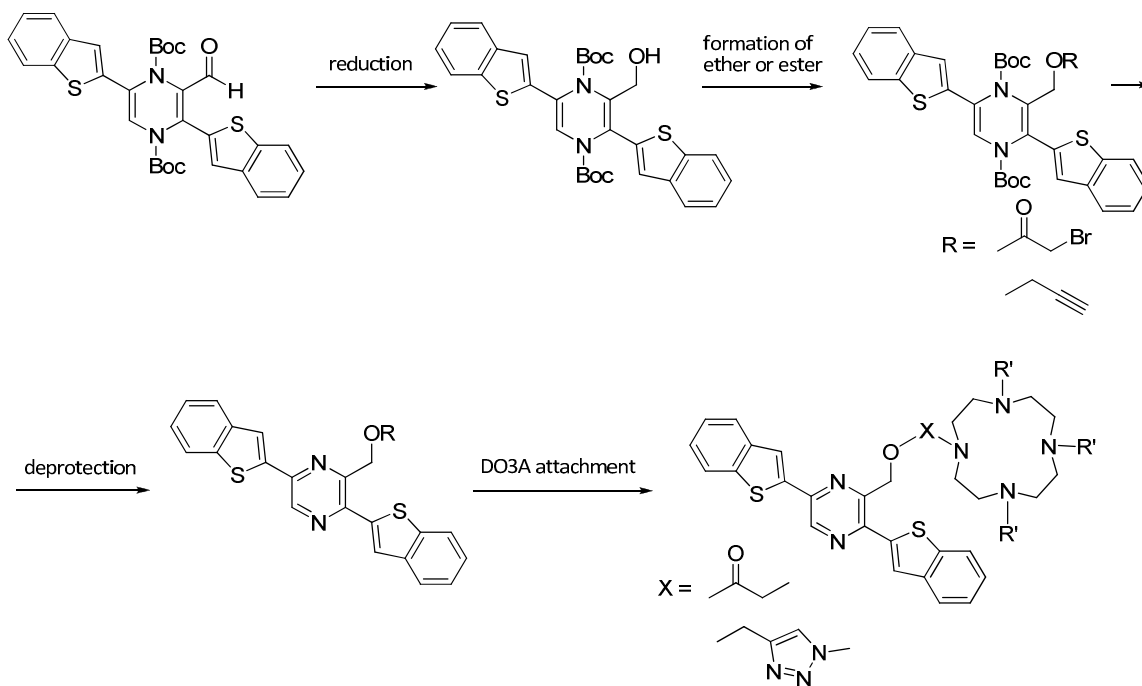


Fig. 124

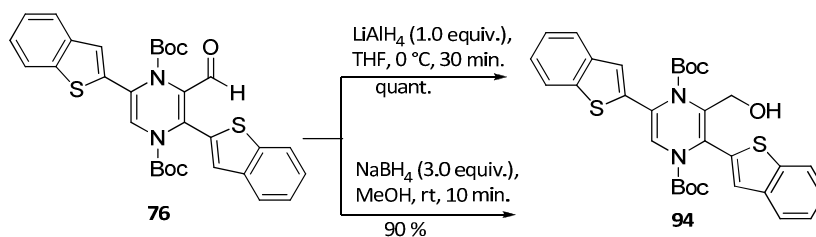
The lanthanide complexes were obtained in high yields 85 % (for Nd³⁺), 82 % (for Yb³⁺) and 83 % (for Gd³⁺). The structures of obtained products were confirmed by high resolution mass spectrometry (HRMS). Their absorption and emission spectra were measured in order to confirm the presence of metal in the chelation center and to estimate the ability of complexes to sensitize the lanthanides (see paragraph II.8).

II.7.2. Reduction of aldehyde and reactivity of obtained alcohol

We envisaged enlarging the scope of possible sensitizers by introduction of a shorter arm based on the ether or ester function. To reach this aim, we need to transform the aldehyde **76** to alcohol, which presumably will react with propargyl bromide to give a terminal alkyne or bromoacetic bromide providing bromated ester.



As mentioned before, the aldehyde function of the dihydropyrazine derivative **76** may be reduced to give appropriate alcohol derivative **94**. We tested the reduction reaction with two reducing agents (LiAlH_4 and NaBH_4) and better yield was obtained in the first case (quantitative compared to 90 %).



The predicted reaction of transformation of alcohol derivative **94** into an ester or ether gave only products of degradation. Any traces of expected products were observed. Therefore, we first anticipated the reaction of deprotection and then, the further modification of alcohol. At the first attempt, the deprotection with TMSI was applied to give a product, which appeared to be 2,5-di(benzo[*b*]thiophen-2-yl)-3-methylpyrazine **95**, the product of deprotection of carbamate and elimination of hydroxyl group in an excellent yield of 90 %. The change of reaction conditions to TFA/TIS did not permit to get expected product. We isolated the same product **95**, but with lower yield (33 %).

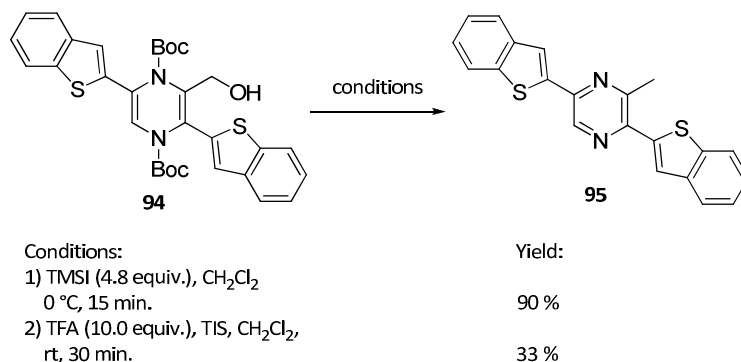


Fig. 126

We abandoned this pathway of synthesis and we tried to undertake the Diels-Alder reaction on alcohol **94** in order to get possibility to link the spacing arm on this system. The same conditions of reaction were applied as for dihydropyrazine derivative (see paragraph II.5.3). The cycloadduct **96** was obtained in low yield (34 %), probably due to the deactivation of diene character by the introduction of a methylhydroxy group.

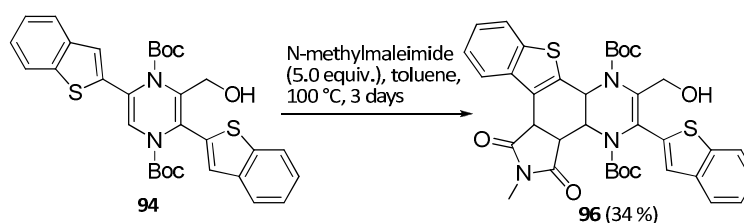


Fig. 127

The deprotection of nitrogen atoms of dihydropyrazine moiety with TMSI or TFA led to the elimination of a water molecule and gave similar to methyl derivative, product **97** (34 %).

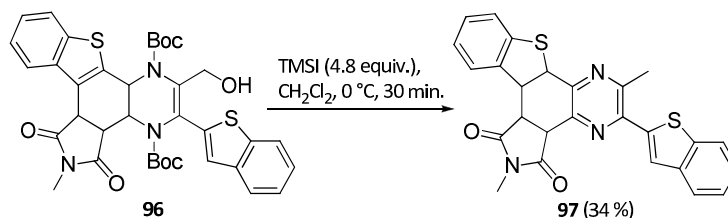


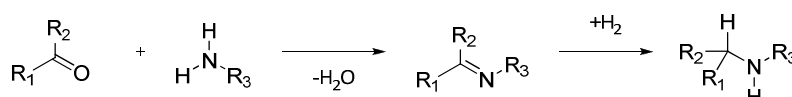
Fig. 128

Unfortunately, this access to construct the spacing arm on the methylhydroxy group had to be abandoned, from one hand due to the difficulty of functionalization of protected compounds and from the other hand, because of the deprotection stage the hydroxyl group is eliminated, required for further modifications. However, this synthetic pathway is not closed and a *trans*-imidation step could be envisaged in order to introduce functional groups allowing the attachment to the cyclen moiety.

II.7.3. Reductive amination

II.7.3.a. Short introduction

Afterwards, we have envisaged the introduction of the spacing arm to the pyrazinic core by a reductive amination. This reaction involves the conversion of carbonyl group (most commonly a ketone or an aldehyde) to an amine *via* an imine intermediate reduced by the use of reduction agents; such as sodium borohydride (NaBH_4) or sodium cyanoborohydride (NaBH_3CN) or sodium triacetoxyborohydride ($\text{NaBH}(\text{OAc})_3$).



Scheme 51 Reductive amination

The amine first reacts with the carbonyl group to form a hemiaminal species, which subsequently loses one molecule of water in a reversible manner by alkylimino-deoxy-bisubstitution to form the imine. The equilibrium between the carbonyl compound and the imine can be shifted toward the imine formation by removal of water. The imine intermediate can be isolated and reduced with suitable reducing agent. However, the direct reductive amination may also take place with reductors, more reactive toward protonated imines than ketones and stable in moderately acidic conditions, such as NaBH_3CN or $\text{NaBH}(\text{OAc})_3$.

II.7.3.b. Examples of reductive amination onto the aldehyde **76**

We tested several primary amines to check the reactivity of our aldehyde **76** in the reductive amination reaction. First, we applied 3-aminopropanol as a substrate offering the free hydroxyl group for further modifications. We used the particular conditions described in a recent publication.²⁰⁷ The solution of aldehyde in MeOH was prepared, then 3-aminopropanol and Et_3N was added, followed by catalyst $\text{Ti}(\text{iPrO})_4$. After 60 h of stirring at room temperature, NaBH_4 was added to reduce an imine. After work-up, the crude product was verified by ^1H NMR to be unreduced imine. The purification by column chromatography resulted in the decomposition of product. Therefore, the reaction was repeated without addition of reducing agent and at the end, the crude was reduced in the presence of H_3BO_3 and sodium borohydride to give expected secondary amine with 30 % of global yield after two steps.

²⁰⁷ A. Novoa, N. Pellegrini-Moise, D. Bechet, M. Barberi-Heyob, Y. Chapleur, *Bioorg. Med. Chem.*, **2010**, *18*, 3285.

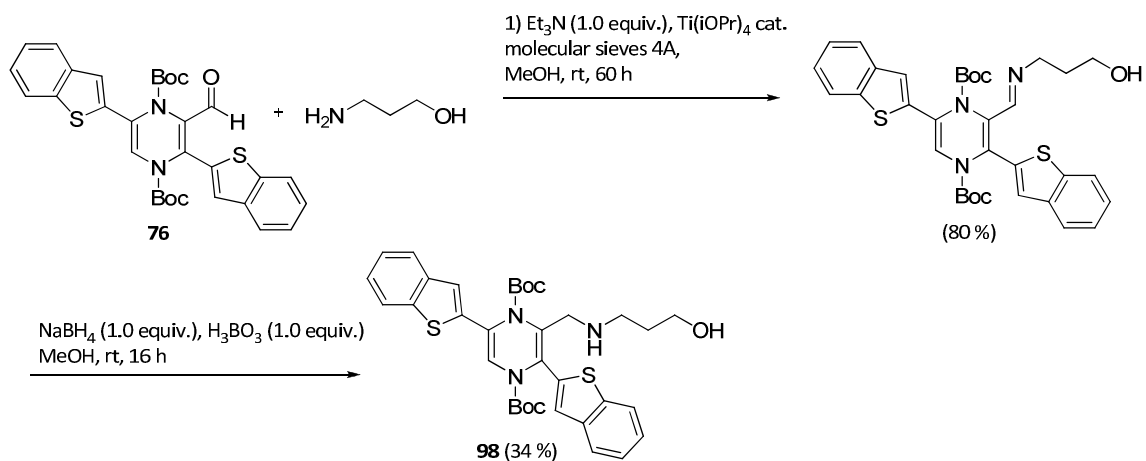


Fig. 129

This reaction gave a secondary amine with a very poor yield. Therefore, we decided to test another reactions with primary amines, such as 2-aminobenzylamine or *N*-benzylethylenediamine. Tested reduction agents were: NaBH(OAc)₃ and NaBH₄ to conduct to the direct reductive amination without the step of isolation of imine. Unfortunately, the reaction between aldehyde derivative **74** and *N*-benzylethylenediamine did not work in both conditions, the formation of imine did not occurred and aldehyde was reduced to the alcohol. At the same time, with 2-aminobenzylamine, we managed to isolate expected product after reduction with NaBH(OAc)₃ with excellent yields.

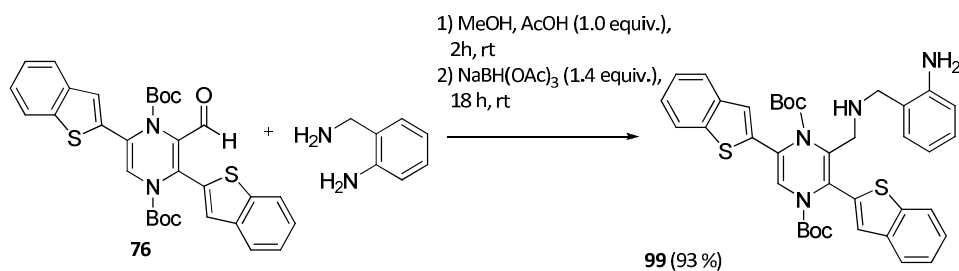
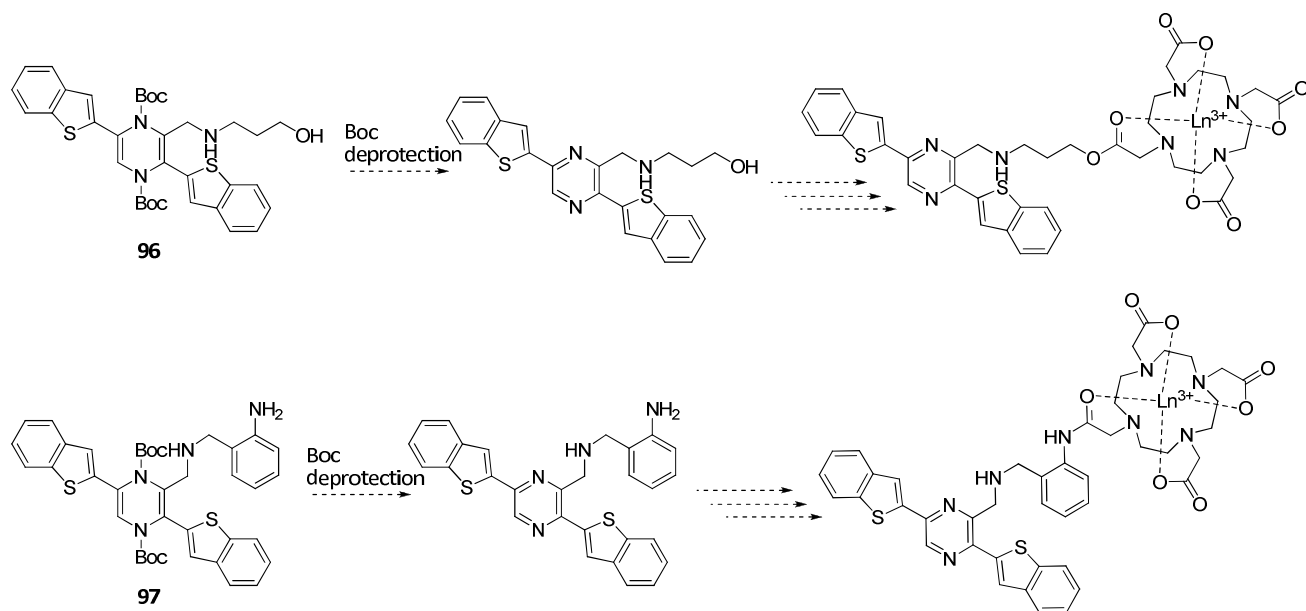


Fig. 130

This reaction shows an opportunity to enlarge the scope of possible reaction of aldehyde **74** and introduce a more complicated molecule by mean of reductive amination in relatively mild conditions. In perspectives, the deprotection of dihydropyraznic moiety and further functionalization of the aromatic amine and the alcohol are envisaged in order to anchor the cyclen derivative and construct the lanthanide complex.



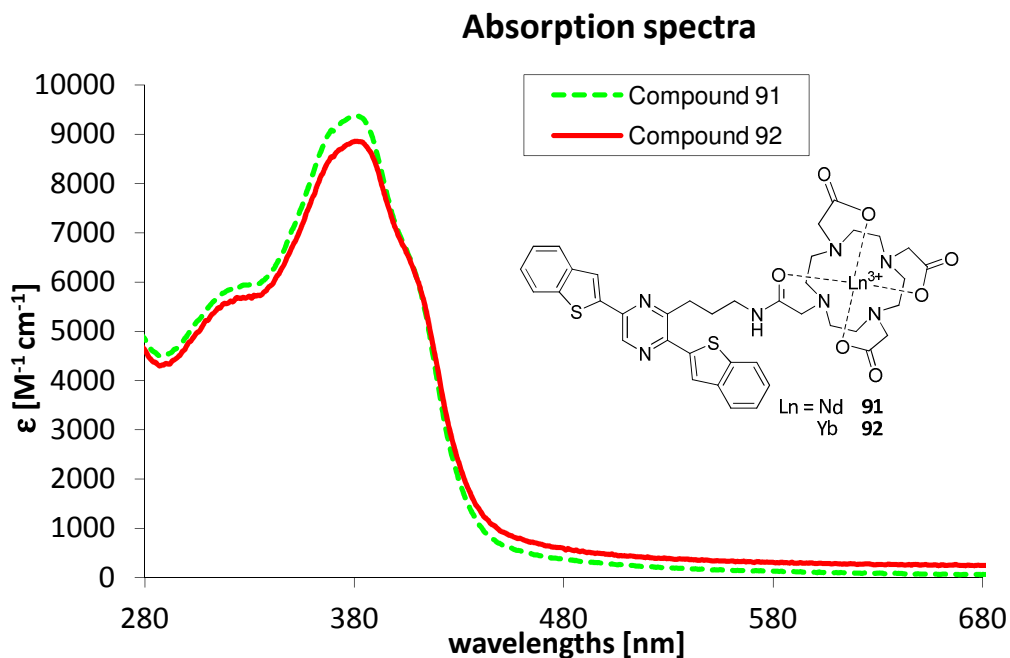
Scheme 52

Notably, the following paragraph will be dedicated the formation of particular chromophores based on azo dyes, which can be attached to the pyrazinic system by the reductive amination.

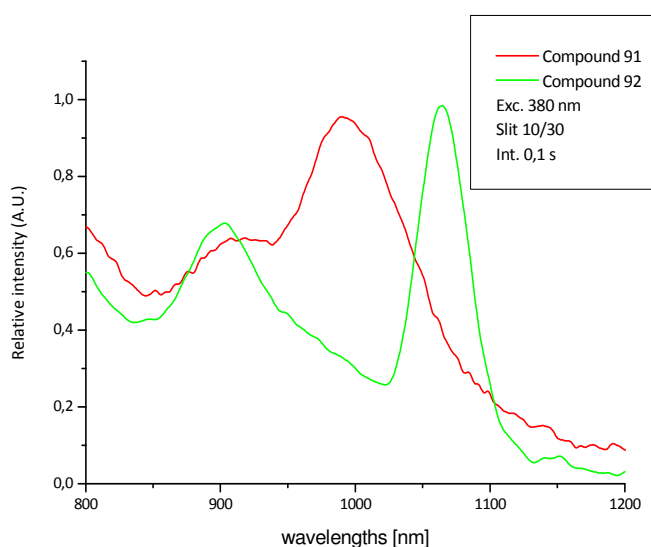
II.8. Spectroscopic properties of compounds 91 and 92

II.8.1. Absorption and emission spectra

The UV-Vis absorption spectra of the lanthanide complexes were measured in solution DMSO/ H₂O (1/9) in concentration 100 µg/mL at room temperature and they are presented in Fig.131.



Both spectra of absorption show apparent maxima at 380 nm. The absorption coefficient ϵ , which quantifies the ability of complex to absorb the light, is equal $8\,700\text{ M}^{-1}\text{cm}^{-1}$ for the complex with neodymium (**91**) and $8\,800\text{ M}^{-1}\text{cm}^{-1}$ for the ytterbium complex (**92**) – for organic chromophores this coefficient is usually in range $5\,000 - 100\,000\text{ [M}^{-1}\text{cm}^{-1}]$.



The Yb^{3+} complex displays a unique NIR emission band ranging from 920 nm to 1050 nm, which is assigned to the ${}^2\text{F}_{5/2} \rightarrow {}^2\text{F}_{7/2}$ transition. The relative intensities of the components of this band reflect the particular symmetry around the metal center. Respectively, for the Nd^{3+} complex, two characteristic bands were observed at 900 nm and 1064 nm. These emission bands are assigned to the transition from the level ${}^4\text{F}_{3/2}$ to the level ${}^4\text{I}_{9/2}$ and ${}^4\text{I}_{11/2}$. The excitation spectra for the respective lanthanide complexes **91** and **92** with the emission monitored at the respective maxima of each lanthanide show the presence of one band with a maximum at 370 nm, which matches the position of the maximum of absorption of both compounds. These results indicate that the electronic levels associated with this band that are located on the chromophore are used for the sensitization of the lanthanide cations. In short, these results demonstrate that this sensitizer can act as an antenna for the sensitization of both Nd^{3+} and Yb^{3+} metal ions.

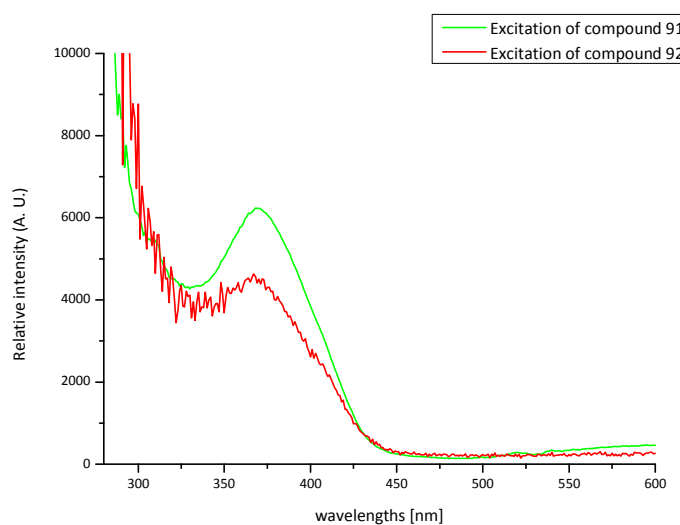


Fig. 133

II.8.2. Emission spectra and determination of energy levels

In the aim of analysis of the photophysical and energy processes occurring in these complexes, energies of the singlet and triplet states located on the ligand bound to the lanthanide cations have been measured. We have recorded the steady-state fluorescence and time-resolved phosphorescence spectra for the ligand coordinated to Gd^{3+} that act as silent metal center. Indeed, the electronic levels of gadolinium complex are too high in energy to allow ligand to lanthanide energy transfer.

The excited chromophore may be in the state S_1 or T_1 , however the experiment in the cool conditions permits to "freeze" the transfer and to increase the signal of phosphorescence. Fluorescence spectrum recorded at room temperature (Fig. 134) shows the presence of a broad band assigned to the $S_1 \rightarrow S_0$ transition with apparent maximum at 450 nm. The phosphorescence spectra recorded at 77K with 50 μs and 100 μs delay after flash (Fig. 135) indicates a presence of a broad band with maximum at 498-503 nm, which is assigned to the transition $T_1 \rightarrow S_0$. The average energy of triplet state is estimated for 19900 cm^{-1} , which makes our complex preferable for the energy transfer to the Yb^{3+} cation.

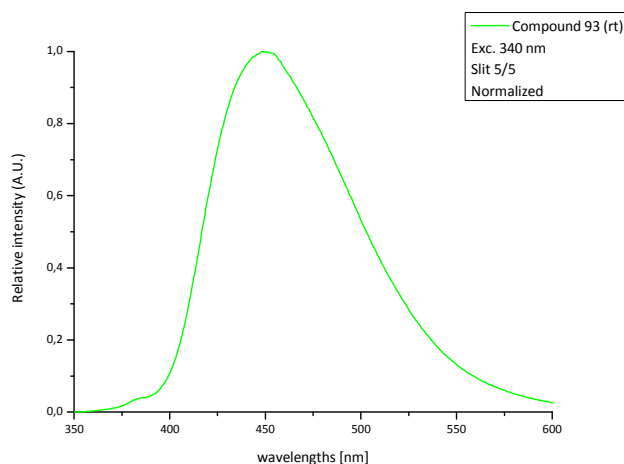


Fig. 134 Fluorescence of gadolinium complex

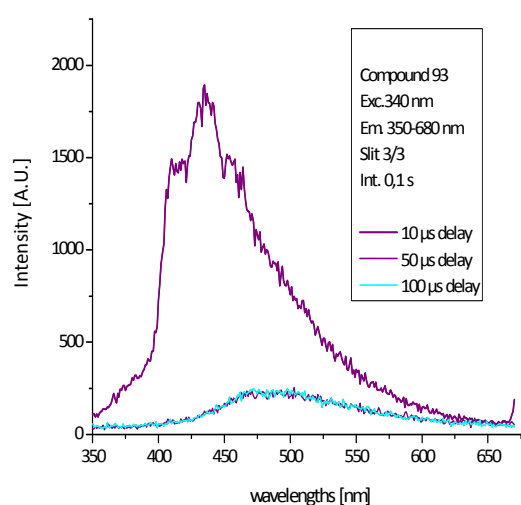


Fig. 135 The comparison of steady state and delayed emission of complex 93.

Having in hand results of our sensitizing system for the energy of singlet and triplet state, we compared them to the sensitizer formed with phenantroline chromophore.¹⁵³ The energy level of triplet states is comparable for both molecules ($19\,900\text{ cm}^{-1}$ for our pyrazinic system *versus* $21\,200\text{ cm}^{-1}$ for phenantroline). However, the energy of singlet is completely different: a cited molecule has a high-energetic level at $29\,200\text{ cm}^{-1}$ and the pyrazinic derivative shows a singlet at $23\,000\text{ cm}^{-1}$, which makes it more valuable in the domain of biological application with lower energy required for the excitation (340 nm).

Table 21

	Compound 93	Reference – phenantroline ¹⁵³
λ_{exc} [nm]	370	264
Singlet state [cm^{-1}]	23 000	29 200
Triplet state [cm^{-1}]	19 900	21 200

II.8.3. Quantum yields and luminescence lifetimes

In order to quantify the ability of our sensitizers to transfer energy to the metal center, we made an experiment to quantify the quantum yield of luminescence emitted *via* the lanthanide. This experiment was carried out in the integration sphere on the Fluorolog - 322. Collecting NIR quantum yields (ϕ) requires the use of both a visible and a NIR detector. A relative quantum yield is measured using a reference sample with a known value (ytterbium tropolonate $[\text{Yb}(\text{trop})_4]^-$ $\phi_{\text{Yb}} = 1.9 \cdot 10^{-2}$ and neodymium tropolonate $[\text{Nd}(\text{trop})_4]^-$ $\phi_{\text{Nd}} = 2.1 \cdot 10^{-3}$).¹³⁶

In the case of our samples, we were measuring the emission of solutions of lanthanide complexes in DMSO/H₂O (1/9) at two excitation wavelengths (340 nm and 380 nm) corresponding to our sensitizer and the tropolonate complexes. In order to get a statistical approval, we have made three repetition of every experiment. The results were placed in Table 22.

Table 22 Relative quantum yields of Nd and Yb complexes

Excitation at 340 nm	QY	Excitation at 380 nm	QY
Nd ³⁺ complex 1	2.03·10⁻⁵	Nd ³⁺ complex 1	1.08·10⁻⁵
Nd ³⁺ complex 2	3.73·10⁻⁵	Nd ³⁺ complex 2	1.05·10⁻⁵
Nd ³⁺ complex 3	1.97·10⁻⁵	Nd ³⁺ complex 3	2.56·10⁻⁵
Average value	2.6·10⁻⁵ (±1.0·10⁻⁵)	Average value	1.6·10⁻⁵ (±0.9·10⁻⁵)
Yb ³⁺ complex 1	3.14·10⁻⁵	Yb ³⁺ complex 1	3.28·10⁻⁵
Yb ³⁺ complex 2	2.80·10⁻⁵	Yb ³⁺ complex 2	2.94·10⁻⁵
Yb ³⁺ complex 3	-	Yb ³⁺ complex 3	2.74·10⁻⁵
Average value	3.0·10⁻⁵ (±0.2·10⁻⁵)	Average value	3.0·10⁻⁵ (±0.3·10⁻⁵)

The quantum yield of Nd³⁺ complex equals **2.58·10⁻⁵** at 340 nm and **1.56·10⁻⁵** at 380 nm and for Yb³⁺ complex is slightly higher: **2.97·10⁻⁵** (340 nm) and **2.99·10⁻⁵** (380 nm). The quantum yields, for each case, are higher for the ytterbium than for the neodymium complex, which means that our chromophore sensitize more efficiently Yb³⁺. The obtained results show that quantum yields of both complexes can appear as low, but are relatively comparable to those obtained with several complexes of DOTA incorporating organic antenna.²⁰⁸

Luminescence lifetimes monitoring the emission of the lanthanide cations were determined in order to analyze the protection of the lanthanide center against non-radiative deactivation and quantify the number of inner sphere water molecules. The analysis of the experimental luminescence decays obtained upon excitation of the complexes at 355 nm in the solution of H₂O/DMSO (9/1) and

²⁰⁸ (a) J.-C. G. Bünzli, A.-S. Chauvin, H. K. Kim, E. Deiters, S. V. Eliseeva, *Coord. Chem. Rev.*, **2010**, 254, 2623; (b) M. V. López, S. V. Eliseeva, J. M. Blanco, G. Rama, M. R. Barnejo, M. E. Vázquez, J.-C. G. Bünzli, *Eur. J. Org. Chem.*, **2010**, 4532, (c) S. Comby, D. Imbert, C. Vandevyver, J.-C. G. Bünzli, *Chem. Eur. J.*, **2007**, 13, 936.

D₂O/DMSO (9/1) revealed the best fittings as single-exponential functions. The fitted lifetimes upon monitoring Nd(⁴F_{3/2}) and Yb(²F_{5/2}) bands are placed in Table 23.

Table 23

Complex	λ_{exc} [nm] for quantum yield measurement	φ , H ₂ O/DMSO (9/1)	τ [μ s]		
			H ₂ O/DMSO (9/1)	D ₂ O/DMSO (9/1)	q
91 (Nd ³⁺)	340	$2.6 \cdot 10^{-5}$	0.089(2)	0.364(1)	0.7
92 (Yb ³⁺)	340	$3.0 \cdot 10^{-5}$	2.48(1)	7.4(2)	0.1

The luminescence lifetime is significantly longer for the Yb³⁺ complex than for Nd³⁺ which is consistent with the literature results; Faulkner¹⁵⁸ reports for example the hydralazine-derived chromophore values 1.87 μ s for Yb³⁺ and 0.09 μ s for Nd³⁺ in H₂O and respectively higher values in the D₂O solution (7.88 μ s and 0.33 μ s). The q parameter for neodymium complex (0.7) means that this lanthanide has one molecule of water coordinated to the metal, however, the value of the q for ytterbium complex (0.1) signifies that no water molecule is complexed to the coordination sphere of this lanthanide. This phenomenon may be explained by the size of ionic radius of Ln³⁺, which equals 116.3 pm for nine-coordinated Nd³⁺ and 98.5 pm for Yb³⁺, thus the smaller ytterbium cation is better shielded in the coordination cavity of cyclen and water molecules have greater difficulty to approach the lanthanide cation.²⁰⁹

II.8.4. Conclusion

The spectroscopic features of an originally synthesized ligand for lanthanide cations show that our system satisfies the condition of a sensitizer for lanthanides. We have quantified and identified the principal properties such as excitation and emission energy, the energy of singlet and triplet state as well as the energy transfer to the metal center (quantum yield). Our molecule is a promising prototype for a family of sensitizers, and its flexible synthetic pathway gives an opportunity to create a library of sensitizers with different spacing arms in order to test the influence of diversity in the system for the lanthanide emission.

²⁰⁹ (a) R. D. Shanon, *Acta Cryst.*, **1976**, A23, 751, (b) S. Faulkner, A. Beeby, R. S. Dickins, D. Parker, J. A. G. Williams, *Journal of Fluorescence*, **1999**, 9, 45.

III. Results and discussion: Sensitizers based on azo compounds

III.1. Bibliography

Azo compounds are chemicals consisted of aryl or alkyl part linked by N=N double bond. According to IUPAC terminology, these compounds are derivatives of diazene (diimide) HN=NH wherein both hydrogens are substituted by hydrocarbone groups, e.g. PhN=NPh azobenzene or diphenyldiazene. The first example of azo compounds - azobenzene was obtained by Alfred Noble in 1856²¹⁰ by heating nitrobenzene with iron filings and acetic acid at the reflux of methanol. This product has an intensive red-yellow color as a consequence of π -delocalized electrons.



Fig. 136 Azobenzene and its chemical aspect

Therefore, the azo compounds found an application as organic dyes and pigments. They have very vivid, intensive colors, which last for a long time. Many of pH indicators are azo compounds, due to their different colors at the basic and acid form. For example, the acid indicator - methyl orange chemically is *p*-dimethylamino-azobenzenesulfonic acid, which in the pH below 3.1 has red color and above 4.4 it takes yellow color.

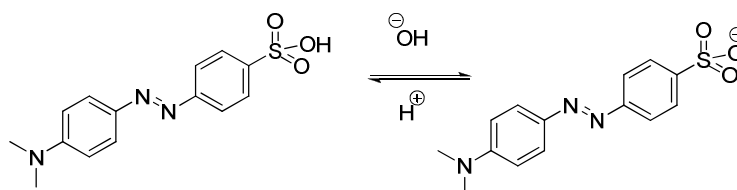


Fig. 137 The acid-base equilibrium in methyl orange

Another azo dye known under name Congo red has not only pH-indication properties, but also it serves as a dye for the cellulose industry owing to its great affinity to cellulose fibers by the hydrogen bonding. Moreover, it is used as a stain for a visual detection of amyloids in muscle and nerve fresh frozen sections in patients who have amyloidosis. In the 1920s Benhold²¹¹ and Divry²¹² established that Congo red bound to amyloid in tissue sections and demonstrated its characteristic yellow-green birefringence under crossed polarizers. The linearity of the dye configuration permits hydrogen bonding of the azo and amine groups of the dye to similarly spaced carbohydrate hydroxyl radicals of the amyloid substance. Since then this birefringence has been used as a diagnostic for amyloid fibrils.²¹³

²¹⁰ A. Nobel, Justus Liebigs Annalen der Chemie, 1856, 98, 253.

²¹¹ H. Benhold, München. Med. Wochenschr., 1922, 69, 1537.

²¹² P. Divry, J. Neurol. Psychiatr., 1927, 27, 643.

²¹³ R. Khurana, V. N. Uversky, L. Nielsen, A. L. Fink, J. Biol. Chem., 2001, 276, 22715.

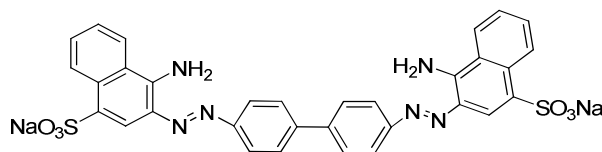


Fig. 138 Congo red

Additionally, Congo red is used in microbiological epidemiology to rapidly identify the presence of virulent serotype 2a *Shigella flexneri* by the binding to the bacterium's unique lipopolysaccharide (LPS) structure.²¹⁴

Non-aromatic azo compounds are noted as radical reaction initiators, because they are unstable at elevated temperature or upon irradiation and they liberate N_2 and free radicals. The very well-known example is azobisisobutyronitrile (AIBN) widely used in industrial scale as initiator of polymerization reaction. Recently, azobenzenes have shown the potential application in the field of nonlinear optics, liquid crystals,²¹⁵ nanotubes,²¹⁶ photochemical molecular switches²¹⁷ and molecular shuttles.²¹⁸ Also in the field of medicine, they supposed to be a therapeutic agents and prodrugs to carry the therapeutic agents.²¹⁹

One of the most intriguing properties of azo compounds is the photoisomerization of *trans* and *cis* isomers. The two isomers can be switched with particular wavelengths of light: ultraviolet light, which corresponds to the energy gap of the $\pi-\pi^*$ (S_2 state) transition, for *trans*-to-*cis* conversion, and blue light, which is equivalent to that of the $n-\pi^*$ (S_1 state) transition, for *cis*-to-*trans* isomerization. The *cis* isomer is less stable due to steric hindrance than the *trans*, it has a distorted configuration and is less delocalized than the *trans* configuration. Thus, *cis*-azo compound will thermally relax back to the *trans* via *cis*-to-*trans* isomerization. The *trans* isomer is more stable by approximately 50 kJ/mol, and the barrier to photoisomerization is approximately 200 kJ/mol.²²⁰

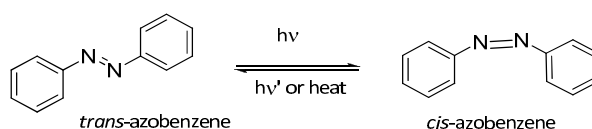


Fig. 139 Photoisomerization of azobenzene

The photoisomerization of azobenzene is extremely rapid, occurring on picosecond timescales. The rate of the thermal back-relaxation varies, greatly depending on the compound: usually hours for azobenzene-type molecules, minutes for aminoazobenzenes, and seconds for the pseudo-stilbenes.

²¹⁴ K. A. Talukder, Z. Islam, M. A. Islam, D. K. Dutta, A. Safa, M. Ansaruzzaman, A. S. G. Faruque, S. N. Shahed, G. B. Nair, D. A. Sack, *J. Clin. Microbiol.*, **2003**, *41*, 110.

²¹⁵ (a) T. Ikeda, O. Tsutsumi, *Science*, **1995**, *268*, 1873; (b) D. Jayalatha, R. Balamurugan, P. Kannan, *High Performance Polymers*, **2009**, *21*, 139.

²¹⁶ I. A. Banerjee, L. Yu, H. Matsui, *J. Am. Chem. Soc.*, **2003**, *125*, 6542.

²¹⁷ B. L. Feringa, R. A. van Delden, N. Koumura, E. M. Geertsema, *Chem. Rev.*, **2000**, *100*, 1789.

²¹⁸ H. Murakami, A. Kawabuchi, K. Kotoo, M. Kitunake, N. Nakashima, *J. Am. Chem. Soc.*, **1997**, *119*, 7605.

²¹⁹ (a) W. J. Sandborn, *Am. J. Gastroenterol.*, **2002**, *97*, 2939 (b) A. Jain, Y. Gupta, S. K. Jain, *Crit. Rev. Ther. Drug Carrier Syst.*, **2006**, *23*, 349.

²²⁰ E. Diau, *J. Phys. Chem. A*, **2004**, *108*, 950.

This feature makes from azo compounds potential candidates to modulate relative movement of different moieties. It has been proven that the motion of one molecule containing an azobenzene group can control the movement of a complementary substrate non-covalently bound to the azobenzene fragment.²²¹ In the biological system, this photoisomerization may enable the control of biomolecules as enzymes of nucleic acids. Liang *et al.*²²² reported that this process of the azobenzene tethered to the third strand of nucleic acid assists a formation and dissociation of DNA triplex.

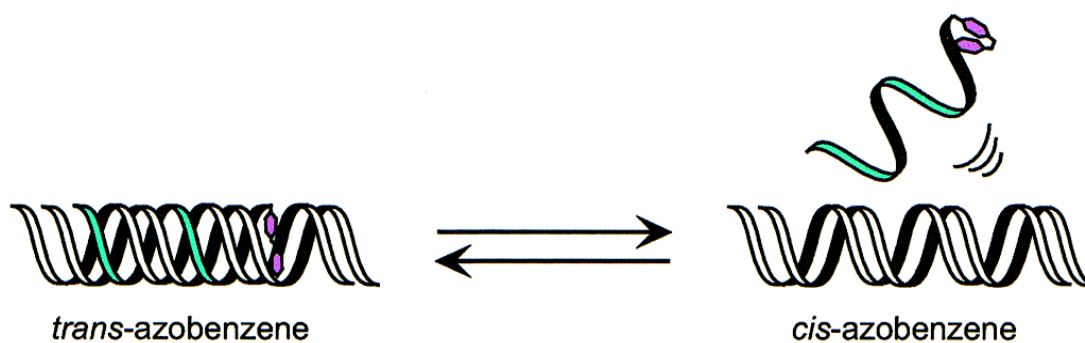


Fig. 140 Photoregulation of formation of DNA triplex

III.2. The synthesis of azo compounds

Several methods of synthesis of azo compounds exist. The classical one is the azo coupling reaction between diazonium salt and electron-rich aromatic compound, the Mills and the Wallach reactions. Recently, some more efficient strategies have been reported by Len *et al.*²²³ with particular emphasis to the carbohydrate domain. In this work, we will focus on the specified methods and we will point out other more particular strategies.

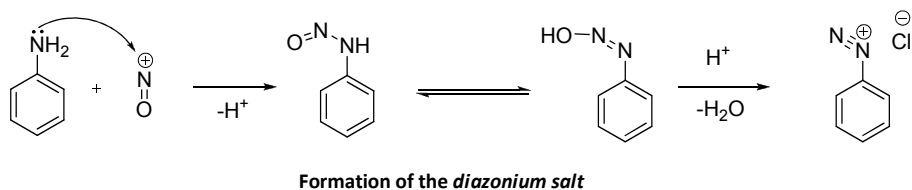
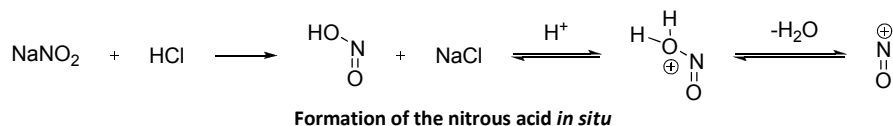
III.2.1. Formation of diazonium salt and azo coupling

Azo coupling is the most widely used industrial reaction in the production of dyes, lakes and pigments. An aromatic diazonium ion acts as electrophile in coupling reactions with activated aromatics such as anilines or phenols. The substitution normally occurs at the *para* position, except when this position is already occupied; in this case *ortho* position is favored. The diazonium salt formation is called diazotation; this process requires aromatic amines (anilines) and the presence of nitrous acid. Usually the nitrous acid is generated *in situ* from sodium nitrite and mineral acid. In aqueous solution diazonium salts are unstable at temperatures above +5 °C; the $-N^+ \equiv N$ group tends to be lost as N_2 (nitrogen gas). Diazonium compounds can be isolated as tetrafluoroborate salts, which are stable at room temperature. Often, diazonium compounds are not isolated and once prepared, used immediately in further reactions.

²²¹ T. Muraoka, K. Kinbara, T. Aida, *Nature*, **2006**, *440*, 512.

²²² X. Liang, H. Asanuma, M. Komiyama, *J. Am. Chem. Soc.*, **2002**, *124*, 1877.

²²³ F. Hamon, F. Djedaini-Pilard, F. Barbot, C. Len, *Tetrahedron*, **2009**, *65*, 10105.



Scheme 53 Mechanism of diazotation

The reaction of diazotation is very pH dependant. For the formation of diazonium salt from an aromatic amine, an acid is indispensable to liberate *in situ* nitrous acid from sodium nitrite(III). Further protonation and water elimination provides the nitrosation agent ($\overset{\oplus}{\text{N}}=\text{O}$), which reacts with the amine group forming *N*-nitroso derivative, the tautomer of diazohydroxide. After a second protonation and H_2O elimination, the diazonium salt is created (Scheme 53); this species is stabilized by resonance.²²⁴

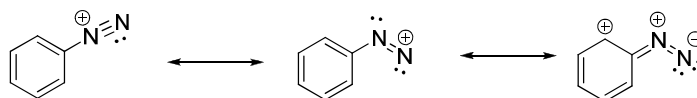


Fig. 141 Mezoforms of arenediazonium ion

Due to the positive charge, diazonium ions, participate in an electrophilic aromatic substitution as an electrophile. The electrophilic reaction center is the terminal nitrogen from the $-\text{N}=\text{N}$ group. The electrophilicity of this group is relatively weak because of the delocalized positive charge. The unsubstituted benzenediazonium ion may react only with strongly activated aromatic compounds, such as phenolates or amines.

The optimal pH for the coupling reaction depends on the nature of reactant. Phenols usually react in slightly alkaline solutions in order to activate the phenol moiety to the highly reactive phenoxide.

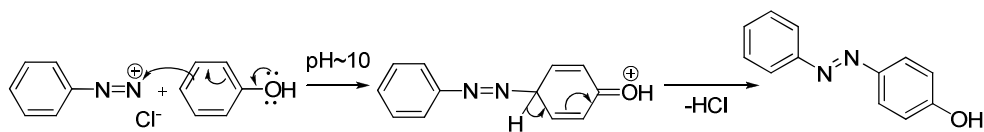


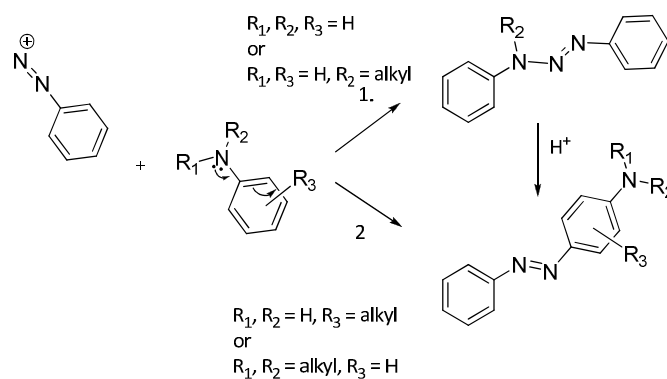
Fig. 142 Diazo coupling with phenol

For aryl amines, the reaction mixture should be considerably acidic or neutral to maintain a high concentration of free amine as well as arenediazonium ions in the solution, because aryl ammonium species are unreactive. When aromatic amines are the nucleophilic reagents, two pathways are possible: the *N-N* bond formation providing the amino diazo compound, further transformed into the azo compound by rearrangement in acidic media.²²⁵ As the reactivity of the aryl group is increased by

²²⁴ I. Svele, H. Zollinger, *Top. Curr. Chem.*, **1983**, 112, 1.

²²⁵ (a) J. R. Penton, H. Zollinger, *Helv. Chim. Acta*, **1981**, 64, 1717, (b) R. P. Kelly, J. R. Penton, H. Zollinger, *Helv. Chim. Acta*, **1982**, 65, 122.

the presence of electron-donating group or fused ring, the direct C-N bond formation occurs (Scheme 54).



Scheme 54 Diazo coupling with amines

By introducing electron-withdrawing substituents in *ortho* or *para* position regarding the azo group, the diazonium ions' electrophilicity may be increased to such a degree that diazonium coupling also occurs with phenols and phenolic ethers, such as anisole.

The azo coupling reaction has been carried out with specialized macrocyclic systems such as porphyrins,²²⁶ metacyclophanes²²⁷ and calixarenes.²²⁸ One of examples is coupling between substituted calixarene with diazonium tetrafluoroborate giving the azo product with 23% isolated yield (Fig. 143). This compound shows the UV band splitting of chromogenic azo-coupled calix[4]crown upon cation complexation.

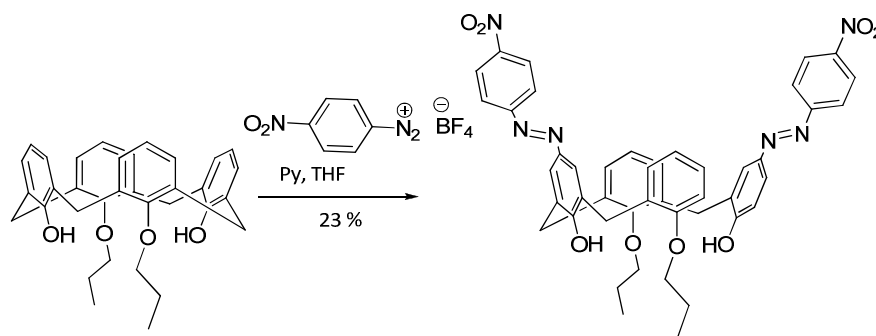


Fig. 143

III.2.2. The Mills reaction

The synthesis of dissymmetrical azobenzenes by aromatic nitroso derivatives with anilines in glacial acetic acid is known as Mills reaction.²²⁹ The aromatic nitroso species can be prepared by oxidation of an aromatic methylhydroxylamine with *tert*-butyl hypochloride at temperature $-78\text{ }^{\circ}\text{C}$. Other oxidation agents may be used: FeCl_3 , Caro's acid (H_2SO_5), sodium or potassium dichromate and sulfuric acid, $\text{AcOH}/\text{H}_2\text{O}_2$, *m*-chloroperbenzoic acid, KMnO_4 , diethyl azodicarboxylate, $\text{I}_2/\text{NaI}/\text{NaOAc}$, Ag_2CO_3 , DDQ and peroxyformic acid.

²²⁶ C. H. Hunter, L. D. Sarson, *Tetrahedron Lett.*, **1996**, 37, 699.

²²⁷ A. Tsuge, T. Moriguchi, S. Mataka, M. Tashiro, *J. Chem. Soc., Perkin Trans. 1*, **1993**, 2211.

²²⁸ J. Y. Kim, G. Kim, C. R. Kim; S. H. Lee, J. S. Kim, *J. Org. Chem.*, **2003**, 68, 1933.

²²⁹ H. H. Davey, R. D. Lee, T. J. Marks, *J. Org. Chem.*, **1999**, 64, 4976.

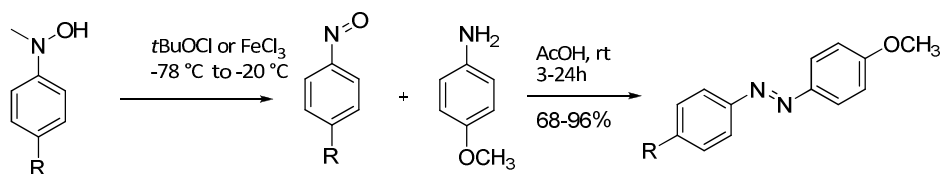
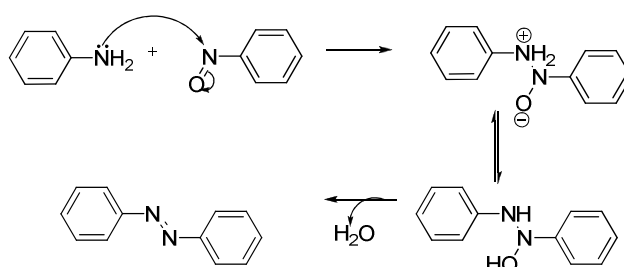


Fig. 144 Example of Mills reaction

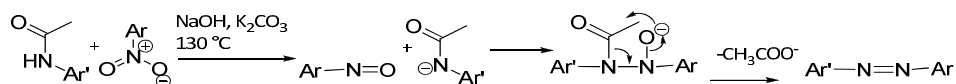
Overall yields of this reaction are good to excellent; it depends on the stability of nitroso compound. It is noteworthy that, applying the Mills reaction, different electron-withdrawing and -donating groups could be present in the *ortho*-, *meta*- and *para*-positions of both aromatic nitroso compounds and the aromatic amines.

The mechanism of Mills reaction involves the attack of aniline onto the nitroso derivative in acidic media. This leads to the azobenzene after dehydration of the intermediate (Scheme 55).²³⁰



Scheme 55 Mechanism of Mills reaction

The nitroso derivative may be obtained by deoxygenation of nitrobenzene. This allows the preparation of asymmetrically substituted azo compounds from the nitro compound and an aromatic *N*-acylamine in the basic conditions (Scheme 56).²³¹



Scheme 56 Mills reaction in basic conditions

Recently, the Mills reaction was applied to synthesized ferrocenylazobenzenes²³² from 3-ferrocenylaniline and nitrosobenzene in acetic acid. It was notable that 2-ferrocenylazobenzene without substituents was obtained in the *Z* configuration.

Also, this method served to synthesize the altering sequences of pyridine-2,6-dicarboxamides and 3-(phenylazo)-azobenzenes, assembled into oligomers of four and eight azobenzene linkages.²³³ X-ray crystallography confirmed a two-turn helical conformation with a helical pitch of approximately 3.4 Å in the solid state.

²³⁰ K. Ueno, S. Akiyoshi, *J. Am. Chem. Soc.*, **1954**, 76, 3670.

²³¹ N. R. Ayyangar, S. N. Naik, K. V. Srinivasan, *Tetrahedron Lett.*, **1989**, 30, 7253.

²³² A. Sakamoto, A. Hirooka, K. Namiki, M. Kurihara, M. Murata, M. Sugimoto, H. Nishihara, *Inorg. Chem.*, **2005**, 44, 7547.

²³³ C. Tie, J. G. Gallucci, J. R. Parquette, *J. Am. Chem. Soc.*, **2006**, 128, 1162.

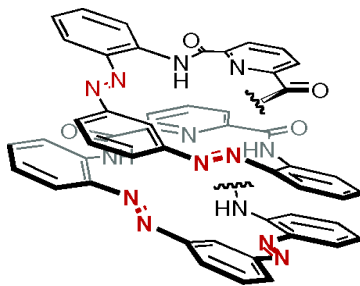


Fig. 145

III.2.3. The Wallach reaction

The Wallach reaction, called also Wallach rearrangement,²³⁴ involves the conversion of an azoxybenzene in the presence of sulfuric acid (60% to 100% are required) to an azo compound with one arene ring substituted by a hydroxyl group in the *para*-position. Conceptually, this reaction is related to Fries rearrangement or benzidine rearrangement. An azoxybenzene is accessible from the reduction of nitrobenzene with alcoholic KOH/CH₃CHO, sodium amalgam, hydrogen/PbO or MeONa or equally from the oxidation of aniline with hydrogen peroxide or permanganic acid/formaldehyde.

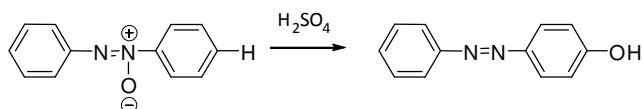
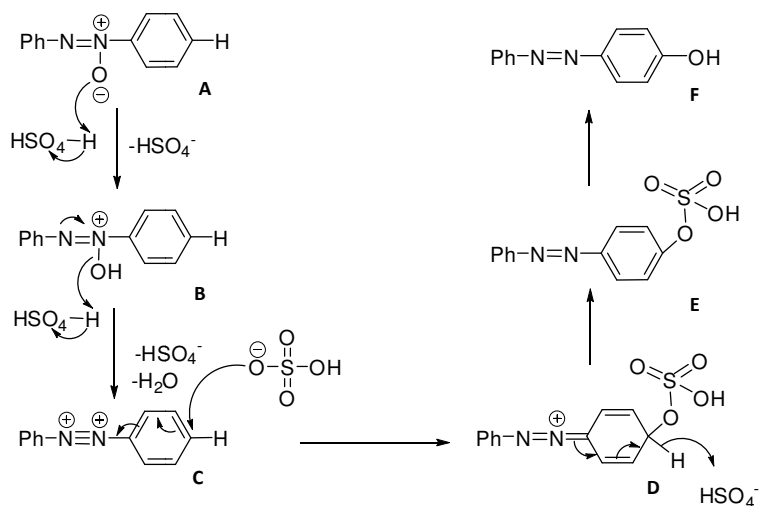


Fig. 146

The mechanism of this reaction is not completely known, but several experimental evidences exist showing the possibility of occurrence this kind of arrangement (Scheme 57):



Scheme 57 Mechanism of Wallach reaction

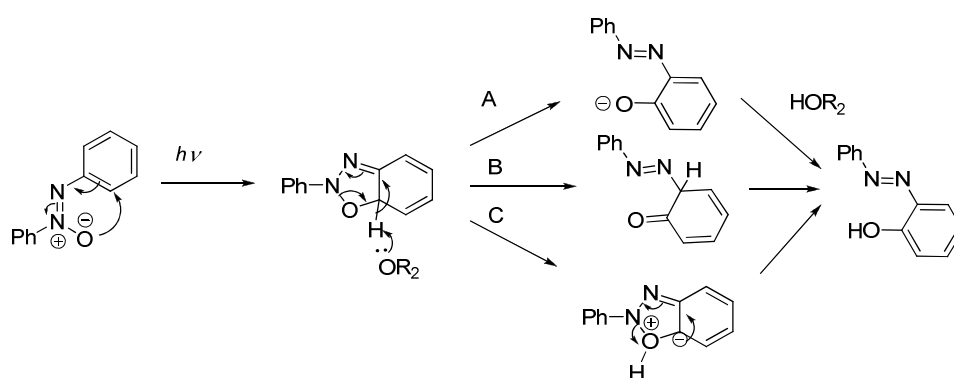
In the first part of the reaction, two equivalents of acid split the oxygen atom off the azoxy group. The resulting dicationic intermediate **C** with an unusual R-N⁺=N⁺-R motif in this scheme has been observed by proton NMR in a system of fluoroantimonic acid and azoxybenzene at -50°C.²³⁵ In the second part of

²³⁴ O. Wallach, E. Belli, *Chem. Ber.*, **1880**, *13*, 525.

²³⁵ G. A. Olah, K. Dunne, D. P. Kelly, Y. K. Mo, *J. Am. Chem. Soc.*, **1972**, *94*, 7438.

the reaction the HSO_4^- anion is a nucleophile in a nucleophilic aromatic substitution to **E** followed by hydrolysis to **F**.

Shemyakin *et al.* described that the formation of 2-hydroxyazobenzene occurs *via* an intermolecular oxygen shift.²³⁶ Also, it was proven that UV irradiation provokes this rearrangement.²³⁷ According to this mechanism, the oxygen atom from the azoxy group is transferred to the benzene ring attached to the fragment $-\text{N}=\text{N}-$ upon exposure to light. The 5-member ring may be formed and its opening leads to 3 different pathways. One of them is ring opening accompanied with deprotonation by basic solvent (A), second is the formation of ketone in *ortho*-position followed by tautomerization (B). The third one is the intramolecular *H*-migration by the [1,5]-sigmatropic rearrangement.



Scheme 58 Formation of 2-hydroxyazobenzene according to Shemyakin

Studies of the Wallach reaction controlled by the presence of Lewis acid were carried out.²³⁸ The formation of Lewis complex was observed and after thermolysis of this complex, desired products with hydroxy-group in the *ortho*-position were obtained. This situation occurred only with SbCl_5 , with other Lewis acids (AlCl_3 , TiCl_4 , FeCl_3 or ZnBr_2) did not give the *ortho*-hydroxy derivatives.

The thermal Wallach reaction is not synthetically useful since, the mixture of products is obtained. At the same time, this reaction is not very efficient and it requires the thermally stable substrate. Therefore, it has not found any application in preparative organic chemistry.

III.2.4. Other reaction providing the azo compounds

Azobenzenes can be also prepared by the reduction of azoxy derivatives in the presence of aluminium in MeOH under reflux or with microwave irradiation.²³⁹ This reaction is very fast and provides azoarenes in excellent yields. Another method is the reductive coupling of aromatic nitro derivatives, such as LiAlH_4 , NaBH_4 , etc.²⁴⁰ It is a useful way to obtain exclusively symmetrical aromatic azo

²³⁶ M. M. Shemyakin, V. I. Maimind, B. K. Vaichunaite, *Chem. Ind.*, **1958**, 755.

²³⁷ W. M. Cumming, G. S. Ferrier, *J. Chem. Soc. Trans.*, **1925**, 127, 2374.

²³⁸ J. Yamamoto, Y. Neshigaki, M. Umezu, *Tetrahedron*, **1980**, 36, 3177.

²³⁹ H. M. Nanjundaswamy, M. A. Pasha, *Synth. Commun.*, **2005**, 35, 2163.

²⁴⁰ (a) R. F. Nystrom, W. G. Brown, *J. Am. Chem. Soc.*, **1948**, 70, 3738; (b) R. O. Hutchins, D. W. Lamson, L. Rua, C. Milewski, B. Maryanoff, *J. Org. Chem.*, **1971**, 36, 803.

compounds. The reductive coupling of 2-nitrotoluene with magnesium/ $\text{HCO}_2\text{HNEt}_3$ in methanol in room temperature gives 2,2'-dimethyl azobenzene in 90 % yield (Fig. 147).²⁴¹

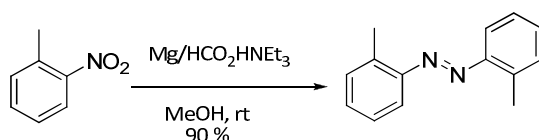


Fig. 147 Reduction of azoxy derivatives

The electrolytic oxidation of anilines is the next method of azobenzene formation. However, the first applied procedure did provide to desired product with low yield,²⁴² the further modification by addition of different oxidizing agent (such as $\text{H}_2\text{O}_2/\text{Na}_2\text{WO}_4$) much improves this methodology (Fig. 148).²⁴³

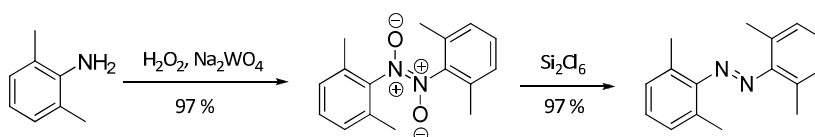


Fig. 148 Oxidation of anilines providing to azo compounds

Several examples exist of azobenzene formation by the dehydrogenation of arylhydrazines. One of them is the reaction of hydrazobenzene with periodate containing polyethylene imine resin.²⁴⁴

Also, dimerization reaction of stable diazonium salts (Fig. 149) is possible in the presence of metallic copper and an acid or with copper(I) salts.²⁴⁵ The mechanism of dimerization probably involves free radicals formed with the aid of copper salts. This process is highly dependent on the nature of the aryl group. If the substrate has electron-withdrawing groups, mainly the C-C coupling will take place. With electron-donating groups only azo compound will be isolated.

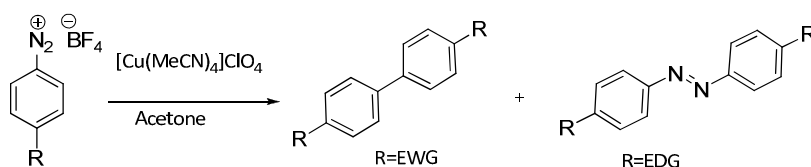


Fig. 149 Dimerization of diazonium salts

Another example is triazene rearrangement, first proposed by Nietzki in 1877. Also, a thermolysis of azides or decomposition of N,N' -*p*-benzoquinonediimine dioxide under the light are particular method for azo compounds formation. An interesting pathway is the reaction of arylcalcium derivatives with nitrous oxide (Fig. 150).²⁴⁶

²⁴¹ G. R. Srinivasa, K. Abiraj, D. C. Gowda, *Aust. J. Chem.*, **2004**, 57, 609.

²⁴² S. Wawzonek, T. W. McIntyre, *J. Electrochem. Soc.*, **1972**, 119, 135.

²⁴³ H. Olsen, P. J. Snyder, *J. Am. Chem. Soc.*, **1977**, 99, 1524.

²⁴⁴ M. Barth, S. Tasadaque, A. Shah, J. Rademann, *Tetrahedron*, **2004**, 60, 8703.

²⁴⁵ T. Cohen, R. J. Lewarchik, J. Z. Tarino, *J. Am. Chem. Soc.*, **1974**, 96, 7753.

²⁴⁶ M. L. Hays, T. P. Hanusa, *Tetrahedron Lett.*, **1995**, 36, 2435.

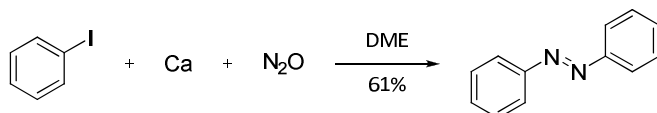


Fig. 150 Arylcalcium derivative forming azo compound

Recently, the metal catalyzed coupling reaction of arylhydrazines became the method of choice for the azo compound's formation. The first described reaction was coupling between *N*-Boc arylhydrazine and aryl halide with Pd(OAc)₂/P(^tBu)₃ as catalyst. The resulting diaryl hydrazines were directly oxidized with NBS/Py to give azobenzenes with good yields (Fig. 151).²⁴⁷

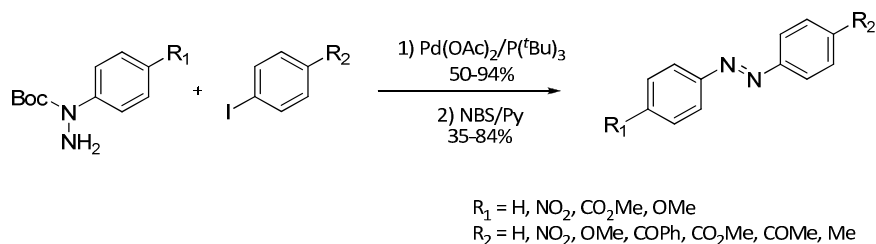


Fig. 151 Palladium catalyzed reaction of azo compound formation

Also, the Cu(I) salts may be applied to oxidize obtained arylhydrazines.²⁴⁸

Ziegler *et al.*²⁴⁹ has described a direct approach of preparation of 2-hydroxyazobenzenes from benzotriazoles by reaction with phenols. Owing to the presence of strongly electron-withdrawing group, the opening of the cycle occurs easily. The azobenzene is obtained after acid hydrolysis with fair to excellent yields (Fig. 152).

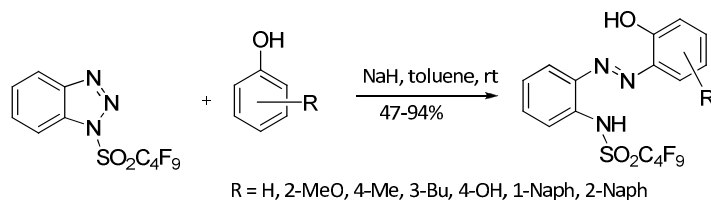


Fig. 152 Application of benzotriazoles in azo compound synthesis

Two last particular methods are: the reaction of quinone with arylhydrazines in acidic conditions and reaction of quinone acetals with arylhydrazines. The reaction between quinone and phenylhydrazine was reported for the first time at 1941 (Fig. 153).²⁵⁰

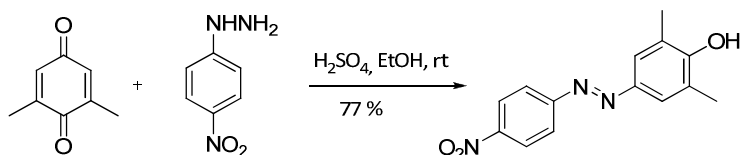


Fig. 153 Application of arylhydrazines to form azo compounds

²⁴⁷ Y.-K. Lim, K.-S. Lee, C.-G. Cho, *Org. Lett.*, **2003**, 5, 979.

²⁴⁸ Y.-K. Lim, S. Choi, K. B. Park, C. G. Cho, *J. Org. Chem.*, **2004**, 69, 2603.

²⁴⁹ X. Álvarez Micó, T. Ziegler, L. R. Subramanian, *Angew. Chem. Int. Ed.*, **2004**, 43, 1400.

²⁵⁰ L. I. Smith, W. B. Irvine, *J. Am. Chem. Soc.*, **1941**, 63, 1036.

Since this time, some modification has been applied like addition of thallium acetate or nitrate²⁵¹ to give rise to desired azo compounds with excellent yields.

Carreño *et al.*²⁵² have presented the formation of azobenzenes from quinone acetals (provided from anodic oxidation of 1,4-dimethoxybenzenes) with aryl hydrazines. The presence of catalytic amounts of cerium ammonium nitrate (CAN) much reduce the reaction times (Fig. 154).

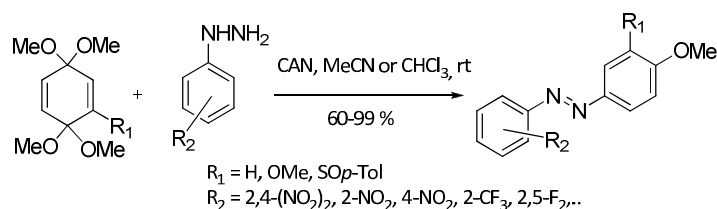


Fig. 154 Carreño approach to azo compounds

III.3. Objectives

Reactions presented above are showing the versatility of synthetic pathways leading to the azo compounds. The interest of formation of new azo derivatives takes its origins in the diversity of application and interesting photophysical properties.

In our strategy of synthesis of azo derivatives, we were focused onto the formation of diazonium ions and subsequent coupling with aromatic amines because of great accessibility of starting materials (aniline derivatives) and short reaction times. Moreover, the isolation of azo compounds from aqueous media by precipitation and filtration was a great advantage. We started with simple diazonium salts with electron withdrawing groups like halides or NO₂ then we moved to more complicated aminobenzylanilines to construct the desired azo compounds with amine group in the *para*-position. This amino group will permit us to perform the reductive amination between azo derivative and our pyrazinic aldehyde in order to get more complex antenna systems where, at the same time, the azo function and pyrazinic core are present. The goal of this part of thesis was to synthesize the original chromophores for lanthanides with cyclen as chelating part and azo compound as an antenna (Fig. 155).

²⁵¹ E. C. Taylor, G. E. Jagdmann Jr., A. McKillop, *J. Org. Chem.*, **1978**, 43 4385.

²⁵² M. C. Carreño, G. Fernández-Mudarra, E. Merino, M. Ribagorda, *J. Org. Chem.*, **2004**, 69, 3413.

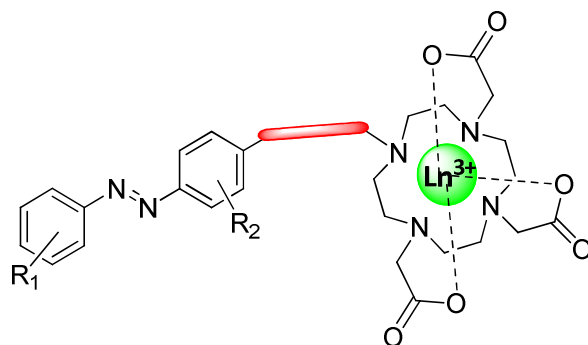


Fig. 155 The scheme of azo sensitizer for lanthanides

III.4. Formation of azo compounds

As a molecule-model, we have chosen the (*E*)-4-((4-bromophenyl)diazenyl)aniline because of the accessibility of starting material, in order to check the regioselectivity of reaction (*ortho* or *para* isomer). The standard condition was the preparation of diazonium salt from 4-bromoaniline in the presence of sodium nitrate and the concentrated hydrochloric acid. This reaction was carried out for 30 min. at 0 °C, till the moment of disappearing of solid in mixture and the change of color of solution from colorless to orange. Then, this diazonium salt was directly introduced drop by drop to the cooled suspension of aniline in the acetic buffer (120 M, pH = 6) (Fig. 156).

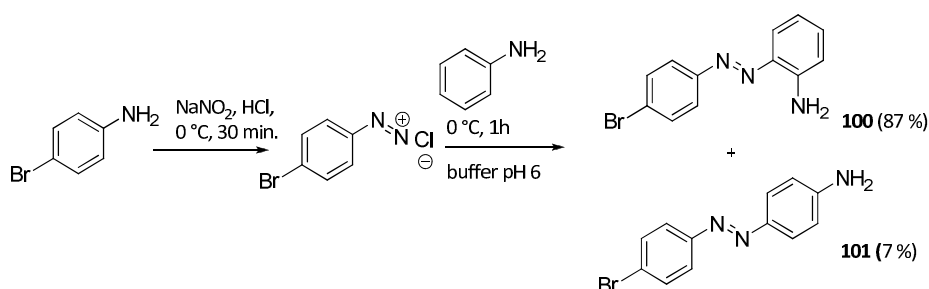


Fig. 156

Unfortunately, in the case of this coupling, the mixture of products was obtained. Moreover, the expected *para* isomer **101** was isolated as a minor fraction (7 %). From this reasons, we moved forward with other nucleophilic aromatic amines. We were searching substrates with blocked *ortho* position to the amine group and at the same time, with potential increased photophysical properties. One of them is 2,5-dimethoxyaniline, the analogue of hydroquinone. The reaction of diazo coupling was tested with the same *para*-bromo diazonium chloride.

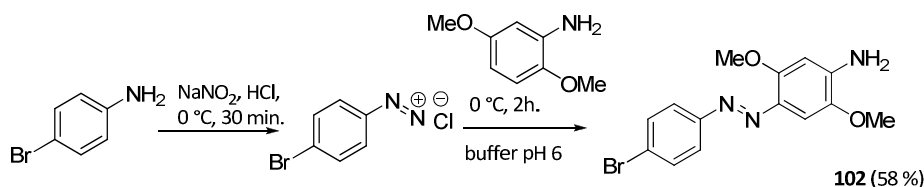


Fig. 157

For this substrate, the aromatic nucleophilic substitution takes place only in preferential *para* position, and we did not have any problems with isolation or purification step. The product **100** was isolated in

58 % yield. The same procedure was repeated for the *para*-chloro and *para*-methoxyanilines to test the reactivity of obtained diazonium salts and to synthesize the diverse chromophores.

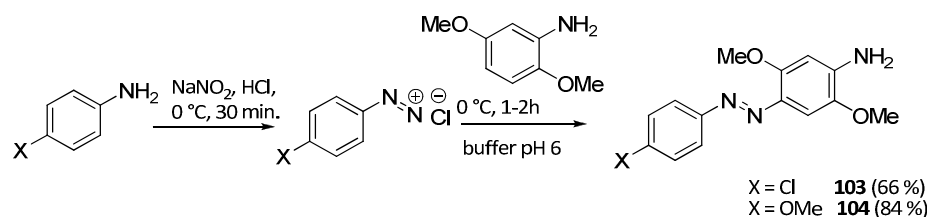


Fig. 158

Finally, 2-aminobenzylaniline was subjected to the formation of diazonium and coupled with 2,5-dimethoxyaniline in order to get the chromophore with the aromatic and aliphatic amino group at the same time. The amino azo compound **105** was obtained with 81 % yield.

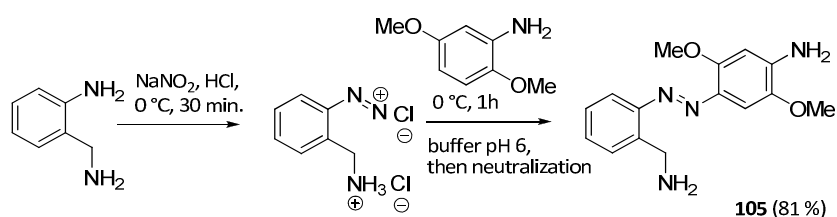
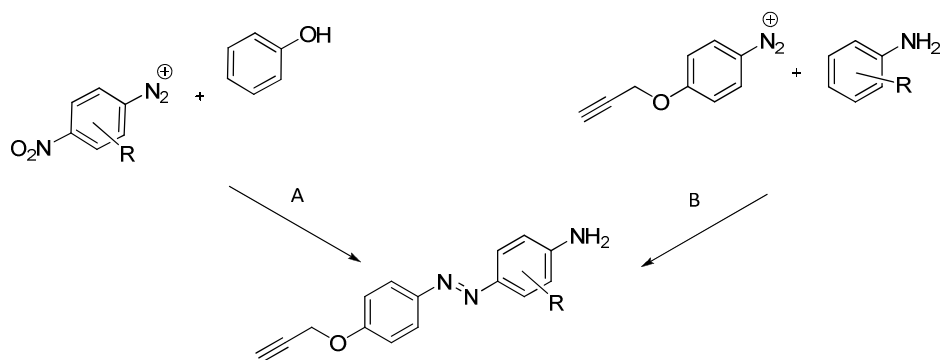


Fig. 159

The last azo compound, which has been envisaged, was product with terminal alkyne. Two synthetic pathways leading to this product were predicted: one through the diazo coupling of activated nitrobenzene and then reduction of obtained azo compound or the synthesis of 4-(prop-2-ynoxy)aniline **106** and formation of diazonium anion from this product (Scheme 59).



Scheme 59

The starting material *para*-nitro phenol was transformed into alkyne ether in the presence of propargyl bromide and K_2CO_3 in DMF. The product was applied for the reduction step without purifying and gave the 4-(prop-2-ynoxy)aniline **106** with good yield (66 % after two steps).²⁵³

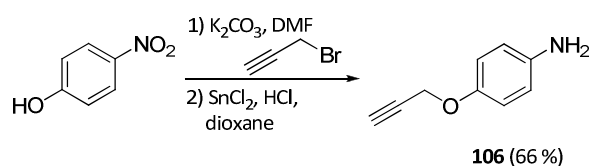


Fig. 160 Preparation of 4-(prop-2-ynoxy)aniline **106**

²⁵³ X. Wang, Y. Zhang, H. Tan, Y. Wang, P. Han, D. Z. Wang, *J. Org. Chem.*, **2010**, *75*, 2403.

This aniline **106** was used in the diazotation reaction in the conditions already stated (NaNO_2 , $\text{HCl}_{\text{conc.}}$, 30 min., 0°C) and then coupled with aniline, giving the mixture of isomers *ortho* and *para*. We tried to separate mixture by column chromatography; however products were not stable in the chromatography conditions.

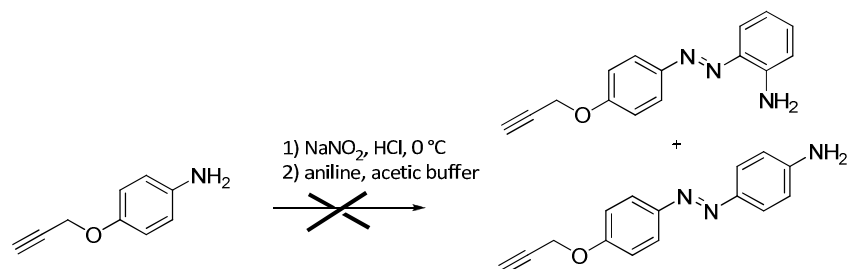


Fig. 161

Simultaneously, we were carrying out the reaction of azo coupling between *para*-nitroaniline and phenol, which provided expected *para*-isomer **107** in 57 % yield. Then, this azo compound was subjected the Williamson ether synthesis with propargyl bromide to give (*E*)-1-(4-nitrophenyl)-2-(4-(prop-2-ynoxy)phenyl)diazene **108** (81 %).

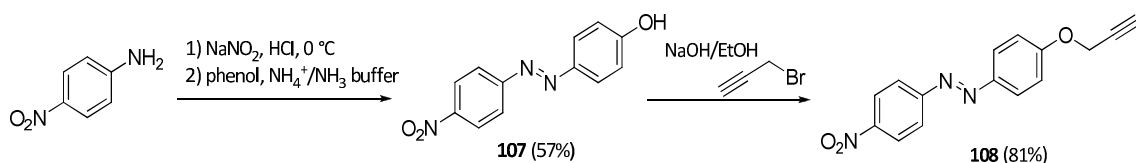


Fig. 162

Unfortunately, the last step of synthesis - the reduction of nitro group in the presence of tin chloride and hydrochloric acid did not work and provided only decomposed product (Fig. 163).

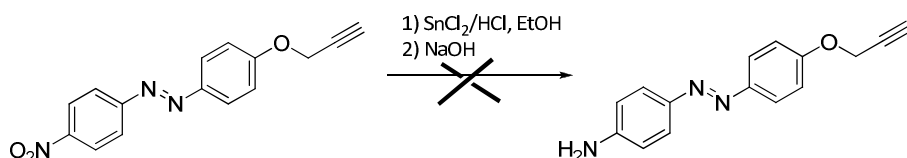


Fig. 163

From the one hand, the application of first pathway seemed to be more accessible, however, the reduction step conferred a problem, therefore the desired product was synthesized *via* the amino alkyne, coupled with 2,5-dimethoxyaniline. We have obtained desired product - the *para*-isomer with 46 % of yield after purification by column chromatography.

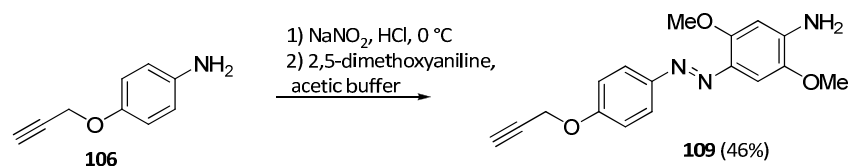


Fig. 164

III.5. Reductive amination with pyrazinic aldehyde

This reaction will permit us to construct the antenna system with pyrazinic core and azo derivative as a spacing arm between the chromophore center and lanthanide chelate. For the best our knowledge, there are no literature examples of this reaction and our approach is completely original. Therefore, we based our first attempt on some examples already conducted with simple primary amines (see paragraph II.7.3). We mixed our product **105** with aldehyde **76** in equimolar amounts in dichloroethane and then reducing agent, $\text{NaBH}(\text{OAc})_3$ (1.4 equiv.) was introduced. Unfortunately, even after overnight vigorous stirring, we did not obtain any traces of expected product. Only both starting materials were recuperated. If so, we changed our strategy, and we used sodium borohydride instead of sodium triacetoxyborohydride. This reaction provided the reduction of aldehyde; therefore we concluded that the nucleophilic attack of the primary amine onto the carbonyl carbon is not spontaneous and needs to be forced by addition of acid.²⁵⁴ We conducted first the formation of imine between an aldehyde and amine (1.2 equiv.) in the presence of acetic acid (1.0 equiv.) for 15 min. at rt and then a reduction agent - NaBH_3CN (1.2 equiv.) - was introduced. Reaction was carried out for 1h at rt and gave a compound **110** with 22% of yield.

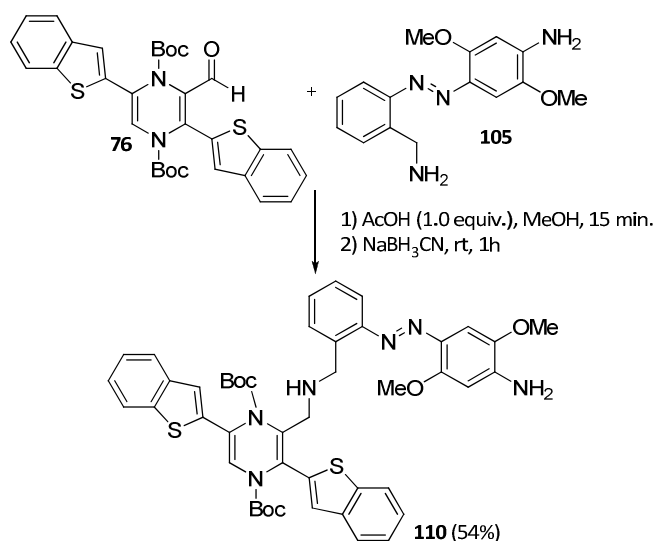


Fig. 165

After optimization of reaction conditions and longer time of stirring with reducing agent, we managed to improve yield of reaction to 54%.

This first attempt showed that the reductive amination of aliphatic group of azo compound **105** is possible. However, the deprotection of the *Boc* group was not succeed for a moment, tested both in acid conditions using TFA at 0 °C and in the presence of TMSI. The further assays are pursuing in the laboratory resulting in a pyrazine derivative with azo spacing arm.

²⁵⁴ (a) A. F. Abdel-Magid, K. G. Carson, B. D. Harris, C. A. Maryanoff, R. D. Shah, *J. Org. Chem.*, **1996**, *61*, 3849; (b) D. C. Beshore, C. J. Dinsmore, *Org. Lett.*, **2002**, *4*, 1201.

III.6. Creation of the spacing arm

The expected final complex should possess the function of attachment with derivatized cyclen molecule. This macrocycle is protected in three positions with acetic acid, but its fourth position stays non-blocked and the connection may be conducted by the secondary amine function. Therefore, the construction of short spacing arm with terminal halogen as candidate for nucleophilic substrate was designed. Besides, this spacing arm should have the carbonyl group in the β position to the nitrogen atom from cyclen in order to provide the oxygen to chelate the metal placed into the center of complex and at the same time to prevent an access for water molecules to the lanthanide center and quenching of fluorescence.

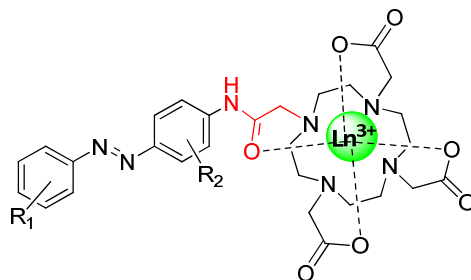
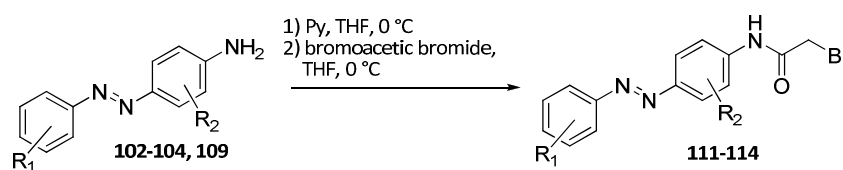


Fig. 166

Bromoacetic bromide was selected as the best spacer. In many synthetic strategies considering the attachment of cyclen moiety to the chromophore, this kind of spacer is used.²⁵⁵ In case of azo derivatives, it suffices to add bromoacetic bromide to the amine compound in the presence of organic base to form the amide with Br-terminal atom. Moreover, the presence of amide bond in the spacing arm gives the possibility to coordinate the eighth position of lanthanide and form the complex insusceptible for quenching in aqueous milieu.

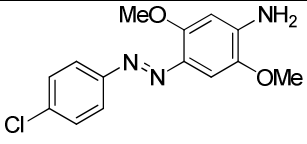
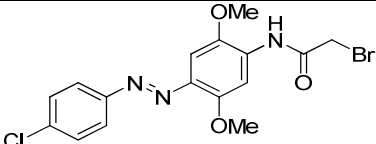
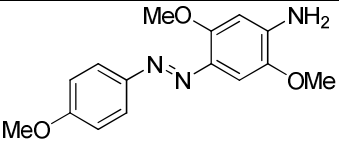
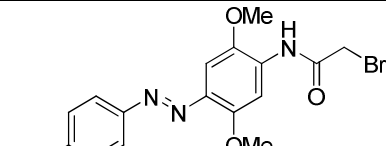
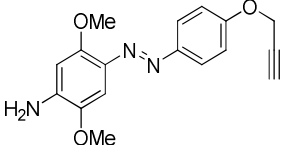
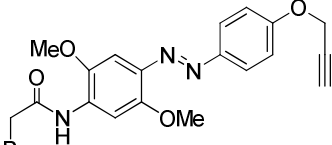
Herein, we report the results of formation of amides from azo derivatives (Table 24).

Table 24



Entry	Substrate	Reaction time	Product	Yield [%]
1	 102	30 min.	 111	95

²⁵⁵ (a) S. Mizukami, K. Tonai, M. Kaneko, K. Kikuchi, *J. Am. Chem. Soc.*, **2008**, *130*, 14376; (b) K. N. Green, S. Viswaiathar, F. A. Rojas-Quijano, Z. Kovacs, D. Shermly, *Inorg. Chem.*, **2011**, *50*, 1648.

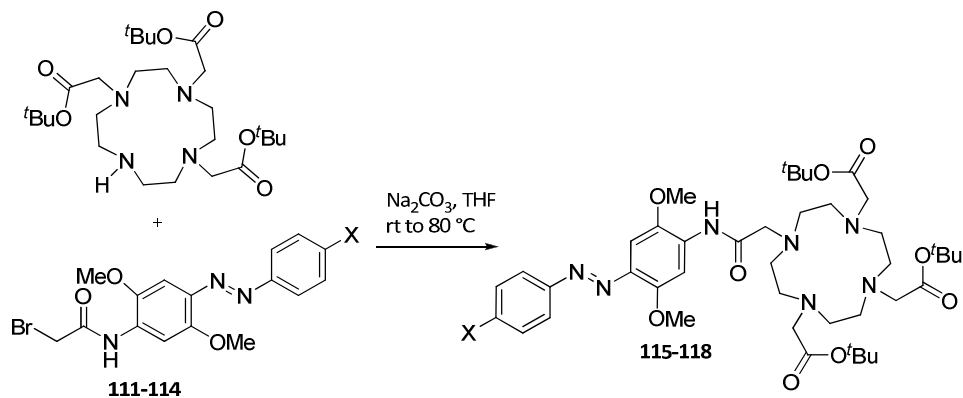
2	 103	30 min.	 112	94
3	 104	60 min.	 113	97
4	 109	30 min.	 114	81

As presented in the Table 8 this reaction gives expected products with excellent yields after 1 hour maximum (Entry 1-3). The product **114** was isolated with 81 % but we suppose that it was due to the lower stability of alkyne in basic conditions. All obtained products were subjected to the nucleophilic substitution with cyclen moiety.

III.7. Nucleophilic substitution with DO3A

The substitution of bromoacetamide of azo compounds by fourth nitrogen atom in DO3A was undertaken in endothermic conditions in the presence of sodium carbonate. First, DO3A was deprotonated by stirring for 30 min. at room temperature in the flask equipped with CaCl₂ trap to avoid the humidity. Then solution of appropriate bromoacetamide was introduced dropwise and the mixture was stirred at the reflux of tetrahydrofuran for several hours. Owing to this methodology, we have obtained expected chromophores in a quantitative manner.

Table 25 Nucleophilic substitution with DO3A



Entry	Substrate	Time	Product/ Yield [%]
1	111 , X = Br	20h	115 / 98
2	112 , X = Cl	18h	116 / 98
3	113 , X = OMe	16h	117 / 57*
4	114 , X = OCH ₂ C≡CH	18h	118 / 95

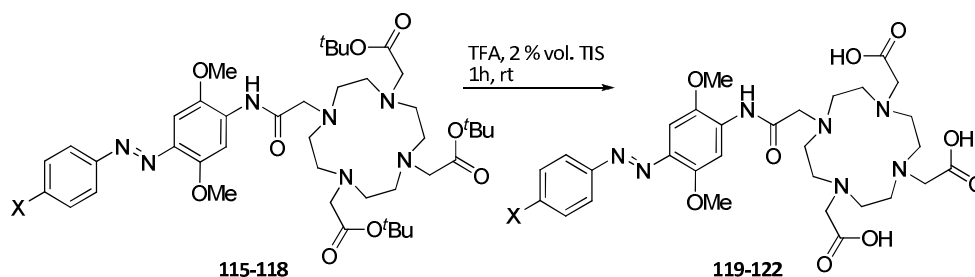
* The complete transformation of starting material, the product partially degraded during purification by column chromatography

Results depicted in Table 25 show the high efficiency of this reaction, all products reacted in the quantitative way; however, the methoxy derivative **117** was isolated with lower yield (57% yield) due to the decomposition on the silica gel in chromatography conditions.

III.8. Deprotection of acetic acid groups in DO3A

The great advantage of application of *tert*-butyl ester group to protect the acetic acid pending arm of cyclen is that this group is stable in nucleophilic substitution condition but also that it is relatively easy to remove in acidic conditions. First, we tested the deprotection in the presence of formic acid in toluene at room temperature. Only the degradation of product and the starting material DO3A were recuperated after this reaction. Afterwards, trifluoroacetic acid was applied in combination with triisopropyl silane (TIS) as a scavenger to trap the free radicals formed during deprotection. This methodology gave a rapid (1 hour of stirring) access to desired acids in a quantitative way.

Table 26 Deprotection of *tert*-butyl esters

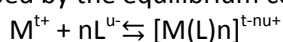


Entry	Substrate	Product/ Yield [%]
1	115 , X = Br	119 / quant.
2	116 , X = Cl	120 / quant.
3	117 , X = OMe	121 / 88
4	118 , X = OCH ₂ C≡CH	122 / 87

The same conditions were applied to the all compounds giving satisfactory results in every case. Compounds **119** and **120** (halogen derivatives) yielded desired acid in quantitative way and compounds **121** (OMe) and **122** (OCH₂C≡CH) showed lower yield, probably due to the difficulty of isolation of products. These products have an aspect of hygroscopic solids and in contact with the air take a form of gum. From these reason, all products were directly used to the step of complexation with corresponding lanthanide salts.

III.9. Formation of lanthanide complexes

The stability of complex is described by the equilibrium constant of formation of complex.



$$K_f = \frac{[M(L)_n]}{[M][L]^n}$$

Equation 12

Stability constants defined in this way, are association constants. This can lead to some confusion as pK_a values are dissociation constants. The relationship between the two types of constant is given in association and dissociation constants.

$$K_a = \frac{1}{K_f}$$

Equation 13

It is known that the stability of the metal complexes with the macrocyclic ligands are much greater than expected in comparison to the stability of the complex with the corresponding open-chain ligands. This phenomenon was named "the macrocyclic effect" and it was also interpreted as an

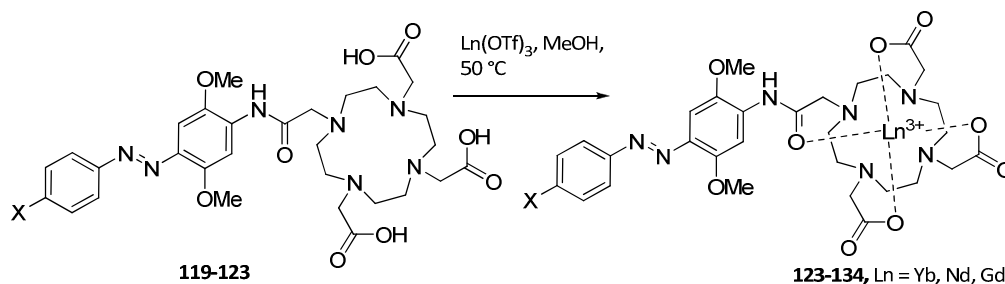
entropy effect. For the lanthanide complexes of DOTA, the value pK_a is very high²⁵⁶ and that indicates the great stability of these assemblies.

As a labile lanthanide complex, we have chosen the trifluoromethanesulfonate salts $\text{Ln}(\text{OTf})_3$ and we conducted the complexation reaction in endothermic conditions (50 °C) in methanol as a solvent. We were using the chromophore triacetic acid derivative without preliminary deprotonation and we recovered the expected complex after precipitation from the mixture with diethyl ether. This method was widely used by the group of Faulkner.²⁵⁷

²⁵⁶ M. F. Loncin, J. F. Desreux, E. Merciny, *Inorg. Chem.*, **1986**, *25*, 2646.

²⁵⁷ A. Dadabhoy, S. Faulkner, P. G. Sammes, *J. Chem. Soc., Perkin Trans.2*, **2002**, 348.

Table 27



Entry	Substrate	Lanthanide complex	Product/Yield [%]
1	<p style="text-align: right;">119</p>	Nd ³⁺	123 (92)
2		Yb ³⁺	124 (73)
3		Eu ³⁺	125 (71)
4	<p style="text-align: right;">120</p>	Nd ³⁺	126 (82)
5		Yb ³⁺	127 (75)
6		Eu ³⁺	128 (81)
7	<p style="text-align: right;">121</p>	Nd ³⁺	129 (90)
8		Yb ³⁺	130 (75)
9		Gd ³⁺	131 (82)
10	<p style="text-align: right;">122</p>	Nd ³⁺	132 (81)
11		Yb ³⁺	133 (quant.)
12		Gd ³⁺	134 (quant.)

We have obtained 12 new complexes of lanthanides with different metals and different substituents in *para* position to azo bond. All complexes were characterized by high resolution mass spectrometry and absorption and emission spectra, their purity were checked by reversed phase HPLC. In our interest was to create the complexes of ytterbium(III) and neodymium(III) in order to observe the

luminescence in the region of near-infrared. The complex of gadolinium serves to verify energy of triplet state of molecule and therefore fully characterize the new sensitizers.

III.10. Vectorization of lanthanide complex by the mean of cyclopeptide RGD

The final aim of this project was to introduce a particular biomolecule to the lanthanide complex, which will show a great affinity to cancer cells and therefore, enables the specific detection of cancerous cells. The biomolecule possessing these features is a cyclopeptide containing a triad RGD.

III.10.1. Cyclopeptide RGD and its role in cancer cell vectorization

Integrines are a family of heterodimeric transmembrane glycoproteins involved in the wide range of cell-to-membrane and cell-to-cell interactions. In general, this kind of biomolecules belongs to the group of cell adhesion molecules (CAM). They play a major role in cell morphology, locomotion, mitosis, phagocytosis and cytokinesis. It is known also that CAMs are responsible for various disease states such as cancer,²⁵⁸ thrombosis,²⁵⁹ rheumatoid arthritis²⁶⁰ and diabetes.²⁶¹

The motif of three amino acids: arginine (R), glycine (G) and aspartic acid (D) has been discovered to be recognizable by the cell adhesion sequence in fibronectin.²⁶² The RGD sequence is the cell attachment site of a number of adhesive surface proteins. It has been proven that nearly half of over 20 integrins recognize this motif in their cell adhesion protein ligands. One of them – integrin $\alpha_v\beta_3$ is expressed on the cell membrane of various tumor cell types such as late stage glioblastoma, melanoma, ovarian, breast and prostate cancer.²⁶³ An integrin $\alpha_v\beta_3$ was shown to play a crucial role in tumor invasion and metastasis resulting from the ability to recruit and activate matrix metalloprotease (MMP), which can degrade components of the basement membrane and interstitial matrix.²⁶⁴

Many of modified structures of molecules containing sequence RGD have been synthesized and valorized since last ten years. Among them, linear and cyclic RGD peptides have been developed as ligands preferentially bound to integrin $\alpha_v\beta_3$, such as c(RGDfK) and c(RGDyK), presented below (Fig. 167).

²⁵⁸ (a) G. Christifori, *EMBO J.*, **2003**, *22*, 2318; (b) K. Maaser, K. Wolf, C. E. Klein, B. Niggemann, K. S. Zanker, E. B. Brocker et al., *Mol. Biol. Cell.*, **1999**, *10*, 3067; (c) E. Ruohlahti, *Nat. Rev. Cancer.*, **2002**, *2*, 83.

²⁵⁹ (a) R. K. Andrews, M. C. Berndt, *Thromb. Res.*, **2004**, *114*, 447; (b) J. M. Gibbins, *J. Cell. Sci.*, **2004**, *117*, 3415.

²⁶⁰ X. Banquy, G. Leclair, J. M. Rabanel, A. Argaw, J. F. Bouchard, P. Hildgen et al., *Bioconjug. Chem.*, **2008**, *19*, 2030.

²⁶¹ K. Ichinose, E. Kawasaki, K. Eguchi, *Am. J. Nephrol.*, **2007**, *27*, 554.

²⁶² (a) M. D. Pierschbacher, E. Ruohlahti, *Nature*, **1984**, *309*, 30; (b) E. Ruohlahti, *Matrix Biol.*, **2003**, *22*, 459.

²⁶³ (a) W. Cai, X. Chen, *Agents. Med. Chem.*, **2006**, *6*, 407; (b) G. J. Mizejewski, *Proc. Soc. Exp. Biol. Med.*, **1999**, *222*, 124; (c) H. Jin, J. Varner, *Br. J. Cancer.*, **2004**, *90*, 561.

²⁶⁴ P. C. Brooks, S. Stromblad, L. C. Sanders, T. L. von Schalscha, R. T. Aimes, W. G. Stetler-Stevenson et al., *Cell.*, **1996**, *85*, 683.

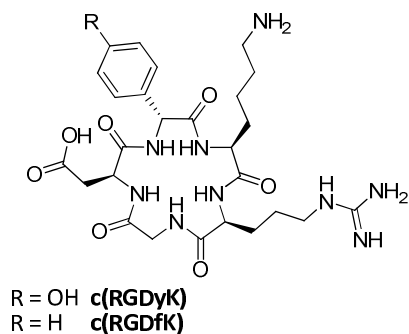


Fig. 167

Cyclopeptides c(RGDyK) and c(RGDfk) are showing high binding affinity and selectivity particularly for this integrin $\alpha_v\beta_3$, thus these peptides are applied as target delivery of therapeutics or diagnostic to tumors.²⁶⁵ Moreover, this kind of peptides may be easily modified by the introduction of azide group in the place of lysine residue, and thus they became interesting substrates in relation to the click reactions.

Taking into account the great affinity of cyclopeptides to integrins, they have found an important application to prepare probes for non-invasive visualization by different media: nuclear media such as SPECT (Single Electron Emission Computed Tomography) and PET (Positron Emission Tomography),²⁶⁶ magnetic resonance (MRI)²⁶⁷ and optical methods dyes (FMT – Fluorescent Mediated Tomography).

III.10.2. Cycloaddition reaction with peptide RGD

Our intention was to use this modified cyclopeptide attached to the lanthanide complex as a marker for cancer cells. Some molecules connected to the macrocycle DO3A have been reported, but they do not serve as chelators for lanthanide emitting in near-infrared, but as a ligands for radiometals such as [¹¹¹In].²⁶⁸ Also, these complexes are chelates for paramagnetic Gd³⁺ as a probe for MRI. To the best of our knowledge, no examples of cyclopeptide RGD attached to the lanthanide complex emitting in near-infrared exist. For the synthesis of biovector for the cancerous cells, we have envisaged to construct the chromophore already complexed with lanthanide, which will have the terminal alkyne to perform cycloaddition reaction with azide-derived cyclopeptide RGD.

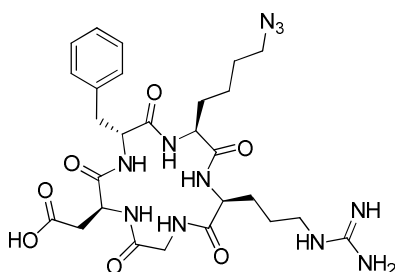


Fig. 168 Cyclopentapeptide RGD

²⁶⁵ K. Temming, R. M. Schiffelers, G. Molema, R. J. Kok, *Drug Resist Updat.*, **2005**, *8*, 381.

²⁶⁶ Z.-B. Li, Z. Wu, K. Chen, F. T. Chin, X. Chen, *Bioconjugate Chem.*, **2007**, *18*, 1987.

²⁶⁷ P. Verwilst, S. V. Eliseeva, S. Carron, L. V. Elst, C. Burtea, G. Dehaen et al., *Eur. J. Inorg. Chem.*, **2011**, 3577.

²⁶⁸ (a) I. Dijgraaf, A. Y. Rijnders, A. Soede, A. C. Dechesne, G. W. van Esse, A. J. Brouwer et al., *Org. Biomol. Chem.*, **2007**, *5*, 935; (b) Y. Zhou, S. Chakraborty, *Theranostics*, **2011**, *1*, 58.

The modified cyclopeptide RGD has been furnished by Dr. V. Aucagne (CBM, Orléans)²⁶⁹ and chromophores containing different lanthanide cations (Yb^{3+} , Nd^{3+} and Gd^{3+}) were synthesized according to our original pathway. The reaction of cycloaddition was carried out in HEPES buffer (pH = 7.5) at room temperature in aqueous solution in the presence of $\text{CuSO}_4 \cdot 5\text{H}_2\text{O}$, THPTA as a ligand for Cu(I), sodium ascorbate and aminoguanidine hydrochloride to protect the peptidic part.²⁷⁰ This methodology has been elaborated and evaluated by equipe of V. Aucagne and A. Delmas for cyclopeptides RGD with terminal azide function. The progress of reaction and purification of products were conducted by HPLC reversed phase.

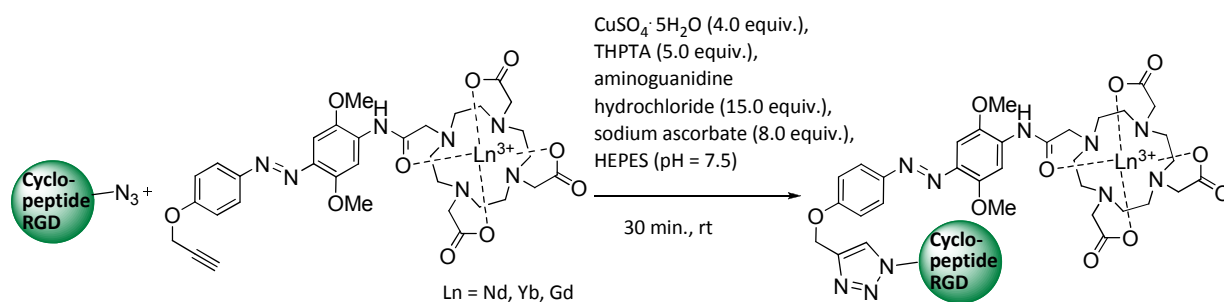


Fig. 169

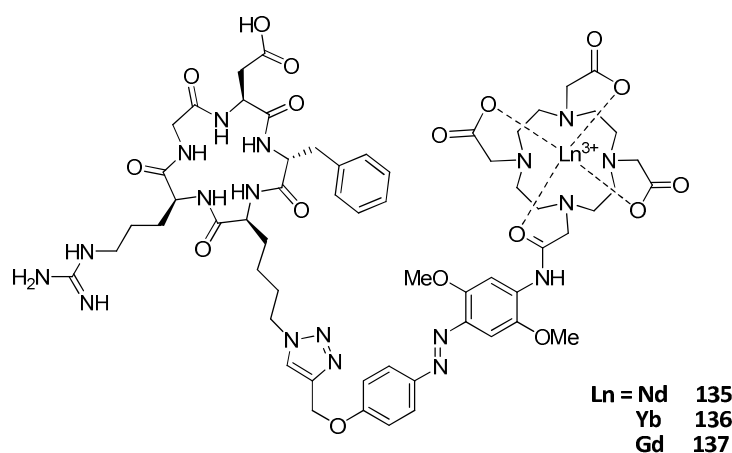


Fig. 170

We have obtained three complexes of target molecules (Fig. 170) with satisfactory yields (up to 40 % after isolation by preparative RP-HPLC) and high purity (99.8%). The structure of products was confirmed by high-resolution mass spectrometry (HRMS), absorption and emission spectra. During the cycloaddition reaction, we did not observe any decomplexation of lanthanide or the cleavage of the azo bond.

²⁶⁹ V. Aucagne, A.F. Delmas, *unpublished results*

²⁷⁰ I. E. Valverde, A. F. Delmas, V. Aucagne, *Tetrahedron*, **2009**, *65*, 7597.

III.11. Spectroscopic properties of azo compounds

III.11.1. Absorption spectra

In order to identify the maximum of excitation wavelength of lanthanide sensitizers, we have collected the absorption spectra in the UV-visible region (Fig. 171). We have worked with diluted aqueous solution of complexes (100 µg/mL for Br-substituted, Cl-substituted and those with cyclopeptide, 50 µg/ mL for OMe-substituted). For the ytterbium and neodymium complexes formed with the ligands that incorporate halogen atom in the position *para* to the azo group **123**, **124**, **126** and **127**, we observed two maxima of absorption at 338 nm and 414 nm. The coefficient of absorption of these compounds is in the range of 6900-9000 [M⁻¹cm⁻¹] (see Table 28). For the compounds containing the methoxy substituent **129** and **130**, two maxima are present and are localized at 350 nm and 410 nm. The highest value of coefficient of absorption equals 9000 [M⁻¹cm⁻¹] for the complex **127** with Nd³⁺. Whereas, for the lanthanide complexes formed with the cyclopeptide **135** and **136**, we have obtained slightly more elevated (11000-11500 M⁻¹cm⁻¹) values. Also maxima of absorption are slightly shifted compared to halogen derivatives: with two apparent maxima located at 350 nm and 410 nm. These values of absorption coefficient are in accordance with those reported for azamacrocyclic europium complexes (11 000-16 000 M⁻¹cm⁻¹).²⁷¹ In comparison with other antennae for lanthanides, they are twice lower than for quantum dots,²⁷² and few-folds smaller than for PAMAM dendrimers²⁷³ due to high concentration of chromophore groups in one molecule.

²⁷¹ A. Bourdolle, M. Allali, J.-C. Mulatier, B. Le Guennic, J. M. Zwier, P. L. Baldeck, J.-C. G. Bünzli, C. Andraud, L. Lamarque, O. Maury, *Inorg. Chem.*, **2011**, *50*, 4987.

²⁷² D. Geißler, L. J. Charbonnière, R. F. Zeissel, N. G. Butlin, H.-G. Löhmansröben, N. Hildebrandt, *Angew. Chem. Int. Ed.*, **2010**, *49*, 1396.

²⁷³ (a) I. Grabchev, J.-M. Chovelon, V. Bojinov, G. Ivanova, *Tetrahedron*, **2003**, *59*, 9591; (b) M. A. Alcalá, C. M. Shade, H. Uh, S. Y. Kwan, M. Bischof, Z. P. Thompson, K. A. Gogick, A. R. Meier, T. G. Strein, D. L. Bartlett, R. A. Modzelewski, Y. J. Lee, S. Petoud, C. K. Brown, *Biomaterials*, **2011**, *32*, 9343.

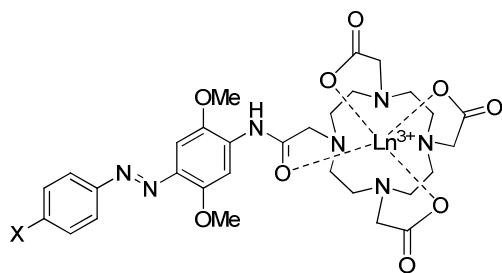


Table 28

X	Ligand	Ln ³⁺	Product
Br	L1	Nd	123
		Yb	124
Cl	L2	Nd	126
		Yb	127
OMe	L3	Nd	129
		Yb	130
cyclopeptide	L4	Nd	135
		Yb	136

Entry	Ligand	Complex	Conc. [mmol/L]	λ_{\max} [nm]	A	ϵ [M ⁻¹ cm ⁻¹]
1	L1	123 (Nd ³⁺)	0.115367	338	1.014	8800
				414	0.958	8300
2	L1	124 (Yb ³⁺)	0.111657	338	1.003	9000
				414	0.947	8500
3	L2	126 (Nd ³⁺)	0.1221	338	0.931	7600
				414	0.848	6900
4	L2	127 (Yb ³⁺)	0.117925	338	1.043	8800
				414	0.967	8200
5	L3	129 (Nd ³⁺)	0.061497	350	0.480	7800
				410	0.553	9000
6	L3	130 (Yb ³⁺)	0.05926	350	0.420	7100
				410	0.498	8400
7	L4	135 (Nd ³⁺)	0.06824	350	0.664	9900
				410	0.770	11500
8	L4	136 (Yb ³⁺)	0.06678	350	0.635	9300
				410	0.750	11000

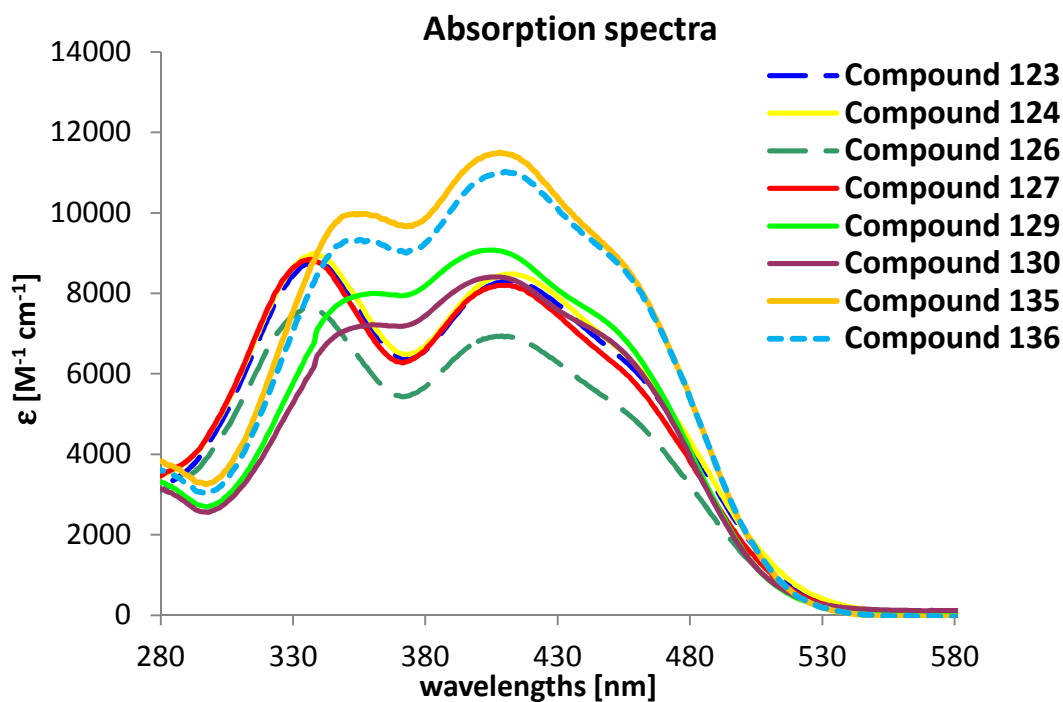


Fig. 171

The tendency can be observed between the different complex containing halogen atom (**123**, **124**, **126**, **127**) and methoxy group and cyclopeptide, that the first maximum of absorption exists for wavelength ($\lambda = 338$ nm) corresponding to higher energies for halogen derivatives and is shifted toward lower energies for other products. However, the second maximum of absorption is located at almost the same wavelength for the different complexes: 410-414 nm and it is significantly shifted toward the red part of spectrum. This observation permits the use of higher wavelengths corresponding to lower energy to induce the sample excitation.

Making comparison between these four groups of chromophores, we can say that the highest efficiency to absorb light (the highest molar absorptivity ϵ) and transfer the energy to the lanthanide cation is found for the compound **135** (cyclopeptide), probably owing to an assembly of chromophore parts (the azo part and triazole moiety joining with the cyclopeptide RGD) in one molecule.

Subsequently, we have tested the photostability of complexes by irradiation in the region of UV-Vis and observation of absorption spectra. We were recording absorption spectra every 15 minutes. The solution of halogenated ligand **123** showed a significant decrease of absorption signal after each 15 minutes of data collection in the maxima of absorptions (indicated by arrows). In the case of the sample test (a green line), the solution was prepared a day before experiment and stored in a dark place. No decrease of signal in the sample test was observed, which means that the irradiation by the excitation source, not the time of storage, is responsible for the decomposition.

Photostability of compound 123

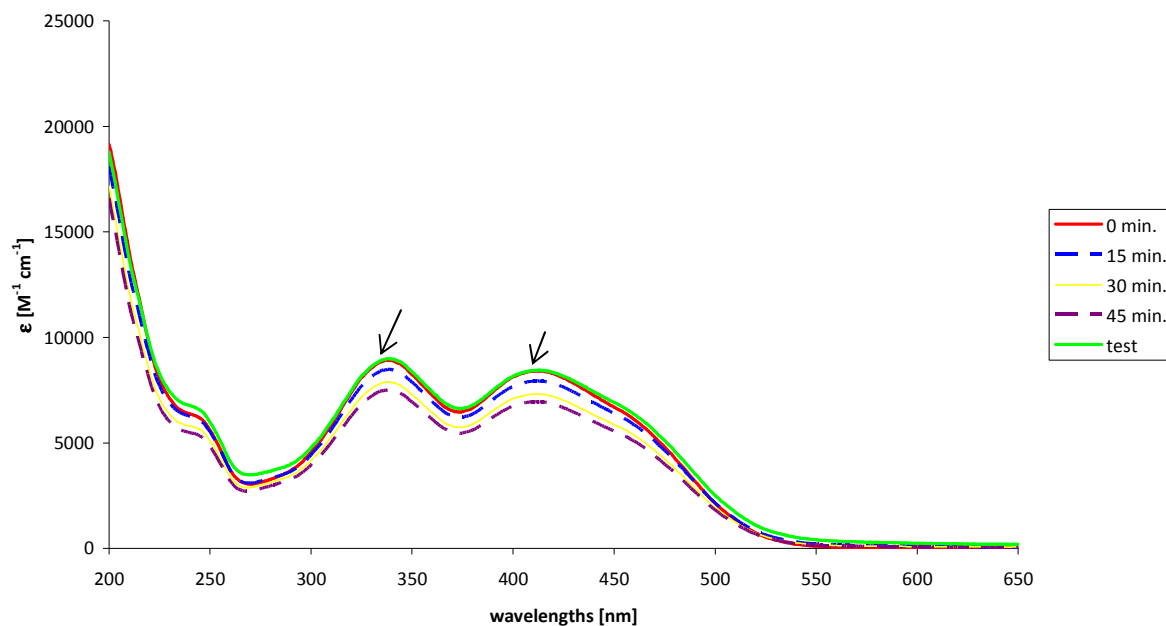


Fig. 172

On the Fig. 172 we can notice a significant decrease of absorption signal after each irradiation. A signal loss of about 20% was observed after four consecutive irradiations. We suppose that this decrease is due to the slow degradation of the chromophore. At the same time, absorption spectra of compound **129** (OMe) counterpart of previously tested product do not show any change of intensity on the absorption spectrum after the repetition of irradiation every 15 min (Fig. 173). That may explain our hypothesis of partial decomposition of complexes containing halides during the irradiation process.

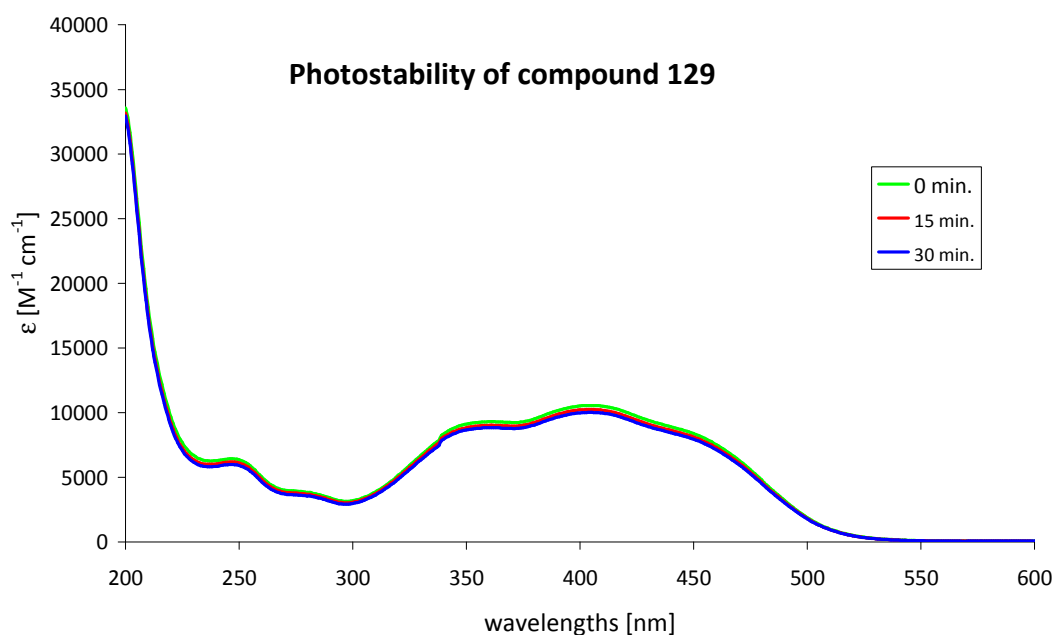


Fig. 173

III.11.2. Emission spectra in the NIR region – luminescence of lanthanide

The emission spectra were recorded on the Fluorolog 322 apparatus in order to quantify the energy which is transferred to the lanthanide chelating system. The stock solution of compounds were prepared prior to use at the concentration 1mg/mL of ultrapure water MiliQ (in the case of compounds **123** and **124**) and in the buffer PBS (pH = 7.5) in the case of products linked to the cyclopeptide RGD (products **135** and **136**). Then these solutions were diluted ten times to the concentration 100 µg/mL to avoid the saturation of the signal on the detector.

At room temperature and upon broad band excitation at 465 nm (**123** and **124**) and 460nm (**135** and **136**), the luminescence spectra display the bands corresponding to the expected emissions. The Nd³⁺ complex **123** displays NIR luminescence in the 800-1200 nm range, the main band being centered at 1064 nm and with a band of lower intensity in the range 875-940 nm, which corresponds to transitions from ⁴F_{3/2} level to the ⁴I_{9/2} sublevel (for lower wavelengths) and to the ⁴I_{11/2} sublevel (for the higher wavelengths). Under the same conditions, the Yb³⁺ complex **124** emits in the 920-1000 nm range, with a band at 950 nm assigned to the ²F_{5/2}→²F_{7/2} transition and a broaden vibronic component at shorter wavelengths.

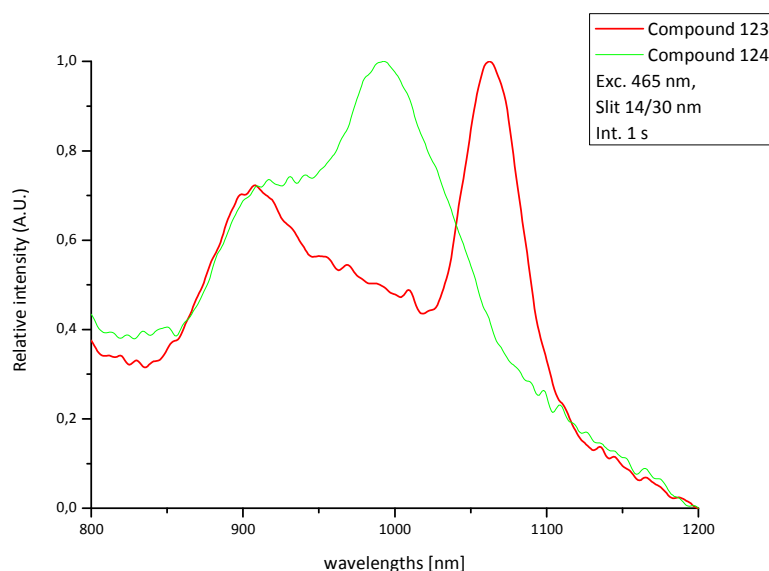


Fig. 174

The compounds **135** and **136** (with cyclopeptide) were equally tested for the energy transfer to the lanthanide center. For the proper acquisition of lanthanide emission spectra, samples were excited at 460 nm, with slit opening 14 nm and 30 nm and integration time 0.5 s. The filter LP700 was applied to remove the contribution of visible photons.

Excitation at 460 nm gave the typical sharp emission bands corresponding to the maxima of Nd³⁺ and Yb³⁺ cations. For the complex **135** (Nd³⁺) two individual apparent emission maxima were observed for

915 nm and 1064 nm attributed to the transitions between $^4F_{3/2}$ level to the $^4I_{9/2}$ and $^4I_{11/2}$ sublevels, respectively. At the same time, Yb^{3+} complex shows the emission band ranging from 920 to 1050 nm ($^2F_{5/2} \rightarrow ^2F_{7/2}$ transition).

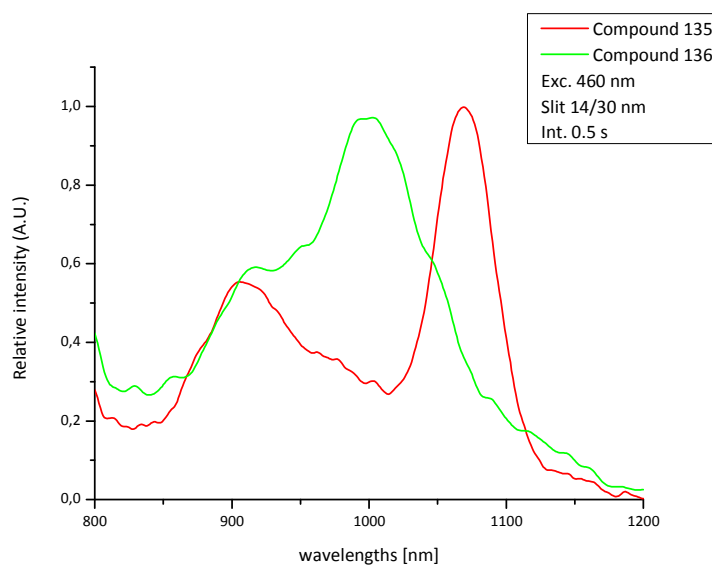


Fig. 175

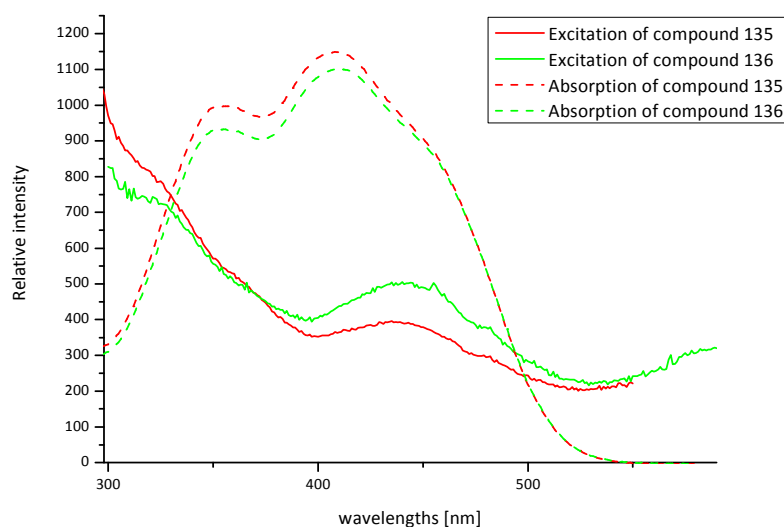


Fig. 176

Excitation spectra for products **135** and **136** presented on Fig. 176 prove that the both complexes can be excited in the range 370 – 500 nm. These excitation spectra can be compared to the absorption spectra of the chromophore **135** and **136**, showing a correct overlap of the chromophore absorption with the excitation spectrum when observing the luminescence of the lanthanide. The red shift of maximum of excitation in comparison to maximum of absorption of ca. 40 nm is probably due to different efficiency of the energy transfer depending on the excited state of the chromophore.

The complexes with cyclopeptide **135** and **136** were synthesized in concept of creation a luminescent biomarkers for tumor cell due to high affinity of cyclopeptide RGD part to the membrane integrines of cancerous cells, as it was described in the introduction. Therefore, we wanted to determine the maximum wavelength of excitation for both complexes, which is still capable to generate the emission of lanthanide cation. Indeed, higher excitation wavelength corresponds to lower energy, and hence provokes less damage in the tested biological material and is preferable for biological tests. Lanthanide emission spectra were recorded with excitation at 370, 410, 460 and 520 nm for solutions of 100 μ g/mL of complexes in PBS buffer (pH = 7.5, physiological conditions) and are presented on the Fig. 177 for Nd³⁺ and Fig. 178 for Yb³⁺ complex. We can notice that at the range of excitation from 370 to 460 nm, the lanthanides have good emission intensities in both cases and the high wavelengths excitation at 520 nm gives some low signal for Nd³⁺ complex **135**, but for Yb³⁺ compound **136** the limit of excitation has been reached, since very low signal can be seen.

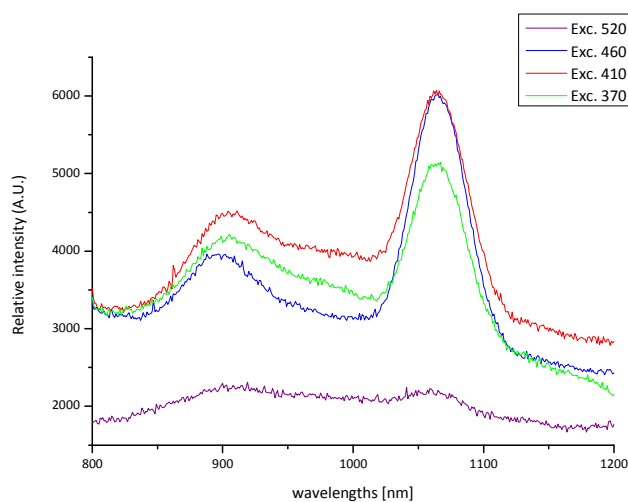


Fig. 177 Emission spectra of the Nd complex 135

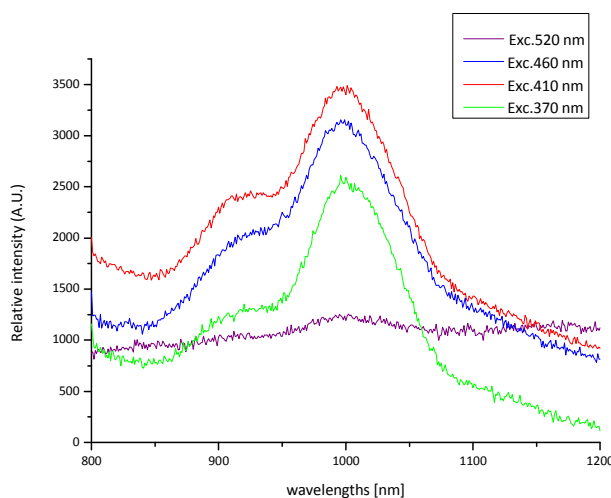


Fig. 178 Emission spectra of the Yb complex 136

In order to establish a proof of principle of the ability of complexes **133** and **134** to act as a luminescent marker for biological imaging, we have decided to record images using Nikon AZ-100 microscope. However, even the concentrated solution did not allow the recording of an image due to the insufficient number of photons.

III.11.3. Emission spectra in UV-Vis – fluorescence of chromophore

It is noteworthy that the solution of product **136** (Yb^{3+} complex) in cold conditions (77K) changes significantly color from yellow to dark violet, indicating a clear change of its absorbance spectrum, which is co-notated with the change of the emission spectrum of chromophore.



Fig. 179 Change of color of the aqueous solution of compound **134** at $-20\text{ }^{\circ}\text{C}$ (on the right)

This red shift of the fluorescence spectrum is presented on Fig. 180. The normalized emission spectra show that at room temperature the maximum of emission is assigned at 550 nm and at the temperature of liquid nitrogen – 594 nm. Moreover, the intensity of this band is about hundred times higher than the intensity at room temperature.

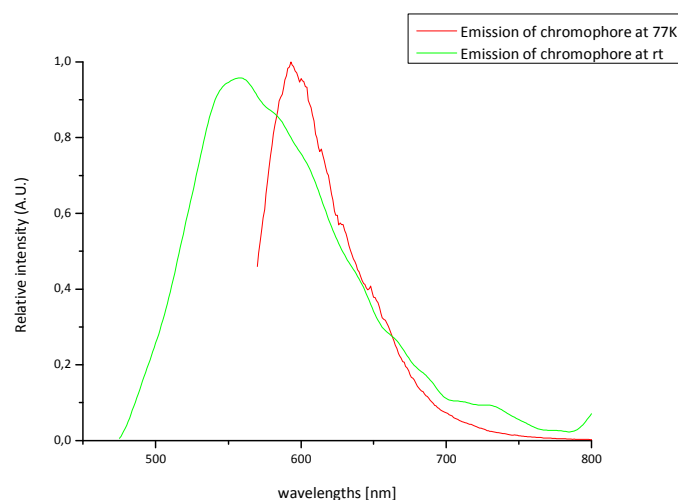


Fig. 180

This is an example of thermochromism, explained as reversible color change of a substance induced by a temperature change. Some examples of this effect were described for compounds with azo bond,²⁷⁴ however, to the best of our knowledge, not with lanthanides complexes.

III.11.4. Lifetime measurements

The lifetime of luminescence of lanthanide complexes for aqueous solutions of compounds **129**, **130**, **135** and **136** were measured to establish the number of inner sphere water molecule, and therefore to consider the protection of lanthanide cation against non-radiative deactivation (Chapter 2, Paragraph I.3).

The analysis of the experimental luminescence decays obtained upon excitation of the complexes at 355 nm revealed the best fittings as single-exponential functions as an indication of the presence of a single-species. The fitted lifetimes upon monitoring Nd(⁴F_{3/2}) and Yb(²F_{5/2}) bands are placed in Table 29.

Table 29

Complex	λ_{exc} [nm]	τ [μs]		
		H ₂ O	D ₂ O	q
129 (Nd ³⁺)	355	0.064(5)	0.230(1)	1.1
130 (Yb ³⁺)	355	0.708(10)	5.85(5)	1.0
135 (Nd ³⁺)	355	0.069(10)	0.238(3)	1.0
136 (Yb ³⁺)	355	0.793(10)	5.84(3)	0.9

The presented luminescence lifetimes are roughly 11-times longer for both Yb³⁺ complexes for the H₂O solutions and about 25-times in the D₂O solution, which is consistent with observations for similar sensitizers.¹⁶⁶ Lifetimes in H₂O solutions are significantly shorter than those reported by Faulkner (1.95 μs and 1.75 μs in water, 5.12 μs and 5.17 μs in the D₂O solution), where the azo sensitizer neodymium complex shows 0.112 μs and our compounds **129** - 0.064 μs and **135** - 0.069 μs . The same tendency occurs for Yb³⁺ complex; the value reported by Faulkner is 1.41 μs and our - 0.708 μs (**130**) and 0.793 μs (**136**). However, in the case of deuterated solutions, values are much closer: the literature ones 0.355 μs (Nd³⁺) and 4.02 μs are close to ours 0.230 (**129**), 0.238 (**135**), 5.853 (**130**) and 5.843 (**136**). In our case, the q parameter is convergent to the unity, which means that we can expect one water molecule in the inner sphere of coordination of the lanthanide cation in synthesized complexes. In the literature this value is rather lower than one, but still means that one molecule is inserted in the coordination sphere of metal center.

²⁷⁴ (a) G. S. Kikot', M. I. Cherkashin, B. S. Kikot', *Russ. Chem. Bull.*, **1981**, *5*, 783; (b) U. Oertel, H. Mart, H. Komber, F. Böhme, *Optical Materials*, **2009**, *32*, 54.

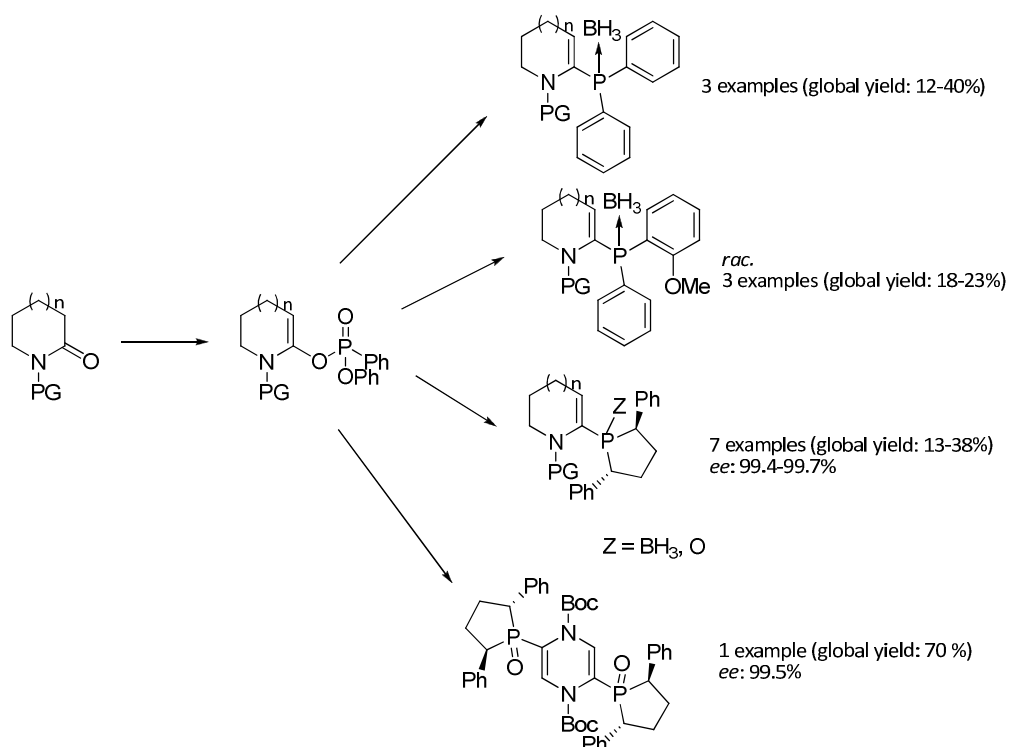
III.11.5. Summary

In conclusion, the spectroscopic features of a newly synthesized chromophore based on azo compounds were presented. These compounds were predicted to sensitize the lanthanide cations and presented results show that our system satisfies the condition of an antenna for lanthanides. The principal properties such as excitation and emission energy were determined. The presented molecules are novel and original examples of azo chromophores linked with cyclen chelate. In our synthetic strategy we have envisaged the attachment of this azo system to the pyrazinic moiety, described before, and this approach will permit to complete studies on original sensitizers.

IV. Conclusion and perspectives

This doctoral dissertation has been devoted to the two complementary topics revolved around the synthesis, reactivity and applications of enecarbamates or enamides and N-heterocycles derived from them. The contribution to the valorization of heterocyclic systems containing the nitrogen atom has been presented on the pages of this thesis. In the first part, the synthesis and evaluation of new organophosphorus compounds starting from enol phosphates was described. Two different synthetic pathways were considered: the first one based on the C-P cross-coupling palladium catalyzed reaction leading to original α -enamido phosphane derivatives and the second one, the nucleophilic addition of phosphides anions to non-activated acyclic enecarbamates. The second part of thesis, in the same assumption of evaluation and valorization of N-heterocycles, was dedicated to the synthesis of original chromophores with pyrazinic core as sensitizers for lanthanide cations emitting in near-infrared.

The lactam derived enol phosphates were starting materials for original C-P cross coupling reaction with borane protected secondary phosphines and phospholane oxides.¹¹⁹ This approach gave us an access to 6- and 7-membered ring α -enamido phosphane products with fair to good yields. 14 novel organophosphorus compounds were obtained: first the strategy was optimized on the achiral series and then, we moved to chiral substrates for coupling (Scheme 60).

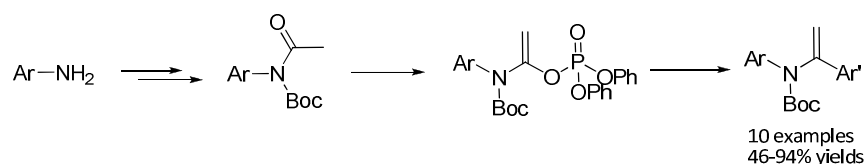


Scheme 60

Unfortunately, we encountered the difficulties on the stage of cross-coupling with enantiopure secondary phosphine borane, where the chiral phosphorus center racemized in the applied thermal conditions. However, in the case of phospholane substrate with chirality placed on two carbons at a position to P-atom, we managed to obtain expected products in an enantioselective way (up to 99.7%

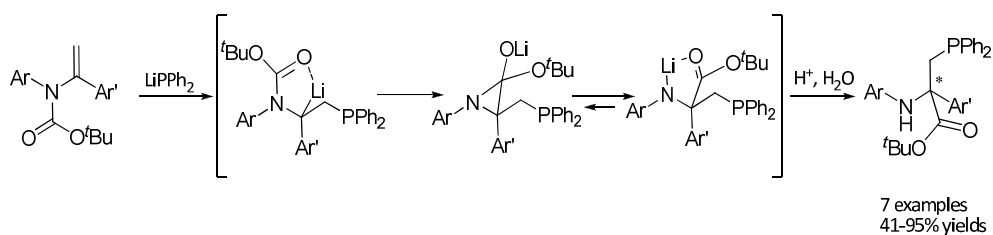
ee). A variety of phosphine derivatives as well as different enol phosphates was coupled, showing the efficiency of this cross-coupling reaction. This strategy may thus provide an access to phosphinoheterocyclic compounds based on privileged substructures with potential biological interest. In perspectives, the problem of racemization could be overcome by using chiral catalysts such as (*R*)-Tol-BINAP or (*S,S*)-Me-DuPHOS, which was recently described in the literature by the team of A.-C. Gaumont.

The second strategy of the synthesis of new organophosphorus compounds was based on the reaction of the nucleophilic addition of lithiated phosphines onto the double bond of acyclic enecarbamates, providing analogues of non-natural amino acids with phosphorus atom in the β position. First, starting from commercial available anilines and benzylamine, after the protection step, we obtained the range of variously substituted enol phosphates. Then, we performed reactions of cross-coupling type Suzuki and Stille on enol phosphates leading to the acyclic enecarbamates with different aryl and heteroaryl groups in an efficient way (46-94% yield for 10 examples).



Scheme 61

These compounds became a starting point for the phospholithiation reaction. The reaction of nucleophilic addition of phosphide anions was inspired by the methodology already elaborated in our laboratory with other nucleophilic agents (RLi, organic bases) and concerned the addition to the double bond of the enecarbamate with concomitant migration of the alkyloxycarbonyl group leading to the derivatives of β -phosphino amino acids. This strategy gave an access to 7 derivatives with moderate to excellent yields (41-95%) (Scheme 62).



Scheme 62

As it is presented on Scheme 62, the quaternary center is created during this reaction, however, the transformation itself is not enantioselective. In order to induce the enantioselectivity during the phospholithiation, we conducted the reaction in the presence of (-)-sparteine as a chiral bidentate ligand to protect the formed carbanion. Nonetheless, even with this modification, we did not manage to obtain the enantiomerically pure compounds. This result signifies that the carbanion formation is

not regioselective and that the alkyloxycarbonyl is equally transferred on both sites on this anion. Also, some attempts with chiral phosphines were undertaken, however in this case, the nucleophilic phosphorus agent could not be formed. In the perspective to this project, the enantiocontrol of this reaction, either by the application of chiral protecting group, or by the chiral organocatalyst or by the application of chiral deprotonation, system is envisaged.

Furthermore, the spontaneous oxidation of the phosphorus atom was observed during the reaction. We tested the influence of the quantity of the nucleophile in the relation to the free phosphine on the *tert*-butyl phenyl(1-phenylvinyl)carbamate. The presence of free phosphine provokes the apparition of non-transferred oxidized and non-oxidized product (Fig. 181), and the excess of the phosphine increases the percentage of this products.

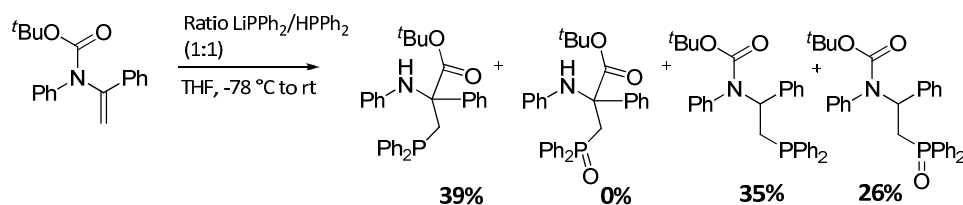
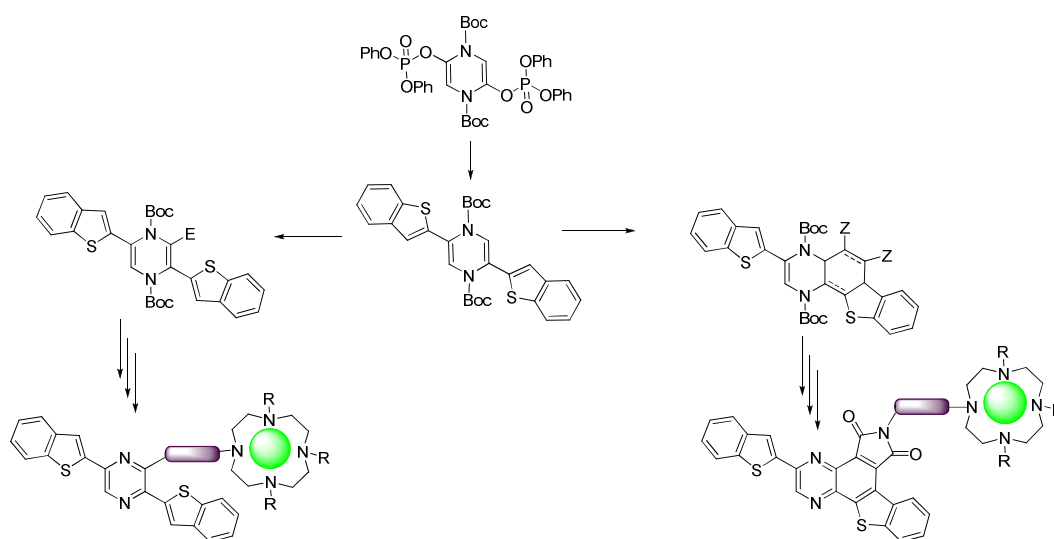


Fig. 181

It means that kinetic influence of reprotonation is much faster than the intramolecular migration of the alkyloxycarbonyl group.

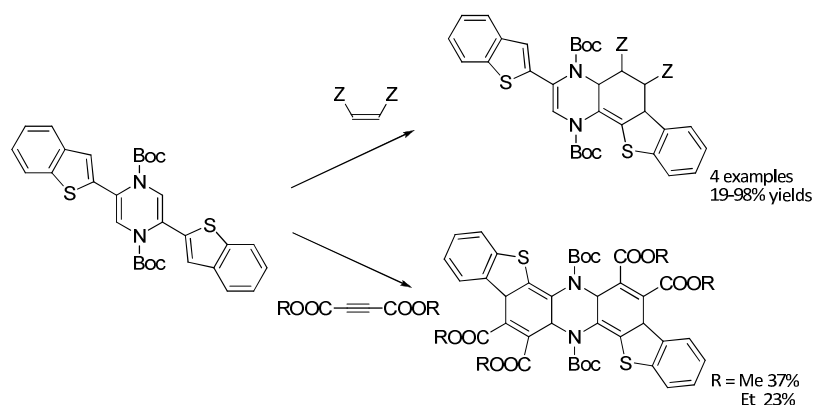
Finally, the structure of five among twenty five novel organophosphorus compounds were determined by structural analysis based on X-ray crystallography.

The second chapter of this dissertation was devoted to the construction of sensitizing systems for lanthanide cations based on pyrazinic chromophores. The pyrazine derivatives were obtained in the reaction of cross-coupling of bisvinyl phosphate of dihydropyrazine with range of aryl and heteroaryl derivatives.



Scheme 63

Considering the photophysical properties of new compounds, a target molecule - 2,5-dibenzo[*b*]thiophenyl dihydropyrazine was chosen for further investigation. Two distinct methodologies were applied in order to functionalize this dihydropyrazine. From the one hand, the reaction of cycloaddition type Diels-Alder was tested with different dienophiles (Scheme 63). This transformation showed that our system is moderate diene and requires an electron-withdrawing dienophile such as *N*-methylmaleimide.



Scheme 64

Therefore, the cyclization with *N*-methylmaleimide led to the monocycloadduct on quantitative manner, which was involved in the reaction of the *Boc* deprotection and aromatization with DDQ. This compound was further functionalized in the *trans*-imidation reaction providing amino- and hydroxyl-derivatives with fair yields (53 and 62%, respectively). The last step of predicted strategy was the attachment with the chelating molecule for lanthanide complexation, either by the halogen derivative or by bromoacetyl function. Notwithstanding, the provided reactions were unsuccessful, making this step impossible (Fig. 182).

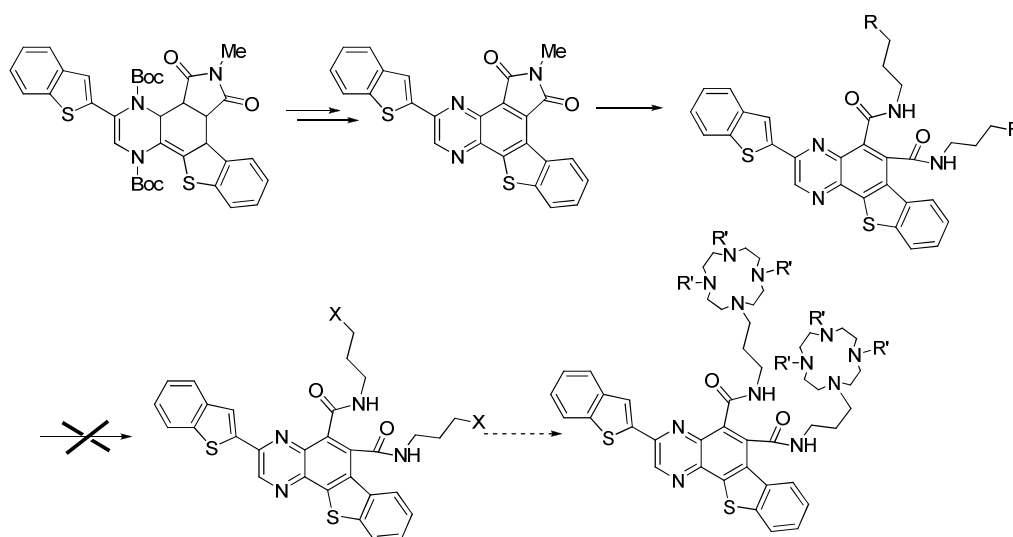
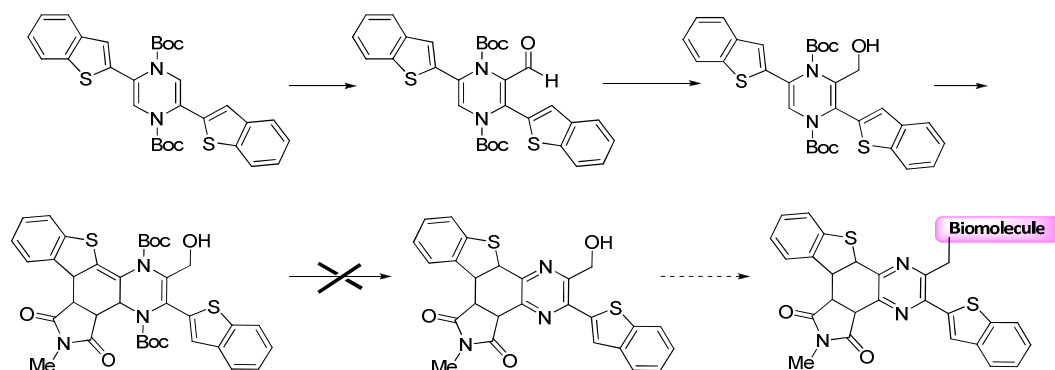


Fig. 182

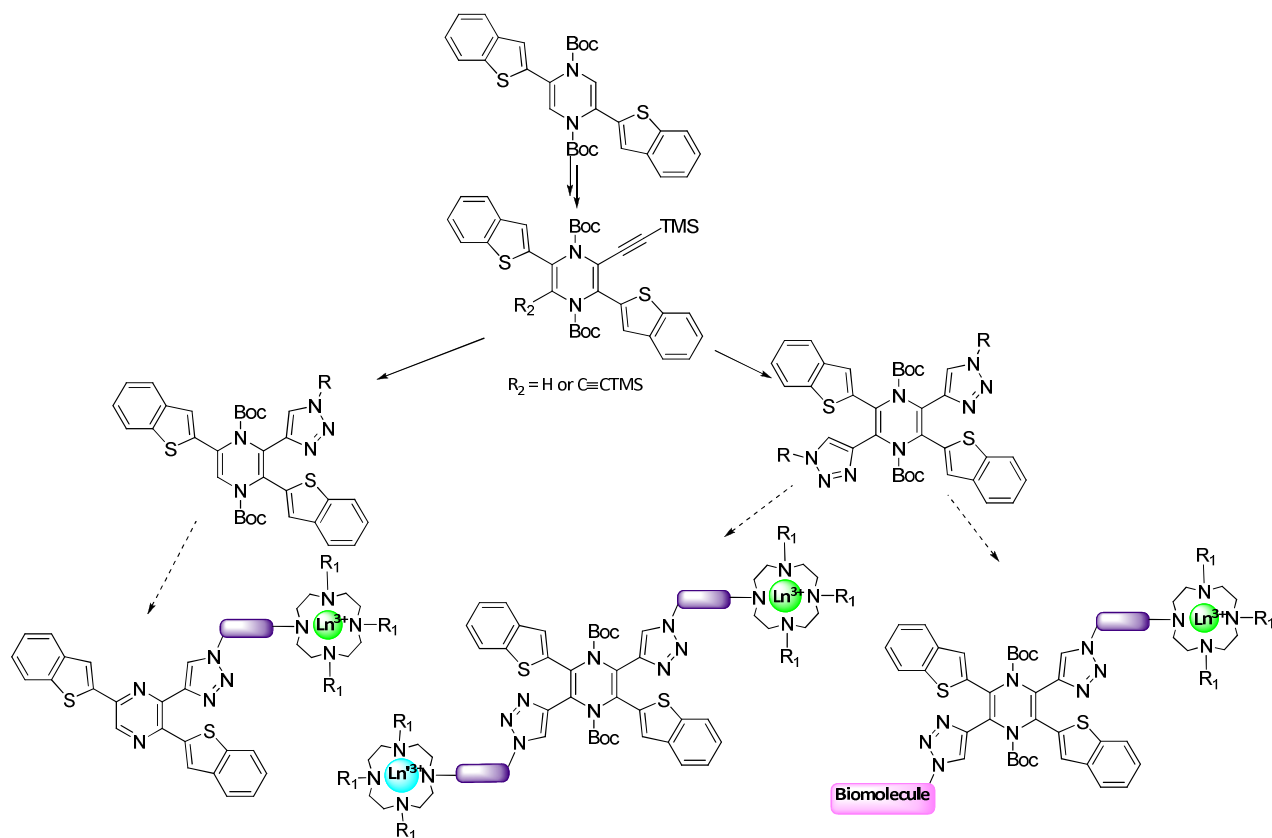
Based on the literature and experiments conducted in the laboratory, we assumed the functionalization of the last free position of dihydropyrazine to construct the additional spacer serving

as an attachment for the biomolecule. We envisaged the introduction of the function compatible with the attachment of the biomolecule to the sensitizer. In this aim, we performed the Diels-Alder reaction on the alcohol derivative, which provides, from the one side, a construction of the spacing arm, and from the other side - the connection to the biomolecule. However, provided pathway was blocked on the deprotection step, preventing the anchoring the active compound.

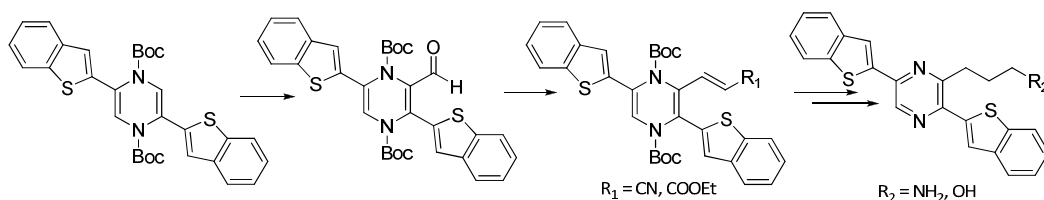


Scheme 65

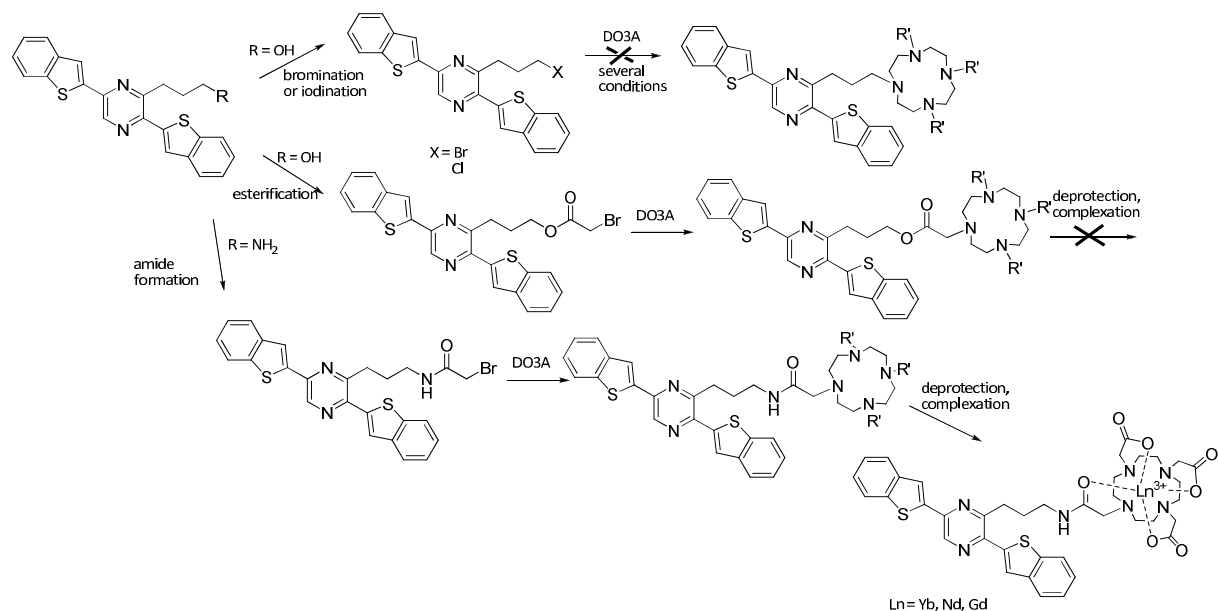
The second pathway to functionalize pyrazinic moiety was to introduce the iodide under anionic conditions and next, to apply the reaction of Sonogashira cross-coupling leading to TMS protected alkyne derivatives. These compounds were tested in the copper-catalyzed cycloaddition reaction ("click reaction") with the deprotection step *in situ*. This strategy had as an aim the valorization of our system in this type of transformation making the field for further application of click reaction to attach the lanthanide chelating system. In the perspective to this pathway, the further deprotection and attachment to the cyclen moiety were predicted. This methodology allows the insertion of two different lanthanide cations as well as the lanthanide and the biomolecule in order to construct the specific bio probe (Scheme 66).



In the third strategy, we predicted the introduction of aldehyde functional group, a useful intermediate for the olefination reaction. We applied the Wittig-Horner-Emmons reaction in order to obtain the nitrile and ester derivatives, which were further modified, first by *Boc* deprotection, then by reduction, to give an access to pyrazines with hydroxyl group and primary amine (Scheme 67).



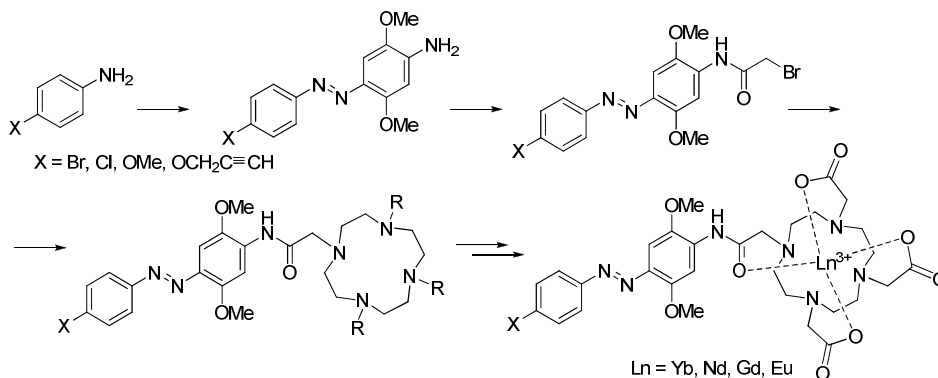
The substitution of an alcohol by different halogens were performed in order to carry out the nucleophilic substitution with cyclen derivative, however, this reaction did not yield an expected product. The amino and hydroxyl derivatives were applied in the esterification or amidation reaction leading to respective brominated ester or amide useful for the DO3A linkage. This methodology permitted to introduce the chelating system for lanthanides in two steps, moreover it gave an access for stable systems for the luminescent experiments.



Scheme 68

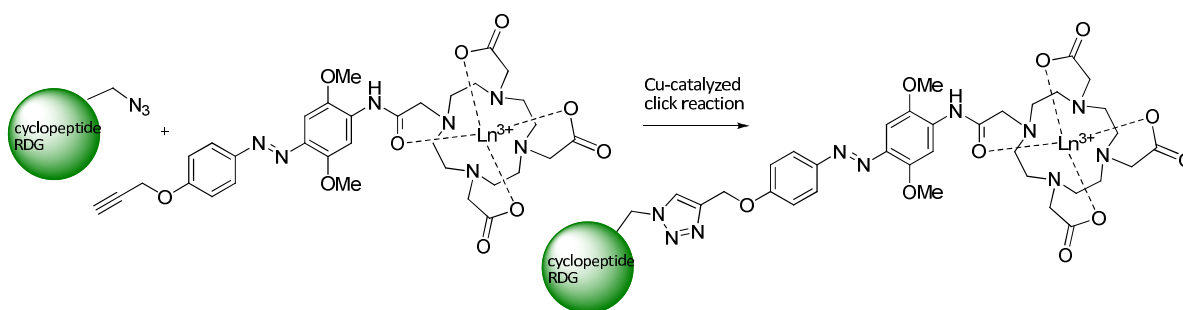
The complexes of Nd^{3+} , Gd^{3+} and Yb^{3+} were obtained and tests for their ability to sensitize lanthanide cations were performed, showing that our chromophore system possesses the electronic structures compatible with lanthanides. In conclusion, a new sensitizing system for near-infrared lanthanides was constructed in an original and flexible strategy that offers the possibility to modulate the electronic structure of this system. Pyrazinic sensitizers showed an efficient energy transfer to the lanthanide cation, resulting in emission in the near-infrared region with quantum yield comparable to other luminescent lanthanide complexes emitting in the NIR and the moderate lifetimes of the emission. The presented sensitizer is the first example of this type of chromophores, not yet described in the literature. Our preliminary studies constitute a proof of principle for the construction of pyrazinic chromophores and open the range of possibilities to versatile modification of synthetic pathways and further functionalizations of these compounds.

Finally, the new family of azo compounds was synthesized and valorized as an original sensitizer alone or in the linkage with the pyrazinic core. These compounds were obtained in the reaction of diazotation of different aromatic amines, followed by the diazo coupling with 2,5-dimethoxyaniline. The resulted products were functionalized to attach the DO3A system in the reaction of nucleophilic substitution and then deprotected and complexed with different lanthanide cations.



Scheme 69

Also, a reaction of copper-catalyzed cycloaddition with the alkyne derivative and cyclopeptide RGD was performed in order to furnish our system with the highly specific for the cancerous cells' biomolecule and hence to make an original near-infrared marker for tumors. This work gives a huge opportunity to valorize the properties of novel systems *in cellulo*.



Scheme 70

The series of azo chromophores were tested for the spectroscopic properties in the visible and near-infrared region. They absorb light in the visible range and transfer energy through the conjugated system to the lanthanide center, provoking an intensive luminescence of metal. Luminescence lifetimes of lanthanide emission are consistent with values reported in the literature.

This original and innovative methodology based on azo dyes permits to apply our sensitizers alone or in the combination with cyclopeptides or other biomolecules. Starting from versatile aromatic amines, the formation of desired sensitizers could be obtained. Moreover, the azo derivatives might be introduced to the pyrazinic system, enhancing thus the spectroscopic properties of the latter.

Experimental part

I. General methods

A) Solvents and reagents

THF was purified with a dry station GT S100 immediately prior to use. Dichloromethane was distilled over CaH₂. Other anhydrous solvents and reagents were distilled according to procedures commonly described. All anionic and moisture-sensitive reactions were carried out in the flame-dried glassware under an argon atmosphere. All reagents were obtained from commercial suppliers unless otherwise stated.

B) Chromatography

Thin layer chromatography (TLC)

The reactions were monitored by thin-layer chromatography (TLC) analysis using silica gel (60 F₂₅₄) plates. Compounds were visualized by UV irradiation (254 and 365 nm) and/or spraying with a solution of potassium permanganate or cerium ammonium nitrate (CAN), followed by charring at 150 °C.

Column chromatography on silica gel

Flash column chromatography was performed on silica gel 60 (230-400 mesh, 0.040-0.063 mm). Ethyl acetate, dichloromethane, acetonitrile and methanol used as eluents are technical grade. Petroleum ether is at 40-60 °C boiling point range.

Determination of enantiomeric excess

Enantiomeric excesses and purity were determined by chiral SFC measurement on a Waters Investigator SFC (Waters, Guyancourt, France) equipped with a Waters 2998 Photodiode Array detector with high-pressure resistant cell. The column was a Lux Cellulose-1 (250 x 4.6 mm, 5 μm) from Phenomenex (Torrance, CA). Operating conditions were always isocratic, with methanol or ethanol modifier. Flow rate was 3 mL/min, outlet pressure 15 MPa, column oven temperature 25°C. Retention times (t_R) are given in minutes. Enantiomers were identified by comparison of retention times, whenever the second enantiomer could be synthesized, and by comparison of UV spectra as provided by the photodiode-array detector.

C) Analysis and identification

Melting points

Melting points (Mp) of solid compounds were determined with WME Kofler apparatus and they are uncorrected.

Infrared spectroscopy

IR spectra were recorded on PERKIN ELMER IRTF spectrometer. Liquids and oils were applied as film between KBr windows and solids were dispersed in a NaCl pastille. Some spectra were recorded with Attenuated Total Reflectance (ATR) device. Absorption bands were given in cm⁻¹.

Nuclear Magnetic Resonance

¹H and ¹³C NMR spectra were recorded on a Brüker Avance spectrometer at 250 MHz (¹³C, 62.9 MHz) or 400 MHz (¹³C, 100 MHz). Chemical shifts were reported in ppm (δ) relative to tetramethylsilane (TMS) as internal reference (δ = 0.0 ppm). ³¹P NMR was recorded on spectrometer Brüker 400 MHz (160 MHz) with complete proton decoupling. The corresponding chemical shifts were reported in [ppm] (δ) relative to external standard – 85% solution of phosphoric acid. The following abbreviations are used for the proton spectra multiplicities: s: singlet, d: doublet, t: triplet, q: quartet, qt: quintuplet, m: multiplet, br: broad signal. Coupling constants (J) are reported in Hertz (Hz).

Optical rotations

Optical rotations were recorded at the sodium D line with a Perkin-Elmer 341 polarimeter.

Mass spectrometry

Low resolution mass spectra (MS) were recorded on a Perkin-Elmer *SCIEX API 3000* spectrometer. Ionspray methodology was used to record mass spectra. High-resolution mass spectra were obtained with a Varian MAT 311 spectrometer using electrospray analysis.

D) Luminescence measurements

Absorption spectra

UV-Vis absorption spectra were recorded at room temperature using Perkin-Elmer Lambda 9 spectrophotometer in quartz cuvette (1 cm).

Emission and excitation

Emission and excitation spectra were measured using a modified Jobin-Yvon Horriba Fluorolog-322 spectrofluorimeter equipped with an Electro-Optical System, Inc. DSS-IGA02TL cooled to 77 K, near-infrared detector. Singlet and triplet states were measured for the Gd³⁺ complexes with excitation at room temperature (fluorescence mode) and at 77 K (phosphorescence mode with 100 and 50 μ s delay).

Quantum yields

Luminescence quantum yields were collected with an integration sphere developed by Frédéric Gummy and Prof. Jean-Claude G. Bünzli (Laboratory of Lanthanide Supramolecular Chemistry, École Polytechnique Fédérale de Lausanne (EPFL), BCH 1402, CH- 1015 Lausanne, Switzerland) and manufactured by GMP SA (Renens Switzerland), using a quartz tube sample holder. Spectra were corrected for variations in excitation lamp output, spectral responses of the excitation and emission gratings, response of the detector, and the use of neutral density filters, when applicable. The calculated values were determined by integrating the emission profiles, averaged from three independent trials, and substitution into the ratio of emitted photons over absorbed photons.

Luminescence quantum yields were determined with an integration sphere using a quartz tube sample holder. Collecting NIR quantum yields (ϕ) requires the use of both a visible and a NIR detector. A relative quantum yield is measured using a reference sample with a known value (ytterbium tropolonate [Yb(trop)₄]⁻ $\phi_{Yb} = 1.9 \cdot 10^{-2}$ and neodymium tropolonate [Nd(trop)₄]⁻ $\phi_{Nd} = 2.1 \cdot 10^{-3}$).¹³⁶ The following steps for collecting a relative quantum yield using the integration sphere are:

- 1) Emission spectra of the lamp (Rayleigh bands) are collected for the sample (R_{S+SB}), the sample solvent (R_{SB}), the reference (R_{R+RB}) and the reference solvent (R_{RB}). The resulting integration values are used to determine the amount of light absorbed by the sample and the reference.
- 2) Emission spectra of the sample (I_{S+SB}), the sample solvent (I_{SB}), the reference (I_{R+RB}) and the reference solvent (I_{RB}) are collected in the NIR range. Emission spectra are corrected for the lamp variation, the solvent spectra are subtracted from the appropriate sample and reference spectra, the resulting spectra are corrected for detector response.
- 3) The known quantum yield of the reference is used to create a scalar ($X_{NIR-VIS}$) which accounts for the use of two different detectors:

$$X_{NIR-VIS} = \frac{\Phi_R R_R}{I_R}$$

- 4) The quantum yield of the sample is calculated using the following equation:

$$\Phi_S = \frac{X_{NIR-VIS} I_S}{R_S}$$

Lifetime determination

Lanthanide-centered luminescence lifetimes were measured at room temperature using Quantel YG 980 (355 nm, third harmonic) as the excitation source. Emission was collected at a right angle to the excitation beam, and wavelengths were selected by an interferential filter (990BP20 for Yb³⁺ and 1063BP175 for Nd³⁺). The signal was monitored by a Hamamatsu H10330-45 near-infrared detector, and was collected on a 500 MHz band-pass digital oscilloscope (Tektronix TDS 724C). The experimental luminescence decay curves were treated with Origin 8.0 software using exponential fitting model. Three decay curves were collected for each sample and fitted separately. The lifetime values were averaged and presented with the calculated error.

II. General procedures

General procedure (A) for the preparation of enol phosphates:

To a solution of the appropriate *N*-COOMe or *N*-Boc protected lactam (**1-4**) (14.6 mmol) in THF (*c* = 0.32M) at -78°C was added dropwise LDA (1.8 M in THF, 1.20 equiv.). The mixture was stirred for 2 h at -78 °C and diphenylchlorophosphate (1.20 equiv.) was subsequently introduced. After stirring for 2 h at -78°C (TLC control), the reaction was quenched by slow addition of distilled water. The resulting mixture was extracted with ethyl acetate. The organic phase was washed with distilled water and brine, dried over MgSO₄ and concentrated. The residue was purified by flash chromatography (silica gel, petroleum ether/ethyl acetate with 0.1 % triethylamine) to provide the desired vinyl phosphates.

General procedure (B) for palladium-catalyzed C-P cross-coupling reaction:

Under argon, enol phosphate **5-8** (120 mg, 0.30 mmol) was dissolved in distilled CH₃CN (2.5 mL) and secondary phosphine borane (diphenylphosphine borane or **13a**) (0.60 mmol, 2.00 equiv.) was added. The content of the flask was evacuated and backfilled with argon three times. Subsequently, dppfPdCl₂ (5 mol% yield) and Cs₂CO₃ (0.60 mmol, 2.00 equiv.) were introduced and the Procedure: of degassing was repeated. Reaction was carried out in a oil bath (65–70°C) for 2 h. The reaction mixture was filtered through Celite[®], washed with CH₃CN and the filtrate was evaporated. The crude product was purified by flash column chromatography (silica gel) to yield the expected alkenylphosphines.

General Procedure (C) for palladium-catalyzed cross-coupling reaction of phospholane borane complex

Under argon, enol phosphate **5-8** (100 mg, 0.248 mmol) was dissolved in CH₃CN (2.1 mL) and chiral phosphine **13b** (0.496 mmol, 2.00 equiv.) was added. The content of the flask was evacuated and backfilled with argon three times. Subsequently, dppfPdCl₂ (10 mol% yield) then Cs₂CO₃ (161.6 mg, 0.496 mmol, 2.00 equiv.) were introduced, and the Procedure: of degassing was repeated. Reaction was carried out in an oil bath (40°C) for 3 h (TLC control). After cooling down the mixture to room temperature, content of flask was filtrated through Celite[®], washed with CH₃CN and the filtrate was evaporated. The crude product was purified by flash column chromatography (silica gel, petroleum ether/ethyl acetate: 7/3 with 1% triethylamine).

General Procedure (D) for palladium-catalyzed cross-coupling of phosphine oxide (**4m-q**).

Under argon, enol phosphate **5-8** (40 mg, 0.09 mmol) was dissolved in DMSO (0.4 mL) and secondary phosphine oxide (**13c**) (0.18 mmol, 2.00 equiv.) was added. The content of the flask was evacuated and backfilled with argon three times. Subsequently, dppfPdCl₂ (10 mol% yield) then *N,N*-diisopropylethylamine (0.06 mL, 0.36 mmol, 4.00 equiv.) were introduced, and the Procedure: of degassing was repeated. Reaction was carried out in an oil bath (100 °C) for 2h (TLC control). After cooling down the mixture to room temperature, water and dichloromethane were added. The resulting mixture was extracted with dichloromethane. The organic phase was washed with brine, dried over MgSO₄ and concentrated. The crude product was purified by flash column chromatography (silica gel) to yield the expected alkenylphosphine oxides.

General Procedure for the preparation of acyclic ene-carbamates **4** via Suzuki coupling (E)

Phosphate (3.2 mmol) was dissolved in degassed THF (10 mL) under argon. Dichloro-bis(triphenylphosphine) palladium (II) (0.32 mmol, 10% mol) was then added and the mixture was degassed and flushed under argon. Boronic acid (8.0 mmol, 2.50 equiv.), aqueous sodium carbonate solution (2M, 3.2 mL) and EtOH (3 drops) were added at once. The reaction mixture was then rapidly degassed, flushed under argon and heated at 60°C for 30 minutes. After cooling, the reaction mixture was filtered through Celite, and was washed with EtOAc (50 mL). The organic phase was washed with brine, dried over MgSO₄ and concentrated. Flash chromatography (silica gel, petroleum ether/EtOAc: 9/1) afforded the desired the pure product.

General Procedure for the synthesis of the ene-carbamates via a Stille cross coupling (F)

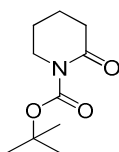
Phosphate (3.2 mmol) was dissolved in degassed toluene (10 mL) under argon. The dichloro-bis(triphenylphosphine) palladium (II) (0.32 mmol, 10% mol) was added and the mixture was degassed and flushed under argon. 2-tributylstannylpyridine (8.0 mmol, 2.50 equiv.) and lithium chloride (6.2 mmol) were added. The reaction mixture was quickly degassed and flushed under argon. The mixture was then heated at 90°C for a night. Brine (50mL) and EtOAc (50mL) were added. The organic phase was separated and the aqueous

phase was extracted with 20 mL of EtOAc. Combined organic phases were dried over MgSO_4 and evaporated under vacuum. Flash chromatography of the crude (silica gel, petroleum ether then petroleum ether/EtOAc: 9/1) provided the pure product.

General Procedure: (G) for the nucleophilic addition of lithiated phosphine onto acyclic ene-carbamates.

Ene-carbamate (0.40 mmol) was dissolved in dry THF (2 mL) and was degassed. The solution was cooled at -78°C . In a separated dried flask, to a degassed solution of diphenylphosphine (1.20 mmol) in dry THF (2 mL) was added *n*-butyllithium (1.20 mmol, 1.6M solution in hexanes) which leads to the apparition of an intense red color. This red solution was slowly canulated into the first flask cooled at -78°C . The cold bath was removed, letting the reaction mixture warm up to room temperature for 15 minutes. The reaction mixture was then quenched with saturated aqueous ammonium chloride (5 mL). EtOAc (5 mL) was added. The organic phase was separated and the aqueous phase was extracted with 20 mL of EtOAc. Combined organic phases were dried over MgSO_4 and evaporated under vacuum. Flash chromatography of the residue (silica gel, PE then PE/EtOAc: 9/1) provided the pure product.

Tert-butyl 2-oxopiperidine-1-carboxylate (1)



Colorless solid

$R_f = 0.58$ (PE/EtOAc: 6/4) revelator KMnO_4

Procedure:

A solution of δ -valerolactam (2.00 g, 20.18 mmol, 1.00 equiv.) was prepared in distilled acetonitrile (30 mL) at room temperature, then DMAP (123 mg, 1.01 mmol, 0.05 equiv.) and Boc_2O (4.85 g, 22.20 mmol, 1.10 equiv.) were added. The mixture was stirred at room temperature for 4 h. The solvent from mixture was evaporated under vacuum and residues were taken up in 20 mL of EtOAc, washed with distilled water (2x15 mL) and brine, dried over MgSO_4 and concentrated. The residue was purified by flash chromatography (silica gel, PE/EtOAc: 7/3 then 6/4) to provide 2.80 g (70 % yield) of the carbamate **1** as a colorless solid.

Analyses:

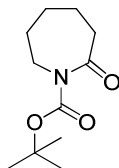
$^1\text{H NMR}$ (250 MHz, CDCl_3) δ [ppm]: 3.86 (t, $J = 6.0$ Hz, 2H), 2.62 (t, $J = 6.3$ Hz, 2H), 1.93-1.90 (m, 4H), 1.51 (s, 9H).

$^{13}\text{C NMR}$ (61 MHz, CDCl_3) δ [ppm]: 171.4 (C=O), 153.2 (C=O), 82.9 (C^{V}), 47.1 (CH_2), 35.2 (CH_2), 28.3 ($3\times\text{CH}_3$), 22.8 (CH_2), 20.7 (CH_2).

MS (ESI) [m/z]: 200.5 [$\text{M}+\text{H}$] $^+$, 222.5 [$\text{M}+\text{Na}$] $^+$.

IR (ATR, neat) ν [cm^{-1}]: 2944, 1777, 1676, 1589, 1485, 1454.

Tert-butyl 2-oxoazepane-1-carboxylate (2)



Colorless oil

$R_f = 0.59$ (PE/EtOAc: 7/3) revelator $KMnO_4$

Procedure:

A solution of ϵ -caprolactam (5.00 g, 44.18 mmol, 1.00 equiv.) was prepared in distilled acetonitrile (60 mL) at room temperature, then DMAP (270 mg, 2.21 mmol, 0.05 equiv.) and Boc_2O (10.89 g, 49.91 mmol, 1.10 equiv.) were added. The mixture was stirred at room temperature for 18 h. The solvent from mixture was evaporated under vacuum and residues were taken up in 20 mL of EtOAc, washed with distilled water (2x15 mL) and brine, dried over $MgSO_4$ and concentrated. The residue was purified by flash chromatography (silica gel, PE/EtOAc: 7/3) to provide 6.14 g (65 % yield) of the carbamate **2** as a colorless oil.

Analyses:

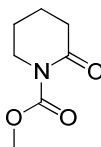
1H NMR (250 MHz, $CDCl_3$) δ [ppm]: 3.76 (m, 2H), 2.65 (m, 2H), 1.73 (m, 6H), 1.52 (s, 9H).

^{13}C NMR (61 MHz, $CDCl_3$) δ [ppm]: 175.9 (C=O), 153.1 (C=O), 82.9 (C^{IV}), 46.3 (CH_2), 39.7 (CH_2), 29.4 (CH_2), 28.8 (CH_2), 28.2 (3x CH_3), 23.7 (CH_2).

MS (ESI) [m/z]: 214.0 [$M+H$] $^+$.

IR (NaCl film) ν [cm^{-1}]: 2979, 2933, 1768, 1715, 1569, 1285.

Methyl 2-oxopiperidine-1-carboxylate (3)



Colorless oil

$R_f = 0.43$ (PE/EtOAc: 4/6) revelator $KMnO_4$

Procedure:

To the solution of δ -valerolactam (1.00 g, 10.09 mmol, 1.00 equiv.) in THF ($c = 0.25$ M) at $-78^\circ C$, a solution of *n*-BuLi (1.6M in hexane, 6.9 mL, 11.10 mmol, 1.1 equiv.) was added dropwise. After stirring at $-78^\circ C$ for 30 minutes, methyl chloroformate (0.86 mL, 11.10 mmol, 1.10 equiv.) was introduced to the yellow solution. The resulting mixture was stirred for an additional 1.5h at $-78^\circ C$. The reaction was quenched with a saturated aqueous NH_4Cl solution. The resulting mixture was extracted with ethyl acetate. The organic phase was washed with distilled water and brine, dried over $MgSO_4$ and concentrated. The residue was purified by flash chromatography (silica gel, petroleum ether/ethyl acetate: 6/4) to provide 1.59 g (52 % yield) of the methyl carbamate **2** as a colorless oil.

Analyses:

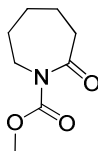
1H NMR (250 MHz, $CDCl_3$) δ [ppm]: 3.83 (s, 3H), 3.74 (t, $J = 6.3$ Hz, 2H), 2.54 (t, $J = 7.1$ Hz, 2H), 1.83 (qt, $J = 3.8$ and 3.1 Hz, 4H).

^{13}C NMR (100 MHz, $CDCl_3$) δ [ppm]: 171.1 (C=O), 154.9 (C=O), 54.9 (CH_3), 46.4 (CH_2), 34.7 (CH_2), 22.5 (CH_2), 20.2 (CH_2).

MS (ESI) [m/z]: 158.5 [$M+H$] $^+$, 175.5 [$M+NH_4$] $^+$.

IR (ATR, neat) ν [cm^{-1}]: 2953, 2875, 1775, 1706, 1436, 1282, 1247, 1142, 1059, 778.

Methyl 2-oxoazepane-1-carboxylate (4)



Colorless oil

$R_f = 0.61$ (PE/Acetone: 6/4) revelator KMnO_4

Procedure:

To the solution of ϵ -caprolactam (2.00 g, 17.67 mmol, 1.00 equiv.) in THF ($c = 0.25$ M) at -78°C , a solution of n -BuLi (1.6M in hexane, 12.15 mL, 19.44 mmol, 1.10 equiv.) was added dropwise. After stirring at -78°C for 30 min., methyl chloroformate (1.50 mL, 19.44 mmol, 1.10 equiv.) was introduced to the yellow solution. The resulting mixture was stirred for an additional 1.75h at -78°C . The reaction was quenched with a saturated aqueous NH_4Cl solution. The resulting mixture was extracted with ethyl acetate. The organic phase was washed with distilled water and brine, dried over MgSO_4 and concentrated. The residue was purified by flash chromatography (silica gel, petroleum ether/acetone: 6/4) to provide 2.00 g (66 % yield) of the methyl carbamate **4** as a creamy oil.

Analyses:

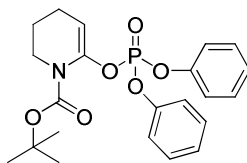
$^1\text{H NMR}$ (400 MHz, CDCl_3) δ [ppm]: 3.85 (s, 5H), 2.69 (m, 2H), 1.77 (s, 6H).

$^{13}\text{C NMR}$ (100 MHz, CDCl_3) δ [ppm]: 175.7 (C=O), 155.2 (C=O), 54.1 (CH_3O), 46.5 (CH_2), 39.6 (CH_2), 29.3 (CH_2), 28.7 (CH_2), 23.7 (CH_2).

MS (ESI) [m/z]: 172.5 [$\text{M}+\text{H}$] $^+$, 194.5 [$\text{M}+\text{Na}$] $^+$.

IR (ATR, neat) ν [cm^{-1}]: 2981, 2952, 2892, 1701, 1287, 1248, 1135, 1061, 854.

Tert-butyl 6-(diphenoxyphosphoryloxy)-3,4-dihydropyridine-1(2H)-carboxylate (5)



Colorless oil

$R_f = 0.50$ (PE/EtOAc: 7/3) revelator KMnO_4

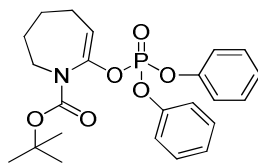
Procedure:

Following the general procedure (A), vinylphosphate **5** was obtained and the crude product was directly used for coupling step, because degradation occurs during purification on column.

Analyses:

$^1\text{H NMR}$ (250 MHz, CDCl_3) δ [ppm]: 7.34-7.16 (m, 10 H), 5.12-5.08 (dd, $J = 2.0$ and 3.0 Hz, 1H), 3.60 (t, $J = 11.0$ Hz, 2H), 2.50 (m, 2H), 1.80 (m, 2H), 1.43 (s, 9H).

Tert-butyl 7-(diphenoxyphosphoryloxy)-2,3,4,5-tetrahydro-1H-azepine-1-carboxylate (6)



Colorless oil

$R_f = 0.57$ (PE/EtOAc: 7/3) revelator KMnO_4

Procedure:

According to general procedure (A), after purification by flash column chromatography (petroleum ether/ethyl acetate: 6/4) vinylphosphate **6** was afforded (83% yield) as a colorless oil.

Analyses:

$^1\text{H NMR}$ (400MHz, CDCl_3) δ [ppm]: 7.40-7.19 (m, 10 H), 5.45 (td, $J = 7.0$ and 3.0 Hz, 1H), 3.55 (m, 2H), 2.14-2.09 (m, 2H), 1.80-1.67 (3, 2H), 1.56-1.47 (m, 9H+2H).

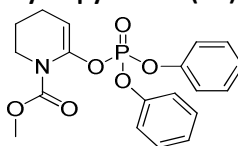
$^{13}\text{C NMR}$ (100MHz, CDCl_3) δ [ppm]: 153.2 (C=O), 150.7, 150.6 (C^{IV}), 145.3 (C^{IV}), 129.9 (4xCH), 125.6 (2xCH), 120.2 (4xCH), 109.7 (CH), 81.3 (C^{IV}), 46.7 (CH_2), 29.5 (CH_2), 28.3 (3x CH_3), 24.5 (CH_2), 24.0 (CH_2).

$^{31}\text{P NMR}$ (160 MHz, CDCl_3) δ [ppm]: -16.50.

MS (ESI) [m/z]: 445.0 [M] $^+$, 468.0 [$\text{M}+\text{Na}$] $^+$.

IR (ATR, neat) ν [cm^{-1}]: 3058, 2977, 2929, 2849, 1712, 1982, 1590, 1482, 1294, 1183, 944, 761.

Methyl 6-(diphenoxyphosphoryloxy)-3,4-dihydropyridine-1(2H)-carboxylate (7)



Colorless oil

$R_f = 0.43$ (PE/EtOAc: 6/4) revelator KMnO_4

Procedure:

According to the general procedure (A), after purification by flash column chromatography (petroleum ether/ethyl acetate: 6/4 with 1% TEA) vinylphosphate **7** was obtained (83% yield) as a colorless oil.

Analyses:

$^1\text{H NMR}$ (400 MHz, CDCl_3) δ [ppm]: 7.38-7.17 (m, 10H), 5.12 (dd, $J_{\text{H,P}} = 3.8$ Hz and $J_{\text{H,H}} = 3.0$ Hz, 1H), 3.65 (t, $J = 5.5$ Hz, 2H), 3.56 (s, 3H), 2.17 (m, 2H), 1.74 (qt, $J = 5.5$ and 6.7 Hz, 2H).

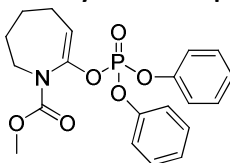
$^{13}\text{C NMR}$ (100 MHz, CDCl_3) δ [ppm]: 154.9 (C=O), 130.1 (C^{IV}), 129.9 (4x CH_{ar}), 125.6 (2x C^{IV}), 129.5 (2x CH_{ar}), 120.4 (4x CH_{ar}), 99.6 (CH_{vinyl}), 54.1 (CH_3), 46.7 (CH_2), 35.0 (CH_2), 22.8 (CH_2).

$^{31}\text{P NMR}$ (160 MHz, CDCl_3) δ [ppm]: -16.11.

MS (ESI) [m/z]: 390.5 [$\text{M}+\text{H}$] $^+$, 412.5 [$\text{M}+\text{Na}$] $^+$.

IR (ATR, neat) ν [cm^{-1}]: 3067, 2956, 2878, 1775, 1712, 1596, 1488, 1294, 1180, 1162, 968, 755.

Methyl 7-(diphenoxyphosphoryloxy)-2,3,4,5-tetrahydro-1H-azepine-1-carboxylate (8)



Yellow oil

$R_f = 0.32$ (PE/EtOAc: 7/3) revelator $KMnO_4$

Procedure:

According to general procedure (A), after purification by flash column chromatography (petroleum ether/ethyl acetate: 8/2 to 7/3) the vinylphosphate **8** was obtained (58% yield) as a yellow oil.

Analyses:

1H NMR (400MHz, $CDCl_3$) δ [ppm]: 7.37-7.20 (m, 10H), 5.48-5.44 (td, $J_{H,P} = 1.8$ Hz and $J_{H,H} = 6.8$ Hz, 1H), 3.59 (s, 5H), 2.08 (m, 2H), 1.74 (t, $J = 3.3$ Hz, 2H), 1.52 (m, 2H).

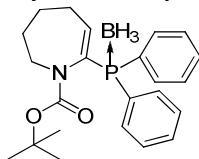
^{13}C NMR (100MHz, $CDCl_3$) δ [ppm]: 154.8 (C=O), 150.9 (2x C^{IV}), 150.8 (C^{IV}), 130.2 (4x CH_{ar}), 125.9 (2x CH_{ar}), 120.5 (2x CH_{ar}), 120.4 (2x CH_{ar}), 110.7 (CH_{vinyl}), 53.5 (CH_3O), 47.8 (CH_2), 29.8 (CH_2), 24.6 (CH_2), 24.3 (CH_2).

^{31}P NMR (160 MHz, $CDCl_3$) δ [ppm]: -17.34.

MS (ESI) [m/z]: 404.5 [$M+H$] $^+$, 426.5 [$M+Na$] $^+$.

IR (ATR, neat) ν [cm^{-1}]: 3058, 2950, 2926, 2852, 1715, 1691, 1593, 1485, 1437, 1285, 1189, 944, 755.

Tert-butyl 7-(diphenylphosphino)-2,3,4,5-tetrahydro-1H-azepine-1-carboxylate borane complex (10)



Colorless oil

$R_f = 0.56$ (PE/EtOAc: 8/2) revelator $KMnO_4$

Procedure:

The general procedure (B) was applied. Purification by flash column chromatography (petroleum ether/ethyl acetate: 9/1) yielded **10** (67 mg, 75% yield) as a colorless oil.

Analyses:

1H NMR (400MHz, DMSO- d_6) δ [ppm]: 7.55 (m, 9H), 7.40 (s, 1H), 6.52 (dd, $J_{H,P} = 7.5$ Hz and $J_{H,H} = 1.3$ Hz, 1H), 2.26 (m, 2H), 1.72 (m, 2H), 1.35 (m, 2H), 1.18 (m, 2H), 0.98 (s, 9H).

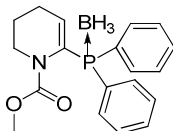
^{13}C NMR (100 MHz, DMSO- d_6) δ [ppm]: 152.2 (C=O), 145.6 (CH_{vinyl}), 136.5 (C^{IV}), 132.9 (4x CH_{ar}), 131.5 (2x CH_{ar}), 128.8 (2x CH_{ar}), 128.7 (2x CH_{ar}), 79.7 (C^{IV}), 59.6 (CH_2), 47.1 (CH_2), 28.9 (CH_2), 27.2 (3x CH_3), 22.7(CH_2).

^{31}P NMR (DMSO- d_6 , 160 MHz) δ [ppm]: 21.94.

HRMS (ESI) [m/z]: calculated for $C_{23}H_{31}^{11}BN^{23}NaO_2P$ [$M+Na$] $^+$: 418.2082, found: 418.2084.

IR (KBr) ν [cm^{-1}]: 3442 (CON lactam), 3051, 2935, 2404, 1697 (C=O), 1435, 1389, 1157.

Methyl 6-(diphenylphosphino)-3,4-dihydropyridine-1(2H)-carboxylate borane complex (**11**)



Yellow oil

$R_f = 0.56$ (PE/acetone: 7/3) revelator KMnO_4

Procedure:

Following the general procedure (B), after purification by flash column chromatography (petroleum ether/acetone: 8/2 to 7/3) phosphine borane **11** was obtained (30 mg, 28% yield) as a yellow oil.

Analyses:

$^1\text{H NMR}$ (250 MHz, CDCl_3) δ [ppm]: 7.60 (m, 4 H), 7.45 (m, 6 H), 5.59-5.51 (dt, $J_{\text{H,P}} = 10.8$ Hz and $J_{\text{H,H}} = 3.8$ Hz, 1H), 3.72-3.67 (m, 2H), 3.11 (s, 3H), 2.25 (m, 2H), 1.88 (m, 2H), 1.00 (m, BH_3).

$^{13}\text{C NMR}$ (100 MHz, CDCl_3) δ [ppm]: 154.3 (C=O), 133.5 ($2\times\text{C}^{\text{IV}}$), 132.8, 132.7 ($4\times\text{CH}_{\text{ar}}$), 130.9 ($2\times\text{CH}_{\text{ar}}$), 130.8 (C^{IV}), 128.6 ($4\times\text{CH}_{\text{ar}}$), 100.2 (CH_{vinyl}), 52.0 (CH_3O), 24.8 (CH_2), 23.1 (CH_2), 20.2 (CH_2).

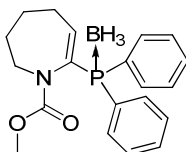
$^{31}\text{P NMR}$ (160 MHz, CDCl_3) δ [ppm]: 27.11.

MS (ESI) [m/z]: 342.5 [$\text{M}+\text{NH}_4\text{-BH}_3$] $^+$, 364.5 [$\text{M}+\text{Na}+\text{NH}_4\text{-BH}_3$] $^+$.

HRMS (ESI) [m/z]: calculated for $\text{C}_{19}\text{H}_{22}\text{NO}_2$ ^{11}BP [M-H] $^+$: 338.1481, found: 338.1449.

IR (NaCl) ν [cm^{-1}]: 3446 (CON lactam), 3210, 2950, 2384, 1712 (C=O), 1438, 1061, 499.

Methyl 7-(diphenylphosphino)-2,3,4,5-tetrahydro-1H-azepine-1-carboxylate borane complex (**12**)



Colorless oil

$R_f = 0.56$ (PE/acetone: 7/3) revelator KMnO_4

Procedure:

Following the general procedure (B), after purification by flash column chromatography (petroleum ether/ethyl acetate: 95/5 to 85/15) product **12** was isolated (100mg, 95% yield) as a colorless oil.

Analyses:

$^1\text{H NMR}$ (400 MHz, CDCl_3) δ [ppm]: 7.58-7.56 (m, 4H), 7.40-7.35 (m, 6H), 6.33 (td, $J_{\text{H,P}} = 6.8$ Hz and $J_{\text{H,H}} = 2.0$ Hz, 1H), 2.96 (s, 3H), 2.27 (q, $J_{\text{H,H}} = 6.0$ Hz, 2H), 1.75 (t, $J_{\text{H,H}} = 5.4$ Hz, 2H), 1.18 (m, 2H), 0.80 (m, BH_3).

$^{13}\text{C NMR}$ (100 MHz, CDCl_3) δ [ppm]: 154.5 (C=O), 144.5 (CH_{vinyl}), 137.6 (C^{IV}), 133.0 ($4\times\text{CH}_{\text{ar}}$), 131.2 ($2\times\text{CH}_{\text{ar}}$), 129.3 ($2\times\text{CH}_{\text{ar}}$), 129.3 (C^{IV}), 128.6 (2CH_{ar}), 52.0 (CH_3), 48.6 (CH_2), 29.7 (CH_2), 28.7 (CH_2), 23.4 (CH_2).

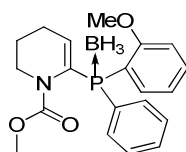
$^{31}\text{P NMR}$ (160 MHz, CDCl_3) δ [ppm]: 24.106.

MS (ESI) [m/z]: 355 [$\text{M}+\text{H}$] $^+$.

HRMS (ESI) [m/z]: [M-BH_3] $^+$ calculated for $\text{C}_{20}\text{H}_{22}\text{NO}_2\text{P}$: 339.1388, found: 339.1379.

IR (KBr) ν [cm^{-1}]: 3416 (CON lactam), 2946, 2389, 1706 (C=O), 1437, 1056, 740.

Methyl 6-((2-methoxyphenyl)(phenyl)phosphino)-3,4-dihydropyridine-1(2H)-carboxylate borane complex (15)



Yellow oil

$R_f = 0.81$ (PE/acetone: 6/4) revelator KMnO_4

Procedure:

According to the general procedure (B), after purification by flash column chromatography (petroleum ether/ethyl acetate: 7/3) product **15** (60 mg, 42% yield) was obtained as a yellow oil.

Analyses:

$^1\text{H NMR}$ (400 MHz, CDCl_3) δ [ppm]: 7.44-7.39 (m, 4H), 7.34-7.24 (m, 5H), 5.75 (dt, $J_{\text{H,P}} = 11.1$ Hz and $J_{\text{H,H}} = 3.8$ Hz, 1H), 3.78 (s, 3H), 3.69 (m, 2H), 3.11 (s, 3H), 2.25 (m, 2H), 1.91 (m, 2H), 1.00 (m, BH_3).

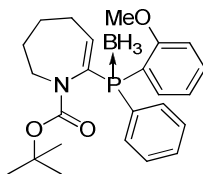
$^{13}\text{C NMR}$ (100 MHz, CDCl_3) δ [ppm]: 154.3 (C=O), 150.9 (C^{IV}), 130.4 ($2 \times \text{CH}_{\text{ar}}$), 129.6 (CH_{ar}), 128.1 (CH_{ar}), 127.9 (CH_{ar}), 124.7 (CH_{ar}), 120.6 (C^{IV}), 120.1 ($2 \times \text{CH}_{\text{ar}}$), 111.4 (CH_{vinyl}), 55.5 (CH_3O), 44.4 (CH_3O), 25.0 (CH_2), 24.4 (CH_2), 23.1 (CH_2).

$^{31}\text{P NMR}$ (160 MHz, CDCl_3) δ [ppm]: 28.11.

HRMS (ESI) [m/z]: calculated for $\text{C}_{19}\text{H}_{19}\text{NO}_3\text{P}$ [$\text{M}-\text{BH}_3-\text{Me}$] $^+$: 340.1102, found: 340.1121.

0% ee as determined by chiral SFC-DAD: CO_2 -methanol 91:9 (v/v), 3 mL/min, 25°C, 15 MPa. $t_{R1} = 6.54$ min., $t_{R2} = 7.02$ min.

Tert-butyl 7-((2-methoxyphenyl)(phenyl)phosphino)-2,3,4,5-tetrahydro-1H-azepine-1-carboxylate borane complex (16)



Yellow oil

$R_f = 0.23$ (PE/EtOAc 8/2) revelator KMnO_4

Procedure:

According to the general procedure (B) and after purification by flash column chromatography (petroleum ether/acetone: 8/2 to 7/3) product **16** was obtained (40 mg, 42% yield) as a yellow oil.

Analyses:

$^1\text{H NMR}$ (250 MHz, $\text{DMSO}-d_6$, 80°C) δ [ppm]: 7.62-7.47 (m, 7H), 7.09-7.05 (m, 2H), 6.48-6.44 (m, 1H), 3.62 (s, 3H), 2.31-2.28 (m, 2H), 1.76 (m, 2H), 1.49 (m, 2H), 1.29 (m, 2H), 1.09 (s, 9H), 0.8-0.5 (m, BH_3).

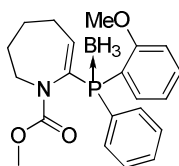
$^{13}\text{C NMR}$ (100 MHz, CDCl_3) δ [ppm]: 154.9 (C=O), 133.7 (CH_{ar}), 131.6 (CH_{ar}), 131.5 (C^{IV}), 130.1 ($2 \times \text{CH}_{\text{ar}}$), 128.2 ($2 \times \text{CH}_{\text{ar}}$), 120.8 ($2 \times \text{CH}_{\text{ar}}$), 120.7 (C^{IV}), 111.4 (CH_{vinyl}), 99.9 (C^{IV}), 80.6 (C^{IV}), 55.3 (CH_3), 47.3 (CH_2), 29.6 (CH_2), 28.1 (CH_2), 27.8 ($3 \times \text{CH}_3$), 23.8 (CH_2).

$^{31}\text{P NMR}$ (160 MHz, CDCl_3) δ [ppm]: 21.88.

HRMS (ESI) [m/z]: calculated for $\text{C}_{24}\text{H}_{30}\text{NO}_3\text{P}$ [$\text{M}-\text{BH}_3$] $^+$: 411.1963, found: 411.1944.

0% ee as determined by chiral SFC-DAD: CO_2 -ethanol 93:7 (v/v), 3 mL/min, 25°C, 15 MPa. $t_{R1} = 7.02$ min., $t_{R2} = 7.90$ min.

Methyl 7-((2-methoxyphenyl)(phenyl)phosphino)-2,3,4,5-tetrahydro-1H-azepine-1-carboxylate borane complex (17).



Yellow oil

R_f = 0.49 (PE/acetone: 7/3) revelator KMnO₄

Procedure:

According to the general procedure (B) and after purification by flash column chromatography (petroleum ether/acetone: 8/2 to 7/3) product **17** was isolated (55 mg, 58% yield) as a yellow oil.

Analyses:

¹H NMR (400 MHz, CDCl₃) δ [ppm]: 7.69 (m, 2H), 7.41 (m, 5H), 6.99-6.90 (m, 2H), 6.45-6.40 (dd, *J*_{H,H} = 3.0 Hz and *J*_{H,P} = 9.5 Hz, 1H), 3.70 (s, 3H), 3.05 (s, 3H), 2.34–2.33 (m, 2H), 1.83-1.82 (m, 2H), 1.26 (m, 2H), 0.89-0.85 (m, BH₃).

¹³C NMR (100 MHz, CDCl₃) δ [ppm]: 154.6 (C=O), 136.7 (C^{IV}), 133.6 (2xCH_{ar}), 132.4 (CH_{ar}), 132.3 (2xCH_{ar}), 130.5(CH_{ar}), 130.4 (CH_{ar}), 128.2 (2xCH_{ar}), 128.1 (C^{IV}), 120.9 (C^{IV}), 120.8 (CH_{ar}), 111.6 (CH), 111.5(C^{IV}), 55.5 (CH₃), 51.9 (CH₃), 29.9 (CH₂), 28.7 (CH₂), 28.6 (CH₂), 23.6 (CH₂).

³¹P NMR (160 MHz, CDCl₃) δ [ppm]: 22.70.

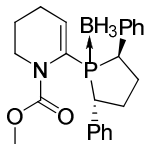
MS (ESI) [m/z]: 368.5 [M + NH₄-BH₃]⁺, 408.5 [M + NH₄-BH₃+Na]⁺.

HRMS (ESI) [m/z]: calculated for C₂₁H₂₄NO₃P [M-BH₃]⁺: 369.1494, found: 369.1476.

IR (NaCl) ν [cm⁻¹]: 3449 (CON lactam), 3056, 2940, 2385, 1709, 1479, 737, 508.

0% ee as determined by chiral SFC-DAD: CO₂-ethanol 80:20 (v/v), 3 mL/min, 25°C, 15 MPa. *t*_{R1}=3.19 min., *t*_{R2}=3.85 min.

Methyl 6-((2S,5S)-2,5-diphenylphospholan-1-yl)-3,4-dihydropyridine-1(2H)-carboxylate borane complex (19)



White semi-solid

R_f = 0.76 (PE/EtOAc: 6/4) revelator KMnO₄

Procedure:

Following the general procedure (C), the product **19** was isolated after purification as a white semi-solid (30 mg, 30% yield).

Analyses:

¹H NMR (400 MHz, CDCl₃) δ [ppm]: 7.35-7.57 (m, 5H), 7.29-7.27 (m, 5H), 5.28-5.22 (q, *J*_{H,P} = 7.2 Hz, 1H), 4.38-4.33 (q, *J*_{H,P} = 7.5 Hz, 1H), 3.95 (m, 2H), 3.67 (s, 1H), 3.52 (m, 3H), 2.63 (m, 2H), 2.24-2.22 (m, 4H), 1.00-0.50 (m, BH₃).

¹³C NMR (100 MHz, CDCl₃) δ [ppm]: 151.7 (C=O), 137.9 (2xC^{IV}), 136.7 (C^{IV}), 129.2 (CH_{ar}), 128.8 (CH_{ar}), 128.7 (CH_{ar}), 128.6 (CH_{ar}), 128.3 (CH_{ar}), 127.6 (CH_{ar}), 127.5 (2xCH_{ar}), 127.4 (2xCH_{ar}), 100.2 (CH), 44.8 (CH₃), 44.5 (CH₂), 41.0 (CH₂), 40.7 (CH₂), 34.9 (CH₂), 34.8 (CH₂), 34.1 (2xCH).

³¹P NMR (160 MHz, CDCl₃) δ [ppm]: 28.74.

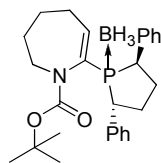
MS (ESI) [m/z]: 397.17 [M-BH₃]⁺, 402.16 [M+Na-BH₃]⁺.

HRMS (ESI) [m/z]: calculated for C₂₃H₃₀NO₂PB [M]⁺: 394.2106, found: 394.2104.

IR (NaCl) ν [cm⁻¹]: 3424, 2960, 2924, 2373, 1720, 1449, 1261, 1063, 801, 699.

[α]_D²⁰ = -20.1 (c=1, CHCl₃); **> 99.5% ee** as determined by chiral SFC-DAD: CO₂-methanol 90:10 (v/v), 3 mL/min, 25°C, 15 MPa. *t*_R (S,S)=17.1 min., *t*_R (R,R) not detected.

Tert-butyl 7-((2*S*,5*S*)-2,5-diphenylphospholan-1-yl)-2,3,4,5-tetrahydro-1*H*-azepine-1-carboxylate borane complex (20**)**



White semi-solid

$R_f = 0.80$ (PE/EtOAc: 8/2) revelator $KMnO_4$

Procedure:

According to the general procedure (C), after purification by flash column chromatography **20** was isolated as a white semi-solid (30 mg, 35% yield).

Analyses:

1H NMR (400 MHz, $CDCl_3$) (rotamers) δ [ppm]: 7.46-7.25 (m, 10H), 6.44-5.99 (m, 1H), 4.55 (m, 1H), 3.74 (m, 2H), 2.50 (br t, 6H), 2.25 (m, 4H), 1.57 (s, 9H), 1.00-0.50 (m, BH_3).

^{13}C NMR (100 MHz, $CDCl_3$) δ [ppm]: 160.9 (C=O), 128.8 (3 \times CH_{ar}), 128.4 (2 \times CH_{ar}), 128.0 (4 \times CH_{ar}), 126.6 (CH_{ar}), 99.9 (CH), 80.5 (C^{IV}), 43.8 (CH₂), 33.8 (2 \times CH₂), 30.7 (CH₂), 28.5 (2 \times CH), 28.4 (3 \times CH₃), 22.8(2 \times CH₂).

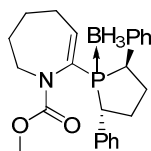
^{31}P NMR (160 MHz, $CDCl_3$) δ [ppm]: 47.30.

MS (ESI) [m/z]: 435.5 [M-BH₃]⁺.

HRMS (ESI) [m/z]: calculated for C₁₉H₁₉NO₂P [M-tBu-BH₃]⁺: 324.1153, found: 324.1145.

$[\alpha]_D^{20} = -13.7$ (c=1, $CHCl_3$); > **99.5% ee** as determined by chiral SFC-DAD: CO₂-methanol 90:10 (v/v), 3 mL/min, 25°C, 15 MPa. t_R (S,S) = 5.9 min.; t_R (R,R) not detected.

Methyl 7-((2*S*,5*S*)-2,5-diphenylphospholan-1-yl)-2,3,4,5-tetrahydro-1*H*-azepine-1-carboxylate borane complex (21**)**



Creamy semi-solid

$R_f = 0.69$ (PE/EtOAc: 6/4) revelator $KMnO_4$

Procedure:

According to the general procedure (C), after purification by flash column chromatography **21** was obtained as a creamy semi-solid (45 mg, 46% yield).

Analyses:

1H NMR (400 MHz, $CDCl_3$) (rotamers) δ [ppm]: 7.36-7.34 (m, 10H), 5.95 and 5.76 (m, 1H), 3.93 (m, 2H), 3.76 (s, 3H), 3.60 (m, 1H), 3.18 (s, 1H), 2.88 (m, 2H), 2.49 (m, 2H), 2.24-2.22 (m, 2H), 1.91 (m, 2H), 1.42 (m, 2H), 0.85 (m, BH_3).

^{13}C NMR (100 MHz, $CDCl_3$) δ [ppm]: 155.3 (C=O), 141.9 (CH_{vinyl}), 133.6 (C^{IV}), 129.0 (CH_{ar}), 128.8 (2 \times CH_{ar}), 128.5 (2 \times CH_{ar}), 128.3 (CH_{ar}), 128.0 (CH_{ar}), 127.0 (CH_{ar}), 126.7 (2 \times CH_{ar}), 53.0 (CH₃), 52.0 (CH), 50.7 (CH), 46.0 (CH₂), 34.7 (CH₂), 30.4 (CH₂), 28.2(CH₂), 22.8 (CH₂), 22.6 (CH₂).

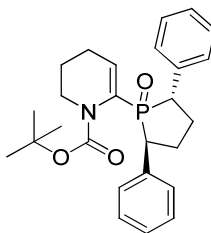
^{31}P NMR (160 MHz, $CDCl_3$) δ [ppm]: 48.20.

MS (ESI) [m/z]: 430.21 [M+Na]⁺.

HRMS (ESI) [m/z]: calculated for C₂₄H₃₁NO₂P¹¹B [M]⁺: 407.2186, found: 407.2175.

$[\alpha]_D^{20} = -26.9$ (c=1, $CHCl_3$); > **99.5% ee** as determined by chiral SFC-DAD: CO₂-methanol 90:10 (v/v), 3 mL/min, 25°C, 15 MPa. t_R (S,S) = 18.08 min., t_R (R,R) not detected.

6-((2S, 5S)-1-oxo-2,5-diphenyl- λ_5 -phospholan-1-yl)-3,4-dihydro-2H-pyridine-1-carboxylic acid *tert*-butyl ester (22)



White semi-solid

$R_f = 0.2$ (EtOAc) revelator $KMnO_4$

Procedure:

Following the general procedure (D), after purification by flash column chromatography (petroleum ether/ethyl acetate: 5/5 to 0/1) yielded the product **22** (43 mg, 28% yield) as a white semi-solid.

Analyses:

1H NMR (400 MHz, $CDCl_3$) δ [ppm]: 7.46-7.16 (m, 10H), 6.19-6.17 (dt, $J_{HP} = 11.7$ Hz, 1H), 4.06 (m, 1H), 3.84-3.75 and 3.59-3.57 (m, 2H), 3.26-3.23 (m, 1H), 2.51-2.43(m, 6H), 2.07 (m, 2H), 1.56 (m, 2H), 1.45 (s, 9H).

^{13}C NMR (100 MHz, $CDCl_3$) δ [ppm]: 152.8 (C=O), 137.4 (C^{IV}), 136.9 (C^{IV}), 132.1 (C_{vinyl}), 129.3 (CH_{ar}), 129.3 (C^{IV}), 129.1 (CH_{ar}), 128.3 (CH_{ar}), 128.2 (CH_{ar}), 127.8 (CH_{ar}), 127.8 (CH_{ar}), 127.5 (CH_{ar}), 126.0 (CH_{ar}), 125.9 (CH_{ar}), 80.4 (C^{IV}), 50.9 (CH), 50.2 (CH), 31.5 (CH_2), 28.3 ($3 \times CH_3$), 27.3-27.2 (CH_2), 23.8(CH_2), 22.3 (CH_2), 20.9 (CH_2).

^{31}P NMR (160 MHz, $CDCl_3$) δ [ppm]: 55.56.

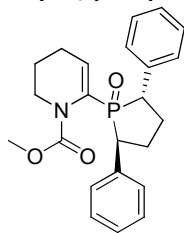
MS (ESI) [m/z]: 438.5 [$M+H$] $^+$, 460 [$M+Na$] $^+$.

HRMS (ESI) [m/z]: calculated for $C_{22}H_{24}NO_3P$ [$M-C_4H_8$] $^+$: 381.1494, found: 381.1490.

IR (KBr) ν [cm^{-1}]: 3443, 2946, 2865, 1689, 1359, 1153, 768, 698.

$[\alpha]_D^{20} = -66.0$ ($c=1$, $CHCl_3$). **99.4% ee** as determined by chiral SFC-DAD: CO_2 -methanol 90:10 (v/v), 3 mL/min, 25°C, 15 MPa. t_R (R,R) = 4.61 min., t_R (S,S) = 5.14 min.

1-(methoxycarbonyl)-6-((2S,5S)-1-oxo-2,5-diphenyl- λ_5 -phospholan-1-yl)-3,4-dihydro-2H-pyridine (23).



Orange oil

$R_f = 0.27$ (EtOAc) revelator $KMnO_4$

Procedure:

According to the general procedure (D) and after purification by flash column chromatography (petroleum ether/ethyl acetate: 5/5 to 0/10 with 1% triethylamine) product **23** was obtained as an orange oil (130 mg, 64% yield).

Analyses:

1H NMR (400 MHz, $CDCl_3$) δ [ppm]: 7.47-7.20 (m, 10H), 5.95 (m, 1H), 3.87-3.76 (m, 2H), 3.42 (s, 3H), 3.23 (m, 1H), 2.61 (m, 1H), 2.49 (m, 2H), 2.42 (m; 2H), 1.99 (m, 2H), 1.58 (m, 2H).

^{13}C NMR (100 MHz, $CDCl_3$) δ [ppm]: 154.3 (C=O), 137.6 (C^{IV}), 137.1 (C^{IV}), 133.9 (C^{IV}), 132.9 (C^{IV}), 129.3 ($2 \times CH_{ar}$), 129.3 ($2 \times CH_{ar}$), 128.3 (CH_{ar}), 128.0 (CH_{ar}), 127.1 (CH_{ar}), 127.1 (CH_{ar}), 126.6 (CH_{ar}), 126.3 (CH_{ar}), 102.0 (CH_{vinyl}), 52.7 (CH_3), 45.8 ($2 \times CH$), 43.7 (CH_2), 23.7 (CH_2), 23.6 (CH_2), 22.2 ($2 \times CH_2$).

³¹P NMR (CDCl₃) δ [ppm]: 54.45.

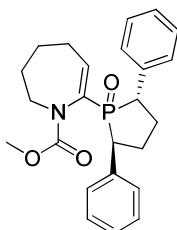
MS (ESI) [m/z]: 396.0 [MH]⁺, 4180 [MNa]⁺, 434.0 [MK]⁺.

HRMS (ESI) [m/z]: calculated for C₂₃H₂₆NO₃P [M]⁺: 395.1650, found: 395.1649.

IR (NaCl) ν [cm⁻¹]: 3386, 2951, 2867, 2354, 1704, 1446, 758, 502.

[α]_D²⁰ = -64.2 (c=1, CHCl₃). **99.4% ee** as determined by chiral SFC-DAD: CO₂-methanol 90:10 (v/v), 3 mL/min, 25°C, 15 MPa. *t_R* (R,R) = 7.62 min., *t_R* (S,S) = 9.14 min.

7-((2S,5S)-1-oxo-2,5-diphenyl-λ₅-phospholan-1-yl)-2,3,4,5-tetrahydro-azepine-1-carboxylic acid methyl ester (24)



Orange oil

R_f = 0.32 (EtOAc) revelator KMnO₄

Procedure:

According to the general procedure (D) and after purification by flash column chromatography (petroleum ether/ethyl acetate: 5/5 to 0/10) compound **24** was obtained (75 mg, 70% yield) as a brown oil.

Analyses:

¹H NMR (250 MHz, CDCl₃) (rotamers) δ [ppm]: 7.43-7.26 (m, 10H), 6.64-6.56 and 6.13 (s, 1H), 4.01 and 3.90 (m, 2H), 3.75 (s, 3H), 3.25 (m, 1H), 3.12 (m, 1H), 2.99 (m, 1H), 2.61 (m, 2H), 2.30 (m, 2H), 2.04 (m, 2H), 1.52 (m, 2H), 1.42 (m, 2H), 1.25 (t, 2H, *J* = 4.6 Hz).

¹³C NMR (63 MHz, DMSO-d₆) δ [ppm]: 154.2 (C=O), 137.9 (C^{IV}), 137.6 (C^{IV}), 137.3 (C^{IV}), 136.4 (C^{IV}), 129.5, 129.3, 128.4, 127.9, 127.4, 127.3, 126.4, 126.2 (10xCH_{ar}), 99.9 (CH), 51.7 (CH), 51.0 (CH), 46.6 (CH₂), 45.3 (CH₂), 36.7 (CH₂), 29.2 (CH₂), 27.3 (CH₂), 27.8 (3xCH₂), 26.4 (CH₂), 22.7 (CH₃).

³¹P NMR (160 MHz, CDCl₃) δ [ppm]: 53.769.

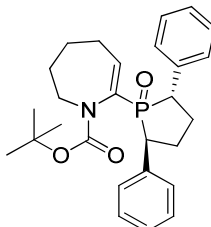
MS (ESI) [m/z]: 410.5 [M+H]⁺, 432.5 [M+Na]⁺.

HRMS (ESI) [m/z]: calculated for C₂₄H₃₁NO₂¹¹BP [M]⁺: 409.1807, found: 409.1799.

IR (NaCl) ν [cm⁻¹]: 3399, 3058, 2933, 2857, 1713, 1450, 1032, 699.

[α]_D²⁰ = -31.0 (c=1, CHCl₃). **99.7% ee** as determined by chiral SFC-DAD: CO₂-methanol 90:10 (v/v), 3 mL/min, 25°C, 15 MPa. *t_R* (R,R) = 9.64 min., *t_R* (S,S) = 14.3 min.

7-((2S,5S)-1-oxo-2,5-diphenyl-1 λ₅-phospholan-1-yl)-2,3,4,5-tetrahydro-azepine-1-carboxylic acid *tert*-butyl ester (25)



Light brown oil

R_f = 0.31 (EtOAc) revelator KMnO₄

Procedure:

Following the general procedure (D) and after purification by flash column chromatography (petroleum ether/ethyl acetate: 5/5 to 0/10) compound **25** was isolated (71 mg, 70% yield) as a light brown oil.

Analyses:

¹H NMR (400 MHz, CDCl₃) (rotamers) δ [ppm]: 7.46 (m, 2H), 7.39 (m, 6H), 7.26 (m, 2H), 6.60 (m, 1H), 4.05 (m, 2H), 3.72 (m, 2H), 2.97 (m, 2H), 2.56 (m, 2H), 2.50 (m, 2H), 2.29 (m, 2H), 2.11 (s, 4H), 1.50 (s, 9H).

¹³C NMR (100 MHz, CDCl₃) δ [ppm]: 154.3 (C=O), 146.2 (CH_{vinyl}), 129.5-126.0 (CH, ar), 80.4 (C^{IV}), 60.4 (CH), 50.3 (CH), 48.2 (CH₂), 44.9 (CH₂), 31.4 (CH₂), 29.7 (CH₂), 28.4 (3xCH₃), 26.7 (CH₂), 22.8 (CH₂).

³¹P NMR (160 MHz, CDCl₃) δ [ppm]: 53.75.

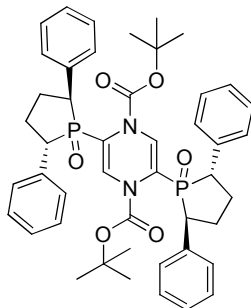
MS (ESI) [m/z]: 452.5 [M+H]⁺, 474.5 [M+Na]⁺.

HRMS (ESI) [m/z]: calculated for C₂₃H₂₅NO₃P [M-tBu]⁺: 394.1572, found: 394.1564.

IR (NaCl) ν [cm⁻¹]: 3373, 3060, 2930, 2859, 2342, 1694, 1454, 1367, 1061, 699.

[α]_D²⁰ = -39.4 (c=1, CHCl₃). **99.5% ee** as determined by chiral SFC-DAD: CO₂-methanol 90:10 (v/v), 3 mL/min, 25°C, 15 MPa. t_R (R,R) = 5.72 min., t_R (S,S) = 5.35 min.

Di-tert-butyl bis(2*S*,5*S*)-1-oxo-2,5-diphenyl-1λ₅-phospholan-1-yl)pyrazine-1,4-dicarboxylate (26**)**



Colorless oil

R_f = 0.13 (EtOAc) revelator KMnO₄

Procedure:

According to the general procedure (D) by doubling the quantity of all reagents, after purification by flash column chromatography (petroleum ether/ethyl acetate: 5/5 to 0/10), product **26** was isolated (220 mg, 75% yield) as a colorless oil.

Analyses:

¹H NMR (400 MHz, CDCl₃) δ [ppm]: 7.41-7.21 (m, 10H), 6.75 (t, J_{H,P} = 5.4 Hz, 1H), 4.67 (m, 1H), 3.95 (dd, J = 3.1 Hz, J = 16.6 Hz, 1H), 3.77 (m, 1H), 2.44 (m, 2H), 2.09 (d, J = 16.6 Hz, 1H), 1.50 (s, 9H).

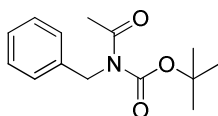
¹³C NMR (100 MHz, CDCl₃) δ [ppm]: 166.6 (C=O), 152.5 (CH_{vinyl}), 136.5 (C^{IV}), 136.0 (C^{IV}), 132.3 (CH_{ar}), 129.2 (2xCH_{ar}), 129.1 (2xCH_{ar}), 128.4 (CH_{ar}), 128.3 (CH_{ar}), 126.9 (CH_{ar}), 126.8 (CH_{ar}), 126.7 (CH_{ar}), 82.3 (C^{IV}), 50.3 (CH), 49.7 (CH), 47.3 (CH₂), 45.7 (CH₂), 28.2 (3xCH₃).

³¹P NMR (160 MHz, CDCl₃) δ [ppm]: 56.83.

MS (m/z): 791.33 [M+H]⁺, 813.8 [M+Na]⁺.

[α]_D²⁰ = -26.4 (c=0.33, CH₃OH). **> 99.5% ee** as determined by chiral SFC-DAD: CO₂-methanol 90:10 (v/v), 3 mL/min, 25°C, 15 MPa. t_R (R,R) = 9.91 min., t_R (S,S) = 11.07 min.

Tert-butyl acetyl-benzyl-carbamate (27)



Colorless oil

$R_f = 0.30$ (PE/EtOAc: 6/4) revelator $KMnO_4$

Procedure:

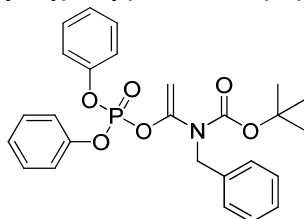
Benzylamine (3.00 g, 27.98 mmol) was added to acetic anhydride (2.64 mL, 27.98 mmol, 1.00 equiv.) and this solution was refluxed 30 min. After cooling down, product was dissolved in dichloromethane and washed with the saturated solution of sodium carbonate, dried over $MgSO_4$ and evaporated under vacuum. After crystallization in Et_2O and drying under vacuum pump, product was taken up in THF (15 mL) and Boc_2O (6.17 g, 28.32 mmol, 1.10 equiv.) was added. Then, DMAP as organocatalyst (346 mg, 2.38 mmol, 10 mol% yield) was introduced and mixture was stirred for 3h at room temperature. Residues were quenched with distilled water, the aqueous phase was extracted with 20 mL of EtOAc. Combined organic phases were dried over $MgSO_4$ and evaporated under vacuum. Flash chromatography (silica gel, petroleum ether/EtOAc: 5/5) yielded carbamate **27** (6.28 g, 90% yield) as a colorless oil.

Analyses:

1H NMR (400 MHz, $CDCl_3$) δ [ppm]: 7.31-7.23 (m, 5H), 4.89 (s, 1H), 2.54 (s, 3H), 1.41 (s, 9H).

^{13}C NMR (100 MHz, $CDCl_3$) δ [ppm]: 173.3 (C=O), 153.3 (C=O), 138.4 (C^{IV}), 128.4 (CH_{ar}), 127.7 (CH_{ar}), 127.2 (CH_{ar}), 83.4 (C^{IV}), 47.2 (CH_2), 28.0 (CH_3), 26.9 (CH_3).

Tert-butyl benzyl(1-(diphenoxyphosphoryloxy) vinyl)carbamate (30)



Colorless oil

$R_f = 0.20$ (PE/EtOAc: 9/1) revelator $KMnO_4$

Procedure:

Starting amide **27** (3.7 mmol) was dissolved in dry THF (15 mL) and the mixture was cooled down to $-78^\circ C$ under argon. A lithium diisopropylamine solution (5.6 mmol, 2 M in THF/n-Heptane, 1.50 equiv.) was then added dropwise and the mixture was stirred at $-78^\circ C$ for 90 minutes. Subsequently, diphenylchlorophosphate (5.6 mmol) was added. After 2h at $-78^\circ C$, the mixture was quenched with water. The aqueous phase was extracted with 20 mL of EtOAc. Combined organic phases were dried over $MgSO_4$ and evaporated under vacuum. Flash chromatography (silica gel, petroleum ether/EtOAc: 1/9) provided pure vinylphosphates **30** (98% yield) as colorless oil.

Analyses:

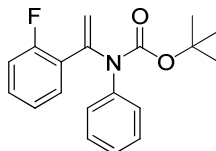
1H NMR (400 MHz, $CDCl_3$) δ [ppm]: 7.19-7.36 (m, 15H), 4.97 (br s, 1H), 4.57 (s, 2H), 4.50 (br s, 1H), 1.42 (s, 9H).

^{13}C NMR (100 MHz, $CDCl_3$) δ [ppm]: 153.8 (C=O), 150.6 (C^{IV}), 146.4 (C^{IV}), 137.7 (C^{IV}), 130.0 (CH_{ar}), 128.2 (CH_{ar}), 128.0 (CH_{ar}), 127.6 (CH_{ar}), 125.8 (CH_{ar}), 120.3 (CH_{ar}), 98.2 (CH_2), 82.7 (C^{IV}), 51.7 (CH_2), 28.3 (CH_3).

^{31}P NMR (162 MHz, $CDCl_3$) δ [ppm]: -18.7.

IR (ATR, neat) ν [cm^{-1}]: 1488, 1193, 1146, 944, 753, 689.

Tert-butyl 1-(2-fluorophenyl) vinyl(phenyl) carbamate (32)



White solid

R_f = 0.57 (PE/EtOAc: 9/1) revelator KMnO₄

Procedure:

According to the general procedure (E) and after purification on the column, product **32** was isolated (46% yield) as a white solid.

Analyses:

¹H NMR (400 MHz, CDCl₃) δ [ppm]: 7.25-7.42 (m, 6H), 7.03-7.20 (m, 3H), 5.42 (s, 1H), 5.16 (s, 1H), 1.25 (s, 9H).

¹³C NMR (100 MHz, CDCl₃) δ [ppm]: 160.4 (C=O), 157.9 (C^{IV}), 152.3 (C^{IV}), 142.4-142.3(F-C^{IV}), 128.6 (CH), 128.5 (CH), 128.1 (CH), 128.0 (CH), 127.9 (CH), 125.2 (CH), 124.7 (CH), 123.2 (CH), 123.1 (CH), 114.9 (CH), 113.8 (CH₂), 80.3 (C^{IV}), 27.0 (CH₃).

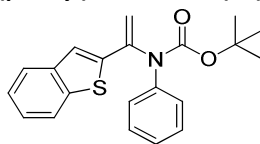
¹⁹F NMR (376.5 MHz, CDCl₃) δ [ppm]: -116.17.

HRMS (ESI) m/z: [M+Na]⁺ calcd for C₁₉H₂₀FNO₂²³Na: 336.1375, found: 336.1369.

IR (neat) ν [cm⁻¹]: 1712, 1365, 1491, 1336, 1218.

Mp < 50°C.

Tert-butyl 1-(benzo[b]thiophen-2-yl) vinyl (phenyl) carbamate (33)



Yellow solid

R_f = 0.50 (PE/EtOAc: 9/1) revelator KMnO₄

Procedure:

According to the general procedure (E), after purification by flash column chromatography, product **33** was isolated as a yellow solid (88% yield).

Analyses:

¹H NMR (400 MHz, CDCl₃) δ [ppm]: 7.71 (m, 1H), 7.66-7.70 (m, 1H), 7.42-7.45 (m, 2H), 7.25-7.34 (m, 5H), 7.14-7.17 (m, 1H), 5.69 (s, 1H), 5.23 (s, 1H), 1.36 (s, 9H).

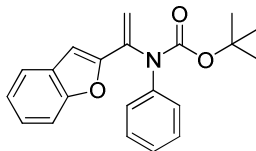
¹³C NMR (100 MHz, CDCl₃) δ [ppm]: 153.4 (C=O), 142.9 (C^{IV}), 142.7 (C^{IV}), 139.9 (C^{IV}), 139.4 (C^{IV}), 128.9 (2CH), 127.5 (CH), 124.9 (CH), 124.8 (CH), 124.7 (CH), 124.5 (CH), 123.1 (CH), 121.5 (CH), 118.5 (CH), 114.5 (CH₂), 81.5 (C^{IV}), 28.1 (CH₃).

HRMS (ESI) m/z [M-tBu]⁺ calcd for [C₁₇H₁₂NO₂S]: 294.0589, found: 294.0593.

IR (neat) ν [cm⁻¹]: 1711, 1503, 1317, 1288, 1251, 1150.

Mp = 117°C.

Tert-butyl 1-(benzofuran-2-yl) vinyl (phenyl) carbamate (34)



Yellow solid

R_f = 0.40 (PE/EtOAc: 9/1) revelator KMnO₄

Procedure:

According to the general procedure (E), after purification by flash column chromatography, product **34** was isolated (74% yield) as a yellow solid.

Analyses:

¹H NMR (400 MHz, CDCl₃) δ [ppm]: 7.14-7.55 (m, 9H), 6.70 (s, 1H), 6.00 (s, 1H), 5.34 (s, 1H), 1.39 (s, 9H).

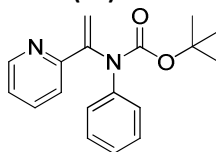
¹³C NMR (100 MHz, CDCl₃) δ [ppm]: 153.9 (C=O), 152.8 (C^{IV}), 152.4 (C^{IV}), 141.3 (C^{IV}), 137.8 (C^{IV}), 127.7 (CH), 127.6 (CH), 124.5 (CH), 123.9 (CH), 122.0 (CH), 120.3(CH), 113.2 (CH₂), 110.1 (CH), 103.2 (CH), 80.4 (C^{IV}), 27.1 (CH₃).

HRMS (ESI) m/z: [M-tBu]⁺ calcd for [C₁₇H₁₂NO₃]: 278.0817, found: 278.0827.

IR (neat, ATR) ν [cm⁻¹]: 1705, 1118, 1063, 988, 711

Mp = 120°C.

Tert-butyl phenyl(1-(pyridin-2-yl) vinyl) carbamate (35)



Brown oil

R_f = 0.15 (PE/EtOAc: 9/1) revelator KMnO₄

Procedure:

According to the general procedure (E), after purification by flash column chromatography, product **35** was isolated (81% yield) as a brown oil.

Analyses:

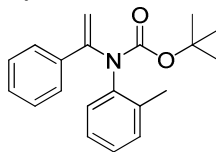
¹H NMR (400 MHz, CDCl₃) δ [ppm]: 8.60 (m, 1H), 7.65 (dt, *J* = 1.6 and 7.6 Hz, 1H), 7.49 (d, *J* = 7.6 Hz, 1H), 7.43 (dd, *J* = 0.8 and 8.8 Hz, 2H), 7.29 (dd, *J* = 8.4 Hz, 2H), 7.11-7.20 (m, 2H), 5.95 (s, 1H), 5.23 (s, 1H), 1.26 (s, 9H).

¹³C NMR (100 MHz, CDCl₃) δ [ppm]: 156.0 (C=O), 153.3 (C^{IV}), 149.2 (CH), 148.2 (C^{IV}), 143.3 (C^{IV}), 136.5 (CH), 128.6 (2CH), 125.5 (2CH), 125.3 (CH), 122.7 (CH), 120.0 (CH), 114.4 (CH₂), 81.0 (C^{IV}), 27.9 (CH₃).

HRMS (ESI) m/z: [M-tBu]⁺ calcd for [C₁₄H₁₁N₂O₂]: 239.0821, found: 239.0838.

IR (neat, ATR) ν [cm⁻¹]: 1707, 1342, 1154, 1100, 746.

Tert-butyl 1-phenylvinyl(o-tolyl)carbamate (36)



Yellow oil

R_f = 0.30 (PE/EtOAc: 9/1) revelator KMnO₄

Procedure:

According to the general procedure (E), after purification by flash column chromatography, product **36** was isolated (90% yield) as a yellow oil.

Analyses:

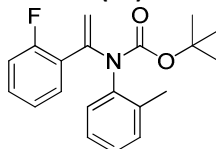
$^1\text{H NMR}$ (400 MHz, CDCl_3) δ [ppm]: 7.55 (d, $J = 7.0$ Hz, 2H), 7.11-7.32 (m, 7H), 5.01 (s, 1H), 4.57 (s, 1H), 2.33 (s, 3H), 1.16 (s, 9H).

$^{13}\text{C NMR}$ (100 MHz, CDCl_3) δ [ppm]: 153.2 (C=O), 149.5 (C^{IV}), 142.5 (C^{IV}), 135.7 (C^{IV}), 131.1 (CH), 128.4 (2CH), 128.1 (CH), 127.6 (CH), 127.2 (2CH), 126.0 (2CH), 107.6 (CH_2), 80.9 (C^{IV}), 27.9 (3 CH_3), 18.2 (CH_3).

HRMS (ESI) m/z : $[\text{M}+\text{Na}]^+$ calcd for $\text{C}_{20}\text{H}_{23}\text{NO}_2^{23}\text{Na}$: 332.1626, found: 332.1633.

IR (neat, ATR) ν [cm^{-1}]: 1709, 1345, 1299, 1163, 768.

Tert-butyl 1-(2-fluorophenyl)vinyl(o-tolyl) carbamate (37)



Yellow oil

$R_f = 0.30$ (PE/EtOAc: 9/1) revelator KMnO_4

Procedure:

According to the general procedure (E), after purification by flash column chromatography, product **37** was isolated (64% yield) as a yellow oil.

Analyses:

$^1\text{H NMR}$ (400 MHz, CDCl_3) δ [ppm]: 7.47 (t, $J = 7.7$ Hz, 1H), 7.01-7.31 (m, 7H), 4.92 (s, 1H), 4.61 (s, 1H), 2.31 (s, 3H), 1.18 (s, 9H).

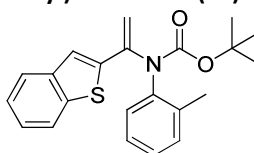
$^{13}\text{C NMR}$ (100 MHz, CDCl_3) δ [ppm]: 160.9 (C=O), 158.5 (C^{IV}), 152.7 (C^{IV}), 143.7, 141.9 (C^{IV}), 136.2 (C^{IV}), 130.8 (CH), 129.3 (2CH), 128.0 (CH), 127.4, (CH), 127.2 (CH), 124.0 (2CH), 115.7 (CH), 115.5 (CH), 109.1, 109.0 (CH_2), 80.9 (C^{IV}), 28.4 (CH_3), 27.8 (3 CH_3).

$^{19}\text{F NMR}$ (376.5 MHz, CDCl_3) δ [ppm]: -116.1.

HRMS (ESI) m/z : $[\text{M}+\text{H}]^+$ calcd for $\text{C}_{20}\text{H}_{23}\text{NO}_2\text{F}$: 328.1699, found: 328.1713.

IR (neat, ATR) ν [cm^{-1}]: 1709, 1307, 1218, 759.

Tert-butyl 1-(benzo[b]thiophen-2-yl)vinyl(o-tolyl)carbamate (38)



Yellow solid

$R_f = 0.55$ (PE/EtOAc: 9/1) revelator KMnO_4

Procedure:

According to the general procedure (E), after purification by flash column chromatography, product **38** was isolated (89% yield) as a yellow solid.

Analyses:

$^1\text{H NMR}$ (400 MHz, CDCl_3) δ [ppm]: 7.71 (m, 2H), 7.42 (s, 1H), 7.12-7.29 (m; 6H), 5.35 (s, 1H), 4.83 (s, 1H), 2.37 (s, 3H), 1.28 (s, 9H).

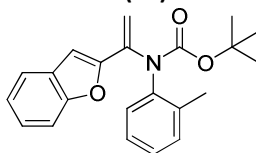
¹³C NMR (100 MHz, CDCl₃) δ [ppm]: 1531 (C=O), 143.3 (C^{IV}), 141.8 (C^{IV}), 139.7 (C^{IV}), 135.3 (C^{IV}), 131.0 (CH), 127.1 (2CH), 126.9 (CH), 124.7 (CH), 124.5 (CH), 123.7 (CH), 122.1 (CH), 121.1 (CH), 110.5 (CH₂), 81.1 (C^{IV}), 27.9 (3CH₃), 18.3 (CH₃).

HRMS (ESI) m/z: [M]⁺ calcd for C₂₂H₂₃NO₂S: 365.1450, found: 365.1470.

IR (neat, ATR) ν [cm⁻¹]: 1707, 1102, 993, 728.

Mp = 130°C.

Tert-butyl 1-(benzofuran-2-yl)vinyl(o-tolyl)carbamate (39)



Yellow solid

R_f = 0.40 (PE/EtOAc: 9/1) revelator KMnO₄

Procedure:

According to the general procedure (E), after purification by flash column chromatography, product **39** was isolated (94% yield) as a yellow solid.

Analyses:

¹H NMR (400 MHz, CDCl₃) δ [ppm]: 7.42-7.56 (m, 2H), 7.12-7.31 (m, 6H), 6.83 (s, 1H), 5.63 (s, 1H), 4.96 (s, 1H), 2.38 (s, 3H), 1.30 (s, 9H).

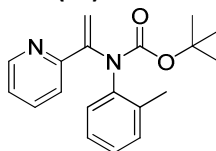
¹³C NMR (100 MHz, DMSO-d₆) δ [ppm]: 154.6 (C=O), 154.3 (C^{IV}), 152.9 (C^{IV}), 141.9 (C^{IV}), 139.7 (C^{IV}), 135.8 (C^{IV}), 131.4 (CH), 128.9 (C^{IV}), 127.9 (CH), 127.2 (CH), 127.7 (CH), 125.4 (CH), 123.7 (CH), 121.8 (CH), 111.5 (CH), 111.0 (CH₂), 104.4 (CH), 81.0 (C^{IV}), 28.1 (3CH₃), 18.1 (CH₃).

HRMS (ESI) m/z/ [M-tBu]⁺ calcd for [C₁₈H₁₄NO₃]: 292.0974, found: 292.0953.

IR (neat, ATR) ν [cm⁻¹]: 1709, 1324, 1108, 994.

Mp = 110°C.

Tert-butyl 1-(pyridin-2-yl)vinyl(o-tolyl)carbamate (40)



Yellow oil

R_f = 0.25 (PE/EtOAc: 9/1) revelator KMnO₄

Procedure:

According to the general procedure (F), after purification by flash column chromatography, product **40** was isolated (78% yield) as a yellow oil.

Analyses:

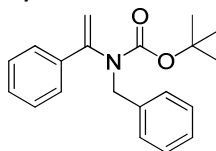
¹H NMR (400 MHz, CDCl₃) δ [ppm]: 8.50 (d, J = 4.7 Hz, 1H), 7.57 (t, J = 7.8 Hz, 1H), 7.45 (m, 1H), 7.06-7.25 (m, 5H), 5.32 (s, 1H), 4.69 (s, 1H), 2.27 (s, 3H), 1.08 (s, 9H).

¹³C NMR (100 MHz, CDCl₃) δ [ppm]: 152.9 (C=O), 148.9 (CH), 148.9 (C^{IV}), 142.3 (C^{IV}), 136.2 (CH), 135.8 (C^{IV}), 130.8 (CH), 127.7 (CH), 127.1 (CH), 126.9 (CH), 122.5 (CH), 120.6 (CH), 109.9 (CH₂), 80.7 (C^{IV}), 27.8 (3CH₃), 17.9 (CH₃).

HRMS (ESI) m/z: [M+H]⁺ calcd for C₁₉H₂₃N₂O₂: 311.1760, found: 311.1754.

IR (neat, ATR) ν [cm⁻¹]: 1709, 1354, 1158, 1082.

Tert-butyl benzyl(1-phenylvinyl)carbamate (41)



Colorless oil

$R_f = 0.60$ (PE/EtOAc: 9/1) revelator KMnO_4

Procedure:

According to the general procedure (F), after purification by flash column chromatography, product **41** was isolated (81% yield) as a colorless oil.

Analyses:

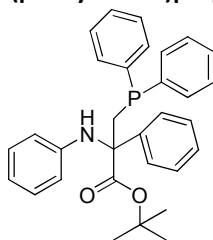
$^1\text{H NMR}$ (400 MHz, CDCl_3) δ [ppm]: 7.11-7.22 (m, 10H), 5.13 (s, 1H), 4.85 (s, 1H), 4.62 (s, 2H), 1.13 (s, 9H).

$^{13}\text{C NMR}$ (100 MHz, CDCl_3) δ [ppm]: 154.7 (C=O), 147.8 (C^{IV}), 138.7 (C^{IV}), 128.6 (CH), 128.5 (CH), 128.2 (CH), 128.1 (CH), 127.5 (CH), 127.1 (CH), 125.8 (CH), 109.5 (CH_2), 80.4 (C^{IV}), 53.2 (CH_2), 27.9 ($3\times\text{CH}_3$).

HRMS (ESI) m/z $[\text{M}+\text{Na}]^+$ calcd for $\text{C}_{20}\text{H}_{23}\text{NO}_2^{23}\text{Na}$: 332.1627, found: 332.1626.

IR (neat, ATR) ν [cm^{-1}]: 1695, 1366, 1153, 696.

Tert-butyl 3-(diphenylphosphino)-2-phenyl-2-(phenylamino)propanoate (42)



White solid

$R_f = 0.70$ (PE/EtOAc: 9/1) revelator KMnO_4

Procedure:

According to the general procedure (F), after purification by flash column chromatography, product **42** was isolated (43% yield) as a white solid.

Analyses:

$^1\text{H NMR}$ (400 MHz, CDCl_3) δ [ppm]: 7.57 (dd, $J = 12.0$ Hz, 2H), 7.43 (dd, $J = 12.0$ Hz, 2H), 7.35 (m, 7H), 7.07 (m, 3H), 6.97 (dd, $J = 7.2$ Hz, 2H), 6.79 (dd, $J = 7.2$ Hz, 2H), 6.47 (dd, $J = 7.2$ Hz, 1H), 6.08 (d, $J = 7.6$ Hz, 2H), 5.57 (s, 1H), 3.42 (ddd, $J = 4.4$ and 14.1 and 26.8 Hz, 2H), 1.22 (s, 9H).

$^{13}\text{C NMR}$ (100 MHz, CDCl_3) δ [ppm]: 209 (C=O), 172.2 (C^{IV}), 144.1 (C^{IV}), 141.3 (C^{IV} , $J = 7$ Hz), 139.6 (C^{IV}), 137.3 (C^{IV}), 133.3 (CH_{ar}), 133.1 (CH_{ar}), 133.0 (CH_{ar}), 132.9 (CH_{ar}), 128.6 ($2\times\text{CH}_{\text{ar}}$), 128.5 (CH_{ar}), 128.4 (CH_{ar}), 128.3 (CH_{ar}), 128.1 (CH_{ar}), 128.0 (CH_{ar}), 127.5 (CH_{ar}), 127.0 (CH_{ar}), 116.9 (CH_{ar}), 115.0 (CH_{ar}), 82.8 (C^{IV}), 66.6 (CH_2 , $J = 7$ Hz), 35.0 (CH_2 , $J = 13$ Hz), 27.6 ($3\times\text{CH}_3$).

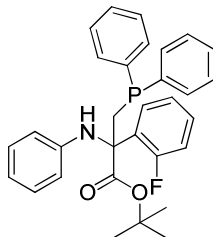
$^{31}\text{P NMR}$ (162 MHz, CDCl_3) δ [ppm]: -22.83.

HRMS (ESI) m/z $[\text{M}+\text{Na}]^+$ calcd for $\text{C}_{31}\text{H}_{32}\text{NO}_2^{23}\text{NaP}$: 504.2068, found: 504.2063.

IR (neat, ATR) ν [cm^{-1}]: 1713, 1504, 1288, 1148, 737.

Mp = 120°C.

Tert-butyl 3-(diphenylphosphino)-2-(2-fluorophenyl)-2-(phenylamino)propanoate (43)



White solid

R_f = 0.65 (PE/EtOAc: 9/1) revelator KMnO₄

Procedure:

According to the general procedure (F), after purification by flash column chromatography, product **43** was isolated (41% yield) as a white solid.

Analyses:

¹H NMR (400 MHz, CDCl₃) δ [ppm]: 7.56 (m, 3H), 7.48 (m, 4H), 7.11-7.33 (m, 6H), 6.89 (m, 3H), 6.57 (dd, *J* = 8.0 Hz, 1H), 6.27 (d, *J* = 8.0 Hz, 2H), 5.13 (s, 1H), 3.38 (ddd, *J* = 4.0 and 12.0 and 36.0 Hz, 2H), 1.24 (s, 9H).

¹³C NMR (100 MHz, CDCl₃) δ [ppm]: 171.0 (C=O), 161.9 (C^{IV}), 159.5 (C^{IV}), 145.205 (C^{IV}), 144.7 (C^{IV}), 139.4 (C^{IV}), 139.3 (C^{IV}), 138.0 (C^{IV}), 137.9 (CH_{ar}), 133.4 (CH_{ar}), 133.2 (CH_{ar}), 132.9 (CH_{ar}), 129.8 (CH_{ar}), 129.7 (CH_{ar}), 128.9 (CH_{ar}), 128.8 (CH_{ar}), 128.7 (CH_{ar}), 128.6 (CH_{ar}), 128.4 (CH_{ar}), 128.2 (CH_{ar}), 123.9 (CH_{ar}), 118.0 (CH_{ar}), 117.8 (CH_{ar}), 116.5 (CH_{ar}), 116.2 (CH_{ar}), 115.7 (CH_{ar}), 115.5 (CH_{ar}), 82.9 (C^{IV}), 37.2 (CH₂, *J* = 15 Hz), 27.7 (3xCH₃).

¹⁹F NMR (376.5 MHz, CDCl₃) δ [ppm]: -109.9.

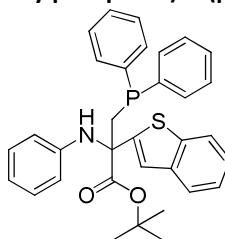
³¹P NMR (162 MHz, CDCl₃) δ [ppm]: -25.0.

HRMS (ESI) *m/z* [M+H]⁺ calcd for C₃₁H₃₂FNO₂P: 500.2155, found: 500.2153.

IR (neat, ATR) *v* [cm⁻¹]: 1720, 1602, 1503, 1281, 1146, 691.

Mp = 120°C.

Tert-butyl 2-(benzo[b]thiophen-2-yl)-3-(diphenylphosphino)-2-(phenylamino)propanoate (44)



White solid

R_f = 0.45 (PE/EtOAc: 9/1) revelator KMnO₄

Procedure:

According to the general procedure (F), after purification by flash column chromatography, product **44** was isolated (95% yield) as a white solid.

Analyses:

¹H NMR (400 MHz, CDCl₃) δ [ppm]: 7.72 (dd, *J* = 8.0 Hz, *J* = 21.0 Hz, 2H), 7.50 (m, 2H), 7.45 (s, 1H), 7.25 (m, 5H), 7.02 (m, 5H), 6.84 (m, 2H), 6.54 (m, 1H), 6.30 (d, *J* = 7.8 Hz, 2H), 5.50 (s, 1H), 3.28-3.53 (ddd, *J* = 2.6 and 14.2 and 80.6 Hz, 2H), 1.25 (s, 9H).

¹³C NMR (100 MHz, CDCl₃) δ [ppm]: 170.7 (C=O), 148.2 (C^{IV}, *J* = 10 Hz), 144.0 (C^{IV}), 140.4 (C^{IV}), 139.9 (C^{IV}), 138.5 (C^{IV}), 137.1 (C^{IV}), 133.0 (4xCH_{ar}, *J* = 10 Hz), 132.8 (CH_{ar}, *J* = 10 Hz), 128.5 (2xCH_{ar}), 128.5 (CH_{ar}), 128.4 (CH_{ar}), 128.4 (CH_{ar}), 128.1 (CH_{ar}), 128.0 (CH_{ar}), 124.0 (CH_{ar}), 123.7 (CH_{ar}), 122.2 (CH_{ar}), 117.8 (CH_{ar}), 115.4 (2xCH_{ar}), 83.4 (C^{IV}), 65.2 (CH₂, *J* = 20 Hz), 37.4 (CH₂, *J* = 10 Hz), 27.5 (3xCH₃).

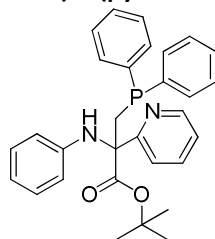
³¹P NMR (162 MHz, CDCl₃) δ [ppm]: -23.4.

HRMS (ESI) m/z $[M+H]^+$ calcd for $C_{33}H_{33}NO_2PS$: 538.1970, found: 538.1964.

IR (neat, ATR) ν $[cm^{-1}]$: 1715, 1602, 1501, 1433, 1288, 1149, 743.

Mp = 178°C.

Tert-butyl 3-(diphenylphosphino)-2-(phenylamino)-2-(pyridin-2-yl)propanoate (46)



White solid

R_f = 0.15 (PE/EtOAc: 9/1) revelator $KMnO_4$

Procedure:

According to the general procedure (F), after purification by flash column chromatography, product **46** was isolated (47% yield) as white solid.

Analyses:

¹H NMR (400 MHz, $CDCl_3$) δ [ppm]: 8.61 (d, J = 4.8 Hz, 1H), 7.51 (dt, J = 2.0, 8.0 Hz, 1H), 7.42 (m, 1H), 7.34 (m, 2H), 7.21 (m, 3H), 7.10 (m, 4H), 6.99 (m, 2H), 6.85 (m, 2H), 6.51 (dd, J = 7.2 Hz, 1H), 6.21 (d, J = 8.0 Hz, 2H), 6.03 (s, 1H), 3.55 (ddd, J = 2.4 and 16.0 and 54.4 Hz, 2H), 1.27 (s, 9H).

¹³C NMR (100 MHz, $CDCl_3$) δ [ppm]: 210.1 (C=O), 172.3 (C^{IV}), 172.2 (C^{IV}), 159.5 (C^{IV}), 159.4 (C^{IV}), 148.7(CH_{ar}), 144.4 (C^{IV}), 139.5 (C^{IV}), 139.4 (C^{IV}), 138.2 (C^{IV}), 138.1 (C^{IV}), 136.8 (CH_{ar}), 134.7 (CH_{ar}), 134.5 (CH_{ar}), 133.5 (CH_{ar}), 133.3 (CH_{ar}), 133.0 (CH_{ar}), 132.9 (CH_{ar}), 128.8 (CH_{ar}), 128.4 (CH_{ar}), 128.3 (CH_{ar}), 128.3 (CH_{ar}), 128.2 (CH_{ar}), 128.1 (CH_{ar}), 128.0 (CH_{ar}), 122.6 (CH_{ar}), 121.5 (CH_{ar}), 121.5 (CH_{ar}), 117.2 (CH_{ar}), 114.8 (CH_{ar}), 82.8 (C^{IV}), 68.1 (CH_2 , J = 20 Hz), 34.4 (CH_2 , J = 10 Hz), 27.8 (3 \times CH_3).

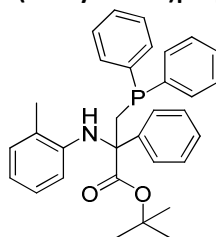
³¹P NMR (162 MHz, $CDCl_3$) δ [ppm]: -25.0.

HRMS (ESI) m/z $[M+H]^+$ calcd for $C_{30}H_{31}N_2O_2P$: 483.2182, found: 483.2201.

IR (neat, ATR) ν $[cm^{-1}]$: 3329, 1729, 1600, 1280, 1147, 740.

Mp = 146°C.

Tert-butyl 3-(diphenylphosphino)-2-phenyl-2-(o-tolylamino)propanoate (47)



Clear yellow solid

R_f = 0.40 (PE/EtOAc: 9/1) revelator $KMnO_4$

Procedure:

According to the general procedure (F), after purification by flash column chromatography, product **47** was isolated (43 % yield) as clear yellow solid.

Analyses:

¹H NMR (400 MHz, CDCl₃) δ [ppm]: 7.59 (d, *J* = 7.9 Hz, 2H), 7.42 (m, 2H), 7.33 (m, 7H), 7.07 (m, 3H), 6.98 (m, 2H), 6.78 (d, *J* = 7.9 Hz, 1H), 6.65 (t, *J* = 7.9 Hz, 1H), 6.45 (t, *J* = 7.3 Hz, 1H), 5.87 (d, *J* = 8.04 Hz, 1H), 5.54 (s, 1H), 3.46 (ddd, *J* = 2.7 and 14.2 and 73.3 Hz, 2H), 2.03 (s, 3H), 1.29 (s, 9H).

¹³C NMR (100 MHz, CDCl₃) δ [ppm]: 172.3 (C=O), 141.7 (C^{IV}), 141.2 (C^{IV}, *J* = 7.0 Hz), 139.7 (C^{IV}, *J* = 11.8 Hz), 136.3 (CH_{ar}, *J* = 11.0 Hz), 133.0 (CH_{ar}), 132.8 (CH_{ar}), 132.8 (CH_{ar}), 132.6 (CH_{ar}), 129.9 (CH_{ar}), 128.5 (CH_{ar}), 128.4 (CH_{ar}), 128.4 (CH_{ar}), 128.2 (CH_{ar}), 128.1 (CH_{ar}), 127.7 (CH_{ar}), 127.6 (CH_{ar}), 127.3 (CH_{ar}), 126.8 (CH_{ar}), 125.7 (CH_{ar}), 123.2 (C^{IV}), 116.6 (CH_{ar}), 112.8 (CH_{ar}), 82.7 (C^{IV}), 66.4 (CH₂, *J* = 21.2 Hz), 34.2 (CH₂, *J* = 13 Hz), 27.6 (3xCH₃), 17.6 (CH₃).

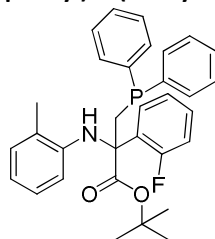
³¹P NMR (162 MHz, CDCl₃) δ [ppm]: -22.6.

HRMS (ESI) *m/z* [M+H]⁺ calcd for C₃₂H₃₅NO₂P: 496.2413, found: 496.2405.

IR (neat, ATR) ν [cm⁻¹]: 1719, 1280, 1150, 734.

Mp = 108°C.

***Tert*-butyl 3-(diphenylphosphino)-2-(2-fluorophenyl)-2-(*o*-tolylamino)propanoate (48)**



White solid

R_f = 0.56 (PE/EtOAc: 9/1) revelator KMnO₄

Procedure:

According to the general procedure (F), after purification by flash column chromatography, product **48** was isolated (55% yield) as a white solid.

Analyses:

¹H NMR (400 MHz, CDCl₃) δ [ppm]: 7.57 (t, *J* = 7.9 Hz, 1H), 7.47 (dt, *J* = 1.4 and 8.0 Hz, 2H), 7.08-7.35 (m, 7H), 6.83 (d, *J* = 7.2 Hz, 1H), 6.70 (t, *J* = 7.6 Hz, 1H), 6.49 (t, *J* = 7.3 Hz, 1H), 6.14 (d, *J* = 8.1 Hz, 1H), 5.18 (s, 1H), 3.45 (ddd, *J* = 2.1 and 14.4 and 60.0 Hz, 2H), 1.95 (s, 3H), 1.26 (s, 9H).

¹³C NMR (100 MHz, CDCl₃) δ [ppm]: 171.0 (C=O), 161.8 (C^{IV}), 159.3 (C^{IV}), 142.4 (C^{IV}), 139.6 (C^{IV}), 137.3 (C^{IV}), 133.1 (CH_{ar}), 132.9 (CH_{ar}), 132.8 (CH_{ar}), 132.6 (CH_{ar}), 130.3 (CH_{ar}), 129.9 (CH_{ar}), 129.6 (CH_{ar}), 129.5 (CH_{ar}), 128.5 (CH_{ar}), 128.1 (CH_{ar}), 127.9 (CH_{ar}), 127.8 (CH_{ar}), 125.8 (CH_{ar}), 123.7 (CH_{ar}), 123.6 (C^{IV}), 117.3 (CH_{ar}), 116.4 (CH_{ar}), 116.2 (CH_{ar}), 112.9 (CH_{ar}), 82.8 (C^{IV}), 65.5 (CH₂, *J* = 19 Hz), 36.5 (CH₂, *J* = 11 Hz), 27.6 (3xCH₃), 17.5 (CH₃).

³¹P NMR (162 MHz, CDCl₃) δ [ppm]: -24.3.

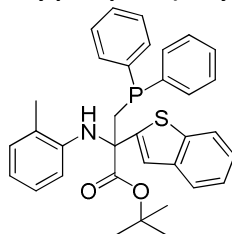
¹⁹F NMR (376.5 MHz, CDCl₃) δ [ppm]: -109.7.

HRMS (ESI) *m/z* [M+H]⁺ calcd for C₃₂H₃₄FNO₂P: 514.2296, found: 514.2311.

IR (neat, ATR) ν [cm⁻¹]: 1731, 1279, 1150, 741, 695.

Mp = 80°C.

***Tert*-butyl 1-(benzo[*b*]thiophen-2-yl)-2-(diphenylphosphino)ethyl(*o*-tolyl)carbamate (49)**



Brown oil

R_f = 0.25 (PE/EtOAc: 9/1) revelator KMnO₄

Procedure:

According to the general procedure (F), after purification by flash column chromatography, product **49** was isolated (54% yield) as a brown solid.

Analyses:

¹H NMR (250 MHz, CDCl₃) δ [ppm]: 7.69 (m, 2H), 7.00-7.39 (m, 13H), 6.81 (m, 1H), 6.67 (t, *J* = 7.5 Hz, 1H), 6.50 (dt, *J* = 1.0 and 7.5 Hz, 1H), 6.2 (d, *J* = 8.0 Hz, 1H), 5.49 (s, 1H), 3.25-3.65 (ddd, *J* = 4.5 and 14.3 and 82.8 Hz, 2H), 2.02 (s, 3H), 1.29 (s, 9H).

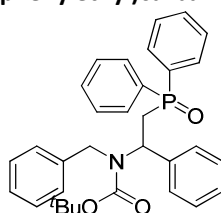
¹³C NMR (100 MHz, CDCl₃) δ [ppm]: 170.9 (C=O), 148.5 (C^{IV}), 141.9 (C^{IV}), 140.4 (C^{IV}), 139.9 (C^{IV}), 138.6 (C^{IV}), 136.4 (C^{IV}), 132.9 (CH_{ar}), 132.7 (CH_{ar}), 130.1 (CH_{ar}), 128.6 (CH_{ar}), 128.5 (CH_{ar}), 128.3 (CH_{ar}), 127.9 (CH_{ar}), 127.8 (CH_{ar}), 127.5 (CH_{ar}), 126.0 (CH_{ar}), 124.0 (CH_{ar}), 123.7 (CH_{ar}), 123.6 (C^{IV}), 122.3 (CH_{ar}), 122.1 (CH_{ar}), 117.6 (CH_{ar}), 113.2 (CH_{ar}), 83.4 (C^{IV}), 65.2 (CH₂, *J* = 20 Hz), 36.5 (CH₂, *J* = 10 Hz), 28.3 (3xCH₃), 17.5 (CH₃).

³¹P NMR (162 MHz, CDCl₃) δ [ppm]: -23.1.

MS (ESI) *m/z* [M+H]⁺ C₃₄H₃₄NO₂PS: 552.

IR (neat, ATR) ν[cm⁻¹]: 1729, 1243, 1045, 694.

Tert-butyl benzyl(2-(diphenylphosphoryl)-1-phenylethyl)carbamate (52)



White solid

R_f = 0.30 (PE/EtOAc: 9/1) revelator KMnO₄

Procedure:

According to the general procedure (F), after purification by flash column chromatography, product **52** was isolated (50% yield) as white solid.

Analyses:

¹H NMR (400 MHz, CDCl₃) δ [ppm]: 7.92 (m, 1H), 7.76 (m, 2H), 7.73 (m, 2H), 7.45 (m, 7H), 7.30-7.12 (m, 8H), 5.37 (dt, *J* = 8Hz and 4Hz, 1H), 4.46 (brs, 1H), 4.05 (brs, 1H), 2.95 (dt, *J* = 5.0 and 12.5 Hz, 1H), 1.27 (s, 9H).

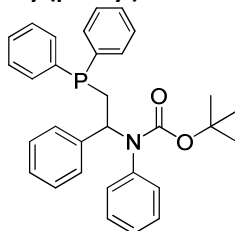
¹³C NMR (100 MHz, CDCl₃) δ [ppm]: 209.9 (C=O), 182.4 (C^{IV}), 154.9 (C^{IV}), 138.9 (C^{IV}), 131.6 (CH_{ar}), 130.8 (CH_{ar}), 130.7 (CH_{ar}), 130.5 (CH_{ar}), 130.4 (CH_{ar}), 128.6 (CH_{ar}), 128.5 (CH_{ar}), 128.2 (CH_{ar}), 127.9 (CH_{ar}), 80.1 (C^{IV}), 59.0-51.2(CH₂), 43.6 (CH), 33.4 (CH), 32.7 (CH), 28.3 (3xCH₃).

³¹P NMR (162 MHz, CDCl₃) δ [ppm]: 28.5.

MS (ESI) *m/z* [M+Na]⁺ C₃₃H₃₄NO₂PNa: 518.

Mp = 150°C.

Tert-butyl 2-(diphenylphosphino)-1-phenylethyl(phenyl)carbamate (42a).



Colorless oil

R_f = 0.50 (PE/EtOAc: 9/1) revelator KMnO₄

Procedure:

According to the general procedure (F) and after purification on the column, the by product **42a** was isolated (35% yield) as a colorless oil.

Analyses:

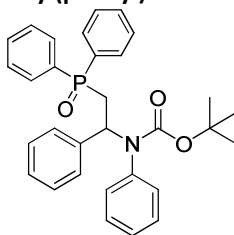
$^1\text{H NMR}$ (400 MHz, CDCl_3) δ [ppm]: 7.49-7.17 (m, 18H), 6.87 (m, 2H), 5.55 (m, 1H), 2.62 (m, 2H), 1.34 (s, 9H).

$^{13}\text{C NMR}$ (100 MHz, CDCl_3) δ [ppm]: 155.1 (C=O), 141.4 (C^{IV}), 139.4 (C^{IV}), 133.4 (C^{IV}), 130.3 (C^{IV}), 130.2 (CH_{ar}), 129.1 (CH_{ar}), 128.9 (CH_{ar}), 128.8 (CH_{ar}), 128.7 (CH_{ar}), 128.5 (CH_{ar}), 128.4 (CH_{ar}), 128.3 (CH_{ar}), 127.7 (CH_{ar}), 127.1 (CH_{ar}), 80.3 (C^{IV}), 57.5 (CH, $J = 18.1$ Hz), 32.4 (CH_2 , $J = 13.7$ Hz), 27.0 (CH_3).

$^{31}\text{P NMR}$ (162 MHz, CDCl_3) δ [ppm]: -22.8.

MS (ESI) m/z $[\text{M}+\text{H}]^+$ $\text{C}_{31}\text{H}_{33}\text{NO}_2\text{P}$: 482.

Tert-butyl 2-(diphenylphosphoryl)-1-phenylethyl(phenyl)carbamate (42b).



Colorless oil

$R_f = 0.10$ (PE/EtOAc: 9/1) revelator KMnO_4

Procedure:

According to the general procedure (F) and after purification on the column, the by product **42b** was isolated (26% yield) as a colorless oil.

Analyses:

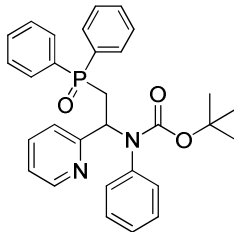
$^1\text{H NMR}$ (400 MHz, CDCl_3) δ [ppm]: 7.70-7.50 (m, 4H), 7.50-7.30 (m, 6H), 7.10 (m, 8H), 6.79-6.76 (m, 2H), 5.65 (m, 1H), 3.36 (m, 1H), 2.86-2.78 (m, 1H), 1.22 (s, 9H).

$^{13}\text{C NMR}$ (100 MHz, CDCl_3) δ [ppm]: 171.1 (C^{IV}), 154.4 (C=O), 140.6 (C^{IV}), 133.8 (C^{IV}), 131.5 (C^{IV}), 130.7 (CH_{ar}), 129.1 (CH_{ar}), 128.5 (CH_{ar}), 128.3 (CH_{ar}), 126.6 (CH_{ar}), 114.3 (CH_{ar}), 80.3 (C^{IV}), 57.1 (CH), 33.4 (CH_2 , $J = 69$ Hz), 28.2 (CH_3).

$^{31}\text{P NMR}$ (162 MHz, CDCl_3) δ [ppm]: 28.6.

MS (ESI) m/z $[\text{M}+\text{H}]^+$ $\text{C}_{31}\text{H}_{33}\text{NO}_3\text{P}$: 498.

Tert-butyl 2-(diphenylphosphoryl)-1-(pyridin-2-yl)ethyl(phenyl)carbamate (45a).



Colorless oil

$R_f = 0.10$ (PE/EtOAc: 9/1) revelator KMnO_4

Procedure:

According to the general procedure (F) and after purification on the column, the by product **45a** was isolated (100% yield) as a colorless oil.

Analyses:

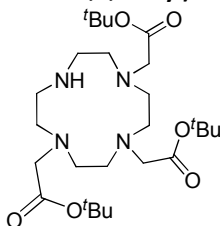
¹H NMR (400 MHz, CDCl₃) δ [ppm]: 8.37 (m, 1H), 7.70-7.20 (m, 16H), 6.94 (m, 2H), 5.93-5.86 (m, 1H), 3.57-3.49 (m, 1H), 3.08 (br s, 1H), 1.32 (s, 9H).

¹³C NMR (100 MHz, CDCl₃) δ [ppm]: 154.5 (C=O), 148.5 (C^{IV}), 140.9 (C^{IV}), 132.0 (CH_{ar}), 131.1 (CH_{ar}), 128.7 (CH_{ar}), 126.5 (CH_{ar}), 122.9 (CH_{ar}), 122.3 (CH_{ar}), 80.9 (C^{IV}), 57.9 (CH), 32.0, 31.3 (CH₂), 28.4 (CH₃).

³¹P NMR (162 MHz, CDCl₃) δ [ppm]: 29.3.

MS (ESI) m/z [M+Na]⁺ C₃₁H₃₃N₂O₃P: 499.

Tert-butyl 2,2',2''-(1,4,7,10-tetraazacyclododecane-1,4,7-triyl)triacetate (53)¹⁸⁴



White solid

R_f = 0.37 (CH₂Cl₂/MeOH: 9/1) revelator KMnO₄

Procedure:

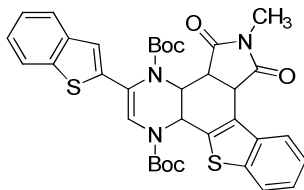
A solution of cyclen (100 mg, 0.58 mmol, 1.00 equiv.) was prepared in distilled acetonitrile (4 mL), cooled down to 0 °C and NaHCO₃ (244 mg, 2.90 mmol, 5.00 equiv.) was added. The mixture was stirred for 30 minutes at 0 °C, then *tert*-butyl bromoacetate (0.28 mL, 1.91 mmol, 3.30 equiv.) was introduced drop by drop during 60 min. at 0 °C. The reaction mixture was left for gentle warming up to room temperature and stirred for next 22h. The residues were filtered through glass frit, washed abundantly with acetonitrile and the filtrate was concentrated. After crystallization in toluene 280 mg (94 % yield) of **53** as a white solid was obtained.

Analyses:

¹H NMR (250 MHz, CDCl₃) δ [ppm]: 3.38 (s, 4H), 3.30 (s, 2H), 3.11 (m, 4H), 2.92-2.89 (m, 12H), 1.47 (s, 27H).

MS (ESI) [m/z]: 515.0 [M+H]⁺, 459.5 [M-*t*Bu]⁺, 403.5 [M-2*t*Bu]⁺, 347.5 [M-3*t*Bu]⁺.

8,11-di-tert-butyl 9-(1-benzothiophen-2-yl)-4-methyl-3,5-dioxo-14-thia-4,8,11-triazapentacyclo[11.7.0.0^{2,6}.0^{7,12}.0^{15,20}]icosa-1(13),9,15,17,19-pentaene-8,11-dicarboxylate (54)



Yellow solid

R_f = 0.52 (PE/EtOAc: 8/2) revelator CAN

Procedure:

A solution of 1,4-dihydropyrazine derivative⁹ (300 mg, 0.55 mmol, 1.00 equiv.) and N-methylmaleimide (305 mg, 2.75 mmol, 5.00 equiv.) in distilled toluene (4 mL, c = 0.14 M) was heated for 24 h at 110 °C in the sealed tube. After cooling down solvent was removed under vacuum and the crude was purified by flash column chromatography (PE then PE/ EtOAc: 9/1) to isolate 360 mg (quantitative) of **54** as a yellow solid.

Analyses:

¹H NMR (400 MHz, CDCl₃) δ [ppm]: 7.99 (d, *J* = 6.4 Hz, 1H), 7.83 (s, 1H), 7.36 (s, 1H), 7.67 (d, *J* = 8 Hz, 3H), 7.15 (m, 6H), 6.72 (s br, 1H), 5.20 (d, *J* = 5.2 Hz, 1H), 4.34 (d, *J* = 7.2 Hz, 1H), 3.13 (m, 1H), 3.09 (s, 3H), 2.77 (t, *J* = 9.6 Hz, 1H), 1.54 (s, 9H), 1.10 (s br, 1H).

¹³C NMR (101 MHz, CDCl₃) δ [ppm]: 177.6 (C=O), 175.2 (C=O), 139.9 (C^{IV}), 139.6 (C^{IV}), 128.5 (CH_{ar}), 126.8 (CH_{ar}), 125.6 (CH_{ar}), 125.0 (C^{IV}), 124.6 (CH_{ar}), 124.5 (CH_{ar}), 123.8 (CH_{ar}), 122.8 (CH_{ar}), 122.1 (CH_{ar}), 121.1 (CH_{ar}), 82.3 (C^{IV}), 60.2 (CH), 47.5 (CH), 46.0 (CH), 44.3 (CH), 28.2 (CH₃), 27.8 (CH₃), 25.1 (CH₃N).

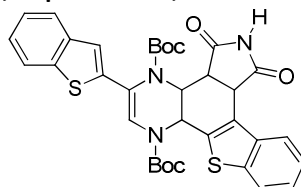
MS (ESI) [m/z]: 680.5 [M+Na]⁺, 696.5 [M+K]⁺.

HRMS (ESI) [m/z]: calculated for C₃₅H₃₅N₃O₆NaS₂ [M+Na]⁺: 680.1865, found: 680.1860.

IR (neat, ATR) ν [cm⁻¹]: 3056 (CH, sp²), 2974 (CH, sp³), 1700 (C=O), 1438, 1347, 1252, 1155, 748.

Mp = 170 °C.

8,11-di-tert-butyl 9-(1-benzothiophen-2-yl)-3,5-dioxo-14-thia-4,8,11-triazapentacyclo[11.7.0.0^{2,6}.0^{7,12}.0^{15,20}]jcosa-1(13),9,15,17,19-pentaene-8,11-dicarboxylate (55)



Yellow solid

R_f = 0.17 (PE/EtOAc: 8/2) revelator CAN

Procedure:

A solution of 1,4-dihydropyrazine derivative⁹ (100 mg, 0.18 mmol, 1.00 equiv.) and maleimide (88 mg, 0.92 mmol, 5.00 equiv.) in distilled toluene (1.5 mL, c = 0.12 M) was heated for 72 h at 110 °C in the sealed tube. After cooling down solvent was removed under vacuum and the crude was purified by flash column chromatography (PE/EtOAc: 9/1 then 8/2 then 7/3) to isolate 72 mg (62% yield) of **55** as a yellow solid.

Analyses:

¹H NMR (400 MHz, CDCl₃) δ [ppm]: 9.32 (s, 1H), 7.98 (d, *J* = 2.6 Hz, 1H), 7.82 (s, 1H), 7.78 (d, *J* = 8.0 Hz, 2H), 7.30-7.18 (m, 6H), 6.90 (s, 1H), 5.47 (s br, 1H), 4.52 (s br, 1H), 3.34 (t, *J* = 8.0 Hz, 1H), 2.93 (t, *J* = 8.0 Hz, 1H).

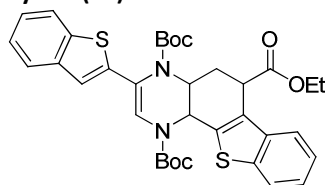
¹³C NMR (101 MHz, CDCl₃) δ [ppm]: 178.2 (C=O), 171.1 (C=O), 151.1 (C^{IV}), 139.9 (C^{IV}), 139.6 (C^{IV}), 138.5 (2xC^{IV}), 135.1 (2xC^{IV}), 128.5 (CH_{ar}), 126.6 (CH_{ar}), 126.2 (CH_{ar}), 125.6 (CH_{ar}), 124.6 (C^{IV}), 122.8 (CH_{ar}), 122.1 (CH_{ar}), 121.1 (2xCH_{ar}), 82.7 (C^V), 60.3 (CH), 47.4 (CH), 45.5 (CH), 28.2 (CH₃), 27.7 (CH₃).

HRMS (ESI) [m/z]: calculated for C₃₄H₃₃N₃O₇NaS₂ [M+Na]⁺: 682.1658, found: 682.1660; calculated for C₃₀H₂₅N₃O₇NaS₂ [M-tBu+Na]⁺: 626.1032, found: 626.1007.

IR (neat, ATR) ν [cm⁻¹]: 3466 (NH imide), 3053 (CH, sp²), 2972 (CH, sp³), 1704 (C=O), 1445, 1347, 1252, 1156, 748.

Mp = 146 °C.

3,6-di-tert-butyl 9-ethyl 5-(1-benzothiophen-2-yl)-17-thia-3,6-diazatetracyclo[8.7.0.0^{2,7}.0^{11,16}]heptadeca-1(10),4,11,13,15-pentaene-3,6,9-tricarboxylate (56)



Orange oil

R_f = 0.21 (PE/EtOAc: 8/2) CAN relevator

Procedure:

In the sealed tube, a solution of starting 1,4-dihydropyrazine derivative⁹ (50 mg, 0.09 mmol, 1.00 equiv.) was prepared in ethyl acrylate (1.0 mL, 9.15 mmol, 100.00 equiv.). The mixture was stirred for 2 days at 110 °C.

After cooling down, the solvent was evaporated under vacuum and a brown oil was recuperated. The crude was purified by column chromatography (8/2) to yield 28 mg of product **56** as an orange oil (47% yield).

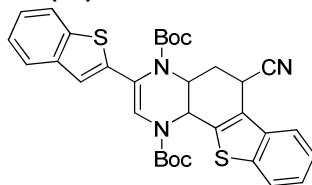
Analyses:

$^1\text{H NMR}$ (400 MHz, CDCl_3) δ [ppm]: 7.98 (m, 2H), 7.79 - 7.75 (m, 2H), 7.63 (s, 1H), 7.52 (m, 4H), 6.97 (s, 1H), 5.08 (s, 1H), 4.59 (m, 1H), 4.21 (q, $J = 5.2$ Hz, 2H), 3.60 (t, $J = 4.0$ Hz, 1H), 2.31 (m, 1H), 2.06 (m, 1H), 1.40 (s, 18H), 1.29 (t, $J = 2.5$ Hz, 3H).

MS (ESI) [m/z]: 647.0 [M+H]⁺, 669.0 [M+Na]⁺, 685.0 [M+K]⁺.

IR (neat, ATR) ν [cm^{-1}]: 3016, 2975 (CH, sp³), 2952 (CH, sp²), 1725, 1706 (C=O), 1505, 1365, 1237, 1180, 730, 484.

3,6-di-tert-butyl 5-(1-benzothiophen-2-yl)-9-cyano-17-thia-3,6-diazatetracyclo[8.7.0.0^{2,7}.0^{11,16}]heptadeca-1(10),4,11,13,15-pentaene-3,6-dicarboxylate (57)



Yellow oil

R_f = 0.21 (PE/ EtOAc: 8/2) CAN relevator

Procedure:

In the sealed tube, a solution of starting 1,4-dihydropyrazine derivative⁹ (100 mg, 0.18 mmol, 1.00 equiv.) was prepared in acrylonitrile (2.0 mL, 31.11 mmol, 170.00 equiv.). The mixture was stirred over 5 days at 110 °C. After cooling down, the solvent was evaporated under vacuum and a brown oil was recuperated. The crude was purified by column chromatography (9/1) to yield 21 mg of product **57** of a yellow oil (19% yield).

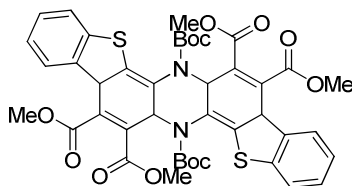
Analyses:

$^1\text{H NMR}$ (400 MHz, CDCl_3) δ [ppm]: 7.65 (m, 2H), 7.35-7.01 (m, 8H), 6.76 (s, 1H), 5.08 (s, 1H), 4.28 (s, 1H), 3.62 (m, 1H), 2.72 (m, 1H), 2.53 (m, 1H), 1.55 (s, 9H), 1.19 (s, 9H).

MS (ESI) [m/z]: 600.5 [M+H]⁺, 622.0 [M+Na]⁺, 638.0 [M+K]⁺.

IR (neat, ATR) ν [cm^{-1}]: 3006, 2975 (CH, sp³), 2951 (CH, sp²), 2245 (CN), 1710 (C=O), 1505, 1365, 1237, 1180, 730, 484.

2,16-di-tert-butyl 13,14,27,28-tetramethyl 5,19-dithia-2,16-diazaheptacyclo[15.11.0.0^{3,15}.0^{4,12}},0^{6,11}.0^{18,26}.0^{20,25}]octacos-3,6,8,10,13,17,20,22,24,27-decaene-2,13,14,16,27,28-hexacarboxylate (58)



Yellow solid

R_f = 0.30 (PE/ EtOAc: 8/2) CAN relevator

Procedure:

In the sealed tube, a solution of starting 1,4-dihydropyrazine derivative⁹ (200 mg, 0.37 mmol, 1.00 equiv.) was prepared in dry toluene (4 mL) and DMAD (0.22 mL, 1.83 mmol, 5.00 equiv.) was introduced. The mixture was stirred over 48 h at 150 °C. After cooling down, a solvent was evaporated under vacuum and a brown oil was recuperated. After trituration in diethyl ether, 117 mg of product **58** a yellow solid was obtained (37% yield).

Analyses:

¹H NMR (250 MHz, DMSO-d₆) δ [ppm]: 9.71 (s, 1H), 8.18 (s, 1H), 8.15 (d, *J* = 8.0 Hz, 1H), 7.90 (d, *J* = 8.0 Hz, 1H), 7.60 (m, 2H), 4.05 (s, 3H), 3.91 (s, 3H), 1.52 (s, 9H).

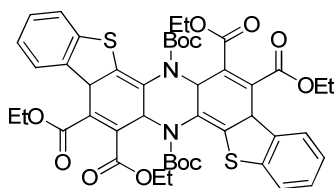
¹³C NMR (101 MHz, DMSO-d₆) δ [ppm]: 168.5 (C=O), 165.3 (C=O), 153.1 (C^{IV}), 139.0 (C^{IV}), 138.6 (C^{IV}), 133.6 (C^{IV}), 132.0 (C^{IV}), 131.5 (C^{IV}), 128.2 (CH_{ar}), 126.6 (C^{IV}), 125.6 (CH_{ar}), 124.1 (CH_{ar}), 123.6 (CH_{ar}), 122.9 (CH), 121.1 (CH), 80.2 (C^{IV}), 53.1 (CH₃), 52.9 (CH₃), 28.1 (3xCH₃).

MS (ESI) [m/z]: 831.0 [M+H]⁺, 853.0 [M+Na]⁺.

IR (neat, ATR) ν [cm⁻¹]: 3305, 2978 (CH, sp³), 2950 (CH, sp²), 1717 (C=O), 1511, 1237, 1150, 730.

Mp = 185 °C.

2,16-di-tert-butyl 13,14,27,28-tetraethyl 5,19-dithia-2,16-diazaheptacyclo[15.11.0.0^{3,15}.0^{4,12}.0^{6,11}.0^{18,26}.0^{20,25}]octacos-3,6,8,10,13,17,20,22,24,27-decaene-2,13,14,16,27,28-hexacarboxylate (59)



Yellow solid

R_f = 0.31 (PE/EtOAc: 8/2) CAN relevator

Procedure:

In the sealed tube, a solution of starting 1,4-dihydropyrazine derivative⁹ (70 mg, 0.13 mmol, 1.00 equiv.) was prepared in dry toluene (2 mL) and DEAD (0.11 mL, 0.64 mmol, 5.00 equiv.) was introduced. The mixture was stirred for 5 days at 150 °C. After cooling down, the solvent was evaporated under vacuum and a brown oil was recuperated. The crude was purified by column chromatography (PE/ EtOAc: 8/2) to yield 26 mg of product **59** of a yellow semi-solid (23% yield).

Analyses:

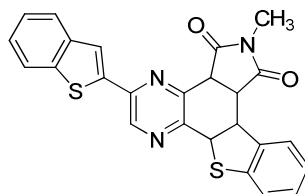
¹H NMR (400 MHz, CDCl₃) δ [ppm]: 9.07 (s, 1H), 8.11 (d, *J* = 5.5 Hz, 1H), 7.93-7.82 (m, 4H), 7.52-7.45 (m, 2H), 7.44-7.37 (m, 2H), 4.61 (q, *J* = 7.2 Hz, 2H), 4.46-4.40 (m, 4H), 4.30-4.25 (m, 2H), 1.48-1.40 (m, 12 H), 1.38-1.26 (m, 18 H).

¹³C NMR (101 MHz, DMSO-d₆) δ [ppm]: 168.4 (C=O), 166.8 (C=O), 165.0 (C=O), 164.9 (C=O), 155.7 (C^{IV}), 151.2 (CH), 142.1 (C^{IV}), 141.8 (C^{IV}), 141.3 (C^{IV}), 140.3 (C^{IV}), 139.7 (C^{IV}), 135.2 (C^{IV}), 134.3 (C^{IV}), 129.5 (C^{IV}), 125.0 (CH_{ar}), 124.4 (CH_{ar}), 124.2 (CH_{ar}), 123.8 (CH_{ar}), 123.3 (CH_{ar}), 123.1 (CH_{ar}), 123.0 (CH_{ar}), 122.8 (CH_{ar}), 117.6 (CH), 80.2 (C^{IV}), 62.7 (CH₂), 62.5 (CH₂), 62.2 (CH₂), 31.6 (CH₃), 30.4 (CH₃), 29.9 (CH₂), 18.5 (CH₃), 14.3 (3xCH₃), 14.2 (CH₃).

MS (ESI) [m/z]: 887.0 [M+H]⁺.

IR (neat, ATR) ν [cm⁻¹]: 3336, 2975 (CH, sp³), 2951 (CH, sp²), 1720 (C=O), 1511, 1237, 1150, 730.

9-(1-benzothiophen-2-yl)-4-methyl-14-thia-4,8,11-triazapentacyclo[11.7.0.0^{2,6}.0^{7,12}.0^{15,20}]icosa-7,9,11,15,17,19-hexaene-3,5-dione (60)



Red-orange solid

R_f = 0.17 (PE/EtOAc: 8/2) revelator CAN

Procedure:

A solution of adduct **54** (100 mg, 0.15 mmol, 1.00 equiv.) in anhydrous distilled dichloromethane (2.5 mL, $c = 0.06$ M) was prepared at room temperature and degassed. Then TMSI (0.13 mL, 0.91 mmol, 6.00 equiv.) was introduced *via* syringe. The solution changed color from yellow to red. After 20 min. of magnetic stirring, the solution was diluted with 10 mL of dichloromethane, hydrolyzed with 10 mL of a saturated solution of NaHCO_3 and extracted three times with dichloromethane (15 mL). All organic phases were recombined and washed with distilled water (30 mL) and brine (20 mL), dried over anhydrous MgSO_4 , filtered and solvent was removed under reduced pressure. The crude was purified by precipitation in diethyl ether to yield 68 mg (98% yield) of **60** as a red-orange solid.

Analyses:

$^1\text{H NMR}$ (250 MHz, CDCl_3) δ [ppm]: 8.63 (s, 1H), 8.31 (d, $J = 5$ Hz, 1H), 7.78 (m, 3H), 7.57 (d, $J = 7.5$ Hz, 1H), 7.47 (m, 4H), 5.32 (d, $J = 7.5$ Hz, 1H), 4.82 (dd, $J = 5$ Hz, 2.5, 1H), 4.58 (dd, $J = 7$ Hz, 2.5, 1H), 4.27 (dd, $J = 7.5$ Hz, 2.5, 1H), 3.05 (s, 3H).

$^{13}\text{C NMR}$ (101 MHz, CDCl_3) δ [ppm]: 176.5 (C=O), 175.1 (C=O), 152.3 (C^{IV}), 151.1 (CH), 141.6 (C^{IV}), 141.5 (C^{IV}), 139.3 (C^{IV}), 139.3 (C^{IV}), 136.9 (C^{IV}), 134.1 (C^{IV}), 126.9 (CH_{ar}), 126.1 (CH_{ar}), 125.1 (CH_{ar}), 125.0 (CH_{ar}), 124.9 (C^{IV}), 124.7 (CH_{ar}), 124.6 (CH_{ar}), 123.5 (CH_{ar}), 122.5 (CH_{ar}), 122.2 (CH_{ar}), 52.2 (CH), 50.5 (CH), 45.5 (CH), 40.0 (CH), 25.2 (CH_3N).

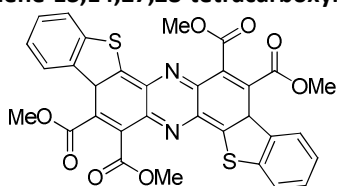
MS (ESI) [m/z]: 456.5 [M+H] $^+$.

HRMS (ESI) [m/z]: calculated for $\text{C}_{25}\text{H}_{17}\text{N}_3\text{O}_2\text{NaS}_2$ [M+Na] $^+$: 478.0660, found: 478.0654.

IR (ATR, neat) $\nu = 3066$ (CH, sp^2), 2973 (CH, sp^3), 1698 (C=O), 1345, 1254, 1156, 749, 697.

Mp = 214 °C (decomposition).

13,14,27,28-tetramethyl 5,19-dithia-2,16-diazaheptacyclo[15.11.0.0^{3,15}.0^{4,12}.0^{6,11}.0^{18,26}.0^{20,25}]octacosane-1,3,6,8,10,13,15,17,20,22,24,27-dodecaene-13,14,27,28-tetracarboxylate (61)



Yellow solid

R_f = 0.27 (PE/EtOAc: 8/2) CAN relevator

Procedure:

To the cooled solution of **58** (52 mg, 62.6 μmol , 1.00 equiv.) in the distilled CH_2Cl_2 (5 mL) under argon at 0 °C, TMSI (21 μL , 0.15 mmol, 2.40 equiv.) was introduced by syringe and the reaction was carried out for 30 min. Then reaction was warmed up and hydrolyzed by addition of 20 mL of a saturated solution of NaHCO_3 . The aqueous phase was extracted twice with CH_2Cl_2 , all organic phases were collected and washed with distilled water and brine, dried over MgSO_4 , filtrated and concentrated. The crude was precipitated with diethyl ether to provide 30 mg of product **61** as a yellow solid (71% yield).

Analyses:

$^1\text{H NMR}$ (250 MHz, CDCl_3) δ [ppm]: 7.96 (m, 2H), 7.49 (m, 2H), 7.35 (s, 1H), 4.11 (s, 3H), 3.92 (s, 3H).

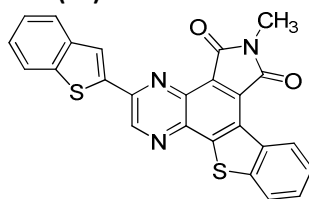
$^{13}\text{C NMR}$ (101 MHz, DMSO-d_6) δ [ppm]: 168.5 (C=O), 165.3 (C=O), 153.1 (C^{IV}), 139.0 (C^{IV}), 138.6 (C^{IV}), 133.6 (C^{IV}), 132.0 (C^{IV}), 131.5 (C^{IV}), 128.2 (CH_{ar}), 126.6 (C^{IV}), 125.6 (CH_{ar}), 124.1 (CH_{ar}), 123.6 (CH_{ar}), 122.9 (CH), 121.1 (CH), 80.2 (C^{IV}), 53.1 (CH_3), 52.9 (CH_3), 28.1 (3 $\times\text{CH}_3$).

MS (ESI) [m/z]: 860.0 [M+H] $^+$.

IR (neat, ATR) ν [cm^{-1}]: 3305, 2978 (CH, sp^3), 2950 (CH, sp^2), 1717 (C=O), 1511, 1237, 1150, 730.

Mp = 185 °C.

9-(1-benzothiophen-3-yl)-4-methyl-14-thia-4,8,11-triazapentacyclo[11.7.0.0^{2,6}.0^{7,12}.0^{15,20}]icosa-1(13),2(6),7,9,11,15,17,19-octaene-3,5-dione (62)



Brown solid

R_f = 0.56 (DCM/EtOAc/MeOH: 6/2/2) revelator CAN

Procedure:

A solution of **60** (90 mg, 0.20 mmol, 1.00 equiv.) in distilled toluene (10 mL, c = 0.02 M) was prepared at room temperature and DDQ (202 mg, 0.75 mmol, 4.50 equiv.) was added. Then solution was heated to 90 °C for 18h. After cooling down, a red precipitate was observed. The volume of solvent was reduced under vacuum to 2 mL and solid was precipitated with diethyl ether, filtered through Milipore and washed twice with diethyl ether to yield after drying 88 mg (98% yield) of **62** as brown solid.

Analyses:

¹H NMR (250 MHz, DMSO-d₆) δ [ppm]: 9.85 (s, 1H), 9.68 (m, 1H), 8.69 (s, 1H), 8.50 (m, 1H), 8.10 (m, 1H), 8.00 (m, 1H), 7.68 (m, 2H), 7.48 (m, 2H), 3.20 (s, 3H).

¹³C NMR (101 MHz, CDCl₃) δ [ppm]: 168.2(C=O), 168.0 (C=O), 153.2 (C^{IV}), 149.0 (CH), 143.4 (C^{IV}), 141.9 (C^{IV}), 140.7 (C^{IV}), 140.3 (C^{IV}), 139.9 (C^{IV}), 139.6 (C^{IV}), 137.9 (C^{IV}), 136.6 (C^{IV}), 134.1 (C^{IV}), 128.0 (C^{IV}), 126.1 (CH_{ar}), 124.9 (C^{IV}), 124.5 (CH_{ar}), 124.4 (CH_{ar}), 124.3 (CH_{ar}), 123.2 (CH_{ar}), 123.0 (CH_{ar}), 122.8 (CH_{ar}), 122.5 (CH_{ar}), 122.1 (CH_{ar}), 25.0 (CH₃N).

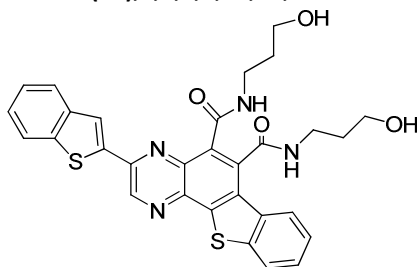
MS (ESI) [m/z]: 452.5 [M+H]⁺, 474.5 [M+Na]⁺.

HRMS (ESI) [m/z]: calculated for C₂₅H₁₃N₃O₂NaS₂ [M+Na]⁺: 474.0347, found: 474.0346.

IR (neat, ATR) ν [cm⁻¹]: 3058 (CH, sp²), 2919 (CH, sp³), 1699 (C=O), 1436, 1391, 1252, 1038, 743.

Mp > 250 °C.

5-(1-benzothiophen-2-yl)-8-N,9-N-bis(3-hydroxypropyl)-17-thia-3,6-diazatetracyclo[8.7.0.0^{2,7}.0^{11,16}]heptadeca-1(10),2,4,6,8,11,13,15-octaene-8,9-dicarboxamide (63)



Orange-brown solid

Procedure:

The product **62** (100 mg, 0.22 mmol, 1.00 equiv.) was added at room temperature to distilled 3-aminopropanol (7.25 mL, 85.0 mmol, 390 equiv.). The mixture was heated at 110 °C for 3h. After cooling down, an orange precipitate was observed. 20 mL of distilled water were added to precipitate the product. Residues were filtered through Milipore and washed twice with distilled water to remove an excess of 3-aminopropanol. After drying under vacuum, 80 mg (62% yield) of **63** were obtained as a brown solid.

Analyses:

¹H NMR (400 MHz, DMSO-d₆) δ [ppm]: 9.79 (s, 1H), 8.66 (m, 1H), 8.63 (s, 1H), 8.32 (m, 1H), 8.17 (m, 1H), 8.06 (m, 1H), 7.99 (m, 1H), 7.64 (m, 2H), 7.46 (m, 2H), 3.63 (m, 2H), 3.57 (m, 4H), 3.49 (m, 6H), 1.87 (t, *J* = 8 Hz, 2H), 1.80 (t, *J* = 8 Hz, 2H).

¹³C NMR (101 MHz, DMSO-d₆) δ [ppm]: 166.0 (C=O), 165.0 (C=O), 148.1 (C^{IV}), 142.2 (CH), 141.6 (C^{IV}), 141.3 (C^{IV}), 140.3 (C^{IV}), 138.8 (C^{IV}), 137.5 (C^{IV}), 136.2 (C^{IV}), 134.3 (C^{IV}), 133.6 (C^{IV}), 130.7 (C^{IV}), 127.6 (CH_{ar}), 126.6 (CH_{ar}), 126.0 (CH_{ar}), 125.3 (CH_{ar}), 125.2 (CH_{ar}), 124.3 (CH_{ar}), 123.6 (CH_{ar}), 123.1 (CH_{ar}), 65.1 (CH₂), 59.0 (CH₂), 58.8 (CH₂), 36.8 (CH₂), 32.8 (CH₂), 32.2 (CH₂).

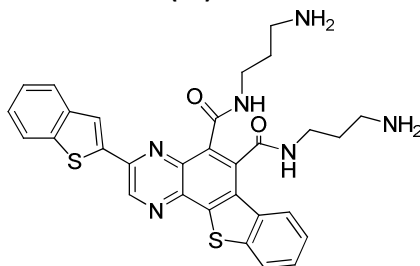
MS (ESI) [m/z]: 452.5 [M+H]⁺, 474.5 [M+Na]⁺.

HRMS (ESI) [m/z]: calculated for C₃₀H₂₆N₄O₄NaS₂ [M+Na]⁺: 593.1293, found: 593.1278.

IR (neat, ATR) ν [cm⁻¹]: 3265 (CONH), 3056 (CH, sp²), 2938 (CH, sp³), 1636 (C=O), 1523, 1327, 1061, 748, 726.

Mp = 256 °C (decomposition).

8-N,9-N-bis(3-aminopropyl)-5-(1-benzothiophen-2-yl)-17-thia-3,6-diazatetracyclo[8.7.0.0^{2,7}.0^{11,16}]heptadeca-1(10),2,4,6,8,11,13,15-octaene-8,9-dicarboxamide (64)



Orange-brown solid

Procedure:

The product **62** (53 mg, 0.12 mmol, 1.00 equiv.) was added at room temperature to diaminopropane (2 mL, 24.0 mmol, 200 equiv.). The mixture was heated at 110 °C for 3h. After cooling down, an orange precipitate was observed. 20 mL of distilled water were added to precipitate the product. Residues were filtered through Milipore and washed twice with distilled water to remove an excess of diaminopropane. After drying under vacuum, 32 mg (53% yield) of product **64** was obtained as an orange-brown solid.

Analyses:

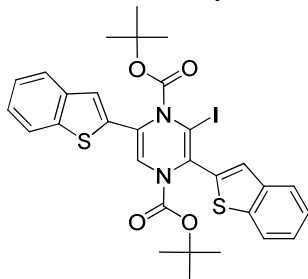
¹H NMR (400 MHz, CDCl₃) δ [ppm]: 8.17 (d, *J* = 8.0 Hz, 1H), 8.08 (m, 1H), 7.93 (s, 1H), 7.85-7.76 (m, 3H), 7.60 (m, 1H), 7.40-7.36 (m, 5H), 3.82 (m, 2H), 3.72 (m, 4H), 2.92 (t, *J* = 6.5 Hz, 2H), 2.89-2.84 (m, 4H), 1.94 (t, *J* = 6.3 Hz, 2H), 1.85-1.80 (m, 4H).

MS (ESI) [m/z]: 569.5 [M+H]⁺, 591.5 [M+Na]⁺.

IR (neat, ATR) ν [cm⁻¹]: 3264 (CONH), 3056 (CH, sp²), 2933 (CH, sp³), 1635 (C=O), 1529, 1433, 1327, 748, 726.

Mp = 224 °C.

2,5-Bis-benzo[b]thiophen-2-yl-3-iodo-pyrazine-1,4-dicarboxylic acid di-*tert*-butyl ester (65)



Yellow solid

R_f = 0.43 (PE/EtOAc: 9/1) revelator CAN

Procedure:

To a solution of starting dihydropyrazine⁹ (570 mg, 1.04 mmol, 1.00 equiv.) in anhydrous THF (30 mL) at -78°C under argon was added dropwise 1.04 mL of LDA (2M in THF, 2.08 mmol, 2.00 equiv.) and the solution was stirred for 45 minutes. The solution of I₂ (662 mg, 2.60 mmol, 2.50 equiv.) in THF was prepared under argon with activated molecular sieves (4A) at room temperature, and after 45 min of stirring, was introduced to the first solution at -78°C. After 1h of reaction, residues were diluted with EtOAc and hydrolyzed with saturated solution of NH₄Cl. Then, the mixture was extracted with EtOAc, washed with a saturated solution of Na₂S₂O₃, distilled water and brine. All organic phases were recombined, dried over MgSO₄, filtered and concentrated. The crude was purified by column chromatography (PE/ EtOAc: 95/5) to yield 635 mg (91% yield) of product **65** as a yellow solid.

Analyses:

¹H NMR (250 MHz, CDCl₃) δ [ppm]: 7.85-7.64 (m, 4H), 7.50 (s, 1H), 7.42-7.27 (m, 4H), 7.24 (s, 2H), 1.41 (s, 9H), 1.16 (s, 9H).

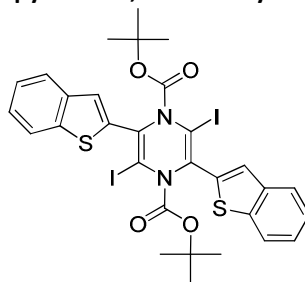
¹³C NMR (63 MHz, CDCl₃) δ [ppm]: 151.53 (C=O), 149.38 (C^{IV}), 140.19 (C^{IV}), 139.74 (C^{IV}), 139.03 (C^{IV}), 138.97 (C^{IV}), 137.55 (C^{IV}), 136.58 (C^{IV}), 135.89 (C^{IV}), 127.66 (CH_{ar}), 125.28 (CH_{ar}), 124.79 (CH_{ar}), 124.73 (CH_{ar}), 124.68 (CH_{ar}), 124.52 (C^{IV}), 124.19 (CH_{ar}), 123.62 (CH_{ar}), 122.39 (CH_{ar}), 122.25 (CH_{ar}), 121.16 (CH_{ar}), 83.94 (C^{IV}), 83.56 (C^{IV}), 28.14 (CH₃), 27.67 (CH₃).

IR (neat, ATR) ν [cm⁻¹]: 3061 (CH sp²), 2974 (CH sp³), 2926 (CH sp³), 1718 (C=O), 1308, 1153, 745 (C-S).

MS (ESI, m/z): 673.0 [M+H]⁺, 695.0 [M+Na]⁺.

Mp = 87°C.

2,5-Bis-benzo[b]thiophen-2-yl-3,6-diiodo-pyrazine-1,4-dicarboxylic acid di-tert-butyl ester (66)



Yellow powder

R_f = 0.52 (PE/ EtOAc: 8/2) revelator CAN

Procedure:

To a solution of starting dihydropyrazine⁹ (250 mg, 0.46 mmol, 1.00 equiv.) in anhydrous THF (14 mL) at -78°C under argon, was added dropwise 1.02 mL of LDA (1.8 M in THF, 1.83 mmol, 4.00 equiv.). The solution was stirred for 45 minutes and HMPA (0.16 mL, 0.87 mmol, 1.90 equiv.) was introduced to the solution. The reaction was stirred for 10 min. The solution of I₂ (580 mg, 2.29 mmol, 5.00 equiv.) in anhydrous THF was prepared under argon, with activated molecular sieves (4A) at room temperature and was introduced to the first solution at -78°C *via* canulla. After 1h of reaction, residues were diluted with EtOAc and hydrolyzed with a saturated solution of NH₄Cl. The mixture was extracted with EtOAc, washed with a 20 % solution of Na₂S₂O₃, distilled water and brine. All organic phases were recombined, dried over MgSO₄, filtered and concentrated. The crude was purified by column chromatography (PE/EtOAc: 95/5 to 90/10) to yield 340 mg (93% yield) of product **66** as a yellow powder.

Analyses:

¹H NMR (400 MHz, DMSO) δ [ppm]: 8.07 – 7.89 (m, 2H), 7.74 (s, 1H), 7.41 (d, J = 4.4 Hz, 2H), 1.22 (s, 9H).

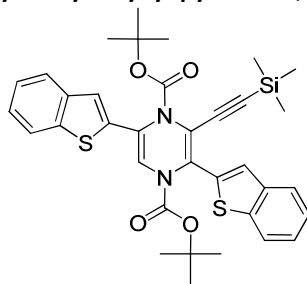
¹³C NMR (101 MHz, DMSO) δ [ppm]: 149.17 (C=O), 139.22 (C^{IV}), 138.96 (C^{IV}), 136.41 (C^{IV}), 136.28 (C^{IV}), 126.22 (CH_{ar}), 125.47 (CH_{ar}), 124.89 (CH_{ar}), 124.27 (CH_{ar}), 122.44 (CH_{ar}), 83.29 (C^{IV}), 27.36 (CH₃).

IR (neat, ATR) ν [cm⁻¹]: 3064 (CH sp²), 2974 (CH sp³), 2932 (CH sp³), 1719 (C=O), 1299, 1154, 747 (C-S).

MS (ESI, m/z): 821.0 [M+Na]⁺.

Mp = 195°C.

2,5-Bis-benzo[b]thiophen-2-yl-3-trimethylsilylanylethynyl-pyrazine-1,4-dicarboxylic acid di-*tert*-butyl ester (67)



Yellow-orange oil

R_f = 0.53 (PE/EtOAc: 9/1) revelator CAN

Procedure:

To a solution of starting iodide **65** (200 mg, 0.29 mmol, 1.00 equiv.) in an freshly distilled triethylamine (8 mL) was added trimethylsilylacetylene (0.09 mL, 0.65 mmol, 2.20 equiv.). The solution was degassed and backfilled with argon for three times. Then, catalysts PdCl₂(PPh₃) (21 mg, 0.029 mmol, 0.10 equiv.) and CuI (14 mg, 0.074 mmol, 0.25 equiv.) were introduced and the reaction was carried out for 40 h at 50°C. The content of flask was filtered through a fritted glass, washed with diethyl ether and concentrated. Then, residues were taken up into diethyl ether, washed with a 5% solution of HCl, distilled water, saturated solution of NaHCO₃ and brine. After drying over MgSO₄, filtration and concentration, the crude was purified by column chromatography (silica gel, PE/EtOAc: 95/5) to give 160 mg (91% yield) of product **67** as a yellow-orange oil.

Analyses:

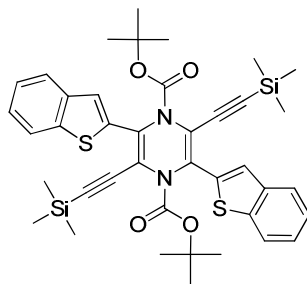
¹H NMR (400 MHz, CDCl₃) δ [ppm]: 7.85-7.64 (m, 5H), 7.42-7.22 (m, 5H), 7.18 (s, 1H), 1.48 (s, 9H), 1.29 (s, 9H), 0.19 (s, 9H).

¹³C NMR (101 MHz, CDCl₃) δ [ppm]: 151.60 (C=O), 149.63 (C^{IV}), 140.02 (C^{IV}), 139.82 (C^{IV}), 139.17 (C^{IV}), 139.07 (C^{IV}), 136.97 (C^{IV}), 135.93 (C^{IV}), 135.79 (C^{IV}), 127.67 (CH_{ar}), 126.46 (CH_{ar}), 126.36 (CH_{ar}), 125.08 (CH_{ar}), 124.68 (CH_{ar}), 124.57 (CH_{ar}), 124.54 (CH_{ar}), 123.86 (CH_{ar}), 123.66 (CH_{ar}), 122.20 (CH_{ar}), 121.40 (CH_{ar}), 99.64 (C≡C), 98.65 (C≡C), 83.65 (C^{IV}), 82.80 (C^{IV}), 28.17 (CH₃), 27.81 (CH₃), -0.24 (TMS).

IR (neat, ATR) ν [cm⁻¹]: 3060 (CH sp²), 2975 (CH sp³), 2253 (C≡C), 2144 (C≡C), 1718 (C=O), 1310, 1139, 843 (C-S).

MS (ESI, m/z): 665.5 [M+Na]⁺.

2,5-Bis-benzo[b]thiophen-2-yl-3,6-bis-trimethylsilylanylethynyl-pyrazine-1,4-dicarboxylic acid di-*tert*-butyl ester (68)



Yellow oil

R_f : 0.65 (PE/EtOAc: 8/2) revelator CAN

Procedure:

To a solution of starting iodide **66** (200 mg, 0.29 mmol, 1.00 equiv.) in an freshly distilled triethylamine (4 mL) was added trimethylsilylacetylene (0.12 mL, 0.83 mmol, 4.40 equiv.). The solution was degassed and backfilled with argon for three times. Then, catalysts PdCl₂(PPh₃) (26 mg, 0.038 mmol, 0.20 equiv.) and CuI (18 mg, 0.094 mmol, 0.50 equiv.) were introduced. The reaction was carried out for 4 h at 50°C. The content of flask was

filtered through a fritted glass, washed with diethyl ether and concentrated. Residues were taken up into diethyl ether, washed with a 5% solution of HCl, distilled water, saturated solution of NaHCO₃ and brine. After drying over MgSO₄, filtration and concentration, the crude was purified on column chromatography (silica gel, PE/EtOAc: 90/10) to give 110 mg (79% yield) of product **68** as a yellow-orange oil.

Analyses:

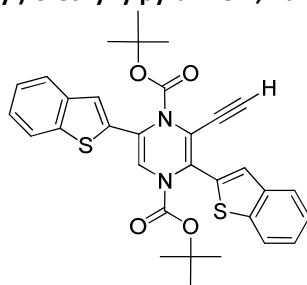
¹H NMR (400 MHz, CDCl₃) δ [ppm]: 7.85-7.75 (m, 2H), 7.43-7.30 (m, 3H), 1.41 (s, 9H), 0.29 (s, 9H).

¹³C NMR (63 MHz, CDCl₃) δ [ppm]: 150.61 (C=O), 140.37 (C^{IV}), 139.56 (C^{IV}), 139.37 (C^{IV}), 137.22 (C^{IV}), 136.75 (C^{IV}), 125.45 (CH_{ar}), 125.09 (CH_{ar}), 124.51 (CH_{ar}), 124.07 (CH_{ar}), 122.30 (CH_{ar}), 102.31 (C≡C), 99.15 (C≡C), 83.35 (C^{IV}), 28.12 (CH₃), -0.16 (TMS).

IR (neat, ATR) ν [cm⁻¹]: 3057 (CH sp²), 2978 (CH sp³), 2158 (C≡C), 1976 (C≡C), 1726 (C=O), 1299, 1141.

MS (ESI, m/z): 627.5 [M-2tBu]⁺, 683.5 [M-tBu]⁺, 739.5 [M]⁺, 761.5 [M+Na]⁺.

Di-tert-butyl 2,5-di(benzo[b]thiophen-2-yl)-3-ethynylpyrazine-1,4-dicarboxylate (69)



Orange oil

R_f : 0.29 (PE/EtOAc: 8/2) revelator CAN

Procedure:

To a solution of starting alkyne **67** (28 mg, 0.05 mmol, 1.00 equiv.) in an freshly distilled THF (3 mL) was added TBAF (0.09 mL, 0.09 mmol, 2.00 equiv.). The reaction was carried out for 3 days at room temperature. The reaction was stopped by dilution with EtOAc and hydrolysis with distilled water. Residues were extracted with EtOAc, washed with distilled water and brine. After drying over MgSO₄, filtration and concentration, the crude was purified on column chromatography (silica gel, PE/EtOAc: 9/1) to give 6.5 mg (25% yield) of product **69** as an orange oil.

Analyses:

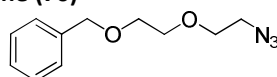
¹H NMR (250 MHz, CDCl₃) δ [ppm]: 7.79-7.69 (m, 4H), 7.63 (s, 1H), 7.38-7.29 (m, 5H), 7.14 (s, 1H), 3.10 (s, 1H), 1.38 (s, 9H), 1.22 (s, 9H).

¹³C NMR (63 MHz, CDCl₃) δ [ppm]: 151.7 (C=O), 149.7 (C=O), 139.9 (C^{IV}), 139.0 (C^{IV}), 138.6 (C^{IV}), 138.5 (C^{IV}), 137.2 (C^{IV}), 136.6 (C^{IV}), 135.6 (C^{IV}), 126.7 (CH_{ar}), 126.1 (C^{IV}), 125.3 (CH_{ar}), 124.8 (CH_{ar}), 124.7 (CH_{ar}), 124.3 (CH_{ar}), 123.7 (CH_{ar}), 122.4 (2xCH_{ar}), 121.6 (C≡C), 121.3 (CH_{ar}), 83.9 (C^{IV}), 83.2 (C^{IV}), 80.3 (C≡CH), 28.2 (3xCH₃), 27.8 (3xCH₃).

IR (neat, ATR) ν [cm⁻¹]: 3060 (CH sp²), 2978 (CH sp³), 2123 (C≡C), 1716 (C=O), 1298, 1140, 748.

MS (ESI, m/z): 459.0 [M-2tBu]⁺, 515.5 [M-tBu]⁺, 571.5 [M+H]⁺, 593.5 [M+Na]⁺.

[2-(2-Azido-ethoxy)-ethoxymethyl]-benzene (70)



Colorless oil

R_f = 0.19 (PE/ EtOAc: 8/2) revelator KMnO₄

Procedure:

The methylsulfonyl chloride (0.095 mL, 1.22 mmol, 1.20 equiv.), was slowly added to the solution of 2-(2-benzyloxy-ethoxy)-ethanol (200 mg, 1.02 mmol, 1.00 equiv.) with triethylamine (0.2 mL, 1.53 mmol, 1.50

equiv.) in anhydrous CH_2Cl_2 (10 mL) at 0 °C. The reaction was left for delicate warming up overnight, hydrolyzed, extracted twice with CH_2Cl_2 and washed with distilled water and brine. All organic phases were resembled, dried over MgSO_4 , filtered and concentrated. The crude was used directly for the next step. To the stirred solution of methanesulfonic acid 2-(2-benzyloxy-ethoxy)-ethyl ester (240 mg) in distilled DMF (10 mL), NaN_3 (99.5 mg, 1.53 mmol, 1.75 equiv.) was added. The reaction was carried out for 48 h at 80 °C. After cooling down to room temperature, the reaction mixture was diluted with CH_2Cl_2 and washed five times with distilled water and brine. The organic phase was dried over MgSO_4 , filtered and concentrated. The crude was purified by column chromatography (silica gel, PE/EtOAc: 9/1) to provide 118 mg of product **70** as a colorless oil (52% after 2 steps).

Analyses:

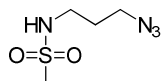
$^1\text{H NMR}$ (250 MHz, CDCl_3) δ [ppm]: 7.44-7.10 (m, 5H), 4.57 (s, 2H), 3.71-3.58 (m, 6H), 3.38 (t, $J = 5.1$, 2H).

$^{13}\text{C NMR}$ (63 MHz, CDCl_3) δ [ppm]: 138.31 (C^{IV}), 128.49 ($2\times\text{CH}_{\text{ar}}$), 127.83 ($2\times\text{CH}_{\text{ar}}$), 127.73 (CH_{ar}), 73.43 (CH_2), 70.86 (CH_2), 70.18 (CH_2), 69.62 (CH_2), 50.83 (CH_2).

IR (neat, ATR) ν [cm^{-1}]: 3031 (CH sp^2), 2860 (CH sp^3), 2097 (N=N), 1679, 1283, 1105, 2737, 698.

MS (ESI, m/z) 222.0 [$\text{M}+\text{H}$] $^+$, 244.0 [$\text{M}+\text{Na}$] $^+$.

N-(3-azidopropyl)methanesulfonamide (71)



Colorless oil

$R_f = 0.39$ (PE/EtOAc: 8/2) revelator KMnO_4

Procedure:

The methylsulfonyl chloride (0.62 mL, 7.99 mmol, 1.20 equiv.) was slowly added to the solution of 3-aminopropanol (500 mg, 6.66 mmol, 1.00 equiv.) with triethylamine (1.39 mL, 9.99 mmol, 1.50 equiv.) in anhydrous CH_2Cl_2 (25 mL) at 0 °C. The reaction was left for delicate warming up overnight and hydrolyzed, extracted twice with CH_2Cl_2 and washed with distilled water and brine. All organic phases were resembled, dried over MgSO_4 , filtered and concentrated. The crude was used directly for the next step.

To the stirred solution of methanesulfonic acid (500 mg) in distilled DMF (10 mL), NaN_3 (425 mg, 6.54 mmol, 2.00 equiv.) was added and the reaction was carried out for 18h at 80°C. After cooling down to room temperature, the reaction mixture was diluted with CH_2Cl_2 and washed five times with distilled water and brine. The organic phase was dried over MgSO_4 , filtered and concentrated. The crude was purified by column chromatography (silica gel, PE/EtOAc: 9/1) to give 240 mg of product **71** as a colorless oil (20% after 2 steps).

Analyses:

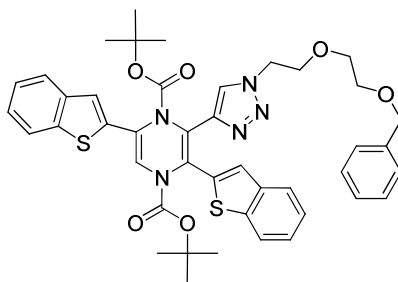
$^1\text{H NMR}$ (250 MHz, CDCl_3) δ [ppm]: 4.42 (s, 1H), 3.47 (t, $J = 6.3$ Hz, 2H), 3.26 (q, $J = 6.5$ Hz, 2H), 2.98 (s, 3H), 1.85 (quint, $J = 6.5$ Hz, 2H).

$^{13}\text{C NMR}$ (63 MHz, CDCl_3) δ [ppm]: 48.5 (CH_2), 40.5 (CH_2), 39.8 (CH_2), 29.2(CH_2).

IR (neat, ATR) ν [cm^{-1}]: 3291 (NHSO_2), 2935 (CH sp^2), 2873 (CH sp^3), 2095 (N=N), 1412, 1310.1, 1082, 974, 764.

MS (ESI, m/z) 179.0 [$\text{M}+\text{H}$] $^+$, 201.0 [$\text{M}+\text{Na}$] $^+$.

2,5-Bis-benzo[b]thiophen-2-yl-3-[1-[2-(2-benzyloxy-ethoxy)-ethyl]-1H-[1,2,3]triazol-4-yl]-pyrazine-1,4-dicarboxylic acid di-tert-butyl ester (72)



Yellow solid

R_f = 0.06 (PE/EtOAc: 8/2) revelator CAN

Procedure:

The solution of TMS alkyne **67** (37 mg, 0.057 mmol, 1.00 equiv.) and azide (13 mg, 0.057 mmol, 1.00 equiv.) was prepared in CH₂Cl₂ at room temperature and TBAF (1.0 M in THF, 0.23 mL, 0.23 mmol, 4.00 equiv.) was added dropwise. Parallel, the solution of CuSO₄·5H₂O (14 mg, 0.057 mmol, 1.00 equiv.) was prepared in distilled water (1 mL) and L-(+) sodium ascorbate was introduced (23 mg, 0.115 mmol, 2.00 equiv.). This solution was immediately added to the alkyne-azide solution and was vigorously stirred for 2h at room temperature. The reaction was stopped by dilution with CH₂Cl₂ and extracted with CH₂Cl₂. The organic phase was washed with distilled water and brine, dried over MgSO₄, filtered and evaporated. Purification by column chromatography (silica gel, PE/EtOAc: 95/5) gave 22 mg (53% yield) of product **72** as a yellow solid.

Analyses:

¹H NMR (400 MHz, CDCl₃) δ [ppm]: 7.77-7.69 (m, 5H), 7.68 (s, 1H), 7.54 (s, 1H), 7.36-7.21 (m, 10H), 4.43 (s, 4H), 3.77 (s, 2H), 3.38 (d, *J* = 4.8 Hz, 4H), 1.26 (s, 9H), 1.20 (s, 9H).

¹³C NMR (101 MHz, CDCl₃) δ [ppm]: 152.2 (C=O), 140.4 (C^{IV}), 140.1 (C^{IV}), 139.2 (C^{IV}), 139.1 (C^{IV}), 138.2 (C^{IV}), 135.8 (C^{IV}), 128.6 (CH_{ar}), 128.4 (CH_{ar}), 127.9 (CH_{ar}), 127.9 (CH_{ar}), 126.1 (C^{IV}), 125.2 (CH_{ar}), 124.7 (CH_{ar}), 124.6 (CH_{ar}), 124.3 (CH_{ar}), 124.1 (CH_{ar}), 123.8 (CH_{ar}), 122.4 (CH_{ar}), 122.3 (CH_{ar}), 121.5 (CH), 83.5 (C^{IV}), 82.4 (C^{IV}), 73.4 (CH₂), 70.8 (CH₂), 69.6 (CH₂), 69.4 (CH₂), 50.5 (CH₂), 28.1 (CH₃), 27.9 (CH₃).

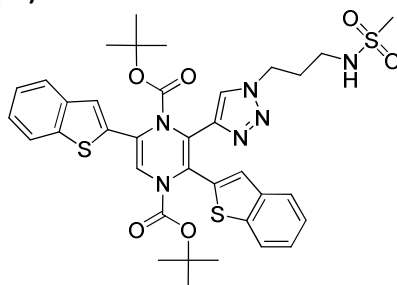
IR (neat, ATR) ν [cm⁻¹]: 3061 (CH sp²), 2971 (CH sp³), 2926, 2852, 1705 (C=O), 1311, 1132, 749.

MS (ESI, m/z): 792.5 [M+H]⁺, 814.5 [M+Na]⁺.

HRMS (ESI, m/z): [M]⁺ calculated for C₄₃H₄₆N₅O₆S₂: 792.2884, found: 792.2886; [M+Na]⁺ calculated for C₄₃H₄₆N₅NaO₆S₂: 814.2704, found: 814.2701.

Mp = 177°C.

2,5-Bis-benzo[b]thiophen-2-yl-3-[1-(3-methanesulfonylamino-propyl)-1H-[1,2,3]triazol-4-yl]-pyrazine-1,4-dicarboxylic acid di-tert-butyl ester (73)



Yellow oil

R_f : 0.30 (PE/EtOAc: 4/6) revelator CAN

Procedure:

The solution of TMS alkyne **67** (50 mg, 0.078 mmol, 1.00 equiv.) and azide (24 mg, 0.135 mmol, 1.70 equiv.) was prepared in CH₂Cl₂ at room temperature and TBAF (1.0 M in THF, 0.27 mL, 0.269 mmol, 3.50 equiv.) was added dropwise. Parallel, the solution of CuSO₄·5H₂O (34 mg, 0.1347 mmol, 1.70 equiv.) was prepared in distilled water (2 mL) and L-(+) sodium ascorbate (53 mg, 0.269 mmol, 3.50 equiv.) was introduced. This solution was immediately added to the alkyne-azide solution and was stirred vigorously for 18h at room temperature. The reaction was stopped by dilution with CH₂Cl₂, then extracted with CH₂Cl₂. The organic phase was washed with distilled water and brine, dried over MgSO₄, filtered and evaporated. Purification by column chromatography (silica gel, PE/EtOAc: 9/5) gave 26 mg (45% yield) of product **73** as a yellow solid.

Analyses:

¹H NMR (400 MHz, CDCl₃) δ [ppm]: 7.77 (dd, *J* = 19.7 and 10.2 Hz, 4H), 7.66 (d, *J* = 11.9 Hz, 2H), 7.51 (s, 1H), 7.31 (ddd, *J* = 17.4 and 14.5 Hz, 7.2, 5H), 4.79 (t, *J* = 6.3 Hz, 1H), 4.36 (t, *J* = 6.1 Hz, 2H), 2.99-2.90 (m, 2H), 2.80 (s, 3H), 2.04 (t, *J* = 5.8 Hz, 2H), 1.26 (s, 9H), 1.19 (s, 9H).

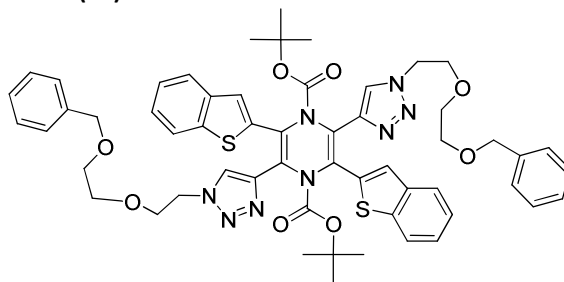
¹³C NMR (101 MHz, CDCl₃) δ [ppm]: 152.3 (C=O), 150.3 (C=O), 142.7 (C^{IV}), 140.4 (C^{IV}), 140.0 (C^{IV}), 139.2 (C^{IV}), 139.0 (C^{IV}), 137.5 (C^{IV}), 135.7 (C^{IV}), 128.4 (CH_{ar}), 125.9 (C^{IV}), 125.3 (CH_{ar}), 124.8 (CH_{ar}), 124.7 (CH_{ar}), 124.3 (CH_{ar}), 129.0 (CH_{ar}), 123.8 (CH_{ar}), 122.6 (CH_{ar}), 122.4 (CH_{ar}), 122.2 (CH_{ar}), 121.4 (CH_{ar}), 83.6 (C^{IV}), 82.6 (C^{IV}), 46.9 (CH₂), 40.1 (CH₃), 39.8 (CH₂), 30.7 (CH₂), 28.1 (CH₃), 27.8 (CH₃).

IR (neat, ATR) ν [cm⁻¹]: 3273 (NHSO₂), 3049 (CH sp²), 2977 (CH sp³), 2929, 1714 (C=O), 1359, 1144, 748.

MS (ESI, m/z): 749.0 [M+H]⁺, 771.5 [M+Na]⁺.

HRMS (ESI, m/z): [M+H]⁺ calculated for C₃₆H₄₁N₆O₆S₃: 749.2244, found: 749.2251; [M+Na]⁺ calculated for C₃₆H₄₀N₆NaO₆S₃: 771.2064, found: 771.2068.

2,5-Bis-benzo[b]thiophen-2-yl-3,6-bis-{1-[2-(2-benzyloxy-ethoxy)-ethyl]-1H-[1,2,3]triazol-4-yl]-pyrazine-1,4-dicarboxylic acid di-tert-butyl ester (**74**)



Yellow oil

R_f = 0.55 (PE/EtOAc: 4/6) revelator CAN

Procedure:

The solution of TMS alkyne **68** (61 mg, 0.083 mmol, 1.00 equiv.) and azide (37 mg, 0.165 mmol, 2.00 equiv.) was prepared in CH₂Cl₂ (1mL) at rt and TBAF (1.0 M in THF, 0.33 mL, 0.33 mmol, 4.00 equiv.) was added dropwise. Parallel, the solution of CuSO₄·5H₂O (21 mg, 0.083 mmol, 1.00 equiv.) was prepared in distilled water (2 mL) and L-(+) sodium ascorbate (33 mg, 0.165 mmol, 2.00 equiv.) was introduced, this solution was immediately added to the alkyne-azide solution and was stirred vigorously for 36h at room temperature. The reaction was stopped by dilution with CH₂Cl₂, then it was extracted with CH₂Cl₂. The organic phase was washed with distilled water and brine, dried over MgSO₄, filtered and evaporated. Purification by column chromatography (silica gel, PE/EtOAc: 6/4 then 5/5 then 4/6) gave 30 mg (35% yield) of product **74** a yellow oil.

Analyses:

¹H NMR (250 MHz, CDCl₃) δ [ppm]: 8.07 (d, *J* = 8.1 Hz, 2H), 7.81-7.65 (m, 2H), 7.35-7.17 (m, 7H), 4.57 (td, *J* = 4.5 and 1.8 Hz, 2H), 4.45 (s, 2H), 3.87 (t, *J* = 5.1 Hz, 2H), 3.62-3.41 (m, 4H), 1.18 (s, 9H).

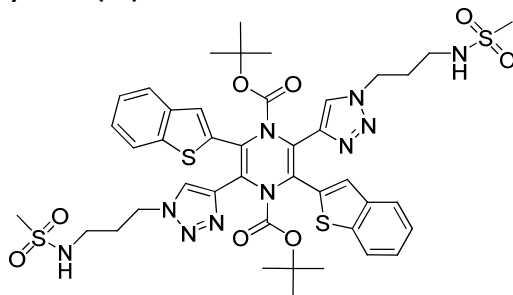
¹³C NMR (63 MHz, CDCl₃) δ [ppm]: 151.5 (C=O), 142.0 (C^{IV}), 140.2 (C^{IV}), 139.7 (C^{IV}), 138.2 (C^{IV}), 137.0 (C^{IV}), 130.9 (C^{IV}), 128.6 (2xCH_{ar}), 127.9 (2xCH_{ar}), 127.4 (CH_{ar}), 126.2 (CH_{ar}), 125.2 (CH_{ar}), 124.9 (CH_{ar}), 124.5 (CH_{ar}), 122.1 (CH_{ar}), 82.7 (C^{IV}), 73.4 (CH₂), 70.9 (CH₂), 69.8 (CH₂), 69.4 (CH₂), 50.7 (CH₂), 28.0 (CH₃).

IR (neat, ATR) ν [cm⁻¹]: 3055 (CH sp²), 2971 (CH sp³), 2926, 2864, 1718 (C=O), 1305, 1144, 745.

MS (ESI, m/z): 1037.5 [M+H]⁺, 1060.5 [M+Na]⁺.

HRMS (ESI, m/z): [M+H]⁺ calculated for C₅₆H₆₁N₈O₈S₂: 1037.4048, found: 1037.4053; [M+Na]⁺ calculated for C₅₆H₆₀N₈NaO₈S₂: 1059.3868, found: 1059.3869.

2,5-Bis-benzo[b]thiophen-2-yl-3,6-bis-[1-(3-methanesulfonylamino-propyl)-1H-[1,2,3]triazol-4-yl]-pyrazine-1,4-dicarboxylic acid di-*tert*-butyl ester (75)



Yellow solid

R_f = 0.18 (PE/EtOAc: 4/6) revelator CAN

Procedure:

The solution of TMS alkyne **68** (50 mg, 0.068 mmol, 1.00 equiv.) and azide (24 mg, 0.135 mmol, 2.00 equiv.) was prepared in CH₂Cl₂ at room temperature and TBAF (1.0 M in THF, 0.27 mL, 0.27 mmol, 4.00 equiv.) was added dropwise. Parallel, the solution of CuSO₄·5H₂O (17 mg, 0.068 mmol, 1.00 equiv.) was prepared in distilled water (2 mL) and L-(+) sodium ascorbate (27 mg, 0.135 mmol, 2.00 equiv.) was introduced. This solution was immediately added to the alkyne-azide solution and was stirred vigorously for 2h at rt. The reaction was stopped by dilution with CH₂Cl₂, then extracted with CH₂Cl₂. The organic phase was washed with distilled water and brine, dried over MgSO₄, filtered and evaporated. Purification by column chromatography (silica gel, PE/EtOAc: 5/5 then 4/6 then 0/10) provided 20 mg (30% yield) of product **75** as a yellow oil.

Analyses:

¹H NMR (400 MHz, CDCl₃) δ [ppm]: 7.99 (d, *J* = 2.8 Hz, 2H), 7.76 (dd, *J* = 19.0 and 7.5 Hz, 2H), 7.28 (dd, *J* = 12.7 and 5.2 Hz, 2H), 5.04 (s, 1H), 4.46 (s, 2H), 3.02 (s, 2H), 2.80 (d, *J* = 3.0 Hz, 3H), 2.11 (s, 2H), 1.17 (d, *J* = 2.8 Hz, 9H).

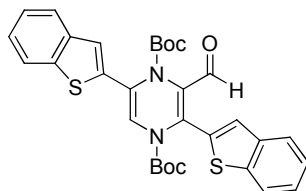
¹³C NMR (101 MHz, CDCl₃) δ [ppm]: 151.4 (C=O), 141.7 (C^{IV}), 139.9 (C^{IV}), 139.3 (C^{IV}), 136.5 (C^{IV}), 131.3 (C^{IV}), 127.1 (CH_{ar}), 125.3 (C^{IV}), 125.0 (2xCH_{ar}), 124.5 (CH_{ar}), 124.2 (CH_{ar}), 122.0 (CH_{ar}), 82.8 (C^{IV}), 47.0 (CH₂), 39.8 (CH₃), 39.7 (CH₂), 30.6 (CH₂), 27.7 (CH₃).

IR (neat, ATR) ν [cm⁻¹]: 3267 (NHSO₂), 2974 (CH sp³), 2929 (CH sp³), 1724 (C=O), 1305, 1144, 749.

HRMS (ESI, m/z): [M+H]⁺ calculated for C₄₂H₅₁N₁₀O₈S₄: 951.2769, found: 951.2781.

Mp = 170°C.

Di-*tert*-butyl 2,5-di(benzo[b]thiophen-2-yl)-3-formylpyrazine-1,4-dicarboxylate (76)



Red-orange glossy solid

R_f = 0.47 (PE/EtOAc: 8/2) CAN relevator

Procedure:

A solution of 1,4-dihydropyrazine derivative⁹ (1.00 g, 1.83 mmol, 1.00 equiv.) was prepared in distilled THF (40 mL) under argon and cooled down to -78 °C. Then, the solution of LDA (2 M in THF, 3.66 mL, 7.32 mmol, 4.00 equiv.) was introduced dropwise and mixture was stirred for 40 minutes at -78 °C. Subsequently, HMPA (0.64 mL, 3.66 mL, 2.00 equiv.) was introduced and the mixture was stirred for 10 min. In a second round bottomed

flask, under argon and with molecular sieves (4A), a solution of DMF (0.71 mL, 9.15 mmol, 5.00 equiv.) was prepared in distilled THF (4 mL) and introduced by cannula to the first flask over 5 min. The resulting mixture was stirred for 2h at -78 °C. Then reaction was hydrolyzed with a saturated solution of NH₄Cl, warmed up and extracted with EtOAc (2x50 mL). All organic phases were collected and washed with distilled water and brine, dried over MgSO₄, filtered and concentrated. The crude was purified by flash column chromatography (PE/EtOAc: 9/1 to 8/2) to isolate 900 mg (86% yield) of a red-orange oil **76** crystallized after stocking.

Analyses:

¹H NMR (250 MHz, DMSO-d₆) δ [ppm]: 9.52 (s, 1H), 8.07-8.00 (m, 1H), 7.99-7.96 (m, 3H), 7.88-7.85 (m, 1H), 7.54 (s, 1H), 7.51-7.47 (m, 2H), 7.38-7.36 (m, 3H), 1.31 (s, 9H), 1.14 (s, 9H).

¹³C NMR (101 MHz, DMSO-d₆) δ [ppm]: 184.7 (CHO), 148.6 (C=O), 145.0 (C=O), 182.5 (C^{IV}), 141.5 (C^{IV}), 139.0 (C^{IV}), 138.2 (C^{IV}), 137.8 (C^{IV}), 133.7 (C^{IV}), 131.5 (CH), 129.8 (CH_{ar}), 125.4 (C^{IV}), 124.9 (CH_{ar}), 124.8 (CH_{ar}), 123.8 (CH_{ar}), 123.7 (CH_{ar}), 122.6 (CH_{ar}), 122.4 (CH_{ar}), 121.5 (CH_{ar}), 84.5 (C^{IV}), 82.0 (C^{IV}), 27.5 (3xCH₃), 27.0 (3xCH₃).

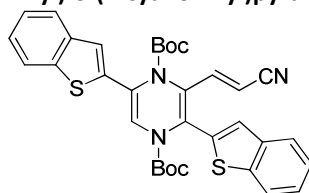
MS (ESI) [m/z]: 597.5 [M+Na]⁺.

HRMS (ESI) [m/z]: calculated for C₃₁H₃₀N₂O₅NaS₂: 597.1494, found: 597.1487.

IR (neat, ATR) ν [cm⁻¹]: 2977 (CH, sp³), 2925 (CH, sp²), 1722 (C=O), 1679, 1306, 1137, 747.

Mp = 113 °C.

(E)-Di-tert-butyl 2,5-di(benzo[b]thiophen-2-yl)-3-(2-cyanovinyl)pyrazine-1,4-dicarboxylate (**77**)



Orange foam

R_f = 0.43 (PE/EtOAc: 8/2) CAN relevator

Procedure:

A solution of sodium hydride (30 mg, 0.743 mmol, 1.10 equiv.) was prepared in distilled THF (5 mL) at 0 °C under argon and diethylcyanomethyl phosphonate (0.12 mL, 0.743 mmol, 1.10 equiv.) was introduced drop by drop. This mixture was stirred for 1h30 at 0 °C. Then, the solution of the aldehyde **76** (388 mg, 0.675 mmol, 1.00 equiv.) prepared in distilled THF (4 mL) was added dropwise *via* cannula and the reaction was left for slow warming up to room temperature for 6 h. The reaction was diluted with EtOAc, hydrolyzed with a saturated solution of NH₄Cl and extracted with EtOAc (2x30 mL). All organic phases were collected and washed with distilled water and brine, dried over MgSO₄, filtered and concentrated. The crude was purified by flash column chromatography (PE/EtOAc: 9/1 to 8/2) to isolate 370 mg (92% yield) of product **77** as an orange foam.

Analyses:

¹H NMR (250 MHz, DMSO-d₆) δ [ppm]: 8.07-7.98 (m, 4H), 7.81 (m, 1H), 7.78 (d, J = 4.8 Hz, 1H), 7.54 (s, 1H), 7.50-7.46 (m, 2H), 7.39 (m, 2H), 7.33 (s, 1H), 6.11 (d, J = 16.0 Hz, 1H), 1.34 (s, 9H), 1.10 (s, 9H).

¹³C NMR (101 MHz, DMSO-d₆) δ [ppm]: 152.0 (C=O), 148.8 (C=O), 142.3 (CH), 140.1 (C^{IV}), 139.6 (C^{IV}), 138.9 (C^{IV}), 138.0 (C^{IV}), 136.6 (C^{IV}), 136.2 (C^{IV}), 133.3 (C^{IV}), 128.4 (C^{IV}), 128.3 (CH_{ar}), 125.8 (C^{IV}), 125.6 (CH_{ar}), 125.0 (CH_{ar}), 124.7 (CH_{ar}), 124.6 (CH_{ar}), 124.1 (CH_{ar}), 123.6 (CH_{ar}), 122.4 (CH_{ar}), 122.3 (CH_{ar}), 121.8 (CH_{ar}), 121.7 (CH_{ar}), 99.5 (C^{IV}), 97.7 (CH), 84.0 (C^{IV}), 80.4 (C^{IV}), 28.2 (3xCH₃), 27.5 (3xCH₃).

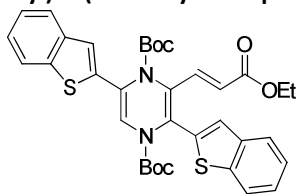
MS (ESI) [m/z]: 598.0 [M+H]⁺, 621.0 [M+Na]⁺.

HRMS (ESI) [m/z]: calculated for C₃₃H₃₁N₃O₄NaS₂ [M+Na]⁺: 620.1654, found: 620.1672.

IR (neat, ATR) ν [cm⁻¹]: 2976 (CH, sp³), 2929 (CH, sp²), 2213 (CN), 1722 (C=O), 1296, 1138, 843, 746.

Mp = 115 °C.

(E)-di-tert-butyl 2,5-di(benzo[b]thiophen-2-yl)-3-(3-ethoxy-3-oxoprop-1-enyl)pyrazine-1,4-dicarboxylate (78)



Orange foam

R_f = 0.5 (PE/EtOAc: 8/2) revelator CAN

Procedure:

A solution of sodium hydride (38 mg, 0.957 mmol, 1.10 equiv.) was prepared in distilled THF (10 mL) at 0 °C under argon and triethyl phosphonate (0.19 mL, 0.957 mmol, 1.10 equiv.) was introduced drop by drop. This mixture was stirred for 1h30 at 0 °C. Then, the solution of aldehyde **76** (500 mg, 0.870 mmol, 1.00 equiv.) prepared in distilled THF (6 mL) was added dropwise *via* cannula and the reaction was left for slow warming up to room temperature for 16 h. The reaction was diluted with EtOAc, hydrolyzed with a saturated solution of NH₄Cl and extracted with EtOAc (2x30 mL). All organic phases were collected and washed with distilled water and brine, dried over MgSO₄, filtered and concentrated. The crude was purified by flash column chromatography (PE/EtOAc: 9/1 to 8/2) to isolate 450 mg (80% yield) of product **78** as an orange foam.

Analyses:

¹H NMR (250 MHz, DMSO-d₆) δ [ppm]: 8.08 (m, 1H), 8.01 (m, 2H), 7.88 (m, 1H), 7.54 (s, 1H), 7.72 (s, 1H), 7.68 (s, 1H), 7.59 (s, 1H), 7.47 (m, 3H), 7.36 (m, 2H), 6.23 (d, *J* = 9.5 Hz, 1H), 4.14 (q, *J* = 4.5 Hz, 2H), 1.32 (s, 9H), 1.19 (t, *J* = 4.3 Hz), 1.16 (s, 9H).

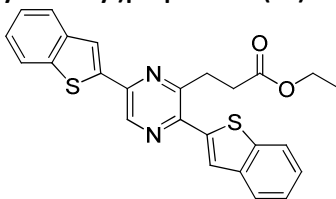
¹³C NMR (101 MHz, DMSO-d₆) δ [ppm]: 165.8 (C=O), 152.0 (C=O), 148.8 (C=O), 140.0 (C^{IV}), 139.6 (C^{IV}), 138.8 (C^{IV}), 136.9 (CH), 133.8 (C^{IV}), 127.8 (CH_{ar}), 125.8 (CH_{ar}), 125.1 (CH_{ar}), 124.9 (CH_{ar}), 124.8 (C^{IV}), 124.7 (CH_{ar}), 124.6 (C^{IV}), 124.5 (CH), 123.7 (CH), 122.5 (CH_{ar}), 122.3 (CH_{ar}), 122.0 (C^{IV}), 120.9 (CH_{ar}), 119.3 (CH_{ar}), 83.9 (C^{IV}), 82.2 (C^{IV}), 60.2 (CH₂), 27.4 (3xCH₃), 26.9 (3xCH₃), 14.1 (CH₃).

MS (ESI) [m/z]: 668.0 [M+Na]⁺.

HRMS (ESI) [m/z]: calculated for C₃₅H₃₆N₂O₆NaS₂ [M+Na]⁺: 667.1913, found: 667.1923.

IR (neat, ATR) ν [cm⁻¹]: 2977 (CH, sp³), 1716 (C=O), 1619, 1297, 1139, 844, 747.

Ethyl 3-(3,6-di(benzo[b]thiophen-2-yl)pyrazin-2-yl)propanoate (79)



Orange solid

R_f = 0.6 (PE/EtOAc: 6/4) revelator CAN

Procedure:

The solution of ester derivative **78** (280 mg, 0.434 mmol) was dissolved in dry CH₂Cl₂ (8 mL), then TMSI (0.296 mL, 2.083 mmol, 4.80 equiv.) was introduced dropwise. The solution was stirred at room temperature for 60 minutes. The mixture was then hydrolyzed with a saturated solution of NH₄Cl (20 mL) and stirred for 10 min. The solution was extracted twice with CH₂Cl₂. All organic phases were collected and washed with distilled water and brine, then dried over MgSO₄, filtered and concentrated under vacuum. The concentrated solution was precipitated with diethyl ether. The brown-beige solid was filtered through Milipore and washed twice with diethyl ether then n-pentane to isolate the product **79** (147 mg, 76% yield) as a orange solid.

Analyses:

¹H NMR (250 MHz, CDCl₃) δ [ppm]: 8.84 (s, 1H), 7.95 (s, 1H), 7.87 (m, 4H), 7.40 (m, 5H), 4.24 (q, *J* = 7.3 Hz, 2H), 3.60 (t, *J* = 6.8 Hz, 2H), 3.08 (t, *J* = 6.8 Hz, 2H), 1.31 (t, *J* = 7.0 Hz, 3H).

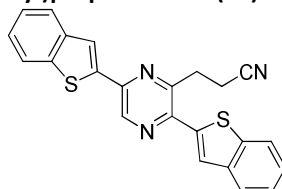
¹³C NMR (101 MHz, CDCl₃) δ [ppm]: 173.2 (C=O), 157.6 (C^{IV}), 147.6 (C^{IV}), 143.9 (C^{IV}), 143.3 (C^{IV}), 143.1 (C^{IV}), 142.3 (CH_{pyr}), 139.6 (2xC^{IV}), 138.6 (C^{IV}), 138.4 (C^{IV}), 125.0 (CH_{ar}), 124.4 (CH_{ar}), 124.3 (CH₂), 124.0 (CH_{ar}), 123.2 (2xCH_{ar}), 122.9 (2xCH_{ar}), 119.6 (CH_{ar}), 119.3 (CH_{ar}), 61.3 (CH₂), 34.2 (CH₂), 33.0 (CH₂), 14.1 (CH₃).

IR (ATR, neat) ν [cm⁻¹]: 3346, 3244, 2983 (CH sp²), 1725, 1646, 1413, 1081, 744.

MS (ESI, *m/z*) 445.1 [M+H]⁺, 467.1 [M+Na]⁺.

Mp = 200 °C

3-(3,6-di(benzo[b]thiophen-2-yl)pyrazin-2-yl)propanenitrile (80)



Beige solid

R_f = 0.8 (PE: EtOAc 6: 4) revelator CAN

Procedure:

The solution of nitrile derivative **77** (200 mg, 0.335 mmol) was dissolved in dry CH₂Cl₂ (8 mL), then TMSI (0.23 mL, 1.606 mmol, 4.80 equiv.) was introduced dropwise. The solution was stirred at room temperature for 90 minutes. The mixture was then hydrolyzed with a saturated solution of NH₄Cl (20 mL) and left to stir for 10 min. The solution was extracted twice with CH₂Cl₂. All organic phases were collected and washed with distilled water and brine, dried over MgSO₄, filtered and concentrated under vacuum. The concentrated solution was precipitated with diethyl ether. The brown-beige solid was filtered through Milipore and washed twice with diethyl ether then n-pentane to isolate the product **80** (130 mg, 99% yield) as a beige solid.

Analyses:

¹H NMR (250 MHz, CDCl₃) δ [ppm]: 9.00 (s, 1H), 7.98 (s, 1H), 7.91-7.88 (m, 4H), 7.45-7.40 (m, 5H), 3.64 (t, *J* = 7.5 Hz, 2H), 3.18 (t, *J* = 7.5 Hz, 2H).

¹³C NMR (101 MHz, DMSO-d₆) δ [ppm]: 157.5 (C^{IV}), 147.5 (C^{IV}), 144.0 (C^{IV}), 143.6 (C^{IV}), 143.4 (C^{IV}), 142.1 (CH_{pyr}), 140.9 (C^{IV}), 140.3 (C^{IV}), 139.6 (2xC^{IV}), 124.6 (2xCH_{ar}), 124.3 (2xCH_{ar}), 122.8 (CH_{ar}), 122.3 (CH_{ar}), 119.5 (2xCH_{ar}), 117.7 (CN), 28.7 (CH₂), 17.9 (CH₂).

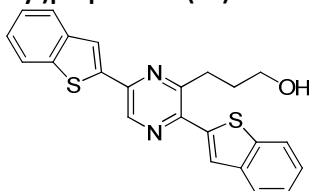
MS (ESI) [*m/z*]: 398.0 [M+H]⁺, 420.0 [M+Na]⁺.

HRMS (ESI) [*m/z*]: calculated for C₃₅H₃₆N₂O₆NaS₂ [M+Na]⁺: 667.1913, found: 667.1923.

IR (neat, ATR) ν [cm⁻¹]: = 3052 (CH, sp³), 2976, 2251, 1563, 1413, 1158, 953, 748.

Mp = 250 °C (decomposition)

3-(3,6-di(benzo[b]thiophen-2-yl)pyrazin-2-yl)propan-1-ol (82)



Yellow solid

R_f = 0.13 (PE/EtOAc: 8/2) revelator CAN

Procedure:

The solution of ester derivative **79** (100 mg, 0.225 mmol) was dissolved in dry THF (15 mL), then cooled down to 0 °C and LiAlH₄ (17 mg, 0.450 mmol, 2.00 equiv.) was introduced in one portion. The solution was stirred at 0 °C for 15 minutes and the mixture was diluted with EtOAc, hydrolyzed with a saturated solution of NH₄Cl (30 mL) and left to warm up. The solution was extracted with EtOAc three times. All organic phases were collected

and washed with distilled water and brine, dried over MgSO_4 , filtered and concentrated under vacuum. The product **82** (90 mg, 100% yield) was obtained as a yellow solid.

Analyses:

$^1\text{H NMR}$ (250 MHz, CDCl_3) δ [ppm]: 8.96 (s, 1H), 7.95 (s, 1H), 7.87 (m, 4H), 7.41 (m, 5H), 3.90 (t, $J = 6.3$ Hz, 2H), 3.43 (t, $J = 7.0$ Hz, 2H), 2.34 (qt, $J = 7.0$ Hz, 2H).

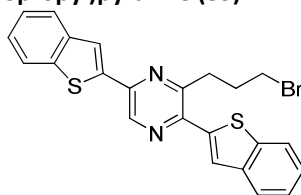
$^{13}\text{C NMR}$ (101 MHz, CDCl_3) δ [ppm]: 156.4 (C^{IV}), 148.6 (C^{IV}), 143.9 (C^{IV}), 143.7 (CH_{pyr}), 143.5 (C^{IV}), 143.3 (C^{IV}), 140.9 (C^{IV}), 140.7 (C^{IV}), 139.6 (C^{IV}), 139.3 (C^{IV}), 124.4 ($2\times\text{CH}_{\text{ar}}$), 124.2 ($2\times\text{CH}_{\text{ar}}$), 132.3 (CH_{ar}), 132.1 (CH_{ar}), 122.8 ($2\times\text{CH}_{\text{ar}}$), 119.5 (CH_{ar}), 119.1 (CH_{ar}), 62.4 (CH_2), 34.5 (CH_2), 31.1 (CH_2).

IR (ATR, neat) ν [cm^{-1}]: 3308 (large), 3055, 2926 (CH sp^2), 2852, 1563, 1411, 1333, 1156, 1048, 744, 724.

HRMS (ESI, m/z) [$\text{M}+\text{H}$] $^+$ calculate for $\text{C}_{23}\text{H}_{19}\text{N}_2\text{OS}_3$: 403.0939, found: 403.0921.

Mp = 185 °C.

2,5-di(benzo[b]thiophen-2-yl)-3-(3-bromopropyl)pyrazine (83)



Red solid

R_f = 0.8 (PE/EtOAc: 6/4) revelator CAN

Procedure:

The solution of alcohol derivative **82** (39 mg, 0.097 mmol) was dissolved in dry DMF (5 mL) under argon, then PPh_3 (89 mg, 0.340 mmol, 3.50 equiv.) and NBS (43 mg, 0.243 mmol, 2.50 equiv.) were introduced. The solution was stirred at 60 °C for 15 minutes. The mixture was cooled down and a red precipitate appeared. The content of the flask was filtered through Milipore, washed four times with Et_2O and dried under vacuum to isolate the product **83** (30 mg, 66% yield) as a red solid.

Analyses:

$^1\text{H NMR}$ (400 MHz, DMSO-d_6) δ [ppm]: 9.61 (s, 1H), 8.47 (s, 1H), 8.40 (s, 1H), 8.08 (m, 4H), 7.61 (m, 4H), 5.16 (t, $J = 8.0$ Hz, 2H), 4.00 (t, $J = 8.0$ Hz, 2H), 2.56 (qt, $J = 8.0$ Hz, 2H).

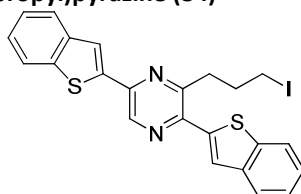
$^{13}\text{C NMR}$ (101 MHz, DMSO-d_6) δ [ppm]: 150.3 (CH_{pyr}), 150.0 (C^{IV}), 148.2 (C^{IV}), 141.6 (C^{IV}), 140.8 (C^{IV}), 140.7 (C^{IV}), 139.5 (C^{IV}), 139.3 (C^{IV}), 132.6 (CH_{ar}), 132.0 (CH_{ar}), 129.2 (C^{IV}), 129.2 (CH_{ar}), 129.1 (CH_{ar}), 128.2 (CH_{ar}), 127.9 (CH_{ar}), 126.4 (CH_{ar}), 126.3 (CH_{ar}), 126.0 (CH_{ar}), 123.3 (CH_{ar}), 122.8 (C^{IV}), 67.8 (CH_2), 12.8 (CH_2), -14.6 (CH_2).

HRMS (ESI) [m/z]: [$\text{M}-\text{Br}+\text{H}$] $^+$ calculated for $\text{C}_{23}\text{H}_{17}\text{N}_2\text{S}_2$: 385.0833, found: 385.0833.

IR (ATR, neat) ν [cm^{-1}]: 3056 (CH sp^3), 2950, 1516, 1371, 1156, 831, 751, 725.

Mp > 260 °C.

2,5-di(benzo[b]thiophen-2-yl)-3-(3-iodopropyl)pyrazine (84)



Dark red solid

R_f = 0.9 (PE/EtOAc: 6/4) revelator CAN

Procedure:

The solution of alcohol derivative **82** (100 mg, 0.248 mmol) was dissolved in distilled toluene (9 mL) under argon, then PPh₃ (85 mg, 0.322 mmol, 1.30 equiv.) and imidazole (51 mg, 0.744 mmol, 3.00 equiv.) were introduced. The solution was stirred at room temperature for 5 minutes and then, I₂ (82 mg, 0.322 mmol, 1.30 equiv.) was added. The mixture was stirred for 30 minutes at 60 °C. After cooling down, a dark red solid appeared. The content of flask was evaporated to reduce the volume of solvent to 2 mL and Et₂O was added to precipitate product with PPh₃O. The crude was purified by column chromatography (PE/EtOAc: 6/4) to isolate the product **84** (85 mg, 67% yield) as a dark red solid.

Analyses:

¹H NMR (250 MHz, DMSO-d₆) δ [ppm]: 9.62 (s, 1H), 8.49 (s, 1H), 8.42 (s, 1H), 8.14 (m, 4H), 7.61 (m, 4H), 5.16 (t, *J* = 7.5 Hz, 2H), 4.02 (t, *J* = 7.6 Hz, 2H), 2.62 (qt, *J* = 7.5 Hz, 2H).

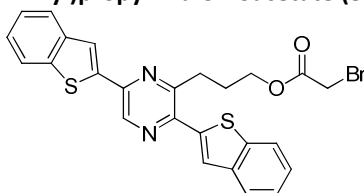
¹³C NMR (101 MHz, DMSO-d₆) δ [ppm]: 149.5 (C^{IV}), 147.4 (C^{IV}), 146.8 (CH_{pyr}), 140.5 (C^{IV}), 140.3 (C^{IV}), 140.2 (C^{IV}), 138.9 (C^{IV}), 138.8 (C^{IV}), 137.3 (C^{IV}), 132.1 (CH_{ar}), 128.8 (CH_{ar}), 129.2 (C^{IV}), 127.2 (CH_{ar}), 127.0 (CH_{ar}), 125.9 (2xCH_{ar}), 125.8 (CH_{ar}), 125.5 (CH_{ar}), 122.8 (CH_{ar}), 122.7 (2xCH_{ar}), 60.5 (CH₂), 33.4 (CH₂), 20.6 (CH₂).

MS (ESI) [m/z] [M-I]⁺: 385.0, [M-I+NH₄]⁺: 401.0.

IR (ATR, neat) ν [cm⁻¹]: 3056 (CH sp³), 2866 (CH sp²), 1515, 1440, 1124, 828, 751.

Mp > 260 °C.

3-(3,6-di(benzo[b]thiophen-2-yl)pyrazin-2-yl)propyl 2-bromoacetate (85)



Orange solid

R_f = 0.44 (PE/EtOAc: 6/4) revelator CAN

Procedure:

The solution of alcohol **82** (90 mg, 0.224 mmol) was dissolved in distilled CH₂Cl₂ (7 mL) under argon and cooled down to 0 °C, then Et₃N (30 μL, 0.224 mmol, 1.00 equiv.) was introduced. In the second flask, the solution of bromoacetic bromide (20 μL, 0.224 mmol, 1.00 equiv.) was prepared in 5 mL of CH₂Cl₂ and added to the first solution dropwise *via* cannula. The solution was stirred at 0 °C for 30 minutes and left to warm up slowly. The mixture was hydrolyzed with 20 mL of a saturated solution of NH₄Cl. The solution was extracted twice with CH₂Cl₂. All organic phases were collected, washed with distilled water and brine, then dried over MgSO₄, filtered and concentrated under vacuum. The crude was purified by flash column chromatography (PE/EtOAc: 9/1 to 8/2) to isolate the product **85** (92 mg, 79% yield) as an orange solid.

Analyses:

¹H NMR (400 MHz, CDCl₃) δ [ppm]: 8.95 (s, 1H), 7.95 (s, 1H), 7.86 (m, 4H), 7.78 (s, 1H), 7.40 (m, 4H), 4.45 (t, *J* = 4.0 Hz, 2H), 3.84 (s, 2H), 3.35 (t, *J* = 8.0 Hz, 2H), 2.43 (qt, *J* = 8.0 Hz, 2H).

¹³C NMR (101 MHz, CDCl₃) δ [ppm]: 167.5 (C=O), 151.8 (C^{IV}), 145.4 (C^{IV}), 145.3 (C^{IV}), 142.5 (C^{IV}), 142.0 (C^{IV}), 141.7 (C^{IV}), 141.6 (C^{IV}), 140.9 (C^{IV}), 140.6 (C^{IV}), 137.5 (CH_{pyr}), 125.9 (CH_{ar}), 125.8 (CH_{ar}), 125.0 (CH_{ar}), 124.9 (CH_{ar}), 124.8 (CH_{ar}), 124.7 (CH_{ar}), 124.7 (CH_{ar}), 122.8 (CH_{ar}), 122.5 (CH_{ar}), 122.4 (CH_{ar}), 66.1 (CH₂), 32.0 (CH₂), 26.1 (CH₂), 26.0 (CH₂).

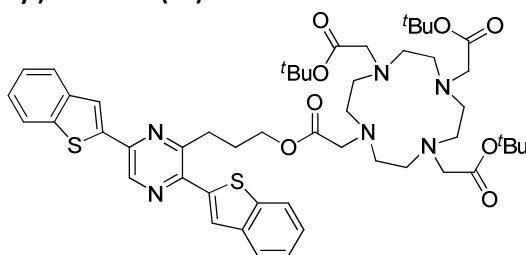
MS (ESI) [m/z]: [M+H]⁺ 523.0.

HRMS (ESI) [m/z]: [M+Na]⁺ calculated for C₂₅H₁₉⁷⁹BrN₂NaO₂S₂: 544.9969, found: 544.9970; [M+K]⁺ calculated for C₂₅H₁₉⁷⁹BrKN₂O₂S₂: 560.9708, found: 560.9725.

IR (ATR, neat) ν [cm⁻¹]: 3056 (CH sp³), 2921, 2848, 1729 (C=O), 1413, 1278, 1164, 951, 748, 726.

Mp = 177 °C.

tert-butyl 2,2',2''-(10-(2-(3-(3,6-di(benzo[b]thiophen-2-yl)pyrazin-2-yl)propoxy)-2-oxoethyl)-1,4,7,10-tetraazacyclododecane-1,4,7-triyl)triacetate (86)



Yellow-brown solid

R_f = 0.38 (CH₂Cl₂/MeOH: 8/2) revelator CAN

Procedure:

The solution of bromide derivative **85** (65 mg, 0.130 mmol) was dissolved in distilled THF (5 mL) under argon. Parallel, the solution of cyclen DO3A (80 mg, 0.156 mmol, 1.20 equiv.) with Na₂CO₃ (32 mg, 0.390 mmol, 3.00 equiv.) in 5 mL of distilled THF was stirred at room temperature for 30 minutes in a flask equipped with a CaCl₂ trap. The solution of bromide derivative was added dropwise to the second flask and the reaction was refluxed for 20h. After cooling down, the content of flask was filtered through glass frit to remove solids and the solvent from filtrate was evaporated to obtain the crude product. After purification by column chromatography (CH₂Cl₂/MeOH: 9/1), the product **86** (90 mg, 73% yield) was obtained as a yellow-brown solid.

Analyses:

¹H NMR (250 MHz, CDCl₃) δ [ppm]: 8.97 (s, 1H), 7.96 (s, 1H), 7.85 (m, 4H), 7.77(s, 1H), 7.41 (m, 4H), 4.31 (m br, 2H), 3.71 (qt, *J* = 5.0 Hz, 2H), 3.33 (m br, 14 H), 2.36 (m br, 12H), 1.45 (s, 27 H).

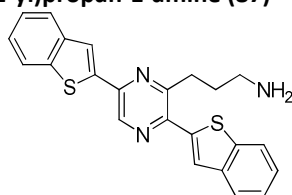
¹³C NMR (61 MHz, CDCl₃) δ [ppm]: 173.6 (C=O), 173.0 (C=O), 172.9 (C=O), 151.7 (C^{IV}), 145.4 (C^{IV}), 145.2 (C^{IV}), 142.5 (C^{IV}), 142.0 (C^{IV}), 141.7 (C^{IV}), 141.6 (C^{IV}), 140.3 (C^{IV}), 137.3 (CH_{pyr}), 125.7 (CH_{ar}), 124.9 (CH_{ar}), 124.8 (CH_{ar}), 124.6 (CH_{ar}), 124.5 (CH_{ar}), 124.4 (2xCH_{ar}), 122.3 (CH_{ar}), 122.3 (CH_{ar}), 122.2 (CH_{ar}), 81.8 (C^{IV}), 64.6 (CH₂), 55.7 (CH₂), 54.8 (CH₂), 52.4 (CH₂), 48.5 (CH₂), 31.3 (CH₂), 27.9 (CH₃), 26.1 (CH₂).

MS (ESI) [*m/z*] [M+Na]⁺ 979.5.

IR (ATR, neat) ν [cm⁻¹]: 2978 (CH sp³), 2827 (CH sp²), 1722 (C=O), 1450, 1367, 1227, 1157, 1105, 753.

Mp = 96 °C.

3-(3,6-di(benzo[b]thiophen-2-yl)pyrazin-2-yl)propan-1-amine (87)



Red glossy solid

R_f = 0.38 (PE/EtOAc: 6/4) revelator CAN

Procedure:

The solution of nitrile derivatives **80** and **81** (130 mg, 0.329 mmol) was dissolved in dry THF (10 mL) under argon, then LiAlH₄ (25 mg, 0.658 mmol, 2.00 equiv.) was introduced in one portion. The solution was stirred at room temperature for 16 hours. The mixture was quenched by addition of 250 μL of a 5% solution of NaOH and let stirring for an hour. Solid residues were separated by filtration on the glass frit, washed three times with THF. After evaporation and drying, the product **87** (100 mg, 76% yield) as a red glossy solid was obtained.

Analyses:

¹H NMR (400 MHz, DMSO-d₆ δ[ppm]: 9.32 (s, 1H), 8.39 (s, 1H), 8.17 (s, 1H), 8.07-7.91 (m, 5H), 7.52-7.39 (m, 5H), 7.25 (s, 1H), 3.38 (s, 3H), 3.10 (t, *J* = 7.2, 2H), 2.37-2.11 (m, 2H).

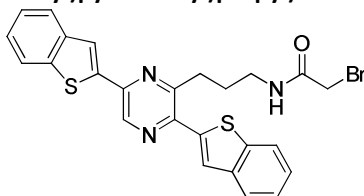
¹³C NMR (101 MHz, DMSO-d₆) δ[ppm]: 154.5 (C^{IV}), 148.6, (C^{IV}), 143.9 (C^{IV}), 143.8 (CH_{pyr}), 143.7 (C^{IV}), 143.0 (C^{IV}), 139.8 (C^{IV}), 136.8 (C^{IV}), 132.0 (C^{IV}), 129.7 (C^{IV}), 127.0 (2xCH_{ar}), 125.9 (CH_{ar}), 124.9 (2xCH_{ar}), 122.8 (CH_{ar}), 122.3 (CH_{ar}), 122.0 (CH_{ar}), 119.8 (CH_{ar}), 118.0 (CH_{ar}), 39.9 (CH₂), 39.7 (CH₂), 38.6 (CH₂).

HRMS (ESI) [m/z]: calculated for C₂₃H₂₀N₃S₂ [M+H]⁺: 402.1099, found: 402.1097.

IR (ATR, neat) ν [cm⁻¹]: 3440, 3242, 3195, 2922 (CH sp²), 1714, 1634, 1077, 800, 748.

Mp = 145 °C.

2-bromo-N-(3-(3,6-di(benzo[b]thiophen-2-yl)pyrazin-2-yl)propyl)acetamide (88)



Orange solid

R_f = 0.29 (CH₂Cl₂/MeOH: 95/5) revelator CAN

Procedure:

The solution of amine derivative **87** (40 mg, 0.099 mmol) was dissolved in dry CH₂Cl₂ (5 mL) under argon and cooled down to 0 °C, then Et₃N (10 μL, 0.099 mmol, 1.0 equiv.) was introduced. In the second flask, the solution of bromoacetic bromide (9 μL, 0.099 mmol, 1.00 equiv.) in 2 mL of CH₂Cl₂ was prepared and added to the first solution dropwise *via* cannula. The solution was stirred at 0 °C for 60 min. and then left to warm up slowly. The mixture was hydrolyzed with 5 mL of distilled water. The solution was extracted with CH₂Cl₂ three times. All organic phases were collected, washed with distilled water and brine, then dried over MgSO₄, filtered and concentrated under vacuum. The crude was purified by flash column chromatography (CH₂Cl₂ to CH₂Cl₂/MeOH: 95/5) to isolate the product **88** (39 mg, 75% yield) as an orange solid.

Analyses:

¹H NMR (400 MHz, CDCl₃) δ [ppm]: 8.96 (s, 1H), 7.95 (s, 1H), 7.84 (m, 4H), 7.71 (s, 1H), 7.38 (m, 4H), 6.83 (s br, NH), 3.88 (s, 2H), 3.50 (q, *J* = 6.0 Hz, 2H), 3.33 (t, *J* = 11.3 Hz, 2H), 2.31 (qt, *J* = 11.1 Hz, 2H).

¹³C NMR (101 MHz, CDCl₃) δ [ppm]: 182.7 (C=O), 155.2 (CH_{pyr}), 148.6 (C^{IV}), 143.9 (C^{IV}), 143.4 (2xC^{IV}), 140.7 (2xC^{IV}), 139.8 (C^{IV}), 139.6 (C^{IV}), 138.5 (C^{IV}), 127.7 (CH_{ar}), 125.9 (CH_{ar}), 125.8 (CH_{ar}), 125.1 (CH_{ar}), 124.9 (CH_{ar}), 124.8 (CH_{ar}), 124.7 (CH_{ar}), 122.8 (CH_{ar}), 122.6 (CH_{ar}), 122.4 (CH_{ar}), 45.2 (CH₂), 39.9 (CH₂), 29.9 (CH₂), 29.5 (CH₂).

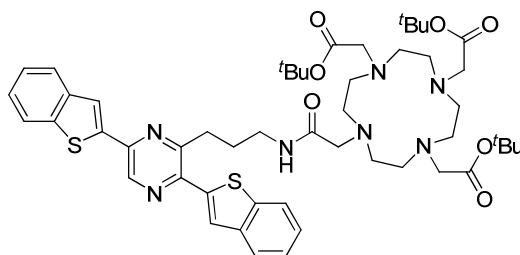
MS (ESI) [m/z]: [M+H]⁺ 524.0

HRMS (ESI) [m/z]: calculated for C₂₅H₂₁BrN₃OS₂: 522.0304, found: 522.0302.

IR (ATR, neat) ν [cm⁻¹]: 3285 (NHCO), 3056 (CH sp³), 2917, 2848, 1728 (C=O), 1646, 1528, 1156, 744, 724.

Mp = 185 °C.

tert-butyl 2,2',2''-(10-(2-(3-(3,6-di(benzo[b]thiophen-2-yl)pyrazin-2-yl)propylamino)-2-oxoethyl)-1,4,7,10-tetraazacyclododecane-1,4,7-triyl)triacetate (89)



Yellow-brown solid

R_f = 0.38 (CH₂Cl₂/MeOH: 8/2) revelator CAN

Procedure:

The solution of bromide derivative **88** (51 mg, 0.098mmol) was dissolved in distilled THF (8 mL) under argon. Parallel, the solution of cyclen DO3A (55 mg, 0.107 mmol, 1.10 equiv.) with Na₂CO₃ (31 mg, 0.293 mmol, 3.00 equiv.) in 8 mL of distilled THF was stirred at room temperature for 30 minutes in a flask equipped with a CaCl₂ trap. The solution of bromide derivative was added dropwise to the second flask and the reaction was refluxed for 20h. After cooling down, the content of flask was filtered through glass frit to remove solids and the solvent from filtrate was evaporated to obtain the crude product. After purification by column chromatography (CH₂Cl₂/MeOH: 9/1), the product **89** (90 mg, 73% yield) was obtained as a yellow-brown solid.

Analyses:

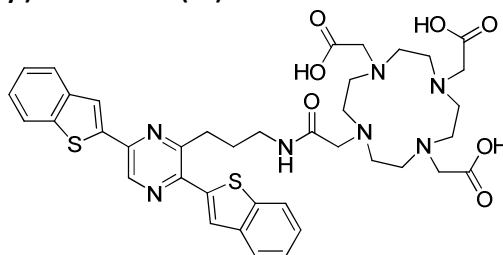
¹H NMR (250 MHz, CDCl₃) δ [ppm]: 8.87 (s, 1H), 8.27 (s, 1H), 7.85 (s, 1H), 7.81 (m, 4H), 7.35 (m, 4H), 3.51 (m br, 2H), 3.41 (m br, 2H), 2.27 (m br, 20H), 1.80 (m br, 4H), 1.44 (s, 27 H).

¹³C NMR (101 MHz, CDCl₃) δ [ppm]: 209.9 (C=O), 182.4 (C=O), 172.3 (C=O), 171.7 (C^{IV}), 170.5 (C^{IV}), 169.6 (C^{IV}), 153.1 (C^{IV}), 144.6 (C^{IV}), 144.4 (C^{IV}), 141.2 (C^{IV}), 140.9 (C^{IV}), 140.4 (C^{IV}), 140.3 (C^{IV}), 136.6 (CH_{pyr}), 128.0 (CH_{ar}), 125.3 (2xCH_{ar}), 124.6 (CH_{ar}), 124.4 (CH_{ar}), 124.3 (CH_{ar}), 122.4 (CH_{ar}), 121.8 (CH_{ar}), 121.6 (CH_{ar}), 81.7 (C^{IV}), 58.1 (CH₂), 56.3 (CH₂), 55.7 (CH₂), 52.4 (CH₂), 49.2 (CH₂), 45.0 (CH₂), 39.0 (CH₂), 33.7 (CH₂), 29.5 (CH₂), 28.2 (CH₃), 27.5 (CH₂).

HRMS (ESI) [m/z] [M+H]⁺ calculated for C₅₁H₇₀N₇O₇S₂: 956.4773, found: 956.4783.

IR (ATR, neat) ν [cm⁻¹]: 3056 (CH sp³), 2866 (CH sp²), 1731, 1516, 1340, 1124, 828, 750.

2,2',2''-(10-(2-(3-(3,6-di(benzo[b]thiophen-2-yl)pyrazin-2-yl)propylamino)-2-oxoethyl)-1,4,7,10-tetraazacyclododecane-1,4,7-triyl)triacetic acid (90)



Yellow-brown solid

R_f = 0.30 (CH₂Cl₂/MeOH: 8/2) revelator CAN

Procedure:

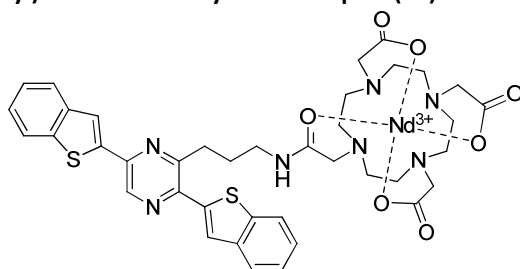
A 2% vol. solution of triisopropyl silane (TIS) was prepared in TFA (10 μL in 0.5 mL of TFA). The solution of ester **89** (34 mg, 0.035 mmol) was prepared in 0.5 mL of CH₂Cl₂ at room temperature. The solution of TFA/TIS was introduced dropwise to the solution of ester **89** and stirred overnight under argon. All solvents were evaporated and recovered solid was precipitated in Et₂O, filtered through Milipore and washed 3 times with Et₂O. 29 mg of product **90** as a yellow-brown solid (94% yield) were recuperated.

Analyses:

¹H NMR (250 MHz, DMSO-d₆) δ [ppm]: 9.28 (s, 1H), 8.39 (s, 1H), 8.02 (m, 4H), 7.44 (m, 5H), 3.42 (s, 2H), 3.03 (m, 6H), 2.74 (m br, 16H), 2.08 (s br, 6H).

HRMS (ESI) [m/z] [M+H]⁺ calculated for C₃₉H₄₅N₇O₇S₂: 779.2662, found: 779.2659.

2,2',2''-(10-(2-(3-(3,6-di(benzo[b]thiophen-2-yl)pyrazin-2-yl)propylamino)-2-oxoethyl)-1,4,7,10-tetraazacyclododecane-1,4,7-triyl)triacetate neodymium complex (91)



Yellow-brown solid

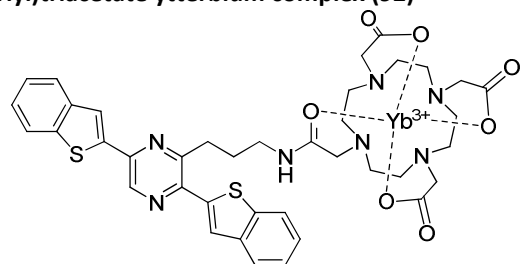
Procedure:

A solution of tricetic acid **90** (10 mg, 12.69 μmol , 1.00 equiv.) was prepared in MeOH (2 mL) and Nd(OTf)₃ (7.5 mg, 12.69 μmol , 1.00 equiv.) was added. The mixture was heated at 50 °C for 18h. The volume solvent was reduced under vacuum to 0.5 mL and the solid was precipitated by addition of Et₂O (2 mL), filtered through Milipore and washed three times with Et₂O. 9.9 mg (85% yield) of yellow-brown solid was obtained.

Analyses:

HRMS (ESI) [m/z] [M+H]⁺ calculated for C₃₉H₄₅N₇Nd O₇S₂: 926.1664, found: 926.1675.

2,2',2''-(10-(2-(3-(3,6-di(benzo[b]thiophen-2-yl)pyrazin-2-yl)propylamino)-2-oxoethyl)-1,4,7,10-tetraazacyclododecane-1,4,7-triyl)triacetate ytterbium complex (92)



Yellow-brown solid

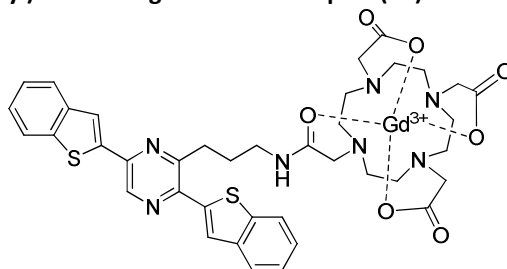
Procedure:

A solution of tricetic acid **90** (10 mg, 12.69 μmol , 1.00 equiv.) was prepared in MeOH (2 mL) and Yb(OTf)₃ (7.9 mg, 12.69 μmol , 1.00 equiv.) was added. The mixture was heated at 50 °C for 18h. The volume solvent was reduced under vacuum to 0.5 mL and the solid was precipitated by addition of Et₂O (2 mL), filtered through Milipore and washed three times with Et₂O. 10 mg (82% yield) of product **92** as a yellow-brown solid was obtained.

Analyses:

HRMS (ESI) [m/z] [M+H]⁺ calculated for C₃₉H₄₅N₇O₇S₂Yb: 961.2210, found: 961.2205.

2,2',2''-(10-(2-(3-(3,6-di(benzo[b]thiophen-2-yl)pyrazin-2-yl)propylamino)-2-oxoethyl)-1,4,7,10-tetraazacyclododecane-1,4,7-triyl)triacetate gadolinium complex (93)



Yellow-brown solid

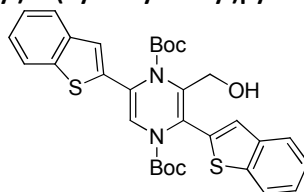
Procedure:

A solution of tricetic acid **90** (6 mg, 7.61 μmol , 1.00 equiv.) was prepared in MeOH (2 mL) and Gd(OTf)₃ (4.6 mg, 7.61 μmol , 1.00 equiv.) was added. The mixture was heated at 50 °C for 16h. The volume solvent was reduced under vacuum to 0.5 mL and the solid was precipitated by addition of Et₂O (2 mL), filtered through Milipore and washed three times with Et₂O. 6 mg (83% yield) of yellow-brown solid **93** was obtained.

Analyses:

HRMS (ESI) [m/z] [M+H]⁺ calculated for C₃₉H₄₅Gd N₇O₇S₂: 945.2055, found: 945.2063.

Di-tert-butyl 2,5-di(benzo[b]thiophen-2-yl)-3-(hydroxymethyl)pyrazine-1,4-dicarboxylate (94)



Yellow solid

R_f = 0.53 (PE/EtOAc: 8/2) CAN relevator

Procedure:

A solution of aldehyde **76** (100 mg, 0.17 mmol, 1.00 equiv.) was prepared in distilled THF (4 mL) under argon and cooled down to 0 °C. Then, LiAlH₄ (6 mg, 0.17 mmol, 1.00 equiv.) was introduced and reaction was stirred for 30 min. at 0 °C. The reaction was hydrolyzed slowly with saturated solution of NH₄Cl, warmed up and extracted with EtOAc (2x10 mL). All organic phases were collected and washed with distilled water and brine, dried over MgSO₄, filtered and concentrated. This reaction does not require further purification because there is no byproduct. After evaporation of solvents, 100 mg (quantitative) of product **94** as a yellow solid was obtained.

Analyses:

¹H NMR (400 MHz, CDCl₃) δ [ppm]: 7.80 (m, 5H), 7.71 (d, *J* = 4.0Hz, 1H), 7.34 (m, 4H), 7.10 (s, 1H), 4.88 (s br, 1H), 4.28 (s br, 2H), 1.26 (s, 9H), 1.19 (s br, 9H).

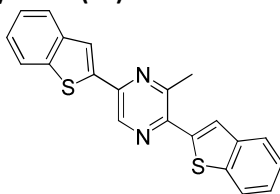
¹³C NMR (101 MHz, CDCl₃) δ [ppm]: 153.8 (C=O), 140.2 (C^{IV}), 139.8 (C^{IV}), 139.7 (C^{IV}), 139.0 (C^{IV}), 138.1 (C^{IV}), 131.4 (C^{IV}), 126.5 (CH_{ar}), 125.0 (C^{IV}), 124.9 (CH_{ar}), 124.8 (CH_{ar}), 124.6 (CH_{ar}), 123.6 (2xCH_{ar}), 122.5 (CH_{ar}), 122.4 (CH_{ar}), 121.9 (2xCH_{ar}), 121.8 (CH), 120.7 (CH_{ar}), 83.8 (C^{IV}), 83.7 (C^{IV}), 62.1 (CH₂), 28.1 (3xCH₃), 27.9 (3xCH₃).

MS (ESI) [m/z]: 599.0 [M+Na]⁺, 615.0 [M+K]⁺.

IR (neat, ATR) ν [cm⁻¹]: 3497 (OH), 2978 (CH, sp³), 1684 (C=O), 1325, 1141, 848, 748.

Mp = 135 °C.

2,5-Di(benzo[b]thiophen-2-yl)-3-methylpyrazine (95)



Beige solid

$R_f = 0.66$ (PE/EtOAc: 8/2) CAN relevator

Procedure:

A solution of the alcohol **94** (50 mg, 0.087 mmol, 1.00 equiv.) was prepared in distilled CH_2Cl_2 (2 mL) under argon and cooled down to 0 °C. Then, TMSI (0.06 mL, 0.416 mmol, 4.80 equiv.) was introduced and reaction was stirred for 15 minutes at 0 °C. The reaction was slowly hydrolyzed with a saturated solution of NaHCO_3 , warmed up and extracted with CH_2Cl_2 (3x10 mL). All organic phases were collected, washed with distilled water, saturated solution of $\text{Na}_2\text{S}_2\text{O}_3$ and brine, dried over MgSO_4 , filtered and concentrated. Residues were precipitated with diethyl ether to obtain 28 mg (90% yield) of product **95** as a beige solid.

Analyses:

$^1\text{H NMR}$ (400 MHz, CDCl_3) δ [ppm]: 8.93 (s, 1H), 7.94 (s, 1H), 7.83 (m, 4H), 7.81 (s, 1H), 7.38 (m, 4H), 2.98 (s, 3H).

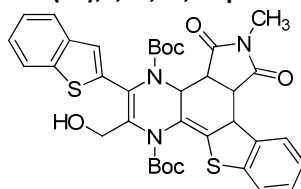
$^{13}\text{C NMR}$ (101 MHz, CDCl_3) δ [ppm]: 150.0 (C^{IV}), 146.2 (C^{IV}), 146.1 (C^{IV}), 142.2 (C^{IV}), 141.6 (C^{IV}), 140.8 (C^{IV}), 140.6 (C^{IV}), 137.6 (CH_{ar}), 125.7 (CH_{ar}), 125.0 (CH_{ar}), 124.8 (CH_{ar}), 124.7 (CH_{ar}), 124.7 (CH_{ar}), 124.6 (CH_{ar}), 122.8 (CH_{ar}), 122.4 (CH_{ar}), 25.1 (CH_3).

MS (ESI) [m/z]: 359.0 [$\text{M}+\text{H}$] $^+$.

IR (neat, ATR) ν [cm^{-1}]: 3053 (CH, sp^2), 2920 (CH, sp^3), 2867, 1702 (C=O), 1458, 1307, 1151, 945, 820, 748.

Mp = 205 °C.

8,11-di-tert-butyl 9-(1-benzothiophen-2-yl)-10-(hydroxymethyl)-4-methyl-3,5-dioxo-14-thia-4,8,11-triazapentacyclo[11.7.0.0^{2,6}.0^{7,12}.0^{15,20}]icosa-1(13),9,15,17,19-pentaene-8,11-dicarboxylate (96)



Orange oil

$R_f = 0.20$ (PE/EtOAc: 8/2) revelator CAN

Procedure:

A solution of the alcohol **94** (50 mg, 0.087 mmol, 1.00 equiv.) and N-methylmaleimide (48 mg, 0.434 mmol, 5.00 equiv.) in distilled toluene (2 mL, c = 0.04 M) was heated for 72 h at 90 °C in the sealed tube. After cooling down solvent was removed under vacuum and the crude was purified by flash column chromatography (PE/EtOAc: 9/1) to isolate 20 mg (34% yield) of **96** as an orange oil.

Analyses:

$^1\text{H NMR}$ (250 MHz, CDCl_3) δ [ppm]: 8.05 (m, 2H), 7.82 (m, 2H), 7.36 (m, 2H), 7.22 (m, 3H), 5.33 (d, $J = 9.0$ Hz, 1H), 4.60 (s br, 1H), 4.43 (m, 2H), 4.26 (s, 1H), 3.26 (t, $J = 7.5$ Hz, 1H), 3.19 (s, 3H), 2.87 (t, $J = 8.0$ Hz, 1H), 1.59 (s, 9H), 1.12 (s, 9H).

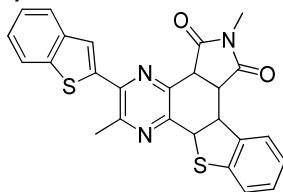
$^{13}\text{C NMR}$ (101 MHz, CDCl_3) δ [ppm]: 177.6 (C=O), 174.7 (C=O), 140.6 (C^{IV}), 139.6 ($2\times\text{C}^{\text{IV}}$), 138.0 (C^{IV}), 128.6 (CH_{ar}), 127.4 (C^{IV}), 126.8 (CH_{ar}), 125.9 (CH_{ar}), 125.8 (CH_{ar}), 124.8 (CH_{ar}), 124.4 (CH_{ar}), 124.2 (CH_{ar}), 122.1 (CH_{ar}), 121.3 (CH_{ar}), 84.2 (C^{IV}), 82.6 (C^{IV}), 62.5 (CH_2), 56.1 (CH), 46.9 (CH), 45.5 (CH), 44.6 (CH), 28.2 (CH_3), 27.6 (CH_3), 25.2 (CH_3N).

MS (ESI) [m/z]: 710.0 [$\text{M}+\text{Na}$] $^+$, 726.0 [$\text{M}+\text{K}$] $^+$.

HRMS (ESI) [m/z]: calculated for $C_{33}H_{37}N_3NaO_7S_2$ $[M+Na]^+$: 710.1965, found: 710.1964.

IR (neat, ATR) ν [cm^{-1}]: 3472 (OH), 3060, 2978 (CH, sp^3), 2927, 1699 (C=O), 1342, 1278, 1159, 750.

9-(1-benzothiophen-2-yl)-4,10-dimethyl-14-thia-4,8,11-triazapentacyclo[11.7.0.0^{2,6}.0^{7,12}.0^{15,20}]jicosa-7(12),8,10,15,17,19-hexaene-3,5-dione (97)



Yellow solid

R_f = 0.21 (PE/EtOAc: 7/3) CAN relevator

Procedure:

A solution of the alcohol **96** (40 mg, 0.058 mmol, 1.00 equiv.) was prepared in distilled CH_2Cl_2 (5 mL) under argon and cooled down to 0 °C. Then, TMSI (0.04 mL, 0.279 mmol, 4.80 equiv.) was introduced and reaction was stirred for 30 minutes at 0 °C. The reaction was slowly hydrolyzed with a saturated solution of $NaHCO_3$, warmed up and extracted with CH_2Cl_2 (3x10 mL). All organic phases were collected, washed with distilled water and brine, dried over anhydrous $MgSO_4$, filtered and concentrated. Residues were purified by column chromatography to yield 24 mg (88% yield) of product **97** as a yellow solid.

Analyses:

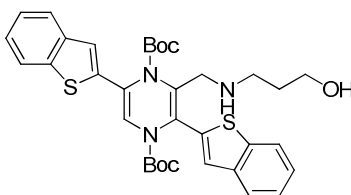
¹H NMR (250 MHz, $CDCl_3$) δ [ppm]: 8.22 (d, J = 8.0 Hz, 1H), 7.69 (m, 3H), 7.50 (s, 1H), 7.36 (m, 4H), 5.17 (d, J = 5.5 Hz, 1H), 4.65 (dd, J = 5.5 Hz, 2.0 Hz, 1H), 4.53 (dd, J = 8.2, 1.5, 1H), 4.23 (dd, J = 8.2 and 2.9, 1H), 3.02 (s, 3H), 2.56 (s, 3H).

¹³C NMR (61 MHz, $CDCl_3$) δ [ppm]: 176.5 (C=O), 175.1 (C=O), 159.1 (C^{IV}), 156.4 (C^{IV}), 140.8 (C^{IV}), 140.3 (C^{IV}), 139.5 (C^{IV}), 139.1 (C^{IV}), 137.2 (C^{IV}), 134.7 (C^{IV}), 126.5 (CH_{ar}), 126.2 (CH_{ar}), 124.8 (2xCH_{ar}), 124.7 (CH_{ar}), 124.6 (CH_{ar}), 124.5 (CH_{ar}), 123.4 (CH_{ar}), 122.2 (CH_{ar}), 53.3 (CH), 50.2 (CH), 45.1 (CH), 40.1 (CH), 25.3 (CH₃), 25.2 (CH₃).

MS (ESI) [m/z]: 470.5 $[M+H]^+$, 486.5 $[M+NH_4]^+$, 502.0 $[M+Na]^+$.

IR (neat, ATR) ν [cm^{-1}]: 3033 (CH, sp^2), 2922 (CH, sp^3), 2867, 1700 (C=O), 1465, 1307, 945, 822, 749, 726.

Di-tert-butyl 2,5-di(benzo[b]thiophen-2-yl)-3-((3-hydroxypropylamino)methyl)pyrazine-1,4-dicarboxylate (98)



Yellow oil

R_f = 0.45 (PE/EtOAc: 4/6) revelator CAN

Procedure:

The solution of aldehyde **76** (50 mg, 0.09 mmol) was prepared in MeOH (2 mL). 3-aminopropanol (20 μ L, 0.26 mmol, 3.00 equiv.), Et_3N (12 μ L, 0.09 mmol, 1.00 equiv.) and $Ti(iPrO)_4$ (10 mg, 0.03 mmol, 0.4 equiv.) were introduced with few molecular sieves (4Å). The mixture was stirred for 60 hours at room temperature (the progress of reaction followed by TLC PE:EtOAc 4: 6). MeOH was evaporated and the mixture was diluted in CH_2Cl_2 , washed with a saturated solution of $NaHCO_3$ and distilled water. The organic phase was dried over $MgSO_4$, filtered and concentrated to give a red-orange oil (characterized by NMR as an imine), which was directly used to the reduction step. The crude (46 mg, 0.07 mmol) was dissolved in MeOH (5 mL) and $NaBH_4$ (4 mg, 0.10 mmol, 1.00 equiv.) with H_3BO_3 (6 mg, 0.10 mmol, 1.00 equiv.) were introduced. A reaction mixture was stirred vigorously overnight, then quenched with distilled water and extracted with CH_2Cl_2 , dried over

MgSO₄, filtered and evaporated. The crude was purified by column chromatography (PE/EtOAc: 5/5) to yield 16.7 mg (30% yield) of product **98** as a yellow oil.

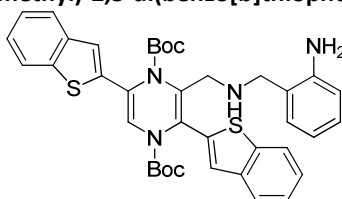
Analyses:

¹H NMR (400 MHz, CDCl₃) δ [ppm]: 7.80-7.70 (m, 4H), 7.41-7.29 (m, 6H), 7.24 (s, 1H), 4.06 (s br, 1H), 3.75 (s, 1H), 3.68 (m, 2H), 2.88 (m, 3H), 2.41 (s, 1H), 1.51 (s, 2H), 1.32 (s, 9H), 1.17 (s, 9H).

¹³C NMR (101 MHz, CDCl₃) δ [ppm]: 152.3 (C=O), 140.1 (C^{IV}), 139.9 (C^{IV}), 139.3 (C^{IV}), 138.7 (C^{IV}), 136.0 (C^{IV}), 132.2 (C^{IV}), 129.3 (C^{IV}), 126.4 (CH_{ar}), 125.3 (CH_{ar}), 124.9 (CH_{ar}), 124.8 (CH_{ar}), 124.8 (CH_{ar}), 124.2 (CH_{ar}), 123.6 (CH_{ar}), 122.4 (CH_{ar}), 122.4 (C^{IV}), 120.4 (CH_{ar}), 83.4 (C^{IV}), 83.1 (C^{IV}), 64.4 (CH₂), 48.4 (CH₂), 47.6 (CH₂), 30.7 (CH₂), 28.1 (3xCH₃), 27.9 (3xCH₃).

MS (ESI) [m/z]: [M+H]⁺: 634.5, [M-tBu]⁺: 578.5.

Di-tert-butyl 3-((2-aminobenzylamino)methyl)-2,5-di(benzo[b]thiophen-2-yl)pyrazine-1,4-dicarboxylate (99)



Orange oil

R_f = 0.36 (PE/EtOAc: 8/2) revelator CAN

Procedure:

The solution of aldehyde **76** (25 mg, 0.05 mmol) was prepared in MeOH (2 mL). 2-(aminomethyl)aniline (5 mg, 0.05 mmol, 1.00 equiv.) was introduced with one drop of acetic acid. The mixture was stirred for 2 hours at room temperature (the progress of reaction followed by TLC PE/EtOAc: 8/2). After whole consumption of starting materials, NaBH(OAc)₃ (13 mg, 0.62 mmol, 1.4 equiv.) was added and mixture was stirred for 18 h at room temperature. A reaction was quenched with distilled water and residues were extracted with EtOAc, washed three times with distilled water, dried over MgSO₄, filtered and evaporated. The crude was purified by column chromatography (PE/EtOAc: 8/2) to yield 27 mg (93% yield) of product **99** as an orange oil.

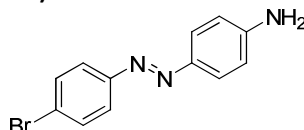
Analyses:

¹H NMR (400 MHz, CDCl₃) δ [ppm]: 7.98-7.80 (m, 4H), 7.63 (s, 2H), 7.51-7.35 (m, 6H), 6.98 (s, 1H), 6.69-6.65 (m, 2H), 5.27 (s, 2H), 3.76 (s, 2H), 3.22 (m, 2H), 2.41 (s, 1H), 1.38 (s, 9H), 1.15 (s, 9H).

¹³C NMR (101 MHz, CDCl₃) δ [ppm]: 148.2 (2xC=O), 146.9 (2xC^{IV}), 140.3 (C^{IV}), 140.2 (C^{IV}), 138.9 (C^{IV}), 138.7 (C^{IV}), 137.4 (C^{IV}), 134.0 (C^{IV}), 129.5 (2xCH_{ar}), 127.6 (2xCH_{ar}), 124.6 (2xCH_{ar}), 124.3 (2xCH_{ar}), 122.3 (CH_{ar}), 121.9 (CH_{ar}), 118.8 (CH_{ar}), 116.2 (CH_{ar}), 116.1 (C^{IV}), 110.4 (2xCH_{ar}), 83.4 (C^{IV}), 83.2 (C^{IV}), 51.9 (CH₂), 46.4 (CH₂), 28.1 (3xCH₃), 27.9 (3xCH₃).

MS (ESI) [m/z]: [M+H]⁺: 682.5, [M+Na]⁺: 704.5.

(E)-4-((4-bromophenyl)diazenyl)aniline (101)



Yellow orange powder

R_f = 0.3 (PE/EtOAc: 6/4) revelator CAN

Procedure:

A solution of NaNO₂ (400 mg, 5.81 mmol, 1.00 equiv.) was prepared in an ice-water mixture and 4-bromoaniline (1.00 g, 5.81 mmol, 1.00 equiv.) was then suspended in this solution. The content of flask was poured into concentrated HCl (2.3 mL) cooled in the ice-water bath. The solution was vigorously stirred for 30 min at 0°C. The solution of diazonium salt was dripped in a suspension of aniline (0.56 mL, 6.10 mmol, 1.05

equiv.) in 100 mL of acetic buffer (1.2 M, pH = 6) at 0°C. A red-orange precipitate appeared. The reaction was carried out for 1h. The red-orange precipitate was filtered through Milipore, rinsed with distilled water and dried under vacuum. The residue was purified by flash column chromatography (PE/EtOAc: 9/1 + 0.5% TEA) to provide 1.49 g (93% yield) of **101** as a yellow-orange powder.

Analyses:

¹H NMR (400 MHz, CDCl₃) δ [ppm]: 7.80 (d, *J* = 8.7 Hz, 2H), 7.72 (d, *J* = 8.7 Hz, 2H), 7.60 (d, *J* = 8.7 Hz, 2H), 6.73 (d, *J* = 8.8 Hz, 2H), 4.13 (s, 2H).

¹³C NMR (101 MHz, CDCl₃) δ [ppm]: 151.7 (C^{IV}), 149.9 (C^{IV}), 145.4 (C^{IV}), 132.1 (CH_{ar}), 132.0 (C^{IV}), 125.3 (CH_{ar}), 123.8 (CH_{ar}), 114.6 (CH_{ar}).

MS (ESI) [*m/z*]: 278.0 [MH]⁺, 280. 0 (isotope ⁸¹Br).

IR (neat, ATR) ν [cm⁻¹]: 3449 (NH₂), 3367 (NH₂), 3211, 2951 (CH, sp³), 2917, 2854, 1614, 1595, 1502.

Mp = 160°C.

(E)-4-((4-bromophenyl)diazenyl)-2,5-dimethoxyaniline (102)



Red solid

R_f = 0.43 (PE/EtOAc: 6/4) revelator CAN

Procedure:

A solution of NaNO₂ (400 mg, 5.81 mmol, 1.00 equiv.) was prepared in an ice-water mixture and 4-bromoaniline (1.00 g, 5.81 mmol, 1.00 equiv.) was then suspended in this solution. The content of flask was poured into concentrated HCl (2.3 mL) cooled in the ice-water bath. The solution was vigorously stirred for 30 min at 0°C. The solution of diazonium salt was dripped in the suspension of 2,5-dimethoxyaniline (934.4 mg, 6.10 mmol, 1.05 equiv.) in 100 mL of acetic buffer (1.2 M, pH = 6) at 0°C. A red-brown precipitate appeared. The reaction was carried out for 2h. The red-orange precipitate was filtered through Milipore, rinsed with distilled water and dried under vacuum. The residue was purified by flash column chromatography (PE/EtOAc +0.5% TEA: 7/3→6/4→5/5) to provide 1.10 g (57% yield) of **102** as a red solid.

Analyses:

¹H NMR (400 MHz, CDCl₃) δ [ppm]: 7.70 (d, *J* = 8.8 Hz, 2H), 7.56 (d, *J* = 8.8 Hz, 2H), 7.36 (s, 1H, ar), 6.35 (s, 1H, ar), 4.37 (s, 1H), 3.94 (s, 3H, CH₃O), 3.89 (s, 3H, CH₃O).

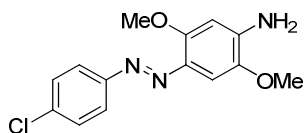
¹³C NMR (101 MHz, CDCl₃) δ [ppm]: 154.8 (C^{IV}), 152.3 (C^{IV}), 142.5 (C^{IV}), 141.8 (C^{IV}), 133.9 (CH_{ar}), 127.5 (CH_{ar}), 124.7 (CH_{ar}), 123.0 (CH_{ar}), 98.2 (CH_{ar}), 98.1 (CH_{ar}), 56.9 (CH₃), 55.8 (CH₃).

MS (ESI) [*m/z*]: 336.0 [MH]⁺, 338. 0 (isotope ⁸¹Br).

IR (neat, ATR) ν [cm⁻¹]: 3479 (NH₂), 3369 (NH₂), 2924 (CH, sp³), 1604, 1505, 1290.

Mp = 125°C.

(E)-4-((4-chlorophenyl)diazenyl)-2,5-dimethoxyaniline (103)



Red needles

R_f = 0.23 (PE/EtOAc: 8/2) revelator CAN

Procedure:

A solution of NaNO₂ (135 mg, 1.96 mmol, 1 equiv.) was prepared in an ice-water mixture and 4-chloroaniline (250 mg, 1.96 mmol, 1 equiv.) was suspended in this solution. The content of flask was poured into

concentrated HCl (1 mL) cooled in the ice-water bath. The solution was vigorously stirred for 30 min at 0°C. The solution of diazonium salt was dripped in the suspension of 2,5-dimethoxyaniline (300 mg, 1.96 mmol, 1.05 equiv.) in 30 mL of acetic buffer (1.2 M, pH = 6) at 0°C. A red precipitate appeared. The reaction was carried out for 1h. The red-orange precipitate was filtered through Milipore, rinsed with distilled water and dried under vacuum. The residue was purified by flash column chromatography (PE/EtOAc: 8/2→6/4) to provide 150 mg (26% yield) of **103** as a red solid.

Analyses:

¹H NMR (400 MHz, CDCl₃) δ [ppm]: 7.77 (d, *J* = 8.8 Hz, 2H), 7.40 (d, *J* = 8.84 Hz, 2H), 7.36 (s, 1H, ar), 6.34 (s, 1H, ar), 4.38 (s, 1H), 3.93 (s, 3H, CH₃O), 3.86 (s, 3H, CH₃O).

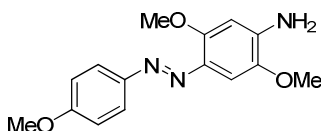
¹³C NMR (101 MHz, CDCl₃) δ [ppm]: 154.9 (C^{IV}), 152.1 (C^{IV}), 142.7 (C^{IV}), 141.0 (C^{IV}), 134.9 (C^{IV}), 133.7 (C^{IV}), 129.3 (2xCH_{ar}), 123.7 (2xCH_{ar}), 98.4 (CH_{ar}), 98.2 (CH_{ar}), 57.1 (CH₃), 56.0 (CH₃).

MS (ESI) [m/z]: 292.0 [MH]⁺, 294.0 (isotope ³⁷Cl).

IR (neat, ATR) ν [cm⁻¹]: 3477 (NH₂), 3354 (NH₂), 2966 (CH, sp³), 16171, 1509, 1301.

Mp = 124°C.

(E)-2,5-dimethoxy-4-((4-methoxyphenyl)diazenyl)aniline (104)



Red-orange needles

R_f = 0.81 (PE/EtOAc: 4/6) revelator CAN

Procedure:

A solution of *p*-anisidine (163 mg, 1.24 mmol, 1 equiv.) in 1 mL of concentrated HCl was prepared at 0°C and then the solution of NaNO₂ (86 mg, 1.24 mmol, 1 equiv.) in iced water was introduced. The solution was vigorously stirred for 30 min at 0°C. The solution of diazonium salt was dripped in the suspension of 2,5-dimethoxyaniline (200 mg, 1.31 mmol, 1.05 equiv.) in 20 mL of acetic buffer (1.2 M, pH = 6) at 0°C. A violet precipitate appeared. The reaction was carried out for 2h, then pH was adjusted to 8.5-9.0 by addition of 5% sodium hydroxide. The precipitate was filtered through Buchner funnel, rinsed with distilled water and dried under vacuum. The residue was purified by flash column chromatography (PE/EtOAc: 7/3) to provide 300 mg (84% yield) of **104** as a red-orange solid.

Analyses:

¹H NMR (400 MHz, CDCl₃) δ [ppm]: 7.83 (d, *J* = 8.0 Hz, 2H), 7.36 (s, 1H, ar), 6.96 (d, 2H, *J* = 8.0 Hz), 6.36 (s, 1H, ar), 4.26 (s, 1H), 3.93 (s, 3H, CH₃O), 3.86 (s, 3H, CH₃O), 3.84 (s, 3H, CH₃O).

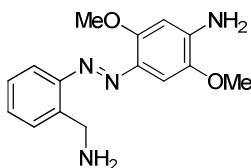
¹³C NMR (101 MHz, CDCl₃) δ [ppm]: 160.9 (C^{IV}), 154.0 (C^{IV}), 148.0 (C^{IV}), 142.1 (C^{IV}), 141.4 (C^{IV}), 133.9 (C^{IV}), 124.2 (2xCH_{ar}), 114.2 (2xCH_{ar}), 98.0 (CH_{ar}), 98.5 (CH_{ar}), 57.3 (CH₃), 56.0 (CH₃), 56.7 (CH₃).

MS (ESI) [m/z]: 288.0 [MH]⁺.

IR (neat, ATR) ν [cm⁻¹]: 3431 (NH₂), 3344 (NH₂), 3222, 3004, 2924 (CH, sp³), 2836, 1633, 1578, 1301, 1035.

Mp = 164°C.

(E)-4-((2-(aminomethyl)phenyl)diazenyl)-2,5-dimethoxyaniline (105)



Dark red powder

R_f = 0.11 (PE/EtOAc: 8/2) revelator CAN

Procedure:

A solution of NaNO₂ (565 mg, 8.19 mmol, 1 equiv.) was prepared in an ice-water mixture and 2-aminobenzylamine (1.00 g, 8.19 mmol, 1 equiv.) was suspended in this solution. The content of flask was poured into concentrated HCl (2.3 mL) cooled in an iced water bath. The solution was vigorously stirred for 30 min at 0°C. The solution of diazonium salt was dripped in the suspension of 2,5-dimethoxyaniline (1.30 g, 8.45 mmol, 1.05 equiv.) in 100 mL of acetic buffer (1.2 M, pH = 6) at 0°C. A red precipitate appeared. The reaction was carried out for 1h and the reaction mixture was neutralized with a 5N solution of potassium hydroxide. The precipitate was filtered through Milipore, rinsed with distilled water and dried under vacuum. The residue was purified by flash column chromatography (PE/EtOAc + 0.5% TEA: 6/4) to provide 1.90 g (81% yield) of **105** as a dark red solid.

Analyses:

¹H NMR (250 MHz, CDCl₃) δ [ppm]: 7.85 (dd, *J* = 1.4 and 7.9 Hz, 1H), 7.39 (m, 2H, ar), 7.33 (s, 1H, ar), 7.30 (m, 1H, ar), 6.35 (s, 1H, ar), 4.64 (s, 2H), 4.48 (s, 2H, NH₂), 3.92 (s, 3H), 3.88 (s, 3H).

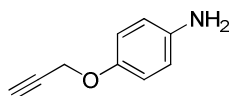
¹³C NMR (101 MHz, CDCl₃) δ [ppm]: 155.0 (C^{IV}), 153.1 (C^{IV}), 143.2 (CH_{ar}), 142.1 (C^{IV}), 134.2 (C^{IV}), 133.4 (C^{IV}), 131.1 (CH_{ar}), 129.1 (CH_{ar}), 128.8 (CH_{ar}), 125.3 (CH_{ar}), 98.5 (CH_{ar}), 97.9 (CH_{ar}), 64.3 (CH₂), 56.7 (CH₃), 56.2 (CH₃).

MS (ESI) [m/z]: 288.0 [MH]⁺.

IR (neat, ATR) ν [cm⁻¹]: 3470 (NH₂), 3330 (NH₂), 3207 (NH₂), 2939 (CH, sp³), 2842, 1634, 1512, 1303.

Mp = 148°C.

(E)-4-((2-(aminomethyl)phenyl)diazenyl)-2,5-dimethoxyaniline (106)²⁵³



White solid

R_f = 0.61 (PE/EtOAc: 4/6) revelator CAN

Procedure:

A solution of *p*-nitrophenol (1.40 g, 10.00 mmol, 1 equiv.) was prepared in DMF (20 mL, *c* = 0.5 M) and K₂CO₃ (4.20 g, 30.00 mmol, 3 equiv.) was added and the mixture was heated at 60 °C for 30 min. The reaction was cooled to room temperature and propargyl bromide (1.34 mL, 12.00 mmol, 1.2 equiv.) was slowly introduced. The content of flask was stirred at room temperature for 60 hours. Solid residues were filtered and the filtrate was reduced under vacuo to recover white solid, which was directly used for a next step. Residues were dissolved in dioxane (30 mL) at 10 °C and the solution of SnCl₂ (11.00 g, 50.00 mmol; 5 equiv.) in concentrated HCl (5 mL) was dripped to the solution for 30 minutes. The reaction was carried out for 30 hours. Distilled water was added and the solution was extracted with CH₂Cl₂ four times, organic phases were collected and dried over MgSO₄. The residue was purified by flash column chromatography (PE/EtOAc: 4/6) to provide 0.97 g (66% yield) of **106** as a white solid.

Analyses:

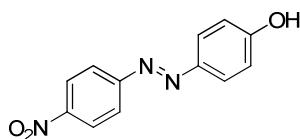
¹H NMR (250 MHz, Acetone) δ [ppm]: 7.46 (d, *J* = 8.0 Hz, 1H), 7.23 (m, 1H, ar), 7.15 (m, 2H, ar), 4.86 (t, *J* = 2.5 Hz, 2H), 3.15 (qt, *J* = 2.5 Hz, 1H).

¹³C NMR (61 MHz, CDCl₃) δ [ppm]: 158.6 (C^{IV}), 157.9 (C^{IV}), 127.4 (CH_{ar}), 127.0 (CH_a), 116.7 (CH_a), 116.3 (CH_a), 79.5 (C^{IV}_r), 77.6 (CH), 56.8 (CH₂).

MS (ESI) [m/z]: 148.0 [M+H]⁺.

IR (neat, ATR) ν [cm⁻¹]: 3251 (NH₂), 2864 (CH, sp³), 2133 (C≡C), 1509, 1246, 1025.

(E)-4-((4-nitrophenyl)diazenyl)phenol (107)



Red-orange solid

R_f = 0.64 (PE/EtOAc: 4/6) revelator CAN

Procedure:

A solution of *p*-nitroaniline (690 mg, 5.00 mmol, 1.00 equiv.) in 2 mL of concentrated HCl was prepared at 0°C and then the solution of NaNO₂ (345 mg, 5.00 mmol, 1.00 equiv.) in iced water was introduced. The solution was vigorously stirred for 30 min at 0°C. The solution of phenol (492 mg, 5.25 mmol, 1.05 equiv.) was prepared in 3.75 mL of solution of NaOH (1.4 M) and added to the 170 mL of buffer NH₄⁺/NH₃. The solution of diazonium salt was dripped in this solution at 0°C and reaction was carried out for 2h. An orange precipitate appeared. The precipitate was filtered through Büchner funnel, rinsed with distilled water and dried under vacuum. The residue was purified by flash column chromatography (PE/EtOAc: 7/3) to provide 692 mg (57% yield) of **107** as a red-orange solid.

Analyses:

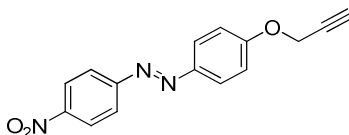
¹H NMR (400 MHz, MeOD) δ [ppm]: 8.34 (d, *J* = 8.7 Hz, 2H), 7.95 (d, *J* = 8.7 Hz, 2H), 7.86 (d, *J* = 8.7 Hz, 2H), 6.93 (d, *J* = 8.7 Hz, 2H).

¹³C NMR (101 MHz, MeOD) δ [ppm]: 162.2 (C^{IV}), 156.1 (C^{IV}), 148.1 (C^{IV}), 146.1 (C^{IV}), 125.5 (2xCH_{ar}), 124.3 (2xCH_{ar}), 122.6 (2xCH_{ar}), 115.6 (2xCH_{ar}).

MS (ESI) [m/z]: 244.0 [MH]⁺.

Mp = 204°C.

(E)-1-(4-nitrophenyl)-2-(4-(prop-2-ynoxy)phenyl)diazene (108)



Red-orange solid

R_f = 0.64 (PE/EtOAc: 4/6) revelator CAN

Procedure:

The solution of **107** (200 mg, 0.82 mg, 1.0 equiv.) in 2 mL of ethanol was prepared, then NaOH (33 mg, 0.82 mmol, 1.0 equiv.) was added and reaction was stirred for 1 h at rt. Propargyl bromide (0.13 mL, 1.23 mmol, 1.5 equiv.) was added dropwise and a solution was left for 18 h at reflux. After cooling down to room temperature, a product was extracted with diethyl ether and washed three times with distilled water and once with brine. The organic phase was dried over anhydrous MgSO₄, filtered and concentrated under vacuo. The crude product was crystallized from EtOH to yield 185 mg of **108** (81 % yield) as red-orange solid.

Analyses:

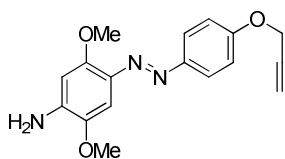
¹H NMR (250 MHz, CDCl₃) δ [ppm]: 8.39 (d, *J* = 8.9 Hz, 2H), 8.00 (d, *J* = 8.8 Hz, 4H), 7.15 (d, *J* = 9.0 Hz, 2H), 4.80 (s, 2H), 2.58 (s, 1H).

¹³C NMR (101 MHz, CDCl₃) δ [ppm]: 210.2 (C^{IV}), 148.5 (C^{IV}), 127.7 (C^{IV}), 125.7 (2xCH_{ar}), 124.9 (2xCH_{ar}), 123.4 (2xCH_{ar}), 115.6 (2xCH_{ar}), 115.5 (C^{IV}), 80.7 (CC), 76.4 (CH), 56.3 (CH₂).

MS (ESI) [m/z]: 282.0 [M+H]⁺, 304.0 [M+Na]⁺, 320.0 [M+K]⁺.

IR (neat, ATR) ν [cm⁻¹]: 3265 (C≡CH), 2927 (CH, sp³), 2129 (C≡C), 1580, 1512, 1335, 1016.

(E)-4-((4-(prop-2-ynoxy)phenyl)diazenyl)aniline (109)



Orange needles

R_f = 0.33 (PE/EtOAc: 6/4) revelator CAN

Procedure:

The starting amine **106** (57 mg, 0.39 mmol, 1 equiv.) was dissolved in HCl concentrated (1mL) and the solution was placed in an ice-water bath, then a cooled solution of NaNO₂ (27 mg, 0.39 mmol, 1 equiv.) was added by syringe. The solution was vigorously stirred for 30 min at 0°C. In the same time, a suspension of 2,5-dimethoxyaniline (63 mg, 0.41 mmol, 1.05 equiv.) was prepared in 20 mL of acetic buffer (pH=6) and transferred to an ice-water bath (0-5°C). The solution of diazonium salt was added dropwise to this suspension and the colour of the mixture changed to deep dark red. The reaction was carried out for 1h, then residues were precipitated in basic conditions (addition dropwise of a 5% solution of sodium hydroxide). A red-orange precipitate was filtered through paper filter and then taken up into solution in acetone. The residue was purified by the flash column chromatography (PE/EtOAc: 6/4) to provide 56 mg (46% yield) of **109** as a red solid.

Analyses:

¹H NMR (250 MHz, CDCl₃) δ [ppm]: 7.82 (d, J = 9.0 Hz, 2H), 7.38 (s, 1H), 7.03(d, J = 9.0 Hz, 2H), 6.39 (s, 1H), 4.74 (d, J = 2.25 Hz, 2H), 4.29 (s, 2H, NH₂), 3.96 (s, 3H), 3.89 (s, 3H), 2.53 (t, J = 2.5 Hz, 1H).

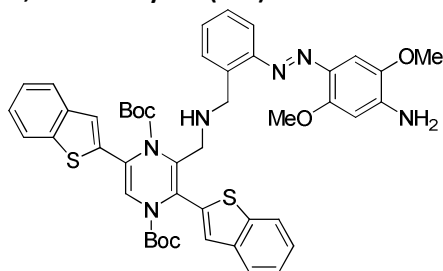
¹³C NMR (101 MHz, CDCl₃) δ [ppm]: 158.76 (C^{IV}), 154.17 (C^{IV}), 148.57 (CH_{ar}), 142.05 (C^{IV}), 141.60 (C^{IV}), 133.92 (CH_{ar}), 124.11 (CH_{ar}), 115.24 (CH_{ar}), 98.90 (CH_{ar}), 98.48 (CH_{ar}), 78.51 (C^{IV}), 75.95 (CH), 57.27 (CH₃), 56.22 (CH₂), 56.06(CH₃).

MS (ESI) [m/z]: 312.0 (MH⁺).

IR (neat, ATR) ν [cm⁻¹]: 3453, 3338, 3285 (NH₂), 2920 (CH₂ sp³), 2128 (C≡C), 1623 (C=O), 1508, 1299, 1018.

Mp = 163°C.

(E)-di-tert-butyl-3-((2-((4-amino-2,5-dimethoxyphenyl)diazenyl)benzylamino)methyl)-2,5-di(benzo[b]thiophen-2-yl)pyrazine-1,4-dicarboxylate (110)



Yellow oil

R_f = 0.20 (PE/EtOAc: 8/2) revelator CAN

Procedure:

The solution of aldehyde **76** (50 mg, 0.09 mmol) was prepared in MeOH (5 mL) and amine **105** (30 mg, 0.10 mmol, 1.20 equiv.) was introduced, followed by AcOH (4 μL, 0.09 mmol, 1.00 equiv.). The mixture was stirred for 1 hour at room temperature and NaBH₃CN (7 mg, 0.10 mmol, 1.20 equiv.) was added. The reaction was continued for 48 h. The mixture was diluted with CH₂Cl₂, washed with distilled water twice and with brine. An organic phase was dried over MgSO₄, filtered and concentrated. The crude was purified by column chromatography (PE/EtOAc: 7/3 to 6/4) to yield 41 mg (54% yield) of product **110** as a yellow oil.

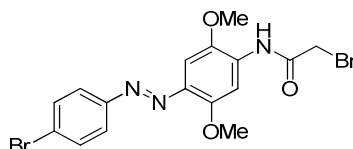
Analyses:

¹H NMR (250 MHz, CDCl₃) δ [ppm]: 7.84-7.82 (m, 2H), 7.74-7.59 (m, 2H), 7.40-7.25 (m, 8H), 7.16-7.15 (m, 2H), 7.02 (s, 1H), 6.51 (s, 1H), 5.82 (s, 1H), 5.66 (m br, 1H), 4.73 (m br, 1H), 4.48-4.38 (m, 3 H), 3.92 (s, 3H), 3.64 (s, 1H), 1.25 (s, 18H).

¹³C NMR (101 MHz, CDCl₃) δ [ppm]: 155.6 (C=O), 152.08 (C^{IV}), 141.7 (C^{IV}), 139.4 (C^{IV}), 139.1 (C^{IV}), 138.5 (C^{IV}), 132.0 (C^{IV}), 131.2 (C^{IV}), 130.5 (C^{IV}), 128.3 (CH_{ar}), 125.4 (CH_{ar}), 124.9 (CH_{ar}), 124.6 (CH_{ar}), 124.3 (CH_{ar}), 123.1 (CH_{ar}), 122.3 (CH_{ar}), 121.9 (CH_{ar}), 97.0 (CH_{ar}), 83.2 (C^{IV}), 82.8 (C^{IV}), 63.9 (CH₂), 56.5 (CH₂), 55.8 (CH₂), 29.7 (CH₂), 27.8 (3xCH₃), 27.7 (3xCH₃).

MS (ESI) [m/z]: [M+H]⁺ 846.5, [M+H-tBu]⁺: 790.0, [M+H-2tBu]⁺: 734.0.

(E)-2-bromo-N-(4-((4-bromophenyl)diazenyl)-2,5-dimethoxyphenyl)acetamide (111)



Dark orange solid

R_f = 0.59 (PE/EtOAc: 6/4)

Procedure:

The starting amine **102** (200 mg, 0.60 mmol, 1.00 equiv.) was dissolved in dry THF (20 mL) and the solution was placed in an ice-water bath, then the pyridine (60 μL, 0.74 mmol, 1.25 equiv.) was introduced. The solution of bromoacetic bromide (52 μL, 0.60 mmol, 1.00 equiv.) in dry THF (3 mL) was prepared and introduced to the first solution by syringe. The reaction was vigorously stirred for 30 min at 0°C. After TLC control, reaction was hydrolyzed with distilled water. The residue was extracted with ethyl acetate, washed twice with distilled water and dried over magnesium sulfate. After filtration, the residue was concentrated and purified by flash column chromatography (PE/EtOAc: 6/4) to provide 258 mg (95% yield) of **111** as a dark orange solid.

Analyses:

¹H NMR (250 MHz, CDCl₃) δ [ppm]: 8.98 (s, 1H, NH), 8.33 (s, 1H, ar), 7.79 (d, J = 8.5 Hz, 2H), 7.63 (d, J = 8.5 Hz, 2H), 7.38 (s, 1H, ar), 4.06 (s, 2H), 4.03 (s, 3H, CH₃O), 3.95 (s, 3H, CH₃O).

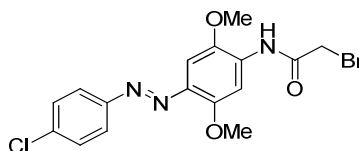
¹³C NMR (63 MHz, CDCl₃) δ [ppm]: 163.8 (C=O), 153.3 (C^{IV}), 152.0 (C^{IV}), 142.9 (C^{IV}), 137.3 (C^{IV}), 132.4 (CH_{ar}), 131.7 (C^{IV}), 124.9 (C^{IV}), 124.5 (CH_{ar}), 104.4 (CH_{ar}), 98.1 (CH_{ar}), 57.2 (CH₃), 56.5 (CH₃), 29.8 (CH₂).

MS (ESI) [m/z]: 458.0 [MH]⁺, 480.0 [MNa]⁺.

IR (neat, ATR) ν [cm⁻¹]: 3391 (NH₂), 3354 (NH₂), 2970, 1690, 1523, 1477, 830.

Mp = 176°C.

(E)-2-bromo-N-(4-((4-chlorophenyl)diazenyl)-2,5-dimethoxyphenyl)acetamide (112)



Dark orange solid

R_f = 0.78 (PE/EtOAc: 6/4) revelator CAN

Procedure:

The starting amine **103** (100 mg, 0.34 mmol, 1.00 equiv.) was dissolved in dry THF (10 mL) and the solution was placed in an ice-water bath, then the pyridine (35 μL, 0.43 mmol, 1.25 equiv.) was introduced. The solution of bromoacetic bromide (30 μL, 0.34 mmol, 1.00 equiv.) in dry THF (2 mL) was prepared and introduced to the first solution by syringe. The reaction was vigorously stirred for 30 min at 0°C. After TLC control, reaction was hydrolyzed with distilled water. The residue was extracted with ethyl acetate, washed twice with distilled water

and dried over magnesium sulfate. After filtration, the residue was concentrated and purified by flash column chromatography (PE/EtOAc: 6/4) to provide 133 mg (94% yield) of **112** as a dark orange solid.

Analyses:

$^1\text{H NMR}$ (250 MHz, CDCl_3) δ [ppm]: 8.96 (s, 1H, NH), 8.33 (s, 1H, ar), 7.84 (d, $J = 8.7$ Hz, 2H), 7.46 (d, $J = 9.43$ Hz, 2H), 7.37 (s, 1H, ar), 4.04 (s, 2H), 4.01 (s, 3H, CH_3O), 3.93 (s, 3H, CH_3O).

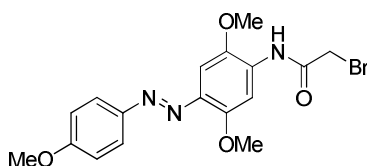
$^{13}\text{C NMR}$ (63 MHz, CDCl_3) δ [ppm]: 163.8 (C=O), 153.3 (C^{IV}), 151.7 (C^{IV}), 142.9 (C^{IV}), 137.3 (C^{IV}), 136.5 (C^{IV}), 131.7 (C^{IV}), 129.5 (CH_{ar}), 124.3 (CH_{ar}), 104.6 (CH_{ar}), 98.1 (CH_{ar}), 57.2 (CH_3), 56.5 (CH_3), 29.8 (CH_2).

MS (ESI) [m/z]: 414.0 [MH^+], 436.0 [MNa^+].

IR (neat, ATR) ν [cm^{-1}]: 3371 (NHCO), 2942 (CH sp^2), 1691 (amide), 1595, 1468, 1035.

Mp = 170°C.

(E)-2-bromo-N-(2,5-dimethoxy-4-((4-methoxyphenyl)diazenyl)phenyl)acetamide (113)



Red solid

R_f = 0.82 (PE/EtOAc: 6/4) revelator CAN

Procedure:

The starting amine **104** (150 mg, 0.52 mmol, 1.00 equiv.) was dissolved in dry THF (20 mL) and the solution was placed in an ice-water bath, then the pyridine (50 μL , 0.65 mmol, 1.25 equiv.) was introduced. The solution of bromoacetic bromide (45 μL , 0.52 mmol, 1.00 equiv.) in dry THF (3 mL) was prepared and introduced to the first solution by cannula. The reaction was vigorously stirred for 60 minutes at 0°C. After TLC control, reaction was hydrolyzed with distilled water. The residue was extracted with ethyl acetate, washed twice with distilled water and dried over magnesium sulfate. After filtration, the residue was concentrated and purified by flash column chromatography (PE/EtOAc: 7/3) to provide 207 mg (97% yield) of **113** as a red solid.

Analyses:

$^1\text{H NMR}$ (250 MHz, CDCl_3) δ [ppm]: 8.97 (s, 1H, NH), 8.32 (s, 1H, ar), 7.93 (d, $J = 7.0$ Hz, 2H), 7.39 (s, 1H, ar), 7.02 (d, $J = 7.0$ Hz, 2H), 4.07 (s, 2H), 4.04 (s, 3H, CH_3O), 3.96 (s, 3H, CH_3O), 3.89 (s, 3H, CH_3O).

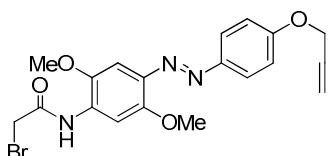
$^{13}\text{C NMR}$ (63 MHz, CDCl_3) δ [ppm]: 163.8 (C=O), 161.9 (C^{IV}), 152.3 (C^{IV}), 147.6 (C^{IV}), 142.9 (C^{IV}), 137.7 (C^{IV}), 130.5 (C^{IV}), 124.9 (2x CH_{ar}), 114.3 (2x CH_{ar}), 104.6 (CH_{ar}), 98.3 (CH_{ar}), 57.2 (CH_3), 56.5 (CH_3), 55.7 (CH_3), 29.8 (CH_2).

MS (ESI) [m/z]: 408.0 [MH^+], 430.0 [MNa^+].

IR (neat, ATR) ν [cm^{-1}]: 3371 (NHCO), 2942 (CH sp^2), 1691 (amide I), 1595, 1468, 1035.

Mp = 152°C.

(E)-2-bromo-N-(2,5-dimethoxy-4-((4-(prop-2-ynoxy)phenyl)diazenyl)phenyl)acetamide (114)



Dark orange powder

R_f = 0.83 (PE/EtOAc: 4/6) revelator CAN

Procedure:

The starting amine **109** (30 mg, 0.10 mmol, 1.00 equiv.) was dissolved in dry THF (3 mL) and the solution was placed in an ice-water bath, then the pyridine (11 μ L, 0.14 mmol, 1.45 equiv.) was introduced. The solution of bromoacetic bromide (10 μ L, 0.11 mmol, 1.45 equiv.) in dry THF (1 mL) was prepared and introduced to the first solution by syringe. The reaction was vigorously stirred for 30 min at 0°C. After TLC control, reaction was hydrolyzed with distilled water. The residue was extracted with ethyl acetate, washed twice with distilled water and dried over magnesium sulfate. After filtration, the residue was concentrated and purified by flash column chromatography (PE/EtOAc: 4/6) to provide 33 mg (81% yield) of **114** as a dark orange solid.

Analyses:

¹H NMR (250 MHz, CDCl₃) δ [ppm]: 8.94 (s, 1H, NH), 8.31 (s, 1H), 7.89 (d, J = 9.1 Hz, 2H), 7.37 (s, 1H), 7.05 (d, J = 9.1 Hz, 2H), 4.75 (d, J = 2.4 Hz, 2H), 4.05 (s, 2H, CH₂), 4.02 (s, 3H), 3.94 (s, 3H), 2.56 (t, J = 2.4 Hz, 1H).

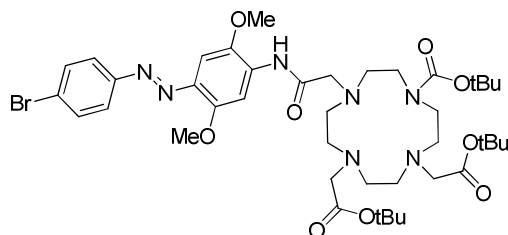
¹³C NMR (101 MHz, CDCl₃) δ [ppm]: 163.70 (C^{IV}, C=O), 159.68 (C^{IV}), 152.53 (C^{IV}), 148.16 (CH_{ar}), 142.86 (C^{IV}), 137.58 (C^{IV}), 130.69 (C^{IV}), 124.77 (CH_{ar}), 115.29 (CH_{ar}), 104.54 (CH_{ar}), 98.26 (CH_{ar}), 78.27 (C^{IV}), 76.13 (CH), 57.19 (CH₃), 56.49 (CH₃), 56.19 (CH₂), 29.80 (CH₂).

MS (ESI) [m/z]: 431.0[M]⁺.

IR (neat, ATR) ν [cm⁻¹]: 3369 (NHCO), 3237, 2924 (CH₂ sp³), 2125 (C \equiv C), 1689 (C=O), 1596, 1480, 1204, 1030, 833.

Mp = 140°C.

(E)-tert-butyl 2,2',2''-(10-(2-(4-((4-bromophenyl)diazenyl)-2,5-dimethoxyphenylamino)-2-oxoethyl)-1,4,7,10-tetraazacyclododecane-1,4,7-triyl)triacetate (115)



Red orange powder

R_f = 0.0 (PE/EtOAc: 6/4) revelator CAN

Procedure:

The solution of DO3A **53** (56 mg, 0.11 mmol, 1.00 equiv.) in anhydrous THF (5 mL) with Na₂CO₃ (34 mg, 0.33 mmol, 3.00 equiv.) was stirred for 30 min. at room temperature. Then, the solution of bromo derivative XX (50 mg, 0.11 mmol, 1.00 equiv.) in anhydrous THF (2 mL) was added dropwise and the reaction was refluxed for 8h and cooled down to room temperature. The residue was filtered through fritting glass, washed with dichloromethane and methanol. The filtrate was concentrated and purified by column chromatography (CH₂Cl₂/MeOH: 95/5) to provide 95 mg (98% yield) of **115** as a red solid.

Analyses:

¹H NMR (400 MHz, CDCl₃) δ [ppm]: 8.63 (s, 1H, NH), 8.10 (s, 1H, ar), 7.75 (d, J = 11 Hz, 2H), 7.60 (d, J = 11 Hz, 2H), 7.35 (s, 1H, ar), 3.92 (s, 3H), 3.89 (s, 3H, CH₃O), 3.69 (m, 2H), 3.10 (m, 8H), 2.27 (m br, 16 H), 1.47 (s, 12H), 1.40 (s, 16H).

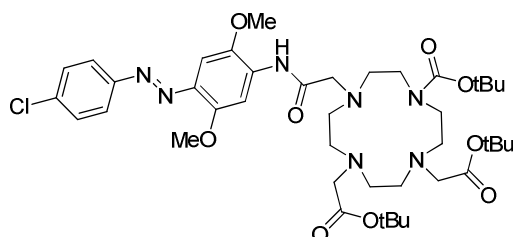
¹³C NMR (101 MHz, CDCl₃) δ [ppm]: 172.9 (C=O), 171.6 (C^{IV}), 153.1 (C^{IV}), 152.0 (C^{IV}), 144.0 (C^{IV}), 137.6 (C^{IV}), 136.5 (C^{IV}), 132.3 (C^{IV}), 132.3 (CH_{ar}), 124.7 (C^{IV}), 124.4 (CH_{ar}), 107.0 (CH_{ar}), 97.9 (CH_{ar}), 82.0 (C^{IV}), 57.6 (CH₃), 56.3 (CH₃), 56.2 (CH₂), 55.6 (CH₂), 28.0 (CH₃).

MS (ESI) [m/z]: 892.5 [MH]⁺, 912.5 [MNa]⁺.

IR (neat, ATR) ν [cm⁻¹]: 3350 (NHCO), 2973 (CH sp²), 2821, 1724 (amide), 1525, 1261, 1223.

Mp = 146°C.

(E)-tert-butyl 2,2',2''-(10-(2-(4-((4-chlorophenyl)diazenyl)-2,5-dimethoxyphenylamino)-2-oxoethyl)-1,4,7,10-tetraazacyclododecane-1,4,7-triyl)triacetate (116)



Red orange powder

R_f = 0.42 (CH₂Cl₂/MeOH: 95/5) revelator CAN

Procedure:

The solution of DO3A **53** (63 mg, 0.12 mmol, 1.00 equiv.) in anhydrous THF (5 mL) with Na₂CO₃ (38 mg, 0.36 mmol, 3.00 equiv.) was stirred for 30 min. at room temperature. Then, the solution of bromo derivative XX (50 mg, 0.12 mmol, 1.00 equiv.) in anhydrous THF (2 mL) was added dropwise. The reaction was refluxed for 18h and then cooled down to room temperature. Residues were filtered through fritting glass, washed with dichloromethane and methanol. Filtrate was concentrated and purified by column chromatography (CH₂Cl₂/MeOH: 95/5) to provide 95 mg (98% yield) of **116** as a red solid.

Analyses:

¹H NMR (250 MHz, CDCl₃) δ [ppm]: 8.60 (s, 1H, NH), 8.10 (s, 1H, ar), 7.82 (d, *J* = 6.8 Hz, 2H), 7.46 (d, *J* = 6.8 Hz, 2H), 7.35 (s, 1H, ar), 3.93 (s, 3H), 3.87 (s, 3H, CH₃O), 3.65 (m, 2H), 3.03 (m, 4H), 2.36 (m br, 16 H), 2.06 (s br, 2H), 1.47 (s, 9H), 1.40 (s, 18H).

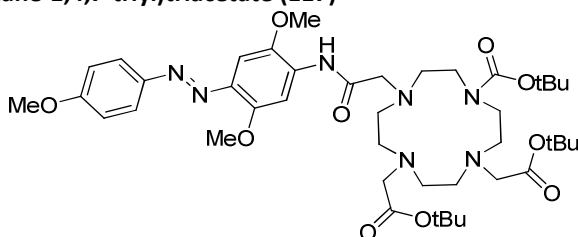
¹³C NMR (61 MHz, CDCl₃) δ [ppm]: 172.9 (C=O), 171.6 (C^{IV}), 153.1 (C^{IV}), 151.6 (C^{IV}), 144.0 (C^{IV}), 137.5 (C^{IV}), 136.2 (C^{IV}), 133.0 (C^{IV}), 129.4 (CH_{ar}), 124.2 (CH_{ar}), 106.9 (CH_{ar}), 97.9 (CH_{ar}), 82.0 (C^{IV}), 57.6 (CH₃), 56.3 (CH₃), 56.2 (CH₂), 55.6 (CH₂), 28.0 (CH₃).

MS (ESI) [m/z]: 790.5 [M-*t*Bu]⁺, 812.5 [M-Cl]⁺, 846.5 [M]⁺, 870.5 [MNa]⁺.

IR (neat, ATR) ν [cm⁻¹]: 3384 (NHCO), 2974, 2828 (CH₂ sp³), 1724 (C=O), 1527, 1223, 1105, 1008.

Mp = 134°C.

(E)-tert-butyl 2,2',2''-(10-(2-(2,5-dimethoxy-4-((4-methoxyphenyl)diazenyl)phenylamino)-2-oxoethyl)-1,4,7,10-tetraazacyclododecane-1,4,7-triyl)triacetate (117)



Red orange solid

R_f = 0.05 (PE/EtOAc: 4/6) revelator CAN

Procedure:

The solution of DO3A **53** (236 mg, 0.46 mmol, 1.00 equiv.) in anhydrous THF (15 mL) with Na₂CO₃ (144 mg, 1.37 mmol, 3.00 equiv.) was stirred for 30 minutes at room temperature. Then the solution of bromo derivative XX (187 mg, 0.46 mmol, 1.00 equiv.) in anhydrous THF (6 mL) was added dropwise. The reaction was refluxed for 16h and cooled down to room temperature. Residues were filtered through fritting glass, washed with dichloromethane and methanol. The filtrate was concentrated and purified by flash column chromatography (PE/EtOAc: 4/6->10->EtOH) to provide 219 mg (57% yield) of **117** as a red-orange solid.

Analyses:

¹H NMR (250 MHz, CDCl₃) δ [ppm]: 8.35 (s, 1H, NH), 8.09 (s, 1H, ar), 7.90 (d, *J* = 6.9 Hz, 2H), 7.35 (s, 1H, ar), 7.01 (d, *J* = 7.1 Hz, 2H), 3.92 (s, 3H), 3.89 (s, 3H, CH₃O), 3.87 (s, 3H, CH₃O), 3.41 (m, 2H), 3.08 (m, 8H), 2.56 (br, 6H), 2.36 (br, 4H), 1.99 (s br, 4 H), 1.47 (s, 9H), 1.40 (s, 18H).

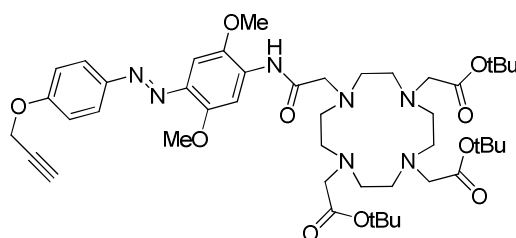
¹³C NMR (61 MHz, CDCl₃) δ [ppm]: 172.8 (C=O), 171.1 (C^{IV}), 161.7 (C^{IV}), 152.2 (C^{IV}), 147.5 (C^{IV}), 143.6 (C^{IV}), 137.8 (C^{IV}), 130.8 (C^{IV}), 124.7 (CH_{ar}), 114.2 (CH_{ar}), 107.1 (CH_{ar}), 98.0 (CH_{ar}), 81.9 (C^{IV}), 57.8 (CH₃), 57.6 (CH₂), 56.2 (CH₃), 56.2 (CH₂), 56.1 (CH₂), 55.6 (CH₃), 55.6 (CH₂), 27.9 (CH₃).

MS (ESI) [m/z]: 842.5 [MH]⁺, 864.5 [MNa]⁺.

IR (neat, ATR) ν [cm⁻¹]: 3406 (NHCO), 2980, 2831 (CH₂ sp³), 1725, 1594, 1225, 1157, 1104.

Mp = 168°C.

(E)-tert-butyl 2,2',2''-(10-(2-(2,5-dimethoxy-4-((4-(prop-2-ynoxy)phenyl)diazenyl)phenylamino)-2-oxoethyl)-1,4,7,10-tetraazacyclododecane-1,4,7-triyl)triacetate (118)



Red solid

R_f = 0.45 (CH₂Cl₂/MeOH: 9/1) revelator CAN

Procedure:

The solution of DO3A **53** (39 mg, 0.08 mmol, 1.00 equiv.) in anhydrous THF (3 mL) with Na₂CO₃ (24 mg, 0.23 mmol, 3.00 equiv.) was stirred for 30 min. at room temperature. Then, the solution of bromo derivative XX (33 mg, 0.08 mmol, 1.00 equiv.) in anhydrous THF (1 mL) was added dropwise. The reaction was refluxed for 18h and cooled down to room temperature. Residues were filtered by fritting glass, washed with dichloromethane and methanol, then filtrate was concentrated and purified by flash column chromatography (CH₂Cl₂/MeOH: 9/1) to provide 63 mg (95% yield) of **118** as a red solid.

Analyses:

¹H NMR (400 MHz, CDCl₃) δ [ppm]: 8.40 (s, 1H, NH), 8.00 (s, 1H, ar), 7.83 (d, *J* = 8.9 Hz, 2H), 7.27 (s, 1H, ar), 7.02 (d, *J* = 12.4 Hz, 2H), 4.69 (s, 2H), 3.85 (s, 3H), 3.79 (s, 3H, CH₃O), 3.25 (m, 16H), 2.50 (t, *J* = 2.3 Hz, 1H), 2.23 (m br, 8H), 1.40 (s, 9H), 1.33 (s, 18H).

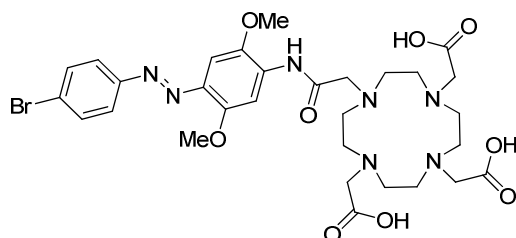
¹³C NMR (101 MHz, CDCl₃) δ [ppm]: 172.8 (C=O), 171.2 (C^{IV}), 159.5 (C^{IV}), 152.4 (C^{IV}), 148.0 (C^{IV}), 143.9 (C^{IV}), 137.8 (C^{IV}), 131.2 (C^{IV}), 124.6 (CH_{ar}), 115.2 (CH_{ar}), 107.2 (CH_{ar}), 98.0 (CH_{ar}), 82.0 (C^{IV}), 78.2 (C≡CH), 76.1 (C≡C), 57.8 (CH₃), 57.5 (CH₂), 56.2 (CH₂), 56.1 (CH₃), 55.6 (CH₃), 27.9 (CH₃).

MS (ESI) [m/z]: 866.5 [MH]⁺, 888.5 [MNa]⁺.

IR (neat, ATR) ν [cm⁻¹]: 3360 (NHCO), 3291, 2974, 2834 (CH₂ sp³), 2107 (C≡C), 1723 (C=O), 1673, 1593, 1250, 1023, 840.

Mp = 143°C.

(E)-2,2',2''-(10-(2-(4-((4-bromophenyl)diazenyl)-2,5-dimethoxyphenylamino)-2-oxoethyl)-1,4,7,10-tetraazacyclododecane-1,4,7-triyl)triacetic acid (119)



Red semi-solid**R_f = 0.0 (CH₂Cl₂/MeOH: 9/1) revelator CAN**Procedure:

A solution of triisopropylsilane (30 μL, 0.25 mmol, 4.72 equiv.) was prepared in trifluoroacetic acid (1.5 mL, 8.83 mmol) and was stirred for 5 minutes. This solution was added to the starting ester **115** (47 mg, 0.053 mmol, 1.00 equiv). The reaction of deprotection was carried out for 60 min. at room temperature. Volatile compounds were evaporated and the product was precipitated with diethyl ether (5 mL). After filtration through Milipore and washings with diethyl ether, the residue was dried under vacuum to provide 38 mg (quantitative) of **119** as a red semi-solid.

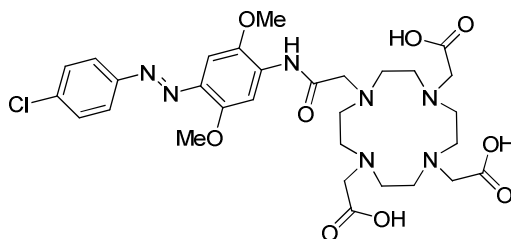
Analyses:

¹H NMR (250 MHz, MeOD) δ [ppm]: 8.28 (d, *J* = 30.0 Hz, 1H), 7.95–7.82 (m, 2H), 7.55 (dd, *J* = 8.6 and 3.2 Hz, 2H), 7.40 (d, *J* = 6.7 Hz, 1H), 4.02 (s, 3H), 3.99 (s, 3H), 3.92 (s, 2H), 3.88 (s, 2H), 3.52 (br m, 6H), 2.76 (br, 14H).

¹³C NMR (101 MHz, MeOD) δ [ppm]: 211.5 (C=O), 184.0 (C^{IV}), 156.5 (C^{IV}), 154.3 (C^{IV}), 133.6 (2xCH_{ar}), 129.0 (CH_{ar}), 125.5 (2xCH_{ar}), 74.1 (CH_{ar}), 56.8 (CH₃), 49.7 (CH₃), 46.6 (CH₂), 28.5 (CH₂), 19.1 (CH₂).

MS (ESI) [m/z] mode negative: 722.5 [M]⁻, 744.0 [M+Na]⁻, 758.0 [M+K]⁻.

IR (neat, ATR) ν [cm⁻¹]: 3375 (OH), 2974, 2852, 1679 (C=O), 1593, 1534, 1454, 1394, 1125, 832, 720.

(E)-2,2',2''-(10-(2-(4-((4-chlorophenyl)diazenyl)-2,5-dimethoxyphenylamino)-2-oxoethyl)-1,4,7,10-tetraazacyclododecane-1,4,7-triyl)triacetic acid (120)**Red-orange semi-solid****R_f = 0.02 (CH₂Cl₂/MeOH: 9/1) revelator CAN**Procedure:

A solution of triisopropylsilane (20 μL, 0.16 mmol, 3.40 equiv.) was prepared in trifluoroacetic acid (1.0 mL, 5.89 mmol) and was stirred for 5 minutes. This solution was added to the starting ester **116** (40 mg, 0.047 mmol, 1.00 equiv). The reaction of deprotection was carried out for 60 min. at rt. Volatile compounds were evaporated and the product was precipitated with diethyl ether (4 mL). After filtration through Milipore and washings with diethyl ether, the residue was dried under vacuum to provide 30 mg (quantitative) of **120** as a red-orange semi-solid.

Analyses:

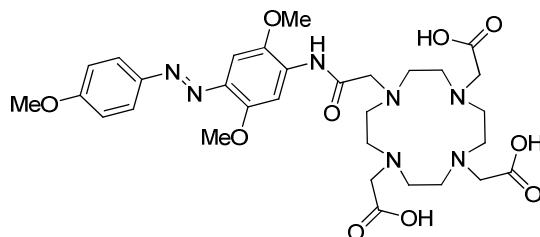
¹H NMR (250 MHz, MeOD) δ [ppm]: 8.34 (s, 1H), 8.22 (s, 1H), 7.88 (m, 2H), 7.56 (m, 2H), 4.02 (s, 3H), 3.99 (s, 3H), 3.92 (d, *J* = 8.9 Hz, 2H), 3.49 (m, 6H), 3.04 (m br, 6H), 2.47 (m br, 8H).

¹³C NMR (101 MHz, MeOD) δ [ppm]: 211.5 (C=O), 184.0, 156.5, 130.6, 130.5, 129.0, 125.4, 125.3, 74.1, 56.8, 49.6, 49.4, 49.2, 19.1.

MS (ESI) [m/z] mode negative: 678.0 [M]⁻, 713.5 [M-3H+K]⁻.

IR (neat, ATR) ν [cm⁻¹]: 3395 (OH), 2971, 2854, 1675 (C=O), 1593, 1183, 721.

(E)-2,2',2''-(10-(2-(2,5-dimethoxy-4-((4-methoxyphenyl)diazenyl)phenylamino)-2-oxoethyl)-1,4,7,10-tetraazacyclododecane-1,4,7-triyl)triacetic acid (121)



Violet gum

R_f = 0.14 (CH₂Cl₂/MeOH: 95/5) revelator CAN

Procedure:

A solution of triisopropylsilane (40 μL, 0.32 mmol, 5.3 equiv.) was prepared in trifluoroacetic acid (2.0 mL, 11.78 mmol) and was stirred for 5 minutes. This solution was added to the starting ester **117** (50 mg, 0.06 mmol, 1.00 equiv). The reaction was carried out for 60 min. at room temperature. Volatile compounds were evaporated and the product was precipitated with diethyl ether (8 mL). After filtration through Milipore and washings with diethyl ether, the residue was dried under vacuum to provide 35 mg (88% yield) of **121** as a dark violet gum.

Analyses:

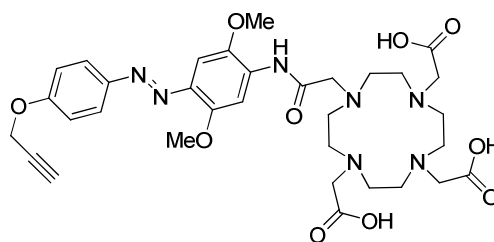
¹H NMR (250 MHz, MeOD) δ [ppm]: 8.32 (s, 1H), 8.11 (s, 1H), 7.91 (d, *J* = 8.7 Hz, 2H), 7.39 (s, 1H), 7.10 (d, *J* = 8.8 Hz, 1H), 4.01 (s, 3H), 3.91 (s, 6H), 3.62 (m, 14H), 2.50 (s br, 10H).

¹³C NMR (101 MHz, MeOD) δ [ppm]: 211.45 (C=O), 183.97, 163.32, 162.97, 156.49, 129.00, 125.94, 125.75, 119.73, 116.83, 115.52, 74.03, 58.03, 56.88, 56.33, 50.00, 49.65, 49.43, 49.22, 46.54, 19.06.

MS (ESI) [*m/z*] mode negative: 672.0 [M-H]⁺, 694.0 [M-H+Na]⁺, 710.0 [M-H+K]⁺.

IR (neat, ATR) ν [cm⁻¹]: 3548, 3468, 3408 (OH), 3094, 2956, 2837, 1682 (C=O), 1594, 1251, 1204, 1012, 842

(E)-2,2',2''-(10-(2-(2,5-dimethoxy-4-((prop-2-ynoxy)phenyl)diazenyl)phenylamino)-2-oxoethyl)-1,4,7,10-tetraazacyclododecane-1,4,7-triyl)triacetic acid (122)



Red-violet semi-solid

R_f = 0.02 (CH₂Cl₂/MeOH: 9/1) revelator CAN

Procedure:

A solution of triisopropylsilane (40 μL, 0.32 mmol, 4.8 equiv.) was prepared in trifluoroacetic acid (2.0 mL, 11.78 mmol) and was stirred for 5 minutes. This solution was added to the starting ester **118** (57 mg, 0.066 mmol, 1.00 equiv). The reaction was carried out for 60 min. at room temperature. Volatile compounds were evaporated and the product was precipitated with diethyl ether (8 mL). After filtration through Milipore and washings with diethyl ether, the residue was dried under vacuum to provide 40 mg (87% yield) of **122** as a red-violet solid was obtained.

Analyses:

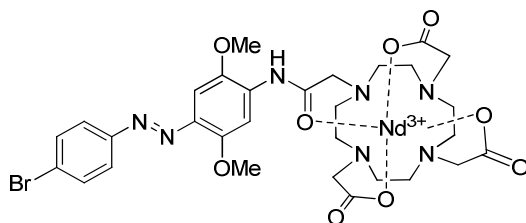
$^1\text{H NMR}$ (250 MHz, MeOD) δ [ppm]: 8.09 (s, 1H), 7.88 (d, $J = 9.2$ Hz, 2H), 7.37 (s, 1H), 7.15 (d, $J = 6.8$ Hz, 2H), 3.95 (s, 3H), 3.88 (s, 3H), 3.58 (m br, 8H), 3.01 (s, 10H), 2.69 (s, 1H), 2.45 (s br, 6H).

$^{13}\text{C NMR}$ (101 MHz, CDCl_3) δ [ppm]: 175.1 (C=O), 163.4, 162.8, 161.6, 153.1, 149.2, 125.8 (2x CH_{ar}), 120.5 (CH_{ar}), 116.5 (2x CH_{ar}), 115.8 (CH_{ar}), 109.4, 99.5, 79.5 (C \equiv CH), 77.4 (C \equiv CH), 58.8 (CH_3), 58.0 (CH_3), 57.1 (CH_2), 28.6 (CH_2), 9.3 (CH_2).

MS (ESI) [m/z] mode positive: 736.5 [M+K] $^+$.

IR (neat, ATR) ν [cm^{-1}]: 3387, 3285 (OH), 2923, 2848, 1674 (C=O), 1591, 1236, 1017, 720.

(E)-2,2',2''-(10-(2-(4-((4-bromophenyl)diazenyl)-2,5-dimethoxyphenylamino)-2-oxoethyl)-1,4,7,10-tetraazacyclododecane-1,4,7-triyl)triacetate neodymium(III) complex (123)



Red-violet solid

R_f = 0.11 (CH₂Cl₂/MeOH: 8/2) revelator CAN

Procedure:

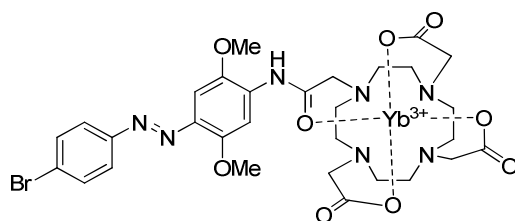
A solution of triacetic acid **119** (10 mg, 13.84 μmol , 1.00 equiv.) was prepared in methanol (2 mL) and then $\text{Nd}(\text{OTf})_3$ (8.2 mg, 13.84 μmol , 1.00 equiv.) was added in one portion. The reaction was carried out for 24 h at 50 $^\circ\text{C}$. Residues were taken up into methanol. Then the volume of solvent was reduced under vacuum and a violet-red solid was precipitated with diethyl ether (5mL). After filtration through Milipore and washings with diethyl ether, the residue was dried under vacuum to provide 11 mg (92% yield) of **123** as a red-violet solid.

Analyses:

MS (ESI) [m/z] mode negative: 863.0 [M] $^-$.

HRMS (ESI) [m/z] positive mode: calculated for $\text{C}_{30}\text{H}_{38}\text{BrN}_7\text{NdO}_9$: 861.0986, found: 861.0978; double charged ion calculated for $\text{C}_{30}\text{H}_{39}\text{BrN}_7\text{NdO}_9$: 431.0529, found: 431.0529.

(E)-2,2',2''-(10-(2-(4-((4-bromophenyl)diazenyl)-2,5-dimethoxyphenylamino)-2-oxoethyl)-1,4,7,10-tetraazacyclododecane-1,4,7-triyl)triacetate ytterbium(III) complex (124)



Red-violet solid

R_f = 0.20 (CH₂Cl₂/MeOH: 8/2) revelator CAN

Procedure:

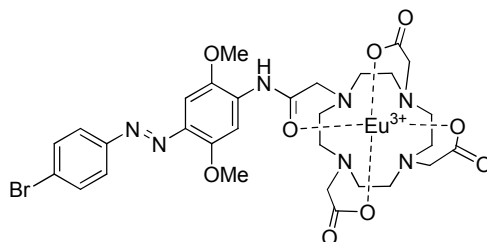
A solution of triacetic acid **119** (10 mg, 13.84 μmol , 1.00 equiv.) was prepared in methanol (2 mL). Then $\text{Yb}(\text{OTf})_3$ (8.6 mg, 13.84 μmol , 1.00 equiv.) was added in one portion. The reaction of complexation was carried out for 24 hours at 50 $^\circ\text{C}$. Residues were taken up into methanol. The volume of solvent was reduced under vacuum and a violet-red solid was precipitated with diethyl ether (5mL). After filtration through Milipore and washings with diethyl ether, the residue was dried under vacuum to provide 9 mg (73% yield) of **124** as a red-violet solid.

Analyses:

MS (ESI) [m/z] mode negative : 889.0 [M-H]⁻.

HRMS (ESI) [m/z] positive mode: calculated for C₃₀H₃₈BrN₇O₉Yb: 893.1285, found: 893.1275; double charged ion calculated for C₃₀H₃₉BrN₇O₉Yb: 447.0679, found: 447.0679.

(E)-2,2',2''-(10-(2-(4-((4-bromophenyl)diazenyl)-2,5-dimethoxyphenylamino)-2-oxoethyl)-1,4,7,10-tetraazacyclododecane-1,4,7-triyl)triacetate europium(III) complex (125)



Orange-red solid

R_f = 0.20 (CH₂Cl₂/MeOH: 8/2) revelator CAN

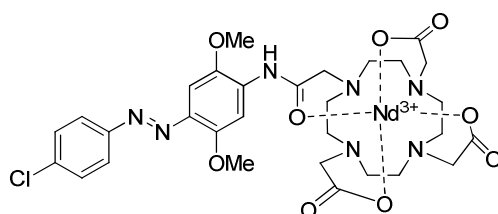
Procedure:

A solution of triacetic acid **119** (20 mg, 27.68 μmol, 1.00 equiv.) was prepared in methanol (4 mL) and then EuCl₃·6H₂O (10.1 mg, 27.68 μmol, 1.00 equiv) was added in one portion. The reaction was carried out for 20 hours at 50 °C. Residues were taken up into methanol. The volume of solvent was reduced under vacuum and a orange-red solid was precipitated with diethyl ether (5mL). After filtration through Milipore and washings with diethyl ether, the residue was dried under vacuum to provide 17 mg (71% yield) of **125** as an orange-red solid.

Analysis:

HRMS (ESI) [m/z] positive mode: calculated for C₃₀H₃₈BrEuN₇O₉: 872.1107, found: 872.1107; double charged ion calculated for C₃₀H₃₉BrEuN₇O₉: 436.5590, found: 436.5594.

(E)-2,2',2''-(10-(2-(4-((4-chlorophenyl)diazenyl)-2,5-dimethoxyphenylamino)-2-oxoethyl)-1,4,7,10-tetraazacyclododecane-1,4,7-triyl)triacetate neodymium(III) complex (126)



Red-violet solid

R_f = 0.11 (CH₂Cl₂/MeOH: 8/2) revelator CAN

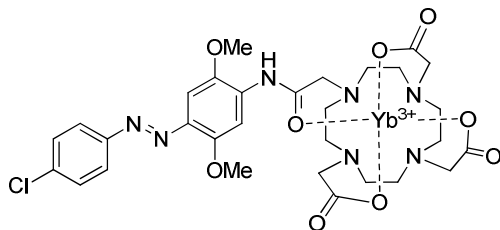
Procedure:

A solution of triacetic acid **120** (8 mg, 11.80 μmol, 1.00 equiv.) was prepared in methanol (2 mL). Then Nd(OTf)₃ (7 mg, 11.80 μmol, 1.00 equiv) was added in one portion. The reaction was carried out for 24 hours at 50 °C. Residues were taken up into methanol. The volume of solvent was reduced under vacuum and a violet-red solid was precipitated with diethyl ether (5mL). After filtration through Milipore and washings with diethyl ether, the residue was dried under vacuum to provide 8 mg (82% yield) of **126** as a red-violet solid.

Analyses:

HRMS (ESI) [m/z] positive mode: calculated for $C_{30}H_{38}ClN_7NdO_9$: 817.1491, found: 817.1484; double charged ion calculated for $C_{30}H_{39}ClN_7NdO_9$: 409.0782, found: 409.0787.

(E)-2,2',2''-(10-(2-(4-((4-chlorophenyl)diazenyl)-2,5-dimethoxyphenylamino)-2-oxoethyl)-1,4,7,10-tetraazacyclododecane-1,4,7-triyl)triacetate ytterbium(III) complex (127)



Red-violet solid

$R_f = 0.11$ ($CH_2Cl_2/MeOH$: 8/2) revelator CAN

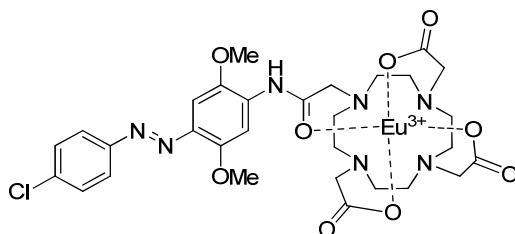
Procedure:

A solution of triacetic acid **120** (8 mg, 11.80 μ mol, 1.00 equiv.) was prepared in methanol (2 mL). Then $Yb(OTf)_3$ (7.3 mg, 11.80 μ mol, 1.00 equiv) was added in one portion. The reaction was carried out for 24 hours at 50 °C. Residues were taken up into methanol. The volume of solvent was reduced under vacuum and a violet-red solid was precipitated with diethyl ether (5mL). After filtration through Milipore and washings with diethyl ether, the residue was dried under vacuum to provide 7.5 mg (75% yield) of **127** as a red-violet solid was obtained.

Analyses:

HRMS (ESI) [m/z] positive mode: calculated for $C_{30}H_{38}ClN_7O_9Yb$: 849.1798, found: 849.1783; double charged ion calculated for $C_{30}H_{39}ClN_7O_9Yb$: 425.0935, found: 425.0931.

(E)-2,2',2''-(10-(2-(4-((4-chlorophenyl)diazenyl)-2,5-dimethoxyphenylamino)-2-oxoethyl)-1,4,7,10-tetraazacyclododecane-1,4,7-triyl)triacetate europium(III) complex (128)



Red-violet solid

$R_f = 0.11$ ($CH_2Cl_2/MeOH$: 8/2) revelator CAN

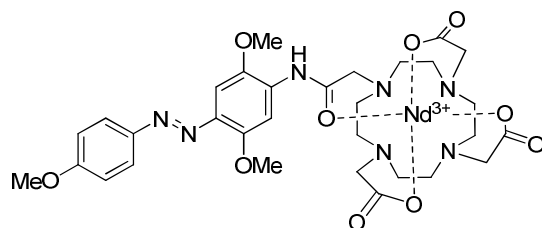
Procedure:

A solution of triacetic acid **120** (10 mg, 14.81 μ mol, 1.00 equiv.) was prepared in methanol (2 mL) and $EuCl_3 \cdot 6H_2O$ (5.4 mg, 14.81 μ mol, 1.00 equiv) was added in one portion. The reaction was carried out for 24 h at 50 °C. Residues were taken up into methanol. The volume of solvent was reduced under vacuum and a violet-red solid was precipitated with diethyl ether (5mL). After filtration through Milipore and washings with diethyl ether, the residue was dried under vacuum to provide 10 mg (81% yield) of **128** as a red violet solid.

Analysis:

HRMS (ESI) [m/z] positive mode: calculated for $C_{30}H_{38}ClEuN_7O_9$: 828.1619, found: 828.1612; double charged ion calculated for $C_{30}H_{39}ClEuN_7O_9$: 414.5846, found: 414.5841.

(E)-2,2',2''-(10-(2-(2,5-dimethoxy-4-((4-methoxyphenyl)diazenyl)phenylamino)-2-oxoethyl)-1,4,7,10-tetraazacyclododecane-1,4,7-triyl)triacetate neodymium(III) complex (129)



Dark violet solid

R_f = 0.11 (CH₂Cl₂/MeOH: 2/8) revelator CAN

Procedure:

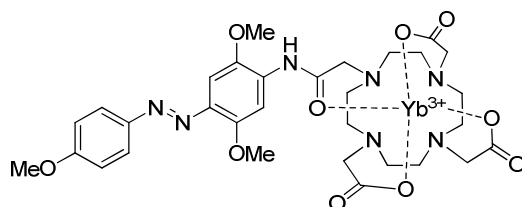
A solution of triacetic acid **121** (10 mg, 14.84 μmol, 1.00 equiv.) was prepared in methanol (2 mL) and then Nd(OTf)₃ (8.8 mg, 14.84 μmol, 1.00 equiv) was added in one portion. The reaction was carried out for 24 h at 50 °C. Residues were taken up into methanol. The volume of solvent was reduced under vacuum and a violet-red solid was precipitated with diethyl ether (5mL). After filtration through Milipore and washings with diethyl ether, the residue was dried under vacuum to provide 10.5 mg (90% yield) of **129** as a dark violet solid.

Analyses:

MS (ESI) [m/z] negative mode: 812.5 [M-H]⁻, positive mode: 814.0 [M+H]⁺, 835.0 [M+Na]⁺.

HRMS (ESI) [m/z] positive mode: calculated for C₃₁H₄₁N₇NdO₁₀: 813.1987, found: 813.1978; double charged ion calculated for C₃₁H₄₂N₇NdO₁₀: 407.1030, found: 407.1031.

(E)-2,2',2''-(10-(2-(2,5-dimethoxy-4-((4-methoxyphenyl)diazenyl)phenylamino)-2-oxoethyl)-1,4,7,10-tetraazacyclododecane-1,4,7-triyl)triacetate ytterbium(III) complex (130)



Dark violet solid

R_f = 0.11 (CH₂Cl₂/MeOH: 2/8) revelator CAN

Procedure:

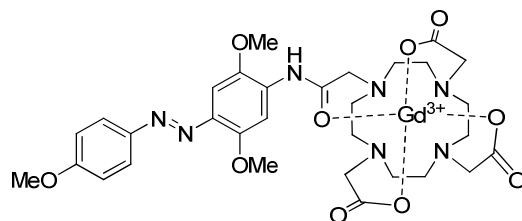
A solution of triacetic acid **121** (29 mg, 43.02 μmol, 1.00 equiv.) was prepared in methanol (6 mL). Then Yb(OTf)₃ (26.7 mg, 43.02 μmol, 1.00 equiv) was added in one portion. The reaction was carried out for 24 h at 50 °C. Residues were taken up into methanol. The volume of solvent was reduced under vacuum and a violet-red solid was precipitated with diethyl ether (10 mL). After filtration through Milipore and washings with diethyl ether, the residue was dried under vacuum to provide 27.4 mg (75% yield) of **130** as a dark violet solid.

Analyses:

MS (ESI) [m/z] negative mode: 842.5 [M-H]⁻, positive mode: 844.5 [M+H]⁺, 867.0 [M+Na]⁺.

HRMS (ESI) [m/z] positive mode: calculated for C₃₁H₄₁N₇O₁₀Yb: 845.2303, found: 845.2308; double charged ion calculated for C₃₁H₄₂N₇O₁₀Yb: 423.1188, found: 423.1196.

(E)-2,2',2''-(10-(2-(2,5-dimethoxy-4-((4-methoxyphenyl)diazenyl)phenylamino)-2-oxoethyl)-1,4,7,10-tetraazacyclododecane-1,4,7-triyl)triacetate gadolinium(III) complex (131)



Dark brown solid

R_f = 0.11 (CH₂Cl₂/MeOH: 2/8) revelator CAN

Procedure:

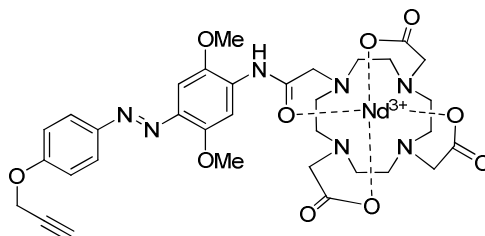
A solution of triacetic acid **121** (10 mg, 14.84 μmol, 1.00 equiv.) was prepared in methanol (2 mL). Then Gd(OTf)₃ (8.9 mg, 14.84 μmol, 1.00 equiv) was added in one portion. The reaction was carried out for 24 h at 50 °C. Residues were taken up into methanol. The volume of solvent was reduced under vacuum and a violet-red solid was precipitated with diethyl ether (5mL). After filtration through Milipore and washings with diethyl ether, the residue was dried under vacuum to provide 9.8 mg (82% yield) of **131** as a dark brown solid.

Analyses:

MS (ESI) [m/z] negative mode: 827.5 [M-H]⁻, positive mode: 829.0 [M+H]⁺, 849.0 [M+Na]⁺.

HRMS (ESI) [m/z] positive mode: calculated for C₃₁H₄₁GdN₇O₁₀: 829.2157, found: 829.2167; double charged ion calculated for C₃₁H₄₂GdN₇O₁₀: 415.1115, found: 415.1122.

(E)-2,2',2''-(10-(2-(2,5-dimethoxy-4-((4-(prop-2-ynoxy)phenyl)diazenyl)phenylamino)-2-oxoethyl)-1,4,7,10-tetraazacyclododecane-1,4,7-triyl)triacetate neodymium(III) complex (132)



Dark violet solid

R_f = 0.11 (CH₂Cl₂/MeOH: 6/4) revelator CAN

Procedure:

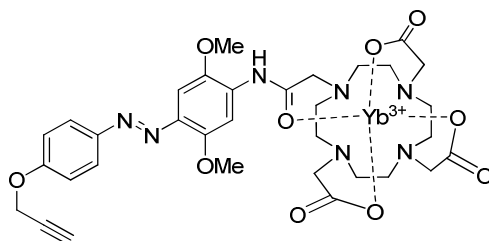
A solution of triacetic acid **122** (10 mg, 14.32 μmol, 1.00 equiv.) was prepared in methanol (2 mL). Then Nd(OTf)₃ (8.5 mg, 14.32 μmol, 1.00 equiv) was added in one portion. The reaction was carried out for 7 h at 50 °C. Residues were taken up into methanol. The volume of solvent was reduced under vacuum and a violet-red solid was precipitated with diethyl ether (5mL). After filtration through Milipore and washings with diethyl ether, the residue was dried under vacuum to provide 10 mg (81% yield) of **132** as dark brown-violet crystals.

Analyses:

MS (ESI) [m/z] positive mode: 839.5 [M+H]⁺, 861.0 [M+Na]⁺.

HRMS (ESI) [m/z] positive mode: calculated for C₃₃H₄₁N₇NdO₁₀: 837.1987, found: 837.1979; double charged ion calculated for C₃₃H₄₂N₇NdO₁₀: 419.1030, found: 419.1035.

(E)-2,2',2''-(10-(2-(2,5-dimethoxy-4-((4-(prop-2-ynoxy)phenyl)diazenyl)phenylamino)-2-oxoethyl)-1,4,7,10-tetraazacyclododecane-1,4,7-triyl)triacetate ytterbium(III) complex (133)



Dark violet solid

R_f = 0.08 (CH₂Cl₂/MeOH: 6/4) revelator CAN

Procedure:

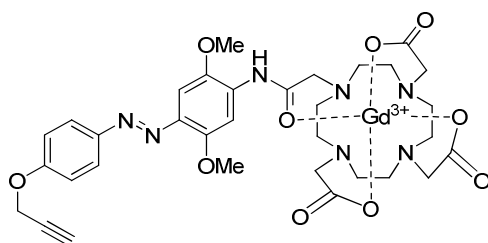
A solution of triacetic acid **122** (10 mg, 14.32 μmol, 1.00 equiv.) was prepared in methanol (2 mL). Then Nd(OTf)₃ (8.9 mg, 14.32 μmol, 1.00 equiv) was added in one portion. The reaction was carried out for 7 h at 50 °C. Residues were taken up into methanol. The volume of solvent was reduced under vacuum and a violet-red solid was precipitated with diethyl ether (5mL). After filtration through Milipore and washings with diethyl ether, the residue was dried under vacuum to provide 12 mg (quantitative) of **133** as dark brown-violet crystals.

Analyses:

MS (ESI) [m/z] positive mode: 869.0 [M+H]⁺, 890.0 [M+Na]⁺.

HRMS (ESI) [m/z] positive mode: calculated for C₃₃H₄₁N₇O₁₀Yb: 869.2303, found: 869.2304; double charged ion calculated for C₃₃H₄₂N₇O₁₀Yb: 435.1188, found: 435.1193.

(E)-2,2',2''-(10-(2-(2,5-dimethoxy-4-((4-(prop-2-ynoxy)phenyl)diazenyl)phenylamino)-2-oxoethyl)-1,4,7,10-tetraazacyclododecane-1,4,7-triyl)triacetate gadolinium(III) complex (134)



Dark brown-violet semi-solid

R_f = 0.08 (CH₂Cl₂/MeOH: 6/4) revelator CAN

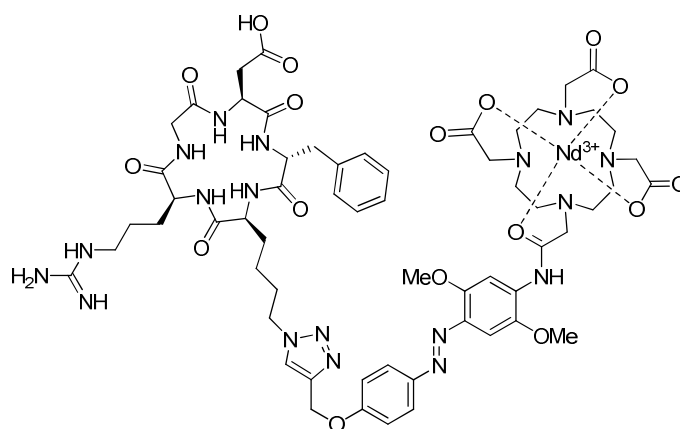
Procedure:

A solution of triacetic acid **122** (13 mg, 18.62 μmol, 1.00 equiv.) was prepared in methanol (2.5 mL). Then Gd(OTf)₃ (11.2 mg, 18.62 μmol, 1.00 equiv) was added in one portion. The reaction was carried out for 7 h at 50 °C. Residues were taken up into methanol. The volume of solvent was reduced under vacuum and a violet-red solid was precipitated with diethyl ether (5mL). After filtration through Milipore and washings with diethyl ether, the residue was dried under vacuum to provide 16 mg (quantitative) of **134** as dark brown-violet semi-solid.

Analyses:

HRMS (ESI) [m/z] positive mode: calculated for C₃₃H₄₁GdN₇O₁₀: 853.5151, found: 853.2158; double charged ion calculated for C₃₃H₄₂GdN₇O₁₀: 427.1114, found: 427.1115.

2,2',2''-(10-(2-(4-((E)-(4-((1-(4-((2S,5S,11S,14R)-14-benzyl-11-(carboxymethyl)-5-(3-guanidinopropyl)-3,6,9,12,15-pentaaxo-1,4,7,10,13-pentaazacyclopentadecan-2-yl)butyl)-1H-1,2,3-triazol-4-yl)methoxy)phenyl)diazenyl)-2,5-dimethoxyphenylamino)-2-oxoethyl)-1,4,7,10-tetraazacyclododecane-1,4,7-triyl)triacetate neodymium(III) complex (135)



Yellow-orange powder

HPLC (Nucleosil^(R) 300-5 RP- C18) gradient CH₃CN:H₂O (0.1% TFA) 22->37%, 3 mL/min. t_R=17.2 min.

Procedure:

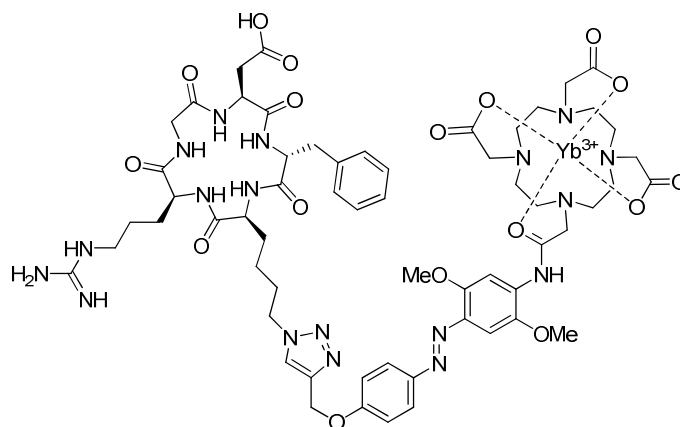
Solution **A**: an Nd complex **132** (15.0 mg, 17.29 μmol, 1.00 equiv.) in MiliQ water (500 μL) was mixed with a solution of cyclopeptide RGD (16.3 mg, 25.94 μmol, 1.50 equiv.) in HEPES buffer (500 μL, 100 mM, pH=7.5). Separately in a small eppendorf, a solution **B** of ligand THPTA (37.3 mg, 85.85 μmol, 5.00 equiv.) and aminoguanidine (28.7 mg, 259.4 μmol, 15.00 equiv.) was prepared in 500 μL of HEPES buffer, then solution of CuSO₄·5H₂O (17.3 mg, 69.16 μmol, 4.00 equiv.) in 200 μL of MiliQ was added (an apparition of intensive blue color), followed by the solution of sodium ascorbate (27.4 mg, 138.32 μmol, 8.00 equiv.) in 250 μL of HEPES (the solution became slightly yellow). The mixture **B** was immediately added to the solution **A**.

The reaction vigorously stirred for 30 minutes at room temperature, checked by HPLC and stopped with addition of 1 mL of MiliQ water with 5% of TFA. The content of flask was centrifuged to remove the precipitate. The supernatant was concentrated to 10 mL and purified by semipreparative HPLC (Nucleosil, RP-C18, gradient CH₃CN/H₂O (+0.1% TFA) 22%/78%-->37%/63%, 3 mL/min., 30 min.). The whole conversion of starting material was observed, the yield after purification was 40%.

Analyses:

HRMS (ESI) [m/z] positive mode: double charged ion calculated for C₆₀H₈₁N₁₈NdO₁₇: 733.7547, found: 733.7550, double charged sodium adduct, calculated for C₆₀H₈₀N₁₈ NaNdO₁₇: 744.7456, found: 744.74520, double charged potassium adduct, calculated for C₆₀H₈₀KN₁₈NdO₁₇: 752.7326, found: 752.7320.

2,2',2''-(10-(2-(4-((E)-(4-((1-(4-((2S,5S,11S,14R)-14-benzyl-11-(carboxymethyl)-5-(3-guanidinopropyl)-3,6,9,12,15-pentaaxo-1,4,7,10,13-pentaazacyclopentadecan-2-yl)butyl)-1H-1,2,3-triazol-4-yl)methoxy)phenyl)diazenyl)-2,5-dimethoxyphenylamino)-2-oxoethyl)-1,4,7,10-tetraazacyclododecane-1,4,7-triyl)triacetate ytterbium(III) complex (135)



Yellow solid.

HPLC (Nucleosil^(R) 300-5 RP- C18) gradient CH₃CN/H₂O (0.1% TFA) 22%→37%, 3 mL/min.

t_R = 17.2 min.

Procedure:

Solution **A**: an Yb complex **133** (15.0 mg, 17.90 μmol, 1.00 equiv.) in MiliQ water (500 μL) was mixed with a solution of cyclopeptide RGD (16.9 mg, 26.85 μmol, 1.50 equiv.) in HEPES buffer (500 μL, 400 mM, pH=7.5), this solution **A** was diluted with 500 μL of water MiliQ, followed by one drop of DMF to solubilise peptide.

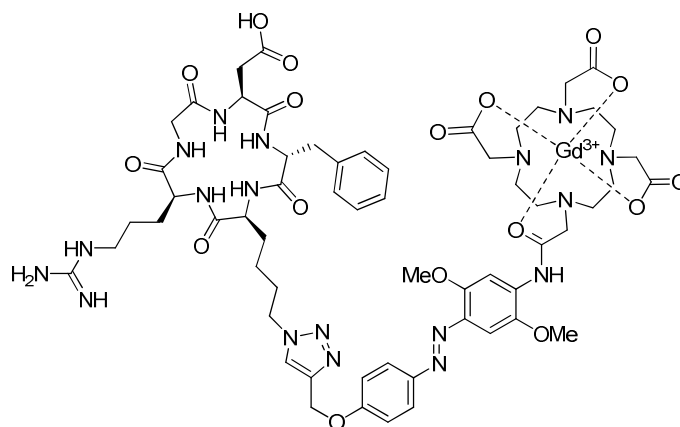
Separately in a small eppendorf, a solution **B** of ligand THPTA (41.27 mg, 94.98 μmol, 5.30 equiv.) and aminoguanidine (29.7 mg, 268.5 μmol, 15.0 equiv.) was prepared in 500 μL of water MiliQ, then solution of CuSO₄·5H₂O (17.88 mg, 71.6 μmol, 4 equiv.) in 200 μL of MiliQ was added (an apparition of intensive blue color), followed by the solution of sodium ascorbate (27.94 mg, 143.2 μmol, 8 equiv.) in 250 μL of HEPES (the solution became slightly yellow). The mixture **B** was immediately added to the solution **A**.

The reaction was vigorously stirred for 30 minutes at room temperature, checked by HPLC and quenched by addition of 1 mL of a 5% TFA MiliQ water. The content of flask was centrifuged to remove the precipitate. The supernatant was concentrated to 10 mL and purified by semipreparative HPLC (Nucleosil, RP-C18, gradient CH₃CN/H₂O (+0.1% TFA) 22%/78%→37%/63%, 3 mL/min., 30 min.). The whole conversion of starting material was observed, the yield after purification on HPLC column was 40%.

Analyses:

HRMS (ESI) [m/z] positive mode: double charged ion calculated for C₆₀H₈₁N₁₈O₁₇Yb: 749.7707, found: 749.7704.

2,2',2''-(10-(2-(4-((E)-(4-((1-(4-((2S,5S,11S,14R)-14-benzyl-11-(carboxymethyl)-5-(3-guanidinopropyl)-3,6,9,12,15-pentaaxo-1,4,7,10,13-pentaazacyclopentadecan-2-yl)butyl)-1H-1,2,3-triazol-4-yl)methoxy)phenyl)diazenyl)-2,5-dimethoxyphenylamino)-2-oxoethyl)-1,4,7,10-tetraazacyclododecane-1,4,7-triyl)triacetate gadolinium(III) complex (136)



Yellow solid.

HPLC (Nucleosil^(R) 300-5 RP- C18) gradient CH₃CN/H₂O (0.1% TFA) 22%→37%, 3 mL/min.

t_R = 15.8 min.

Procedure:

Solution **A**: an Gd complex **134** (18.0 mg, 21.55 μmol, 1.00 equiv.) in MiliQ water (500μL) was mixed with a solution of cyclopeptide RGD (20.3 mg, 32.32 μmol, 1.50 equiv.) in HEPES buffer (500μL, 100 mM, pH=7.5). Separately in a small eppendorf, a solution **B** of ligand THPTA (46.8 mg, 107.75 μmol, 5.00 equiv.) and aminoguanidine (35.7 mg, 323.25 μmol, 15.00 equiv.) was prepared in 500 μL of HEPES buffer, then solution of CuSO₄·5H₂O (21.5 mg, 86.2 μmol, 4.00 equiv.) in 200 μL of MiliQ was added (an apparition of intensive blue color), followed by the solution of sodium ascorbate (34.2 mg, 172.4 μmol, 8.00 equiv.) in 250 μL of HEPES (the solution became slightly yellow). The mixture **B** was immediately added to the solution **A**.

The reaction was vigorously stirred for 30 minutes at room temperature, checked by HPLC and stopped with addition of 1mL of MiliQ water with 5% of TFA. The content of flask was centrifuged to remove the precipitate. The supernatant was concentrated to 10 mL and purified by semipreparative HPLC (Nucleosil, RP-C18, gradient CH₃CN/H₂O (+0.1% TFA) 22%/78%→37%/63% , 3mL/min., 30 min.). The whole conversion of starting material was observed, the yield after purification on HPLC column was 36%.

Analyses:

HRMS (ESI) [m/z] positive mode: mono charged ion calculated for C₆₀H₈₀GdN₁₈O₁₇: 1482.5201, found: 1482.5175; double charged ion calculated for C₆₀H₈₁GdN₁₈O₁₇: 741.7636, found: 741.7639; triple charged ion calculated for C₆₀H₈₂GdN₁₈O₁₇: 494.8448, found: 494.8450.

Annexes

I. Determination of the enantiomeric excess of chiral compounds

Supercritical fluid chromatography (SFC) is a relatively recent chromatographic technique, commercially available since only about 1982. What differentiates SFC from other chromatographic techniques (gas chromatography (GC) and high performance liquid chromatography (HPLC)) is the use of a supercritical fluid as the mobile phase.

Supercritical fluid chromatography has several main advantages over other conventional chromatographic techniques (GC and HPLC). Compared with HPLC, SFC provides rapid separations without or with small quantity of organic solvents, such as methanol or ethanol. Because SFC generally uses carbon dioxide collected as a byproduct of other chemical reactions or is collected directly from the atmosphere, it contributes no new chemicals to the environment. In addition, SFC separations can be done faster than HPLC separations because the diffusion of solutes in supercritical fluids is about ten times greater than that in liquids (and about three times less than in gases). This results in a decrease in resistance to mass transfer in the column and allows for fast high resolution separations. Compared with GC, capillary SFC can provide high resolution chromatography at much lower temperatures. This allows fast analysis of thermo labile compounds.

I.1. Analysis of organophosphorus chiral compounds by SFC

Enantiomeric excesses and purity were determined by chiral SFC measurement on a Waters Investigator SFC (Waters, Guyancourt, France) equipped with a Waters 2998 Photodiode Array detector with high-pressure resistant cell. The column was a Lux Cellulose-1 (250 x 4.6 mm, 5 μ m) from Phenomenex (Torrance, CA). Operating conditions were always isocratic, with methanol or ethanol modifier. Flow rate was 3 mL/min, outlet pressure 15 MPa, column oven temperature 25°C. Retention times (t_R) are given in minutes. Enantiomers were identified by comparison of retention times, whenever the second enantiomer could be synthesized, and by comparison of UV spectra as provided by the photodiode-array detector.

Below we present the chromatograms of synthesized enantiomeric couples for compounds **22-25**, which served as a model for the calculation of enantiomeric excess and permits to optimize the separation conditions.

Compound 22

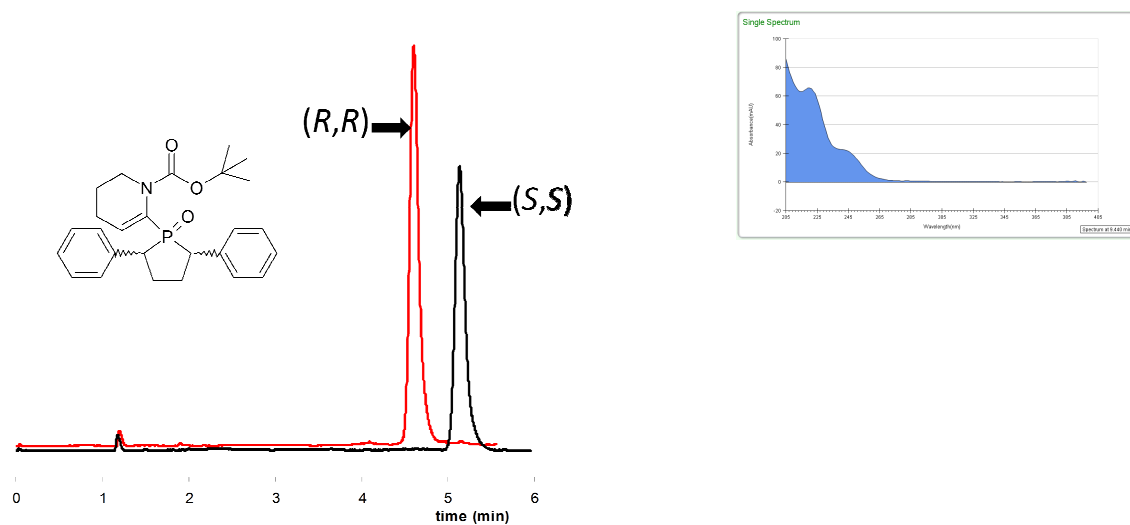


Fig. 183 Lux Cellulose-1 (250 x 4.6 mm, 5 μ m), CO₂-methanol 90:10 (v/v), 3 mL/min, 25°C, 15 MPa.

t_R (R,R): 4.61; t_R (S,S): 5.14.

Compound 23

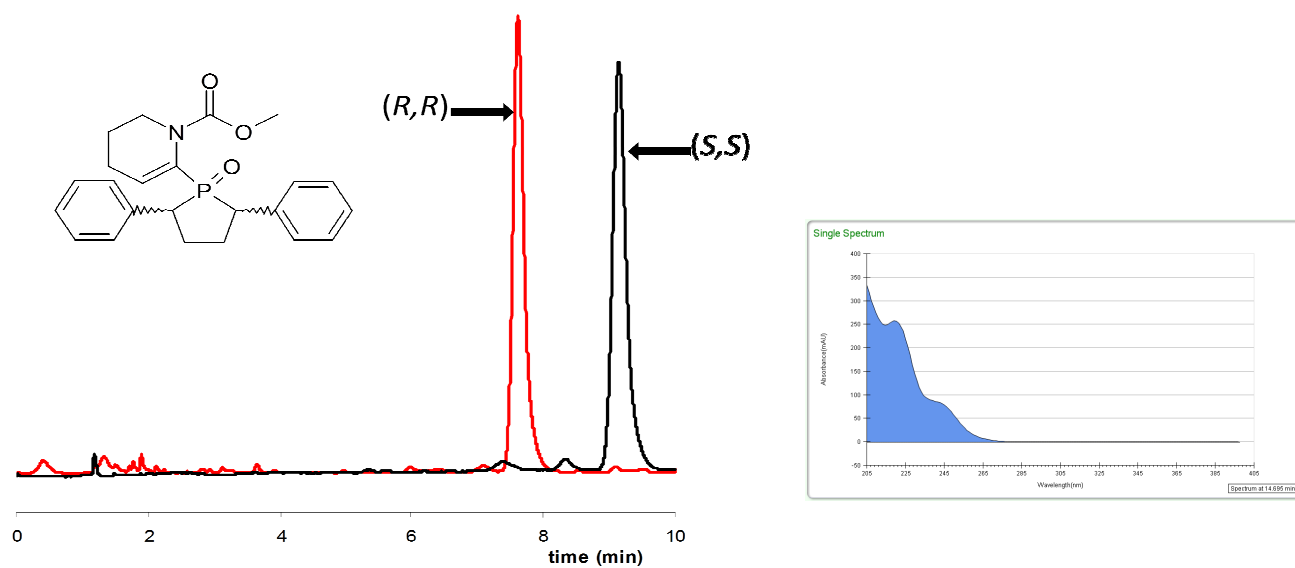


Fig. 184 Lux Cellulose-1 (250 x 4.6 mm, 5 μ m), CO₂-methanol 90:10 (v/v), 3 mL/min, 25°C, 15 MPa.

t_R (R,R): 7.62; t_R (S,S): 9.14.

Compound 24

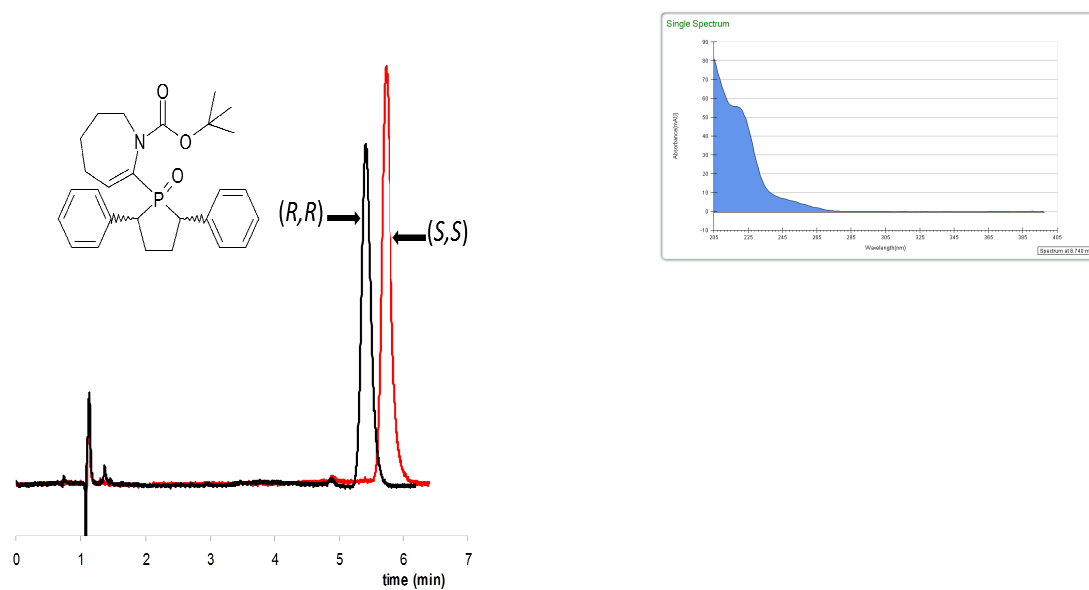


Fig. 185 Lux Cellulose-1 (250 x 4.6 mm, 5 μ m), CO₂-methanol 90:10 (v/v), 3 mL/min, 25°C, 15 MPa.

t_R (R,R): 5.72; t_R (S,S): 5.35.

Compound 25

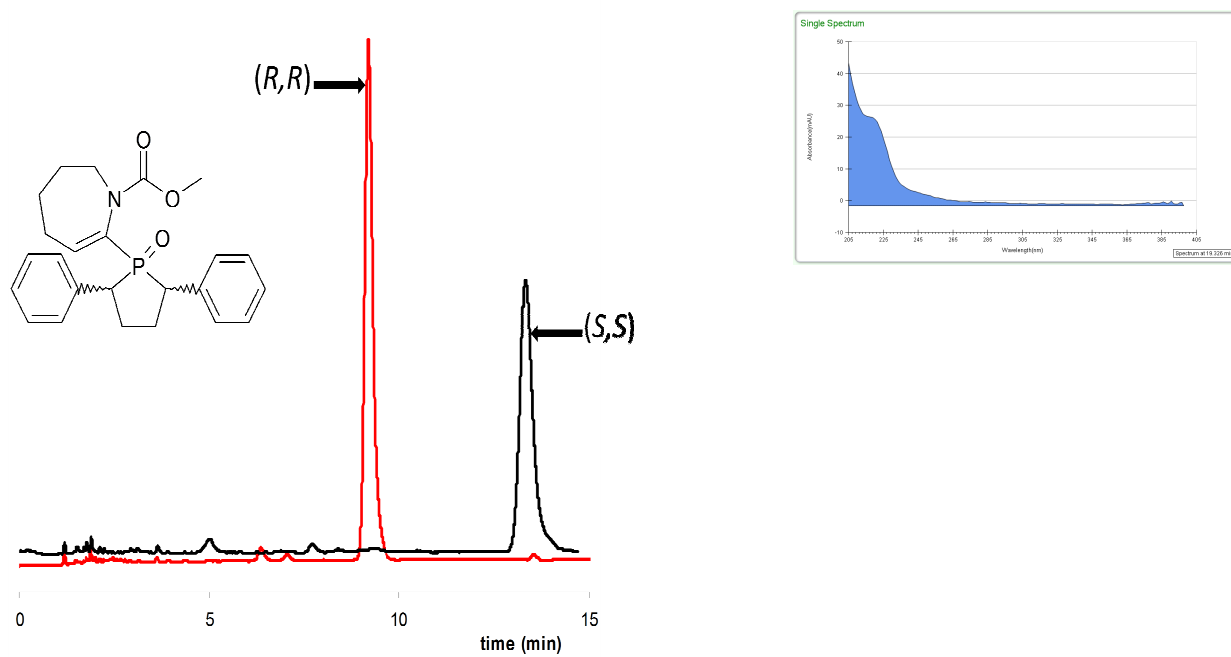


Fig. 186 Lux Cellulose-1 (250 x 4.6 mm, 5 μ m), CO₂-methanol 90:10 (v/v), 3 mL/min, 25°C, 15 MPa.

t_R (R,R): 9.64; t_R (S,S): 14.3.

I.2. SFC separation of racemic mixtures of phosphine-containing non-natural amino acids

All synthesized products were subjected to chiral separation by Supercritical Fluid Chromatography. As stated before, conducted reactions were not stereoselective, even in the case of (-)-sparteine application, thus the purification of enantiomers was required. The purification on the semi-preparative SFC system on the column Lux Cellulose-1 (the packing with cellulose tris(3,5-dimethylphenylcarbamate)) and Lux Cellulose-2 (cellulose tris(3-chloro-4-methylphenylcarbamate)) were performed.²⁷⁵ Separation conditions were optimized to achieve the highest resolution in face of short purification time. On the Fig. 187 we presented five chromatograms of representative products with high resolution, every separation completed upon 10 minutes with optimized gradients.

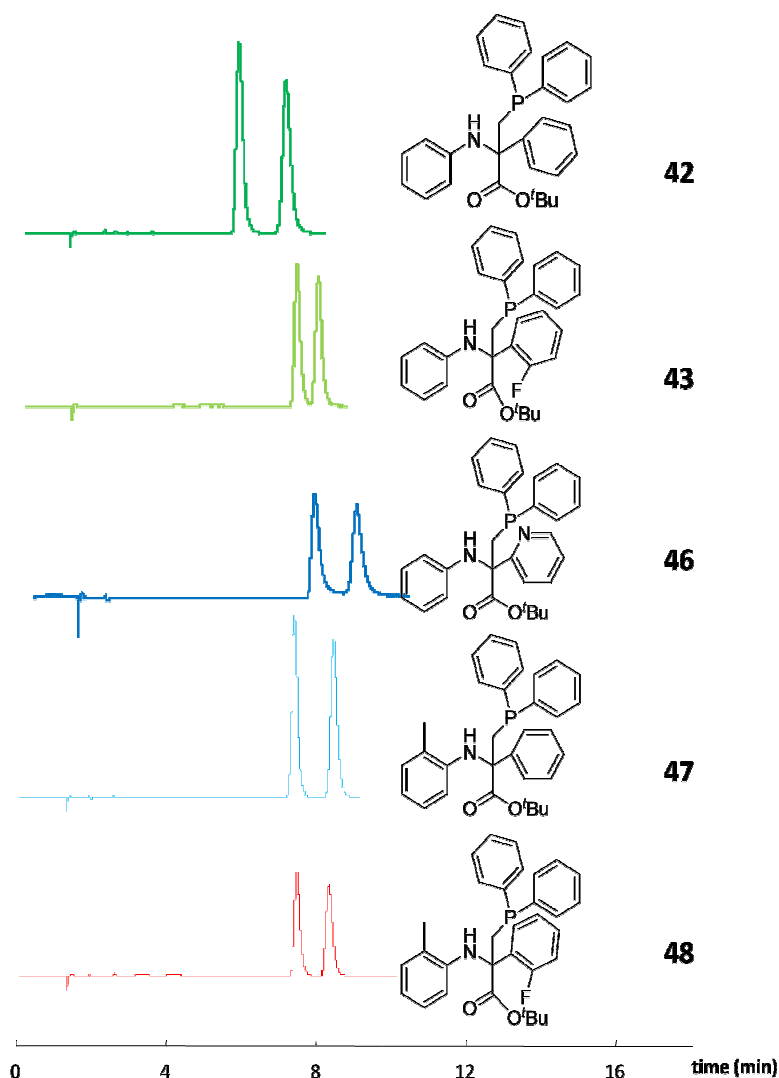


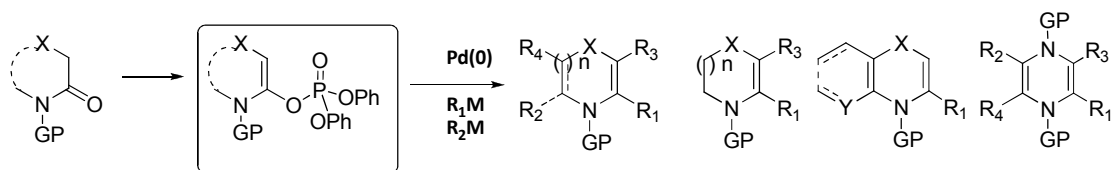
Fig. 187 The best separation conditions: 5% of EtOH, 30 °C, 150 bar backpressure, 3 mL/min, column Lux 1 for compounds 43,47, 48 and Lux 2 for 42 and 46.

²⁷⁵ C. West, A. Bouet, I. Gillaizeau, G. Coudert, M. Lafosse, E. Lesellier, *Chirality*, **2010**, *22*, 245.

Streszczenie

Związki heterocykliczne zawierające atom azotu stanowią ważną grupę produktów syntetycznych, są one obecne w większości biologicznie czynnych cząsteczek, takich jak kwasy nukleinowe, witaminy, przekaźniki energii chemicznej w metabolizmie komórek (ATP), kofaktory białek i wiele innych. Występują one również w przemyśle chemicznym (barwniki, konserwanty, perfumy), farmaceutycznym i rolnictwie jako środki ochrony roślin. Ze względu na ich wszechobecność i biologiczne zapotrzebowanie, syntezywanie nowych pochodnych jest centralnym zagadnieniem w chemii heterocyklicznej. Enkarbaminiany i enamidy to grupa nieaktywowanych enamin, należąca do wszechstronnych produktów pośrednich w syntezie związków heterocyklicznych zawierających atom azotu.

Reakcje sprzęgania krzyżowego pochodnych eterów enolowych katalizowane związkami palladu stanowią korzystne podejście do syntezy enkarbaminianów i enamidów spośród dostępnych metod. Wiele grup badawczych zaprezentowało użyteczność pochodnych laktamów i imidów do otrzymywania fosforanów enolowych jako produktów przejściowych w syntezie enamidów. Zdolność do przekształcenia powyższych fosforanów enoli w reakcji sprzęgania krzyżowego typu Suzuki-Miyaura, Stille, Sonogashira, itp. w obecności różnych heteroatomów czyni je użytecznymi substratami w konstrukcji różnorodnych systemów heterocyklicznych. W oparciu o tą metodę, opracowaną i udoskonalaną od kilku lat w laboratorium prof. I. Gillaizeau, cały szereg struktur heterocyklicznych (tj. pochodne 1,4-dihydropirydiny, 1,4-oksazyny, 1,4-dihydropirazyiny) posiadających ugrupowanie enkarbaminianu zostało zsyntezowane (Schemat 1).



GP = C(O)OR₂ (enkarbaminian), C(O)R₂ (enamid)
R₁, R₂, R₃, R₄ = Alkyl, alkenyl, acyl, aryl, heteroaryl, alkil ...
X = O, CR₂, NR₂
Y = CH, N
n = 1, 2, 8

Schemat 1

Biorąc pod uwagę ekspertyzę i badania przedsięwzięte w grupie prof. Gillaizeau dotyczące otrzymywania i reaktywności enkarbaminianów, niniejsza rozprawa doktorska będzie podejmowała tematykę syntezy nowych związków heterocyklicznych i ich wszechstronne zastosowanie. Pierwsza

część rozprawy doktorskiej zostanie poświęcona reaktywności enkarbaminianów i enamidów w reakcji sprzęgania krzyżowego katalizowanej kompleksami palladowymi, tworząc bezpośrednio wiązanie C-P oraz w reakcji addycji nukleofilowej anionu fosfinowego w celu utworzenia nowych bloków syntetycznych zawierających atom fosforu. Druga część pracy doktorskiej będzie dotyczyć otrzymywania i charakteryzacji oryginalnych chromoforów opartych na rdzeniu pirazynowym, wywodzących się z ugrupowania dihydropirazynowego. Powyższe związki chromoforowe zostały zaprojektowane w celu utworzenia systemów sensybilizujących kationy lantanowców i tym samym, mogą zostać one wykorzystane jako oryginalne sensybilizatory organiczne do obrazowania molekularnego w bliskiej podczerwieni.

Pierwszy rozdział: Heterocykliczne związki organofosforowe - tworzenie wiązania C-P

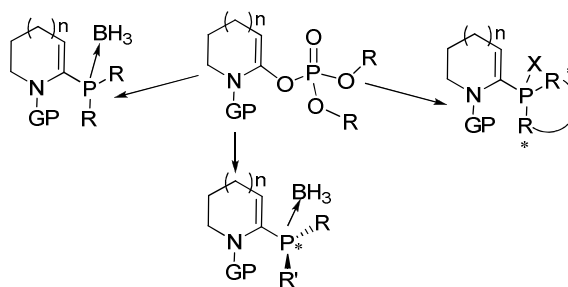
Podstawowym celem pierwszej części pracy doktorskiej było zsyntetyzowanie nowych, na stan obecny nieopublikowanych, produktów organofosforowych na drodze oryginalnych ścieżek syntezy opracowanych w grupie prof. Gillaizeau.

Otrzymywanie nowych związków zawierających atom fosforu jest tematem stale budzącym zainteresowanie w chemii organicznej ostatnich lat. Produkty organofosforowe mają szerokie zastosowanie w wielu dziedzinach życia codziennego oraz przemysłu chemicznego. Z biologicznego punktu widzenia, pełnią one istotną rolę w procesach przemiany materii (ATP), w przekazie materiału genetycznego (DNA, RNA) oraz stanowią materiał budulcowy błon komórkowych (fosfolipidy). Ze względu na izosteryczność grupy fosforowej z grupą karboksylową, fosforowe analogi aminokwasów i peptydów są ważną grupą związków farmaceutycznych stosowanych jako inhibitory enzymów, związki antybakteryjne i anty-HIV. Dodatkowo, organofosforany posiadają właściwości inhibujące acetylocholinesterazę przez co są szeroko stosowane jako pestycydy, insektycydy i herbicydy oraz jako gazy bojowe.

W przemyśle chemicznym są one wykorzystywane jako chiralne ligandy dla kompleksów metali przejściowych w reakcjach katalizy. Umożliwiają one otrzymywanie enancjomerycznie czystych produktów w asymetrycznych przemianach, takich jak uwodornienie, utlenianie, nukleofilowa addycja organometalicznych reagentów do aldehydów, ketonów i imidów, reakcje aldolowe, reakcje cyklizacji i wiele innych. Dużą zaletą ligandów zawierających atom fosforu jest różnorodność możliwych kombinacji podstawników oraz ewentualność wprowadzenia centrum asymetrycznego zarówno na atomie fosforu, jak i na atomie węgla sąsiadującym z fosforem oraz poprzez chiralność osiową. Ponadto, związki organofosforowe znalazły zastosowanie jako organokatalizatory, ze względu na ich właściwości jednocześnie nukleofilu i kwasu Brønsteda (pod postacią aksjalnie chiralnych kwasów fosforowych).

Część literaturowa pierwszego rozdziału rozprawy doktorskiej zostanie poświęcona reakcjom tworzenia wiązania C-P. Najstarszą, lecz ciągle używaną metodą, jest reakcja Arbuzowa opierająca się na nukleofilowym ataku fosforynu na halogenek alkilowy tworząc fosfiniany dialkilowe. Kolejna cytowana metoda to reakcja fosfa-Michaela, addycja nukleofilowego reagenta fosforowego do olefinowego akceptora. Reakcja ta stała się wszechstonną ścieżką syntezy licznych asymetrycznych pochodnych fosforowych w łagodnych warunkach reakcji. Następną metodą otrzymywania tytułowych związków jest hydrofosfonylacja - przyłączenie fosfonianu do aktywowanego wiązania podwójnego. Reakcja sprzęgania krzyżowego katalizowana kompleksami metali przejściowych to ostatnia i najszerzej opisana metoda syntezy związków organofosforowych. Niniejszy podrozdział został poświęcony licznym przykładom tych reakcji z różnymi substratami fosforowymi (tlenkami fosfin, trialkil- lub triarylfosfinami, boranowymi kompleksami fosfin i chlorkami fosfin) jako partnerami w sprzęganiu. Dodatkowo sprzęganie tworzące wiązanie C(sp)-P oraz C(sp³)-P i przykłady reakcji asymetrycznych zostały zaprezentowane.

Część eksperymentalną pierwszego rozdziału zadedykowano syntezie oryginalnych pochodnych α -amidofosfin na drodze nowatorskiej metody sprzęgania krzyżowego pomiędzy fosforanami enolu oraz boranowymi kompleksami fosfin. Zastosowana metoda prowadząca bezpośrednio do tworzenia wiązania C-P nigdy dotychczas nie została opisana. Produkty pośrednie syntezy - fosforany enolu - to łatwo dostępne, stabilne i mniej kosztowne odpowiedniki trifluorometanosulfonianów i tosylianów, stosowane szeroko w laboratorium. Do optymalizacji warunków reakcji zastosowano niechiralny kompleks boranowy difenylofosfiny. Stosując różne zasady nieorganiczne, rozpuszczalniki, czas i temperaturę reakcji wytypowano najlepszy układ katalizujący, a następnie rozszerzono powyższą syntezę o związki chiralne - z centrum asymetrycznym umieszczonym na atomie fosforu i na atomie węgla w pozycji α do atomu fosforu (Schemat 2).

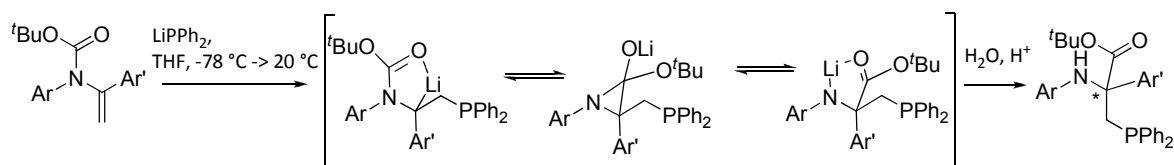


Schemat 2

Na podstawie badań czystości enancjomerycznej otrzymanych produktów, poprzez superkrytyczną chromatografię cieczą z chiralną fazą stacjonarną, stwierdzono, że reakcja substratów z asymetrycznym atomem fosforu spowodowała racemizację centrum chiralnego. Natomiast w przypadku związków niosących centrum asymetryczne na atomach węgla α w stosunku do fosforu,

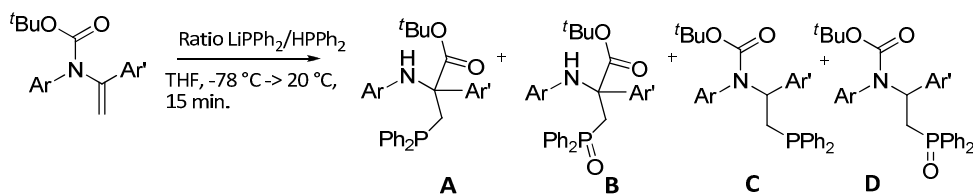
chiralność reakcji została zachowana. Cykliczne kompleksy fosfin i cykliczne tlenki fosforanów zostały otrzymane z umiarkowanymi do dobrych wydajnościami i wysokimi nadmiarami enancjomerycznymi.

W drugiej części pierwszego rozdziału niniejszej rozprawy opisano reakcję nukleofilowej addycji aninów fosfinowych do niecyklicznych enkarbaminianów, prowadzącą do fosfinowych pochodnych nienaturalnych aminokwasów. Zaprojektowana ścieżka syntezy opiera się na specyficznej spontanicznej migracji grupy alkoksykarbonylowej od atomu azotu do czwartorzędowego atomu węgla poprzez formację cyklu azirydynowego jako stanu pośredniego (Schemat 3).



Schemat 3

Powyższa ścieżka syntezy zaproponowana została na podstawie badań z innymi czynnikami nukleofilowymi takimi jak litowe zasady organiczne (MeLi, PhLi, n-BuLi oraz LDA) opisanymi w literaturze, a mechanizm wewnątrzcząsteczkowej migracji grupy alkoksykarbonylowej poparty został obliczeniami teoretycznymi. Dodatkowo, wyizolowano z mieszaniny reakcyjnej związku zawierające utleniony atomu fosforu, co świadczy o reaktywności tych fosfin. Przeprowadzono więc doświadczenie badające wpływ ilości nukleofilowego substratu fosforowego w stosunku do wyjściowego enkarbaminianu na proporcje otrzymanych produktów: z transferem grupy alkoksykarbonylowej lub bez transferu, z utlenionym atomem fosforu lub zachowanym P(III) (Schemat 4).



Schemat 4

Na podstawie tego doświadczenia stwierdzono, iż zmniejszenie ilości nukleofila w układzie prowadzi do zwiększenia wydajności produktu nietransferowanego C, co świadczy iż kinetyczny wpływ reprotonacji jest znacznie szybszy niż wewnątrzcząsteczkowa migracja grupy *tert*-butoksykarbonylowej.

Otrzymane fosforowe pochodne nienaturalnych aminokwasów posiadają czwartorzędowy atom węgla, jednakże niemożliwa była stereokontrola tej reakcji addycji. Przeprowadzono więc próby z (-)-sparteiną jako chiralnym ligandem kompleksującym utworzony anion, jednakże bezskutecznie.

Dodatkowo zastosowano chiralne fosfiny jako substraty w reakcji, niemniej jednak utworzenie anionu fosfinowego w tym przypadku było niemożliwe.

Struktury pięciu spośród dwudziestu dwóch nowo otrzymanych produktów zostały zbadane metodami dyfrakcyjnymi monokryształów. Potwierdzono charakterystyczną architekturę wokół atomów fosforu, stan utlenienia oraz chiralność centrów asymetrycznych.

Wobec zaprezentowanych w niniejszej rozprawie doktorskiej badań i obserwacji można stwierdzić, iż cel badań został osiągnięty i zaproponowane ścieżki syntetyczne dają dostęp do oryginalnych związków organofosforowych. Przedstawione metody syntezy są nowatorskie i umożliwiają rozszerzenie syntezy na dowolne produkty wyjściowe, pochodne fosforanów enolu. W przypadku pochodnych nienaturalnych aminokwasów odpowiedni dobór substratów do reakcji sprzęgania krzyżowego oraz reagentów fosforowych otwiera możliwość syntezy bibliotek interesujących produktów. Ponadto, możliwe jest zastosowanie innych czynników nukleofilowych (dla przykładu, związków krzemu).

Drugi rozdział: Oryginalne sensybilizatory kompleksów lantanowców wywodzące się z pochodnych pirazynowych

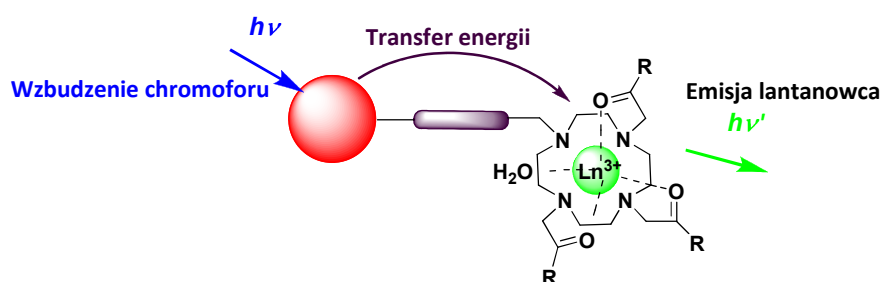
Luminescencyjne właściwości kompleksów lantanowców są szeroko badane pod kątem technologii konwertujących światło, takich jak lasery, diody emitujące światło, wyświetlacze plazmowe i katodowe. Związki lantanowców posiadają dobrze zdefiniowane, nienakładające się na siebie wąskie pasma emisyjne w zakresie widzialnym widma elektromagnetycznego i w bliskiej podczerwieni. Od ostatniej dekady, ich szczególne własności spektroskopowe znalazły zastosowanie w dziedzinie obrazowania medycznego. Zwłaszcza związki kompleksowe neodymu i iterbu, wykazujące intensywne pasma emisyjne wokół 1000 nm, budzą zainteresowanie w optycznej diagnostyce medycznej, ponieważ ich widma wpisują się w zakres "okna biologicznego" do badań spektroskopowych, niezaburzonych poprzez fluorescencję pochodzącą od płynów biologicznych i od hemoglobiny. Co więcej, fotony z zakresu bliskiej podczerwieni nie ulegają fotowysielaniu, mogą być selektywnie wzbudzone poprzez zastosowanie charakterystycznych długości fal, rozpraszają się w tkankach biologicznych w znacznie mniejszym stopniu niż fotony z zakresu widzialnego oraz mogą przechodzić przez tkanki na odległość kilku centymetrów bez ich uszkodzenia. Wszystkie wymienione cechy czynią kompleksy neodymu i iterbu obiecującymi sondami biologicznymi. Mają one jednakże jedną ujemną stronę, a mianowicie, ich bezpośrednie wzbudzenie jest prawie niemożliwe (współczynniki absorpcji są zakresu $1-10 \text{ M}^{-1}\cdot\text{cm}^{-1}$). Wymagają one zastosowania systemu wzbudzającego, który absorbuje energię pod postacią fotonów, a następnie poprzez szereg przejść wewnątrz- i międzysystemowych przenosi ją do stanu wzbudzonego lantanowca, prowokując jego

emisję. Ten układ sensybilizujący, zwany również anteną, może być cząsteczką organiczną, nanokryształem, strukturą metalo-organiczną lub dendrymerem.

Celem niniejszego rozdziału jest przedstawienie systemów sensybilizujących zbudowanych ze związków organicznych oraz opisanie syntezy oryginalnych sensybilizatorów opartych na rdzeniu pirazynowym i z cząsteczką cyklenu jako ligandem chelatującym kation lantanowca. Rozdział ten został podzielony na część literaturową wprowadzającą do tematyki pracy, ze szczególnym naciskiem położonym na systemach anten organicznych, na część eksperymentalną opisującą otrzymywanie poszczególnych związków, na część dyskusyjną i opisanie rezultatów, wyniki spektroskopowe oraz podsumowanie. Krótki podrozdział, zawierający opis otrzymywania oraz badania spektroskopowe chromoforów z grupy związków azowych, został zawarty na końcu pracy.

Część bibliograficzna tegoż rozdziału obejmuje opis zagadnień dotyczących aktywności luminescencyjnej cząsteczek na przykładzie diagramu Jabłońskiego oraz zjawiska sensybilizacji. Zawiera ona przegląd współczesnej literatury naukowej związanej z organicznymi systemami sensybilizującymi i opisuje przykłady zastosowania lantanowców jako sond molekularnych w bliskiej podczerwieni. Kolejne fragmenty części literaturowej poświęcone są chromoforom pirazynowym i ich właściwościom.

Część eksperymentalna zawiera szczegółowy opis zastosowanych ścieżek syntezy prowadzących do oryginalnych systemów sensybilizujących dla lantanowców. Badania te zostały zainspirowane na wcześniejszych, zachęcających wynikach dla układów dihydropirazynowych. Według zaproponowanego konceptu, zamierzony sensybilizator będzie posiadał rdzeń pirazynowy, połączony ramieniem łącznikowym z cząsteczką cyklenu, który tworzy termodynamicznie i kinetycznie stabilne kompleksy z kationami lantanowców (Schemat 5).



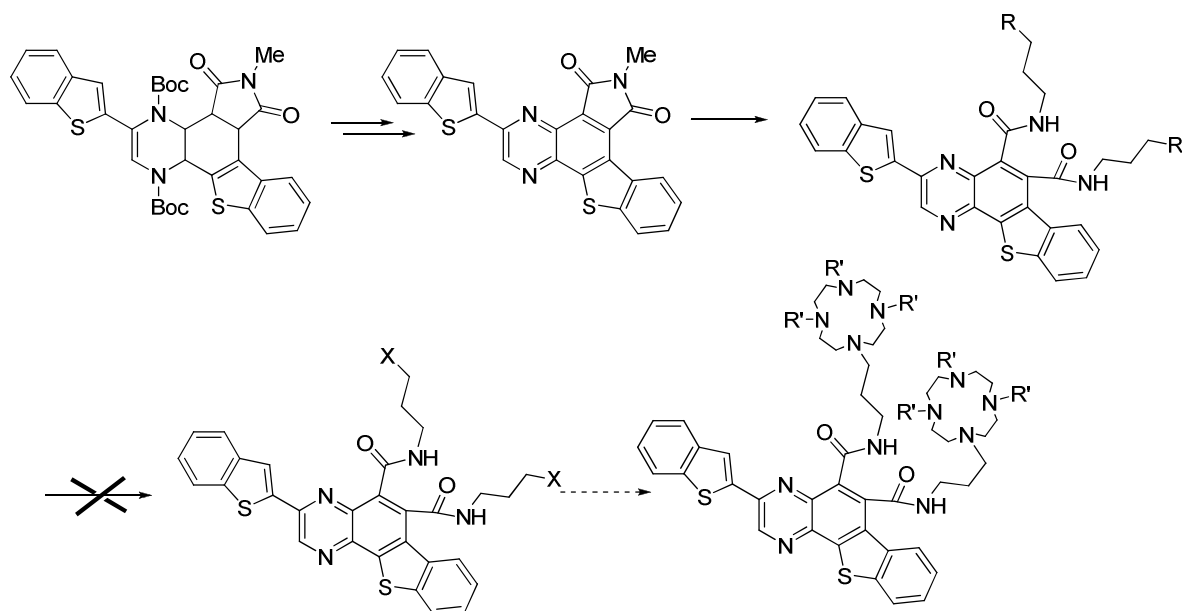
Schemat 5

Na podstawie wstępnych badań przeprowadzonych na ugrupowaniu dihydropirazynowym ustalono, iż system ten nadaje się do wprowadzenia licznych modyfikacji i grup funkcyjnych umożliwiających przyłączenie cyklenu. Zaproponowano dwie oddzielne drogi syntezy:

- poprzez reakcję cykloaddycji Diels-Aldera z gamą różnych dienofili
- przez funkcjonalizację związku wyjściowego w warunkach anionowych, przyłączając rozmaite elektrofile poddające się standardowym transformacjom.

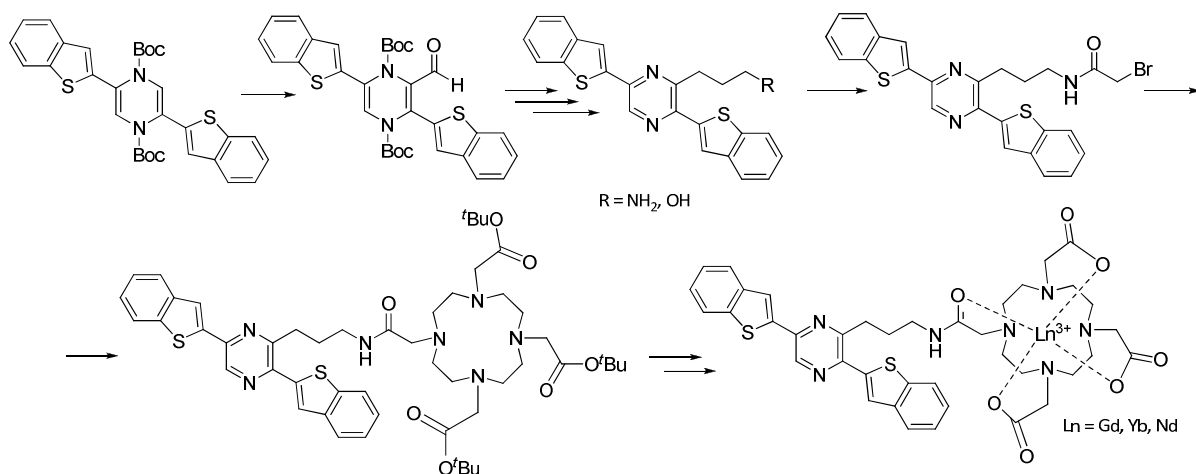
Finalnym krokiem konstrukcji systemów antenowych jest reakcja odłączenia grupy blokującej i aromatyzacja prowadząca do oczekiwanego rdzenia pirazyнового.

Na kolejnych stronach niniejszej rozprawy opisano zastosowane metody syntetyczne. Najpierw wykonano szereg badań pozwalających na wytypowanie najlepszego dienofila w reakcji Diels-Aldera, następnie skupiono się na systemie czterocyklicznym dającym najlepsze wyniki. Związek ten został poddany reakcji aromatyzacji i trans-imidyfikacji, dając dostęp do dwóch pochodnych, potencjalnych systemów antenowych ze skondensowanym, sprzężonym systemem chromoforowym. Jednakże ostatni etap przewidzianej syntezy - przyłączenie cyklenu, na dany moment, nie został zrealizowany ze względu na brak reaktywności otrzymanych pochodnych hydroksylowych i aminowych w zastosowanych przemianach (Schemat 6). W perspektywach do tej części pracy przewidziana jest zmiana zastosowanych grup funkcyjnych.



Schemat 6

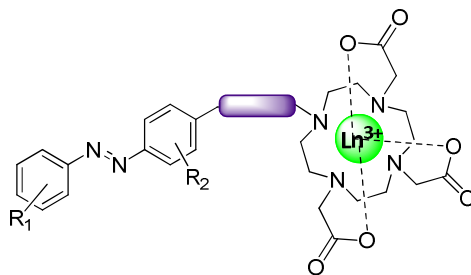
Następnie przeprowadzono próby funkcjonalizacji układu dihydropirazyнового poprzez przyłączenie atomu jodu oraz grupy aldehydowej. Zaproponowane podejście daje dostęp do licznych pochodnych - substratów w reakcji sprzężenia typu Sonogashira, produktów wyjściowych w reakcji olefinacji typu Wittig-Horner-Emmons, w reakcji redukcji i reduktywnej aminacji. Spośród przeprowadzonych licznych reakcji chemicznych, wytypowano najefektywniejszą ścieżkę syntezy poprzez aldehyd do pochodnej bromoamidowej pirazyны, która została przyłączona do cząsteczki cyklenu z odpowiednio zmodyfikowanymi grupami aminowymi, tak aby po odblokowaniu grup funkcyjnych otrzymać chelat zdolny do kompleksowania kationu lantanowca (Schemat 7).



Schemat 7

Otrzymano kompleksy neodymum iterbu i gadolinu z oryginalnymi sensybilizatorami i zbadano ich właściwości spektroskopowe. Widma absorpcyjne, ekscytacyjne i emisyjne w zakresie widzialnym i w bliskiej podczerwieni zostały zarejestrowane dla tych związków kompleksowych. Zmierzono również wydajność kwantową emisji lantanowców oraz czas życia fluorescencji w celu oszacowania zdolności sensybilizujących oryginalnych systemów antenowych. Powyższe badania zostały przeprowadzone w Centrum Biofizyki Molekularnej w Orleanie pod opieką dr S. Petoud i dr S. Villette. Otrzymane wyniki wskazują, iż badany system sensybilizujący jest wydajny, niezawodny, daje możliwość testowania równolegle kilku kationów lantanowców.

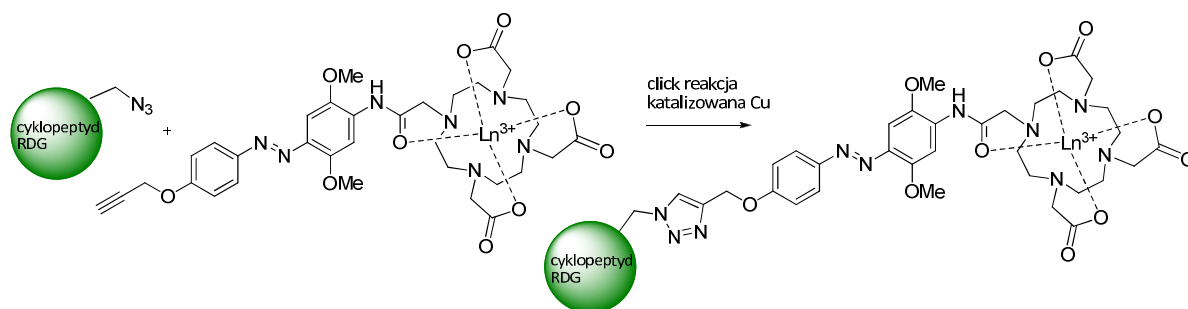
Ostatni podrozdział pracy doktorskiej został poświęcony otrzymywaniu nowych chromoforów opartych na systemach azowych. Związki azowe charakteryzują się absorpcją w zakresie widzialnym widma elektromagnetycznego, posiadają intensywne i nieblaknące kolory, dzięki czemu znalazły zastosowanie w chemii barwników i indykatorów chemicznych. Biorąc pod uwagę ich właściwości spektroskopowe, przewidziano użyteczność tych związków jako sensybilizatorów oraz grup łącznikowych do systemamów pirazynowych zwiększających ich zdolność do sensybilizacji.



Schemat 8

Otrzymano szereg związków azowych na drodze reakcji diazotacji i sprzężenia diazowego z pochodnymi aniliny, a następnie sfunkcjonalizowano powyższe produkty w reakcji z bromkiem bromoacetylu, aby przyłączyć je do pochodnych cyklicznych i skompleksować z kationami lantanowców.

Dodatkowo przeprowadzono badania mające na celu przyłączenie powyższych związków do ugrupowania dihydropirazynowego i do biocząsteczek o wysokim powinowactwie do komórek nowotworowych, tj. cyklopeptyd RGD (Schemat 9).



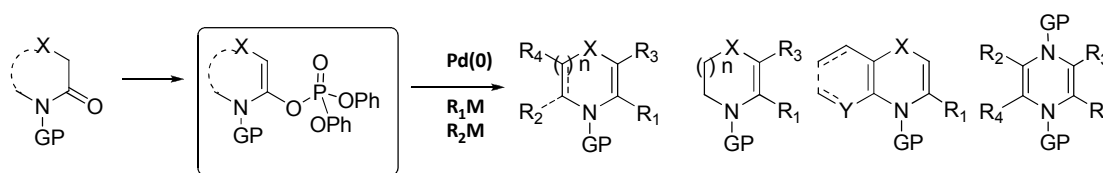
Schemat 9

Przedstawione badania ukazują dużą przydatność powyższych systemów jako sond molekularnych w zakresie bliskiej podczerwieni. Wykazują one wzbudzenie w szerokim zakresie długości fali (aż do 500 nm) dając intensywne pasma emisyjne badanych kompleksów lantanowców. Czas życia fluorescencji badanych związków mieści się w zakresie kilkuset nanosekund do kilku mikrosekund, co plasuje je w obrębie dobrych układów sensybilizujących.

Wobec zaprezentowanych w niniejszej rozprawie doktorskiej badań, spostrzeżeń i konkluzji można stwierdzić, iż postawiony cel został osiągnięty, a zaproponowane strategie syntezy dają dostęp do nowej, dotychczas nieopisanej grupy systemów sensybilizujących dla kompleksów lantanowców. Przedstawione wstępne badania spektroskopowe ukazują zdolność pochodnych pirazynowych do efektywnego przekazu energii do systemu chelatującego metalu. Dodatkowo możliwość wprowadzenia modyfikacji na każdym etapie syntezy oraz elastyczność funkcjonalizacji jest dużym atutem przedstawionych badań. W perspektywach do tego projektu, przewidziane jest przyłączenie poszczególnych systemów sensybilizujących do biomolekuł specyficznie wykrywających komórki i tkanki rakowe w celu stworzenia markerów cząsteczkowych do badań w zakresie bliskiej podczerwieni. Ponadto, przewidziane jest przyłączenie do sensybilizatora więcej niż jednej cząsteczki cyklenu, co pozwoli na różnicowanie odpowiedzi spektralnej lub wzmocnienie rejestrowanego sygnału.

Résumé

Les composés hétérocycliques azotés représentent une classe importante de produits synthétiques. Ils sont présents dans de nombreuses molécules biologiquement actives telles que les acides nucléiques, les vitamines, les relais de l'énergie chimique dans le métabolisme cellulaire (ATP), les cofacteurs de protéines et beaucoup d'autres encore. Les hétérocycles azotés sont également utilisés dans l'industrie chimique (colorants, conservateurs, parfums), les produits pharmaceutiques, ainsi qu'en agriculture comme produits phytosanitaires. En raison de leur omniprésence et leur intérêt biologique, une attention particulière est accordée au développement de méthodologie pour leur synthèse et leur fonctionnalisation. Dans ce but, la conception de nouvelles voies de synthèse pour la fonctionnalisation d'énamides constitue une thématique importante pour la communauté des chimistes et des biologistes car ces motifs s'avèrent être des intermédiaires synthétiques polyvalents permettant d'introduire une fonctionnalité azotée dans de nombreux composés plus complexes. Les réactions de couplage pallado-catalysées constitue une méthode de choix rapide et éco-efficente pour la synthèse d'énamides et/ou de ènecarbamates. Cette méthodologie décrite depuis plusieurs années dans l'équipe du Pr. I. Gillaizeau permet d'accéder à des énamides variés via des couplages métallo-catalysés (ex. Suzuki-Miyaura, Stille, Sonogashira) de phosphates d'énols issus de lactames, d'imides ou d'amides, intermédiaires facilement accessibles. Ainsi, un grand nombre de structures hétérocycliques (dérivés 1,4-dihydropyridine; 1,4-oxazines; 1,4-dihydropyrazines ...) originales ou difficilement accessibles ont été synthétisées (Schéma 1).



GP = C(O)OR₂ (ènecarbamate), C(O)R₂ (énamide)
R₁, R₂, R₃, R₄ = Alkynyl, alkenyl, acyl, aryl, heteroaryl, alkyl ...
X = O, CR₂, NR₂
Y = CH, N
n = 1, 2, 8

Schéma 1

Tenant compte de l'expertise et des recherches entreprises dans le groupe du Prof. I. Gillaizeau sur l'obtention, la polyvalence et la réactivité des ènecarbamates, cette thèse a pour but la synthèse et l'identification structurale de nouveaux composés hétérocycliques porteurs d'un groupe

organophosphorés d'une part, ainsi que de nouvelles sondes pyraziniques pour la détection en proche infra-rouge.

Première chapitre : Synthèse de dérivés de phosphines originaux

Le premier chapitre de la thèse porte sur l'étude de la réactivité d'énamides pour la préparation de dérivés alpha-enamido-phosphines ou d'acides aminés non naturels porteurs d'un groupe organophosphorés en bêta, blocs synthétiques pouvant être utilisés pour accéder à des molécules plus complexes.

Une partie bibliographique introduit l'ensemble de ce chapitre mettant en évidence l'intérêt des produits organophosphorés, largement utilisés dans de nombreux domaines de la vie quotidienne et l'industrie chimique. D'un point de vue biologique, ils jouent un rôle important dans le métabolisme (ATP), le transfert de matériel génétique (ADN, ARN) et sont les éléments constitutifs des membranes cellulaires (phospholipides). En raison des groupes phosphate isostériques avec le groupe carboxyle, les analogues phosphatés d'acides aminés et des peptides sont des groupes importants de composés pharmaceutiques utilisés comme inhibiteurs de réactions enzymatiques, composés antibactériens et anti-HIV. En outre, les composés organophosphorés ont des propriétés d'inhibition d'acétylcholinestérase et sont donc largement utilisés comme pesticides, insecticides et herbicides ainsi que comme gaz toxiques. Dans l'industrie chimique, ils sont utilisés comme ligands chiraux pour des complexes de métaux de transition dans les réactions catalytiques. Ils permettent d'obtenir des produits énantiomériquement purs dans de nombreuses transformations asymétriques. L'avantage de ligands contenant un atome de phosphore est la versatilité de ses substituants et la possibilité d'introduire d'un centre asymétrique soit sur l'atome de phosphore, soit sur l'atome de carbone adjacent au phosphore, ou encore par chiralité axiale. Une étude bibliographique concernant les réactions de formation des liaisons C-P est également décrite.

Le couplage organopalladié C-P de phosphines boranes secondaires chirales ou achirales avec des phosphates d'alpha-amido-énol a été étudié donnant des énamido-phosphines boranes correspondantes avec 28 à 95 % de rendement (Schéma 2). Ce couplage C-P original qui est réalisé dans des conditions douces avec des dérivés cétoniques de nature différente, offre de nombreuses possibilités pour la constitution d'une librairie de phosphines fonctionnalisées originales. Il est à noter que dans le cas d'une phosphine secondaire borane P-chirogénique, l'analyse du mélange réactionnel par chromatographie supercritique sur phase chirale, indique que le couplage est racémisant dans les conditions de réaction. Ce phénomène peut s'expliquer par une inversion de l'anion phosphore-borane en milieu basique, avant l'échange de ligand dans la sphère de coordination du palladium. Les études qui ont été menées en changeant la température de réaction

(TA à 60°C, avec ou sans activation microonde), le solvant (CH₃CN, DMSO) ou encore les conditions de réaction par l'ajout de BH₃ supplémentaire, conduisent toujours au produit racémique.

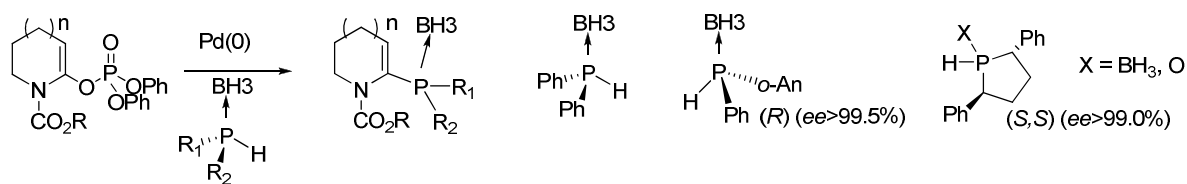


Schéma 2

En revanche, lorsque la réaction est réalisée avec une phosphine secondaire borane cyclique, porteuse de la chiralité non plus sur l'atome de phosphore mais sur le cycle phospholane, le produit de couplage est obtenu stéréosélectivement avec une excellente pureté énantiomérique (Schéma 3) (ee > 99.4%).

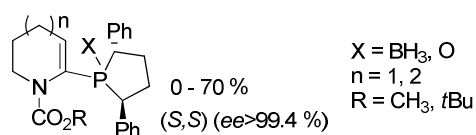


Schéma 3

La structure par diffraction de RX de ces composés a été réalisée en collaboration avec Pr. K. Lewinski de l'Université de Jagellonne à Cracovie en Pologne.

Parallèlement à ce travail, l'addition nucléophile de phosphures sur divers éne-carbamates acycliques préparées par couplage à partir de phosphates d'énol acyclique, a été étudiée. Il a ainsi été montré qu'il était possible d'accéder par carbolithiation intermoléculaire à divers éne-carbamates acycliques, qui réagissent ensuite avec un phosphure pour donner des acides alpha-aminés bêta-phosphorés originaux, porteurs d'un carbone quaternaire en alpha de l'azote. La réaction de carbolithiation se déroule avec une migration concomitante du groupement Boc de l'atome azote sur le carbone placé en alpha *via* la formation d'une aziridine intermédiaire. Des études concernant l'addition d'organophosphorés chiraux (phosphines ou oxydes de phosphine) ont également été menées, malheureusement sans succès.

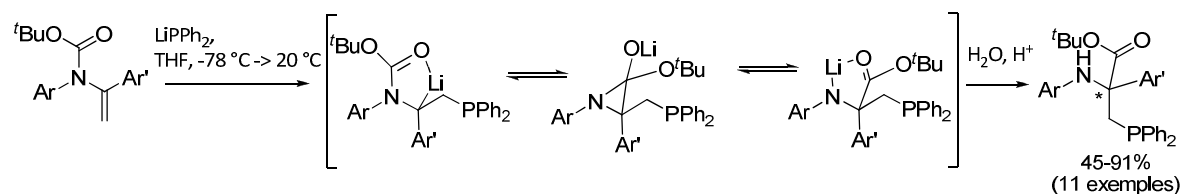


Schéma 4

Il est à noter que des composés constitués d'un atome de phosphore oxydé ont également été isolés. Toutefois, en augmentant la quantité d'anion phosphure au sein du milieu réactionnel, la réaction d'oxydation de la phosphine est limitée. Par ailleurs, une diminution de la quantité d'anion phosphure induit une diminution de la migration de l'alkoxyde N-> C, nous permettant ainsi de

conclure que la cinétique de reprotonation est beaucoup plus rapide que la migration intramoléculaire d'un groupe de *tert*-butoxycarbone.

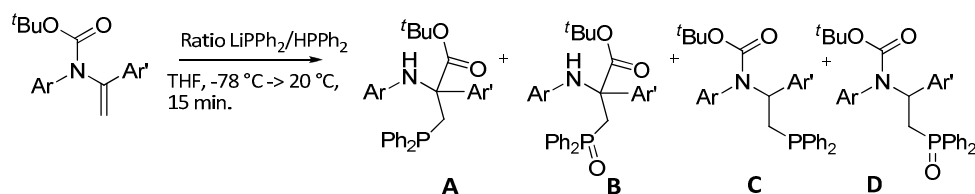


Schéma 5

Les dérivés phosphorés des acides aminés non naturels possèdent un atome de carbone quaternaire en alpha de l'azote dont la stéréochimie n'est pas contrôlable au cours de la réaction d'addition nucléophile. Différents test avec notamment l'utilisation d'inducteur chiral telle que la (-)-spartéine ont été effectués, mais en vain. L'utilisation d'une phosphine chirale pour induire un stéréo-contrôle lors de l'étape de transfert du groupement *tert*-butoxycarbone n'a pas aboutit, l'anion lithé n'ayant pu être obtenu.

Les structures de cinq des vingt-deux produits nouvellement obtenus ont été analysées par la méthode de diffraction des monocristaux. Cela a permis de confirmer l'architecture caractéristique autour des atomes de phosphore, son état d'oxydation et la configuration des centres asymétriques.

Les buts et objectifs fixés en début de thèse ont été atteints et les voies de synthèse proposées ont permis l'obtention de composés organo-phosphorés originaux. Les méthodes de synthèse développées sont innovantes et peuvent s'étendre à la synthèse de nombreux autres composés à partir d'énol éthers variés. Dans le cas des dérivés non-naturels d'acides aminés, une sélection appropriée des substrats et des réactifs phosphorés engagés dans la réaction de couplage croisé palladocatalysée ouvre une perspective intéressante pour la conception d'une bibliothèque de produits originaux. Deux publications correspondent à ce sujet.

Deuxième chapitre : Sensibilisateurs originaux de complexes de lanthanides basés sur les dérivés pyraziniques

Le deuxième chapitre de la thèse porte sur la préparation et la caractérisation de chromophores organiques originaux sur la base d'un noyau pyrazinique et qui sont susceptibles de présenter des propriétés de fluorescence. Ces composés sont conçus pour former des nouveaux systèmes sensibilisateurs de cations de lanthanides, et donc être utilisés comme sensibilisateurs organiques pour l'imagerie moléculaire dans le proche infrarouge.

Les propriétés luminescentes des complexes de lanthanides sont testés pour les technologies de conversion de lumière telles que les lasers, les diodes émettrices de lumière ou encore les écrans à plasma. Ces composés ont des bandes d'émission bien définies et étroites, qui se ne superposent pas dans le domaine visible du spectre électromagnétique et dans le proche infrarouge. Durant la dernière décennie, la spécificité de leurs propriétés spectroscopiques ont été utilisées dans le domaine de l'imagerie médicale. En particulier, des complexes de néodyme et de l'ytterbium, montrant une bande d'émission forte à environ 1000 nm, possèdent un intérêt pour le diagnostic médical optique. En raison de leur spectre en proche infrarouge, ils émettent dans la "fenêtre biologique" pour des études spectroscopiques, non perturbées par la fluorescence provenant de fluides biologiques et de l'hémoglobine. En outre, les photons dans le proche infrarouge ne montrent pas de photo-blanchiment. Ils peuvent être excités sélectivement en appliquant des longueurs d'onde caractéristiques et leur dispersion dans les tissus biologiques est bien moindre que les photons de la lumière visible. Ils peuvent traverser les tissus sur plusieurs centimètres sans les endommager. Toutes ces caractéristiques rendent prometteuse l'utilisation des complexes de néodyme et d'ytterbium comme sondes biologiques et notamment la possibilité de développer des sondes non-invasives pour la détection tumorale par imagerie proche infrarouge. Les cations lanthanides ont toutefois un inconvénient, leur excitation directe est presque impossible (les coefficients d'absorption sont dans la plage $1-10 \text{ M}^{-1} \text{ cm}^{-1}$) et ils exigent l'application d'un système d'excitation (système sensibilisateur) permettant l'absorption d'énergie sous forme de photons via une série de transitions intra- et inter-système jusqu'à l'état excité des lanthanides. S'en suit une émission de photons dans le proche infrarouge. Ce système sensibilisateur, également appelé "antenne", peut être une molécule organique, un nanocrystal, la structure métallo-organique ou de dendrimère.

Le but de ce chapitre est de fournir des systèmes sensibilisateurs fabriqués à partir de composés organiques, et de décrire la synthèse de sensibilisateurs originaux basés sur un noyau pyrazinique et un dérivé de cyclène comme ligand chélateur de cations lanthanides. Ce chapitre est divisé en deux parties; la partie bibliographique décrit le thème du travail, avec un accent particulier sur les systèmes d'antennes organiques; la partie expérimentale décrit la préparation de chaque composé, une discussion sur les résultats obtenus, les études spectroscopiques et un résumé. Une courte section décrivant la préparation et les études spectroscopiques du groupe chromophore azoïque, a été incluse à la fin des travaux.

La partie bibliographique comprend une introduction dédiée à l'activité de molécules luminescentes à l'aide du diagramme de Jablonski et du phénomène de sensibilisation. Il contient un aperçu de la littérature scientifique contemporaine liée aux systèmes sensibilisateurs organiques et

décrit des exemples d'utilisation des lanthanides comme sonde moléculaire dans le proche infrarouge.

La partie principale de ce chapitre contient une description détaillée des voies de synthèse conduisant à des sensibilisateurs originaux pour les systèmes de lanthanides. Ces études ont été inspirées par des résultats encourageants de propriétés de fluorescence obtenus en série pyraziniques et conduits au sein dans notre laboratoire. Le concept proposé est constitué d'un sensibilisateur de nature pyrazinique relié par un bras espaceur à une molécule du cyclène, qui forme un complexe thermodynamiquement et cinétiquement stable avec des cations lanthanides (Schéma 6).

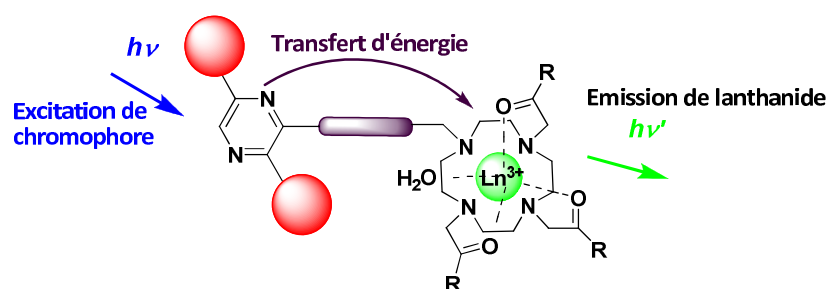


Schéma 6

Basé sur des études préliminaires effectuées sur le motif dihydropyrazinique, il a été constaté que le système est adapté pour l'introduction de nombreuses modifications et groupes fonctionnels, permettant l'ancrage du cyclène. Nous avons proposé deux voies distinctes de synthèse de ces composés cibles:

- Par cycloaddition de Diels-Alder en faisant réagir une large gamme de différents diénophiles,
- Par fonctionnalisation du composé de départ en conditions anioniques avec une variété d'électrophiles et en appliquant des transformations classiques.

Dans les deux cas, l'étape finale dans la construction de ces systèmes d'antennes est la réaction de coupure du groupe protecteur suivi d'une aromatisation, conduisant à la base pyrazine prévue.

Concernant l'approche *via* la cycloaddition de Diels Alder, plusieurs études ont été réalisées afin de choisir le meilleur diénophile, la N-méthylmaléimide. Après déprotection des atomes d'azote suivie d'une étape d'aromatisation, nous avons envisagé introduire le bras espaceur suivant une réaction de trans imidification, malheureusement sans succès. Des travaux sur ce sujet sont actuellement en cours dans le laboratoire.

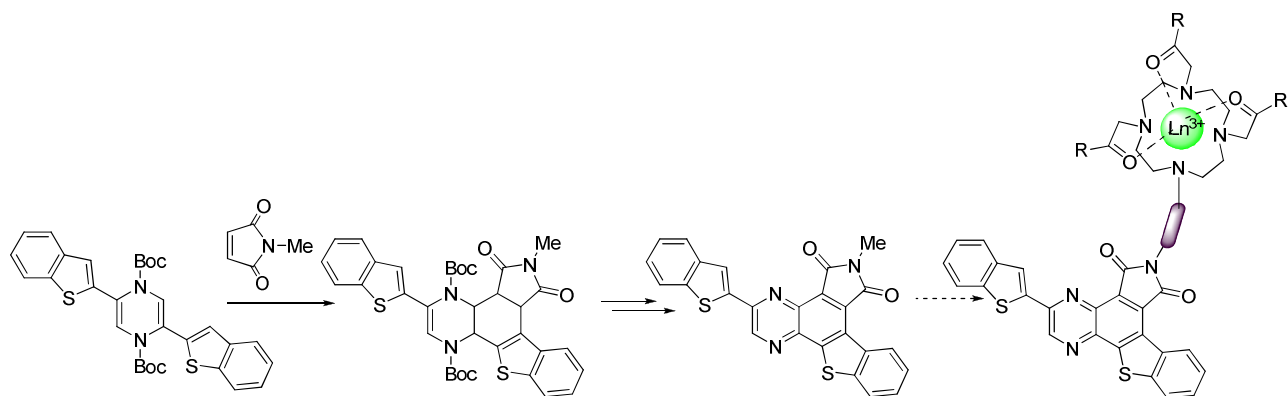


Schéma 7

Parallèlement, la fonctionnalisation du noyau dihydropyrazinique a été réalisée soit *via* une réaction de couplage de type Sonogashira, selon une réaction d'olefination de Wittig-Horner-Emmons, et selon une réaction d'amination réductrice par fixation d'un atome d'iode ou d'un groupe aldéhyde. Les méthodes proposées offrent l'accès à plusieurs dérivés, la voie la plus efficace étant décrite dans le Schéma 8.

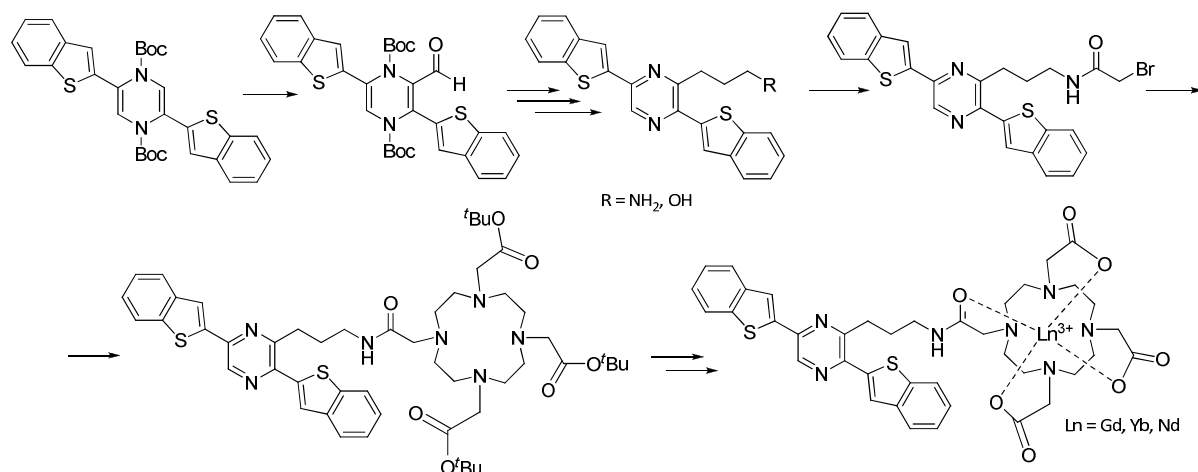


Schéma 8

Les sensibilisateurs originaux résultant de la complexation de cations de l'ytterbium, du neodymium et du gadolinium ont été obtenus et leurs propriétés spectroscopiques ont été étudiées. Les spectres d'absorption et d'émission dans le domaine visible et du proche infrarouge ont été enregistrés pour ces composés. Nous avons mesuré le rendement quantique de l'émission des lanthanides et le temps de vie de fluorescence pour estimer la capacité de ces systèmes d'antenne originaux. Ces études ont été menées au Centre de Biophysique Moléculaire à Orléans sous la responsabilité du Dr. S. Petoud et Dr. S. Villette. Les résultats montrent que le système sensibilisateur est efficace, fiable, et qu'il permet parallèlement plusieurs tests de cations lanthanides.

Le dernier sous-paragraphe de ce chapitre est consacré à la préparation de nouveaux chromophores basés sur des systèmes azoïques. Les composés azoïques sont caractérisés par une absorption dans le domaine visible du spectre électromagnétique. Ils ont une couleur intense, si bien

que ces produits chimiques sont utilisés dans les colorants et les indicateurs chimiques. Compte tenu de leurs propriétés spectroscopiques, ces composés peuvent être utilisés comme sensibilisateurs, soit seuls soit ancrés sur un système pyrazinique permettant l'amélioration de leur capacité de sensibilisation.

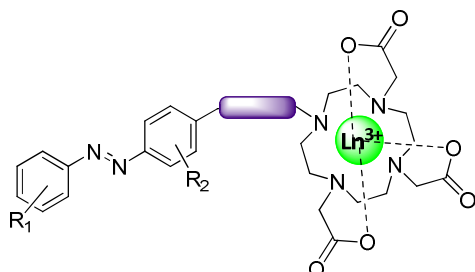


Schéma 9

Une série de composés azoïques a été obtenue par réaction de diazotation et de couplage diazoïque sur des dérivés de l'aniline. Ces produits ont été fonctionnalisés par réaction avec le bromure de bromoacétyle pour fixer le cyclène. La deprotection des groupements protecteurs du cyclène suivie par la complexation avec des cations de lanthanides, ont permis d'obtention de différents composés. Une étape supplémentaire a été réalisée en collaboration avec l'équipe d'Agnès Delmas et de Vincent Aucagne au CBM d'Orléans en accrochant une biomolécule à haute affinité pour les cellules cancéreuses, la cyclopeptide RGD (Schéma 10).

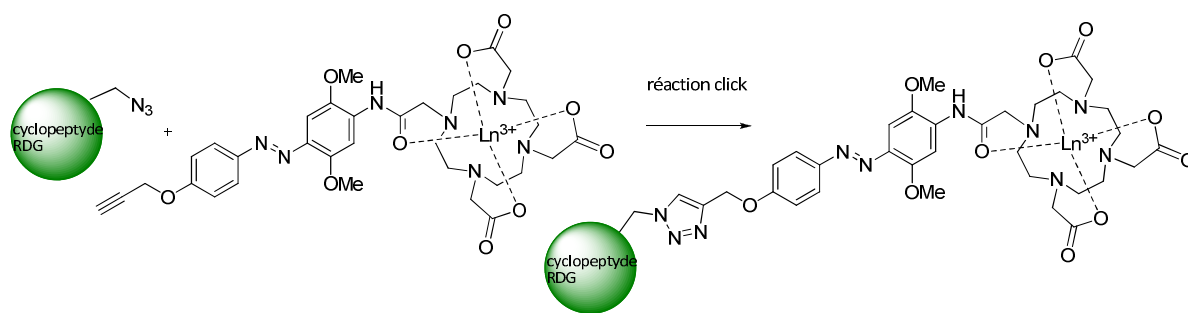


Schéma 10

Des études préliminaires montrent une grande utilité de ces systèmes en tant que sondes moléculaires dans le proche infrarouge. Ils présentent un large éventail de longueurs d'onde d'excitation (jusqu'à 500 nm), ce qui donne une bande d'émission intense de complexes de lanthanides. Les temps de vie de fluorescence des composés testés sont dans la gamme de quelques nanosecondes à quelques microsecondes, ce qui les place au sein des sensibilisateurs efficaces.

A la vue des résultats présentés dans cette thèse, nous pouvons affirmer que les objectifs ambitieux de départ ont été atteints. Nous avons proposé des stratégies des synthèses pour l'accès à de nouveaux groupes de systèmes sensibilisateurs pour les complexes de lanthanides. Les études préliminaires spectroscopiques montrent l'aptitude des dérivés pyraziniques à transférer d'énergie

au système de chélation de métal. En outre, la possibilité d'apporter des modifications à n'importe quel stade de la synthèse et la flexibilité de fonctionnalisation est un atout majeur pour cette recherche. Les perspectives de ce projet sont de relier les différents systèmes de sensibilisateurs et avec des biomolécules afin de détecter spécifiquement les cellules et les tissus cancéreux et de développer des marqueurs moléculaires dans le proche infrarouge. En outre, il est prévu pour connecter plusieurs dérivés cyclène sur un sensibilisateur, ce qui permettrait de distinguer la réponse spectrale ou d'améliorer le signal enregistré.

Bibliography

- [1] (a) K. Turner, *Org. Process Res. Dev.*, **2007**, *11*, 663; (b) K. Turner, *Org. Process Res. Dev.*, **2007**, *11*, 802.
- [2] A. F. Pozharski, A. T. Soldatenkov, A. R. Katritzky, *Heterocycles in life and society*, John Wiley & Sons Ltd., **1997**.
- [3] A. Burger, *Medicinal Chemistry*, Wiley-Interscience, **1970**.
- [4] K. C. Nicolaou, K. Namoto, *Chem. Commun.*, **1998**, 1757.
- [5] (a) A. L. Hansen, J.-P. Ebran, T. Gøgsig, T. Skrydstrup, *Chem. Commun.*, **2006**, 4137; (b) A. L. Hansen, J.-P. Ebran, T. M. Gøgsig, T. Skrydstrup, *J. Org. Chem.*, **2007**, *72*, 6464.
- [6] H. Fuwa, M. Sasaki, *J. Org. Chem.*, **2009**, *74*, 212.
- [7] F. Lepifre, S. Clavier, P. Bouyssou, G. Coudert, *Tetrahedron*, **2001**, *57*, 6969.
- [8] B. Cottineau, I. Gillaizeau, J. Farard, M.-L. Auclair, G. Coudert, *Synlett*, **2007**, *12*, 1925.
- [9] M. Chaignaud, I. Gillaizeau, N. Ouhamou, G. Coudert, *Tetrahedron*, **2008**, *64*, 8059.
- [10] H. Uh, S. Petoud, *CR Chimie*, **2010**, *13*, 668.
- [11] P. Savignac, B. Iorga, *Modern Phosphonate Chemistry*, CRC, New York, **2003**.
- [12] M. Mikołajczyk, P. Bałczewski, *Top. Curr. Chem.*, **2003**, *223*, 161.
- [13] A. Börner, *Phosphorus Ligands in Asymmetric Catalysis: Synthesis and Applications*, Wiley-VCH, Weinheim, **2008**.
- [14] (a) W.S. Wadsworth Jr., W.D. Emmons, *J. Am. Chem. Soc.* **1961**, *83*, 1733; (b) B.H. Lipshutz, D.W. Chung, B. Rich, R. Corral, *Org. Lett.*, **2006**, *8*, 5069; (c) M. Shi, Y.-H. Liu, *Org. Biomol. Chem.*, **2006**, *4*, 1468.
- [15] (a) N.T. McDougal, S.E. Schauls, *J. Am. Chem. Soc.*, **2003**, *125*, 12094; (b) Y.K. Chung, G.C. Fu, *Angew. Chem. Int. Ed.*, **2009**, *48*, 2225.
- [16] (a) T. Akiyama, J. Itoh, K. Yokota, K. Fuchibe, *Angew. Chem. Int. Ed.*, **2004**, *43*, 1566; (b) M. Rueping, A. P. Antonchick, T. Theissmann, *Angew. Chem. Int. Ed.*, **2006**, *45*, 3683; (c) S. Hoffmann, A. M. Seayad, B. List, *Angew. Chem. Int. Ed.*, **2005**, *44*, 7424; (d) S. Hoffmann, S. Nicoletti, B. List, *J. Am. Chem. Soc.*, **2006**, *128*, 13074; (e) S. J. Connon, *Angew. Chem. Int. Ed.*, **2006**, *45*, 3909.
- [17] W. Tang, X. Zhang, *Chem. Rev.*, **2003**, *103*, 3029.
- [18] (a) F. Palacios, C. Alonso, J. M. Santos, *Chem. Rev.*, **2005**, *105*, 899; (b) J. G. Allen, F. R. Atherton, M. J. Hall, C. H. Hassall, S. W. Holmes, L. W. Lambert, L. J. Nisbet, P. S. Ringrose, *Nature*, **1978**, *272*, 56; (c) S. Fushimi, K. Furihata, H. Seto, *J. Antibiot (Tokyo)*, **1989**, *42*, 1019.
- [19] (a) K. Morita, Z. Suzuki, H. Hirose, *Bull. Chem. Soc. Jpn*, **1968**, *41*, 2815; (b) T. Hayase, T. Shibata, K. Soai, Y. Wakatsuki, *Chem. Commun.*, **1998**, 1271.
- [20] M. Shi, L.-H. Chen, C.-Q. Li, *J. Am. Chem. Soc.*, **2005**, *127*, 3790.
- [21] (a) B. M. Trost, U. Kazmaier, *J. Am. Chem. Soc.*, **1992**, *114*, 7933; (b) C. Guo, X. Lu, *J. Chem. Soc., Perkin Trans. 1*, **1993**, 1921.
- [22] (a) C. Zhang, X. Lu, *J. Org. Chem.*, **1995**, *60*, 2906; (b) J. E. Wilson, G. C. Fu, *Angew. Chem. Int. Ed.*, **2006**, *45*, 1426.
- [23] (a) X.-F. Zhu, J. Lan, O. Kron, *J. Am. Chem. Soc.*, **2003**, *125*, 4716; (b) R. P. Wurz, G. C. Fu, *J. Am. Chem. Soc.*, **2005**, *127*, 12234.
- [24] R. B. Grossman, S. Comesse, R. M. Rasne, K. Hattori, M. N. DeLong, *J. Org. Chem.*, **2002**, *68*, 871.
- [25] T. Akiyama, J. Itoh, K. Yokota, K. Fuchibe, *Angew. Chem. Int. Ed.*, **2004**, *43*, 1566.
- [26] D. Uraguchi, M. Terada, *J. Am. Chem. Soc.*, **2004**, *126*, 5356.
- [27] R. I. Storer, D. E. Carrera, Y. Ni, D. W. C. MacMillan, *J. Am. Chem. Soc.*, **2006**, *128*, 84.
- [28] M. Rueping, A. P. Antonchick, T. Theissmann, *Angew. Chem. Int. Ed.*, **2006**, *45*, 3683.
- [29] T. Akiyama, H. Morita, J. Itoh, K. Fuchibe, *Org. Lett.*, **2005**, *7*, 2583.
- [30] T. Akiyama, Y. Tamura, J. Itoh, H. Morita, K. Fuchibe, *Synlett.*, **2006**, 141.
- [31] J. Jiang, J. Yu, X.-X. Sun, Q.-Q. Rao, L.-Z. Gong, *Angew. Chem. Int. Ed.*, **2008**, *47*, 2458.
- [32] D. Nakashima, H. Yamamoto, *J. Am. Chem. Soc.*, **2006**, *128*, 9626.
- [33] M. Rueping, W. Ieawsuwan, A. P. Antonchick, B. J. Nachtsheim, *Angew. Chem. Int. Ed.*, **2007**, *46*, 2097.
- [34] (a) S. W. Knowles, M. J. Sabacky, *Chem. Commun.*, **1968**, 1445; (b) L. Horner, H. Siegel, H. Bütthe, *Angew. Chem. Int. Ed. Engl.*, **1968**, *7*, 941.
- [35] (a) W. S. Knowles, *Acc. Chem. Res.*, **1983**, *16*, 106; (b) W. S. Knowles, *Angew. Chem. Int. Ed.*, **2002**, *41*, 1999.
- [36] (a) T. P. Dang, H. B. Kagan, *J. Chem. Soc. Chem. Commun.*, **1971**, 481; (b) T. Satyanarayana, S. Abraham, H. B. Kagan, *Angew. Chem. Int. Ed.*, **2009**, *48*, 456.
- [37] M. J. Burk, J. E. Feaster, W. A. Nugent, R. L. Harlow, *J. Am. Chem. Soc.*, **1993**, *115*, 10125.
- [38] A. Miyashita, A. Yasuda, H. Takaya, K. Toriumi, T. Ito, T. Souchi, R. Noyori, *J. Am. Chem. Soc.*, **1980**, *102*, 7932.
- [39] T. Ohkuma, H. Ooka, T. Ikariya, R. Noyori, *J. Am. Chem. Soc.*, **1995**, *117*, 10417.
- [40] S. Prevost, S. Gauthier, M. C. C. de Andrade, C. Mordant, A. R. Touati, P. Lesot, P. Savignac, T. Ayard, P. Phansavath, V. Ratovelomana-Vidal, J.-P. Genêt, *Tet.:Asym.*, **2010**, *21*, 1436.
- [41] I. G. Rios, A. Rosas-Hernandez, E. Martin, *Molecules*, **2011**, *16*, 970.
- [42] Y. Wei, M. Shi, *Acc. Chem. Res.*, **2010**, *43*, 1005.
- [43] C. Lexer, D. Burtscher, B. Perner, E. Tzur, N. G. Lemcoff, C. Slugov, *J. Org. Chem.* **2011**, *696*, 2466.
- [44] (a) F. Orsini, G. Sello, M. Sisti, *Curr Med Chem*, **2010**, *17*, 264; (b) E. D. Naydenova, P. T. Todorov, K. D. Troev, *Amino Acids.*, **2010**, *38*, 23.

- [45] W. W. Smith, P. A. Bartlett, *J. Am. Chem. Soc.*, **1998**, *120*, 4622.
- [46] J. G. Allen, F. R. Artherton, M. J. Hall, C. H. Hassall, S. W. Holmes, R. W. Lambert, L. J. Nisbet, P. S. Ringrose, *Nature*, **1978**, *272*, 56.
- [47] E. Alonso, E. Alonso, A. Solis, C. del Pozo, *Synlett*, **2000**, 698.
- [48] H. Gali, K. R. Prabhu, S. R. Karra, K. V. Katti, *J. Org. Chem.*, **2000**, *65*, 676.
- [49] F. Palacios, A. M. Ocha de Retana, E. Martinez de Marigorta, J. M. de los Santo, *Org. Prep. Proc. Int.*, **2002**, *34*, 219.
- [50] (a) D. V. Patel, K. Reilly-Gauvin, D. E. Ryono, C. A. Free, W. L. Rogers, S. A. Smith, J. M. DeForrest, R. S. Oehl, E. W. Pertillo Jr., *J. Med. Chem.*, **1995**, *38*, 4557; (b) B. Stowasser, K.-H. Budt, L. Jian-Qi, A. Peyman, D. Ruppert, *Tetrahedron Lett.*, **1992**, *33*, 6625.
- [51] C. de Risi, D. Perrone, A. Dondoni, G. P. Pollini, V. Vertolasi, *Eur. J. Org. Chem.*, **2003**, 1904.
- [52] S. Ikeda, J. A. Ashley, P. Wirsching, K. D. Janda, *J. Am. Chem. Soc.*, **1992**, *114*, 7604.
- [53] L. W. Peterson, M. Sala-Rabanal, I. S. Krylov, M. Serpi, B. A. Kashemirov, C. E. McKenna, *Molecular Pharmaceutics*, **2010**, *7*, 2349.
- [54] R. S. Gilbertson, G. Chen, M. MacLoughlin, *J. Am. Chem. Soc.*, **1994**, *116*, 4481.
- [55] P. Knochel, M. Ch. P. Yeh, S. C. Berk, J. Talbert, *J. Org. Chem.*, **1988**, *53*, 2390.
- [56] (a) S. J. Greenfield, S. R. Gilbertson, *Synthesis*, **2001**, *15*, 2337; (b) A. Agarkov, S. J. Greenfield, D. Xie, R. Pawlick, G. Starkley, S. R. Gilbertson, *Peptide Science*, **2006**, *84*, 48.
- [57] S. R. Gilbertson, G. W. Starkey, *J. Org. Chem.*, **1996**, *61*, 2922.
- [58] A. Agarkov, S. J. Greenfield, T. Ohishi, S. E. Collibee, S. R. Gilbertson, *J. Org. Chem.*, **2004**, *69*, 8077.
- [59] (a) F. Meyer, A. Laaziri, A. M. Papini, J. Uziel, S. Jugé, *Tetrahedron: Asymm.*, **2003**, *14*, 2229; (b) F. Meyer, A. Laaziri, A. M. Papini, J. Uziel, S. Jugé, *Tetrahedron*, **2004**, *60*, 3593.
- [60] F. Real-Fernandez, A. Colson, J. Bayardon, F. Nuti, E. Peroni, R. Meunier-Prest, F. Lolli, M. Chello, C. Daracel, S. Jugé, A. M. Papini, *Peptide Science*, **2008**, *90*, 488.
- [61] G. G. Rajeshwaran, M. Nandakumar, R. Sureshbabu, A. K. Mohanakrishnan, *Org. Lett.*, **2011**, *13*, 1270.
- [62] (a) T. Hirao, T. Masunaga, Y. Ohshiro, T. Agawa, *Tetrahedron Lett.*, **1980**, *21*, 3595; (b) T. Hirao, T. Masunaga, N. Yamada, Y. Ohshiro, T. Agawa, *Bull. Chem. Soc. Jpn.*, **1982**, *55*, 909.
- [63] D. Enders, A. Saint-Dizier, M.-I. Lannou, A. Lenzen, *Eur. J. Org. Chem.*, **2006**, 29.
- [64] C. Larpent, H. Patin, *Tetrahedron*, **1988**, *44*, 6107.
- [65] H.-J. Cristau, J.-P. Vors, H. Christol, *Tetrahedron Lett.*, **1961**, *20*, 2377.
- [66] G. Knühl, P. Sennhenn, G. Helmchen, *J. Chem. Soc., Chem. Commun.*, **1995**, 1845.
- [67] T. Minami, Y. Okada, T. Otaguro, S. Tawaraya, T. Furuichi, T. Okauchi, *Tetrahedron: Asymmetry*, **1995**, *6*, 2469.
- [68] M. Léautey, G. Castelot-Deliencourt, P. Jubault, X. Pannecoucke, J.-C. Quirion, *Tetrahedron Lett.*, **2002**, *43*, 9237.
- [69] L. Tedeschi, D. Enders, *Org. Lett.*, **2001**, *22*, 3515.
- [70] X. Fu, Z. Jiang, C.-H. Tan, *Chem. Commun.*, **2007**, 5058.
- [71] B. Cho, C.-H. Tan, M. W. Wong, *Org. Biomol. Chem.*, **2011**, *9*, 4550.
- [72] F. Lemasson, H.-J. Gais, J. Runsink, G. Raabe, *Eur. J. Org. Chem.*, **2010**, 2157.
- [73] X. Luo, Z. Zhou, X. Li, X. Liang, J. Ye, *RCS Adv.*, **2011**, *1*, 698.
- [74] (a) C. Baillie, J. Xiao, *J. Curr. Org. Chem.*, **2003**, *7*, 477; (b) M. Tanaka, *Top. Curr. Chem.*, **2004**, *232*, 25; (c) J.-L. Montchamp, *J. Organomet. Chem.* **2005**, *690*, 2388; (d) D. Enders, A. Saint-Dizier, Lannou, M.-I.; Lenzen, A. *Eur. J. Org. Chem.*, **2006**, 29; (e) F. Alonso, I. P. Beletskaya, M. Yus, *Chem. Rev.* **2004**, *104*, 3079; (f) I. P. Beletskaya, M. A. Kazankova, *Russ. J. Org. Chem.* **2002**, *38*, 1391; (g) L. Coudray, J.-L. Montchamp, *Eur. J. Org. Chem.* **2008**, 3601.
- [75] N. Pudovik, A. Arbuzov, *Dokl. Akad. Nauk. SSSR*, **1950**, *73*, 327.
- [76] F. Yang, D. Zhao, J. Lan, P. Xi, L. Yang, S. Xiang, J. You, *Angew. Chem. Int. Ed.*, **2008**, *47*, 5646.
- [77] R. G. de Noronha, P. J. Costa, C. C. Romão, M. J. Calhorda, A. C. Fernandes, *Organometallics*, **2009**, *28*, 6206.
- [78] E. Balaraman, V. Srinivas, K. C. Swamy, *Tetrahedron*, **2009**, *65*, 7603.
- [79] T. Bunlaksanusorn, P. Knochel, *Tetrahedron Lett.*, **2002**, *43*, 5817.
- [80] T. Bunlaksanusorn, K. Polbron, P. Knochel, *Angew. Chem. Int. Ed.*, **2003**, *42*, 3941.
- [81] D. Mimeau, A.-C. Gaumont, *J. Org. Chem.*, **2003**, *68*, 7016.
- [82] M. Nielsen, C. B. Jacobsen, K. A. Jørgensen, *Angew. Chem. Int. Ed.*, **2011**, *50*, 3211.
- [83] (a) W. Chodkiewicz, *Ann. Chim. Paris*, **1957**, *2*, 819; (b) P. Cadiot, W. Chodkiewicz, *Chemistry of Acetylenes*; H. G. Viehe Ed., Marcel Dekker: New York, **1969**, 597.
- [84] S. E. Tunney, K. J. Stille, *J. Org. Chem.*, **1987**, *52*, 748.
- [85] L. Kurz, G. Lee, D. Morgans Jr., M. J. Waldyke, T. Ward, *Tetrahedron Lett.*, **1990**, *31*, 6321.
- [86] A. Miyashita, A. Yasuda, H. Takaya, K. Toriumi, T. Ito, T. Souchi, R. Noyori, *J. Am. Chem. Soc.*, **1980**, *102*, 7932.
- [87] D. Cai, J. F. Payack, D. R. Bender, D. L. Hughes, T. R. Verhoeven, P. J. Reider, *J. Org. Chem.*, **1994**, *59*, 7180.
- [88] T. Imamoto, T. Oshiki, T. Onozawa, M. Matsuo, T. Hikosaka, M. Yanagawa, *Heteroat. Chem.*, **1992**, *3*, 563.
- [89] B. H. Lipshutz, D. J. Buzard, C. S. Yun, *Tetrahedron Lett.*, **1999**, *40*, 201.
- [90] M. Al-Masum, T. Livinghouse, *Tetrahedron Lett.*, **1999**, *40*, 7731.
- [91] M. Al-Masum, G. Kumaraswamy, T. Livinghouse, *J. Org. Chem.*, **2000**, *65*, 4776.
- [92] S. R. Gilbertson, Z. Fu, G. W. Starkley, *Tetrahedron Lett.*, **1999**, *40*, 8509.
- [93] D. Julienne, J.-F. Lohier, O. Delacroix, A.-C. Gaumont, *J. Org. Chem.*, **2007**, *72*, 2247.
- [94] D. Julienne, O. Delacroix, A.-C. Gaumont, *C. R. Chimie*, **2010**, *13*, 1099.
- [95] (a) J. Uziel, C. Darcel, D. Moulin, C. Bauduin, S. Jugé, *Tetrahedron: Asymmetry*, **2001**, *12*, 1441 ; (b) S. Jugé, M. Stephan, J. A. Laffitte, J. P. Genêt, *Tetrahedron Lett.*, **1990**, *31*, 6357.
- [96] F. Y. Kwong, K. S. Chan, *Organometallics*, **2001**, *20*, 2570.
- [97] H.-J. Cristau, A. Chêne, H. Christol, *J. Organomet. Chem.*, **1980**, *185*, 283.
- [98] D. J. Ager, B. E. East, A. Eisenstadt, S. A. Laneman, *Chem. Comm.*, **1997**, 23590.

- [99] (a) I. P. Beletskaya, M. A. Kazankova, I. V. Efimova, *Org. Lett.*, **2003**, *5*, 4309; (b) V. V. Afanasiev, I. P. Beletskaya, M. A. Kazankova, I. V. Efimova, M. U. Antipin, *Synthesis*, **2003**, 2835.
- [100] M. Arisawa, M. Onoda, C. Hori, M. Yamaguchi, *Tetrahedron Lett.*, **2006**, *47*, 5211.
- [101] K. Bravo-Altamirano, Z. Huang, J.-L. Montchamp, *Tetrahedron*, **2006**, *61*, 6315.
- [102] (a) M.-A. David, S. N. Paisner, D. S. Glueck, *Organometallics*, **1995**, *14*, 17; (b) V. P. W. Böhm, M. Brookhart, *Angew. Chem. Int. Ed.*, **2001**, *40*, 4694.
- [103] J. R. Moncarz, N. F. Laritcheva, D. S. Glueck, *J. Am. Chem. Soc.*, **2002**, *124*, 13356.
- [104] J. R. Moncarz, T. J. Brunker, D. S. Glueck, R. D. Sommer, A. L. Rheingold, *J. Am. Chem. Soc.*, **2003**, *125*, 1180.
- [105] T. J. Brukner, B. J. Anderson, N. F. Blank, D. S. Glueck, A. L. Rheingold, *Org. Lett.*, **2007**, *9*, 1109.
- [106] V. S. Chan, R. G. Bergman, F. D. Toste, *J. Am. Chem. Soc.*, **2007**, *129*, 15122.
- [107] C. Scriban, D. S. Glueck, *J. Am. Chem. Soc.*, **2006**, *128*, 2788; C. Scriban, D. S. Glueck, J. A. Golen, A. L. Rheingold, *Organometallics*, **2007**, *26*, 1788.
- [108] V. S. Chan, I. C. Steward, R. G. Bergman, F. D. Toste, *J. Am. Chem. Soc.*, **2006**, *128*, 2786.
- [109] D. Julienne, O. Delacroix, A.-C. Gaumont, *Phosphorus, Sulfur and Silicon*, **2009**, *184*, 846.
- [110] (a) C. Dobrota, A. Durand, M. Toffano, *Eur. J. Org. Chem.*, **2008**, *14*, 2439; (b) J.-C. Fiaud, M. Toffano, C. Dobrota, J.-C. Fiaud, *Eur. J. Org. Chem.*, **2006**, 650; (c) F. Guillen, M. Rivard, M. Toffano, J.-Y. Legros, J.-C. Daran, J.-C. Fiaud, *Tetrahedron*, **2002**, *58*, 5895.
- [111] (a) C. Buon, P. Bouyssou, G. Coudert, *Tetrahedron Lett.*, **1999**, *40*, 701; (b) F. Lepifre, C. Buon, R. Rabot, P. Bouyssou, G. Coudert, *Tetrahedron Lett.*, **1999**, *40*, 6373.
- [112] (a) D. Mousset, I. Gillaizeau, A. Sabatié, P. Bouyssou, G. Coudert, *J. Org. Chem.*, **2006**, *71*, 5993; (b) E. Cleaveau, I. Gillaizeau, J. Blu, A. Bruel, G. Coudert, *J. Org. Chem.*, **2007**, *72*, 4832; (c) M. Chaignaud, I. Gillaizeau, N. Ouhamou, G. Coudert, *Tetrahedron*, **2008**, *64*, 8059.
- [113] K. C. Nicolaou, G.-Q. Shi, J. L. Gunzner, P. Gärtner, Z. Yang, *J. Am. Chem. Soc.*, **1997**, *119*, 5467.
- [114] U. S. Larsen, L. Martiny, M. Begtrup, *Tetrahedron Lett.*, **2005**, *46*, 4261.
- [115] O. Navarro, Y. Oonishi, R. A. Kelly, D. E. Stevens, O. Briel, S. P. Nolan, *J. Organomet. Chem.*, **2004**, *689*, 3722.
- [116] C. Bauduin, D. Moulin, El B. Kaloun, C. Darcel, S. Jugé, *J. Org. Chem.*, **2003**, *68*, 4293.
- [117] J. S. Harvey, V. Gouverneur, *Chem. Commun.*, **2010**, *46*, 7477.
- [118] (a) F. Palacios, A. M. O. de Retana, J. I. Gil, R. L. de Munain, *Org. Lett.*, **2002**, *4*, 2405; (b) M. E. Fox, M. Jackson, I. C. Lennon, J. Klosin, K. A. Abboud, *J. Org. Chem.*, **2008**, *73*, 775; (c) E. L. Deal, C. Petit, J. L. Montchamp, *Org. Lett.*, **2011**, *13*, 3270.
- [119] M. Cieslikiewicz, A. Bouet, S. Jugé, M. Toffano, J. Bayardon, C. West, K. Lewinski, I. Gillaizeau, *Eur. J. Org. Chem.*, **2012**, 1101.
- [120] K. N. Houk, N. G. Rondan, P. V. R. Schleyer, E. Kaufman, T. J. Clark, *J. Am. Chem. Soc.*, **1985**, *107*, 2821.
- [121] W. F. Bailey, A. D. Khnaolkar, K. Gavaskar, T. V. Ovaska, K. Rossi, Y. Thiel, K. B. Wiberg, *J. Am. Chem. Soc.*, **1991**, *113*, 2925.
- [122] (a) D. R. Anderson, N. C. Faibish, P. Beak, *J. Am. Chem. Soc.*, **1999**, *121*, 7553; (b) K. M. Gross, P. Beak, *J. Am. Chem. Soc.*, **2001**, *123*, 315.
- [123] E. Maerten, S. Cabrera, A. Kjærsgaard, K. A. Jørgensen, *J. Org. Chem.*, **2007**, *72*, 8893.
- [124] G. Knühl, P. Sennhenn, G. J. Helmchen, *Chem. Commun.*, **1995**, 1845.
- [125] S. N. Arbuzova, N. K. Gusarova, B. A. Trofimov, *Arkivoc*, **2006**, *V*, 12.
- [126] A. Bouet, M. Cieslikiewicz, K. Lewinski, G. Coudert, I. Gillaizeau, *Tetrahedron*, **2010**, *66*, 498.
- [127] Y. Uozumi, T. Hayashi, *J. Am. Chem. Soc.*, **1991**, *113*, 9887.
- [128] A. Page, J. Clayden, *Beilstein J. Org. Chem.*, **2011**, *7*, 1327.
- [129] (a) Z. Otwinowski, W. Minor, *Macromolecular Crystallography*, Part A; (b) C. W. Jr. Carter, R. M. Sweet, Eds.; Academic Press: New York, **1997**; *Methods in Enzymology*, Vol. 276, 307.
- [130] A. Altomare, G. Cascarno, G. Giacovazzo, A. Guagliardi, M. C. Burla, G. Polidori, M. Camalli, *J. Appl. Cryst.*, **1994**, *27*, 435.
- [131] G. M. Sheldrick, *Acta Crystallogr.*, **2008**, *A64*, 112.
- [132] (a) S. V. Eliseeva, J.-C. G. Bünzli, *Chem. Soc. Rev.*, **2010**, *39*, 189; (b) J.-C. G. Bünzli, S. V. Eliseeva, *J. Rare Earths*, **2010**, *28*, 824; (c) J.-C. G. Bünzli, *Chem. Rev.*, **2010**, *110*, 2729; (d) C. P. Montgomery, B. S. Murray, E. J. New, R. Pal, D. Parker, *Acc. Chem. Res.*, **2009**, *42*, 925; (e) K. Binnemans, *Chem. Rev.*, **2009**, *109*, 4283; (f) E. G. Moore, A. P. S. Samuel, K. N. Raymond, *Acc. Chem. Res.*, **2009**, *42*, 542; (g) C. M. G. Dos Santos, A. J. Harte, S. J. Quinn, T. Gunnlaugsson, *Coord. Chem. Rev.*, **2008**, *252*, 2512; (h) J.-C. G. Bünzli, C. Piguet, *Chem. Soc. Rev.*, **2005**, *34*, 1048.
- [133] (a) D. Parker, *Chem. Soc. Rev.*, **2004**, *33*, 156; (b) D. Parker, R. S. Dickens, H. Puschmann, C. Crossland, J. A. K. Howard, *Chem. Res.*, **2002**, *102*, 1977; (c) J.-C. G. Bünzli, *Acc. Chem. Res.*, **2006**, *39*, 53.
- [134] C. M. G. dos Santos, P. B. Fernandez, S. E. Plush, J. P. Leonard, T. Gunnlaugsson, *Chem. Commun.*, **2007**, 3389.
- [135] S. Aime, S. G. Crich, E. Gianolio, G. B. Giovenzana, L. Tei, E. Terreno, *Coord. Chem. Rev.*, **2006**, *250*, 1562.
- [136] J. Zhang, P. D. Badger, S. J. Geib, S. Petoud, *Angew. Chem. Int. Ed.*, **2005**, *44*, 2508.
- [137] G. A. Wagnieres, W. M. Star, B. C. Wilson, *Photochem Photobiol.*, **1998**, *68*, 603.
- [138] (a) Y. Oshishi, T. Kanamori, T. Kitagawa, S. Takahashi, E. Snitzer, G. H. Sigel, *Opt. Lett.*, **1991**, *16*, 1747; L. H. Slooff, A. Polman, M. P. O. Wolbers, F. van Veggel, D. N. Reinhoudt, J. W. Hofstraat, *J. Appl. Phys.*, **1998**, *83*, 497.
- [139] L. Armelao, S. Quici, F. Barigelletti, G. Accorsi, G. Bottar, M. Cavazzini, E. Tondello, *Coord. Chem. Rev.*, **2010**, *254*, 487.
- [140] S. Hirano, K. T. Suzuki, *Environ. Health. Perspect.*, **1996**, *104*, 85.
- [141] K. W.-Y. Chan, W. T. Wong, *Coord. Chem. Rev.*, **2007**, *251*, 2428.
- [142] P. G. Sammes, G. Yahioglu, *Nat. Prod. Rep.*, **1996**, *13*, 1.
- [143] S. Aime, A. S. Batsanov, M. Botta, J. A. K. Howard, D. Parker, K. Senanayake, G. Williams, *Inorg. Chem.*, **1994**, *33*, 4696.
- [144] (a) D. Meyer, M. Sheaffer, B. Bonnemain, *Invest. Radiol.*, **1988**, *23*, S232; (b) K. Nwe, M. Bernardo, C. A. Regino, M. Williams, M. W. Brechbiel, *Bioorg. Med. Chem.*, **2010**, *18*, 5925.

- [145] (a) A. Beeby, B. P. Burton-Pye, S. Faulkner, G. R. Motson, J. Jeffery, J. A. McCleverty, M. D. Ward, *Dalton Trans.*, **2002**, 19, 1923; (b) Faulkner, A. Beeby, M. C. Carrie, A. Dadabhoy, A. M. Kenwright, P. G. Sammes, *Inorg. Chem. Commun.*, **2001**, 4, 187.
- [146] A. Beeby, I. M. Clarkson, R. S. Dickins, S. Faulkner, D. Parker, L. Royle, A. S. de Sousa, J. A. G. Woods, *J. Chem. Soc., Perkin Trans.*, **1999**, 3, 493.
- [147] H. Uh, S. Petoud, *CR Chimie*, **2010**, 13, 668.
- [148] M. Latva, H. Takalo, V.-M. Mikkala, C. Matachescu, J. C. Rodriguez-Ubis, J. Kankare, *J. Lumin.*, **1997**, 75, 149.
- [149] (a) T. Förster, *Discuss. Faraday Soc.*, **1959**, 27, 7; (b) D. L. Dexter, *J. Chem. Phys.*, **1953**, 21, 836; (c) T. Lazarides, D. Sykes, S. Faulkner, A. Barbieri, M. D. Ward, *Chem. Eur. J.*, **2008**, 14, 9389.
- [150] W. de W. Horrocks, M.-J. Rhee, A. P. Snyder, D. R. Sudnick, *J. Am. Chem. Soc.*, **1980**, 102, 3650.
- [151] (a) A. P. S. Samuel, E. G. Moore, M. Melchior, J. Xu, K. N. Raymond, *Inorg. Chem.*, **2008**, 47, 7535; (b) E. G. Moore, J. Xu, C. J. Jocher, I. Castro-Rodriguez, K. N. Raymond, *Inorg. Chem.*, **2008**, 47, 3105.
- [152] (a) J.-C. G. Bünzli, *Chem. Rev.*, **2010**, 110, 2729, (b) S. Faulkner, S. J. A. Pope, B. P. Burton-Pye, *Appl. Spectr. Reviews*, **2005**, 40, 1.
- [153] S. Quici, G. Marzanni, M. Cavazzini, P. L. Anelli, M. Botta, E. Gianolio, G. Accorsi, N. Armaroli, F. Barigelletti, *Inorg. Chem.*, **2002**, 41, 2777.
- [154] A. Beeby, R. S. Dickins, S. FitzGerald, L. J. Govenlock, C. L. Maupin, D. Parker, J. P. Riehl, G. Siligardi, J. A. G. Williams, *Chem. Commun.*, **2000**, 1183.
- [155] S. I. Klink, H. Keizer, F. C. J. M. van Veggel, *Angew. Chem. Int. Ed.*, **2000**, 39, 4319.
- [156] M. Li, P. R. Selvin, *J. Am. Chem. Soc.*, **1995**, 117, 8132.
- [157] A. Dadabhoy, S. Faulkner, P. G. Sammes, *J. Chem. Soc., Perkin Trans. 2*, **2002**, 348.
- [158] B. P. Burton-Pye, S. L. Heath, S. Faulkner, *Dalton Trans.*, **2005**, 146.
- [159] F. Rizzo, A. Papagni, F. Meinardi, R. Tubino, M. Ottonelli, G. F. Musso, G. Dellapiane, *Synthetic Metals*, **2004**, 147, 143.
- [160] D. Maffeo, J. A. G. Williams, *Inorg. Chimica Acta*, **2003**, 355, 127.
- [161] M. Andrews, L. H. Laye, L. P. Harding, S. J. A. Pope, *Polyhedron*, **2008**, 27, 2365.
- [162] C. P. Montgomery, D. Parker, L. Lamarque, *Chem. Commun.*, **2007**, 3841.
- [163] L.S. Natrajan, A.-J. L. Villaraza, A. M. Kenwright, S. Faulkner, *Chem. Commun.*, **2009**, 6020.
- [164] M.P. Placidi, A.-J.L. Villaraza, L.S. Natrajan, D. Sykes, A.M. Kenwright, S. Faulkner, *J. Am. Chem. Soc.* **2009**, 131, 9916.
- [165] K. Aita, T. Temma, Y. Kuge, K. Seki, H. Saji, *Luminescence*, **2010**, 25, 19.
- [166] D. Parker, P. K. Senanayake, J. A. G. Williams, *J. Chem. Soc., Perkin Trans. 2*, **1998**, 2129.
- [167] J. B. Coldwell, C. E. Felton, L. P. Harding, R. Moon, J. A. Pope, C. Rice, *Chem. Commun.*, **2006**, 5048.
- [168] A. Bodi, K. E. Borbas, J. I. Bruce, *Dalton Trans.*, **2007**, 4352.
- [169] S. He, H. Li, Y.-W. Yip, C.-T. Yeung, Y. O. Fung, H.-K. Kong, H.-L. Yeung, G.-L. Law *et al.*, *Org. Lett.*, **2011**, 13, 5036.
- [170] F.-L. Jiang, C.-T. Poon, W.-K. Wong, H.-K. Koon, N.-K. Mak, C. Y. Choi, D. W. J. Kwong, Y. Liu, *Chem. Bio. Chem.*, **2008**, 9, 1034.
- [171] P. Zhang, W. Steelant, M. Kumar, M. Scholfield, *J. Am. Chem. Soc.*, **2007**, 129, 4526.
- [172] M. A. Alcalá, C. M. Shade, H. Uh, S. Y. Kwan, M. Bishhof, Z. P. Thompson, K. A. Gogick, A. R. Meier, T. G. Strein, D. L. Bartlett, R. A. Modzelewski, Y. J. Lee, S. Petoud, C. K. Brown, *Biomaterials*, **2011**, 32, 9343.
- [173] A. Thibon, V. C. Pierre, *Anal. Bioanal. Chem.*, **2009**, 394, 107.
- [174] S. Mizukami, K. Tonai, M. Kaneko, K. Kikuchi, *J. Am. Chem. Soc.*, **2008**, 130, 14376.
- [175] E. Pazos, D. Torrecilla, M. V. López, L. Castedo, J. L. Mascareñas, A. Vidal, M. E. Vázquez, *J. Am. Chem. Soc.*, **2008**, 130, 9652.
- [176] (a) K. Hori, M. J. Cormier, *Proc. Natl. Acad. Sci. U.S.A.*, **1973**, 14, 120; (b) O. Shimomura, F. H. Johnson, *Proc. Nat. Acad. Sci.*, **1975**, 72, 1546; (c) C. M. Thomson, P. J. Herring, A. K. Campbell, *J. Biolumin. Chemilumin.*, **1997**, 8, 87; (d) K. Jones, F. Hibbert, M. Keenan, *Trends Biotechnol.*, **1999**, 17, 477; (e) J. W. Hastings, C. H. Johnson, *Methods Enzymol.*, **2000**, 305, 75.
- [177] D. J. Mitchell, G. B. Schuster, H. G. Drickamer, *J. Chem. Phys.*, **1979**, 70, 2443.
- [178] Z. Li, S. Wu, *J. Fluorescence*, **1997**, 7, 237.
- [179] J. D. Lee, L. M. Vrana, E. R. Bullock, K. J. Brewer, *Inorg. Chem.*, **1998**, 37, 3575.
- [180] K. Sugou, K. Sasaki, K. Kitajima, T. Iwaki, Y. Kuroda, *J. Am. Chem. Soc.*, **2002**, 124, 1182.
- [181] W. Ming, L. Ying, X. ZhiYuan, W. LiXiang, *Science China, chemistry*, **2011**, 54, 656.
- [182] N. Maindron, S. Poupard, M. Hamon, J.-B. Langlois, N. Plé, L. Jean, A. Romieu, P.-Y. Renard, *Org. Biomol. Chem.*, **2011**, 9, 2357.
- [183] (a) X. Zhang, Z. Sui, *Tetrahedron*, **2006**, 47, 5953; (b) D. Aparicio, O. A. Attanasi, P. Filippone, R. Ignacio, S. Lillini, F. Mantellini, F. Palacios, J. M. de los Santos, *J. Org. Chem.*, **2006**, 71, 5897.
- [184] S. Mizukami, K. Tono, M. Kaneko, K. Kikuchi, *J. Am. Chem. Soc.*, **2008**, 130, 14376.
- [185] O. Diels, K. Alder, *Justus Liebigs. Ann. Chem.*, **1928**, 460, 98.
- [186] I. Fleming, *Frontier Orbitals and Organic Chemical Reactions*, Wiley, London, **1976**, p.110, 161.
- [187] (a) G. Coudert, F. Lepifre, D. H. Caignard, P. Renard, J. Hickman, A. Pierré, L. Kraus-Berthier, *FR 2002-12964 A* 18 oct. 2002 – WO 2003-FR3068 W 17 oct. 2003; (b) G. Coudert, N. Ayerbe, F. Lepifre, S. Routier, D. H. Caignard, P. Renard, J. Hickman, A. Pierré, S. Léonce, *FR 2002-12965 A* 18 oct. 2002 – WO 2003-FR3069 W 17 oct. 2003.
- [188] M. A. Alcalá, S. Y. Kwan, C. M. Shade, M. Lang, H. Uh, M. Wang, S. G. Weber, D. L. Bartlett, S. Petoud, Y. J. Lee, *Nanomedicine*, **2011**, 7, 249.
- [189] (a) A. Bourderioux, V. Bénéteau, J.-Y. Mérour, B. Baldeyrou, C. Ballot, A. Lansiaux, C. Bailly, R. Le Guével, C. Guillouzo, S. Routier, *Org. Biomol. Chem.*, **2008**, 6, 2108; (b) N. Ayerbe, S. Routier, I. Gillaizeau, S. Tardy, G. Coudert, *Lett. Org. Chem.*, **2010**, 7, 121.
- [190] R. Appel, *Angew. Chem. Int. Ed.*, **1975**, 14, 801.

- [191] K. Sonogashira, Y. Tohda, N. Hagihara, *Tetrahedron Lett.*, **1975**, 16, 4467.
- [192] R. Chinchilla, C. Nájera, *Chem. Rev.*, **2007**, 107, 874.
- [193] (a) H. A. Dieck, F. R. Heck, *J. Organomet. Chem.*, **1975**, 93, 259; (b) L. Cassar; *J. Organomet. Chem.*, **1975**, 93, 253.
- [194] C. W. Tornøe, C. Christensen, M. Meldal, *J. Org. Chem.*, **2002**, 67, 3057.
- [195] V. V. Rostovtsev, L. G. Green, V. V. Fokin, K. B. Sharpless, *Angew. Chem. Int. Ed.*, **2002**, 41, 2596.
- [196] B. C. Boren, S. Narayan, L. K. Rasmussen, L. Zhang, H. Zhao, Z. Lin, G. Jia and V. V. Fokin, *J. Am. Chem. Soc.*, **2008**, 130, 8923.
- [197] F. Himo, T. Lovell, R. Hilgraf, V. V. Rostovtsev, L. Noodleman, K. B. Sharpless, V. V. Fokin, *J. Am. Chem. Soc.*, **2005**, 127, 210.
- [198] C. Li, E. Henry, N. K. Mani, J. Tang, J.-C. Bronchon, E. Deprez, J. Xie, *Eur. J. Org. Chem.*, **2010**, 2395.
- [199] L. Horner, H. Hoffmann, H. G. Wippel, G. Klahre, *Chem. Ber.*, **1959**, 92, 2499.
- [200] K. C. Nicolau, M. W. Härter, J. L. Gunzner, A. Nadin, *Eu. J. Org. Chem.*, **1997**, 7, 1283.
- [201] G. Pattenden, A. Walter, S. J. Woodhead, *Natural Product Synthesis*, **2004**, 101, 12024.
- [202] (a) J. M. Robinson, G. T. Daniel, S. J. Hale, *J. Org. Chem.*, **1986**, 51, 109; (b) T. Sakai, K. Miyata, M. Utaka, A. Takeda, *Bull. Chem. Soc. Jpn.*, **1987**, 60, 1063.
- [203] S. Irifune, T. Kibayashi, Y. Ishii, M. Ogawa, *Synthesis*, **1988**, 5, 366.
- [204] M. Botta, S. Quici, G. Pozzi, G. Marzanni, R. Pagliarin, S. Barra, S. G. Crich, *Org. Biomol. Chem.*, **2004**, 2, 570
- [205] N. Raghunani, G. P. Guntle, V. Gokhale, G. S. Nichol, E. A. Mash, B. Jagadish, *J. Med. Chem.*, **2010**, 18, 6746
- [206] C. Tu, E. A. Osborne, A. Y. Louie, *Tetrahedron*, **2009**, 65, 1241.
- [207] A. Novoa, N. Pellegrini-Moise, D. Bechet, M. Barberi-Heyob, Y. Chapleur, *Bioorg. Med. Chem.*, **2010**, 18, 3285.
- [208] (a) J.-C. G. Bünzli, A.-S. Chauvin, H. K. Kim, E. Deiters, S. V. Eliseeva, *Coord. Chem. Rev.*, **2010**, 254, 2623; (b) M. V. López, S. V. Eliseeva, J. M. Blanco, G. Rama, M. R. Barnejo, M. E. Vázquez, J.-C. G. Bünzli, *Eur. J. Org. Chem.*, **2010**, 4532, (c) S. Comby, D. Imbert, C. Vandevyver, J.-C. G. Bünzli, *Chem. Eur. J.*, **2007**, 13, 936.
- [209] (a) R. D. Shanon, *Acta Cryst.*, **1976**, A23, 751, (b) S. Faulkner, A. Beeby, R. S. Dickins, D. Parker, J. A. G. Williams, *Journal of Fluorescence*, **1999**, 9, 45.
- [210] A. Nobel, *Justus Liebigs Annalen der Chemie*, 1856, 98, 253.
- [211] H. Benhold, *München. Med. Wochenschr.*, **1922**, 69, 1537.
- [212] P. Divry, *J. Neurol. Psychiatr.*, **1927**, 27, 643.
- [213] R. Khurana, V. N. Uversky, L. Nielsen, A. L. Fink, *J. Biol. Chem.*, **2001**, 276, 22715.
- [214] K. A. Talukder, Z. Islam, M. A. Islam, D. K. Dutta, A. Safa, M. Ansaruzzaman, A. S. G. Faruque, S. N. Shahed, G. B. Nair, D. A. Sack, *J. Clin. Microbiol.*, **2003**, 41, 110.
- [215] (a) T. Ikeda, O. Tsutsumi, *Science*, **1995**, 268, 1873; (b) D. Jayalatha, R. Balamurugan, P. Kannan, *High Performance Polymers*, **2009**, 21, 139.
- [216] I. A. Banerjee, L. Yu, H. Matsui, *J. Am. Chem. Soc.*, **2003**, 125, 6542.
- [217] B. L. Feringa, R. A. van Delden, N. Koumura, E. M. Geertsema, *Chem. Rev.*, **2000**, 100, 1789.
- [218] H. Murakami, A. Kawabuchi, K. Kotoo, M. Kitunake, N. Nakashima, *J. Am. Chem. Soc.*, **1997**, 119, 7605.
- [219] (a) W. J. Sandborn, *Am. J. Gastroenterol.*, **2002**, 97, 2939 (b) A. Jain, Y. Gupta, S. K. Jain, *Crit. Rev. Ther. Drug Carrier Syst.*, **2006**, 23, 349.
- [220] E. Diau, *J. Phys. Chem. A*, **2004**, 108, 950.
- [221] T. Muraoka, K. Kinbara, T. Aida, *Nature*, **2006**, 440, 512.
- [222] X. Liang, H. Asanuma, M. Komiyama, *J. Am. Chem. Soc.*, **2002**, 124, 1877.
- [223] F. Hamon, F. Djedaini-Pilard, F. Barbot, C. Len, *Tetrahedron*, **2009**, 65, 10105.
- [224] I. Svelle, H. Zollinger, *Top. Curr. Chem.*, **1983**, 112, 1.
- [225] (a) J. R. Penton, H. Zollinger, *Helv. Chim. Acta*, **1981**, 64, 1717, (b) R. P. Kelly, J. R. Penton, H. Zollinger, *Helv. Chim. Acta*, **1982**, 65, 122.
- [226] C. H. Hunter, L. D. Sarson, *Tetrahedron Lett.*, **1996**, 37, 699.
- [227] A. Tsuge, T. Moriguchi, S. Mataka, M. Tashiro, *J. Chem. Soc., Perkin Trans. 1*, **1993**, 2211.
- [228] J. Y. Kim, G. Kim, C. R. Kim; S. H. Lee, J. S. Kim, *J. Org. Chem.*, **2003**, 68, 1933.
- [229] H. H. Davey, R. D. Lee, T. J. Marks, *J. Org. Chem.*, **1999**, 64, 4976.
- [230] K. Ueno, S. Akiyoshi, *J. Am. Chem. Soc.*, **1954**, 76, 3670.
- [231] N. R. Ayyangar, S. N. Naik, K. V. Srinivasan, *Tetrahedron Lett.*, **1989**, 30, 7253.
- [232] A. Sakamoto, A. Hirooka, K. Namiki, M. Kurihara, M. Murata, M. Sugimoto, H. Nishihara, *Inorg. Chem.*, **2005**, 44, 7547.
- [233] C. Tie, J. G. Gallucci, J. R. Parquette, *J. Am. Chem. Soc.*, **2006**, 128, 1162.
- [234] O. Wallach, E. Belli, *Chem. Ber.*, **1880**, 13, 525.
- [235] G. A. Olah, K. Dunne, D. P. Kelly, Y. K. Mo, *J. Am. Chem. Soc.*, **1972**, 94, 7438.
- [236] M. M. Shemyakin, V. I. Maimind, B. K. Vaichunaite, *Chem. Ind.*, **1958**, 755.
- [237] W. M. Cumming, G. S. Ferrier, *J. Chem. Soc. Trans.*, **1925**, 127, 2374.
- [238] J. Yamamoto, Y. Neshigaki, M. Umezu, *Tetrahedron*, **1980**, 36, 3177.
- [239] H. M. Nanjundaswamy, M. A. Pasha, *Synth. Commun.*, **2005**, 35, 2163.
- [240] (a) R. F. Nystrom, W. G. Brown, *J. Am. Chem. Soc.*, **1948**, 70, 3738; (b) R. O. Hutchins, D. W. Lamson, L. Rua, C. Milewski, B. Maryanoff, *J. Org. Chem.*, **1971**, 36, 803.
- [241] G. R. Srinivasa, K. Abiraj, D. C. Gowda, *Aust. J. Chem.*, **2004**, 57, 609.
- [242] S. Wawzonek, T. W. McIntyre, *J. Electrochem. Soc.*, **1972**, 119, 135.
- [243] H. Olsen, P. J. Snyder, *J. Am. Chem. Soc.*, **1977**, 99, 1524.
- [244] M. Barth, S. Tasadaque, A. Shah, J. Rademann, *Tetrahedron*, **2004**, 60, 8703.
- [245] T. Cohen, R. J. Lewarchik, J. Z. Tarino, *J. Am. Chem. Soc.*, **1974**, 96, 7753.
- [246] M. L. Hays, T. P. Hanusa, *Tetrahedron Lett.*, **1995**, 36, 2435.

- [247] Y.-K. Lim, K.-S. Lee, C.-G. Cho, *Org. Lett.*, **2003**, *5*, 979.
- [248] Y.-K. Lim, S. Choi, K. B. Park, C. G. Cho, *J. Org. Chem.*, **2004**, *69*, 2603.
- [249] X. Álvarez Micó, T. Ziegler, L. R. Subramanian, *Angew. Chem. Int. Ed.*, **2004**, *43*, 1400.
- [250] L. I. Smith, W. B. Irvine, *J. Am. Chem. Soc.*, **1941**, *63*, 1036.
- [251] E. C. Taylor, G. E. Jagdmann Jr., A. McKillop, *J. Org. Chem.*, **1978**, *43*, 4385.
- [252] M. C. Carreño, G. Fernández-Mudarra, E. Merino, M. Ribagorda, *J. Org. Chem.*, **2004**, *69*, 3413.
- [253] X. Wang, Y. Zhang, H. Tan, Y. Wang, P. Han, D. Z. Wang, *J. Org. Chem.*, **2010**, *75*, 2403.
- [254] (a) A. F. Abdel-Magid, K. G. Carson, B. D. Harris, C. A. Maryanoff, R. D. Shah, *J. Org. Chem.*, **1996**, *61*, 3849; (b) D. C. Beshore, C. J. Dinsmore, *Org. Lett.*, **2002**, *4*, 1201.
- [255] (a) S. Mizukami, K. Tonai, M. Kaneko, K. Kikuchi, *J. Am. Chem. Soc.*, **2008**, *130*, 14376; (b) K. N. Green, S. Viswaiathar, F. A. Rojas-Quijano, Z. Kovacs, D. Shermy, *Inorg. Chem.*, **2011**, *50*, 1648.
- [256] M. F. Loncin, J. F. Desreux, E. Merciny, *Inorg. Chem.*, **1986**, *25*, 2646.
- [257] A. Dadabhoy, S. Faulkner, P. G. Sammes, *J. Chem. Soc., Perkin Trans.2*, **2002**, 348.
- [258] (a) G. Christifori, *EMBO J.*, **2003**, *22*, 2318; (b) K. Maaser, K. Wolf, C. E. Klein, B. Niggemann, K. S. Zanker, E. B. Brocker et al., *Mol. Biol. Cell.*, **1999**, *10*, 3067; (c) E. Ruohlahti, *Nat. Rev. Cancer.*, **2002**, *2*, 83.
- [259] (a) R. K. Andrews, M. C. Berndt, *Thromb. Res.*, **2004**, *114*, 447; (b) J. M. Gibbins, *J. Cell. Sci.*, **2004**, *117*, 3415.
- [260] X. Banquy, G. Leclair, J. M. Rabanel, A. Argaw, J. F. Bouchard, P. Hildgen et al., *Bioconjug. Chem.*, **2008**, *19*, 2030.
- [261] K. Ichinose, E. Kawasaki, K. Eguchi, *Am. J. Nephrol.*, **2007**, *27*, 554.
- [262] (a) M. D. Pierschbacher, E. Ruoslahti, *Nature*, **1984**, *309*, 30; (b) E. Ruoslahti, *Matrix Biol.*, **2003**, *22*, 459.
- [263] (a) W. Cai, X. Chen, *Agents. Med. Chem.*, **2006**, *6*, 407; (b) G. J. Mizejewski, *Proc. Soc. Exp. Biol. Med.*, **1999**, *222*, 124; (c) H. Jin, J. Varner, *Br. J. Cancer.*, **2004**, *90*, 561.
- [264] P. C. Brooks, S. Stromblad, L. C. Sanders, T. L. von Schalscha, R. T. Aimes, W. G. Stetler-Stevenson et al., *Cell.*, **1996**, *85*, 683.
- [265] K. Temming, R. M. Schiffelers, G. Molema, R. J. Kok, *Drug Resist Updat.*, **2005**, *8*, 381.
- [266] Z.-B. Li, Z. Wu, K. Chen, F. T. Chin, X. Chen, *Bioconjugate Chem.*, **2007**, *18*, 1987.
- [267] P. Verwilst, S. V. Eliseeva, S. Carron, L. V. Elst, C. Burtea, G. Dehaen et al., *Eur. J. Inorg. Chem.*, **2011**, 3577.
- [268] (a) I. Dijkstra, A. Y. Rijnders, A. Soede, A. C. Dechesne, G. W. van Esse, A. J. Brouwer et al., *Org. Biomol. Chem.*, **2007**, *5*, 935; (b) Y. Zhou, S. Chakraborty, *Theranostics*, **2011**, *1*, 58.
- [269] V. Aucagne, A.F. Delmas, *unpublished results*
- [270] I. E. Valverde, A. F. Delmas, V. Aucagne, *Tetrahedron*, **2009**, *65*, 7597.
- [271] A. Bourdolle, M. Allali, J.-C. Mulatier, B. Le Guennic, J. M. Zwier, P. L. Baldeck, J.-C. G. Bünzli, C. Andraud, L. Lamarque, O. Maury, *Inorg. Chem.*, **2011**, *50*, 4987.
- [272] D. Geißler, L. J. Charbonnière, R. F. Zeissel, N. G. Butlin, H.-G. Löhmansröben, N. Hildebrandt, *Angew. Chem. Int. Ed.*, **2010**, *49*, 1396.
- [273] (a) I. Grabchev, J.-M. Chovelon, V. Bojinov, G. Ivanova, *Tetrahedron*, **2003**, *59*, 9591; (b) M. A. Alcalá, C. M. Shade, H. Uh, S. Y. Kwan, M. Bischof, Z. P. Thompson, K. A. Gogick, A. R. Meier, T. G. Strein, D. L. Bartlett, R. A. Modzelewski, Y. J. Lee, S. Petoud, C. K. Brown, *Biomaterials*, **2011**, *32*, 9343.
- [274] (a) G. S. Kikot', M. I. Cherkashin, B. S. Kikot', *Russ. Chem. Bull.*, **1981**, *5*, 783; (b) U. Oertel, H. Mart, H. Komber, F. Böhme, *Optical Materials*, **2009**, *32*, 54.
- [275] C. West, A. Bouet, I. Gillaizeau, G. Coudert, M. Lafosse, E. Lesellier, *Chirality*, **2010**, *22*, 245.

Monika CIEŚLIKIEWICZ-BOUET

Synthèse, étude structurale et évaluation de sensibilisateurs pyraziniques de lanthanides émettant dans le proche infrarouge et de nouvelles phosphines

Résumé :

En raison de l'omniprésence des hétérocycles azotés et de leurs propriétés biologiques, une attention particulière est accordée au développement de méthodologie pour leur synthèse et leur fonctionnalisation. L'étude de la fonctionnalisation d'énamides constitue une thématique importante car ces motifs s'avèrent être des outils synthétiques polyvalents permettant d'accéder à des dérivés hétérocycliques complexes. Les réactions de couplage Pd-catalysées constituent une méthode de choix rapide et efficace pour la synthèse d'énamides, notamment à partir de phosphates d'énols issus de lactames, d'imides ou d'amides.

Le premier chapitre de ce travail porte sur le couplage organopalladié C-P de phosphines boranes secondaires chirales ou achirales avec des phosphates d'énols. Ce couplage C-P original, réalisé dans des conditions douces, conduit aux énamido-phosphines boranes correspondantes et offre de nombreuses possibilités pour la constitution d'une librairie de phosphines originales. Parallèlement à ce travail, l'addition nucléophile d'anions phosphures sur divers éne-carbamates acycliques conduit à des acides alpha-aminés bêta-phosphorés originaux, porteurs d'un carbone quaternaire en alpha de l'azote.

Le deuxième chapitre de la thèse porte sur la préparation et la caractérisation de chromophores organiques originaux basés sur un noyau pyrazinique et qui sont susceptibles de présenter des propriétés de fluorescence. Ces composés sont conçus pour former des nouveaux systèmes sensibilisateurs de cations de lanthanides, et être utilisés comme sensibilisateurs organiques pour l'imagerie moléculaire dans le proche infrarouge.

Mots clés : Enamides, phosphate d'énol, couplage C-P pallado-catalysé, énamido-phosphines boranes, acides alpha-aminés bêta-phosphorés, complexes de lanthanides, antenne hétérocyclique, proche infrarouge.

Synthesis, structural investigations and evaluation of pyrazine sensitizers for lanthanides emitting in near-infrared and novel phosphine derivatives

Summary:

On account of the ubiquity of nitrogen heterocycles and their biological properties, the great attention is paid to developing methodologies of their synthesis and functionalization. For this purpose, the study of functionalization of enamides constitutes an important topic due to the utility of these motifs in the construction of complex heterocyclic derivatives. Palladium-catalyzed reactions of cross-coupling are rapid and efficient methods of choice for synthesis of enamides particularly starting from enol phosphates derived from lactams, imides or amides.

The first chapter of the thesis evokes the original C-P coupling reaction of chiral and achiral secondary phosphine boranes with different enol phosphates in mild reaction conditions, leading to corresponding enamido-phosphine boranes. This methodology permits the construction of libraries of novels phosphines. Also, the reaction of nucleophilic addition of phosphide anions onto various enecarbamates acyclic was elaborated, giving an access to original beta-phosphino alpha-amino acids, bearing the quaternary carbon on alpha position to nitrogen.

The second chapter is devoted to the preparation and characterization of organic chromophores based on the pyrazinic core, which are likely to exhibit the fluorescence properties. These compounds were designed to form new sensitizing systems for lanthanide cations and could be used as organic sensitizers for molecular imaging in near infrared.

Keywords: Enamides, vinyl phosphate, C-P palladium catalyzed cross-coupling, enamido-phosphine boranes, beta-phosphino alpha-amino acids, lanthanide complexes, heterocyclic antenna, near infrared



Institut de Chimie Organique et Analytique,
UMR 7311, Rue de Chartres,
45067 Orléans cedex 2

